Stability and stabilization of linear parameter-varying and time-varying delay systems with actuators saturation

Viet Long Bui-Tuan

THÈSE DE DOCTORAT

Mention **:** ***Sciences pour l'Ingénieur***
Spécialité **:** ***Automatique***

présentée à l'École Doctorale en Sciences Technologie et Santé (ED 585)

DE L'UNIVERSITE DE PICARDIE JULES VERNE

par

Viet Long Bui-Tuan

pour obtenir le grade de docteur de l'Université de Picardie Jules Verne

---

Stability and Stabilization of Linear Parameter-Varying and Time-Varying Delay Systems with Actuator Saturation

---

Soutenue le 21 juillet 2022, après avis des rapporteurs, devant le jury d'examen :

M. Thierry Guerra	Professeur des Universités *Université Polytechnique Hauts-de-France*	Rapporteur
M. Michel Zasadzinski	Professeur des Universités *Université de Lorraine*	Rapporteur
M. Abdellah Benzaouia	Professeur des Universités *Université Cadi Ayyad*	Examinateur
M. Driss Mehdi	Professeur des Universités *Université de Poitiers*	Examinateur
M. Ahmed El Hajjaji	Professeur des Universités *Université de Picardie Jules Verne*	Directeur de thèse
M. Olivier Pages	Maître de Conférences *Université de Picardie Jules Verne*	Co-encadrant

Remerciements

Tout d'abord, je tiens à remercier mon directeur de thèse, qui m'a accepté au sein de l'équipe de recherche Commande Véhicule (CoVE) pour mon doctorat, M. Ahmed El Hajjaji. Je lui dois ma reconnaissance pour son aide concernant les démarches administratives que j'ai eu à effectuer et pour son soutien lors des périodes difficiles durant ma thèse. Je tiens également à remercier M. Olivier Pages, mon co-encadrant, qui a toujours été très minutieux et m'a corrigé dans les moindres détails mes résultats et mes publications. J'espère pouvoir continuer à collaborer avec vous dans le futur.

Je remercie M. Thierry Guerra, et M. Michel Zasadzinski, les rapporteurs de ce mémoire qui ont accepté de consacrer une partie de leur précieux temps pour me faire part de leurs remarques et questions. Je remercie également M. Driss Mehdi, et M. Abdellah Benzaouia, les examinateurs de mon jury de soutenance, pour avoir accepté et participé à ce jury et montré l'intérêt et la suggestion dans mon travail. Je les remercie tous d'avoir participé à la soutenance et d'avoir contribué à faire de cette journée un grand moment pour moi.

J'aimerais aussi exprimer ma reconnaissance aux membres du secrétariat du laboratoire MIS, et du département de l'EEA : Juliette, Gaël, Laetitia, Isabelle, etc. Ils ont beaucoup souffert dans le passé à cause de mon vocabulaire français « *riche et garnis* » et phonétique de l'autre bout du monde. Ils ont probablement dû user de beaucoup d'habileté pour comprendre mes intentions et m'aider à remplir certains formulaires, ordres de mission... Par ailleurs, le *responsable du labo*, Gilles et Jérôme ont été très aimables en m'aidant dans certaines situations difficiles lors du processus d'inscription ainsi que lors de la mise en place des confinements nationaux.

L'ambiance conviviale et chaleureuse était ma première impression en arrivant dans la ville d'Amiens et surtout au laboratoire MIS. Les doctorants et stagiaires : Clément, Jordan, Doha, Nathan, Eder, Monika, Seif, ... étaient toujours là pour moi que ça soit pour améliorer mon français, pour les procédures d'inscription, pour les cours, et surtout au début, en me traduisant en anglais leurs conversations pour que je puisse être plus intégré au sein du groupe.

Cinq ans, c'est un temps ni trop long ni trop court pour vivre de nouvelles aventures, faire de nouvelles connaissances et apprendre de nouvelles cultures. Les amis mystérieux sont venus en cadeau du désert. Des amis de Tunisie qui avaient chassé le froid des jours d'hiver. Said B., Dhouha, Amin, Salama, Imen, Amel, … ne sont pas seulement mes collègues mais aussi « *le vent* » qui m'emportent vers le ciel et que je contemplais avec admiration. J'ai beaucoup appris de vous les *adorables*.

Le Groupe d'amis des fêtes bruyantes et des rires, Noureddine, Farouk, des anniversaires inoubliables, des dîners de réveillon chez Richie (Richardson). Tausif, Yassine, je me

souviendrai sûrement encore du moment où j'ai montré mes talents de barista à 22 rue Vauban. L'atmosphère chaleureuse, la façon rustique de parler, pas de frontières religieuses, pas de distance nationale, pas de différence ethnique, vivre à chaque instant est ce dont je me souviens de vous.

En tant que gars doux et timide, Soufyane a toujours essayé de me supporter et de me soutenir au début, lorsque nous sortions avec des filles que nous venions de rencontrer. Bien sûr, nous avons toujours eu des discussions animées sur les matchs de football internationaux, nous avons longuement parlé des systèmes dynamiques, mais surtout, j'ai beaucoup appris de lui sur la façon de présenter et d'interpréter les problèmes, ainsi que sur le système d'onduleurs AC-DC et les systèmes d'alimentation.

Pendant les moments difficiles, les doctorants aiment apporter une brise fraîche d'air, l'odeur de sable marin, la pureté et le silence de la forêt, Zeineb, Laila, Hamza, *notre violoniste* Khelil, Soufyane, Amin, nous avons gardé de beaux souvenirs à Amiens. Soirées barbecue, querelles passionnées à propos de l'attribution de la vaisselle, paris sur les jeux, comparaison des scores au bowling. Amis de la jeunesse. Et puis après, l'arrivée des amis Algériens, distractions et perturbations illimitées, Khalil O., Issam, m'ont d'abord rendu fou et irrité. Cependant, ce sont les amis qui ont le plus laissé leur place après leurs départs. « *Dieu merci* », il y a peut-être un an, ce dicton avait un sens différent, mais maintenant cela signifie vrai d'apprendre beaucoup de vous. Je me souviens toujours de votre devise, « un pour tous, tous pour un ».

Il serait négligent de ne pas mentionner les colocataires sympathiques, Clara, Natali, Linh, Imen, Raja. Chacun de vous a apporté un parfum floral distinctif à la maison. Le plus spécial est probablement « » comme la motivation pour moi de surmonter de nombreuses difficultés ainsi que d'oublier toute la fatigue en rentrant après un travail de recherche laborieux.

Des amis précieux, comme les frères, Bình, Hoài, Tân, Laurent, Japhet, Ahmed M., Ahmed B., Reda, colocs Salama, Louis, Ismaël ont partagé de nombreuses perspectives différentes de vie, d'amour, de la foi, d'aspiration et de tolérance.

En outre, en tant qu'élément indispensable pour améliorer la vie mentale et réformer les performances au travail, le club de footing MIS comprend Jérôme, Hervé, Hamza, Amin, Stéphane avec des séances d'entraînement ensemble. Grâce aux membres du club US Camon, l'AUC qui cherchent toujours à offrir de bonnes conditions pour que je m'intègre dans la communauté des coureurs et améliorer mes capacités. Grâce à Alex avec ses plans d'entraînement fous, le sentier imprévu se déroule à Cottenchy. Merci Mouloud, Patrice de m'avoir accueilli lors de mes premiers jours au club de tennis TCAM. Vos conseils m'ont aidé pour m'améliorer dans les matchs et à élaborer une stratégie mentale. Merci Hamza, Amin, Daniel pour les balades à vélo relaxantes dans la nature, le long des canaux de la Somme, ou rouler sous la pluie et le vent, nager dans la boue (la folie des cyclistes extrêmes). Merci aux membres du club de football UPJV, Anas, Morguant, Noureddine, Khalil B., Carlos, Daniel, ... qui partent à la recherche d'un terrain de foot pendant 50 minutes pour ne jouer que 5 minutes.

Je voudrais remercier également les membres de l'équipe qui travaillent pour l'école Esiee (Uni Lasalle), comme Alan et ses collègues, les agents de sécurité de l'école : David, ...,

les personnels de nettoyage, les personnels travaillant à la cafétéria du Crous de l'école Esiee, ou à la cafétéria de Saint-leu. Pendant mon séjour et mon travail à Amiens, et surtout pendant le confinement et le couvre-feu, votre aide enthousiaste, vos demandes passionnées, votre accueil chaleureux, vous m'avez toujours fait sentir comme si j'étais chez moi. Un sincère merci pour vous ne suffira peut-être pas, je voudrais garder les meilleures choses dans mon cœur. Au cours de mes cinq années d'utilisation du service de restauration de Crous, la soupe du chef d'Esiee me manque le plus, et à ce jour, je n'ai pas eu un seul mal de ventre.

Au cours de ce séjour, je tiens à remercier la ville Amiens pour m'avoir accueilli chaleureusement, et de m'avoir fait vivre de nombreuses expériences émouvantes. Merci mesdames, votre acuité, votre charisme seront une saveur inoubliable pour ce voyage.

Et enfin, merci du fond du cœur à ma famille et mes amis qui ont toujours été avec moi ces derniers temps. Sans eux, je n'aurais pas eu le courage et la motivation pour tenir jusqu'au bout. Tout ce travail est grâce à vous.

Merci.

Viet Long.

Acknowledgments

I would like to express my sincere gratitude to the anonymous reviewers for taking the time to review and provide comments. Your criticism and suggestions help me significantly progress the results and improve the writing style of the PhD dissertation.

In addition, I would like to thank the professors and technicians who enthusiastically responded to my questions. I have learned and improved a lot from your dedicated help. Also, I would like to mention Prof. Löfberg has guidance on the academic problems of the Interior-point method and share advice to improve the convergence results involving the Yalmip toolbox. And I would like to thank Professor Tarbouchie for taking her precious time during December 2021 holiday to answer questions and provide valuable comments on the open problems.

Thanks to Mohamed Z., Hari for the discussion and exchange that I have learned a lot from you with the advanced use of Carsim simulation. You are exceptional intelligence, full of energy, and desire to contribute. Thanks to Albert (my English teacher), Mohamad, and Homa for helping me correct my English pronunciation and vocabulary. I hope you can understand what I mean now.

Financial resources

The work resulting in this thesis has been funded by the Ministry of Education and Training of Vietnam for three years (2016-2019) under grant project 911, along with the tuition fee and insurance policy supported by the Ministry of Foreign Affairs of the French Republic for five years is gratefully acknowledged.

Viet Long.

Introduction Générale et Résume

Avant-propos

La thèse a été menée au sein de l'équipe de recherche COVE (Commande et Vehicles) du laboratoire MIS (Modélisation, Information et Systèmes) réalisée dans le cadre d'un doctorant. Le sujet de la thèse porte sur la « Stabilité et stabilisation des systèmes de retard à paramètres linéaires et variables dans le temps avec saturation des actionneurs ». Nous nous concentrons sur la résolution des problèmes de stabilité et de stabilisation des systèmes LPV et quasi-LPV incluant certaines contraintes de performances (retard variable dans le temps, saturation des actionneurs, variations de paramètres, perturbations externes, etc.).

Contexte et motivations

Les systèmes physiques contiennent des non-linéarités et des dynamiques variant dans le temps. Il est possible d'approximer le comportement non linéaire d'un état du système à partir de la linéarisation. Les méthodes de linéarisation envisagées pour les systèmes non linéaires pourraient être divisées en trois catégories (Vidyasagar, 1992): 1-Linéarisation autour d'un équilibre; 2-Linéarisation globale; et 3-Linéarisation autour d'une trajectoire d'état. Cette représentation des systèmes LPV sera étudiée ici.

L'intérêt des techniques LPV consiste en une approximation des systèmes non linéaires par des systèmes dépendant de paramètres avec l'hypothèse où l'ensemble des paramètres est supposé compact. Le comportement du système non linéaire est linéarisé localement autour de la trajectoire des paramètres variant dans le temps. Sur la base de ces hypothèses, l'analyse des critères de robustesse, de stabilité et de performance des systèmes LPV sont déduites. L'analyse de la robustesse des incertitudes dynamiques (non-linéarités, dynamique négligée, etc.) et des paramètres incertains (connaissance incertaine sur les grandeurs physiques simulées) a reçu une attention considérable. La théorie de la commande linéaire à paramètres variables (LPV) joue un rôle clé dans la gestion des incertitudes ou des inexactitudes. Les transformations fractionnaires linéaires (LFT) et les inégalités matricielles linéaires (LMI) ont été développées pour traiter l'analyse robuste de la stabilité et les performances des systèmes LPV et quasi-LPV.

D'une manière générale, la fonction de Lyapunov quadratique (QLF) joue un rôle central dans l'analyse de la stabilité et la stabilisation des systèmes LPV via les LMI. Cependant, une fonction de Lyapunov quadratique peut être trop conservatrice pour une analyse de stabilité robuste car elle impose l'existence d'une seule matrice définie positive de Lyapunov vérifiant un ensemble de LMI. Il en résulte une dégradation des performances (conservatisme) pour des exigences multi-objectifs, par exemple, contraintes sur les entrées et les sorties, saturation des actionneurs, retard variant dans le temps, etc. Suite à cet argument, une condition de stabilité robuste dérivée du lemme réel borné à l'échelle est

généralement moins conservatrice que le QLF. Une question intéressante ressort de cette discussion : comment pourrions-nous exploiter plus d'informations sur le système et améliorer la flexibilité des conditions de conception ? Ainsi, la première motivation consiste à assouplir les conditions de stabilité basées sur les QLF.

En raison de la nature des systèmes paramétriques, un problème dans la technique d'analyse LPV repose sur les formulations dérivées associées à l'ensemble compact de paramètres réellement représentés comme des conditions de dimension infinie. Ainsi, des méthodes de relaxation des LMI paramétrés ont été proposées pour formuler efficacement des problèmes d'analyse base sur l'optimisation convexe impliquant des contraintes LMI de finie dimension. En conséquence, une synthèse des méthodes de relaxation pour les LMI paramétrés a été proposée dans (Apkarian & Tuan, 2000b; Gahinet et al., 1996; Tuan & Apkarian, 1999).

De manière générale, la stabilité robuste utilisant une fonction de Lyapunov dépendante des paramètres (PDLF, qui semble plus adaptée à la synthèse de contrôle LPV) a été bien étudiée. Cependant, le problème de conception de la commande n'est pas entièrement résolu en présence de contraintes de saturation des actionneurs. Ce problème crucial sera étudié en détail et constitue l'une des principales contributions.

Dans l'analyse de la conception des systèmes de commande, un phénomène observé dans de nombreux systèmes d'ingénierie est la saturation des actionneurs. À première vue, l'effet de cette non-linéarité peut paraître simple, mais une analyse inappropriée ou ignorant ses effets peuvent entraîner une dégradation des performances ou une instabilité du système. La saturation des actionneurs est inévitable dans l'ingénierie des systèmes dynamiques pratiques concernant les limites physiques (vitesse, tension, cycle, etc.) et les contraintes de sécurité (pression, température, puissance, consommation d'énergie, etc.). C’est pourquoi nous devons trouver une méthode de stabilisation consistant à replacer les points de fonctionnement du système d'asservissement dans la région sans élément sature. Au cours des dernières décennies, une attention considérable a été accordée aux systèmes LTI soumis à la saturation des actionneurs, voir par exemple (Hu & Lin, 2001; Tarbouriech et al., 2011; Zaccarian & Teel, 2011) et les références qui s'y trouvent.

D'une manière générale, il existe deux approches principales pour effectuer l'analyse de stabilisation dans la littérature. La première considère les bornes de saturation dans la stratégie de conception. Dans la seconde part, une synthèse stabilisante asymptotique proposée pour un système en boucle fermée ne tient pas compte des bornes de commande. Ensuite, une stratégie de conception appropriée analysera pour compenser la saturation, telle que *Direct Linear Anti-windup* (DLAW) ou *Model Recovery Anti-windup* (MRAW). Le domaine anti-windup a fait l'objet de discussions approfondies au cours des dernières décennies. Nous pouvons nous rendre compte que l'analyse de stabilisation en boucle fermée pour DLAW et MRAW est plus compliquée en tenant compte de l'effet du comportement non linéaire et de la dynamique incertaine. Néanmoins, la construction DLAW dépasse le cadre de la thèse, elle ne sera donc pas incluse.

Enfin, une autre contribution porte sur les retards, des phénomènes de retard temporel sont observés dans divers systèmes d'ingénierie tels que les procédés chimiques, les transmissions mécaniques, les transmissions hydrauliques, les processus métallurgiques et les

systèmes de contrôle en réseau. La stabilité et la stabilisation des systèmes retards (TDS) ont reçu une attention considérable dans la pratique et la théorie du contrôle. Le retard peut être classé en différentes approches en fonction de la caractéristique ou du comportement de réponse du retard au système. La littérature sur la stabilité et la stabilisation des systèmes retardés porte sur les systèmes LTI, les systèmes LPV, le domaine temporel l'analyse de stabilité basée sur Lyapunov et l'approche basée sur les valeurs propres.

De plus, les conditions dépendantes du retard dérivées de l'analyse de stabilité et de stabilisation via la technique LMI basée sur la fonction de Lyapunov-Krasovskii sont rencontrées dans de nombreux articles de la littérature. La majorité des résultats de la littérature concerne les systèmes LPV/quasi-LPV avec retards sans prise en compte des effets de saturation des actionneurs. Peu de techniques de synthèse sont disponibles pour la stabilisation robuste des systèmes LPV retards avec des actionneurs contraints ce sera notre contribution. De plus, les conditions de stabilisation de ces classes de systèmes sont généralement des inégalités matricielles non linéaires (NMI ou NLMI), qui sont généralement des problèmes polynomiaux non déterministes (NP-*hard*).

Une structure appropriée de LKF peut faire référence aux termes intégraux supplémentaires, aux vecteurs d'état croissants et aux approches de partitionnement de retard/fragmenté qui se sont révélées extrêmement efficaces pour réduire la résolution des conditions de stabilité. Il convient de noter que plus les matrices de variables d'écart utilisées sont nombreuses, plus l'analyse des conditions de stabilité dépendantes au retard est compliquée. En conséquence, ces approches sont le compromis entre la relaxation de la condition de stabilité et celle du calcul.

Le troisième objectif de cette thèse est de fournir la stratégie de conception de contrôle la moins restrictive pour les systèmes LPV et quasi-LPV avec des contraintes de retard variant dans le temps et de saturation. Outre l'utilisation de LKF appropriés, de variables d'écart et de bornes de saturation, pour obtenir des conditions plus flexibles, la méthode proposée est un équilibre entre conservatisme et réduction de la complexité de calcul.

Plan de thèse

Cette thèse est organisée selon les chapitres suivants :

Le Chapitre 1 donne une introduction générale et un résumé de la thèse.

Le Chapitre 2 donne un aperçu des représentations de la famille des systèmes LPV. Ensuite, les propriétés dépendantes des paramètres implicites dans les LMIs dérivées sont linéarisées par les méthodes de relaxation. La convergence asymptotique peut être obtenue lors de la résolution d'un ensemble de conditions d'inégalité matricielle. Enfin, une synthèse détaillée de la stabilité des approches non quadratiques de Lyapunov donne une approche pour stabiliser les systèmes LPV.

Le Chapitre 3 est consacré à l'analyse de la stabilité et de la stabilisation robuste de systèmes dépendant de paramètres sans contraintes de saturation. La première contribution sur l'algorithme d'itération optimale concave utilisant des blocs de paramètres diagonaux est présentée et comparée à la littérature existante.

Le Chapitre 4 traite l'analyse et la synthèse du contrôleur de programmation de gain saturé avec des inégalités de stabilisation plus strictes basées sur la fonction paramétrique de Lyapunov telle que PDLF et la fonction floue de Lyapunov (FLF). Les résultats ont été obtenus par la méthode de relaxation appliquée aux conditions PDLMI obtenues. Le chapitre se termine par la troisième contribution de l'analyse de stabilisation pour les systèmes LPV avec contraintes de saturation.

Le Chapitre 5 traite de l'analyse de stabilité et de la conception de contrôle pour les systèmes LPV avec retard utilisant une fonction convexe appropriée basée sur la fonction de Lyapunov-Krasovskii. Une nouvelle condition de stabilité dépendante du retard est donnée à l'aide de la fonctionnelle de Lyapunov-Krasovskii dépendante des paramètres (PDLKF) combinée à la *bounding technique*. Cette approche fournit une inégalité plus étroite pour délimiter l'intégrale quadratique d'un vecteur étendu. Plusieurs types de stabilité dans les cadres de valeur de retard de mémoire exacte et de retard approximatif sont étudiés. La condition de stabilité du retard de mémoire incertaine est considérée comme convenant à l'exigence de mise en œuvre. Enfin, l'efficacité des conditions PDLMI proposées est démontrée par des résultats d'analyse de stabilité par rapport aux méthodes existantes pour les systèmes linéaires invariants dans le temps et LPV.

Le Chapitre 6 contribue à la stabilisation des systèmes à retard variable dans le temps LPV avec saturation de l'actionneur. En incluant le délai de mémoire approché, un contrôleur par retour d'état et par retour de sortie dynamique sont présenté. Ensuite, des conditions PLMI nécessaires et suffisantes ont été proposées pour garantir une stabilisation résiliente à mémoire respectant les contraintes de saturation. Par rapport aux résultats existants récents, cette méthode fournit une performance améliorée avec une borne supérieure du retard. La discussion finale démontre les caractéristiques efficaces de cette stabilisation.

Table of Content

Remerciements i

Acknowledgments iv

Introduction Générale et Résume v

Table of Content ix

List of Figures xii

List of Tables xiv

Notation xv

Acronyms xvi

Chapter 1. General Introduction and Summary 1
1.1. Context and motivations ... 1
1.2. Contributions ... 3
1.3. Thesis outline ... 3
1.4. Publications ... 5

Chapter 2. Overview Linear Parameter-Varying Systems 7
2.1. Introduction of LPV/quasi-LPV systems ... 9
2.1.1. Affine LPV Systems ... 11
2.1.2. Polynomial Systems ... 11
2.1.3. Polytopic Systems ... 11
2.1.4. Takagi-Sugeno Fuzzy Systems ... 13
2.1.4.1. Sector Nonlinearity ... 14
2.1.4.2. Polynomial Fuzzy Model ... 15
2.1.5. Example ... 15
2.1.6. Applications ... 18
2.1.6.1. Automotive Chassis Systems ... 18
2.1.6.2. Aircrafts Systems ... 20
2.1.6.3. Mechatronics and Robotics Systems ... 22
2.1.6.4. Other applications ... 23
2.2. Stability of LPV/quasi-LPV Systems ... 24
2.2.1. Stability of Polytopic Systems ... 27
2.2.2. Stability of Polynomial Parameter-Dependent Systems ... 28
2.2.3. Stability of T-S Fuzzy Systems ... 29
2.2.3.1. Non-quadratic Stability (Bounded Parameters) ... 29
2.2.3.2. Non-quadratic Stability (Sum of Squares) ... 30
2.2.4. Relaxation of the Parameterized Linear Matrix Inequality ... 31
2.2.4.1. Relaxation of Parametrized LMIs by Discretization ... 32

2.2.4.2. Relaxation of Parametrized LMIs by Sum-of-Squares Decomposition ... 33
2.2.5. Example ... 34
2.2.5.1. Relaxation of Parameter-Dependent Lyapunov Function ... 34
2.2.5.2. The Conservativeness of Fuzzy and Fuzzy Polynomial Lyapunov Functions ... 37
2.3. The Saturation Nonlinearity – Stabilization Analysis ... 41
2.3.1. Sector Nonlinearity Model ... 42
2.3.1.1. Asymptotical stabilization. ... 42
2.3.1.2. Region of Attraction. ... 44
2.3.1.3. Ellipsoidal Set of Stability. ... 44
2.3.1.4. Optimization problems. ... 46
2.3.2. Saturated Feedback Control Synthesis ... 46
2.3.2.1. Parameterized State Feedback Controller ... 47
2.3.2.2. Parameterized Static Output Feedback Controller ... 48
2.3.2.3. Parameterized Observer-Based Output Feedback Controller ... 49
2.3.2.4. Parameterized Dynamic Output Feedback Controller ... 50
2.4. Conclusions ... 52

Chapter 3. Quadratic Stabilization Analysis for LPV/quasi-LPV Systems with Actuators Saturation 53
3.1. Stabilization Analysis ... 54
3.1.1. Norm-Bounded Input ... 54
3.1.2. Observer-based control stabilization ... 56
3.1.3. Concave Nonlinearity – Cone Complementarity Linearization ... 59
3.2. Reduction to Finite-Dimensional Problems ... 62
3.2.1. Finite Discretization of Parametrized LMIs via ... 62
3.2.2. Polynomial Parameter-Dependent LMIs via Sum-of-Squares ... 63
3.2.3. Parametrical Dependent LMIs via Convex Combination ... 66
3.2.3.1. T-S Fuzzy Controller Stabilization Construction ... 67
3.2.3.2. Reducing Conservatism – Parameter-Dependent Scaling ... 70
3.3. Example ... 70
3.4. Conclusions ... 77

Chapter 4. Stabilization Synthesis for LPV/quasi-LPV Systems with Actuators Saturation 79
4.1. State Feedback Stabilization ... 79
4.1.1. Sector Nonlinearity Models ... 79
4.1.2. Example ... 81
4.1.2.1. Ellipsoidal regions of stability ... 82
4.1.2.2. The comparison of conservativeness of conditions ... 83
4.1.2.3. Generalized Sector Condition ... 85
4.2. Static Output Feedback Stabilization ... 87
4.3. Observer-based Feedback Stabilization ... 90
4.3.1. Generalization of Young's Inequality ... 90
4.3.2. Generalization of Finsler's Lemma ... 91
4.4. Dynamic Output Feedback Stabilization ... 94
4.5. Examples ... 97
4.5.1. Saturated Feedback Controller Comparison ... 98
4.5.2. Evaluation of the performance and stability of the saturated system ... 105
4.5.3. Quadratic and Non-Quadratic Stabilization ... 108

4.6. Conclusions 109

Chapter 5. Stability Analysis of the LPV/Quasi-LPV Time-Delay Systems 111
5.1. Introduction to LPV Time-Delay Systems 112
5.1.1. Representation of LPV System with Single Delay 113
5.1.2. Delay-Dependent LKF Stability – Convex function 114
5.1.2.1. Jensen's Inequality and Extended Approach 114
5.1.2.2. Discretized Convex Function 116
5.1.3. Delay-Dependent Stability – Input-Output Approach 117
5.2. Stability Analysis of Lyapunov-Krasovskii functional 118
5.2.1. Single Delay-Dependent LKF Stability and associated relaxation 118
5.2.1.1. Jensen's Inequality 118
5.2.1.2. Wirtinger-Based Inequality 119
5.2.1.3. Auxiliary Function-Based Integral Inequality 123
5.2.2. Decomposition Lyapunov-Krasovskii Functional Stability 124
5.2.3. Uncertain Delay-Dependent Lyapunov-Krasovskii Functional Stability .. 129
5.2.4. Memory-Resilient Delay-Dependent Lyapunov-Krasovskii Functional Stability 130
5.2.4.1. Jensen's Inequality 130
5.2.4.2. Wirtinger-Based Inequality 131
5.2.5. Example 135
5.3. Conclusions 139

Chapter 6. Stabilization Synthesis for the LPV/quasi-LPV Time-delay Systems with Actuators Saturation 141
6.1. Problem Formulation and Preliminaries 142
6.1.1. Sector Nonlinearity Model Approach 142
6.1.2. Parameterized State Feedback Controller 143
6.1.3. Parameterized Dynamic Output Feedback Controller 145
6.2. State Feedback Controllers 146
6.2.1. Memoryless Delay-Dependent Stabilization 146
6.2.2. Approximated Delay-Dependent Stabilization 149
6.2.3. Optimization problem – Maximization Domain of Attraction 151
6.2.4. Example 152
6.2.4.1. Memory-resilient saturated controller synthesis 152
6.2.4.2. Maximization of the set of admissible initial conditions 155
6.3. Dynamic Output Feedback Controllers 157
6.3.1. Exact Memory Delay-Dependent Stabilization 157
6.3.2. Approximate Delay-Dependent Stabilization 160
6.3.3. Optimization problem – Maximization Domain of Attraction 164
6.3.4. Example 164
6.3.4.1. Memory saturated controller synthesis 165
6.3.4.2. Optimization Problems 168
6.4. Conclusions 171

Chapter 7. Conclusions and Perspectives 173

Appendix 175

Bibliography 215

List of Figures

Figure 2-1. *Polytopic parametrization*. 12
Figure 2-2. *Illustrates fuzzy model construction by sector nonlinearity*. 14
Figure 2-3. *Vehicle lateral dynamics.* 19
Figure 2-4. *LPV modelling and control of robotic systems.* 22
Figure 2-5. *Time transient of Lyapunov function*. 36
Figure 2-6. *Dead-zone nonlinearity.* 43
Figure 2-7. *The level set of ellipsoidal domains.* 45
Figure 2-8. *The closed-loop diagram of saturated feedback controllers.* 47
Figure 3-1. *The extreme points of the polynomial in the interval* $[-6, 12]$. 65
Figure 3-2. *The diagram of quadruple-tank process model.* 72
Figure 3-3. *The evolution of dynamic states and estimations under disturbance and uncertain dynamics.* 73
Figure 3-4. *The observer performance – error estimations* (*left*); *and the DC-Motor pumps signal control* (*right*). 74
Figure 4-1. *The estimate of feasibility regions with* $a \in [-25,\ 20], b \in [-0,\ 25]$. 84
Figure 4-2. *The improvement of the controller performance with LMI* $\mathcal{D}$*-Region*, *via Polytopic quadratic stability condition.* 86
Figure 4-3. *a. The simulated constrained responses of the state-feedback SF controller* (*colored solid line*), *the static-output feedback SOF controller* (*colored dash-dotted line*), *the observer-based feedback OBF controller* (*colored dashed line*), *and the dynamic output feedback DOF controller* (*colored dotted line*). *b. The time-evolution of external disturbance.* 102
Figure 4-4. *The stabilized states of the closed-loop systems are regulated, respectively, by the gain-scheduled SF controller* (*colored solid line*), *SOF controller* (*colored dash-dotted line*), *OBF controller* (*colored dashed line*), *DOF controller* (*colored dotted line*) *conforming to the simulated parameter* (*green solid line in the last frame*). 103
Figure 4-5. *The comparison of the closed-loop systems regulated, respectively, by the saturated gain-scheduled SF controller (colored solid line), and nominal state feedback controller (colored dotted line).* 106
Figure 4-6. *The comparison of the closed-loop systems regulated, respectively, by the saturated gain-scheduled SOF controller (colored solid line), and nominal static output feedback controller (colored dash-dotted line).* 107
Figure 4-7. *Region of stability. Trajectories of the closed-loop systems respond from the same initial conditions during 10 seconds of simulation.* 108
Figure 5-1. *Graph of a convex function.* 116

Figure 5-2. *The evolutions of quasi-LPV time-delay system* (5.68) with the slow-varying delay $h(t) \le 20.4917,\ \dot{h}(t) \le 0.1$. 137
Figure 6-1. *The responses of the bounded controllers correspond to saturation limit* $\overline{u} = 5, with\ \overline{h} = 1, \mu = 0.9$. 154
Figure 6-2. *The evolutions of the LPV time-delay system regulate by saturated state feedback and dynamic output feedback controllers.* 167
Figure 6-3. *The responses of the stabilizing gain-scheduling controllers solved by Theorem* 6.2.2, *and Theorem* 6.3.1 *corresponding to saturation limit* $\overline{u} = 5$, *with* $\overline{h} = 1, \mu = 0.5,$ and $\gamma = 2.5$. 168
Figure 6-4. *Example 6.3.1 — designed controllers. The estimates of region of stability using sector nonlinearities approaches with different criteria. Asymptotically stabilized* (*green solid-lines*) *and destabilized trajectories* (*brown dotted-lines*) *of the closed-loop systems from the initial conditions* (o). 170

List of Tables

Table 2.1. *The Conservativeness of Parametrized LMI Conditions.* 38
Table 3.1. *Observer-Based Feedback Robust Stabilization and Performance with Saturation actuators.* 75
Table 4.1. *Multi-objective optimization - Problem* 4.1.1 83
Table 4.2. *Robust Pole Placement in LMI Regions.* 86
Table 4.3. *Multi-objective optimization* $-\gamma_{opt}$ and η_{opt}. 99
Table 4.4. *Minor Axis Maximization* $-\gamma = 10$. 105
Table 4.5. *Actuator Saturation – Optimization Problems.* 108
Table 4.6. *Multi-objective optimization - Example* 4.5.1. 109
Table 5.1. *The maximum admissible upper bound MAUB for delay* $h(t) \in \mathcal{H}_0$. 135
Table 5.2. *The maximum admissible upper bound for delay* $h(t) \in \mathcal{H}_0$. 136
Table 6.1. *The optimization of* $\mathcal{H}_\infty$ *performance criterion* $-\gamma_{opt}$. 153
Table 6.2. *Domain of attraction, with* $\overline{h} = 1$. 156
Table 6.3. *Multi-criteria optimization.* 169

Notation

$\mathbb{N}$	Set of natural numbers, positive integers
$\mathbb{R}$, $\mathbb{R}_+$, $\mathbb{R}_{++}$	Set of real numbers, nonnegative real numbers, strictly positive real numbers
$\mathbb{R}^n$,	Space of $n\times 1$ real vectors
$\mathbb{C}$	Set of complex numbers
$\mathbb{S}^n$, $\mathbb{S}^n_+$, $\mathbb{S}^n_{++}$	Cone of $n\times n$ symmetric matrices, $n\times n$ symmetric positive semi definite matrices, $n\times n$ symmetric positive definite matrices
$\mathcal{C}_1(J,K)$	Set of continuously differentiable functions from set J to K
$\mathcal{F}(J,K)$	Set of functions from set J to K
I_n	Identity matrix of dimension n
$0_{n\times m}$	$n\times m$ matrix with entries equal to 0
A^T	Transpose matrix of A
A^*	Conjugate transpose of A
A^{-1}	Inverse of matrix A
A^{-T}	Transpose of the inverse of A
A^+	Moore-Penrose pseudoinverse of A
trace (A)	Trace of A
det (A)	Determinant of A
$\lambda(A)$	Set of eigenvalues of A
$\lambda_{\min}(A)$, $\underline{\lambda}(A)$	Minimal eigenvalue of A
$\lambda_{\max}(A)$, $\overline{\lambda}(A)$	Maximal eigenvalue of A
$\sigma(A)$	Set of singular values of A : $\sqrt{\lambda(A^*A)}$
$\overline{\sigma}(A)$	Maximal singular value of A
$\otimes$	Kronecker product
$A \succ (\succeq) 0$	A is a positive (semi) definiteness matrix
$A \prec (\preceq) 0$	A is a negative (semi) definiteness matrix
$:=$, $\stackrel{\Delta}{=}$	Denoted as, assigned to
$\cong$	Approximated by
$sym\{A\}$, A^S	Hermitian operator defined as $sym\{A\} := A^S := A + A^T$
ρ	Parameter in generic LPV systems
h	Delay in time-delay systems
$\|v\|_q$	q-norm of the vector $v \in \mathbb{R}^n$ defined as $\|v\|_q := (\|v_1\|^q + \|v_2\|^q + \cdots + \|v_n\|^q)^{1/q}$
$\mathcal{L}_q$	Space of functions with finite $\mathcal{L}_q$-norm
$\|z(t)\|_{\mathcal{L}_q}$	$\mathcal{L}_q$-norm of the function $z(t):\mathbb{R}_+ \to \mathbb{R}^n$ defined as $\|z(t)\|_{\mathcal{L}_q} := (\int_0^\infty \|z(t)\|_q^q \, dt)^{1/q}$
$\square$	End of the proof

Acronyms

LTI	Linear Time–Invariant
TDS	Time–Delay System
LPV	Linear Parameter Varying
quasi–LPV, qLPV	Quasi Linear Parameter Varying
LFT	Linear Fractional Transformation
TS	Takagi–Sugeno
PDC	Parallel Distributed Compensation
LMI	Linear Matrix Inequality
PDLMI	Parameter–Dependent Linear Matrix Inequality
PLMI	Parameterized Linear Matrix Inequality
NMI	Nonlinear Matrix Inequality
BMI	Bilinear Matrix Inequality
JBI	Jensen–Based Inequality
WBI	Wirtinger–Based Inequality
AFB	Auxiliary Function–Based
RCC	Reciprocal Convex Combination
CCL	Cone Complementary Linearization
PDLF	Parameter Dependent Lyapunov Function
QLF	Quadratic Lyapunov function
MPLF	Multiple piecewise Lyapunov function
FLF	Fuzzy Lyapunov function
PFLF	Polynomial Fuzzy Lyapunov function
LKF	Lyapunov–Krasovskii functional
PDLKF	Parameter–Dependent Lyapunov–Krasovskii functional
SF	State Feedback
OBF	Observer Based Feedback
SOF	Static Output Feedback
DOF	DOF Dynamic Output Feedback
GSC	Generalized Sector Condition
DLAW	Direct Linear Anti–windup
MRAW	Model Recovery Anti–windup
RAS	Region of Asymptotical Stability
DoA	Domain of Attraction
SDP	Semidefinite Program
CP	Cone Program

Chapter 1.

General Introduction and Summary

Foreword

The thesis was conducted at the "COVE" research team of MIS laboratory throughout a Ph.D. research. The subject of the dissertation is "Stability and Stabilization of linear parameter-varying and time-varying delay Systems with Actuators Saturation." We focus on solving the stability and stabilization problems for the LPV and quasi-LPV systems including some performance constraints (time-varying delay, actuator saturation, parameter variations, external disturbances, etc.).

1.1. Context and motivations

Since the last decade of the 20th century, the guarantee of the stability and the robustness analysis of the system robustly against the influence of dynamical uncertainties (nonlinearities, neglected dynamics, etc.) and uncertain parameters (uncertain knowledge about simulated physical values, the time variations of these values during operation) have received considerable attention of engineering control community. The robustness analysis and linear parameter-varying (LPV) control theory plays a key role in handling *uncertainties* or *inaccuracies*. The Linear Fractional Transformations (LFTs) and Linear Matrix Inequalities (LMIs) have been developed to deal with the robust stability and performance analysis for both LPV and quasi-LPV systems.

Generally speaking, the quadratic Lyapunov function (QLF) plays a central role in analyzing the stability and stabilization of LPV systems via LMIs. However, a quadratic Lyapunov function may be too conservative for robust stability synthesis because it imposes the existence of a single Lyapunov positive definite matrix verifying a set of LMIs. But, due to some particular properties of the implementation, a considerable approach has been developed or analyzed the $\mathscr{H}_\infty$ gain-scheduling controller with this modest case. And, because it cannot characterize slow variation parameters, it results in a degradation performance (conservatism) for multi-objective requirements, for example, hard time constraints, actuators saturation, time-varying delay, etc. Followed this argument, a robust stability condition derived from the scaled-bounded real lemma is typically less conservative than the QLF. An interesting question arises from this discussion: how could we exploit more system information and improve the *flexibility* of design conditions? So, the first motivation engages in relaxing the QLF-based stability conditions by taking advantage of the parametric properties of the scaling structure.

Due to the nature of parametric systems, one critical issue in the LPV analysis technique

is the derived formulations associated with the compact set of parameters actually represented as infinite dimension LMI conditions. Thereby, popular relaxation methods of Parameterized LMIs have been proposed to efficiently formulate analysis problems as convex optimization problems involving a finite LMI constraints. Generally speaking, the robust stability using a parameter-dependent Lyapunov function (PDLF, which seems more suitable for LPV control synthesis) is well-studied and well-advanced. However, the control design issue is not completely resolved in the presence of actuator saturation constraints. This crucial problem will be studied in detail and constitutes one of the main motivations of this thesis.

It is well known that actuator saturation can lead to performance degradation or even instability in several engineering systems. As a result, actuator saturation is considered as an exciting challenge in control system design. The problem of the saturated feedback controller design for these classes of dynamics systems constitutes an interesting problem for both theoretical and practical reasons. Stability analysis and control synthesis of saturated LPV systems are generally divided into two different strategies: (1) *Anti-windup scheme*, (2) *Saturation nonlinearities*.

It can be seen that the conventional input constraint imposed by a small-gain theorem is related to the input-output approach in a strict manner. So, the less conservative method, such as *generalized sector condition* (GSC), gives an extra degree of freedom in the stabilization synthesis used in this literature. Besides, the GSC is appropriate for the parameter-dependent LMI conditions and well suits extension for delay-dependent stabilization.

On the other side, the delay-dependent conditions derived from the stability and stabilization analysis via the Lyapunov-Krasovskii functional based LMI technique is encountered in many papers of literature. The majority of the results in the literature concerns LPV/quasiLPV systems with time delay without taking into account the actuator saturation effects. Few synthesis techniques are available for the robust stabilization of timed LPV systems with constrained actuators. Moreover, the stabilization conditions for these classes of systems are usually nonlinear matrix inequalities (NMI or NLMI), which are usually nondeterministic (NP-hard) polynomial problems. Therefore, the stability analysis and stabilization of saturated LPV/quasi-LPV systems with time delay become a more attractive challenge.

The third objective of this thesis is to propose less restrictive control design strategy for LPV and quasi-LPV systems with time-varying delay and saturation constraints. Besides, the use of appropriate LKFs, slack-variables, saturation bounds, to obtain more flexible design conditions, the proposed method is a balance between conservatism and computational complexity reduction.

1.2. Contributions

Inspired by the convex and quasi-convex optimization problem, in this dissertation, we address the stability and stabilization of the LPV/quasi-LPV and time-delay systems derived from the parameter-dependent Lyapunov function involving the control saturation problems. The relaxation of PLMI would be performed with the derived analysis and synthesis. This additional design step in the controller synthesis allows for consideration

of a more generalized formulation and affords a flexible implementation.

Methodological developments and scientific contributions are in both stability analysis and controller design that is summarized as follows:

- Concave-optimization iterative algorithm: quasi-convex forms of robust stabilization conditions associated with the application of Young's inequality are linearized by the CCL algorithm. However, the primitive algorithm is too conservative because of the strong mathematical constraints (the *pseudo*-matrix ranks). So, by adopting the scaling techniques relating to block-structured uncertainty, an improved algorithm provides the less conservative conditions.
- Parameter-dependent Lyapunov functions: a generalized parameter-dependent Lyapunov function is considered to handle the stability and stabilization analysis of the LPV/ quasi-LPV and time-delay systems. The relaxation methods such as parameter discretization, the multiconvexities, and the sum of squared (SoS) approaches are employed for the PDLMI.
- Saturation LPV/quasi-LPV systems: more general stabilization conditions are delivered for the state feedback (FB), static output feedback (SOF), observer-based feedback (OBF), and dynamic output feedback (DOF) controllers. Following LPV control design strategies, the generalized sector nonlinearity condition is injected in the stabilization analysis to guarantee the constrained bounds.
- Saturation LPV/quasi-LPV time-varying delay systems: an appropriate Lyapunov–Krasovskii functional is utilized to deliver a better stabilization result characterizing both memoryless and exact-memory (non-implementable in practice) controllers regarding the saturated limits. Then, due to the difficulty of estimating delays, a new stabilizing condition is proposed to enforce the saturation bound on memory–resilient gain-scheduled controllers. It has not been investigated so far followed the best of the author's knowledge in the literature.

1.3. Thesis outline

This monograph is organized by the following content sections, corresponding to a construction shown in the next figure:

Chapter 1 provides a general introduction and summary of the Thesis.

Chapter 2 gives an overview of representations of the family of LPV systems. It recalls basic concepts and definitions of parametric dependent stability analyzed based on Lyapunov function. Then, the implicit parameter-dependent properties in the derived LMI are linearized by the relaxation methods. The asymptotic convergence can be achieved upon the satisfaction of a set of matrix inequality conditions. A better parameter characterization provides a higher relaxation PLMI method with significant system performance improvement results. Finally, a detailed stability synthesis of the *non-quadratic* Lyapunov approaches gives a premise for stabilizing LPV systems with the saturation actuators.

Chapter 3 is devoted to the analysis of Robust Stability and Stabilization of parameter-dependent systems without saturation constraints. An improved solution of the Robust T-S Fuzzy controller stabilizing analysis with $\mathscr{L}_2$ norm-bounded input constraints is presented. The first contribution about the concave optimal iteration algorithm using diagonal parameter blocks is presented and compared with the existing literature.

Chapter 4 discusses the analysis and synthesis of the saturated gain-scheduling controller with tighter stabilizing inequalities based on the parametric Lyapunov function such as PDLF and fuzzy Lyapunov function (FLF). The less conservative results were attained by the proposed relaxation method applied to the designed PDLMI conditions. The chapter is concluded with the third contribution of stabilization analysis for LPV systems with saturation constraints.

Chapter 5 deals with stability analysis and control design for LPV time-delay systems using an appropriated Lyapunov-Krasovskii functional based convex function. A new delay-dependent stability condition is addressed using parameter-dependent Lyapunov-Krasovskii functional (PDLKF) combined with the advanced bounding technique. This approach provides a tighter inequality for bounding the quadratic integral of an extended vector. Several types of stability in both exact-memory delay value and approximate delay frameworks are studied. The uncertain-memory delay stability condition is considered suiting the implementation requirement. Finally, the effectiveness of the proposed PDLMI conditions are demonstrated through stability analysis results compared with the existing methods for both linear time-invariant (LTI) and LPV time-delay systems.

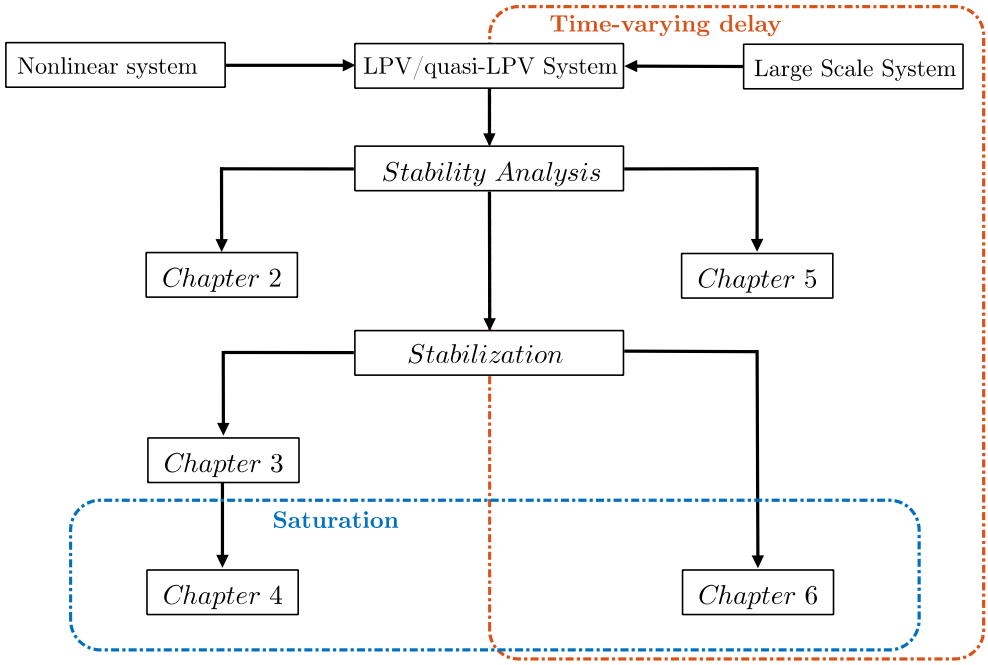

Chapter 6 contributes to the stabilization of LPV time-varying delay systems with actuator saturation. Including the approximated-memory delay, a more general controller is introduced for both state feedback and dynamic output feedback controllers. Then, necessary and sufficient PLMI conditions have been proposed

to guarantee a memory-resilient stabilization respecting the saturation constraints (sector nonlinearities). Besides, the optimization of the estimation of the domain of attraction (DOA) is analyzed. The proposed method is validated by considering several numerical examples. Compared to the recent existing results, this method provides an enhanced performance conforming to a higher upper bound of the delay value. The final discussion demonstrates the efficient characteristics of saturation stabilization.

1.4. Publications

The thesis is based on the following publications and other studies in the process of being submitted.

Bui Tuan, V. L., & Hajjaji, A. El. (2018). Robust Observer-Based Control for T-S Fuzzy Models Application to Vehicle Lateral Dynamics. *2018 26th Mediterranean Conference on Control and Automation (MED)*, 1–6.

Bui Tuan, V. L., Hajjaji, A. El., & Naami, G. (2019). Robust T-S fuzzy observer-based control for Quadruple-Tank system. *2019 12th Asian Control Conference, ASCC 2019*.

Bui Tuan, V. L., Pages, O., & Hajjaji, A. El. (2021). Robust T-S fuzzy output feedback controller synthesis for saturated vehicle System. *Proceedings of the American Control Conference*, *2021-May*, 142–147.

Bui Tuan, V. L., Hajjaji, A. El., & Pages, O. (2021). Further Results of Robust Observer-Based Control Synthesis for Saturated Linear Parameter Varying Systems. *2021 Australian New Zealand Control Conference (ANZCC)*, pp.

Bui Tuan, V. L., Hajjaji, A. El., & Pages, O. (2021). L2 -Stabilization of anti-windup compensators subject to actuator saturation and disturbance. *2021 Australian New Zealand Control Conference (ANZCC)*, pp.

Chapter 2.

Overview Linear Parameter-Varying Systems

Physical systems are practically involved with nonlinearities and time-varying dynamics. It is possible to approximate the nonlinear behavior of a system state in the range of *nominal operating conditions*, usually referred to as linearization (Isidori, 1995; Khalil, 1996). The linearization methods considered for nonlinear systems could be supposedly characterized into three categories (Vidyasagar, 1992): 1-Linearization around an equilibrium; 2-Global linearization; and 3-Linearization around a state trajectory.

- Linear Time-Invariant (LTI) system as a representative for first method related with the simplest analysis and synthesis techniques, which is expressed by linearizing the dynamic systems around the neighborhood of equilibrium points. During the operation, the presence of nonlinearities with a wide range of variation (include dynamical uncertainty, saturation, and inaccurate knowledge of dynamics....) causes the *inaccurate* linearization occurs over equilibrium conditions.

- The multi-model representation of Linear Time Varying (LTV) systems also called Linear Differential Inclusions (LDI) is used to represent trajectories of a nonlinear system by a set of trajectories of LDI in the entire operating range. Nevertheless, this linearization method could be conservative because the approximated trajectories that are sometimes not actual trajectories of the given system.

- Parameter Dependent systems as a typical for third method where the nonlinear system can be approximated by a family of linearization or the parameterized linearization. Since the proposed method is valid around a state trajectory rather than a single equilibrium point, then it can characterize a nonlinear system in a wider range of operating conditions than LTI. This representation of the LPV systems that will intensively study here.

This chapter provides a non-exhaustive overview of the linear parameter-varying (LPV) systems used to approximate nonlinear systems according to the trajectories of parameters. Depending on the characteristics of the parameter, it can classify as linear time-varying (LTV), LPV systems (Briat, 2008; Lim, 1998; Mohammadpour & Scherer, 2012; Shamma, 1988; Wu, 1995), or quasi-linear parameter varying (quasi-LPV or qLPV) systems, for example, the representation of T-S fuzzy systems (Lam, 2016; Takagi & Sugeno, 1985; Tanaka & Wang, 2001). In addition, LPV systems can also classify according to the parameter properties, e.g., the intrinsic (endogenous) or extrinsic (exogenous), the physical properties (e.g., parametric uncertainty, and dynamical parameters), and mathematical significance (continuous/discrete, smooth or non-smooth, continuous derivative, etc.).

The benefit of LPV techniques consists in an approximation of the characterizations of

the nonlinear systems to the parameter-dependent systems. Where the compact sets of parameters and their derivatives are the prerequisite of the system design hypothesis. The behavior of the nonlinear system is linearized locally around the trajectory of the time-varying parameters. Based on these assumptions, the analysis of robustness, stability, and performance criteria of the LPV systems thus *simplifies* as on LTV or LTI systems (Apkarian, Feron, et al., 1995; Apkarian & Gahinet, 1995; Gahinet et al., 1996).

In the first part, in section 2.1, we discuss commonly used framework to represent LPV systems along with some applications. Corresponding to each representation is a characteristic approach for the stability analysis provided in section 2.2. The stability synthesis for the LPV system via the Lyapunov function results in the parametric conditions. In which the convex optimization linear matrix inequality (LMI) tools cannot solve these conditions directly. As a result, a synthesis of relaxing methods for the parameterized LMIs has been methodically discusses in (Apkarian & Tuan, 2000b; Gahinet et al., 1996; Tuan & Apkarian, 1999) including:

- The gridding technique with uniform density (Wu, 1995; Wu et al., 1996), and the meshing parametric affine (Apkarian & Tuan, 1998; Lim, 1998).
- The convex combination of *multi*-LTI systems is known as the polytopic paradigm (Apkarian, Gahinet, et al., 1995; Apkarian & Tuan, 2000b; Gahinet et al., 1996), and the T-S fuzzy model (Tanaka & Wang, 2001; Tuan et al., 2004; Tuan, Apkarian, et al., 2001).
- The multiplier-based linear fraction transformation (LFT) use $\mathcal{D}$-scaling to capture the behavior of the parameter with the additional inequality on the multiplier quadratic in the scheduling block (Apkarian & Gahinet, 1995; Packard, 1994). The matrix algebraic transformations of LFT LPV based on $\mathcal{S}$-procedure can be found at (Boyd et al., 1994; Pólik & Terlaky, 2007).
- The sum of squares (SoS) relaxation-based LPV stability synthesis on the SoS decomposition for multivariate polynomials can be efficiently computed using semi-definite programming (Parrilo, 2000, 2003).

The parameterized linear matrix inequality (PLMI) can be converted into finite-dimensional inequalities. Where the feasible solution is obtained by solving the LMI conditions. The methodologies and numerical examples of LPV stability synthesis are introduced at the end of section 2.2. It should be notice that the design requirements conformed to the LPV framework such as, robust stability and performance e.g., $\mathcal{H}_\infty$ criterion, or the full-block $\mathcal{S}$-procedure (FBSP) will be presented in Appendix B.

In section 2.3, we recall some fundamental definitions like the region of linearity, region of attraction and regions of asymptotic stability and the developments concerned within the dissertation, with respect to main problems of the stability analysis and the stabilization of linear parameter-varying and time-delay systems with saturating inputs. The characterization of sets of admissible initial states and admissible disturbances plays a central role in stability analysis as well as in the synthesis of stabilizing control laws when saturation occurs.

2.1. Introduction of LPV/quasi-LPV systems

Let us introduce a generalized expression of the LPV system that is studied throughout this dissertation under the forms of a non-autonomous non-stationary system of ordinary differential equations:

$$\begin{aligned} \dot{x}(t) &= A(\rho(t))x(t) + B(\rho(t))u(t) + B_w(\rho(t))w(t), \\ y(t) &= C(\rho(t))x(t) + D(\rho(t))u(t) + D_w(\rho(t))w(t), \\ z(t) &= H(\rho(t))x(t) + J(\rho(t))u(t) + J_w(\rho(t))w(t), \\ x(0) &= x_0, \ t \geq 0 \end{aligned} \tag{2.1}$$

where vectors $x(t) \in \mathbb{R}^n, y(t) \in \mathbb{R}^p, z(t) \in \mathbb{R}^r, u(t) \in \mathbb{R}^m, w(t) \in \mathbb{R}^d$ are respectively the state of the system, the measured output, the regulated output, the control input and the external disturbance. The behavior of LPV system (2.1) depends on the behavior of the parameters. From the point of view of the physical meaning of parameters (e.g., measurability, endogenous or exogenous parameters, etc.), or mathematical properties (i.e., continuous/discontinuous parameters, differentiable/non-differentiable parameter, etc.), that provides a classification for LPV modeling or the appropriate method for system stability analysis and control system design strategy.

Endogenous Parameters and Exogenous Parameters

Let consider a time-continuous state space system:

$$\begin{aligned} \dot{x}_1(t) &= x_1(t) + \sin(2\pi t)x_2(t), \\ \dot{x}_2(t) &= \cos(\pi t + \pi/3)x_1(t). \end{aligned} \tag{2.2}$$

can be represented to the LPV system

$$\begin{bmatrix} \dot{x}_1(t) \\ \dot{x}_2(t) \end{bmatrix} = \begin{bmatrix} 1 & \rho_1(t) \\ \rho_2(t) & 0 \end{bmatrix} \begin{bmatrix} x_1(t) \\ x_2(t) \end{bmatrix}. \tag{2.3}$$

where the *exogenous parameters* $\rho_1(t) = \sin(2\pi t), \ \rho_2(t) = \cos(\pi t + \pi/3) \in [-1, \ 1]$ are independent of the system state. It can be noticed that these parameters have continuous and bounded derivatives.

On the other hand, the time-varying parameters can also characterize the states of the nonlinear system, for instance

$$\begin{aligned} \dot{x}_1(t) &= x_1(t) + x_2^2(t), \\ \dot{x}_2(t) &= \frac{x_1(t)}{1 - \sin(x_2(t))}. \end{aligned} \tag{2.4}$$

The defined domain of the system is $x_2(t) \neq \pi/2 \pm 2k\pi, k \in \mathbb{N}$. Let's set the parameters as follows $\rho_1(x(t)) = x_2(t) \neq \pi/2 \pm 2k\pi$, and $\rho_2(x(t)) = (1 - \sin(x_2(t)))^{-1}$, then the approximation of system (2.4) under LPV formulation is given by:

$$\begin{bmatrix} \dot{x}_1(t) \\ \dot{x}_2(t) \end{bmatrix} = \begin{bmatrix} 1 & \rho_1(x(t)) \\ \rho_2(x(t)) & 0 \end{bmatrix} \begin{bmatrix} x_1(t) \\ x_2(t) \end{bmatrix}. \tag{2.5}$$

In this case, when the parameters are functions of states, they are usually classified as *endogenous parameters*. The representation systems are referred to as a quasi-LPV system (Briat, 2015a; Hoffmann & Werner, 2015; Lovera et al., 2013; Rotondo et al., 2013;

Shamma, 2012). It is interesting to note that systems (2.3) and (2.5) have a similar LPV representation.

Continuous (*discontinuous*) *parameter values with continuous* (*discontinuous*) *derivative*

In addition, parameter behaviors can also be classified by mathematical properties such as discrete or continuous value, smooth or non-smooth functions, and differentiability or non-differentiability. Let's consider an example:

$$\begin{aligned} \rho: \quad & \mathbb{R}_+ \to \mathbb{B} \\ & t \to \{0,1\} \end{aligned} \tag{2.6}$$

where $\mathbb{B}$ is the image set of function $\rho(t)$ maps from $t \in \mathbb{R}_+$ to $\mathbb{B} := \{0,1\}$. In this case, the parameter trajectory is a continuous switching between the piecewise constants. The systems involved in *the function* described the discrete value parameter could be considered as Hybrid Systems (deterministic and stochastic switched cases). The interested readers can refer to the literature (Alwan & Liu, 2018; Boukas, 2006; Briat, 2018, 2021; Chatterjee & Liberzon, 2006; Colaneri, 2009; Teel et al., 2014).

Let's consider a continuous parameter with discontinuous trajectory:

$$\rho(t) = \begin{cases} \sin(t) & t \in [2k\pi,\ \pi + 2k\pi) \\ (-1)^k + \cos(t) & t \in [\pi + 2k\pi, 2(k+1)\pi) \end{cases} \qquad k \in \mathbb{N}. \tag{2.7}$$

There is no existence of the continuous derivative function $f(t) = \dot{\rho}(t)$. This function is discontinuous at times $t = k\pi$. Instead, it takes left and right values by -1 and 1, respectively.

Generally, the bounding derivative of the parameters often interferes with stability analysis. The dynamics of state are theoretically unbounded, but with the definition, the parameters do. Nonetheless, if considered that functions mapping from state to parameter domain are bounded on each state, it is a too strong assumption. Let borrow a simple example from (Briat, 2008) to make this clear: in the synthesis of stabilization conditions of single input single output SISO LPV system is ensued in condition $\dot{x} = \dot{\rho}(t) \in [a,\ b]$. Then, by implementing the closed-loop system with the found controller, the system's trajectory exhibits a stable characteristic, but the behavior of the derivative of the state goes outside the bounded region, e.g., $[a-1,\ b+1]$. So, it is not reasonable to *confirm* that the closed-loop system is stable in the domain $[a,\ b]$, and then the analysis should start over with an expansion of the bounds on the derivative of the state, e.g., $[a-2,\ b+2]$. But, the increase of the limits also leads to the conservative results.

Throughout this dissertation, we are only interested in the systems that are assumed to depend on continuous time-varying parameters $\rho(t) = [\rho_1(t), \rho_2(t), \ldots, \rho_{N_p}(t)]$, which have the continuous derivatives and respectively belong to parameter spaces

$$\rho(t) \in \mathcal{U}_p = \{\rho_i \in [\underline{\rho}_i, \overline{\rho}_i], i = 1, \ldots, N_p\} \subset \mathbb{R}^{N_p}, \tag{2.8}$$

$$\dot{\rho}(t) \in \mathcal{U}_\nu = \{\nu_i \in [\underline{\nu}_i, \overline{\nu}_i], |\dot{\rho}_i| < \nu_i,\ i = 1, \ldots, N_p\} \subset \mathbb{R}^{N_p}. \tag{2.9}$$

The compact parameter sets can be symbolized as follows $(\rho(t), \dot{\rho}(t)) \in \mathcal{U}_p \times \text{conv}\{\mathcal{U}_\nu\}$. Hereafter, we inherit the mathematical definition of convex optimization from (Boyd et al., 1994; Boyd & Vandenberghe, 2004) and use the computational toolboxes such as

LMI toolbox MATLAB (Gahinet & Laub, 1994), Yalmip toolbox (Lofberg, 2004), semidefinite programming problems - SDP Sedumi toolbox (Sturm, 1999), cone programming Mosek toolbox (E D Andersen et al., 2003; Erling D Andersen & Andersen, 2000) to solve the convex optimization problems.

In the following sections, the presentations of the LPV/qLPV paradigms are provided along with the summarizing stability synthesis of LPV systems based on Lyapunov technique expressing in the parameterized LMIs.

2.1.1. *Affine LPV Systems*

An affine LPV (ALPV) system is linear parameter-varying systems whose matrices are affine functions of the scheduling parameters. Considering a dynamic system depend *affinely* on the parameter vector $\rho(t) = [\rho_1(t), \rho_2(t), ..., \rho_{Np}(t)]$ presented under the general expression:

$$\begin{aligned} \dot{x}(t) &= A(\rho)x(t) + B_w(\rho)w(t) \\ z(t) &= H(\rho)x(t) + J_w(\rho)w(t) \end{aligned} \tag{2.10}$$

where matrices function $A: \mathcal{U}_p \to \mathbb{R}^{n\times n}$, $B_w: \mathcal{U}_p \to \mathbb{R}^{n\times d}$, $H: \mathcal{U}_p \to \mathbb{R}^{r\times n}$, $J_w: \mathcal{U}_p \to \mathbb{R}^{r\times d}$, can be expressed by $A(\rho) = A_0 + \sum_{i=1}^{N_p} A_i \rho_i(t)$. Then, the parameter-dependent state space matrices could represent in the following form:

$$\left[\begin{array}{c|c} A(\rho) & B_w(\rho) \\ \hline H(\rho) & J_w(\rho) \end{array}\right] = \left[\begin{array}{c|c} A_0 & B_{w,0} \\ \hline H_0 & J_{w,0} \end{array}\right] + \sum_{i=1}^{N_p} \left[\begin{array}{c|c} A_i & B_{w,i} \\ \hline H_i & J_{w,i} \end{array}\right] \rho_i(t). \tag{2.11}$$

For the sake of simplicity, parametric dependent matrix expression $A(\rho(t))$ are reduced to $A(\rho)$. This is one of the most common LPV system formulations encountered in control synthesis, where the affine-dependent system leads to a low degree of conservatism of stability conditions.

2.1.2. *Polynomial Systems*

The parameter polynomial formulations are widely concerned to the modeling and control system design of the LPV systems. A polynomial system relating to the parameter-dependent state-space representation could express by the following form:

$$\left[\begin{array}{c|c} A(\rho) & B_w(\rho) \\ \hline H(\rho) & J_w(\rho) \end{array}\right] = \left[\begin{array}{c|c} A_0 & B_{w,0} \\ \hline H_0 & J_{w,0} \end{array}\right] + \sum_{i=1}^{N_p} \sum_{j=1}^{N} \left[\begin{array}{c|c} A_{ij} & B_{w,ij} \\ \hline H_{ij} & J_{w,ij} \end{array}\right] \rho_i^j(t). \tag{2.12}$$

It should note that a polynomial system is directly approximated by Taylor's expansion of the nonlinear expressions. A general formulation could find in the literature (Parrilo, 2000, 2003; Sato & Peaucelle, 2006).

2.1.3. *Polytopic Systems*

The polytopic LPV formulation is a linear combination of a convex set of dependent parameters, widely used in the framework for control synthesis of LPV systems. Introduced the early 90s in the literatures (Apkarian & Tuan, 2000b; Feron et al., 1996; Gahinet et

al., 1994, 1996) which address robust stability and robust performance of the uncertainty systems. Generally, a polytopic system is defined by the following equations:

$$\begin{cases} \dot{x}(t) = \sum_{i=1}^{N_l} \lambda_i(\rho(t))(A_i x(t) + B_{w,i} w(t)) \\ z(t) = \sum_{i=1}^{N_l} \lambda_i(\rho(t))(H_i x(t) + J_{w,i} w(t)) \end{cases}, i = 1,2,\ldots,N_l, \tag{2.13}$$

where the polytopic coordinates $\sum_{i=1}^{N_l} \lambda_i(\rho(t)) = 1,$ and $\lambda_i(\rho(t)) \in [0,1].$

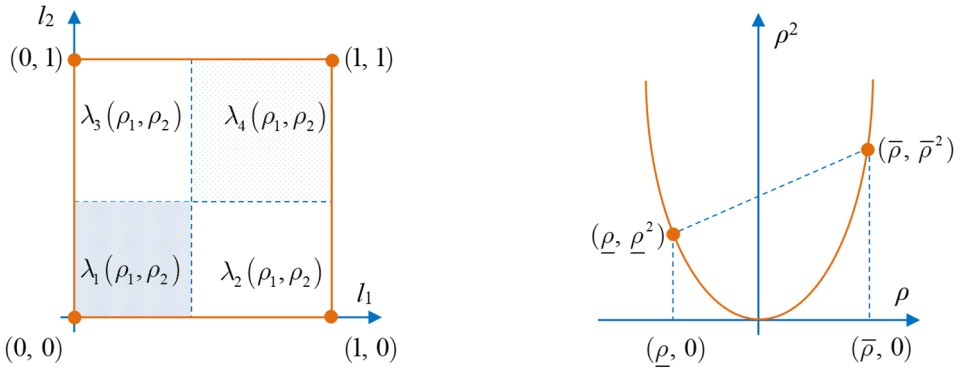

a. Distribution domain of the parameters *b. Parabola of parameters*

Figure 2-1. *Polytopic parametrization*.

Example 2.1.1. (Briat, 2008) Considering an affine system with 2 parameters:

$$\dot{x}(t) = (A_{p1}\rho_1(t) + A_{p2}\rho_2(t))x(t) \tag{2.14}$$

Let's define a polytope 4 vertices $\mathcal{P}_\rho = \{(\underline{\rho}_1, \underline{\rho}_2); (\overline{\rho}_1, \underline{\rho}_2); (\underline{\rho}_1, \overline{\rho}_2); (\overline{\rho}_1, \overline{\rho}_2)\}$ encloses the set parameters $\rho(t) = \{(\rho_1(t), \rho_2(t)) \in \mathbb{R}^2 \mid \underline{\rho}_1 \le \rho_1(t) \le \overline{\rho}_1,\ \underline{\rho}_2 \le \rho_2(t) \le \overline{\rho}_2\}.$

The conversion of an affine system into a polytopic system carries out by the following coordinate system transform:

$$\begin{aligned} \lambda_1(t) &= \frac{(\overline{\rho}_1 - \rho_1(t))(\overline{\rho}_2 - \rho_2(t))}{(\overline{\rho}_1 - \underline{\rho}_1)(\overline{\rho}_2 - \underline{\rho}_2)}, & \lambda_2(t) &= \frac{(\overline{\rho}_1 - \rho_1(t))(\rho_2(t) - \underline{\rho}_2)}{(\overline{\rho}_1 - \underline{\rho}_1)(\overline{\rho}_2 - \underline{\rho}_2)}, \\ \lambda_3(t) &= \frac{(\rho_1(t) - \underline{\rho}_1)(\overline{\rho}_2 - \rho_2(t))}{(\overline{\rho}_1 - \underline{\rho}_1)(\overline{\rho}_2 - \underline{\rho}_2)}, & \lambda_4(t) &= \frac{(\rho_1(t) - \underline{\rho}_1)(\rho_2(t) - \underline{\rho}_2)}{(\overline{\rho}_1 - \underline{\rho}_1)(\overline{\rho}_2 - \underline{\rho}_2)}. \end{aligned} \tag{2.15}$$

The coordinates are illustrated in Figure 2-1.a. By using the transformation (2.15) the polytopic system are presented as follows:

$$\dot{x}(t) = \sum_{i=1}^{4} \lambda_i(\rho(t)) A_i x(t) \tag{2.16}$$

Where $A_1 = A_{p1}\underline{\rho}_1,\ A_2 = A_{p1}\overline{\rho}_1,\ A_3 = A_{p2}\underline{\rho}_2,$ and $A_4 = A_{p2}\overline{\rho}_2.$

Example 2.1.2. Let's analyze a polynomial system with bounded parameters:

$$\dot{x}(t) = \left(A_{p0} + A_{p1}\rho(t) + A_{p2}\rho(t)^2\right)x(t), \tag{2.17}$$

where the parameter $\rho(t) \in [\underline{\rho},\ \overline{\rho}]$ can be transferred coordinate to polytopic system by 4

vertices (visualized in Figure 2-1.*b*) as follows:

$$\begin{bmatrix}\rho(t)\\ \rho(t)^2\end{bmatrix}=\lambda_1(t)\begin{bmatrix}\underline{\rho}\\ 0\end{bmatrix}+\lambda_2(t)\begin{bmatrix}\overline{\rho}\\ 0\end{bmatrix}+\lambda_3(t)\begin{bmatrix}\underline{\rho}\\ \underline{\rho}^2\end{bmatrix}+\lambda_4(t)\begin{bmatrix}\overline{\rho}\\ \overline{\rho}^2\end{bmatrix}, \tag{2.18}$$

The polytopic coordinate $\lambda_i(t),\ i=1,...,4$ are employed similarly to (2.15), but $\rho(t)$ and $\rho(t)^2$ are not two separate parameters. In the work of literature (Briat, 2008), the author has used this example as a simple way to demonstrate the drawback of the polytopic approach. As seen in Figure 2-1.b, the polytope lost its parametric dependence since the two vertices of the system are not related to the parameter domain $(\rho(t),\rho(t)^2)$ resulting in the conservative stability conditions. Consequently, a uncertain polytope method (Appendix A.1.4) that reshapes the quasi-convex vertex containing the parameter curve presented in (Briat, 2008) and (Gonçalves et al., 2006) to reduce this conservatism.

2.1.4. *Takagi-Sugeno Fuzzy Systems*

Since introduced by (Takagi & Sugeno, 1985), the T-S fuzzy model has shown the effective linearization of the nonlinear systems by using logical rules (fuzzy sets). Following this research direction, (Tanaka & Wang, 2001) presented the control and observation analysis for nonlinear systems that could reformulate to the T-S fuzzy framework. Like the LPV system, the T-S fuzzy systems grow the influence in multidisciplinary applications of the robust stability control analysis. Now, let's consider a nonlinear system:

$$\begin{cases}\dot{x}(t)=f(x(t),w(t))\\ z(t)=g(x(t),w(t))\end{cases} \tag{2.19}$$

where vectors $x(t)\in\mathbb{R}^n, z(t)\in\mathbb{R}^r,$ are respectively the state of the system and the controlled output. The *i-th* rule of continuous local linear model approximated from system (2.19) is given under the following form:

if $\rho_1(t)\in M_{i1}$ and … and $\rho_p(t)\in M_{ip}$

then $\begin{cases}\dot{x}_i(t)=A_ix(t)+B_{w,i}w(t)\\ z(t)=H_ix(t)+J_{w,i}w(t)\end{cases},\quad i=1,2,...,r.$

Where *j-th* premise variable $\rho_j(t)\in M_{ij}$ may be functions of state variables $x(t),$ internal parameters, etc., distributed under the rules of fuzzy set $M_{ij},$ and local linear matrices $A_i\in\mathbb{R}^{n\times n}, B_i\in\mathbb{R}^{n\times m},$ and $C_i\in\mathbb{R}^{p\times n}$. The aggregation of the subsystems is based on membership function $\rho_j(t)$ in M_{ij}

$$\rho_j(t)\in[\underline{\rho}_j,\ \overline{\rho}_j]\ \rightarrow\ \theta_j(\rho(t))\in[0,\ \overline{\rho}_j-\underline{\rho}_j]\ \rightarrow\ \lambda_i(\rho(t))=\theta_j(\rho(t))\Big/\sum\nolimits_{j=1}\theta_i(\rho(t)),$$
$$\text{with } \lambda_i(\rho(t))\in[0,\ 1] \text{ and } \sum\nolimits_{i=1}^{N_l}\lambda_i(\rho(t))=1. \tag{2.20}$$

A similarity can be found in this expression of the membership function and the polytopic coordinate system (2.13). Then, the defuzzification process of this model can derive by:

$$\begin{cases}\dot{x}(t)=\sum_{i=1}^{N_l}\lambda_i(\rho(t))\left(A_ix(t)+B_{w,i}w(t)\right)\\ z(t)=\sum_{i=1}^{N_l}\lambda_i(\rho(t))\left(H_ix(t)+J_{w,i}w(t)\right)\end{cases},\quad i=1,2,...,N_l. \tag{2.21}$$

It should note that the commonly used notations in the fuzzy logic control community are

denoted by $h_i(z(t)) \leftarrow \lambda_i(\rho(t)),\ r \leftarrow N_l,$ etc. Nonetheless, to unify the symbolizations on the control system in this dissertation, $h(t)$ is signified for the time-varying delay, and $z(t)$ is used for the regulated output. And parameters $\theta_i(\rho(t))$ is a monochromatic transformation from $\rho_j(t) \in M_{ij}$, for more details refer to (Tanaka & Wang, 2001).

The fuzzification is convenient for modeling dynamic systems, complex non-smooth nonlinear systems, chaotic systems, etc. The choice of distribution law and member functions is dependent on the purpose of system design, more specific of the fuzzification and defuzzification referred to (Tanaka & Wang, 2001). In the next section, we briefly describe the mathematical formula of membership function $\lambda_i(\rho(t))$ of a bounded nonlinear system (local sector) and unbounded nonlinear system (global sector).

2.1.4.1. *Sector Nonlinearity*

As discussed in (Tanaka & Wang, 2001), T-S fuzzy modeling has two typical approaches. In the one hand, the fuzzy identification modeling using input-output relation is difficult to analyze the control design for physical models. On the other hand, the nonlinear dynamic models obtained from the Lagrange equation or the Newton-Euler theorem are fuzzificated by "sector nonlinearity."

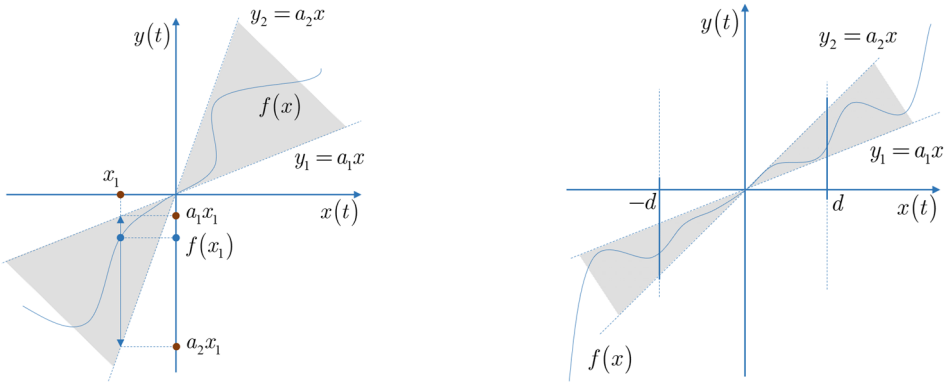

a. Global sector *b. Local sector*

Figure 2-2. *Illustrates fuzzy model construction by sector nonlinearity.*

The sector nonlinearity method introduced by (Kawamoto et al., 1992) and generalized by (Tanaka & Wang, 2001) can interpret as follows: in the specified time domain of state $x(t) \in \mathcal{D}_x \subset \mathbb{R}$, give a finite nonlinear function $f(x(t)) \in \mathbb{R}$, such that the upper and lower bound functions of $f(x(t))$ are finite over certain time-domain of $x(t)$.

As shown in Figure 2-2 is the Cartesian coordinate system (Oxy) representing nonlinear function $f(x(t))$ is locally or globally bounded by two linear function $y_2(x(t)) = a_2x(t)$ and $y_1(x(t)) = a_1x(t)$. Where Figure 2-2.*a*, the construction of T-S fuzzy model for the nonlinear system $f(x(t))$ is illustrated at point $(x_1, f(x_1))$ as follows:

$$f(x_1) = \lambda y_1(x_1) + (1-\lambda)y_2(x_1) = \lambda a_1x_1 + (1-\lambda)a_2x_1, \text{with } \lambda = \frac{a_2f^{-1}(x_1) - f(x_1)}{(a_2 - a_1)f^{-1}(x_1)}. \quad (2.22)$$

Similarly, Figure 2-2.*b* shows a fuzzyfication of the system in local region $x(t) \in [-d, d]$, where the fuzzification of the function $f(x(t))$ is so-called local sector linearization. In this

case, nonlinear systems are approximated around a local bound on each state. However, there are no prerequisites requirements for the dynamics of system states, e.g., the upper bound of the derivative $\dot{x}(t) \leq ?$. Usually, these constraints are often involved in the stability synthesis with the parameter-dependent Lyapunov functions (i.e., fuzzy Lyapunov function - FLF).

A computational load requirement for the sector nonlinearity approach is to simplify the original nonlinear system with fewer model rules (vertices) as possible so that the reduction of the effort for analysis and design of control systems does not degrade the performance of the modeling process. In the work of (Tanaka & Wang, 2001) a local approximation in fuzzy partition spaces was used to simplify the system with a significant decrease of the model rules. In the other direction, the combination of fuzzification with the monomial formulation will balance less conservative condition and computational synthesis complexity.

2.1.4.2. *Polynomial Fuzzy Model*

The polynomial fuzzy proposed for the SoS-based state-space approach in (Tanaka et al., 2009) is more effective for representing nonlinear control systems and providing less conservative stability analysis and synthesis than the traditional T-S fuzzy model. The main difference between T-S fuzzy model (2.21) and a polynomial fuzzy model is indicated in the following formulation of a local linear model.

$$\textbf{\textit{if}} \qquad \rho_1(t) \in M_{i1} \text{ and } \ldots \text{ and } \rho_p(t) \in M_{ip} \tag{2.23}$$

$$\textbf{\textit{then}} \qquad \begin{cases} \dot{x}_i(t) = A_i(x(t))Z(x(t)) + B_{w,i}(x(t))w(t) \\ z(t) = H_i(x(t))Z(x(t)) + J_{w,i}(x(t))w(t) \end{cases}, \quad i = 1,2,\ldots,N_l \tag{2.24}$$

Where $A_i(x(t)) \in \mathbb{R}^{n \times N}$, $C_i(x(t)) \in \mathbb{R}^{p \times N}$, $B_{w,i}(x(t))$, and $J_{w,i}(x(t))$ are the polynomial matrices in $x(t)$. The term $Z(x(t)) \in \mathbb{R}^N$ signifies a column vector of monomial in $x(t) \in \mathbb{R}^n$, e.g., a second order monomial $Z(x) = [x_1(t)\ x_2(t)\ x_1(t)x_2(t)\ x_1(t)^2\ x_2(t)^2]^T$.

2.1.5. *Example*

In this section, a nonlinear system is used to illustrate the representation to all the discussed types of LPV/quasi-LPV systems.

Example 2.1.3. Let's consider a nonlinear system (Tanaka & Wang, 2001):

$$\begin{bmatrix} \dot{x}_1(t) \\ \dot{x}_2(t) \end{bmatrix} = \begin{bmatrix} -x_1(t) + x_1(t)x_2^3(t) \\ 3x_1^3(t) - x_2(t) + x_1^3(t)x_2(t) \end{bmatrix}. \tag{2.25}$$

with state vector $x(t) = [x_1(t),\ x_2(t)]^T$, and $x_1(t)$, $x_2(t)$ belong to domain $\mathcal{D}_x = [-1,1]$.

Affine system

Let's define a parameters vector $\rho(x(t)) = (\rho_1(x(t)), \rho_2(x(t))) \in \mathcal{U}_\rho \subset \mathbb{R}^2$, with

$$\rho_1(x(t)) = x_1(t)x_2^2(t),\ \rho_2(x(t)) = x_1^2(t)(3 + x_2(t)). \tag{2.26}$$

are constrained by:

$$-1 \leq \rho_1(x(t)) \leq 1,\ 0 \leq \rho_2(x(t)) \leq 4. \tag{2.27}$$

Then, system (2.25) is represented by LPV formulation as follows:

$$\dot{x}(t) = A(\rho(x(t)))x(t) = (A_0 + A_1\rho_1(x(t)) + A_2\rho_2(x(t)))x(t), \tag{2.28}$$

with $A(\rho(x(t))) = \begin{bmatrix} -1 & \rho_1(x(t)) \\ \rho_2(x(t)) & -1 \end{bmatrix}$, $A_0 = \begin{bmatrix} -1 & 0 \\ 0 & -1 \end{bmatrix}$, $A_1 = \begin{bmatrix} 0 & 1 \\ 0 & 0 \end{bmatrix}$, and $A_2 = \begin{bmatrix} 0 & 0 \\ 1 & 0 \end{bmatrix}$.

Polynomial formulation

Now, by defining a monomial vector in $x : Z(x) = [x_1(t)\ x_2(t)\ x_1(t)x_2(t)]^T$, then system (2.25) is expressed by the following polynomial equation:

$$\dot{x}(t) = A(x)Z(x). \tag{2.29}$$

with $A(x) = \begin{bmatrix} -1 & 0 & x_2^2(t) \\ 3x_1^2(t) & -1 & x_1^2(t) \end{bmatrix}$.

It should be noted that system (2.28) depends affinely on the time-varying parameters and is presented as a first-order polynomial matrix. The expression $\rho(t)$ can be implicitly considered as an uncertain parameter (either *endogenous parameters* or *exogenous parameters*). Whereas system (2.29) is an explicit state-dependent polynomial.

T-S Fuzzy Model

Let's designate the local sector nonlinearities:

$$\rho_1(x(t)) = x_1(t)x_2^2(t),\ \rho_2(x(t)) = x_1^2(t)(3 + x_2(t)), \tag{2.30}$$

which vary respect to $-1 \le \rho_1(x(t)) \le 1,\ 0 \le \rho_2(x(t)) \le 4$.

From the designed operation range, the nonlinear system (2.25) is represented by the following fuzzy models

Model rule 1:

if $\rho_1(x(t)) \in [0, 1]$ and $\rho_2(x(t)) \in [2, 4]$

then $\dot{x}(t) = A_1x(t)$, $A_1 = \begin{bmatrix} -1 & 1 \\ 4 & -1 \end{bmatrix}$,

Model rule 2:

if $\rho_1(x(t)) \in [0, 1]$ and $\rho_2(x(t)) \in [0, 2)$

then $\dot{x}(t) = A_2x(t)$, $A_2 = \begin{bmatrix} -1 & 1 \\ 0 & -1 \end{bmatrix}$,

Model rule 3:

if $\rho_1(x(t)) \in [-1, 0)$ and $\rho_2(x(t)) \in [2, 4]$

then $\dot{x}(t) = A_3x(t)$, $A_3 = \begin{bmatrix} -1 & -1 \\ 4 & -1 \end{bmatrix}$,

Model rule 4:

if $\rho_1(x(t)) \in [-1, 0)$ and $\rho_2(x(t)) \in [0, 2)$

then $\dot{x}(t) = A_4x(t)$, $A_4 = \begin{bmatrix} -1 & -1 \\ 0 & -1 \end{bmatrix}$,

Corresponding to the membership functions:

$$\begin{aligned}\lambda_1 &= \frac{(\rho_1(x(t))+1)}{2}\frac{\rho_2(x(t))}{4}, \qquad \lambda_2 = \frac{(\rho_1(x(t))+1)}{2}\frac{4-\rho_2(x(t))}{4},\\ \lambda_3 &= \frac{(1-\rho_1(x(t)))}{2}\frac{\rho_2(x(t))}{4}, \qquad \lambda_4 = \frac{(1-\rho_1(x(t)))}{2}\frac{4-\rho_2(x(t))}{4},\end{aligned} \tag{2.31}$$

with $\sum_{i=1}^{4}\lambda_i(\rho(x(t))) = 1,\ \lambda_i(\rho(x(t))) \in [0,\ 1],\ i = 1,\ldots,4.$

Finally, the defuzzification is carried out as

$$\dot{x}(t) = \sum_{i=1}^{4}\lambda_i(\rho(x(t)))A_i x(t). \tag{2.32}$$

This quasi-LPV representation is expressed by a convex combination of the four vertices of the nonlinear system (2.25) in the specified domain. The linear combinational representation is convenient for stability and stabilization analysis. As stated in the discussion of Polytopic systems, the convexity conditions are directly delivered. The conservatism of the convex envelope is illustrated in Figure 2-1.*b*, and the computational burden increases exponentially with the number of vertices of the system (i.e., the number of membership functions).

In the other aspect, the polynomial formulation more accurately describes the nonlinear behaviors. But it depends on the selection of the monomial vector $Z(x)$ to have a reasonable number of polynomial order (a higher degree leads to complexity in the stability analysis and increased computational load). Accordingly, a fuzzy polynomial system balances conservatism with numerical complexity is considered as follows.

Polynomial Fuzzy Model

Using the same monomial vector $Z(x) = [x_1(t)\ x_2(t)\ x_1(t)x_2(t)]^T$, and designates the nonlinear term

$$\rho(x(t)) = x_1^2(t), \tag{2.33}$$

belongs to $0 \le \rho(x(t)) \le 1$. Then, matrix

$A(x) = \begin{bmatrix} -1 & 0 & x_2^2(t) \\ 3x_1^2(t) & -1 & x_1^2(t) \end{bmatrix}$ is fuzzificated by the following rules:

Model rule 1:

if $\rho(x(t)) \in (\frac{1}{2},\ 1]$,

then $\dot{x}(t) = A_1(x)x(t), \qquad A_1(x) = \begin{bmatrix} -1 & 0 & x_2^2(t) \\ 3 & -1 & 1 \end{bmatrix}.$

Model rule 2:

if $\rho(x(t)) \in [0,\ \frac{1}{2}]$,

then $\dot{x}(t) = A_2(x)x(t), \qquad A_2(x) = \begin{bmatrix} -1 & 0 & x_2^2(t) \\ 0 & -1 & 0 \end{bmatrix}.$

Consistent with the membership functions:

$$\lambda_1(\rho(x)) = \rho(x(t)), \qquad \lambda_2(\rho(x)) = 1 - \rho(x(t)). \tag{2.34}$$

Then, the defuzzification of polynomial fuzzy is approved by

$$\dot{x}(t) = \sum_{i=1}^{2} \lambda_i(\rho(x)) A_i(x) Z(x). \tag{2.35}$$

The vertices of system (2.35) is halved compared to system (2.32), which also has a simpler polynomial matrix structure than system (2.29).

An appropriate stability analysis method will be delivered for each presented model in section 2.2, including the advantages and disadvantages suitable for the implementation. Then, in section 2.2.5 with these representation, the appropriate stability conditions will be developed on each LPV model corresponding to an LMI relaxation method.

2.1.6. *Applications*

Linear Parameter-Varying (LPV) systems have been extensively studied over the last three decades to approximate the nonlinear systems and provide a systematic design framework of gain-scheduled controllers robust again the uncertain information. Their applications have been found in various fields such as automotive systems, aircraft systems, robotic manipulators, mechatronic systems see, for example, (Briat, 2015a; Giri & Bai, 2013; Hoffmann & Werner, 2015), etc. From a theoretical perspective, in addition to choosing an appropriate LPV model, the online measurement feature also plays a decisive role in accurately restructuring the system trajectories and linearizing the behavior of the nonlinear dynamics. However, in some LPV control applications, not all scheduling parameters are available for measuring. The high-precision engineering systems are even more demanding on requirements and system performances, e.g., aerospace application, Unmanned aircraft systems (Marcos & Balas, 2004; Marcos & Bennani, 2009). It can be found that increasing the number of scheduling parameters enhances the simulation accuracy and the system validation process. However, it also burdens the computational load, increases memory requirements, and growths the synthesis complexity, see, e.g., (Hoffmann et al., 2014; Hoffmann & Werner, 2014, 2015). So, depending on the design requirements, we have appropriate analysis and synthesis tools. Now, let's discuss some applications of the LPV modeling.

2.1.6.1. *Automotive Chassis Systems*

In the last decades, LPV control synthesis has been addressed the robust stability and performance of the lateral dynamic stabilizing system integrated on-road vehicles, see, for example, in (Dahmani et al., 2014; Doumiati et al., 2013; Ono et al., 1998, 1999; Zhang et al., 2014). The simplified lateral dynamic stabilization system (illustrated in Figure 2-3.*b*) can be described by the following equations:

$$\begin{cases} m\dot{v}_y(t) = 2F_{yf}(\alpha_f(t)) + 2F_{yr}(\alpha_r(t)) - m\dot{\psi}(t)v_x(t) \\ I_z\ddot{\psi}(t) = 2F_{yf}(\alpha_f(t))l_f - 2F_{yr}(\alpha_r(t))l_r \end{cases} \tag{2.36}$$

where the full description of the physical parameters is detailed in Appendix E.2. This dynamic system depends on the lateral friction forces $F_{yf}(\alpha), F_{yr}(\alpha)$ (also called cornering forces), described by the nonlinear equations of the tire slip angle at the contact point of front tires $\alpha_f(t)$ (rear tires $\alpha_r(t)$) and road surface, see, e.g., (Bakker et al., 1989; Dugoff et al., 1970; Kiencke & Nielsen, 2005).

LTI and LTV systems

Considering linear cornering forces, i.e., $F_{yf}(\alpha)=C_f\alpha_f(t),\ F_{yr}(\alpha)=C_r\alpha_r(t)$. Where the dynamics $\alpha_f(t),\alpha_r(t)$ could approximate by the following expression:

$$\alpha_f(t)\cong-\frac{v_y(t)}{v_x(t)}-l_f\cdot\frac{\dot\psi(t)}{v_x(t)}+\delta_f(t),\ \text{and}\ \alpha_r\cong-\frac{v_y(t)}{v_x(t)}+l_r\cdot\frac{\dot\psi(t)}{v_x(t)}. \tag{2.37}$$

If longitudinal speed v_x is constant, then the vehicle system is regarded with LTI system (Farrelly & Wellstead, 1996; Fukada, 1999; Guldner et al., 1996).

$$\begin{bmatrix}\dot v_y(t)\\ \ddot\psi(t)\end{bmatrix}=\begin{bmatrix}\frac{-2(C_f+C_r)}{mv_x} & \frac{-2(C_fl_f-C_rl_r)}{mv_x}-v_x\\ \frac{-2(C_fl_f-C_rl_r)}{I_zv_x} & \frac{-2(C_fl_f^2+C_rl_r^2)}{I_zv_x}\end{bmatrix}\begin{bmatrix}v_y(t)\\ \dot\psi(t)\end{bmatrix}+\begin{bmatrix}\frac{2C_f}{m}\\ \frac{2C_fl_f}{I_z}\end{bmatrix}\delta_f(t). \tag{2.38}$$

The state-space is obtained by setting variables $x_1(t)=v_y(t),\ x_2(t)=\dot\psi(t),\ u(t)=\delta_f(t)$. If the system considers uncertain force models, e.g., $F_{yf}(\alpha)=(C_f+\Delta C_f)\alpha_f(t)$ (the variation cornering stiffness shows in Figure 2-3.*a*), then it is characterized by LTV systems discussed in (Ono et al., 1999; Zhang et al., 2014).

$$\begin{bmatrix}\dot v_y(t)\\ \ddot\psi(t)\end{bmatrix}=\begin{bmatrix}\frac{-2(C_f+C_r)-2(\Delta C_f+\Delta C_r)}{mv_x} & \frac{-2(C_fl_f-C_rl_r)-2(\Delta C_fl_f-\Delta C_rl_r)}{mv_x}-v_x\\ \frac{-2(C_fl_f-C_rl_r)-2(\Delta C_fl_f-\Delta C_rl_r)}{I_zv_x} & \frac{-2(C_fl_f^2+C_rl_r^2)-2(\Delta C_fl_f^2+\Delta C_rl_r^2)}{I_zv_x}\end{bmatrix}\begin{bmatrix}v_y(t)\\ \dot\psi(t)\end{bmatrix}+\begin{bmatrix}\frac{2(C_f+\Delta C_f)}{m}\\ \frac{2(C_f+\Delta C_f)l_f}{I_z}\end{bmatrix}\delta_f(t) \tag{2.39}$$

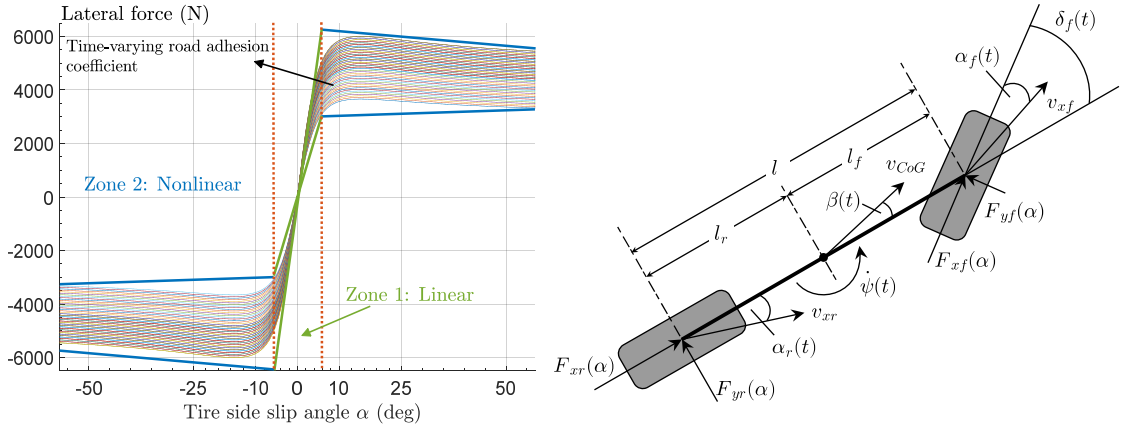

a. Tire sideslip angle – local sectors *b. Single-track parameter description*

Figure 2-3. *Vehicle lateral dynamics.*

Exogenous Parameters (*LPV systems*) *and Endogenous Parameters* (*quasi-LPV systems*)

Consider a constant longitudinal speed v_x. By approximating the nonlinear friction forces $F_{yf}(\alpha),F_{yr}(\alpha)$ to a parametric affine model, a convex combination form (e.g., T-S fuzzy forces model & sector nonlinearity as shown in Figure 2-3.a, with $F_{yf}(\alpha_f(t))\cong(h_1(\alpha)C_{f1}+h_2(\alpha)C_{f2})\alpha_f(t)$), that results in a quasi-LPV formulization.

$$\begin{bmatrix}\dot v_y(t)\\ \ddot\psi(t)\end{bmatrix}=\sum_{i=1}^{4}\lambda_i(\alpha(t))\left(\begin{bmatrix}\frac{-2(C_{f,i}+C_{r,i})}{mv_x} & \frac{-2(C_{f,i}l_f-C_{r,i}l_r)}{mv_x}-v_x\\ \frac{-2(C_{f,i}l_f-C_{r,i}l_r)}{I_zv_x} & \frac{-2(C_{f,i}l_f^2+C_{r,i}l_r^2)}{I_zv_x}\end{bmatrix}\begin{bmatrix}v_y(t)\\ \dot\psi(t)\end{bmatrix}+\begin{bmatrix}\frac{2C_{f,i}}{m}\\ \frac{2C_{f,i}l_f}{I_z}\end{bmatrix}\delta_f(t)\right). \tag{2.40}$$

Since slip coefficients (2.37) are functions of the states, then the membership functions

$\lambda_i(\alpha)$ are *intrinsic* parameters of these qLPV systems, see, e.g., (Bui Tuan & El Hajjaji, 2018; Dahmani et al., 2014; Dahmani, Chadli, et al., 2015; Dahmani, Pages, & El Hajjaji, 2015; El Hajjaji et al., 2006; Latrech et al., 2015).

The coordinate parameters $\lambda_i(\alpha)$ are usually accompanied by the assumption that the scheduling parameters can be *measured*. However, the stabilization chassis control system (2.40) is involved with an unmeasurable dynamic - tire sideslip angle $\alpha(t)$. The problem of an *inexact parameter* $\lambda_i(\hat{\alpha})$ has been addressed for the LPV system, see, e.g., (Daafouz et al., 2008; Heemels et al., 2010; Rotondo et al., 2014; Sato & Peaucelle, 2013) and the T-S fuzzy system (Li & Yang, 2014; Yang et al., 2019; Zhang & Wang, 2017). Using the estimates of membership function improve the performance of the control system but increases the complexity of the stability condition.

Now, let's consider a time-varying longitudinal velocity $\rho(t) = v_x(t)$. A compact set of the parameter transformed to the polytopic formulation discussed in (Bosche & El Hajjaji, 2008; A. T. Nguyen, Guerra, et al., 2018; Zhang et al., 2014, 2015).

$$\begin{bmatrix} \dot{v}_y(t) \\ \ddot{\psi}(t) \end{bmatrix} = \sum_{i=1}^{4} \lambda_i(\alpha(t)) \left(\begin{bmatrix} \frac{-2(C_{f,i}+C_{r,i})}{m\rho(t)} & \frac{-2(C_{f,i}l_f - C_{r,i}l_r)}{m\rho(t)} - \rho(t) \\ \frac{-2(C_{f,i}l_f - C_{r,i}l_r)}{I_z\rho(t)} & \frac{-2(C_{f,i}l_f^2 + C_{r,i}l_r^2)}{I_z\rho(t)} \end{bmatrix} \begin{bmatrix} v_y(t) \\ \dot{\psi}(t) \end{bmatrix} + \begin{bmatrix} \frac{2C_{f,i}}{m} \\ \frac{2C_{f,i}l_f}{I_z} \end{bmatrix} \delta_f(t) \right), \quad (2.41)$$

In this case, the representation is considered as an extrinsic LPV system because $v_x(t)$ is a state-independent parameter. If a global chassis system is used (Kiencke & Nielsen, 2005; Poussot-vassal, 2008), this parameter is now an implicit function of the states $x_1(t)$, $x_2(t)$. So, the definition is *quite abstract* and depends on the specific design purpose. In addition, $v_x(t)$ is measurable, so it suits the gain-scheduling controller technique.

Generally, depending on the system requirements (such as robust stability, robust performance, fast response, good tracking, etc.) and the *accessibility* of state variables and parameters, we have an appropriate approach for the analysis and design of control systems. Another application of LPV control relates to the improvement of performance and comfort of the automotive chassis system. The recent advances technique can find for instance in (Do, 2011; Do et al., 2010; Doumiati et al., 2012; Giri & Bai, 2013; M. Q. Nguyen, 2016; Poussot-vassal, 2008; Savaresi et al., 2010; Tuan, Ono, et al., 2001; Vu et al., 2016), and the reference therein.

2.1.6.2. *Aircrafts Systems*

The physical properties of the flight dynamics (high velocity, large number of degrees of freedom, aerodynamic influence, etc.) characterize the aviation control systems. The requirements, therefore, are more demanding in terms of robustness, system performance, and stability compared to the ground vehicles. The LPV theory is suitable for enhancing performance, robustness, and ensuring accuracy and safety during operation against the influence of aerodynamics. See, for example, analysis robustness margins (Schug et al., 2016), robust $\mathscr{H}_\infty$ control (Papageorgiou et al., 2000), high performance on F-16 Aircraft System (Shin et al., 2001) on F-14 and F-18 Aircraft System (Balas et al., n.d., 1997), LPV modeling and controller design for Boeing 747-100/200 (Ganguli et al., 2002; Marcos & Balas, 2001, 2004), and developments of LPV controllers for an unmanned air

vehicle (UAV) (Chen et al., 2008; Natesan et al., 2007; Rotondo et al., 2017). The application of gain-scheduling applies to missile autopilot LPV systems (Pellanda et al., 2002; Shamma & Cloutier, 1992; Wu et al., 1995).

Let's consider a qLPV modeling of Boeing 747-100/200 longitudinal motion (Marcos, 2001; Marcos & Balas, 2004) as follows:

$$\begin{bmatrix} \dot{\alpha}(t) \\ \dot{q}(t) \\ \dot{V}_{tas}(t) \\ \dot{\theta}(t) \\ \dot{h}_e(t) \end{bmatrix} = A\big(\alpha(t), V_{tas}(t), h_e(t), \theta_{eq}\big) \begin{bmatrix} \alpha(t) \\ q(t) \\ V_{tas}(t) \\ \nabla_\theta \\ h_e(t) \end{bmatrix} + B\big(\alpha(t), V_{tas}(t), h_e(t)\big) \begin{bmatrix} \delta_E(t) \\ \sigma(t) \\ T_{n,i}(t) \end{bmatrix} + f\big(\alpha(t), V_{tas}(t), h_e(t), \theta_{eq}, q_{eq}\big). \tag{2.42}$$

with

$$A\big(\alpha(t), V_{tas}(t), h_e(t), \theta_{eq}\big) = \begin{bmatrix} 0 & A_{12} & 0 & \frac{g}{V_{tas}(t)}(s_\alpha c_{\theta_{eq}} - c_\alpha s_{\theta_{eq}}) & 0 \\ 0 & A_{22} & 0 & 0 & 0 \\ 0 & \frac{-gS}{m}\frac{\partial C_{D_{Mach}}}{\partial q}\Big|_{eq} & 0 & -g(c_\alpha c_{\theta_{eq}} + s_\alpha s_{\theta_{eq}}) & 0 \\ 0 & 1 & 0 & 0 & 0 \\ 0 & 0 & (c_\alpha s_{\theta_{eq}} - s_\alpha c_{\theta_{eq}}) & V_{tas}(t)\cdot(c_\alpha c_{\theta_{eq}} + s_\alpha s_{\theta_{eq}}) & 0 \end{bmatrix},$$

$$A_{12} = \{1 - \tfrac{\bar{q}S\bar{c}}{2mV_{tas}(t)^2}(1.45 - 1.8x_{cg})\tfrac{dC_L(h_e(t),M)}{dq}\},$$

$$A_{22} = \tfrac{c_7\bar{q}S\bar{c}^2}{2V_{tas}}\{\tfrac{dC_{m025}(h_e(t),M)}{dq} - \tfrac{1}{\bar{c}}(1.45 - 1.8x_{cg})\tfrac{dC_L(h_e(t),M)}{dq}\cdot(c_\alpha\bar{x}_{cg} + s_\alpha\bar{z}_{cg})\} + c_7\bar{q}S\tfrac{\partial C_{D_{Mach}}}{\partial q}\Big|_{eq}\cdot(c_\alpha\bar{z}_{cg} + s_\alpha\bar{x}_{cg}),$$

$$B\big(\alpha(t), V_{tas}(t), h_e(t)\big) = \begin{bmatrix} B_{11} & 0 & \frac{-1}{mV_{tas}(t)}(s_\alpha + 0.0436c_\alpha) \\ B_{21} & c_7\bar{q}S\bar{c}K_\alpha\big(\delta_{f,i}(t), \alpha_w(t)\big)\frac{dC_{m025}(h_e(t),M)}{d\sigma} & c_7 z_{eng,i} \\ 0 & 0 & \frac{1}{m}(c_\alpha - 0.0436s_\alpha) \\ 0 & 0 & 0 \\ 0 & 0 & 0 \end{bmatrix},$$

$$B_{11} = \tfrac{-\bar{q}S}{mV_{tas}(t)}K_\alpha\big(\delta_{f,i}(t), \alpha_w(t)\big)\{\tfrac{dC_L(h_e(t),M)}{d\delta_{E_I}} + \tfrac{dC_L(h_e(t),M)}{d\delta_{E_O}}\},$$

$$B_{21} = c_7\bar{q}S\bar{c}K_\alpha(\delta_{f,i}(t), \alpha_w(t))\{\tfrac{dC_{m025}(h_e(t),M)}{d\delta_{E_I}} + \tfrac{dC_L(h_e(t),M)}{d\delta_{E_O}} - \tfrac{1}{\bar{c}}[\tfrac{dC_L(h_e(t),M)}{d\delta_{E_I}} + \tfrac{dC_L(h_e(t),M)}{d\delta_{E_O}}]\cdot(c_\alpha\bar{x}_{cg} + s_\alpha\bar{z}_{cg})\}.$$

The states of the system $x(t) = [z(t) \;\; w(t)]^T$ are decomposed by the scheduling state $z(t)$ includes angle of attack $\alpha(t)$, true airspeed $V_{tas}(t)$, altitude $h_e(t)$, and non-scheduling states $w(t)$ involves with pitch rate $q(t)$, and pitch angle $\theta(t)$. A linearization with respect to a trim value is performed for the pitch angle to transform the nonlinear entries, where ∇_θ is the difference between the state and a trim point:

$$\begin{aligned} c_{\theta_{eq}} &\triangleq \cos(\theta_{eq}) = \cos(\theta_{eq}) - \sin(\theta_{eq})\cdot\nabla_\theta \\ s_{\theta_{eq}} &\triangleq \sin(\theta_{eq}) = \sin(\theta_{eq}) + \cos(\theta_{eq})\cdot\nabla_\theta \end{aligned} \tag{2.43}$$

The angle of attack and true airspeed are *altitude*-dependence. And, the control vector $u(t) = [\delta_E(t) \;\; \sigma(t) \;\; T_{ni}(t)]^T$, where longitudinal control is regulated through a movable horizontal stabilizer with four elevator segments, and the thrust from the four engines $T_{n,i}(t), i = 1,2,3,4$. And pitch trim is performed by the horizontal stabilizer, under normal

operation the inboard $\delta_{E_I}(t)$ and outboard elevators $\delta_{E_O}(t)$ move together, $\delta_E(t) = \delta_{E_I}(t) = \delta_{E_O}(t)$. For more details about the state transformation quasi-LPV Model of the Boeing 747-100/200 longitudinal motion, refer to (Marcos, 2001).

2.1.6.3. *Mechatronics and Robotics Systems*

Another application of the LPV control system concerns the stabilization of the nonlinear robotic arm system depending on the parameter dynamics and nonlinearities. Two common modeling examples are usually used to develop the gain-scheduling controllers for LPV systems and Parallel Distributed Compensators (PDC) for qLPV T-S fuzzy systems.

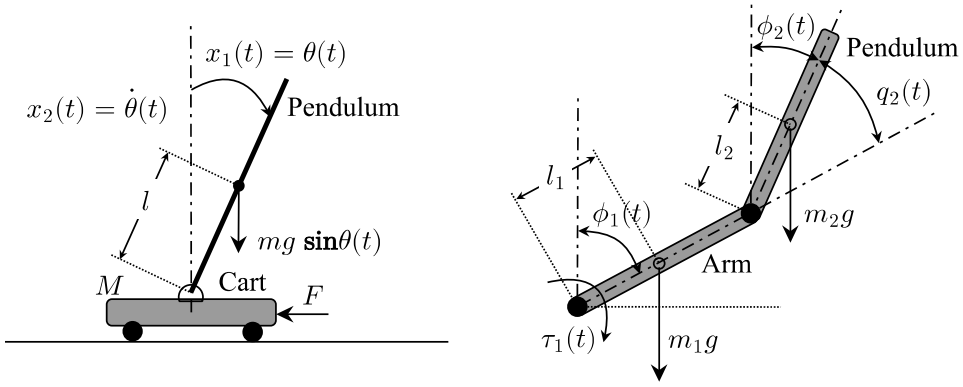

a. The inverted pendulum on cart *b. The two-link arm-driven inverted pendulum*

Figure 2-4. *LPV modelling and control of robotic systems.*

Showing in Figure 2-4.*a* is the force diagram of another example of an inverted pendulum analyzed in (Tanaka & Wang, 2001; Wang, 1996). The nonlinear state-space equations governing the *two*-link dynamic system are given by:

$$\begin{bmatrix}\dot{x}_1(t)\\ \dot{x}_2(t)\end{bmatrix} = \begin{bmatrix}0 & 1\\ 0 & \dfrac{\boldsymbol{a}x_2(t)\sin 2x_1(t)}{2(\frac{4}{3}-\boldsymbol{a}\cos^2 x_1(t))}\end{bmatrix}\begin{bmatrix}x_1(t)\\ x_2(t)\end{bmatrix} + \begin{bmatrix}0\\ \dfrac{\boldsymbol{a}\cos x_1(t)}{ml(\frac{4}{3}-\boldsymbol{a}\cos^2 x_1(t))}\end{bmatrix}u(t) + \frac{g\sin x_1(t)}{l(\frac{4}{3}-\boldsymbol{a}\cos^2 x_1(t))}, \tag{2.44}$$

where $\boldsymbol{a} = m/(m+M)$ can consider as an uncertainty, then followed the definition of (Tanaka & Wang, 2001), we have the following membership functions:

$$\begin{aligned}
&\rho_1(x(t)) = \frac{1}{l(\frac{4}{3}-\boldsymbol{a}\cos^2 x_1(t))},\\
&\rho_2(x(t)) = \sin x_1(t),\\
&\rho_3(x(t)) = x_2(t)\sin 2x_1(t),\\
&\rho_4(x(t)) = \cos x_1(t),
\end{aligned} \tag{2.45}$$

As presented before, the local sector linearization method could transform the nonlinear system (2.44) into the qLPV (T-S fuzzy) system as follows:

$$\dot{x}(t) = \sum_{i=1}^{N_l}\lambda_i(\rho_j(x))(A_i x(t) + B_i u(t)),\ i = 1,2,...,N_l. \tag{2.46}$$

However, this T-S fuzzy system representation requires $N_l = 2^4$ linear combination of

membership functions (2.45). This number increase exponentially in control design analysis (fuzzy PDC controller). The computational burden is a hindrance of the implementation. In addition, the following LPV system (2.47) is based on assumptions about the bounded region of the parameter $\rho(t)$, but qLPV system (2.46) is involved with the constraints bounding on the state $x_1(t)$. This association cause trouble in the design prerequisites such as initial condition $x(0)$ and the upper bound of the derivative $d\lambda_i(\rho_j(x))/dt$.

Illustrated in Figure 2-4.*b* is the diagram of the physical parameters and force diagram of the arm-driven inverted pendulum (ADIP) system (Kajiwara et al., 1999; Canudas-de-Wit et al., 1996). The approximation of this LPV model is presented as follows:

$$\begin{bmatrix} \dot{z}(t) \\ \ddot{z}(t) \\ \dot{r}_x(t) \\ \ddot{\phi}_1(t) \end{bmatrix} = A(\rho) \begin{bmatrix} z(t) \\ \dot{z}(t) \\ r_x(t) \\ \dot{\phi}_1(t) \end{bmatrix} + \begin{bmatrix} 0 \\ 0 \\ 0 \\ \frac{K_a}{T_a} \end{bmatrix} u(t), \tag{2.47}$$

with $r_x(t) \coloneqq 2l_1 \sin\phi_1(t)$, $\rho(t) = r_y(t) \coloneqq 2l_1 \cos\phi_1(t)$, $z(t) \coloneqq r_x(t) + \frac{4}{3} l_2 \phi_2(t)$,

$$A(\rho) = \begin{bmatrix} 0 & 1 & 0 & 0 \\ 0 & 0 & 0 & 0 \\ 0 & 0 & 0 & 0 \\ 0 & 0 & 0 & \frac{-1}{T_a} \end{bmatrix} + \frac{3}{4l_2} \begin{bmatrix} 0 \\ 1 \\ 0 \\ 0 \end{bmatrix} \begin{bmatrix} 1 & 0 & -1 & 0 \end{bmatrix} + \rho(t) \begin{bmatrix} 0 \\ 0 \\ 1 \\ 0 \end{bmatrix} \begin{bmatrix} 0 & 0 & 0 & 1 \end{bmatrix},$$

$u(t)$ is control signal of the electric motor, m_1, m_2, l_1, l_2 are respectively the mass and the half of the length of the arm and the pendulum. The control objective is to maintain the pendulum in a reference vertical position (inverted pendulum motion) using the generated torque from the arm. This moment is regulated by a motor power amplifier voltage, with K_a, T_a are constant mechanic-electric parameters.

To facilitate for developing a gain-scheduling controller, $\rho(t)$ and $z(t)$ are assumed to be measurable in this two-link robot manipulator example. This intrinsic parameter is *state independent*. The further discussions about robot dynamics models can find at (Canudas-de-Wit et al., 1996), for the LPV application on robot-arm control, see, e.g., (Halalchi et al., 2014; Robert et al., 2010; Sename et al., 2008), for the fuzzy application and control (Roose et al., 2017; Tanaka & Wang, 2001; Wang, 1996; Yi & Yubazaki, 2000).

2.1.6.4. *Other applications*

From the above discussion, the LPV modeling and control design provide wide-range applications such as automobile engine systems, photovoltaic systems, electronic circuit systems, Etc. Another application that we would like to mention here is the LPV modeling and control for the tokamak fusion reactor (Ariola & Pironti, 2016; Wesson & Campbell, 2004). A control-oriented distributed model discussed in (Witrant et al., 2007), then an approximation of an LPV system deployed in (Bribiesca Argomedo et al., 2011) from heterogeneous transport partial differential equation (PDE) model of dynamics of the poloidal flux. Thereby, developing a polytopic feedback control law for the non-inductive lower hybrid current drive (LHCD) is proposed (Bribiesca Argomedo et al., 2011), that regulates the current and heat source on the plasma. This method shows an efficient reduction in computational cost, and easier to integrate the saturated constraint than to seek

for the weight matrices for the linear–quadratic regulator (LQR) method by solving the algebraic Riccati equation (ARE) (Bribiesca Argomedo et al., 2014, 2010). Readers interested in this topic can refer to the monographs (Ariola & Pironti, 2016; Bribiesca Argomedo et al., 2014). More discussion and analysis on nonlinear dynamics motion, and methods of identification and linearizing LPV models refers to (Tóth, 2010).

2.2. Stability of LPV/quasi-LPV Systems

Before going into the stability analysis of the parameter-dependent system, let's revise the fundamental control system theory by analyzing the stability of the equilibrium point at the origin of a pendulum system

$$\begin{aligned} \dot{x}_1(t) &= x_2(t), \\ \dot{x}_2(t) &= -a\sin(x_1(t)) - bx_2(t). \end{aligned} \tag{2.48}$$

with $a, b \in \mathbb{R}_{++}$. The system stability in the sense of Lyapunov function is to find a continuously differentiable energy function $V(x(t))$ that decreases over time, and the solutions of the system starting in the vicinity of the equilibrium point will be nearby or converge to the equilibrium point as the time approaches infinity. For more details on stability of dynamical systems, the reader could refer to (Khalil, 1996; Scherer & Weiland, 2005; Vidyasagar, 1992).

Theorem 2.2.1: *Lyapunov Theorem* (Khalil, 1996), *consider the following nonlinear dynamical system*

$$\dot{x}(t) = f(x(t)), \tag{2.49}$$

with an equilibrium point $x_e = 0$. *There exist a locally Lipchitz function* $V(x(t))$ *that is assumed to have continuous derivative across the defined domain of* $x(t) \in \mathcal{D}_x$ *such that* $\alpha(\|x(t)\|) \leq V(x(t)) \leq \beta(\|x(t)\|)$, *with* α, β *are* $\mathcal{K}$ *function* [1], *then system* (2.49) *is*

1 - *Stable if*

$$\frac{dV(x(t))}{dt} \leq 0, \ \forall x(t) \in D \setminus \{0\}$$

2 - *Asymptotically stable if exits a* $\mathcal{K}$ *function* γ *such that*

$$\frac{dV(x(t))}{dt} \leq -\gamma(\|x(t)\|), \ \forall x(t) \in D \setminus \{0\}$$

A Lyapunov function candidate of system (2.48) is given by (Khalil, 1996) as follows:

$$V_1(x(t)) = a(1-\cos(x_1(t))) + \tfrac{1}{2}x_2(t)^2 \geq \tfrac{1}{2}x_2(t)^2. \tag{2.50}$$

The derivative of $V_1(x(t))$ along the trajectories of the nonlinear system

$$\dot{V}_1(x(t)) = a\dot{x}_1(t)\sin(x_1(t)) + x_2(t)\dot{x}_2(t) = -bx_2(t)^2 \leq 0. \tag{2.51}$$

Since $\dot{V}_1(x(t)) = 0$ along the $x_1 -$ axis, we can only confirm that the system is stable at origin using the Lyapunov function (2.50). However, the phase portrait of the dynamic

[1] (Khalil, 1996), chapter 4

system exhibits asymptotically convergence to this equilibrium. So let include a quadratic term to the previous Lyapunov function:

$$V_2(x(t)) = \tfrac{1}{2}[x_1(t) \;\; x_2(t)]\underbrace{\begin{bmatrix} p_{11} & p_{12} \\ p_{12} & p_{22} \end{bmatrix}}_{P\in\mathbb{R}^2_{++}}\begin{bmatrix} x_1(t) \\ x_2(t) \end{bmatrix} + a(1-\cos(x_1(t))) \geq \lambda_{\min}(P)\left\|x(t)\right\|^2.$$

The derivative $\dot{V}_2(x(t))$ is expressed by

$$\begin{aligned}\dot{V}_2(x(t)) &= [x_1(t) \;\; x_2(t)]\begin{bmatrix} p_{11} & p_{12} \\ p_{12} & p_{22} \end{bmatrix}\begin{bmatrix} x_2(t) \\ -a\sin(x_1(t)) - bx_2(t) \end{bmatrix} + a\dot{x}_1(t)\sin(x_1(t)) \\ &= a(1-p_{22})x_2(t)\sin(x_1(t)) - ap_{12}x_1(t)\sin(x_1(t)) + (p_{11} - p_{12}b)x_1(t)x_2(t) \\ &\quad + (p_{12} - p_{22}b)x_2(t)^2. \end{aligned} \tag{2.52}$$

With the choice of $0 < p_{12} < b,\ p_{11} = p_{12}b,\ p_{22} = 1$, then

$$\dot{V}_2(x(t)) = -ap_{12}x_1(t)\sin(x_1(t)) + (p_{12} - p_{22}b)x_2(t)^2$$

is negative definite over the domain $\mathcal{D}_x = \{x(t)\in\mathbb{R}^2,\ k\pi < |x_1(t)| < (k+1)\pi,\ k\in\mathbb{N}\}$. As discussed in the literature (Khalil, 1996), the failure of Lyapunov function does not imply that the equilibrium of the system is stable nor asymptotically stable. It can only emphasize that the stability of the system cannot be guaranteed with these inappropriate Lyapunov candidates. Let's move forward to discuss the necessary and sufficient Lyapunov conditions addressed for the stability of a linear system.

Theorem 2.2.2: *Let us consider the time-continuous LTI system*

$$\begin{aligned} \dot{x}(t) &= Ax(t) \\ x(0) &= x_0 \end{aligned} \tag{2.53}$$

is obtained as the linearization around an equilibrium point. The following statements are equivalent

1 - *The system* (2.53) *is globally asymptotically stable*.
2 - *The system* (2.53) *is globally exponentially stable*.
3 - *The matrix A is Hurwitz* (*i.e.*, *the eigenvalues of matrix A have negative real part*).
4 - *There exist matrices* $P,Q\in\mathbb{S}^n_{++}$ *such that the Lyapunov equation*

$$A^TP + PA + Q = 0,$$

is satisfied.
5 - *There exist matrices* $P,Q\in\mathbb{S}^n_{++}$ *such that the Lyapunov inequality holds.*

$$A^TP + PA \prec 0,$$

By linearizing the system (2.48) around the origin $x_{eq1} = [0 \;\; 0]^T$, the Jacobian matrix:

$$A_1 = \left.\frac{\partial f(x(t))}{\partial x(t)}\right|_{x_{eq1}=0} = \begin{bmatrix} 0 & 1 \\ -a & -b \end{bmatrix}, \text{is a Hurwitz matrix}$$

with the eigenvalues $\lambda(A_1) = -\frac{1}{2}b \pm \frac{1}{2}\sqrt{b^2 - 4a}$ have negative real part. It can conclude that this equilibrium is asymptotically stable for $a,b > 0$. But, the eigenvalues will slide

on the imaginary axis for $b=0$. In this case, it is not possible to determine the stability feature at the origin by this linearization system. Similarly, linearizing the system (2.48) at the equilibrium $x_{eq2}=[\pi \ \ 0]^T$, we obtain

$$\text{matrix } A_2=\left.\frac{\partial f(x(t))}{\partial x(t)}\right|_{x_{eq2}=[\pi \ \ 0]^T}=\begin{bmatrix}0 & 1\\ a & -b\end{bmatrix},$$

has one of the eigenvalues $\lambda(A_2)=-\frac{1}{2}b\pm\frac{1}{2}\sqrt{b^2+4a}$ in the open right-half plane for all $a,b>0$. Thus, this equilibrium is unstable. It can be checked that there will be no matrix $P\succ 0$ satisfies $A_2^TP+PA_2\prec 0,\ \forall a,b>0$.

Quadratic Stability and Non-Quadratic Stability Analysis

The stability analysis for the LTI system using the Lyapunov function can be easily performed. But the linearizing characteristic of the nonlinear system in the form of an LTI system does not accurately describe the behaviors of the original system.

In this case, by approximating the nonlinear system as a parametric affine is much more convenient for the analysis and synthesis of system design. In the early 90s, the term *parametric uncertainties* or *parameter-dependent* is related to two commonly analytical methods, robust stability for LTV system (Dullerud & Paganini, 2000; Khargonekar et al., 1990; Zhou et al., 1996; Zhou & Doyle, 1998; Zhou & Khargonekar, 1988) and quadratic stability (Apkarian & Gahinet, 1995; Becker & Packard, 1994). To ensure stability and performance against uncertainty parameters, Apkarian has presented two different approaches in the middle 90s. On one side, according to the linear fraction dependence and linear fractional transformation (LFT) technique (Apkarian & Gahinet, 1995), the parametric-dependency extraction from the nominal plant using an uncertainty structure (Doyle, 1985; Doyle et al., 1991). Followed the scaling commuting structure, LFT approach shows the efficiency in dealing with uncertainties and provides more relaxation than old-fashioned conditions. Besides, the bounded real lemma (Feron et al., 1996; Gahinet & Apkarian, 1994; Scherer, 1990) also plays a central role in robust $\mathscr{H}_\infty$ performance synthesis during this time.

However, these stability conditions capture only fast variation parameters that become very conservative with slowly varying parameters. So, the affine quadratic Lyapunov formulation (Apkarian, Feron, et al., 1995; Gahinet et al., 1994) is proposed to address the stability of the LPV system. Where the scaled-bounded real lemma can enhance the robustness and performance requirements. The parameter-dependent Lyapunov functions (PDLF) consider for stability analysis and gain-scheduling controller synthesis of LPV systems that better describe the behavior of parameters, see for example, in the literature (Apkarian & Adams, 1998; Apkarian & Tuan, 2000b; Gahinet et al., 1996; Gahinet & Laub, 1994; Lim & How, 1997; Tuan & Apkarian, 1999; Wu et al., 1996), for the qLPV T-S fuzzy systems (Tanaka et al., 2003, 2009; Tuan et al., 2004; Tuan, Apkarian, et al., 2001), for the LPV time-delay systems (Briat, 2008, 2015b) and the references therein.

The leverage of the development of convex optimization programing and the relaxation PLMI methods, it makes the use of PDLF widespread in the stability and stabilization analysis for the parameter-dependent systems. The following sections are devoted to the

stability analysis for the LPV/quasi-LPV systems using Lyapunov function via parameterized LMI conditions.

2.2.1. *Stability of Polytopic Systems*

This issue was *excavated* decades ago because of its effectiveness in analyzing for robust stability and robust performance (Feron et al., 1996; Gahinet et al., 1994, 1996). The quadratic (Boyd et al., 1994; Scherer & Weiland, 2005) and non-quadratic stability (Apkarian & Adams, 1998; Apkarian & Tuan, 2000b; Tuan, Apkarian, et al., 2001; Tuan & Apkarian, 1999) are discussed for the polytopic systems. Generally, the open loop polytopic LPV system is obtained under the form:

$$\begin{aligned} &\dot{x}(t) = \sum\nolimits_{i=1}^{N_l} \lambda_i(\rho(t)) A_i x(t), \\ &x(0) = x_0, \end{aligned} \tag{2.54}$$

Theorem 2.2.3: *Consider system* (2.54), *if there exists a symmetric positive matrix* $P \in \mathbb{S}_{++}^n$ *such that*

$$A_i^T P + P A_i \prec 0, \tag{2.55}$$

hold for $\forall i = 1, 2, \ldots, N_l$, *then, LPV polytopic system* (2.54) *is quadratic stable.*

Proof.

The proof is directly inferred from the application of Theorem 2.2.2 to finding a matrix P such that the following condition is satisfied.

$$\sum\nolimits_{i=1}^{N_l} \lambda_i(\rho(t)) A_i^T P + P \sum\nolimits_{i=1}^{N_l} \lambda_i(\rho(t)) A_i \prec 0, \tag{2.56}$$

By applying the property of linear combination $\forall \lambda_i(\rho(t)) \in [0,\ 1]$, then the latter condition holds if all of LMIs (2.55) are satisfied.

□

However, considering only a *common* matrix to guarantee the quadratic stability for the multi-convex system is conservative. In some cases, it doesn't exist a candidate matrix $P \in \mathbb{S}_{++}^n$ that satisfies stability conditions (2.55). Hence, it makes more sense to consider the parameter-dependent Lyapunov function PDLF or the piece-wise Lyapunov function approach introduces in (Johansson, 1999) to relax the conservativeness.

Theorem 2.2.4: (Briat, 2015a) *Polytopic system* (2.54) *is robust stability*, *if there exist symmetric positive matrices* $P_i \in \mathbb{S}_{++}^n$, $P(\lambda(\rho)) = \sum_{i=1}^{N_l} \lambda_i(\rho) P_i$, *such that*

$$A(\lambda(\rho))^T P(\lambda(\rho)) + P(\lambda(\rho)) A(\lambda(\rho)) + \sum\nolimits_{i=1}^{N_l} \sum\nolimits_{j=1} \frac{\partial \lambda_i}{\partial \rho_j} \dot{\rho}_j(t) P_i \ \prec\ 0, \tag{2.57}$$

hold for $\forall i = 1, 2, \ldots, N_l$, *with* $A(\lambda(\rho)) = \sum_{i=1}^{N_l} \lambda_i(\rho(t)) A_i$ *is a convex combination.*

When the relationship between the parameters and its derivations is undetermined, these conditions will be more difficult to deal with. By assuming the derivatives of parameters $\left| \sum_{j=1} (\partial \lambda_i / \partial \rho_j)\, \dot{\rho}_j(t) \right| < \nu_i$, then parametric matrix inequality (2.57) are multi-affine in $\lambda_i(\rho(t)) \in [0,\ 1]$, $\forall i = 1, 2, \ldots, N_l$. Actually, there is no method to adequately describe the

upper bound the rate variation of the parameter. An exciting transformation method introduced in (Briat, 2008) uses the differential-algebraic equation to transfer the coordinate of the vertices enclosed in the unknown derivate parameters.

2.2.2. *Stability of Polynomial Parameter-Dependent Systems*

One of the most effective ways to approximate the nonlinear systems is to represent as polynomials of the Taylor expansion. The polynomial form of state and time-varying parameters is a regular representation in a company with trigonometric forms, for example, diodes system (Khalil, 1996), jet engines (Azuma et al., 2000; Fakhri, 2005; Watanabe, 1993), and the academic applications (Sala, 2010, 2019; Sala & Ariño, 2009; Sato & Peaucelle, 2007a; Scherer, 2006; Tanaka et al., 2009; Wu & Prajna, 2004), etc. Let's introduce a parameter-dependent system expressed as a polynomial formulation:

$$\begin{aligned} &\dot{x}(t) = A(\rho(t))x(t) = (A_0 + \textstyle\sum_{i=1}^{N_p}\sum_{j=1}^{N} A_{ij}\rho_i^j(t))x(t), \\ &x(0) = x_0, \end{aligned} \tag{2.58}$$

and a parameter-dependent Lyapunov function:

$$V(x(t),\rho(t)) = x^T(t)P(\rho(t))x(t) = x^T(t)(P_0 + \textstyle\sum_{i=1}^{N_p}\sum_{j=1}^{N} P_{ij}\rho_i^j(t))x(t). \tag{2.59}$$

with parameters $\rho(t) \in \mathcal{U}_p$ has the highest number of polynomial degrees is N.

Theorem 2.2.5: *Polynomial system* (2.58) *is robust stability, if there exist symmetric matrices* $P_0, P_{ij} \in \mathbb{S}^n$ *such that the following PLMI holds.*

$$\begin{aligned} &A_0^T P_0 + P_0 A_0 + \sum_{i=1}^{N_p}\sum_{j=1}^{N}(A_0^T P_{ij} + P_{ij}A_0 + A_{ij}^T P_0 + P_0 A_{ij})\rho_i^j(t) \\ &\quad + \sum_{i,k=1}^{N_p}\sum_{j,l=1}^{N}(A_{ij}^T P_{kl} + P_{kl}A_{ij})\rho_i^j(t)\rho_k^l(t) + \sum_{i=1}^{N_p}\sum_{j=1}^{N} P_{ij}\rho_i^{j-1}(t)\dot{\rho}_i^j(t) \prec 0. \end{aligned} \tag{2.60}$$

Proof.

The derivative of PDLF (2.59) along the trajectories of LPV system (2.58) is given by:

$$\begin{aligned} \frac{dV}{dt} &= A(\rho(t))^T P(\rho(t)) + P(\rho(t))A(\rho(t)) + \dot{P}(\rho(t)) \\ &= \Big(A_0 + \sum_{i=1}^{N_p}\sum_{j=1}^{N} A_{ij}\rho_i^j(t)\Big)^T \Big(P_0 + \sum_{i=1}^{N_p}\sum_{j=1}^{N} P_{ij}\rho_i^j(t)\Big) + \sum_{i=1}^{N_p}\sum_{j=1}^{N} P_{ij}\rho_i^{j-1}(t)\dot{\rho}_i^j(t) \\ &\quad + \Big(P_0 + \sum_{i=1}^{N_p}\sum_{j=1}^{N} P_{ij}\rho_i^j(t)\Big)\Big(A_0 + \sum_{i=1}^{N_p}\sum_{j=1}^{N} A_{ij}\rho_i^j(t)\Big) \\ &= A_0^T P_0 + P_0 A_0 + \sum_{i=1}^{N_p}\sum_{j=1}^{N}(A_0^T P_{ij} + P_{ij}A_0 + A_{ij}^T P_0 + P_0 A_{ij})\rho_i^j(t) \\ &\quad + \sum_{i,k=1}^{N_p}\sum_{j,l=1}^{N}(A_{ij}^T P_{kl} + P_{kl}A_{ij})\rho_i^j(t)\rho_k^l(t) + \sum_{i=1}^{N_p}\sum_{j=1}^{N} P_{ij}\rho_i^{j-1}(t)\dot{\rho}_i^j(t) \prec 0. \end{aligned} \tag{2.61}$$

The stability condition is presented as a matrix polynomial inequality that can be casted in terms of convex problems LMIs by the gridding method (meshing affine) or Sum of Square decomposition technique.

2.2.3. *Stability of T-S Fuzzy Systems*

The stability analysis for this class of nonlinear systems based on the Lyapunov theory expanded via LMI conditions. The overview of the PDC controller strategy analyzes systematically for this class of systems are introduced in (Tanaka & Wang, 2001). The design analysis of the fuzzy control system at this stage is essentially a matter of finding a quadratic Lyapunov function for all stability conditions, see, e.g., (Tanaka et al., 1998; Tanaka & Wang, 2001) and the references therein. The relaxing stabilization conditions methods (Tanaka & Wang, 2001; Tuan, Ono, et al., 2001) or the non-quadratic Lyapunov function NQLF approach (Rheex & Won, 2006; Sala, 2010; Sala & Ariño, 2009; Tanaka et al., 2003) are considered to reduce the conservatism of the design conditions. However, the proposed conditions do not exactly describe the behavior of membership function rate but instead are subdivision into local stability by the linear combinatorial method applied to non-quadratic Lyapunov functions.

Let's consider an open-loop T-S fuzzy system:

$$\begin{aligned} &\dot{x}(t) = \sum\nolimits_{i=1}^{N_l} \lambda_i(\rho(t)) A_i x(t), \qquad \dim A_i = n, i = 1,2,...,N_l, \\ &x(0) = x_0. \end{aligned} \tag{2.62}$$

Both quadratic and non-quadratic stability is delivered and well-developed and studied in the framework of the T-S fuzzy system. It can state that the quadratic stability condition of T-S fuzzy system is essentially the same formulation as condition (2.55). It frequently encounters in the analyzing stability of the nonlinear systems approaching via linear combination. These conditions are solved at each vertex of a convex polyhedron encapsulates the behavior of the parameters. As mentioned, there does not always exist a global solution $P \in \mathbb{S}_{++}^n$ that can satisfy all LMI conditions (2.55). So, the relaxation of LMI condition has been considered to reduce conservativeness, see, for example (Tanaka et al., 1998; Tuan, Apkarian, et al., 2001). In this period, the piecewise Lyapunov functions effectively reducing the conservativeness of stability and stabilization problems have received attention, see e.g., (Johansson, 1999; Xie et al., 1997). Based on this approach, the Fuzzy Lyapunov Function (FLF) is delivered for the non-quadratic stability analysis, provides the less conservative condition.

Most of the challenges are related to the derivative development of the membership functions (constrains this value also leads to limitation of the system dynamics). Perhaps, for this reason, much effort of the early work of the stabilizing implementations for T-S fuzzy systems focused on quadratic stability. The fuzzy Lyapunov function is implemented later in (Mozelli et al., 2009; Sala & Ariño, 2009; Tanaka et al., 2003, 2009), Etc.

2.2.3.1. *Non-quadratic Stability* (*Bounded Parameters*)

The PDLF is expanded as a fuzzy Lyapunov function under form:

$$V(x,t) = x^T P(\lambda(\rho)) x = \sum\nolimits_{i=1}^{N_l} \lambda_i(\rho(t)) x(t)^T P_i x(t) \succ 0. \tag{2.63}$$

Where membership function $\lambda_i(\rho(t)) \in [0,\ 1]$, $\sum_{i=1}^{N_l} \lambda_i(\rho(t)) = 1$, and the piecewise decision matrices $P_i \in \mathbb{S}_{++}^n$ are considered to relax the PLMI stability condition.

Theorem 2.2.6: (Tanaka et al., 2003) *The equilibrium of the continuous T-S fuzzy system* (2.62) *is asymptotically stable if there exist matrices* $P_i \in \mathbb{S}^n_{++}$ *such that*:

$$\frac{1}{2}(A_i^T P_j + P_j A_i + A_j^T P_i + P_i A_j) + \sum_{k=1}^{N_l-1}\sum_{l=1}\left|\frac{\partial \lambda_k}{\partial \rho_l}\dot{\rho}_l\right|(P_k - P_{N_l}) \prec 0, \tag{2.64}$$

hold for $\forall i \geq j$, *with* $i, j = 1,2,\ldots,N_l$, *and* $P_k \succeq P_{N_l}$ *with* $k = 1,2,\ldots,N_l - 1$.

This condition is also derived from a relaxing form of the parameter-dependent stability condition (2.61). The FLF has gained considerable attention in the field of wide application. Most of the work focuses on the relaxation of the stability conditions relates to the derivative of the parameter dependency matrix $P(\lambda(\rho))$. In which the local boundaries are set for the nonlinearities $(\partial\lambda_k/\partial\rho_l)\dot{\rho}_l$. Inheriting the properties of the membership function, if transformation $\rho_l(t) \rightarrow \lambda_k(t)$ are composed of logical laws, it does not exist a continuous derivative over time! On the contrary, if it expresses the nonlinearity dynamics (depends on the states), then the bounded partial derivative of MF could be addressed like (Guerra & Bernal, 2009; Mozelli et al., 2009; Sala, 2010, 2019; Sala & Ariño, 2009).

2.2.3.2. *Non-quadratic Stability* (*Sum of Squares*)

A generalization of fuzzy modeling and control presented in (Lam, 2016; Tanaka et al., 2009) shows the refinement of nonlinearities as the fuzzy polynomial model. In which the stability and stabilizability conditions can convert to the SoS problem based on polynomial Lyapunov function (Guerra & Bernal, 2009; Jaadari, 2013; Sala & Ariño, 2009) develop the local sector for the polynomial-fuzzy system. The polynomial condition can be checked as an SoS or consider as the parametric polynomial matric inequality.

The defuzzification process discussed in section 2.1.4.2 can applied as follows:

$$\begin{aligned} &\dot{x}(t) = \sum\nolimits_{i=1}^{N_l} \lambda_i(\rho(t)) A_i(x) Z(x), \qquad \dim A_i = n, i = 1,2,\ldots,N_l, \\ &x(0) = x_0. \end{aligned} \tag{2.65}$$

where $A_i(x)$ are polynomial matrices in $x(t)$, and $Z(x) \in \mathbb{R}^N$ is a column vector whose entries are all of monomials in $x(t)$. For example, a second order monomial vector of a state vector: $x(t) = [x_1,\ x_2]^T$ are given by $Z(x) \triangleq [x_1, x_2, x_1x_2, x_1^2, x_2^2]^T$, with $n = 2, N = 5$.

Let's consider a Lyapunov function candidate $V(x) = Z(x)^T P(x) Z(x)$ for the polynomial system. The preliminary concepts and the prerequisites will be covered in section 2.2.4.2. According to the SoS argument, the stability analysis for quasi-LPV system (2.65) is usually characterized by the following results.

Theorem 2.2.7: (Tanaka et al., 2009) *Polynomial fuzzy system* (2.65) *is stable, if there exists a polynomial matrix* $P(x) \in \mathbb{S}^N_{++}$, *the coefficients polynomials in* x, $\epsilon_1(x)$, $\epsilon_2(x) > 0$, *such that the following expressions:*

$$Z(x)^T (P(x) - \epsilon_1(x) I) Z(x), \tag{2.66}$$

$$\begin{aligned} -Z(x)^T \{ &P(x)M(x)A_i(x) + A_i(x)^T M(x)^T P(x) + \cdots \\ &\sum\nolimits_{j=1}^{n} \frac{\partial P(x)}{\partial x_j} A_i(x)_{(j)} + \epsilon_2(x) I \} Z(x), \end{aligned} \tag{2.67}$$

are sum of square. Where $i = 1, 2, \ldots, N_l$, $A_i(x)_{(j)}$ *denotes the* j^{th} *row of matrix* $A_i(x)$ *and*

$$M(x) = \partial Z(x)/\partial x \triangleq \left[\frac{\partial Z(x)}{\partial x_1} \quad \frac{\partial Z(x)}{\partial x_2} \quad \cdots \quad \frac{\partial Z(x)}{\partial x_n}\right].$$

If the condition (2.67) is satisfied with $\epsilon_2(x) > 0$, for $x \neq 0$, then the equilibrium is asymptotical stable. If $P(x)$ is a constant matrix, the stability condition holds globally. Hence, the polynomial SoS relaxation method provides a more general condition. But the coefficients associated with irreducible polynomials in the solutions ensues in the polynomial dependencies with utopian exponents.

2.2.4. *Relaxation of the Parameterized Linear Matrix Inequality*

The parameter-dependent characterization of the stability conditions is an infinite set of LMIs across the parameter space domain. For delivering the convexity argument, the commonly used relaxations of PLMIs condition include:

- Gridding technique (Wu, 1995) is fragmented *N*-finite parameter operation range, and affine meshing parameter space (Apkarian & Tuan, 2000b; Lim, 1998).
- Convex combination or multi-convexities (Gahinet et al., 1996; Tuan & Apkarian, 2002) – Fuzzy Lyapunov Function (Guerra & Bernal, 2009; Sala, 2010; Tanaka et al., 2003).
- Generalization of Filner's Lemma: (1)-Sum of squares (SoS) decomposition for polynomial systems (Papachristodoulou & Prajna, 2002; Parrilo, 2003) - for fuzzy systems (Lam, 2016; Sala & Ariño, 2009; Tanaka et al., 2009). (2)-Slack variable or $\mathcal{S}$-variable (Sato & Peaucelle, 2006, 2007b).

The gridding technique is simple and can be deployed directly on the parameter dependence condition. Following the argument of (Apkarian & Tuan, 2000a, 1998; Wu, 1995): with finite intervals, it is impossible to verify whether it captures all of the critical points or describes the nonlinear behavior of the parameters $\rho(t)$ within their defined boundaries $[\underline{\rho},\ \overline{\rho}]$. In the work of (Apkarian & Tuan, 1998; Lim, 1998), the author has introduced an approach solving the parameterized LMIs (PLMIs), which only need to grid a surface of lower dimension whenever the function is quasi-convex or convex along some direction. But it costs in high computation load.

During this time, the relaxation based on the sum of squares decomposition has also gained considerable attention that separates of the polynomial parameters and can be cast as a semidefinite programming problem, see, e.g., the convex optimization SoS toolbox (Papachristodoulou et al., 2013; Prajna et al., 2004). This approach promises less conservative results for the relaxation of the PLMI conditions. It is also widely employed for the analysis of stabilizing analysis of the qLPV & T-S fuzzy systems in the literature such as (Gahlawat et al., 2011; Sala, 2010; Sala & Ariño, 2009; Tanaka et al., 2009). But the fractional form involving the polynomial gains is an obstacle of the implementation. For example: a feedback gain $K(\rho(t)) = Y(\rho(t))X(\rho(t))^{-1}$, where a polynomial decision matrix $X(\rho(t)) = X_0 + \rho(t)X_1 + \rho(t)^2 X_2$. Then, how to perform the inverse of $X(\rho(t))$?

An alternative method is to convert the polynomial parameter-dependent condition into a

Slack-Variable formulation (Ebihara et al., 2015; Hosoe & Peaucelle, 2017; Sato & Peaucelle, 2007a, 2007b). This method, also based on Finsler's generalization, shows a computational advantage over SoS decomposition. Furthermore, the $\mathcal{S}$-variable allows to manipulate $X(\rho(t)) = \mathcal{X}\Theta(\rho(t)), \mathcal{X}$ is $\rho(t) - independent$ variable matrix, and $\Theta(\rho(t))$ is a column of parameters. A numerical computation comparison of the two methods is given in (Sato & Peaucelle, 2007a, 2007b), and a numerical comparison of the optimization of polynomial methods provides in Section 3.2.2. More details on the $\mathcal{S}$-variable application to the robustness and stability analysis of the system based on LMI conditional developments refers to (Ebihara et al., 2006, 2015; Hosoe & Peaucelle, 2017; Dimitri Peaucelle & Ebihara, 2014).

The proposed methods have distinctive advantages and disadvantages, which may be the trade-off between conditional conservatism and computational complexity. For example, the gridding method simplifies the parameter-dependent conditions into a set of LMI conditions, but the weakness of this linearization is whether it covers all the critical points or how to accurately describe specific characteristics of parameters on operating conditions. On the other hand, the SoS method is characterized by the polynomial Lyapunov functional formulation. Giving more tight relaxation on variation of the $\mathcal{S}$-procedure constraints are exchanged with complexity in parametric decomposition. Finally, the multi-convexities Lyapunov function is a linear combination between vertices, covering the trajectories of the parameter within the convex domain for analyzing controller design.

The synthesis of relaxing PLMI methods discusses in the literature (Apkarian & Tuan, 2000b; El Ghaoui & Niculescu, 2000; Tuan & Apkarian, 1999). The promising fruition of the LPV control system in this time inherited the growth of linear programming or convex optimization tools (Erling D Andersen & Andersen, 2000; Boyd et al., 1994; Boyd & Vandenberghe, 2004; Gahinet & Laub, 1994; Lofberg, 2004; Papachristodoulou et al., 2013). Which converts the linear matrix inequality (LMI) constraint derived from the stability analysis into barrier function conditions. Readers interested in the interior-point methods or the other contemporary methods, for example, conjugate gradient, golden section, the wider scope of polynomial-time complexity, can refer to the monographs (Bertsimas, 1999; Bertsimas & Tsitsiklis, 1997; Konno et al., 1997). Bertsimas describes in more detail algorithm problems (i.e., gradient descent, update step size, etc.). For optimization problems and global optimization can be found in (Tuy, 2016). The work of literature (Hiriart-Urruty & Lemaréchal, 1993a, 1993b) provides multiple sections appropriately devoted to readers.

2.2.4.1. *Relaxation of Parametrized LMIs by Discretization*

It is possible to refer the finite discretizing methods over time-varying intervals (Apkarian & Tuan, 1998; Lim, 1998) and time-independent intervals (Wu, 1995). The LMI relaxation proposed by (Wu, 1995), well-known as a "***gridding***" method, illustrates in the following example.

Example 2.2.1. Let consider polynomial system (2.28):

$$\begin{bmatrix}\dot{x}_1(t)\\ \dot{x}_2(t)\end{bmatrix} = \begin{bmatrix}-1 & \rho_1(x(t))\\ \rho_2(x(t)) & -1\end{bmatrix}\begin{bmatrix}x_1(t)\\ x_2(t)\end{bmatrix} = (A_0 + A_1\rho_1(x(t)) + A_2\rho_2(x(t)))\begin{bmatrix}x_1(t)\\ x_2(t)\end{bmatrix}. \tag{2.68}$$

with $A_0 = \begin{bmatrix} -1 & 0 \\ 0 & -1 \end{bmatrix}, A_1 = \begin{bmatrix} 0 & 1 \\ 0 & 0 \end{bmatrix}$, and $A_2 = \begin{bmatrix} 0 & 0 \\ 1 & 0 \end{bmatrix}$.

Since the LPV system is affine in $\rho_1(x), \rho_2(x)$, then choosing a polynomial matrix Lyapunov as follows:

$$P(\rho(x)) = P_0 + P_1\rho_1(x) + P_2\rho_2(x) \succ 0. \tag{2.69}$$

Following condition (2.61), the LPV system (2.68) is robustly stable if and only if the matrix inequality

$$sym\{(P_0 + P_1\rho_1(x) + P_2\rho_2(x))(A_0 + A_1\rho_1(x) + A_2\rho_2(x))\} \pm \nu_1 P_1 \pm \nu_2 P_2 \prec 0, \tag{2.70}$$

hold, for $P_0, P_1, P_2 \in \mathbb{S}^2$ and $\rho_1(x), \rho_2(x)$ within the specified range:

$$\{\rho_1(x), \rho_2(x)\} \in [-1,1]\times[0,4] \subset \mathbb{R}^2,\ \dot{\rho}(x) \in \mathcal{U}_\nu = \{|\dot{\rho}_i| < \nu_i,\ i = 1,2\} \subset \mathbb{R}^2. \tag{2.71}$$

Indeed, the LMI conditions are derived from (2.70) by equally discretized N_i points in the intervals of parameters (2.27). If the conditions hold throughout the parameter domain, then the stability of LPV system (2.68) is ensured robustly in the presence of the time-varying parameters.

This approach bases on the discretizing parameter space. So, what is a "good" density to be able to cover most of critical points? The *critical points* are a set of $\rho_i(x) \in \mathcal{U}_\rho$, for which the LMI is unfeasible in $\mathcal{D}_x$. For example, system (2.68) is unstable in the interval of parameter $\rho_1(x)\rho_2(x) \le 1$. In addition, what are the appropriate parameter density, and its determination remains a difficult question. It is difficult to assert an ideal density of a parameter domain because their unfeasible regions are ambiguous information. The unfeasible set is estimated only when the infeasibility of the problem finds. That can visualize by adjusting the sound of an instrument that has to hit a chord to adjust the correct range. We cannot fine-tune before playing an instrument, and we cannot copy the tuning of one musical accessory to another. Like the lament of Briat: "*This paradox shows that probably no method to find a perfect gridding would develop someday*."

On the other hand, the piecewise affine parameter-dependent (PAPD) approaches introduced as multi-switch partitioned parameter space, see, e.g., (Apkarian & Tuan, 1998; Lim, 1998), could provide less conservative stability conditions. The parametric switch subsystem is recalled in Appendix 1.4.2. But the number of LMI condition that must check is overwhelming. For example, given a LPV system depend on *p* parameters, each parameter is partitioned into N_i subspace, so the number of conditions that need to be checked is about $2^p \prod_{i=1}^{p} N_i$.

2.2.4.2. *Relaxation of Parametrized LMIs by Sum-of-Squares Decomposition*

Generally, the stability conditions based on the parameter-dependent Lyapunov function has difficulty expressing the derivative expansion of the parameter. But the polynomials allow for easier development and expand the partial derivation of state with the endogenous parameter polynomial formulation. Let's recall some mathematical premises mainly introduced by (Parrilo, 2000, 2003; Prajna et al., 2004).

Lemma 2.2.1. (Parrilo, 2003) *Let $f(x)$ be a polynomial in $x \in \mathbb{R}^n$ of degree 2d. And let $Z(x)$ be a column vector whose entries are all monomials in x with degree no greater than d. Then $f(x)$ is a sum of squares if and only if there exists a positive semidefinite matrix Q such that*

$$f(x) = Z^T(x)QZ(x). \tag{2.72}$$

The canonical decomposition of a polynomial is expanded to SoS that can be converted to a semidefinite programming problem. The analysis of polynomials are introduced by (Papachristodoulou et al., 2013; Papachristodoulou & Prajna, 2002; Prajna et al., 2004) could handle the stabilization PLMI condition as SoS expressions.

Lemma 2.2.2. (Prajna et al., 2004) *Let $F(x)$ be an $N \times N$ polynomial matrix degree 2d in $x \in \mathbb{R}^n$. Moreover, let $Z(x)$ be a column vector whose entries are all monomials in x with degree no greater than d, then the following statements*

(1) $F(x) \succeq 0$ *for all* $x \in \mathbb{R}^n$.
(2) $v^T F(x) v$ *is a sum of squares, where* $v \in \mathbb{R}^n$.
(3) *There exists a matrix* $Q \in \mathbb{S}_+$ *such that* $v^T F(x) v = \left\| Q^{\frac{1}{2}} (v \otimes Z(x)) \right\|_2$.

in accordance with the relationships (1) $\Leftarrow$ (2) $\Leftrightarrow$ (3).

The polynomial LMI stability are the infinite-dimensional parameter-dependent conditions. Following the SOS-based polynomial method (Parrilo, 2000, 2003), the monomial in x (*variables*) are apart from its coefficients (*decision variables*) in the polynomial conditions. Then, some slack variables are injected during the $\mathcal{S}$-procedure, which converts the infinite parametric conditions into a finite LMIs (that able to be solved by the interior-point method with solvers such as Mosek, Sedumi, SDPT3, SDPA, etc.). The variation of the $\mathcal{S}$-procedure constraints provides significantly relaxed condition than the existing approaches (discretization in section 2.2.4.1, or convex combination in section 2.2.1 and 2.2.3.1). In addition, there are other methods to decompose the polynomial matrix inequalities, see, for example the $\mathcal{S}$-variable approach (Ebihara et al., 2006; Sato & Peaucelle, 2006, 2007a).

2.2.5. *Example*

According to the representation for each model (i.e., LPV, T-S fuzzy, Polynomial, Polynomial Fuzzy) discussed in Section 2.1.5, the characteristic stability analysis will be deployed by a suitable approach (e.g., gridding, convex combination, SoS, etc.).

2.2.5.1. *Relaxation of Parameter-Dependent Lyapunov Function*

It should be noted that the stability analysis using the Lyapunov quadratic form i.e., condition (2.55) of Theorem 2.2.2 fails to verify the stability of T-S fuzzy system (2.32).

Example 2.2.2. Let's consider the representations of nonlinear system (2.25), including affine system (2.28), polynomial system (2.29), T-S fuzzy system, (2.32) and fuzzy polynomial (2.35).

LPV model & Gridding

The stability for LPV system (2.28) is analyzed using the compact set of the parameters defined in (2.71). Like section 2.2.4.1, we now seek for the symmetric positive matrices $P_0, P_1, P_2, P_{12}, P_{11}, P_{22} \in \mathbb{S}^2$ such that the following conditions hold

$$sym\{P(\rho)(A_0 + A_1\rho_1(x) + A_2\rho_2(x))\} \pm \nu_1 \partial P(\rho)/\partial\rho_1 \pm \nu_2 \partial P(\rho)/\partial\rho_2 \prec 0, \tag{2.73}$$

with

$$P(\rho) = P_0 + P_1\rho_1(x) + P_2\rho_2(x) + P_{12}\rho_1(x)\rho_2(x) + P_{11}\rho_1(x)^2 + P_{22}\rho_2(x)^2,$$
$$\partial P(\rho)/\partial\rho_1 = P_1 + P_{12}\rho_2(x) + 2P_{11}\rho_1(x),\ \partial P(\rho)/\partial\rho_2 = P_2 + P_{12}\rho_1(x) + 2P_{22}\rho_2(x),$$
$$A_0 = \begin{bmatrix} -1 & 0 \\ 0 & -1 \end{bmatrix},\ A_1 = \begin{bmatrix} 0 & 1 \\ 0 & 0 \end{bmatrix}, \text{ and } A_2 = \begin{bmatrix} 0 & 0 \\ 1 & 0 \end{bmatrix}.$$

For $\rho_1(x), \rho_2(x)$ varying in the range:

$$\{\rho_1(x), \rho_2(x)\} \in [-1,1]\times[0,4] \subset \mathbb{R}^2,\ |\dot{\rho}_i| < \nu_i,\ i = 1,2,\ \nu_1 = \nu_2 = 1. \tag{2.74}$$

Verifying the LMI (2.73) over a grid of $N_g = 121$ points that yields:

$$P_0 = \begin{bmatrix} 0.2139 & 0.2088 \\ 0.2088 & 0.2139 \end{bmatrix},\ P_1 = \begin{bmatrix} -0.1849 & -0.1799 \\ -0.1799 & -0.1849 \end{bmatrix},\ P_2 = \begin{bmatrix} 0.1384 & 0.1949 \\ 0.1949 & 0.1384 \end{bmatrix},$$
$$P_{12} = \begin{bmatrix} 0.0553 & 0.0362 \\ 0.0362 & 0.0553 \end{bmatrix},\ P_{11} = \begin{bmatrix} -0.0260 & -0.0280 \\ -0.0280 & -0.0260 \end{bmatrix},\ P_{22} = \begin{bmatrix} -0.0880 & -0.1244 \\ -0.1244 & -0.0880 \end{bmatrix}.$$

Polytope & Multi-convexities

Let analysis the local stability for T-S fuzzy system (2.32), with the nonlinear terms:

$$\theta_1(x) = x_1(t)x_2^2(t) \in [-1,1],\ \theta_2(x) = x_1^2(t)(3 + x_2(t)) \in [0,4], \tag{2.75}$$

and the membership functions

$$\begin{aligned} \lambda_1(x(t)) &= \frac{(\theta_1(x)+1)}{2}\frac{\theta_2(x)}{4}, & \lambda_2(x(t)) &= \frac{(\theta_1(x)+1)}{2}\frac{4-\theta_2(x)}{4}, \\ \lambda_3(x(t)) &= \frac{(1-\theta_1(x))}{2}\frac{\theta_2(x)}{4}, & \lambda_4(x(t)) &= \frac{(1-\theta_1(x))}{2}\frac{4-\theta_2(x)}{4}, \end{aligned} \tag{2.76}$$

are assumed to be continuous in the time domain and have continuous and bounded derivatives $\left|\dot{\lambda}_i(x(t))\right| \le \nu_i,\ i = 1,2,3,4.$

By applying Theorem 2.2.6, fuzzy system (2.32) is stable if and only if there are the symmetric positive matrices $P_1, P_2, P_3, P_4 \in \mathbb{S}^2_{++}$ such that the following LMI conditions

$$\frac{1}{2}(A_i^T P_j + P_j A_i + A_j^T P_i + P_i A_j) + \sum_{k=1}^{3} \nu_k (P_k - P_4) \prec 0, \text{ with } \forall i \ge j, \tag{2.77}$$

hold with $i, j = 1,2,3,4$, and

$$A_1 = \begin{bmatrix} -1 & 1 \\ 4 & -1 \end{bmatrix}, A_2 = \begin{bmatrix} -1 & 1 \\ 0 & -1 \end{bmatrix}, A_3 = \begin{bmatrix} -1 & -1 \\ 4 & -1 \end{bmatrix}, A_4 = \begin{bmatrix} -1 & -1 \\ 0 & -1 \end{bmatrix}.$$

As in the previous example, selects $\nu_i = 1$ and solves the LMIs (2.77) we obtain:

$$P_1 = \begin{bmatrix} 0.0632 & -0.0250 \\ -0.0250 & 0.0632 \end{bmatrix},\ P_2 = \begin{bmatrix} 0.1105 & -0.0701 \\ -0.0701 & 0.1105 \end{bmatrix},$$

$$P_3 = \begin{bmatrix} 0.0590 & -0.0206 \\ -0.0206 & 0.0590 \end{bmatrix},\ P_4 = \begin{bmatrix} 0.2375 & 0.2349 \\ 0.2349 & 0.2375 \end{bmatrix}.$$

As discussed in section 2.2, these conditions can either handle by the sum of squares decomposition method, or directly treated by the SoS toolbox. Both methods are based on a generalization of Finsler's lemma. In this example, the polynomial matrix conditions are converted to the SoS expressions and solved by SoS toolbox. The higher number of the monomial degree increases the computational complexity, so if the polynomials with the highest degree are fuzzification, then the fuzzy polynomial model is theoretically more advantageous than the original polynomial model.

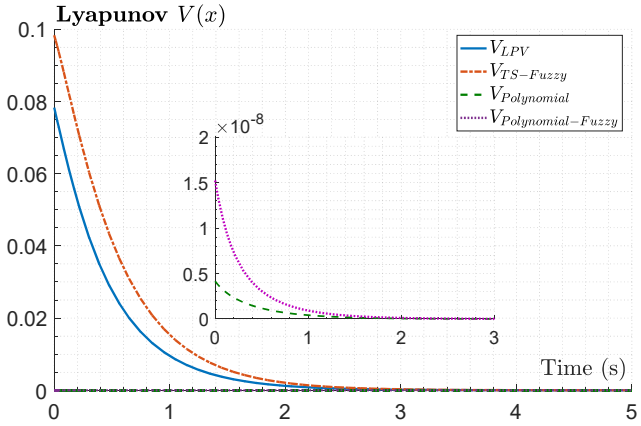

Figure 2-5. *Time transient of Lyapunov function.*

Polynomial model & SoS

Followed the line of Theorem 2.2.7, *polynomial system* (2.29) *is stable, if there exists a polynomial matrix* $P(x) \in \mathbb{S}^N_{++}$, *the coefficients polynomials in* x, $\epsilon_1(x)$, $\epsilon_2(x) > 0$, *such that the expressions:*

$$Z(x)^T(P(x) - \epsilon_1(x)I)Z(x), \tag{2.78}$$

$$-Z(x)^T\{P(x)M(x)A(x) + A(x)^T M(x)^T P(x) + \cdots \sum_{j=1}^{n} \frac{\partial P(x)}{\partial x_j} A(x)_{(j)} + \epsilon_2(x)I\}Z(x), \tag{2.79}$$

are sum of square. Where $A(x)_{(j)}$ *denotes the* j^{th} *row of matrix* $A(x)$, $Z(x) = [x_1\ x_2\ x_1x_2]^T$,

$$M(x) = \partial Z(x)/\partial x \triangleq \begin{bmatrix} \frac{\partial Z(x)}{\partial x_1} & \frac{\partial Z(x)}{\partial x_2} \end{bmatrix},\ A(x) = \begin{bmatrix} -1 & 0 & x_2^2(t) \\ 3x_1^2(t) & -1 & x_1^2(t) \end{bmatrix}.$$

Using SoS toolbox to verify the expressions (2.78), (2.79) are sum of square with $\epsilon_1(x) = \epsilon_2(x) = 10^{-9}(x_1^2 + x_2^2)$, we get:

$$P(x) = 10^{-9} \cdot \begin{bmatrix} P_{11} & P_{12} & P_{13} \\ * & P_{22} & P_{23} \\ * & * & P_{33} \end{bmatrix}, \text{ with}$$

$$P_{11} = -2.301 \cdot 10^{-5} x_1^2 - 1.009 \cdot 10^{-5} x_1x_2 + 0.453x_1 - 2.194 \cdot 10^{-4} x_2^2 + 0.749x_2 + 3.881,$$
$$P_{12} = 1.304 \cdot 10^{-5} x_1^2 + 2.849 \cdot 10^{-5} x_1x_2 + 0.284x_1 + 1.412 \cdot 10^{-5} x_2^2 + 7.157 \cdot 10^{-2} x_2 - 1.566,$$

$$P_{13} = 2.036\cdot10^{-5}x_1^2 - 1.822\cdot10^{-6}x_1x_2 - 0.436x_1 + 1.576\cdot10^{-4}x_2^2 - 0.364x_2 - 0.827,$$
$$P_{22} = -9.019\cdot10^{-6}x_1^2 + 2.715\cdot10^{-6}x_1x_2 + 0.207x_1 - 1.329\cdot10^{-5}x_2^2 + 6.498\cdot10^{-2}x_2 + 1.482,$$
$$P_{23} = 2.994\cdot10^{-5}x_1^2 - 2.267\cdot10^{-5}x_1x_2 - 3.475\cdot10^{-2}x_1 + 3.784\cdot10^{-5}x_2^2 + 1.846\cdot10^{-2}x_2 - 0.506,$$
$$P_{33} = 4.215\cdot10^{-6}x_1^2 - 2.074\cdot10^{-6}x_1x_2 - 0.192x_1 - 1.700\cdot10^{-5}x_2^2 - 0.365x_2 + 0.682.$$

Polynomial Fuzzy Model & SoS

Using SoS toolbox to solve the expressions of Theorem 2.2.7 with $\epsilon_1(x) = \epsilon_2(x) = 10^{-9}(x_1^2 + x_2^2)$, and

$M(x) = \begin{bmatrix} \frac{\partial Z(x)}{\partial x_1} & \frac{\partial Z(x)}{\partial x_2} \end{bmatrix}, A_1(x) = \begin{bmatrix} -1 & 0 & x_2^2(t) \\ 3 & -1 & 1 \end{bmatrix}, A_2(x) = \begin{bmatrix} -1 & 0 & x_2^2(t) \\ 0 & -1 & 0 \end{bmatrix}$, we obtain:

$P(x) = 10^{-9} \cdot \begin{bmatrix} P_{11} & P_{12} & P_{13} \\ * & P_{22} & P_{23} \\ * & * & P_{33} \end{bmatrix}$, with

$$P_{11} = -1.960\cdot10^{-3}x_1^2 - 8.877\cdot10^{-3}x_1x_2 + 1.076x_1 + 7.663x_2^2 + 9.176x_2 + 20.89,$$
$$P_{12} = 6.401\cdot10^{-5}x_1^2 + 2.215\cdot10^{-5}x_1x_2 + 0.448x_1 - 3.197x_2^2 + 0.073x_2 - 1.877,$$
$$P_{13} = -2.845\cdot10^{-4}x_1^2 + 1.209\cdot10^{-4}x_1x_2 - 1.044x_1 + 1.806\cdot10^{-4}x_2^2 - 6.542x_2 - 6.958,$$
$$P_{22} = -1.904\cdot10^{-3}x_1^2 + 1.719\cdot10^{-4}x_1x_2 + 0.308x_1 + 3.489x_2^2 - 1.850x_2 + 2.095,$$
$$P_{23} = 3.469\cdot10^{-5}x_1^2 - 2.125\cdot10^{-4}x_1x_2 + 0.564x_1 - 1.215\cdot10^{-4}x_2^2 + 2.200x_2 - 2.305,$$
$$P_{33} = 3.781\cdot10^{-4}x_1^2 - 1.529\cdot10^{-3}x_1x_2 - 1.171x_1 + 2.798\cdot10^{-4}x_2^2 - 2.186x_2 + 4.347.$$

The computational time is taken to solve the conditions by Gridding and convex combinations methods is 14.4237 and 0.2297 seconds, respectively, while the time spent on sum-squared polynomials is 19.1659 and 24.6257 seconds. The characteristic convergence of the region of stability is shown in Figure 2-5. However, we cannot draw any further conclusions. Each relaxation method has its own advantages and disadvantages, which are compatible with each type of LPV representation.

Theoretically, the SoS decomposition should give the least conservative results. But up to now, the limitations of numerical computation (e.g., SoS toolbox), have not allowed to take full advantage of the lossless transformation. Specifically, the time takes to process sorting, separating the variables, and solving the conditions will increase exponentially. Besides, this numerical computation tool is sensitive to complex conditions (e.g., a large scale PLMI condition). On the other hand, the convex polyhedron method (such as the stability conditions of T-S fuzzy or polytopic systems) provides solutions with a reasonable algorithmic time is 0.2297s compared to 24.6257s of the polynomial-fuzzy SoS method. Finally, the gridding method is straightforward to handle the parameter-dependent conditions by discretizing the parameter domain. However, the computational time to treat the LMI conditions also increases exponentially with the number of parameters. *There's always a price to pay*!

2.2.5.2. *The Conservativeness of Fuzzy and Fuzzy Polynomial Lyapunov Functions*

In the last section, the relaxation of PLMI stability conditions analyzed for LPV systems has delivered satisfactory results (except for the quadratic Lyapunov, which returns an

infeasible result). Right after, an example of (Sala & Ariño, 2009) is used to show conservatism of the parameter-dependent LMI conditions where traditional relaxation methods do not work (as illustrated in Table 2.1). The approximations of the nonlinear model to the LPV representations can be fulfilled similarly to section 2.1.5. For details of the transformation can be found in the literature cited below.

Table 2.1. *The Conservativeness of Parametrized LMI Conditions.*

	Quadratic LF	**Parameter-Dependent LF**			
LPV System	**T-S fuzzy**	**Affine**	**T-S fuzzy**	**Polynomial**	**Poly-fuzzy**
Stability *Relaxation*	Theorem 2.2.3	Theorem 2.2.5 *Gridding*	Theorem 2.2.6 *Multi-convex*	Theorem 2.2.5 *SoS*	Theorem 2.2.7 *SoS*
Example 2.1.3	(2.32)	(2.28)	(2.32)	(2.29)	(2.35)
	infeasible	*feasible*	*feasible*	*feasible*	*feasible*
Example 2.2.3	(2.83)	(2.81)	(2.83)	(2.82)	(2.84)
	infeasible	*feasible*	*infeasible*	*infeasible*	*infeasible*
Imprv	[ref1]		[ref2]		[ref3]
	infeasible		*feasible*		*feasible*
0	1	2	3	4	5

Imprv is the improvement of the respective stability conditions combining with the following methods:
[ref1] – Relaxed Stability LMI conditions (Tuan, Apkarian, et al., 2001),
[ref2] – Locality and Shape-Dependent Conditions (Sala, 2009),
[ref3] – Positivstellensatz Relaxation (Furqon et al., 2017; Sala & Ariño, 2009).

Example 2.2.3. Let's consider a nonlinear system (Sala & Ariño, 2009):

$$\begin{aligned}\dot{x}_1(t) &= -3x_1(t) + 0.5x_2(t)\\ \dot{x}_2(t) &= -2x_2(t) + 3\sin(x_1(t))x_2(t)\end{aligned} \tag{2.80}$$

with state vector $x(t) = [x_1(t),\ x_2(t)]^T$, and $x_1(t),\ x_2(t)$ belong to domain $\mathcal{D}_x = [-1,\ 1]$.

First, an affine system gives as follows:

$$\dot{x}(t) = \begin{bmatrix} -3 & 0.5 \\ 0 & -2 + 3\rho(t) \end{bmatrix} x(t). \tag{2.81}$$

with parameter $\rho(t) = \sin(x_1(t)) \in [-0.8415,\ 0.8415],\ \dot{\rho}(t) \in [-1,\ 1]$.

Then, using a third-order polynomial of Taylor series of the sinusoid around $x_1 = 0$, we get a polynomial system:

$$\dot{x}(t) = \begin{bmatrix} -3 & 0.5 \\ 0 & -2 + 3x_1(t) - 0.5x_1^3(t) \end{bmatrix} x(t). \tag{2.82}$$

By applying the fuzzy modeling (Sala & Ariño, 2009), we obtain a representation of T-S fuzzy system

$$\dot{x}(t) = \left(\lambda_1(t) \begin{bmatrix} -3 & 0.5 \\ 0 & -5 \end{bmatrix} + \lambda_2(t) \begin{bmatrix} -3 & 0.5 \\ 0 & 1 \end{bmatrix} \right) x(t). \tag{2.83}$$

and a fuzzy polynomial system

$$\dot{x}(t)=\left(\lambda_1(t)\begin{bmatrix}-3 & 0.5\\ 0 & -2+3x_1(t)-0.4755x_1^3(t)\end{bmatrix}+\lambda_2(t)\begin{bmatrix}-3 & 0.5\\ 0 & -2+3x_1(t)-0.5031x_1^3(t)\end{bmatrix}\right)x(t). \tag{2.84}$$

Analyzing a parameter-dependent stability for system (2.81) that yields to the following condition

$$sym\left\{P(\rho)\begin{bmatrix}-3 & 0.5\\ 0 & -2+3\rho(t)\end{bmatrix}\right\}\pm\nu\partial P(\rho)/\partial\rho \prec 0, \tag{2.85}$$

with $P(\rho)=P_0+P_1\rho(t)+P_2\rho(t)$, $\partial P(\rho)/\partial\rho=P_1+P_2\rho(t)$. Following the line of Theorem 2.2.5, and using gridding technique to the latter PLMI over a grid of $N_g=121$ points for $\rho(t)$ in the range $[-0.8415,\ 0.8415]$, $|\dot{\rho}|<1$, we obtain the symmetric positive matrices

$$P_0=\begin{bmatrix}0.2521 & 0.1105\\ 0.1105 & 0.1581\end{bmatrix},\ P_1=\begin{bmatrix}-0.0296 & -0.0295\\ -0.0295 & -0.0316\end{bmatrix},\ P_2=\begin{bmatrix}-0.0689 & -0.0650\\ -0.0650 & -0.0902\end{bmatrix}.$$

It should be noted that for given domain, we have:

$$|\dot{\rho}(t)=\cos x_1(t)\dot{x}_1(t)| \ \le\ \|[-3\ \ 0.5]x(t)\|_2 \ \le\ \sqrt{(3^2+0.5^2)1}\ \approx\ 3.0414. \tag{2.86}$$

The feasible polynomial matrices are obtained at the bounded rate of the parameter $\rho(t)$ of 1 and 13.5125 for PLMI (2.85), respectively. But, with $|\dot{\rho}(t)|\le\nu=1$, the multi-convex method using a fuzzy Lyapunov function fails to prove the stability. Likewise, the parameter-dependent LMI stability conditions of the polynomial systems (2.83), (2.84) do not return satisfactory solutions due to accuracy complication. It could be elucidated that although the SoS toolbox returns the "positive" information s.t., *feasible ratio* = 0.9921, *numerical problems* = 0, *Primal and Dual feasible*[2].

However, by checking the eigenvalues of the polynomial matrix $P(x)$ over the domain of $\{x_1(t),x_2(t)\}\in[-1,1]\times[-1,1]$, that yields the smallest eigenvalues are slightly negative with a norm approximately equal to the default precision level of the interior-point optimization (Sedumi), $\epsilon=10^{-9}$. If this designed accuracy radius is achieved, then *info.numerr* is set to 0 (Sturm, 1999). A way out of these misunderstandings is to "transform" all semi-definite inequalities into definite inequalities (Labit et al., n.d.; Dimitri Peaucelle et al., 2002). In this work, we introduce a positive definite scalar in all inequalities s.t.,

$$P_0\succeq 0,\ P_0\in\mathbb{R}^{n\times n}\ \rightarrow\ P_0\succeq\delta I_n, \tag{2.87}$$

with a small arbitrary constant $\delta\ge\epsilon$. This constraint transformation *is expected* do not add some extra conservatism and tune the solver convergence without strongly modifying the feasibility radius. It should be noted that a strict inequality $P_0\succ 0$ is not recommended on the current numerical computation tools such as Yalmip. So, numerical adjustment (2.87) provides an appropriate modification to the linear matrix inequalities (e.g., the stability condition of the T-S fuzzy multi-convex system), but it doesn't fit the SoS constraints. There are two reasons, first it can be asserted that there is no solution, and the

[2] The polynomial condition is executed on Matlab v2020b, using the SoS toolbox v4.00 with Interior-point solvers, Sedumi v1.03 and Mosek v9.3 respectively.

second is that the polynomial matrix inequality can be positive but not a sum of squares. Accordingly, we applied a refinements of the sum of squares polynomials proposed by (Sala & Ariño, 2009) to verify the stability of the polynomial systems (2.82), (2.83).

Corollary 2.2.1. *Giving a set* $F = \{f_1(x), f_2(t), ..., f_{n_1}(t)\} \in \mathbb{R}$, *then define a region*

$$\mathcal{D}_x \subset \{x(t) \in \mathbb{R}^n \mid \ \forall f \in F,\ f_i(x) \geq 0,\ i = 1, ..., n_1\},$$

and arbitrary polynomials $g_j(x), j = 1, ..., n_2$ *are composed of products of F. Then, a sufficient condition for polynomials* $\Omega(x)$ *are positive* $\forall x \in \mathcal{D}_x$, *if there exist multiplier SoS polynomial* $q_j(x) \geq 0,\ j = 1, ..., n_2$, *such that the following expressions:*

$$v^T\Big(\Omega(x) - \sum\nolimits_{j=1}^{n_2} q_j(x) g_j(x)\Big) v, \tag{2.88}$$

are sum of squares for arbitrary appropriate dimension vector v.

Using a third order Taylor expansion method similar to (Sala & Ariño, 2009), combining the relaxed SoS condition (2.88) with the PLMI stability condition analyzed for fuzzy polynomial system (2.84), we obtain a second degree decision matrix:

$$P(x) = \begin{bmatrix} P_{11} & P_{12} \\ * & P_{22} \end{bmatrix} \succ 0, \text{ for } \forall x \in \mathcal{D}_x, \text{ where}$$

$$\begin{aligned}
P_{11} &= 4.688 \cdot 10^{-4} x_1^2 - 1.249 \cdot 10^{-4} x_1 x_2 - 2.398 \cdot 10^{-4} x_1 + 0.3182 x_2^2 + 2.463 \cdot 10^{-5} x_2 + 7.401 \cdot 10^{-5}, \\
P_{12} &= -8.674 \cdot 10^{-8} x_1^2 - 0.3181 x_1 x_2 + 8.474 \cdot 10^{-6} x_1 - 4.0 \cdot 10^{-7} x_2^2 - 1.141 \cdot 10^{-6} x_2 - 6.987 \cdot 10^{-6}, \\
P_{22} &= 0.3181 x_1^2 + 3.134 \cdot 10^{-7} x_1 x_2 - 1.181 \cdot 10^{-6} x_1 + 5.805 \cdot 10^{-9} x_2^2 + 1.024 \cdot 10^{-7} x_2 + 1.397 \cdot 10^{-6},
\end{aligned}$$

with local constraints $g_1(x) = 1 - x_1^2$, $g_2(x) = 1 - x_2^2$, and the polynomial Positivstellensatz multipliers of second degree

$$\begin{aligned}
q_1(x) &= 10^{-9} \begin{bmatrix} x_1 \\ x_2 \end{bmatrix}^T \begin{bmatrix} 5.3566 & 0 \\ -0.4254 & 2.5644 \end{bmatrix} \begin{bmatrix} x_1 \\ x_2 \end{bmatrix} \succeq 0, \\
q_2(x) &= 10^{-9} \begin{bmatrix} x_1 \\ x_2 \end{bmatrix}^T \begin{bmatrix} 4.6983 & 0 \\ 0.0527 & 6.6968 \end{bmatrix} \begin{bmatrix} x_1 \\ x_2 \end{bmatrix} \succeq 0.
\end{aligned}$$

And, even with the *quadratic case* that returns a feasible solution

$$P = 10^{-6} \cdot \begin{bmatrix} 9.7014 & -0.2101 \\ -0.2101 & 1.9633 \end{bmatrix} \succ \epsilon I_2, \text{ for } \epsilon = 10^{-7}, \text{ and arbitrary polynomials}$$

$$\begin{aligned}
q_1(x) &= 10^{-9} \begin{bmatrix} x_1 \\ x_2 \end{bmatrix}^T \begin{bmatrix} 6.2579 & 0 \\ -1.1414 & 2.6545 \end{bmatrix} \begin{bmatrix} x_1 \\ x_2 \end{bmatrix} \succeq 0, \\
q_2(x) &= 10^{-9} \begin{bmatrix} x_1 \\ x_2 \end{bmatrix}^T \begin{bmatrix} 5.6823 & 0 \\ 0.0823 & 8.0597 \end{bmatrix} \begin{bmatrix} x_1 \\ x_2 \end{bmatrix} \succeq 0.
\end{aligned}$$

Though the old-fashioned sum of squares decomposition method failed to approve the stability of the fuzzy polynomial system, the obtained results demonstrate the effectiveness of the Positivstellensatz multipliers polynomial approaches. However, this method is also sensitive to the numerical problem, which regularly entails unsatisfactory results related to, e.g., the complex stabilization conditions (Furqon et al., 2017; Sala & Ariño, 2008). On the other hand, the arbitrary uniform discretization over the parameter domain

(i.e., gridding) delivers promising results (as observed in Table 2.1), with the advantage of being straightforward to perform on the polynomial LMI conditions.

Through these two examples, it can be emphasized that all the stabilization conditions developed for saturated LPV systems in this thesis are formulated by the parameter dependency matrix inequalities, e.g., condition (2.73), which are solved by the gridding over the defined domain of parameters. The decision matrices such as Lyapunov candidate will be chosen polynomial form, for example:

$$P(\rho) = P_0 + P_1\rho_1(t) + P_2\rho_2(t) + P_{12}\rho_1(t)\rho_2(t) + P_{11}\rho_1(t)^2 + P_{22}\rho_2(t)^2.$$

This polynomial expression is simpler to unify than other nonlinear forms such as trigonometric forms.

2.3. The Saturation Nonlinearity – Stabilization Analysis

In control system design analysis, a phenomenon observed in many engineering systems, chemical processes, biology, and even economics, is saturation in actuators. At first glance, the effect of this nonlinearity is quite simple, but analysis inappropriately or ignoring its effects can lead to performance degradation or system instability. Actuator saturation is unavoidable in engineering practical dynamics systems concerning physical limits (velocity, voltage, cycle, etc.) and safety constraints (pressure, temperature, power, energy consumption, etc.). Besides, the saturation effect characterized as nonlinearity cannot linearize. That must find a stabilization method of replacing the operating points of the feedback control system into the region without element saturates. In the last decades, considerable attention has been devoted to LTI systems subject to actuator saturation, see for instance (Hu & Lin, 2001; Tarbouriech et al., 2011; Zaccarian & Teel, 2011) and the references therein.

There are two main approaches to carry out the stabilization analysis in the literature. The first one considers the saturation bounds like a prerequisite in the design strategy (João Manoel Gomes da Silva & Tarbouriech, 1999; Henrion et al., 2005; Henrion & Tarbouriech, 1999; Hu et al., 2002; Hu & Lin, 2003; Tarbouriech et al., 2006). On the other side, an asymptotical stabilizing synthesis proposed for a closed-loop system disregards the control bounds. Then, a suitable design strategy will analyze to compensate for the saturation, such as Direct Linear Anti-windup (DLAW) or Model Recovery Anti-windup (MRAW). The anti-windup domain has been discussed thoroughly in recent decades, see for example (Galeani, Massimetti, Teel, & Zaccarian, 2006; Galeani et al., 2009; Gomes da Silva & Tarbouriech, 2005; Grimm et al., 2003; Hu, Teel, & Zaccarian, 2008; F. Wu, Grigoriadis, & Packard, 2000; Zaccarian & Teel, 2002, 2005, 2011) and the references therein. It can realize that the closed-loop stabilization analysis for DLAW and MRAW is more complicated in considering the effect of the nonlinear behavior and uncertain dynamics. Nonetheless, the DLAW construction is beyond the scope of the dissertation, so it will not be included. Instead, controversial analyzes of the Anti-windup compensator issue using the differential-algebraic equations to constrain the DOF controller are presented in (Bui Tuan et al., 2021).

It can be emphasized that many cited research papers and books are devoted to LTI sys-

tems. Obviously, the saturated synthesis for the LPV/quasi-LPV systems isn't fit in stabilization analysis for saturated LTI systems. However, just several works in the literature subject to the saturation problems analyzed for nonlinear systems or parametric dependence systems, for example, the LPV systems (Cao, Lin, & Shamash, 2002; Forni & Galeani, 2007, 2010; Kapila & Grigoriadis, 2002; A. T. Nguyen, Chevrel, et al., 2018; Roos et al., 2007; Theis et al., 2020; Wu et al., 2000) or T-S fuzzy systems (Benzaouia & Hajjaji, 2014; Dey et al., 2018). So, let's discuss one stability analysis tool used for the saturated LPV systems and LPV time-delay systems.

2.3.1. *Sector Nonlinearity Model*

A representation of LPV systems with actuator saturation gives under the forms:

$$\begin{aligned} \dot{x}(t) &= A(\rho)x(t) + B(\rho)\text{sat}(u) + B_w(\rho)w(t), \\ y(t) &= C(\rho)x(t) + D(\rho)\text{sat}(u) + D_w(\rho)w(t), \\ z(t) &= H(\rho)x(t) + J(\rho)\text{sat}(u) + J_w(\rho)w(t), \end{aligned} \tag{2.89}$$

where nonlinear saturation function $\text{sat}(u) \in \mathbb{R}^m$ will be defined right after, and the parameters are assumed to belong to spaces (2.8)-(2.9).

2.3.1.1. *Asymptotical stabilization.*

Both local and global stabilization is well suited regarding strategy control synthesis for LPV systems with actuator saturation. The global, semi-global, and local stabilization were discussed in detail in (Tarbouriech et al., 2011), with the assumptions that open-loop poles are located in the closed left-half plane, and the set of admissible-initial conditions is explicitly defined. But it can notice that the stabilizing condition analysis for system (2.1) is typically localized corresponding to the assumptions about the compact set of the parameters (2.8)-(2.9). Similar to the LPV system, the T-S fuzzy system is characterized by the operating ranges of the *fuzzificated* functions. Perceptibly, the global stabilization condition does exist in control synthesis for this class of systems. But when saturation limits are involved, the local stabilization condition is more reasonable.

Saturation nonlinearity.

Following this approach, it is generally classified into three representations used for closed-loop system with saturated actuators:

(1)-Polytopic models,

(2)-Sector nonlinearity models, and

(3)-Regions of saturation models.

Giving a control input vector $u(t) = [u_1(t), u_2(t), \ldots, u_m(t)]^T \in \mathbb{R}^m$ that corresponds with the saturation limits $u_i(t) \in [\min u_i(t), \max u_i(t)]$, $i = 1, 2, \ldots, m$, are usually expressed by the following nonlinear function:

$$\text{sat}\, u_i(t) = \begin{cases} \overline{u}_i & u_i(t) \in [\max u_i(t), +\infty] \\ u_i(t) & u_i(t) \in (\min u_i(t), \max u_i(t)) \\ \underline{u}_i & u_i(t) \in [-\infty, \min u_i(t)] \end{cases} \tag{2.90}$$

The notations $\overline{u}_i := \max u_i(t)$, $\underline{u}_i := \min u_i(t)$ are used for the purpose of simplifying the presentation. As analyzed in the literature (Tarbouriech et al., 2011), the polytopic bounds technique and regions of saturation might result in higher computational complexity, respectively, with 2^m, and 3^m conditions compared with sector nonlinearity has only m conditions. Furthermore, it worthy to note that the region of stability of the first two approaches seem to be equally scaled (under the same primary assumptions), if not to say the local sector bounding provides better performance. Since mentioned works are commonly imposed on a symmetric saturation (there is rare work realizing for asymmetric saturation) so the lower bounded is typically set by $\underline{u}_i = -\overline{u}_i$, with $\overline{u}_i > 0$.

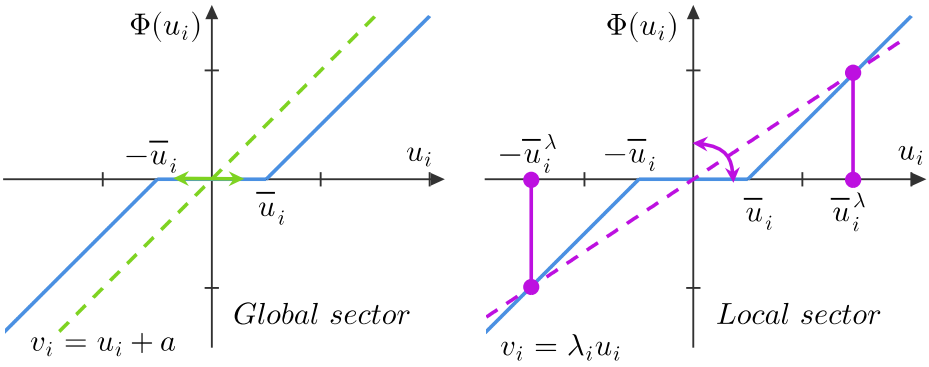

Figure 2-6. *Dead-zone nonlinearity.*

Accordingly, let's introduce with the dead-zone nonlinearity associated with a symmetric saturation function $\text{sat}(u) = u(t) - \Phi(u)$:

$$\Phi(u_i) = \begin{cases} u_i - \text{sign}(u_i)\overline{u}_i & \text{if } |u_i| \geq \overline{u}_i \\ 0 & \text{if } |u_i| < \overline{u}_i \end{cases} \quad i = 1,2\ldots m. \tag{2.91}$$

Given a vector $v(t) = [v_1(t), v_2(t), \ldots, v_m(t)]^T \in \mathbb{R}^m$ and defined an auxiliary control vector $\vartheta(t) = u(t) - v(t)$, belong to the polyhedral set

$$\mathcal{S}(u-v, \overline{u}) = \{u, v \in \mathbb{R}^m : -\overline{u}_i \leq \vartheta_i = u_i - v_i \leq \overline{u}_i,\ i = 1,2\ldots m\}. \tag{2.92}$$

Then, a generalized sector condition (GSC) is introduced as follows.

Lemma 2.3.1. *Given* $u(t), \vartheta(t) \in \mathcal{S}$, *and a diagonal matrix function* $T : \mathcal{U}_p \to \mathbb{R}_{++}^{m\times m}$, *then nonlinearity* $\Phi(u) = u(t) - \text{sat}(u)$ *satisfies the following inequality*

$$\Phi^T(u) T^{-1}(\rho)(\text{sat}(u) - \vartheta(t)) \geq 0. \tag{2.93}$$

Proof.

Consider the dead-zone nonlinear function (2.91) conceding the following properties:

$$\begin{array}{ll} u_i \geq \Phi(u_i) \geq 0 & \text{if } u_i \geq 0 \\ u_i < \Phi(u_i) \leq 0 & \text{if } u_i < 0 \end{array} \quad \text{with } i = 1,2\ldots m. \tag{2.94}$$

This is illustrated in Figure 2-6 (*left*), where nonlinear function $\Phi(u_i)$ is the solid blue line, and linear function u_i is the green dashed line. For all $\lambda_i > 0$, define $v_i = \lambda_i u_i$, we look for a vector $\vartheta = [\vartheta_1, \vartheta_2, \ldots, \vartheta_m]^T \in \mathcal{S}(u-v, \overline{u})$ s.t.

$$-\overline{u}_i \leq \vartheta_i \leq \overline{u}_i,\ \vartheta_i = u_i - v_i = (1-\lambda_i)u_i, \text{ with } i = 1,2,\ldots,m, \tag{2.95}$$

that satisfy, for

$$\begin{aligned} &\overline{u}_i \le u_i < +\infty, \quad \text{sat}(u_i) - \vartheta_i = \overline{u}_i - \vartheta_i \ge 0. \\ &0 \le u_i < \overline{u}_i, \qquad \text{sat}(u_i) - \vartheta_i = u_i - (u_i - v_i) \ge 0,\ \forall \lambda_i > 0,\ v_i = \lambda_i u_i. \end{aligned}$$

Then, for $u_i \ge 0$ there exist functions $T_i : \mathcal{U}_p \to \mathbb{R}_{++}$ such that

$$\Phi^T(u_i) T_i^{-1}(\rho)(\text{sat}(u_i) - \vartheta_i) \ge 0, \text{ for all } -\overline{u}_i \le \vartheta_i \le \overline{u}_i,\ i = 1,2,...,m. \tag{2.96}$$

Similarly, for

$$\begin{aligned} &-\overline{u}_i < u_i < 0, \qquad \text{sat}(u_i) - \vartheta_i = u_i - (u_i - v_i) < 0,\ \forall \lambda_i > 0,\ v_i = \lambda_i u_i. \\ &-\infty < u_i \le -\overline{u}_i, \quad \text{sat}(u_i) - \vartheta_i = -\overline{u}_i - \vartheta_i \le 0. \end{aligned}$$

Hence, for $u_i < 0$ there exist functions $T_i : \mathcal{U}_p \to \mathbb{R}_{++}$ such that

$$\Phi^T(u_i) T_i^{-1}(\rho)(\text{sat}(u_i) - \vartheta_i) \ge 0, \text{ for all } -\overline{u}_i \le \vartheta_i \le \overline{u}_i,\ i = 1,2,...,m. \tag{2.97}$$

It follows immediately from condition (2.96), (2.97), there exists a diagonal matrix function $T : \mathcal{U}_p \to \mathbb{R}_{++}^{m \times m},\ T(\rho) := \text{diag}\{T_1(\rho), T_2(\rho), ..., T_m(\rho)\}$ such that (2.93) holds.

□

By substituting $\text{sat}(u) = u(t) - \Phi(u),\ \vartheta(t) = u(t) - v(t)$, for the condition (2.93), we get $\Phi^T(u) T^{-1}(\rho)(-\Phi(u) + v(t)) \ge 0$, which can be recognized as the *prototype* GSC condition in (Tarbouriech et al., 2011). However, the existence of vector $v(t)$ in the GSC condition and polyhedral set $\mathcal{S}(u - v, \overline{u})$ would lead to the unnecessarily difficult in analyzing saturation constraints. Instead, the GSC condition is reformatted by finding a vector $\vartheta(t)$, a feedback control law $u(t)$, and a nonlinear function $\Phi(u)$.

Corollary 2.3.1 *Given $u(t), \vartheta(t) \in \mathcal{S}$, and a diagonal matrix function $T : \mathcal{U}_p \to \mathbb{R}_{++}^{m \times m}$, then nonlinearity $\Phi(u) = u(t) - \text{sat}(u)$ satisfies the following inequality*

$$\Phi^T(u) T^{-1}(\rho)(u(t) - \vartheta(t) - \Phi(u)) \ge 0. \tag{2.98}$$

From now on, this formulation will be essentially implemented for the saturated LPV and LPV time-delay system in the following chapters. Where the definition of the polyhedron $\mathcal{S}(\vartheta, \overline{u})$ is recalled as an alternative of $\mathcal{S}(u - v, \overline{u})$.

2.3.1.2. *Region of Attraction.*

The defined domain of states of the system (2.1) is denoted by $\mathcal{D}_x$. Without effect of disturbance $w(t) = 0$, the region of attraction of the LPV system is defined as a set of $x(t) \in \mathcal{D}_x$ such that from specified initial condition, the trajectory $x(t, x(0))$ converges asymptotically to the origin.

$$\mathcal{R}_A = \left\{ x(t) \in \mathcal{D}_x \subset \mathbb{R}^n \,\middle|\, x(t, x(0)) \to 0 \text{ as } t \to \infty \right\}. \tag{2.99}$$

2.3.1.3. *Ellipsoidal Set of Stability.*

It is possible to find the feedback control laws (e.g. $u(t) = K(\rho)x(t)$) so that the unsaturated closed-loop system is *stable* (*i.e.* $A(\rho) + B(\rho)K(\rho)$ is Hurwitz $\forall \rho(t) \in \mathcal{U}_p$). Due to actuator saturation, there exist initial conditions that could lead to divergence of the

closed-loop system, an incorrect convergence of the equilibrium point away from the origin, or a destabilization (Tarbouriech et al., 2011). However, determining the initial conditions such that the trajectories of the closed-loop system are asymptotical stable is not simple as it seems. Therefore, the estimation of $\mathcal{R}_A$ related with the admissible set of initial conditions is generally encountered in saturation control synthesis, see for examples (Cao, Lin, & Ward, 2002; João Manoel Gomes da Silva & Tarbouriech, 2001, 2005; Hu et al., 2002, 2008). In this thesis, a stability analysis tool for the dynamic system primarily deploys by considering the various forms of Lyapunov function. The associated level sets are given by the characterized domains corresponding to:

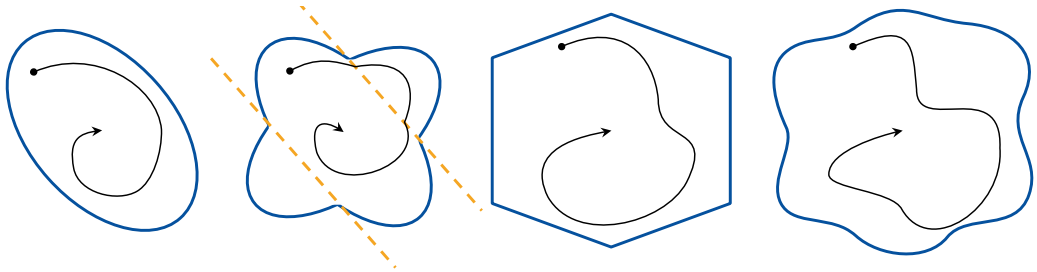

a. QLF *b. MPLF* *c. FLF* *d. PFLF*

Figure 2-7. *The level set of ellipsoidal domains.*

Quadratic Lyapunov function (QLF) candidate:

$$\mathcal{E}(P,\eta)=\left\{x(t)\in\mathcal{D}_x\middle|\ V(x(t))=x(t)^T Px(t)\le\eta^{-1}\right\}. \tag{2.100}$$

Multiple piecewise Lyapunov function (MPLF) candidate:

$$\mathcal{E}(P_i,\eta)=\left\{x(t)\in\mathcal{D}_x\middle|\ V(x(t))=x(t)^T P_i x(t)\le\eta^{-1}, i=1,2,\ldots,N\right\}. \tag{2.101}$$

Parameter-Dependent Lyapunov function candidate:

$$\mathcal{E}(P,\eta,\rho)=\left\{x(t)\in\mathcal{D}_x\middle|\ V(x(t),\rho(t))=x(t)^T P(\rho)x(t)\le\eta^{-1},\ \rho(t)\in\mathcal{U}_p\right\}. \tag{2.102}$$

Fuzzy Lyapunov function (FLF) candidate:

$$\mathcal{E}(P,\eta,\lambda)=\left\{x(t)\in\mathcal{D}_x\middle|\ V(x(t),\lambda(\rho))=\sum\nolimits_{i=1}^{N_l}\lambda_i(\rho)x(t)^T P_i x(t)\le\eta^{-1}\right\}, \tag{2.103}$$

$$\lambda(\rho)\in\mathcal{U}_l=\left\{\lambda_i(\rho)\in[0,\ 1], i=1,\ldots,N_l, \sum\nolimits_{i=1}^{N_l}\lambda_i(\rho(x))=1\right\}\subset\mathbb{R}^{N_l}. \tag{2.104}$$

Polynomial Fuzzy Lyapunov function (PFLF) candidate:

$$\mathcal{E}(P,\eta,\lambda)=\left\{x(t)\in\mathcal{D}_x\middle|\ V(t)=\sum\nolimits_{i=1}^{N_l}\lambda_i(\rho)x(t)^T P_i(x)x(t)\le\eta^{-1},\lambda(\rho)\in\mathcal{U}_l\right\}. \tag{2.105}$$

Then, the problem is formulated by finding the matrices P are defined in (2.100)-(2.105) so that the given level sets $\mathcal{E}(P,\eta)$ are regions of asymptotical stability for the closed-loop system. Since the parameter dependency form (2.102) able to present both (2.103), (2.105), and if $\rho(t)$ is constant then it yields to quadratic form, so this formulation is more general. Henceforth, this parameter-dependent elliptical domain is employed mostly, the remaining forms are only considered in specific cases.

Among the Lyapunov functions are derived for stability analysis of LPV system (2.1)

(without external disturbance), the quadratic formulation generally leads to strict conditions (illustrated by the smallest ellipsoid, as seen in Figure 2-7.a). The next figure shows the piecewise Lyapunov function commonly delivered for switching LTI systems. In visualization, we can see that the estimates of the region of asymptotic stability of the parametric Lyapunov functions (FLF and PFLF) are significantly larger. Nevertheless, the optimization problems such as the size or performance criteria results in the parameterized conditions. The relaxation of these PLMIs depends on the structure of transformation used for the stabilization condition.

2.3.1.4. *Optimization problems.*

The elliptic domain optimization discussed in (Boyd et al., 1994) could convert to convex optimization methods such as maximization matrix volume - $\log(\det(\eta P))$; generalized eigenvalue problems by maximizing the minor axis of ellipsoid - $\mathcal{E}(P,\eta)$; and minimizing the sum eigenvalues - $\text{trace}(\eta P)$. In addition, the maximization method in certain directions are discussed by considering a quadratic Lyapunov function (João Manoel Gomes da Silva & Tarbouriech, 2001, 1999; Hu et al., 2002, 2008) or a convex combination piecewise Lyapunov function (Hu & Lin, 2003). Without loss generality, we might consider the unit level set $\eta = 1$, to simplify the optimization problems involved in bilinear couple between η and P. In Chapter 4, the maximization of the minor axis carries out for the parametric ellipsoidal set (2.102). The optimization problem is even more interesting in implemented on an LPV time-delay system with stability analysis based on the Lyapunov- Krasovskii function discussed in Chapter 6.

On the other side, in consideration of the effect of the external disturbances and the initial condition, the optimization of performance requirement consisted of finding the $\mathcal{L}_2$-gain scheduling controller for saturated system (2.1) so that the criterion is satisfied:

$$\gamma^{-1}\|z(t)\|_{\mathcal{L}_2}^2 < \gamma\|w(t)\|_{\mathcal{L}_2}^2 + \eta_0^{-1} \tag{2.106}$$

where η_0 is maximum of the non-null admissible initial conditions $\mathcal{E}(P,\eta_0)$. And, an energy bounded exogenous signal such as: $\mathcal{W}(w,\sigma) = \{w \in \mathbb{R}^d \mid \|w(t)\|_{\mathcal{L}_2} < \sigma^{-1}\}$.

Actually, the optimization problem is the trade-off between the estimation of the region of asymptotical stability (RAS), the level of attenuated disturbances, and the region of linear behavior (characterized by the unsaturated regulation region).

2.3.2. *Saturated Feedback Control Synthesis*

The feedback controller structures illustrated in Figure 2-8 are proposed to stabilize the saturated LPV systems. The PLMI stabilization conditions are derived from stability analysis using parameter-dependent Lyapunov (2.102). Concerning constraints defined by polyhedrons $\mathcal{S}(\vartheta,\overline{u})$, the analysis of the saturation bounds address as follows:

$$(\eta\overline{u}_s^2)^{-1}\|\vartheta(t)_{(s)}\|^2 \le V(x(t),\rho(t)) = x(t)^T P(\rho(t))x(t),\ s = 1,2,...,m, \tag{2.107}$$

$$\textit{if } w(t) = 0:\ V(x(t),\rho(t)) \le V(x(0),\rho(0)) \le \eta_0^{-1} \le \eta^{-1}, \tag{2.108}$$

$$\textit{if } w(t) \neq 0:\ V(x(t),\rho(t)) \le V(x(0),\rho(0)) + \gamma\|w(t)\|_{\mathcal{L}_2}^2 \le \eta_0^{-1} + \gamma\sigma^{-1} \le \eta^{-1}. \tag{2.109}$$

The necessary condition (2.107) is set directly for each auxiliary controller $\vartheta_s(t)$. And,

the sufficient conditions (2.108)-(2.109) related to the stabilization condition (with and without the influence of disturbance), it is guaranteed that the closed-loop system trajectories is confined within the level set of the ellipsoidal domain $\mathcal{E}(P(\rho(t)),\eta)$ from the initial conditions are belonged to this domain. The satisfaction of the necessary and sufficient conditions means that the ellipsoid is included in the polyhedron set $\mathcal{S}(\vartheta,\overline{u})$. From Corollary 2.3.1, the following GSC condition holds

$$\Phi^T(u)T^{-1}(\rho)(u(t)-\vartheta(t)-\Phi(u))\geq 0. \tag{2.110}$$

So, depending on the feedback controller structure $u(t)$, we will choose the appropriate auxiliary controller structure $\vartheta(t)$, so that the combination of these two vectors in the latter GSC condition is convenient for the designed purpose. In the following sections, the necessary conditions are specifically designed for each controller structure (state feedback, observer-based feedback, static output feedback, and dynamic output feedback) correspond to each optimization method.

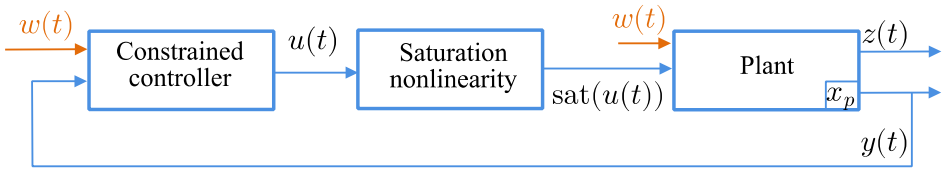

State Feedback

$u(t) = K(\rho)x(t)$

Observer-Based Feedback

$u(t) = K(\rho)\widehat{x}(t)$

Static Output Feedback

$u(t) = K(\rho)y(t)$

Dynamic Output Feedback

$$\begin{cases} \dot{x}_c(t) &= A_c(\rho)x_c(t)+B_c(\rho)y(t) \\ u(t) &= C_c(\rho)x_c(t)+D_c(\rho)y(t) \end{cases}$$

Figure 2-8. *The closed-loop diagram of saturated feedback controllers.*

2.3.2.1. *Parameterized State Feedback Controller*

The simplest method of robust stabilizing and performance analysis for the LPV system is evident the development of the state feedback law. Where the stabilization problem can express directly as the PLMI condition. The studies have been coherently discussed for the continuous and discrete LTI system in the work of (J.M. Gomes da Silva & Tarbouriech, 1998; João Manoel Gomes da Silva et al., 2003; João Manoel Gomes da Silva & Tarbouriech, 1999; Hu et al., 2002, 2006, 2008; Tarbouriech et al., 2006, 2011).

Considering compact sets of parameters (2.8)-(2.9) and a gain-scheduled state feedback controller $u(t)=K(\rho)x(t)$, $\text{sat}(u)=K(\rho)x(t)-\Phi(u)$. Then, the closed-loop system is obtained by substitute this gain-scheduled state feedback controller to saturated LPV system (2.89) as follows:

$$\begin{aligned} \dot{x}(t) &= (A(\rho)+B(\rho)K(\rho))x(t)-B(\rho)\Phi(u)+B_w(\rho)w(t), \\ z(t) &= (H(\rho)+J(\rho)K(\rho))x(t)-J(\rho)\Phi(u)+J_w(\rho)w(t), \end{aligned} \tag{2.111}$$

From initial condition $x(0)\in\mathcal{E}_0(P(\rho_0),\eta_0)$, $\rho_0 := \rho(0)$, the stabilization analysis related to the constraint saturation (i.e., GSC condition) is seek an auxiliary vector $\vartheta(t)=G(\rho)x(t)$ belong to polyhedron set $\mathcal{S}(\vartheta,\overline{u})$ such that:

$$
\begin{aligned}
&(\eta\overline{u}_s^2)^{-1}\left\|\vartheta_s(t)\right\|^2 = (\eta\overline{u}_s^2)^{-1}x(t)^T G(\rho)_{(s)}^T G(\rho)_{(s)}x(t) \le x(t)^T P(\rho)x(t),\\
&\textit{if } w(t)=0:\ x(t)^T P(\rho)x(t)\le x(0)^T P(\rho_0)x(0)\le \eta_0^{-1}\le \eta^{-1},\\
&\textit{if } w(t)\neq 0:\ x(t)^T P(\rho)x(t)\le x(0)^T P(\rho_0)x(0)+\gamma\left\|w(t)\right\|_{\mathcal{L}_2}^2\le \eta_0^{-1}+\gamma\sigma^{-1}\le \eta^{-1}. \quad (2.112)
\end{aligned}
$$

$G(\rho)_{(s)}$ symbolizes s-th row of with $s=1,2,\ldots m$. The satisfaction of the above conditions implies ellipsoid $\mathcal{E}(P(\rho(t)),\eta)$ is included in the polyhedral set $\mathcal{S}(\vartheta,\overline{u})$.

In Section 4.1.2, the optimization problems involve in the sets of the admissible initial condition η_0, the estimation of the ellipse domain η, the upper bound of the disturbance σ^{-1} and the rejection disturbance level γ is investigated. But, the minimization of disturbance attenuation entailing the decline of the linear operating area (region of unsaturated control signals), and predominantly effects on the generalized sector condition. So, an enhancement of the control system's performance could be done by utilizing the $\mathcal{D}$-stable LMI method to relocate the pole of the closed-loop system.

2.3.2.2. *Parameterized Static Output Feedback Controller*

Since a relevant design case impractical control engineering as some states is unmeasurable, the full-state feedback controller is not appropriate for the implementation. But, solving the stabilization condition of static output feedback (SOF) is much more difficult, usually leading to a nonconvex, bilinear matrix inequality (BMI) (Sadabadi & Peaucelle, 2016; Syrmos et al., 1997).

On the one side, the iterative LMI algorithm (Cao et al., 1998; He & Wang, 2006), the algebraic equation (Gossmann & Svaricek, 2019; Syrmos et al., 1997), the iterative global optimization CCL algorithm (El Ghaoui et al., 1997), the two-steps algorithm with output structural constraints (D. Peaucelle & Arzelier, 2001), the congruence transformation (Dong & Yang, 2013; Prempain & Postlethwaite, 2001) and the $\mathcal{S}$-variable method (Ebihara et al., 2015; Pipeleers et al., 2009) have been proposed to cope with SOF control design problem. Besides, the other unsaturated SOF controller synthesis could refer to (Chang & Yang, 2014; Gossmann & Svaricek, 2019; Kau et al., 2007; A. T. Nguyen et al., 2017; A. T. Nguyen, Chevrel, et al., 2018; Qiu et al., 2013), where a gain-scheduled static output feedback (SOF) controller law is generally designed with the form $u(t)=K(\rho)y(t)$. However, there is still room for researching and developing the *saturated* SOF structure implemented in the LPV systems.

On the other side, a controller gain could be considered by $K(\rho)=Y(\rho)W(\rho)^{-1}$, and a congruent transformation is deployed like (Dong & Yang, 2013; Nguyen et al., 2018). Let's consider SOF controller $u(t)=Y(\rho)W(\rho)^{-1}y(t)$ for saturated LPV system (2.89), then a closed-loop system is represented as a parametric dependence formulation:

$$
\begin{aligned}
\dot{x}(t)&=\left(A(\rho)+B(\rho)K(\rho)C(\rho)\right)x(t)-B(\rho)\Phi(u)+B_w(\rho)w(t),\\
z(t)&=\left(H(\rho)+J(\rho)K(\rho)C(\rho)\right)x(t)-J(\rho)\Phi(u)+J_w(\rho)w(t),\\
y(t)&=C(\rho)x(t),\\
u(t)&=K(\rho)y(t)=Y(\rho)W(\rho)^{-1}C(\rho)x(t).
\end{aligned}
\quad (2.113)
$$

The stabilization PLMI condition is derived from a congruence transformation treated the

bilinear structure matrix $Y(\rho)W(\rho)^{-1}C(\rho)$ without using the *strong* mathematical constraints. Due to this specific construction, some scalar variable injects into the design condition. Generally, the gridding logarithm searches linearly on a scale in the interval, e.g., $[10^{-n},10^{n}]$, with $n \in \mathbb{N}_{++}$ is a positive integer. In Section 4.2, we use this controller structure to analyze the local stabilization involved in the expansions of the polyhedron set provided in conditions (2.107)-(2.109).

2.3.2.3. *Parameterized Observer-Based Output Feedback Controller*

In the branch using measurement outputs to design control systems, the dynamic output feedback (DOF[3]) and observer-based feedback controller (OBF) have gained considerable attention in recent decades. Each approach has its benefits and drawbacks. The observer-based controller structure is an exceptional form of DOF, introduced by (Cristi et al., 1990), provided a simple construction and easier to implement. Alternatively, the DOF full-block design analysis was presented by (Chilali et al., 1996; Gahinet et al., 1996; Gahinet & Apkarian, 1994; Scherer et al., 1997) for the LTI systems proposed a congruence transformation with new substitution of variables. Both approaches have been analyzed and implemented in a wide range of system engineering.

Besides, it can mention that there are two common approaches for observer-based controller synthesis: the 2-step separated strategy and the full-block observer-based output feedback control framework. Whereas one method separates the design of the observer from the controller, it is common to apply to accurately known systems (the states are not influenced by the uncertainties).

On the other hand, the simultaneous design method of the extended system includes system dynamics, and the estimated error could handle the parameter uncertainty. In this case, the observation error involves in the input control and state of the plant with the feedback controller $u(t) = K(\rho)\hat{x}(t)$. The second method focused in this thesis shows many difficulties and more challenges for control design strategy. For readers interested, more details about observer-based controller develop for LTI systems (Lien, 2004), for nonlinear Lipschitz systems (Ahmad et al., 2016; Ibrir et al., 2005; Zemouche, Rajamani, Kheloufi, et al., 2017; Zemouche, Rajamani, Trinh, et al., 2017; Zemouche & Boutayeb, 2013), for nonlinear systems represented by T-S fuzzy model (Benzaouia & Hajjaji, 2014; Bui Tuan et al., 2019; Bui Tuan & El Hajjaji, 2018; Dahmani et al., 2014; Dahmani, Pages, El Hajjaji, et al., 2015; Gassara et al., 2017), for LPV system (Briat, 2015a; Heemels et al., 2010), for the LTI saturated system (Tarbouriech et al., 2011), and the references therein.

This section targets to deliver necessary conditions of feedback control based on the structure observer as follows:

$$\begin{aligned} \dot{\hat{x}}(t) &= A(\rho)\hat{x}(t) + B(\rho)u(t) - B(\rho)\Phi(u) + L(\rho)\left(C(\rho)x(t) - C(\rho)\hat{x}(t)\right), \\ u(t) &= K(\rho)\hat{x}(t), \end{aligned} \tag{2.114}$$

where $L(\rho) \in \mathbb{R}^{n\times p}$ is the observer gains to be determined, then by denoting an error estimate $e(t) = x(t) - \hat{x}(t)$, then an augmented closed-loop system can be rewritten as:

[3] The Degree of Freedom is denoted as DoF throughout this dissertation.

$$\begin{aligned}\begin{bmatrix}\dot{x}(t)\\ \dot{e}(t)\end{bmatrix}&=\begin{bmatrix}A(\rho)+B(\rho)K(\rho) & -B(\rho)K(\rho)\\ 0 & A(\rho)-L(\rho)C(\rho)\end{bmatrix}\begin{bmatrix}x(t)\\ e(t)\end{bmatrix}+\begin{bmatrix}-B(\rho)\\ 0\end{bmatrix}\Phi(u)+\begin{bmatrix}B_w(\rho)\\ B_w(\rho)\end{bmatrix}w(t),\\ z(t)&=\begin{bmatrix}H(\rho)+J(\rho)K(\rho) & -J(\rho)K(\rho)\\ 0 & H_e(\rho)\end{bmatrix}\begin{bmatrix}x(t)\\ e(t)\end{bmatrix}+\begin{bmatrix}-J(\rho)\\ 0\end{bmatrix}\Phi(u)+\begin{bmatrix}J_w(\rho)\\ 0\end{bmatrix}w(t).\end{aligned}\tag{2.115}$$

The stabilization of closed-loop system (2.115) is analysis like unsaturated observer-based feedback control system, with an additional reform in the constrained control conditions that deploy the same in section 2.3.2.1. Now, considering an ellipsoid as region of asymptotic stability for system (2.115),

$$\begin{aligned}\mathcal{E}(P_1(\rho),P_2(\rho),\eta)=\big\{x(t)\in\mathcal{D}_x, e(t)\in\mathcal{D}_e\big|\ V(x(t),e(t),\rho(t))=x(t)^T P_1(\rho)x(t)\\ +e(t)^T P_2(\rho)e(t)\le\eta^{-1},\ \rho(t)\in\mathcal{U}_p\big\},\end{aligned}\tag{2.116}$$

a level set of admissible initial conditions,

$$\mathcal{E}_0(P_1(\rho_0),P_2(\rho_0),\eta_0)=\big\{x(0)^T P_1(\rho_0)x(0)+e(0)^T P_2(\rho_0)e(0)\le\eta_0^{-1}\big\}.\tag{2.117}$$

and a polyhedral set to reinforces the constraints on auxiliary controller:

$$\vartheta(t)=G_1(\rho)x(t)+G_2(\rho)e(t),\tag{2.118}$$

From initial condition $\mathcal{E}_0$, the stabilization analysis related to the constraints on auxiliary vector $\vartheta(t)=[\vartheta_1(t),...,\vartheta_s(t),...]$, $|\vartheta_s(t)|\le\overline{u}_s, s=1,2,...,m$, are developed as follows:

$$\begin{aligned}&(\eta\overline{u}_s^2)^{-1}\|\vartheta_s(t)\|^2=(\eta\overline{u}_s^2)^{-1}\left\|\begin{bmatrix}G_1(\rho)_{(s)} & G_2(\rho)_{(s)}\end{bmatrix}\begin{bmatrix}x(t)\\ e(t)\end{bmatrix}\right\|^2\le\begin{bmatrix}x(t)\\ e(t)\end{bmatrix}^T\begin{bmatrix}P_1(\rho) & 0\\ 0 & P_2(\rho)\end{bmatrix}\begin{bmatrix}x(t)\\ e(t)\end{bmatrix},\\ &\textit{if } w(t)=0:\ \begin{bmatrix}x(t)\\ e(t)\end{bmatrix}^T\begin{bmatrix}P_1(\rho) & 0\\ 0 & P_2(\rho)\end{bmatrix}\begin{bmatrix}x(t)\\ e(t)\end{bmatrix}\le\begin{bmatrix}x(0)\\ e(0)\end{bmatrix}^T\begin{bmatrix}P_1(\rho_0) & 0\\ 0 & P_2(\rho_0)\end{bmatrix}\begin{bmatrix}x(0)\\ e(0)\end{bmatrix}\le\eta_0^{-1}\le\eta^{-1},\\ &\textit{if } w(t)\ne0:\ \begin{bmatrix}x(t)\\ e(t)\end{bmatrix}^T\begin{bmatrix}P_1(\rho) & 0\\ 0 & P_2(\rho)\end{bmatrix}\begin{bmatrix}x(t)\\ e(t)\end{bmatrix}\le\begin{bmatrix}x(0)\\ e(0)\end{bmatrix}^T\begin{bmatrix}P_1(\rho_0) & 0\\ 0 & P_2(\rho_0)\end{bmatrix}\begin{bmatrix}x(0)\\ e(0)\end{bmatrix}+\gamma\|w(t)\|_{\mathcal{L}_2}^2.\\ &\qquad\le\eta_0^{-1}+\gamma\sigma^{-1}\le\eta^{-1}\end{aligned}\tag{2.119}$$

However, the traditional approach of analytical stabilization conditions for this controller has a major drawback (the conservatism will expose in Section 4.2 and 4.5.1).

2.3.2.4. *Parameterized Dynamic Output Feedback Controller*

The full-block output-feedback control law framework has also earned a lot of interest in a wide range of control syntheses. The early methodologies of the dynamic output feedback controller synthesis could mention (Chilali et al., 1996; Gahinet, 1996; Gahinet & Apkarian, 1994; Scherer et al., 1997) employed on the LTI systems; (Apkarian & Adams, 1998; Apkarian & Gahinet, 1995; Apkarian & Tuan, 2000b, 1998; Tuan & Apkarian, 2002) deployed for uncertain parameters and LPV systems, the LPV time-delay systems discussed in (Briat, 2008, 2015a), and a dynamic parallel distributed compensation (DPDC) analyzed for the T-S fuzzy systems in (Tanaka & Wang, 2001) via LMI conditions for both cubic, quadratic and linear parameterizations. The synthesis methods is presented by Gahinet, but the $\mathscr{H}_\infty$ performance synthesis is widely known by (Scherer et al., 1997) especially for the LTI systems. In essence, the stabilization problem for saturated DOF controllers is alternatively approached for the anti-windup strategy (DLAW

or MRAW). In monograph (Tarbouriech et al., 2011) has presented and discussed the two separate step design for the LTI systems.

Now, let's introduce a dynamic controller feedback law derived for LPV system (2.89) by the following equation:

$$\begin{aligned} \dot{x}_c(t) &= A_c(\rho)x_c(t) + B_c(\rho)y(t), \\ u(t) &= C_c(\rho)x_c(t) + D_c(\rho)y(t). \end{aligned} \tag{2.120}$$

with output measurement $y(t) = C(\rho)x(t) + D_w(\rho)w(t)$, the goal is to seek a saturation conditional stabilizing structure with proposed DOF (2.120). By replacing the controller in the system (2.89), the extended closed-loop system is obtained:

$$\begin{aligned} \dot{\zeta}(t) &= \mathbb{A}\,\zeta(t) + \mathbb{B}_1\Phi(u) + \mathbb{B}_2 w(t), \\ z(t) &= \mathbb{C}\,\zeta(t) + \mathbb{D}_1\Phi(u) + \mathbb{D}_2 w(t). \end{aligned} \tag{2.121}$$

with $\zeta(t) = \begin{bmatrix} x(t)^T & x_c(t)^T \end{bmatrix}^T$,

$$\mathbb{A} = \begin{bmatrix} A(\rho) + B(\rho)D_c(\rho)C(\rho) & B(\rho)C_c(\rho) \\ B_c(\rho)C(\rho) & A_c(\rho) \end{bmatrix},\ \mathbb{B}_1 = \begin{bmatrix} -B(\rho) \\ 0 \end{bmatrix},\ \mathbb{B}_2 = \begin{bmatrix} B(\rho)D_c(\rho)D_w(\rho) + B_w(\rho) \\ B_c(\rho)D_w(\rho) \end{bmatrix},$$

$$\mathbb{C} = \begin{bmatrix} H(\rho) + J(\rho)D_c(\rho)C(\rho) & J(\rho)C_c(\rho) \end{bmatrix},\ \mathbb{D}_1 = -J(\rho),\ \mathbb{D}_2 = J(\rho)D_c(\rho)D_w(\rho) + J_w(\rho).$$

From this point, the stabilization analysis for saturated DOF is quite challenging, in which the system (2.121) contains nonlinear couples concerned with the variable matrices. Now, let's assign the following parameter-dependent Lyapunov variables:

$$P(\rho) = \begin{bmatrix} \boldsymbol{Y}(\rho) & N(\rho) \\ N(\rho)^T & \star \end{bmatrix},\ P(\rho)^{-1} = \begin{bmatrix} \boldsymbol{X}(\rho) & M(\rho) \\ M(\rho)^T & \star \end{bmatrix}, \tag{2.122}$$

where $\star$ we don't care, $P(\rho) \in \mathbb{S}^{2n}_{++}$ is Lyapunov matrix belong to ellipsoid as region of asymptotic stability of system (2.121),

$$\mathcal{E}(P(\rho),\eta) = \left\{ \zeta(t) = [x(t)^T \quad x_c(t)^T]^T \middle|\ V(\zeta,\rho,t) = \zeta(t)^T P(\rho)\zeta(t) \le \eta^{-1},\ \rho(t) \in \mathcal{U}_p \right\}. \tag{2.123}$$

A level set of admissible initial conditions,

$$\mathcal{E}_0(P(\rho_0),\eta_0) = \left\{ \zeta(0) = [x(0)^T \quad x_c(0)^T]^T \middle|\ \zeta(0)^T P(\rho_0)\zeta(0) \le \eta_0^{-1},\ \rho_0 \in \mathcal{U}_p \right\}. \tag{2.124}$$

Then, expanding the structure of the DOF controller as follows:

$$u(t) = \mathbb{K}\zeta(t) + D_c(\rho)D_w(\rho)w(t),\ \text{with}\ \mathbb{K} = [D_c(\rho)C(\rho) \quad C_c(\rho)], \tag{2.125}$$

and defining an auxiliary dynamic controller

$$\vartheta(t) = \mathbb{G}\zeta(t),\ \text{with}\ \mathbb{G} = [G_c(\rho)C(\rho) \quad F_c(\rho)]. \tag{2.126}$$

From initial condition $\mathcal{E}_0$, the analysis of saturation constraints on auxiliary vector $\vartheta(t)$ are expanded similarly to the previous sections.

$$(\eta\overline{u}_s^2)^{-1}\left\|\vartheta_s(t)\right\|^2 = (\eta\overline{u}_s^2)^{-1}\left\|\mathbb{G}\zeta(t)\right\|^2 \le \zeta(t)^T \begin{bmatrix} \boldsymbol{Y}(\rho) & N(\rho) \\ N(\rho)^T & \star \end{bmatrix} \zeta(t),$$

$$
\begin{aligned}
&\textit{if } w(t)=0: \ \zeta(t)^T \begin{bmatrix} \boldsymbol{Y}(\rho) & N(\rho) \\ N(\rho)^T & \star \end{bmatrix} \zeta(t) \leq \zeta(0)^T \begin{bmatrix} \boldsymbol{Y}(\rho_0) & N(\rho_0) \\ N(\rho_0)^T & \star \end{bmatrix} \zeta(0) \leq \eta_0^{-1} \leq \eta^{-1}, \\
&\textit{if } w(t)\neq 0: \ \zeta(t)^T \begin{bmatrix} \boldsymbol{Y}(\rho) & N(\rho) \\ N(\rho)^T & \star \end{bmatrix} \zeta(t) \leq \zeta(0)^T \begin{bmatrix} \boldsymbol{Y}(\rho_0) & N(\rho_0) \\ N(\rho_0)^T & \star \end{bmatrix} \zeta(0) + \gamma \|w(t)\|_{\mathcal{L}_2}^2 . \\
&\qquad\qquad\qquad\qquad\qquad\qquad\qquad\qquad \leq \eta_0^{-1} + \gamma\sigma^{-1} \leq \eta^{-1}
\end{aligned} \tag{2.127}
$$

The nonlinear terms in the stabilization conditions related to system construction (2.121), or the heterogeneous form with the occurrence of $\star$ in the latter conditions, will be thoroughly handled thanks to a congruence transform presented in Section 4.4.

2.4. Conclusions

In this chapter, the fundamental concepts of LPV/quasi-LPV systems have been recapitulated. Thereby, three usual approximation forms: polytopic system, polynomial system, and polynomial-fuzzy system have been delivered, corresponding to the stability analysis and synthesis for each representation.

The stability conditions derived from the analysis of the parameter dependent Lyapunov function are presented as parametric linear matrix inequalities. Then, the relaxation methods of parameterized LMI: the gridding, the sum of squares, and the convex combination that convert the infinite-dimension conditions into the finite-dimension constraints as linear matrix inequalities. It can be solved by numerical mathematic tools (SDP, CP, etc.). Then, the design specifications and requirements for the saturated control system are discussed and analyzed based on the Lyapunov technique. The necessary and sufficient conditions deliver for the stabilization of saturation LPV systems corresponding to constrained feedback control systems.

Chapter 3.

Quadratic Stabilization Analysis for LPV/quasi-LPV Systems

In this chapter, the stability of LPV systems is solved by using an observer-based feedback control law corresponds to the $\mathscr{H}_\infty$ performance criterion. The first section devotes to the stabilizing analysis of LPV/quasi-LPV systems including:

- The observer-based feedback control stabilization delivers for the LPV systems considering the influence of disturbance and uncertain parameter. The non-convex problem related to coupling variable matrices is handled by the generalized of Young's inequality. This controller design improves the results of the quadratic conditions (Dahmani et al., 2014, 2015) and presents an adjustment to optimize the concave condition using the scaling-commuting sets, that is addressed in sections 3.1.3 and 3.2.3.2. The results show a significant enhancement in the stabilization condition application of Young's inequality (relates to the scalars considering as the weighted geometric mean).
- The stabilization condition delivered on the parametric linear matrix inequalities (PLMIs) formulation are infinite dimension, which could not solve directly by semidefinite programming (SDP) or cone programming (CP). So, the relaxation of PLMI methods is represented in section 3.2 to reformulate the design conditions to finite convex optimization problems.

A raised question about the content focuses on the stabilization analysis of the observer-based controller for the LPV system. First, it can realize that feedback control synthesis for this class of systems is well-investigated and developed. However, the conventional approach of the observer-based feedback design is conservative. In addition, the analysis and synthesis of controllers (i.e., state feedback, new observer-based feedback, output static and dynamic feedback) for the LPV saturation system will deliver in the next chapter using parameter-dependent Lyapunov functions. Therefore, this chapter is devoted to addressing the concave problem relating to quadratic stabilizing conditions and presenting the relaxation methods of the parametrized LMI conditions. A global optimization method *cone complementarity linearization* (CCL) has effectively reduced the gaps in Young's inequality and enhanced the system's performance. A quadratic Lyapunov candidate is applied to demonstrate the conservative relaxation using the CCL method for the performance and robustness requirements. Accordingly, the scaling parameters method combined with the CCL algorithm provides smaller optimal disturbance rejection values confirming the system performance improvement. In addition, the parameter-dependent conditional relaxation methods such as Gridding, parametric matrix polynomials

($\mathcal{S}$-variable, Sum of squares), convex combination (polytopic/T-S fuzzy) are presented along with the further discussions. Finally, the illustrated examples, a design PDC controller validates on a vehicle lateral stabilization and a quadruple–tank process systems.

3.1. Stabilization Analysis

3.1.1. *Norm-Bounded Input*

An unsaturated LPV system introduces by the following equations:

$$\begin{aligned} \dot{x}(t) &= A(\rho)x(t) + B(\rho)u(t) + B_w(\rho)w(t), \\ y(t) &= C(\rho)x(t) + D(\rho)u(t) + D_w(\rho)w(t), \\ z(t) &= H(\rho)x(t) + J(\rho)u(t) + J_w(\rho)w(t), \end{aligned} \tag{3.1}$$

where $x(t) \in \mathbb{R}^n$ is state vector; $y(t) \in \mathbb{R}^p, z(t) \in \mathbb{R}^r$ are measured output and regulated output vectors; $u(t) \in \mathbb{R}^m, w(t) \in \mathbb{R}^d$ are control input and disturbance input vectors. The parameters $\rho(t)$ belong to parameter spaces (2.8) - (2.9).

Now, let's consider the uncertain models for this LPV system:

$$\begin{aligned} [\Delta A(\rho) \quad \Delta B(\rho) \quad \Delta B_w(\rho)] &= M(\rho)F(t)[N_A(\rho) \quad N_B(\rho) \quad N_W(\rho)], \\ \Delta C(\rho) &= M_C(\rho)F(t)N_C(\rho), \end{aligned} \tag{3.2}$$

with the assumption $F(t)^T F(t) \preceq I,$ and a simplification on the output, then the uncertain parametric system is rewritten by:

$$\begin{aligned} \dot{x}(t) &= (A(\rho) + \Delta A(\rho))x(t) + (B(\rho) + \Delta B(\rho))u(t) + (B_w(\rho) + \Delta B_w(\rho))w(t), \\ y(t) &= (C(\rho) + \Delta C(\rho))x(t), \end{aligned} \tag{3.3}$$

This section targets to deliverer sufficient stabilized conditions for a feedback control law based on the structure observer as follows:

$$\begin{aligned} \dot{\hat{x}}(t) &= A(\rho)\hat{x}(t) + B(\rho)u(t) + L(\rho)\big(y(t) - C(\rho)\hat{x}(t)\big), \\ u(t) &= K(\rho)\hat{x}(t), \end{aligned} \tag{3.4}$$

where $K(\rho) \in \mathbb{R}^{m \times n}$ is controller gain, $L(\rho) \in \mathbb{R}^{n \times p}$ is the observer gains to be sought. Then, denoting an error estimate $e(t) = x(t) - \hat{x}(t)$ the augmented closed-loop system can be rewritten as:

$$\begin{aligned} \begin{bmatrix} \dot{x}(t) \\ \dot{e}(t) \end{bmatrix} &= \begin{bmatrix} A(\rho) + B(\rho)K(\rho) + \Delta A(\rho) + \Delta B(\rho)K(\rho) & -B(\rho)K(\rho) - \Delta B(\rho)K(\rho) \\ \Delta A(\rho) - L(\rho)\Delta C(\rho) + \Delta B(\rho)K(\rho) & A(\rho) - L(\rho)C(\rho) - \Delta B(\rho)K(\rho) \end{bmatrix} \begin{bmatrix} x(t) \\ e(t) \end{bmatrix} \\ &\quad + \begin{bmatrix} B_w(\rho) + \Delta B_w(\rho) \\ B_w(\rho) + \Delta B_w(\rho) \end{bmatrix} w(t) \\ \tilde{z}(t) &= \begin{bmatrix} H(\rho) + J(\rho)K(\rho) & -J(\rho)K(\rho) \\ 0 & H_e(\rho) \end{bmatrix} \begin{bmatrix} x(t) \\ e(t) \end{bmatrix} + \begin{bmatrix} J_w(\rho) \\ 0 \end{bmatrix} w(t). \end{aligned} \tag{3.5}$$

where $\tilde{z} \in \mathbb{R}^{r+r_e}$ is controlled output, $H_e(\rho) \in \mathbb{R}^{r_e \times n}$. Now, considering a quadratic Lyapunov function for the closed-loop system as follows:

$$x(t) \in \mathcal{D}_x, e(t) \in \mathcal{D}_e, \quad V(x,e,t) = x(t)^T P_1 x(t) + e(t)^T P_2 e(t), \tag{3.6}$$

Bases on this ellipsoidal set, a inputs with bounded $\mathcal{L}_2$-norm impose by small-gain theorem (Boyd et al., 1994). The norm-bounded conditions set directly to the input control

such that $\|u_s(t)\|^2 \leq \max|u_s(t)| \coloneqq \overline{u}_s^2,\ s=1,2,...,m.$ Imposing the constraints on observer-based feedback controller law (3.4) leads to the following result.

Lemma 3.1.1. *Giving a set of initial condition, positive scalars* $\varepsilon, \overline{u}_s$ *and a feedback control law* (3.4), *then the constraints on input signal control are enforced* $\forall t \in [0,+\infty)$ *if the following matrix inequalities hold*

$$\begin{bmatrix} 1 & * & * \\ x(0) & P_1^{-1} & * \\ P_2 e(0) & 0 & P_2 \end{bmatrix} \succeq 0, \tag{3.7}$$

$$\begin{bmatrix} P_1^{-1} & Y_1(\rho)_{(s)}^T & 0 \\ * & \overline{u}_s^2 & Y_1(\rho)_{(s)} \\ * & * & \varepsilon^{-1} P_1^{-1} \end{bmatrix} \succeq 0, \quad \begin{bmatrix} P_2 & I \\ * & \varepsilon P_1^{-1} \end{bmatrix} \succeq 0, \text{ with } s=1,2,...,m, \tag{3.8}$$

with $Y_1(\rho)_{(s)}$ symbolizes s-th row of $Y_1(\rho)$, gains controller $K(\rho) = Y(\rho)P_1^{-1}$, and ellipsoid $\mathcal{E} = \{x(t), e(t) \in \mathcal{D} \,|V(t) = x(t)^T P_1 x(t) + e(t)^T P_2 e(t) \leq 1\}$.

Proof.

Condition (3.7) directly implies the initial condition:

$$x(0)^T P_1 x(0) + e(0)^T P_2 e(0) \ \leq \ 1. \tag{3.9}$$

The limit constraints $\|u_s(t)\|^2 \leq \overline{u}_s^2$ are guaranteed if the following conditions hold:

$$\frac{1}{\overline{u}_s^2} \left\| \begin{bmatrix} K(\rho) & -K(\rho) \end{bmatrix}_{(s)} \begin{bmatrix} x(t) \\ e(t) \end{bmatrix} \right\|^2 \leq (x(t)^T P_1 x(t) + e(t)^T P_2 e(t)), \tag{3.10}$$

$$(x(t)^T P_1 x(t) + e(t)^T P_2 e(t)) \ \leq \ x(0)^T P_1 x(0) + e(0)^T P_2 e(0) \ \leq \ 1. \tag{3.11}$$

Let's set $Y(\rho) = K(\rho)X$. By using Schur's complement and then doing a congruence transformation by $diag\{X, I, I\}$ for condition (3.10) yields to:

$$\begin{bmatrix} P_1^{-1} & 0 & Y_1(\rho)_{(s)}^T \\ 0 & P_2 & -K(\rho)_{(s)}^T \\ Y_1(\rho)_{(s)} & -K(\rho)_{(s)} & \overline{u}_s^2 \end{bmatrix} \succeq 0. \tag{3.12}$$

However, the remnant of $K(\rho)_{(s)}$ in these conditions leads to a heterogeneous form. By deploying a matricial generalization of Young's inequality to eliminate these non-convex problems, we have:

$$\begin{bmatrix} 0 \\ 0 \\ -K(\rho)_{(s)} \end{bmatrix} \begin{bmatrix} 0 \\ I \\ 0 \end{bmatrix}^T + \begin{bmatrix} 0 \\ I \\ 0 \end{bmatrix} \begin{bmatrix} 0 \\ 0 \\ -K(\rho)_{(s)}^T \end{bmatrix}^T \succeq -\varepsilon^{-1} \begin{bmatrix} 0 \\ I \\ 0 \end{bmatrix} P_1 \begin{bmatrix} 0 \\ I \\ 0 \end{bmatrix}^T - \varepsilon \begin{bmatrix} 0 \\ 0 \\ Y_1(\rho)_{(s)} \end{bmatrix} P_1 \begin{bmatrix} 0 \\ 0 \\ Y_1(\rho)_{(s)} \end{bmatrix}^T. \tag{3.13}$$

Substituting (3.13) into (3.12), continually applying Schur's Lemma that entails in condition LMI (3.8).

It concludes the proof. □

The LMIs (3.8) are conservative conditions, and there is a small probability of finding a feasible solution that satisfies the stabilization problems with a preselected ε value. However, better results could be obtained if this scalar were a variable. Besides, the satisfaction of (3.8) only guarantees a necessary condition. Sufficient condition (3.11) is satisfied if the derivative of Lyapunov function (3.6) along the trajectory of the closed-loop system is negative. Further analysis will deliver in section 3.1.2.

Remark 3.1.1. The norm-bounded conditions are given in Lemma 3.1.1, and the observer-based control stabilization had been addressed in (Bui Tuan & El Hajjaji, 2018). But, the bounds on the control input has not been properly treated.

3.1.2. *Observer-based control stabilization*

In consideration of the effect of external disturbances the robustness and performance requirements of system (3.1) are consisted on finding the $\mathcal{L}_2$-gain scheduling controller $K(\rho)$ and observer $L(\rho)$ given in (3.4) that guarantee a stabilization condition concerns to a minimize disturbance rejection level $\gamma > 0$ across the frequency domain as follows:

$$\gamma^{-1}\|z(t)\|_{\mathcal{L}_2} < \gamma\|w(t)\|_{\mathcal{L}_2} \tag{3.14}$$

Use quadratic Lyapunov function (3.6) for stabilizing analysis associated with this $\mathscr{H}_\infty$ performance that leads to the following result.

Theorem 3.1.1: *In presence of parametric uncertainties and disturbances, for the positive scalars* ε_3, γ, *then closed-loop system* (3.5) *is robustly asymptotical stable corresponding to energy-to-energy index* (3.14), *if there exist matrices* $X, P_2 \in \mathbb{S}^n_{++}$, *continuously matrices function* $Y_1 : \mathcal{U}_p \to \mathbb{R}^{m\times n}$, $Y_2 : \mathcal{U}_p \to \mathbb{R}^{n\times p}$, *and scalars function* $\varepsilon_i : \mathcal{U}_p \to \mathbb{R}$, $i = 1,2,4$, *such that the PLMI*:

$$\begin{bmatrix} \Xi(\rho) & \Psi(\rho) \\ * & \Theta(\rho) \end{bmatrix} \prec 0, \tag{3.15}$$

is satisfied. Where the scheduling controller and observer gains are $K(\rho) = Y_1(\rho)X^{-1}$, $L(\rho) = P_2^{-1}Y_2(\rho)$, *and*

$$\Xi(\rho) = \begin{bmatrix} \{A(\rho)X + B(\rho)Y_1(\rho)\}^S & * & * & * & * \\ 0 & \{P_2A(\rho) - Y_2(\rho)C(\rho)\}^S & * & * & * \\ B_w^T(\rho) & B_w^T(\rho)P_2 & -\gamma I_d & * & * \\ H(\rho)X + J(\rho)Y_1(\rho) & 0 & J_w(\rho) & -\gamma I_r & * \\ 0 & H_e(\rho) & 0 & 0 & -\gamma I_{r_e} \end{bmatrix},$$

$$\Phi(\rho) = \begin{bmatrix} M(\rho) & (N_A(\rho)X + N_B(\rho)Y_1(\rho))^T & 0 & XN_C(\rho)^T & 0 & B(\rho)Y_1(\rho) & 0 \\ P_2M(\rho) & 0 & Y_2(\rho)M_C(\rho) & 0 & I & 0 & 0 \\ 0 & N_W(\rho)^T & 0 & 0 & 0 & 0 & 0 \\ 0 & 0 & 0 & 0 & 0 & J(\rho)Y_1(\rho) & 0 \\ 0 & 0 & 0 & 0 & 0 & 0 & 0 \end{bmatrix},$$

and

$$\Theta(\rho)=diag\left\{\frac{-\varepsilon_1(\rho)\varepsilon_4(\rho)I}{\varepsilon_1(\rho)+\varepsilon_4(\rho)}, -\varepsilon_1(\rho)^{-1}I, -\varepsilon_2(\rho)I, -\varepsilon_2(\rho)^{-1}I, -\varepsilon_3 X, \left[\begin{array}{c|c} -\varepsilon_3^{-1}X & * \\ \hline N_B(\rho)Y_1(\rho) & -\varepsilon_4(\rho)^{-1}I \end{array}\right]\right\}.$$

Proof.

For the sake of simplicity, the time-varying "(t)" and parameter-dependent expressions "(ρ)" are omitted from next inequality. Takes the derivative of the Lyapunov function (3.6) along the trajectories of LPV system (3.5), combines with $\mathscr{H}_\infty$ performance (3.14) that exposes:

$$2\begin{bmatrix}x\\e\end{bmatrix}^T\begin{bmatrix}X^{-1} & 0\\ 0 & P_2\end{bmatrix}\begin{bmatrix}A+BK+\Delta A+\Delta BK & -BK-\Delta BK\\ \Delta A-L\Delta C+\Delta BK & A-LC+\Delta BK\end{bmatrix}\begin{bmatrix}x\\e\end{bmatrix}+2\begin{bmatrix}x\\e\end{bmatrix}^T\begin{bmatrix}X^{-1} & 0\\ 0 & P_2\end{bmatrix}\begin{bmatrix}B_w+\Delta B_w\\ B_w+\Delta B_w\end{bmatrix}w$$
$$\gamma^{-1}\begin{bmatrix}x\\e\\w\end{bmatrix}^T\begin{bmatrix}H+JK & -JK & J_w\\ 0 & H_e & 0\end{bmatrix}^T\begin{bmatrix}H+JK & -JK & J_w\\ 0 & H_e & 0\end{bmatrix}\begin{bmatrix}x\\e\\w\end{bmatrix}-\gamma w^T w<0. \qquad (3.16)$$

Reorganizing stabilization condition (3.16) yields to:

$$\begin{bmatrix}\Omega_{11} & * & * & * & *\\ 0 & \Omega_{22} & * & * & *\\ \Omega_{31} & B_w^T(\rho)P_2 & -\gamma I_d & * & *\\ H(\rho)X+J(\rho)Y_1(\rho) & 0 & J_w(\rho) & -\gamma I_r & *\\ 0 & H_e(\rho) & 0 & 0 & -\gamma I_{r_e}\end{bmatrix}+\Omega_K+\Omega_\Delta\prec 0, \qquad (3.17)$$

with $X^{-1}=P_1,\ Y_2(\rho)=P_2L(\rho)$,

$$\Omega_K=sym\left\{\begin{bmatrix}X^{-1}(B(\rho)-\Delta B(\rho))K(\rho)\\ P_2\Delta B(\rho)K(\rho)\\ 0\\ J(\rho)K(\rho)\\ 0\end{bmatrix}\begin{bmatrix}0\\I\\0\\0\\0\end{bmatrix}^T\right\},\qquad \begin{aligned}\Omega_{11}&=sym\left\{X^{-1}A(\rho)+X^{-1}B(\rho)K(\rho)\right\},\\ \Omega_{31}&=B_w(\rho)^T X^{-1},\\ \Omega_{22}&=\left\{P_2A(\rho)-Y_2(\rho)C(\rho)\right\},\end{aligned}$$

$$\Omega_\Delta=sym\left\{\begin{bmatrix}X^{-1}M(\rho)\\ P_2M(\rho)\\ 0\\ 0\\ 0\end{bmatrix}F(t)\begin{bmatrix}(N_A(\rho)+N_B(\rho)K(\rho))^T\\ 0\\ N_W(\rho)^T\\ 0\\ 0\end{bmatrix}^T+\begin{bmatrix}0\\ -Y_2(\rho)M_C(\rho)\\ 0\\ 0\\ 0\end{bmatrix}F(t)\begin{bmatrix}N_C(\rho)^T\\ 0\\ 0\\ 0\\ 0\end{bmatrix}^T\right\}.$$

The uncertainties can be suppressed using Young's inequality (Appendix A.4):

$$\Omega_\Delta\preceq\varepsilon_1(\rho)\begin{bmatrix}(N_A(\rho)+N_B(\rho)K(\rho))^T\\ 0\\ N_W(\rho)^T\\ 0\\ 0\end{bmatrix}\begin{bmatrix}(N_A(\rho)+N_B(\rho)K(\rho))^T\\ 0\\ N_W(\rho)^T\\ 0\\ 0\end{bmatrix}^T+\varepsilon_2(\rho)\begin{bmatrix}N_C(\rho)^T\\ 0\\ 0\\ 0\\ 0\end{bmatrix}\begin{bmatrix}N_C(\rho)^T\\ 0\\ 0\\ 0\\ 0\end{bmatrix}^T$$

$$+\varepsilon_1(\rho)^{-1}\begin{bmatrix}X^{-1}M(\rho)\\P_2M(\rho)\\0\\0\\0\end{bmatrix}\begin{bmatrix}X^{-1}M(\rho)\\P_2M(\rho)\\0\\0\\0\end{bmatrix}^T+\varepsilon_2(\rho)^{-1}\begin{bmatrix}0\\Y_2(\rho)M_C(\rho)\\0\\0\\0\end{bmatrix}\begin{bmatrix}0\\Y_2(\rho)M_C(\rho)\\0\\0\\0\end{bmatrix}^T. \tag{3.18}$$

Parametric LMI (3.17) contains bilinear forms Ω_K presented in places that is difficult to perform a congruence transformation. Continue applies the tedious matrix transformation (Young's inequality) for this non-convex problem that results in:

$$\Omega_K \preceq \varepsilon_3^{-1}\begin{bmatrix}0\\I\\0\\0\\0\end{bmatrix}X^{-1}\begin{bmatrix}0\\I\\0\\0\\0\end{bmatrix}^T+\varepsilon_3\begin{bmatrix}X^{-1}(B(\rho)-\Delta B(\rho))Y_1(\rho)\\P_2\Delta B(\rho)Y_1(\rho)\\0\\J(\rho)Y_1(\rho)\\0\end{bmatrix}X^{-1}\begin{bmatrix}X^{-1}(B(\rho)-\Delta B(\rho))Y_1(\rho)\\P_2\Delta B(\rho)Y_1(\rho)\\0\\J(\rho)Y_1(\rho)\\0\end{bmatrix}^T. \tag{3.19}$$

Combining conditions (3.18), (3.19) with PLMI (3.17), consecutively deploys congruence transformation by $diag\{X,I,I,I,I\}$, and Schur's complement that ensues in:

$$\begin{bmatrix}\Xi_{11} & \Xi_{12}\\ * & \Xi_{22}\end{bmatrix} \prec 0, \tag{3.20}$$

where $\Xi_{11} \coloneqq \Xi(\rho)$ gives in (3.15), and

$$\Xi_{12}=\begin{bmatrix}M(\rho) & (N_A(\rho)X+N_B(\rho)Y_1(\rho))^T & 0 & XN_C(\rho)^T & 0 & (B(\rho)-\Delta B(\rho))Y_1(\rho)\\P_2M(\rho) & 0 & Y_2(\rho)M(\rho) & 0 & I & P_2\Delta B(\rho)Y_1(\rho)\\0 & N_W(\rho)^T & 0 & 0 & 0 & 0\\0 & 0 & 0 & 0 & 0 & J(\rho)Y_1(\rho)\\0 & 0 & 0 & 0 & 0 & 0\end{bmatrix},$$

$$\Xi_{22}=diag\left\{-\varepsilon_1(\rho)I,-\varepsilon_1(\rho)^{-1}I,-\varepsilon_2(\rho)I,-\varepsilon_2(\rho)^{-1}I,-\varepsilon_3X,-\varepsilon_3^{-1}X\right\}.$$

The uncertainties can be eliminated similarly as follows:

$$sym\begin{bmatrix}-\Delta B(\rho)Y_1(\rho)\\P_2\Delta B(\rho)Y_1(\rho)\\0\\\vdots\\0\end{bmatrix}=sym\left\{\begin{bmatrix}M(\rho)\\P_2M(\rho)\\0\\\vdots\\0\end{bmatrix}F(t)\begin{bmatrix}0\\0\\0\\\vdots\\(N_B(\rho)Y_1(\rho))^T\end{bmatrix}^T\right\}\preceq\varepsilon_4(\rho)^{-1}\begin{bmatrix}M(\rho)\\P_2M(\rho)\\0\\\vdots\\0\end{bmatrix}\begin{bmatrix}M(\rho)\\P_2M(\rho)\\0\\\vdots\\0\end{bmatrix}^T$$

$$+\varepsilon_4(\rho)\begin{bmatrix}0\\0\\0\\\vdots\\(N_B(\rho)Y_1(\rho))^T\end{bmatrix}\begin{bmatrix}0\\0\\0\\\vdots\\(N_B(\rho)Y_1(\rho))^T\end{bmatrix}^T \tag{3.21}$$

Substitutes inequality (3.21) into condition (3.20), then repeatedly applies Shur's complement that results in (3.15).

It completes the proof. □

The stability development for the feedback control system is guaranteed robustly against the influence of external disturbance and the model uncertainty conforming to the selected design values (e.g., $\gamma, \varepsilon_i, i = 1,...,4$).

Remark 3.1.2. The transformation (3.19) provides a tractable condition without imposing strong constraints like the rank of the matrix. But the use of the Young inequality (bounding lemma) usually leads to conservation. That can point out two weaknesses of this inequality. First, the upper bound is always positive, and this disadvantage is at the primary of the transform method (which cannot be improved). Second, as we can see that this approach is dependent on a wise choice of scalars $\varepsilon_i(\rho)$. If it was set as variables which turn conditions (3.18), (3.19) and (3.21) are nonconvex with bilinearity $\varepsilon_i X, \varepsilon_i(\rho), \varepsilon_i(\rho)^{-1}$.

The cone complementarity linearization CCL method (El Ghaoui et al., 1997) has been employed to handle with concave problems involved with the strategic SOF or observer-based controller designs. Nonetheless, this iterative optimization algorithm could deliver positive results if the constraints are not too complex, other than there are no guarantees for the larger scale of stability conditions.

3.1.3. *Concave Nonlinearity – Cone Complementarity Linearization*

The nonconvex or quasi-convex problem relate to nonlinearity matrix structure is frequently encountered in the stabilization condition via LMI synthesis. These problems are not easy to handle directly or cannot solve successfully by standard techniques (convex programming). A relaxation method reformates as a global optimization problem - cone complementary linearization Algorithm (El Ghaoui et al., 1997) provides a useful tool that consists in linearizing a nonconvex problem to a *canonical* form: minimizing a linear function over a difference of two convex sets. This method is commonly found in the robust control system design involving SOF synthesis or parameter uncertainty such as (Cao et al., 1998; Moon et al., 2001; Sun et al., 2009). Most of them could solve practically only problem instances of very limited size, as would be expected from the NP-hardness of these problems. In another aspect, for a more exhaustive and comprehensive analysis of this issue and other approaches of global optimization should refer to the following monographs (Konno et al., 1997; Tuy, 2016).

On the other hand, Young's inequality plays an essential role in the observer-based controller analysis method for nonlinear systems (Zemouche et al., 2017; Zemouche & Boutayeb, 2013), most of which are pre-selected or gridding within reasonable intervals with these variables. But it is *tricky* to pick the appropriate ranges of the scalars to deliver good results, which may lead to conservative design conditions.

Iterative algorithm

We now discuss a concave problem encountered in robust stabilizing conditions of the observer-based control analysis (3.15), related to bi-linearity forms εX, $\varepsilon^{-1} X$.

$$\left[\begin{array}{cc|cc} * & \cdots & I & 0 \\ * & \ddots & \vdots & \vdots \\ \hline * & * & -\varepsilon X & 0 \\ * & * & * & -\varepsilon^{-1}X \end{array}\right] \succeq 0, \tag{3.22}$$

As discussed in Appendix A.4, the role of slack-variable ε is to tighten the gaps of these inequalities and is essential to the relaxation of Young's inequality. Then, an iterative algorithm is provided to seek for the globally optimal value of the stabilization condition for the substitutions shown in (Bui Tuan et al., 2019; Bui Tuan & El Hajjaji, 2018).

Gives a new scalar $\alpha = \sqrt{\varepsilon}$, then let's assign $U = \alpha^{-1} X \alpha^{-1}$, and $S = \alpha X \alpha$. Because existing LMI tools cannot handle α and α^{-1} at the same time, so we assign a new variable $U \coloneqq \overline{\alpha} X \overline{\alpha}$, with $\overline{\alpha}$ is as a pseudo of α^{-1}. Then, in accordance with CCL method, the solution of $U \coloneqq \overline{\alpha} X \overline{\alpha}$ is to look for variables $X, U, \overline{U}, \overline{\alpha}$ such that the following problem is satisfied

$$\begin{cases} \overline{\alpha} X \overline{\alpha} \geq U, \\ \textbf{Minimize } \operatorname{Trace}\left(\overline{\alpha} X \overline{\alpha} \overline{U} + U \overline{U}\right). \end{cases} \tag{3.23}$$

Moreover, from above inequality $\overline{\alpha} X \overline{\alpha} \overline{U} \geq U \overline{U} \geq I$. Therefore, the optimal solution of the latter condition is the convergence of $\overline{U} \to U^{-1}$, and $\overline{\alpha} X \overline{\alpha} \to U$.

Now we analyze this problem by the approach of (Bui Tuan et al., 2019), then nonconvex problems (3.22) are transformed into the optimization problem as follows:

$$\textbf{Minimize } \operatorname{Trace}\left(\overline{\alpha}\alpha I_n + 0.25\left(\overline{U}U + \overline{S}S + \overline{\alpha} X \overline{\alpha} \overline{U} + \alpha X \alpha \overline{S}\right)\right) \tag{3.24}$$

subject (3.22) and the inequalities,

$$\begin{bmatrix} \overline{\alpha} & 1 \\ * & \alpha \end{bmatrix} \succeq 0, \begin{bmatrix} \overline{U} & I_n \\ * & U \end{bmatrix} \succeq 0, \begin{bmatrix} \overline{S} & I_n \\ * & S \end{bmatrix} \succeq 0, \begin{bmatrix} X & \overline{\alpha} I_n \\ * & \overline{S} \end{bmatrix} \succeq 0, \begin{bmatrix} X & \alpha I_n \\ * & \overline{U} \end{bmatrix} \succeq 0. \tag{3.25}$$

where matrix $\overline{\bigcirc}$ is as a pseudo of $\bigcirc^{-1}$, etc.

Furthermore, to *reduce* the complexity of problem (3.24) and the number of LMI constraints (3.25), then conditions (3.22) can also be reformatted to an alternative approach:

$$\left[\begin{array}{cc|cc} * & \cdots & \overline{\alpha} I & 0 \\ * & \ddots & \vdots & \vdots \\ \hline * & * & -X & 0 \\ * & * & * & -U \end{array}\right] \succeq 0, \tag{3.26}$$

with $U \coloneqq \overline{\alpha} X \overline{\alpha}$, and $\alpha \coloneqq \varepsilon^{0.5}$, $\overline{\alpha} \coloneqq \varepsilon^{-0.5}$. Pursuant to this formulation that makes conditions (3.24) and (3.25) decrease computational efforts by almost half. We obtain a reducing optimization version of original problem (3.24):

$$\textbf{Minimize } \operatorname{Trace}\left(\overline{\alpha}\alpha I_n + 0.5(\overline{U}U + \overline{\alpha} X \overline{\alpha} \overline{U})\right) \tag{3.27}$$

subject (3.22) and the inequalities,

$$\begin{bmatrix} \overline{\alpha} & 1 \\ * & \alpha \end{bmatrix} \succeq 0, \begin{bmatrix} \overline{U} & I_n \\ * & U \end{bmatrix} \succeq 0, \begin{bmatrix} X & \alpha I_n \\ * & \overline{U} \end{bmatrix} \succeq 0. \tag{3.28}$$

Then, the Cone Complementary Algorithm allows converting concave problems (3.24), (3.25) (or reduced conditions (3.27), (3.28)) into the following iterative optimization.

Algorithm 3.1. *Adapted CCL & Multi-optimization Objective*

Step 1: Choose any initial values $\gamma, \ldots$ s.t. the conditions (3.22)-(3.25) are feasible.

Step 2: Assigning above solutions be initial set $(\overline{\alpha}_0, \alpha_0, X_0, U_0, S_0, \overline{U}_0, \overline{S}_0)$ then set $k = 0$.

Step 3: Find new solution at k^{th} by solving LMI problem given as:

$$\textbf{Minimize } \text{Trace}\left(J_{1,k} + J_{2,k} + 0.25 J_{3,k}\right) \tag{3.29}$$

subject to (3.22)-(3.25), with

$$\begin{aligned} J_{1,k} &= \left(\alpha\overline{\alpha}_k + \alpha_k\overline{\alpha}\right) I_n, \\ J_{2,k} &= \overline{U}U_k + \overline{U}_k U + \overline{S}S_k + \overline{S}_k S, \\ J_{3,k} &= \overline{\alpha}X_k\overline{\alpha}_k\overline{U}_k + \overline{\alpha}_k X\overline{\alpha}_k\overline{U}_k + \overline{\alpha}_k X_k\overline{\alpha}\overline{U}_k + \overline{\alpha}_k X_k\overline{\alpha}_k\overline{U} + \\ &\quad \alpha X_k\alpha_k\overline{S}_k + \alpha_k X\alpha_k\overline{S}_k + \alpha_k X_k\alpha\overline{S}_k + \alpha_k X_k\alpha_k\overline{S}. \end{aligned}$$

Setting k^{th} optimal solution of (3.29)

Step 4: Fix a positive scalar $\delta \in \mathbb{R}^+$, and a sufficient small tolerance ϵ, if

$$\begin{aligned} &\text{Trace}\left(J_{1,k} + J_{2,k} + 0.25 J_{3,k}\right) - 14n < \delta, \\ &\text{or } \left\|\alpha_k - \overline{\alpha}_k^{-1}\right\| < \epsilon, \ \left\|U_k - \overline{U}_k^{-1}\right\| < \epsilon, \text{ and } \left\|S_k - \overline{S}_k^{-1}\right\| < \epsilon. \end{aligned} \tag{3.30}$$

satisfied, then adjusting the k^{th} optimum value of γ and go back to Step 2.

Otherwise, increase the count value-*k* by 1 and go to Step 3 within a specified iteration loop number $k < N_{\max}$. Return $\gamma^* = \gamma_k$, then exit.

By seeking for the new variables $\overline{\alpha}, \alpha, X, U, \overline{U}, S, \overline{S}$ at each loop such that the conditions (3.22)-(3.25) hold. A better value γ^* is achieved by increasing (or decreasing) their value each time the conditions (3.30) are satisfied. But it does not guarantee the *accurate* convergence of the solution. So, we only use this method just to find the epsilon coefficients, and then deploy a conjoint algorithm to efficiently achieve a better *local optimization*.

Algorithm 3.2. *Enhanced CCL & Local Optimization*

Step 1: Choose on purpose initial values $\eta, \ldots$ s.t. the conditions (3.22)-(3.25) are feasible.

Step 2: Solve steps 2 through 4 of Algorithm 3.1 to find a solution α_k that satisfies conditions (3.30), then set $\varepsilon = \alpha_k^2$.

Step 3: Optimizing γ under design stabilization LMI conditions.

The proposed iterative algorithm able to converge directly a better local region for design condition, e.g., better performance attenuation $\gamma\ldots$ It should remind that the above CCL algorithms have been improved to be better adapt to the concave structure and to converge faster to the optimal solution. As illustrated in the example section, the *varying scalars*

reduces effectively the conservation of stabilization conditions that some existing approaches are confused to find a feasible solution.

3.2. Reduction to Finite-Dimensional Problems

The purpose of this section is to present the scaling-parameter method that can be combined with the optimization algorithms in the previous section to increase the performance of the control system. As discussed in chapter two, the PLMI relaxation methods could be straightforwardly applied for stabilization condition (3.15) in Theorem 3.1.1. Hereafter, the design conditions for the saturated LPV system in the next chapters will only be presented in the parametric formulation.

It should remind that the proposed stabilizing conditions expresses as parametric dependence matric inequalities, which are infinite-dimensional problems characterized by infinite space in the range of parameters. The relaxation PLMI methods generally reformulate design condition to finitely LMIs. One of the widely known relaxation methods is the finite-dimensional meshing – *gridding techniques*, or the affine parameter-dependence distributed over each parameter subspace. The limitation of the methods is how approximate the behavior of the parameters in their operating range, including the critical points with the smallest number of discrete points.

Besides, the parameterized LMI conditions could represent as multiconvexities by polytopic or T-S fuzzy representations or tensor product transformation, that shows efficiency in reducing the numerical computation, the number of iterations, etc. An alternative approach uses the polynomial expression converted to a SoS problem is treated effectively by the SoS toolbox. The semi-definite programming (SDP) problems derived from the polynomial matrix and SoS constraints could be solved by the interior-point techniques. However, the computational time and numerical resources reserved for this method is enormous. This is a trade-off between conservative and reasonable computational efforts. In the first part, the piecewise-affine parameter, the sum of squares, and the convex combination (fuzzification) are manipulated to relax the parametric LMIs.

3.2.1. *Finite Discretization of Parametrized LMIs via*

The first discussion deserves for the discretization of parametrized LMIs into finite multiple subspaces without knowledge of the density of the parameters. Define a parameter set as follows:

$$\mathcal{F}_p \coloneqq \{\rho \in \mathcal{C}^1([t_0,\ \infty), \mathbb{R}^{N_p}) : \rho(t) \in \mathcal{U}_p\}. \tag{3.31}$$

This approach is applicable for almost all types of parameterized LMIs conditions.

Example 3.2.1 Let us consider the PDLF candidates such as:

$$X(\rho) = X_0 + X_1 \sin(\rho) + X_2 \cos(\rho), \text{with } \rho(t) \in [-\pi/2,\ \pi/2], \tag{3.32}$$

$$\text{or in the form } X(\rho) = X_0 + X_1\rho(t) + X_2\rho(t)^2, \text{with } \rho(t) \in [-1,\ 1]. \tag{3.33}$$

We now seek for symmetric matrices X_0, X_1, X_2 such that $X(\rho) \succ 0$ for $\forall \rho(t) \in \mathcal{U}_p$ has

belonged to a subset $\rho(t) \in [-\pi/2,\ \pi/2]$ (or $\rho(t) \in [-1, 1]$). These conditions need to *simultaneously verify* the feasibility at *N*- discretized points of the parameter range.

It should mention that the parametric-dependent conditions are converted effortlessly into the multiple LMIs, but there is a probability of missing essential information (critical points). Precisely, the gridding points must be enormous to cover exactly the behavior of the parameters. That entails in the exponentially increasing number of the solved conditions. Alternatively, the piecewise affine parameter-dependent is introduced in the works (Apkarian & Tuan, 2000; Lim, 1998; Tuan & Apkarian, 1999) assigning continuous subspace domains.

Let us now introduce a simplification of the method piecewise switching-dependent functional. Giving the set of parameters $\rho(t) \in \mathcal{U}_p$, then it is distributed into *m* subspace parameter domains as follows:

$$\theta_k(t) \in \overline{\mathcal{U}_p} := \cap_{k=1}^{m} \mathcal{U}_{p,k} \subset \mathbb{R}^m,\ \forall \theta_k(t) \in [\rho_k, \rho_{k+1}],\ k = 1,\ldots,m, \tag{3.34}$$

and define a piecewise function:

$$\sigma_k(\rho) = \begin{cases} 1 & \text{if } \rho(t) \in \mathcal{U}_{pk} \\ 0 & \text{otherwise} \end{cases},\ \text{with } k = 1,\ldots,m. \tag{3.35}$$

By using the local affine parameter-dependent subsets, the parameter is represented by:

$$\rho(t) = \sum_{k=1}^{m} \sigma_k(\rho) \sum_{i=1}^{2} \lambda_{ki}(\theta_k)\, \rho_{k+i-1},\ \text{with } \sum_{i=1}^{2} \lambda_{ki}(\theta_k) = 1\ ,\ k = 1,\ldots,m. \tag{3.36}$$

where $\rho(t) \in [\underline{\rho}, \overline{\rho}]$, divided into *m* segments $\rho_k = k\Delta\rho + \underline{\rho}$, and $\Delta\rho = (\overline{\rho} - \underline{\rho})/m$.

The association of gridding and local affine provides a less conservative and smoother model than the traditional one. It is worth noting that we can check for the *m*-points of the continuous subset converted to convex linear combinations of $\theta_k(t)$.

3.2.2. *Polynomial Parameter-Dependent LMIs via Sum-of-Squares*

As introduced in Chapter 2, a polynomial of parameter dependence matrices inequality could address by the SoS approach or Slack-Variable (SV) approach. This method decomposes the sum-of-squares polynomials, then converts them to a convex coordinate transformation (related to the coefficients of the polynomials over the defined domain of the parameter). This parametrized relaxation converts the parameter-dependence matrix inequalities to the Sum-of-Squares expression, which means *positive definite* (guaranteed with a minor deviation). As mentioned by (Prajna et al., 2004), the scalar variables defined by a set of polynomial inequalities (*vars* and *decvars*) concerned the variation of the $\mathcal{S}$-procedure constraints where the pre-selected scalars. In such an approach, the parameter values are not constant, giving more relaxation in stability conditions.

The sum of squares decomposition has limitations in the experiment application, even for a simple structure of the polynomial gain-scheduling e.g., $X(\rho) = X_0 + \rho X_1 + \rho^2 X_2$, the feasible solution of the stabilization conditions results in higher orders of the polynomials. For example, a structured controller classically decomposes by $K(\rho) = Y(\rho)X(\rho)^{-1}$, that

ensues in a complicated fraction form in monomials. This method is evident an illustration of trade-off between computational burden and conservativeness.

SV-LMI-based control design

The slack-variable method has shown convenience for control synthesis and applicability in analyzing the parametric polynomial dependency matrix structure. This relaxation method based on the generalization of Finsler's lemma characterized via quadratic relations generalized $\mathcal{S}$-Lemma (so-called $\mathcal{S}$-procedure). In this aspect, a comparison between the SoS formulation and the $\mathcal{S}$-variable approach has been delivered in (Sato & Peaucelle, 2007a, 2007b).

Based on the SoS decomposition, this methodology cast the polynomial expression as a semidefinite programming problem. Let assign $Z(\rho)$ are vector of monomials in $\rho=[\rho_1,\rho_2,...,\rho_{N_p}]\in\mathcal{U}_p$ (*vars*) and coefficients $a_{i,j}(\rho)$ are decision variables (*decvars*). Then, the parameter dependent matrix involving in constructing vectors of monomials introduced as follows:

$$\mathcal{M}(a,\rho)=\mathcal{M}_0(a)+\sum\nolimits_j^{N_p}\mathcal{M}_j(a)Z_j(\rho). \tag{3.37}$$

where $\mathcal{M}_j(a)\in\mathbb{S}^n$, and $a\in\mathbb{R}^c$.

Lemma 3.2.1. (Apkarian & Tuan, 2000) *Let us consider a parameterized linear matrix* (3.51) *is represented as a spectral formulation of polynomial matrix inequality constraint*

$$\Theta(\rho)_\perp^T\mathcal{M}(a)\Theta(\rho)_\perp \succ 0, \tag{3.38}$$

The condition (3.38) *is satisfied* $\forall\rho\in\mathcal{U}_p$, *if exits the symmetric matrix* $\mathcal{M}(a), a\in\mathbb{R}^c$, *decomposed in* (3.37), *and a slack-variable matrix* $\mathcal{P}$ *with appropriate dimensions such that the following parameterized condition*

$$\mathcal{M}(a)+\mathcal{P}^T\Theta(\rho)+\Theta(\rho)^T\mathcal{P} \succ 0. \tag{3.39}$$

hold, where $\Theta(\rho)_\perp$ *is an orthogonal matrix gathering monomials occurring in the PLMIs.*

With an appropriate choice of $\Theta(\rho)_\perp$ could yield to $\Theta(\rho)=\sum_j^{N_p}\Theta_j\rho_j$.

Example 3.2.2. Consider the following polynomial

$$\begin{aligned}&\mathcal{M}(a,\rho)=a_4\rho^4+a_3\rho^3+a_2\rho^2+a_1\rho+a_0,\\&\text{with } a_4=-1,\ a_3=10,\ a_2=18,\ a_1=-86,\ a_0=102,\ \rho\in\mathbb{R}.\end{aligned} \tag{3.40}$$

Since, a_4 – the coefficient of highest order monomial is negative and the derivative $\partial\mathcal{M}(a,\rho)/\partial\rho=0$ has three distinct solutions, then polynomial (3.40) exists a global extreme. We seek the maximum value of this polynomial by using the $\mathcal{S}$-variable method then compare it with the SoS method and theoretical one. The problem rewrites into the following statement:

minimize γ such that,

$$\mathcal{M}(a,\rho,\gamma)=\mathcal{M}(a,\rho)-\gamma \le 0,\ \ \forall\rho\in\mathbb{R}. \tag{3.41}$$

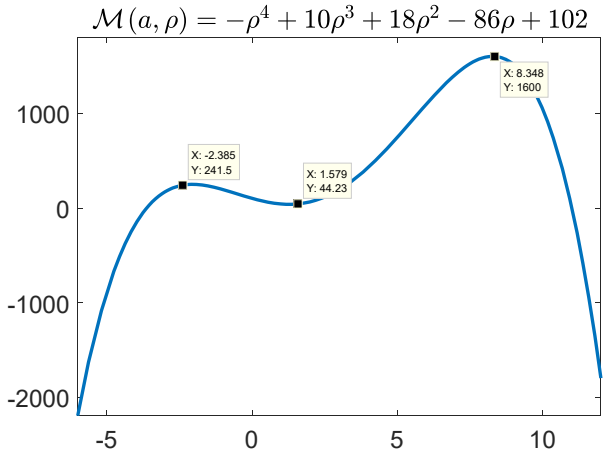

Figure 3-1. *The extreme points of the polynomial in the interval* $[-6, 12]$.

Uses the decomposition method for polynomial (3.40), then the optimization problem (3.41) is rewrite in the spectral form:

$$\mathcal{M}(a,\rho,\gamma) = \begin{bmatrix} 1 \\ \rho \\ \rho^2 \end{bmatrix}^T \underbrace{\begin{bmatrix} -\gamma+102 & -43 & 6 \\ * & 6 & 5 \\ * & * & -1 \end{bmatrix}}_{\mathcal{M}(a,\gamma)} \underbrace{\begin{bmatrix} 1 \\ \rho \\ \rho^2 \end{bmatrix}}_{\Theta(\rho)_\perp} \leq 0 \tag{3.42}$$

Applying Lemma 3.2.1 to PLMI (3.42), we have a following condition:

$$\mathcal{M}(a,\gamma) + \mathcal{P}^T\Theta(\rho) + \Theta(\rho)^T\mathcal{P} \preceq 0, \tag{3.43}$$

where $\mathcal{P}$ is slack-variable matrix and $\Theta(\rho)\Theta(\rho)_\perp = 0$. One reasonable choice is given by

$$\Theta(\rho) = \begin{bmatrix} \rho & -1 & 0 \\ 0 & \rho & -1 \end{bmatrix}. \tag{3.44}$$

Although the polynomial (3.43) has a global extreme, we cannot solve the above optimization problem on the whole domain of ρ. For simplicity, we choose a local domain $\rho \in [\underline{\rho}, \overline{\rho}]$ so that could cover all 3 extreme points $\partial\mathcal{M}(a,\rho)/\partial\rho = 0$. In combining with PLMI (3.43) and optimization problem (3.41), we get:

minimize γ with $\rho \in [\underline{\rho}, \overline{\rho}]$, such that:

$$\mathcal{Q}(\rho,\gamma) = \begin{bmatrix} -\gamma+102 & -43 & 6 \\ * & 6 & 5 \\ * & * & -1 \end{bmatrix} + \mathcal{P}^T \begin{bmatrix} \rho & -1 & 0 \\ 0 & \rho & -1 \end{bmatrix} + \begin{bmatrix} \rho & -1 & 0 \\ 0 & \rho & -1 \end{bmatrix}^T \mathcal{P} \preceq \tag{3.45}$$

We now compare the results in turn using the following methods:

- The $\mathcal{S}$-variable LMI polytope $\gamma_{SV1} = \gamma_{opt}$:

  minimize γ s.t.,

  $$\mathcal{Q}(\underline{\rho},\gamma) \preceq 0, \qquad \mathcal{Q}(\overline{\rho},\gamma) \preceq 0. \tag{3.46}$$

- The $\mathcal{S}$-variable LMI Gridding-N $\gamma_{SV2} = \gamma_{opt}$:

  minimize γ s.t.,

  $$\mathcal{Q}(\underline{\rho}, \gamma) \preceq 0, \qquad \mathcal{Q}(\underline{\rho} + i\delta, \gamma) \preceq 0, \qquad \mathcal{Q}(\overline{\rho}, \gamma) \preceq 0, \tag{3.47}$$

  with $i = 1, \ldots, N-1$, and interval $\delta = (\overline{\rho} - \underline{\rho})/N$.

- The sum of squares decomposition $\gamma_{SoS} = \gamma_{opt}$:

  minimize γ s.t., $\quad \gamma - \mathcal{M}(a, \rho) \succeq 0, \quad$ with $\rho \in [\underline{\rho}, \overline{\rho}]$. (3.48)

- The theoretical approach:

  $$\gamma_T = \sup_{\rho \in [\underline{\rho}, \overline{\rho}]} \mathcal{M}(a, \rho). \tag{3.49}$$

With $\underline{\rho} = -6$, $\overline{\rho} = 12$, solving SDPs (3.46), we obtain slack-variable matrix

$$\mathcal{P} = \begin{bmatrix} 13.9073 & 40.0716 & -2.4979 \\ -22.7663 & -2.2947 & 0.3019 \end{bmatrix}, \tag{3.50}$$

and the optimal values, respectively,

$$\begin{aligned} \gamma_T &= 1600.358242052000, \\ \gamma_{SV1} &= 1600.358239279673, \quad \rightarrow \quad e_1 = \gamma_T - \gamma_{SV1} = 2.772326524791424 \cdot 10^{-6}, \\ \gamma_{SV2} &= 1600.358242271239, \quad \rightarrow \quad e_2 = \gamma_T - \gamma_{SV2} = 2.192391548305750 \cdot 10^{-7}, \\ \gamma_{SoS} &= 1600.358215350658, \quad \rightarrow \quad e_3 = \gamma_T - \gamma_{SoS} = 2.670134199433960 \cdot 10^{-5}. \end{aligned}$$

The $\mathcal{S}$-variable approach provides better results, and closes to the theoretical technique (error e_1, e_2). The interesting point is that the $\mathcal{S}$-variable is solved at the boundaries (two points) also gives a positive result where error e_1 approximates to error e_2 obtained by 19 points gridding in the range $[-6, 12]$. When solving simple parameter dependency conditions, the $\mathcal{S}$-variable gives better convergence results than SoS decomposition. However, for large-scale conditions, the SoS toolbox handles the PLMI conditions more delicately with fewer additional slack variables.

Besides, the mathematical programming software such as MATLAB® effortlessly returns the invertible matrix as fractions of the parameters with large polynomial exponents. But, the possibility of the implementation in practice is questionable. Another approach, more conservative, the LMI conditions are directly delivered by the linear combination of the vertices of the parametric convex domain. The two well-known methods are the T-S fuzzy and Polytopic models. There was no difference in the representations of the two systems but a distinction in the stabilizing control synthesis for the PDC scheme and polytopic gain-scheduling, respectively.

3.2.3. *Parametrical Dependent LMIs via Convex Combination*

Given compact parameter set $\rho(t) \in \mathcal{U}_p$. There exists a linear parallel to transform the basis conversion bilinear mapping and linear conservation from the parametric dependent function $\mathcal{F}_{\mathcal{P}} := \{\rho \in \mathcal{C}^1([t_0, \infty), \mathbb{R}^{N_p}) \mid \rho_i(t) \in \mathcal{U}_p, \ i = 1, \ldots, N_p\}$ to

$$\mathcal{F}_{\mathcal{Q}} := \left\{\theta \in \mathcal{C}^1([t_0,\ \infty), \mathbb{R}_+^{N_p}) |\ \theta_i(t) \in \mathcal{U}_p,\ i = 1,\ldots,N_p\right\}. \tag{3.51}$$

where $\mathcal{U}_q = \{\theta_i \in [0,\ 1], i = 1,\ldots,N_p\} \subset \mathbb{R}^{N_p}$.

The conversion of the parametric coordinate system to the convex coordinate system

$$\rho_i(t) \to \theta_i(t) \to \lambda_j(t),\ \sum_{j=1}^{N_l} \lambda_j(t) = 1,\ j = 1,\ldots,N_l \tag{3.52}$$

has been discussed in Chapter 2. However, the reverse transformation is rarely mentioned in many documents. Such an algebraic transformation method is presented in Appendix A.1.4.1, which allows for the generalization of the coordinates expression of the multi-convex system. In the next section, a Lyapunov quadratic is considered for the stability analysis of a T-S fuzzy system.

3.2.3.1. *T-S Fuzzy Controller Stabilization Construction*

The fuzzification and defuzzification are applied to convert the parametric dependent conditions to the linear combination forms. Let's introduce a convex combination of affine system (3.5) and a feedback parallel distributed compensation controller by using rules (3.52) as follows:

$$\begin{aligned}
\begin{bmatrix}\dot{x}(t)\\ \dot{e}(t)\end{bmatrix} &= \sum_{i,j=1}^{N_l} \lambda_i(t)\lambda_j(t) \begin{bmatrix} A_i + B_iK_j + \Delta A(\rho) + \Delta B_iK_j & -B_iK_j - \Delta B_iK_j \\ \Delta A_i - L_i\Delta C_i + \Delta B_iK_j & A_i - L_iC_i - \Delta B_iK_j \end{bmatrix} \begin{bmatrix} x(t)\\ e(t)\end{bmatrix} \\
&\quad + \sum_{i=1}^{N_l} \lambda_i(t) \begin{bmatrix} B_{w,i} + \Delta B_{w,i} \\ B_{w,i} + \Delta B_{w,i}\end{bmatrix} w(t), \\
z(t) &= \sum_{i,j=1}^{N_l} \lambda_i(t)\lambda_j(t) \begin{bmatrix} H_i + J_iK_j & -J_iK_j \\ 0 & H_{e,i}\end{bmatrix} \begin{bmatrix} x(t)\\ e(t)\end{bmatrix} + \sum_{i=1}^{N_l} \lambda_i(t) \begin{bmatrix} J_{w,i}\\ 0\end{bmatrix} w(t), \\
u(t) &= \sum_{j=1}^{N_l} \lambda_j(t) [K_j \quad -K_j] \begin{bmatrix} x(t)\\ e(t)\end{bmatrix}.
\end{aligned} \tag{3.53}$$

where the parametric matrix is convexified by the membership function (3.52) as follows

$$\{A(\rho),\ B(\rho),\ K(\rho),\ B_w(\rho),\ldots\} = \sum_{i=1}^{N_l} \lambda_i(t) \{A_i,\ B_i,\ K_i,\ B_{w,i},\ldots\}. \tag{3.54}$$

By considering a quadratic Lyapunov function candidate (3.6) that leads to the following relaxation of stabilization PLMI condition.

Theorem 3.2.1: (Bui Tuan et al., 2019) *In presence of parametric uncertainties and disturbances, for the positive scalars* $\varepsilon_k, \gamma,$ *with* $k = 1,\ldots,4,$ *closed-loop system* (3.53) *is asymptotically stable corresponding to energy-to-energy index* γ *given in* (3.14), *if there exist matrices* $X, P_2 \in \mathbb{S}_{++}^n,$ *and matrices* $Y_{1,j} \in \mathbb{R}^{m\times n}$, $Y_{2,i} \in \mathbb{R}^{n\times p},$ *such that the linear matrix inequality* :

$$\frac{1}{2}\begin{bmatrix}\Xi_{ij} & \Psi_{ij}\\ * & \Theta_{ij}\end{bmatrix} + \frac{1}{2}\begin{bmatrix}\Xi_{ji} & \Psi_{ji}\\ * & \Theta_{ji}\end{bmatrix} \prec 0,\ \ with\ i \geq j,\ i,j = 1,2,\ldots,N_l, \tag{3.55}$$

are satisfied, then the controller gains and the observer gains are given by $K_j = Y_{1,j}X^{-1}$, $L_i = P_2^{-1}Y_{2,i}$, *where*

$$\Xi_{ij}=\begin{bmatrix}\{A_iX+B_iY_{1,j}\}^S & * & * & * & *\\ 0 & \{P_2A_i-Y_{2,i}C_i\}^S & * & * & *\\ B_{w,i}^T & B_{w,i}^TP_2 & -\gamma I_d & * & *\\ H_iX+J_iY_{1,j} & 0 & J_{w,i} & -\gamma I_r & *\\ 0 & H_{e,i} & 0 & 0 & -\gamma I_{r_e}\end{bmatrix},$$

$$\Phi_{ij}=\begin{bmatrix}M_i & (N_{A,i}X+N_{B,i}Y_{1,j})^T & 0 & XN_{C,i}^T & 0 & B_iY_{1,j} & 0\\ P_2M_i & 0 & Y_{2,i}M_i & 0 & I & 0 & 0\\ 0 & N_{W,i}^T & 0 & 0 & 0 & 0 & 0\\ 0 & 0 & 0 & 0 & 0 & J_iY_{1,j} & 0\\ 0 & 0 & 0 & 0 & 0 & 0 & 0\end{bmatrix},$$

and

$$\Theta_{ij}=diag\left\{-\frac{\varepsilon_{1,i}\varepsilon_{4,i}}{\varepsilon_{1,i}+\varepsilon_{4,i}}I,\ -\varepsilon_{1,i}^{-1}I,\ -\varepsilon_{2,i}I,\ -\varepsilon_{2,i}^{-1}I,\ -\varepsilon_3X,\ \left[\begin{array}{c|c}-\varepsilon_3^{-1}X & *\\ \hline N_{B,i}Y_{1,i} & -\varepsilon_{4,i}^{-1}I\end{array}\right]\right\}.$$

Proof.

The demonstration is directly inferred from the parameter-dependent condition in Theorem 3.1.1 with the use of linear convex combinations (3.52). We now look for a stabilization feedback control $K(\rho)=\sum_{j=1}^{N_l}\lambda_j(t)K_j=\sum_{j=1}^{N_l}\lambda_j(t)Y_{1,j}X^{-1}$, and observer gain $L(\rho)=\sum_{i=1}^{N_l}\lambda_i(t)L_i=P_2^{-1}\sum_{i=1}^{N_l}\lambda_i(t)Y_{2,i}$, such that closed-loop system (3.53) ensures the designed robustness and performance requirements. Similarly, from PLMI condition (3.15) yields to the following LMIs:

$$\sum\nolimits_{i,j=1}^{N_l}\lambda_i(t)\lambda_j(t)\begin{bmatrix}\Xi_{ij} & \Psi_{ij}\\ * & \Theta_{ij}\end{bmatrix}\prec 0,\ \text{with}\ \sum_{i=1}^{N_l}\lambda_i(t)=1,\ \forall\lambda_i(t)\in[0,\ 1],i,j=1,...,N_l. \qquad (3.56)$$

Then, following the property of convex combinations, if each condition at each vertex is satisfied, condition (3.56) holds. Next, by applying a relaxation of the stabilization condition approach (Tanaka et al., 1998) that yields to (3.55).

□

The stabilizability of PDC controller and relaxing LMI conditions can find in (Tanaka & Wang, 2001; Tuan et al., 2001) for quadratic Lyapunov function and for fuzzy Lyapunov function (Tanaka et al., 2003). It should note that the fuzzy Lyapunov functions (FLF) reduces conservatism in design conditions. And, the derivative of the membership function relates to $\dot{X}(\rho)=\sum_{k=1}^{N_l}\dot{\lambda}_k(t)X_k$ could expand as method of (Sala & Ariño, 2009). This issue is encountered in the next chapter.

Now, let impose the constraints for the PDC control law of system (3.53) by taking advantage of PLMI condition (3.7), (3.8) that entails in the following results.

Lemma 3.2.2. *Giving a set of initial condition, positive scalars* $\varepsilon,\overline{u}_s$ *and a feedback control law* (3.53)*. Then constraints on input signal control is enforced* $\forall t\in[0,+\infty)$ *if the following matrix inequalities hold*

$$\begin{bmatrix} 1 & * & * \\ x(0) & X & * \\ P_2 e(0) & 0 & P_2 \end{bmatrix} \succeq 0, \tag{3.57}$$

$$\begin{bmatrix} X & \frac{1}{2}\left(Y_{1,i(s)}^T + Y_{1,j(s)}^T\right) & 0 \\ * & \overline{u}_s^2 & \frac{1}{2}\left(Y_{i(s)} + Y_{j(s)}\right) \\ * & * & \varepsilon^{-1} P_1^{-1} \end{bmatrix} \succeq 0, \quad \begin{bmatrix} P_2 & I \\ * & \varepsilon X \end{bmatrix} \succeq 0, \text{ if } i \geq j, \tag{3.58}$$

where ellipsoid $\mathcal{E}\left(X^{-1}, P_2, 1\right) := \{x(t), e(t) \in \mathcal{D} \,|V(t) = x(t)^T X^{-1} x(t) + e(t)^T P_2 e(t) \leq 1\}$ and gains controller $K_i = Q_{1i} X^{-1}$, with $i, j = 1, \ldots, N_l$, and $s = 1, 2, \ldots, m$.

Proof.

The proof is omitted because it is deduced as a linear combination version of the PLMI condition in Lemma 3.1.1.

□

Remark 3.2.1. The norm bounded condition in Lemma 3.2.2 is purposely associated with the stabilization condition (3.55) to demonstrate the effectiveness of the relaxation method – CCL algorithm on a T-S fuzzy system and compares to the generalized sector condition. In the result section, we show a comparison of the pre-selection epsilon method (Benzaouia & Hajjaji, 2014; Dahmani et al., 2014, 2015; El Hajjaji et al., 2006; Kheloufi et al., 2013b; Zemouche et al., 2017) with the CCL iteration algorithms (combining with scaling parameters).

Problem 3.2.1. For the control synthesis based on convex combination framework:

What is an essential distinction between the stabilized condition structure analyzed for a T-S fuzzy system and a Polytopic system?
(*In another view, what is the difference between a structure PDC controller and a polytopic gain-scheduling controller in control system design?*)

Let's consider a state feedback controller construction

$$u(t) = \sum\nolimits_{i=1}^{N_l} \lambda_i(t) K_i x(t), \quad \sum_{i=1}^{N_l} \lambda_i(t) = 1, \ \forall \lambda_i(t) \in [0, \ 1], \ i = 1, \ldots, N_l. \tag{3.59}$$

At first glance, it does not show difference in the control analysis of the two approaches. Supposes the parameters $\rho(t)$ belongs to $[\underline{\rho}, \ \overline{\rho}]$, then the rules set on local system:

$$\textit{T-S Fuzzy}: \ \dot{x}(t) = A_i x(t) + B_i \sum\nolimits_{j=1}^{N_l} \lambda_j(t) K_j x(t), \qquad A_{cl,ij} = A_i + B_i K_j, \tag{3.60}$$

$$\textit{Polytopic}: \ \dot{x}(t) = A_i x(t) + B_i K_i x(t), \qquad A_{cl,i} = A_i + B_i K_i. \tag{3.61}$$

Based on Lyapunov quadratic stability analysis, we have the following statements:
If there exists a common positive definite matrix $P \succ 0$ *such that*

$$\textit{T-S Fuzzy}: \ \tfrac{1}{2}\left(A_{cl,ij}^T P + A_{cl,ji}^T P\right) + \tfrac{1}{2}\left(P A_{cl,ij} + P A_{cl,ji}\right) \prec 0, \text{ with } i \geq j, \ i, j = 1, \ldots, N_p. \tag{3.62}$$

Polytopic: $A_{cl,i}^T P + P A_{cl,i} \prec 0,\ i = 1,\ldots,N_p.$ (3.63)

The control analysis of the Polytopic system seems to be the switching of the ***individual*** stabilized LTI systems corresponding to the operating regions of the parameter coordinates. The T-S fuzzy system is an ***alternate*** combination of LTI systems that in each operating area is a stabilized PDC control rule (even gain control K_j are sometimes not stabilization law of local linear systems A_i, B_i, with $i \neq j$). Specifically, in some case $(A_{cl,ij}^T P + P A_{cl,ij}) \succeq 0$, but $\frac{1}{2}(A_{cl,ij}^T P + A_{cl,ji}^T P) + \frac{1}{2}(P A_{cl,ij} + P A_{cl,ji}) \prec 0$, that gives more relaxation of the stabilizing conditions.

3.2.3.2. *Reducing Conservatism – Parameter-Dependent Scaling*

It can realize that the scalars $\varepsilon_i(\rho)$ related to the Young inequality parameterized in the design conditions of theorems Theorem 3.1.1, e.g., inequalities (3.18), (3.19), and (3.21). In the conventional approaches using CCL, authors often simplify scalars $\varepsilon_i \in \mathbb{R}$. In this section, an enhancement of the CCL condition associated with a set of uncertain parameters develops via the linear combinations.

In robust control theory, the set of scaling associated with the uncertain structure is considered to be compatible with the LPV control synthesis. In this approach, the *scaling small-gain theorem* or *structured-robust stability* (Apkarian & Adams, 1998; Apkarian & Gahinet, 1995) is probably the most commonly known, which delivers a less conservative stabilizing condition associated with the scaling matrices depends on uncertain parameters. We employ the scaled parameters to conditions (3.18), (3.19), and (3.21) concerning with the following three cases:

- *Variables*: looking for $\varepsilon_1, \varepsilon_2, \varepsilon_4 \in \mathbb{R}$.
- *Polytope*: searching for scalars $\varepsilon_{1,j}, \varepsilon_{2,j}, \varepsilon_{4,j} \in \mathbb{R}$, where $\varepsilon_i(\rho) = \sum_{j=1}^{N_l} \lambda_j(t) \varepsilon_{i,j}$, with $i = 1,2,4,\ j = 1,2,\ldots,N_l$ acts as a scaling-scalar in these conditions.
- *Scaling matrix*: seeking diagonal matrices $\Lambda_{1,j}, \Lambda_{2,j}, \Lambda_{4,j}$ s.t. $\Lambda_i(\rho) = \sum_{j=1}^{N_l} \lambda_j(t) \Lambda_{i,j}$, with $i = 1,2,4,\ j = 1,2,\ldots,N_l$, and $\Lambda_i(\rho)$ replace of $\varepsilon_i(\rho) I$ in these conditions.

which provide an efficiency improvement system performance and reduce conservatism of design conditions. It can more accurately describe the behavior of the gain scheduling on uncertain parameters $\rho(t)$. When the scalars are considered as variables, the nonconvex problems relating to nonlinearity $\varepsilon_{ij}, \varepsilon_{ij}^{-1}$, and $\varepsilon_3 W, \varepsilon_3^{-1} W$ can be handled by the global optimization algorithm in section 3.1.3.

3.3. Example

In this section, the numerical results are implemented to demonstrate the performance and robustness improvements using the CCL method, a quadratic Lyapunov candidate is applied on the most conservative condition – observer-based control stabilization.

We employ the design controller based on the structure observer to stabilize the quadruple–tank process system, and the vehicle lateral dynamic system with the influence of

external disturbance and uncertain parameters. The PLMI stabilization conditions in Theorem 3.1.1 (without saturation constraint) is relaxed to the stabilizing LMIs, respectively, conditions of Theorem 3.2.1. Firstly, we discuss on the results of (Bui Tuan et al., 2019), demonstrating the effectiveness of the proposed method when using Young's inequality in combination with the global optimal algorithm CCL.

In the following analysis, the results of (Bui Tuan et al., 2021; Bui Tuan & El Hajjaji, 2018) will be reproduced to compare with the other results. In this section, At the same time, we deploy the stabilization condition of Theorem 3.2.1 associated with norm bounded inputs of Lemma 3.2.2 for system (3.70) compared with the stabilization condition of feedback control. By pre-selecting the initial conditions and using Algorithm 3.1 (CCL1) & Algorithm 3.2 (CCL2) to minimize the performance criterion γ, the comparison are given.

Quadruple–tank process system

Let's consider a quadruple–tank process system (Johansson, 1997) with diagram shown in Figure 3-2.

Example 3.3.1: The continuous–time nonlinear dynamical system is represented by the following equations:

$$\begin{aligned}
\dot{h}_1(t) &= -\frac{a_{s,1}}{A_{s,1}}\sqrt{2gh_1(t)} + \frac{a_{s,3}}{A_{s,1}}\sqrt{2gh_3(t)} + \frac{\gamma_1(t)k_{v,1}}{A_{s,1}}V_1(t),\\
\dot{h}_2(t) &= -\frac{a_{s,2}}{A_{s,2}}\sqrt{2gh_2(t)} + \frac{a_{s,4}}{A_{s,2}}\sqrt{2gh_4(t)} + \frac{\gamma_2(t)k_{v,2}}{A_{s,2}}V_2(t),\\
\dot{h}_3(t) &= -\frac{a_{s,3}}{A_{s,3}}\sqrt{2gh_3(t)} + \frac{(1-\gamma_2(t))k_{v,2}}{A_{s,3}}V_2(t),\\
\dot{h}_4(t) &= -\frac{a_{s,4}}{A_{s,4}}\sqrt{2gh_4(t)} + \frac{(1-\gamma_1(t))k_{v,1}}{A_{s,4}}V_1(t),
\end{aligned} \tag{3.64}$$

where $h_i(t)$ are the liquid level in tank $-i$, $i=1,2,3,4$; $A_{s,i}$ are the cross sectional area of tank $-i$; $a_{s,i}$ are the outlet cross-sectional area of tank $-i$; $\gamma_j(t)\in[0,\ 1], j=1,2$ are time-varying valve flow ratio; $V_j(t)$ are the voltage control signal of Pump $-j$ with the corresponding coefficient $k_{v,j}$. The measurement voltage (V) on output signal $y(t)\in\mathbb{R}^p$, are assumed proportional to level measurement (cm) of tank 1 and tank 2. For further description of the parameters of tank process model and fuzzyfication analysis, refer to Appendix E.1. Based on this T-S fuzzy rules and the set of membership function, the quadruple–tank process can be represented as follows:

$$\begin{aligned}
\dot{x}(t) &= \sum\nolimits_{i=1}^{8}\mu_i(\lambda,\theta)\big((A_i+\Delta A_i(t))x(t)+B_iu(t)\big)+B_ww(t),\\
y(t) &= (C+\Delta C(t))x(t).
\end{aligned} \tag{3.65}$$

The flow disturbance from pump to tanks is presented by the following equation:

$$w(t) = [\sin(30\pi t)\quad \cos(20\pi t)\quad -\sin(26\pi t)\quad \sin(31\pi t)]^T. \tag{3.66}$$

The nominal constant matrices $A_i\in\mathbb{R}^{4\times4}, B_i\in\mathbb{R}^{4\times2},$ and $C\in\mathbb{R}^{2\times4}$ are given:

$$A_i = \begin{bmatrix} \frac{-a_{s,1}\sqrt{2g}C_{fz,j}}{A_{s,1}} & 0 & \frac{a_{s,3}\sqrt{2g}C_{fz,j}}{A_{s,1}} & 0 \\ 0 & \frac{-a_{s,2}\sqrt{2g}C_{fz,j}}{A_{s,2}} & 0 & \frac{a_{s,4}\sqrt{2g}C_{fz,j}}{A_{s,2}} \\ 0 & 0 & \frac{-a_{s,3}\sqrt{2g}C_{fz,j}}{A_{s,3}} & 0 \\ 0 & 0 & 0 & \frac{-a_{s,4}\sqrt{2g}C_{fz,j}}{A_{s,4}} \end{bmatrix},$$

coefficients $C_{fz,j}$, $j=1,2$ follow the rules: if $j=1$ set $i=1,\ldots,4$, if $j=2$ set $i=5,\ldots,8$,

$$B_{1,5} = \begin{bmatrix} \frac{2k_{v,1}}{A_{s,1}} & 0 \\ 0 & 0 \\ 0 & 0 \\ 0 & 0 \end{bmatrix}, \; B_{2,6} = \begin{bmatrix} 0 & 0 \\ 0 & \frac{2k_{v,2}}{A_{s,2}} \\ 0 & 0 \\ 0 & 0 \end{bmatrix}, \; B_{3,7} = \begin{bmatrix} 0 & 0 \\ 0 & 0 \\ 0 & \frac{2k_{v,2}}{A_{s,3}} \\ 0 & 0 \end{bmatrix}, \; B_{4,8} = \begin{bmatrix} 0 & 0 \\ 0 & 0 \\ 0 & 0 \\ \frac{2k_{v,1}}{A_{s,4}} & 0 \end{bmatrix}, \; C = \begin{bmatrix} 1 & 0 & 0 & 0 \\ 0 & 1 & 0 & 0 \end{bmatrix},$$

and $B_w = 10^{-2} \cdot \mathrm{diag}\{2.2,\ 1.5,\ -4.8,\ 5.7\}$.

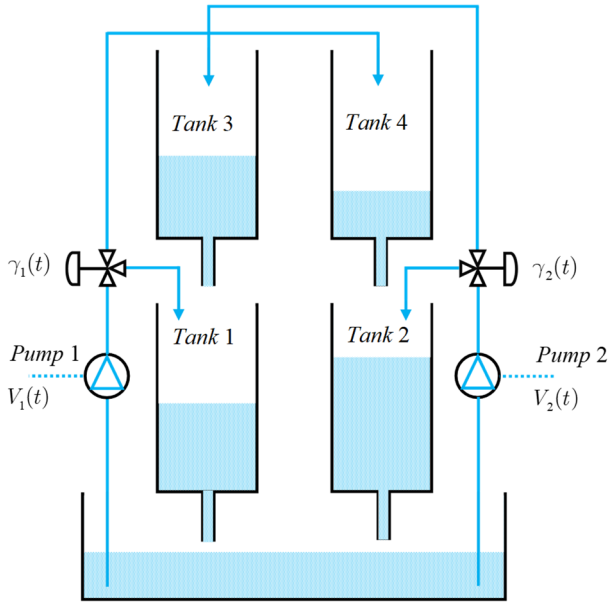

Figure 3-2. *The diagram of quadruple-tank process model.*

The uncertain matrices $\Delta A_i(t)$ and $\Delta C(t)$ are unknown time–varying parameter deployed consistent with the hypothesis. The unit for measuring the height of the water level in the tank is cm (0.01 m).

$$M_i = [0.1 \quad 0.1 \quad 0.1 \quad 0.1]^T, \qquad N_{A,i} = \delta_i[0.1 \quad 0.1 \quad 0.1 \quad 0.1]^T,$$
$$M_C = [0.1 \quad 0.1]^T, \qquad N_C = [0.1 \quad 0.1]^T.$$

The fuzzy controller gains given in Appendix E.1 obtained by using toolbox Yalmip (Lofberg, 2004) with solver Sedumi (Sturm, 1999) to solve optimization Algorithm 3.1 and the stabilization condition in Theorem 3.2.1 (with $J_i, J_{w,i}$, $\Delta B_{w,i}$, and $\Delta B_i = 0$).

The uncertain parameters are the unmodeled and neglected dynamics, and error linearization, modified by varying $\delta_i \in [1,\ 100],\ i = 1..8$. We consider the flow distribution rate in the tanks placed by the position of the regulating valve $\gamma_1(t)$ and $\gamma_2(t)$, is adjusted according to the following rules:

$$\begin{cases} \text{if } t_{sim} = 0 \cdots 20(s) & \text{then } \gamma_1(t) + \gamma_2(t) \in [1,\ 2] & MP \\ \text{if } t_{sim} = 20 \cdots 120(s) & \text{then } \gamma_1(t) + \gamma_2(t) \in [0,\ 1] & NMP \\ \text{if } t_{sim} = 120 \cdots 220(s) & \text{then } \gamma_1(t) + \gamma_2(t) \in [1,\ 2] & MP \\ \text{if } t_{sim} = 220 \cdots 300(s) & \text{then } \gamma_1(t) + \gamma_2(t) \in [0,\ 1] & NMP \end{cases} \tag{3.67}$$

where *MP* is minimum phase setting (Johansson, 1997), and *NMP* is non–minimum phase setting. The simulation starts from the *operating points*:

$$x(0) = [0.15 \quad 0.2 \quad 0.13 \quad 0.23]^T, \text{and } \hat{x}(0) = [0.12 \quad 0.08 \quad 0.02 \quad 0.05]^T.$$

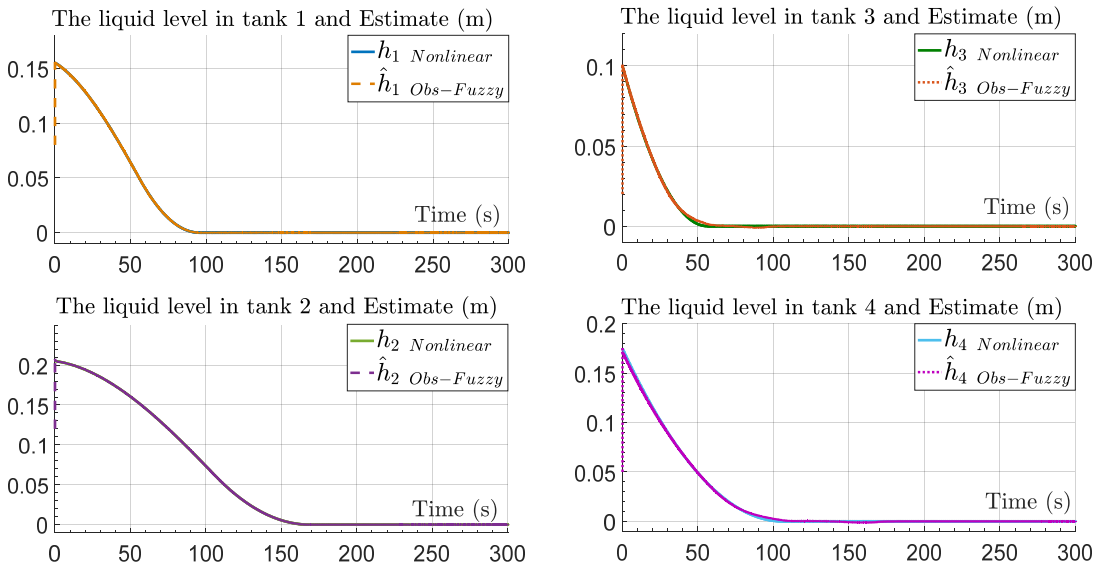

Figure 3-3. *The evolution of dynamic states and estimations under disturbance and uncertain dynamics.*

The time-evolutions of the liquid level in tanks including the measurable states (h_1, h_2), the unmeasurable states (h_3, h_4), respectively, and its estimations shown in Figure 3-3 that have demonstrated the good performance of the designed observer-based control strategy. The minimization of disturbance effects on the system is enhanced by using the CCL algorithm. As we can see in Figure 3-3 and Figure 3-4 (left), the error estimate of liquid level in tanks 1st, 2nd is smaller than 0.6 *mm*, corresponding to level in tank 3rd being less than 3 *mm* and level tank 4 is less than 5 *mm*. And the stabilized control signal of the observer-based controller design for the quadruple-tank process system gives in Figure 3-4 (right). With the limited voltage of each pump is 12 (V), the maximum flow of each pump is 40 (ml. s^{-1}) corresponding to 2.4 (l. mn^{-1}). The illustrative simulation results show the high performances of the proposed design technique.

The norm-bounded constraint (Boyd et al., 1994) increases the conservatism of the stabilization condition, rendering unsatisfactory results obtained from the preselected scalars

methods. The *scaling* scalars method does indeed relax the proposed conditions. However, the above results do not expose the effectiveness of *scaling*-parameter transformation combined with the CCL algorithm. So, the optimal disturbance rejection for each design case is discussed just below, where the $\mathcal{L}_2$ norm-bounded condition is compared with the other works.

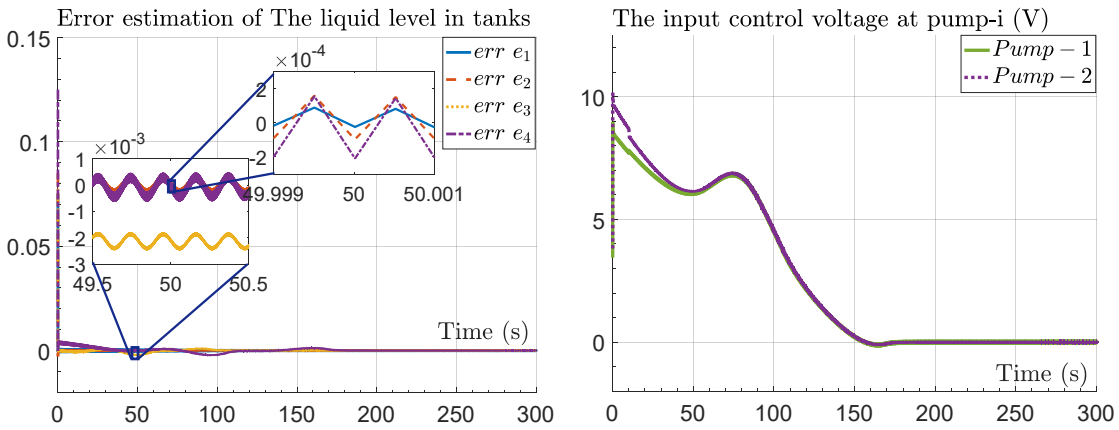

Figure 3-4. *The observer performance – error estimations* (*left*); *and the DC-Motor pumps signal control* (*right*).

Vehicle chassis stabilization system

Let's recall an example discussed in Section 2.1.6.1, with the dynamic states govern the lateral velocity $\dot{v}_y(t)$ and the yaw rate dynamic $\dot{\psi}(t)$. The design objective is to improve vehicle's handling and lateral safety in hazardous situations based on the limited steering-wheel adjusted angle $\delta_c(t)$ is governed by the Active Steering actuator and active yaw moment $M_\psi(t)$. The design limit for $u_1(t)-\delta_c$ is 0.0524 *rad*, while the limit set for $u_2(t)-M_\psi$ is 2842 *Nm*.

Example 3.3.2: Considering the effect of external crosswind disturbances $F_{wY}(t)$, $M_{wZ}(t)$, the reduced nonlinear vehicle model is presented by the equations:

$$\begin{cases} m\dot{v}_y(t) = 2F_{yf}(\alpha_f(t)) + 2F_{yr}(\alpha_r(t)) - m\dot{\psi}(t)v_x(t) + F_{wY}(t) \\ I_z\ddot{\psi}(t) = 2F_{yf}(\alpha_f(t))l_f - 2F_{yr}(\alpha_r(t))l_r + M_\psi(t) + M_{wZ}(t) \end{cases} \tag{3.68}$$

The member function coefficients, the calibration of lateral forces and steering angle on the single-track model, and vehicle simulation parameters, etc., are all detailed in Appendix E.2. The crosswind side force effect and yawing moment $d(t) = [F_{wY}(t)\ M_{wZ}(t)]^T$ and unknown steering wheel of driver $\delta_d(t)$ are assumed $\mathcal{L}_2$-Bounded disturbance.

$$\mathcal{W}(w(t),\sigma) := \{w(t) = [\delta_d(t)\ d(t)^T]^T \in \mathbb{R}^d \mid \|\delta_d(t)\|_2^2 < \sigma_\delta^{-1}, \|d(t)\|_2^2 < \sigma_d^{-1}\}, \tag{3.69}$$

By replacing the T-S fuzzy forces model into the equation (3.68), then a T-S fuzzy observer-based control system is presented as follows:

$$\begin{bmatrix} \dot{x}(t) \\ \dot{e}(t) \end{bmatrix} = \sum_{i,j=1}^{4} \lambda_i(\alpha)\lambda_j(\alpha) \begin{bmatrix} A_i + B_iK_j + \Delta A & -B_iK_j \\ \Delta A_i - L_i\Delta C_i & A_i - L_iC_i \end{bmatrix} \begin{bmatrix} x(t) \\ e(t) \end{bmatrix} + \sum_{i=1}^{4} \lambda_i(\alpha) \begin{bmatrix} B_{w,i} \\ B_{w,i} \end{bmatrix} w(t),$$

$$\begin{aligned}\tilde{z}(t) &= \sum_{i}^{4} \lambda_i(\alpha) \begin{bmatrix} H_i & 0 \\ 0 & H_{e,i} \end{bmatrix} \begin{bmatrix} x(t) \\ e(t) \end{bmatrix}, \\ u(t) &= \sum_{j=1}^{4} \lambda_j(\alpha) \begin{bmatrix} K_j & -K_j \end{bmatrix} \begin{bmatrix} x(t) \\ e(t) \end{bmatrix},\end{aligned} \tag{3.70}$$

with $\tilde{z}(t) \in \mathbb{R}^4$ is controlled outputs. The simulation uses four vertices to validate of proposed model, where the controller design considering a simplification model of system based on two vertices of the front wheel slip angle. Respectively, the local linear systems give as follows:

$$\begin{aligned} A_1 &= \begin{bmatrix} -10.3925 & -18.9120 \\ 0.7416 & -15.2311 \end{bmatrix}, & A_2 &= \begin{bmatrix} -0.0515 & -19.9951 \\ 0.0034 & -0.0752 \end{bmatrix}, \\ B_1 &= \begin{bmatrix} 117.3336 & 0 \\ 94.3627 & 0.0004 \end{bmatrix}, & B_2 &= \begin{bmatrix} 0.5840 & 0 \\ 0.4697 & 0.0004 \end{bmatrix}, \\ B_{w,1} &= \begin{bmatrix} 0.5459 & 0 & 117.3336 \\ 0 & 0.3720 & 94.3627 \end{bmatrix}, & B_{w,2} &= \begin{bmatrix} 0.5459 & 0 & 0.5840 \\ 0 & 0.3720 & 0.4697 \end{bmatrix}, \\ H &= H_e = I_2, \; J_i = 0, \; J_{w,i} = 0. \end{aligned} \tag{3.71}$$

The robust quadratic stabilization conditions are solved at 10% – 30% uncertainty of cornering forces with ΔB_i, and $\Delta B_{w,i} = 0 \rightarrow \varepsilon_4(\alpha) = 0$. And the limits set on inputs control are $|u_1(t)| < \overline{u}_1 = 0.0524\ (rad)$, and $|u_2(t)| < \overline{u}_2 = 2820\ (Nm)$.

Table 3.1. *Observer-Based Feedback Robust Stabilization and Performance with Saturation actuators.*

$\mathscr{H}_\infty$	**Norm bounded** Lemma 3.2.2 & **Stabilization Condition** Theorem 3.2.1									
	Fix ε_i	*Variable* $-\varepsilon_i$			*Polytope* $-\varepsilon_{i,j}$			*Affine scaling* $-\Lambda_{i,j}$		
	[ref]	**T3.3.1**	**T3.3.1**	**Redn**	**T3.3.1**	**T3.3.1**	**Redn**	**T3.3.1**	**T3.3.1**	**Redn**
	$\varepsilon_i = 1$	CCL1	CCL2	CCL1	CCL1	CCL2	CCL1	CCL1	CCL2	CCL1
γ_{opt}	*inf*	53.7486	50.3045	54.7086	5.6668	5.6283	5.2818	5.0952	5.0646	5.1002
0	1	2			3			4		

$i = 1,2,3,\ j = 1,2$; *inf* – infeasible.

T3.3.1 – Stabilization LMI conditions of Theorem 3.2.1&Lemma 3.2.2;

Redn – Reduced conditional form as given in (3.26)-(3.28);

[ref] – Stabilization LMI conditions (Dahmani et al., 2014, 2015; El Hajjaji et al., 2006; Kheloufi et al., 2013b, 2013a).

Cone Complementarity Linearization and Scaling-Parameters

As can be seen in Table 3.1, if the scalars ε_i are pre-selected, these stabilization inequalities become more conservative, causing a decline in system performance (with a larger value of γ or even infeasible conditions). When the *variables* $-\varepsilon_i$ are considered, as a way of envisioning that makes appropriately rotates the self-selected barriers to reduce the inequality gap (as illustrated in Figure A-5). The feasible solutions are obtained at the permissible errors of iterative Algorithm 3.1 CCL1. Then, taking advantage of the new sought scalars ε_i to locally optimize (using iterative Algorithm 3.2 CCL2) that affords a

better minimum value. For found values $-\varepsilon_i$, the best relaxations are attained for stabilization conditions corresponding to each design case.

Besides, the conservation drops significantly by considering the slack variables corresponding from the 2nd catalog to the 4th catalog. It can realize that the stabilization conditions are infeasible with fixing constant values $-\varepsilon_i$, however the CCL algorithm provides the feasible solutions. Moreover, CCL1 (Algorithm 3.1 - global optimization) always returns to a higher rejection level than CCL2 (Algorithm 3.2 - local optimization). But algorithm CCL2 achieves good results inheriting from the set of optimal values $-\varepsilon_i$, derived from algorithm CCL1. Without these data, algorithm CCL2 cannot converge to the local optimal region.

On one hand, performance degradation can observer in Table 3.1 as a result of applying a quadratic Lyapunov function to enforce the stabilizing condition of the parameter-dependent system. For example, let's consider a diagonal slack variable matrix

$$\Theta = diag\{-\varepsilon_1 I, -\varepsilon_2 I, -\varepsilon_3 X, -\varepsilon_1^{-1} I, -\varepsilon_2^{-1} I, -\varepsilon_3^{-1} X\}, \tag{3.72}$$

in LMI conditions (3.55) in Table 3.1. It can interpret that each epsilon $\varepsilon_1, \varepsilon_2, \varepsilon_3$ must be satisfied all LMIs $-ij$ corresponding to all vertex of condition (3.55), which makes the stabilization conditions *claustrophobic*.

In this case, the parameterization is a more reasonable choice for the parameter-dependent conditions. As discussed in section 3.2.3.2, the improvement includes by changing e.g., ε_1 to $\varepsilon_1(\alpha) = \sum_j^2 \lambda_i(t)\varepsilon_{1,j}$, with $j = 1,2$, provides significant relaxation (from 2nd to 3rd catalog). In the second case – *Polytope*, diagonal slack-variables matrix (3.72) represents as convex combination formulation:

$$\Theta = diag\{-\varepsilon_{1,j} I, -\varepsilon_{2,j} I, -\varepsilon_3 X, -\varepsilon_{1,j}^{-1} I, -\varepsilon_{2,j}^{-1} I, -\varepsilon_3^{-1} X\},\ j = 1,2. \tag{3.73}$$

Precisely, the attenuation optimum of stabilization condition of Theorem 3.2.1 associated with Lemma 3.2.2 and algorithm CCL1 is considerably declined from 53.7486 to only 5.6668 by using the proposed method.

On the other hand, consider the set of positive definite similarity scaling associated with structure uncertainty (Apkarian & Adams, 1998; Apkarian & Gahinet, 1995):

$$\Lambda_\Delta := \{\Lambda_{i,j} = diag\{\varepsilon_{i,j1}, ..., \varepsilon_{i,jk}\} \succ 0 \mid \Lambda_{i,j}\alpha(t) = \alpha(t)\Lambda_{ij},\ \forall \alpha(t) \in \Delta_\alpha\}, \tag{3.74}$$

where $i = 1,2, j = 1,2,$ and $k = 1,2,...,$ rank $(\Lambda_{i,j})$. Then, given a symmetric matrix $Y(t)$ associates with the scaling set of parameters enjoys $\Lambda_{i,j}Y(t) = Y(t)\Lambda_{i,j}$, we have:

$$\begin{aligned} & 0 \le \left(\Lambda_{i,j}^{-0.5} X^T \mp \Lambda_{i,j}^{0.5} YZ\right)^T \left(\Lambda_{i,j}^{-0.5} X^T \mp \Lambda_{i,j}^{0.5} YZ\right), \\ \Leftrightarrow\ & \pm XY(t)Z \pm Z^T Y(t)^T X^T \le X\Lambda_{i,j}^{-1} X^T + Z^T Y(t)^T \Lambda\, Y(t) Z, \\ & \le X\Lambda_{i,j}^{-1} X^T + Z^T \Lambda Z. \end{aligned} \tag{3.75}$$

And the last case – *scaling*, we have the following change in the variable matrix (3.72) by applying about development:

$$\Theta = diag\{-\Lambda_{1j}, -\Lambda_{2j}, -\varepsilon_3 X, -\Lambda_{1j}^{-1}, -\Lambda_{2j}^{-1} I, -\varepsilon_3^{-1} X\},\ j = 1,2. \tag{3.76}$$

By deploying the *affine scaling* formulation to the stabilization conditions (3.56)-(3.58)

leads to a better performance from $\gamma^* = 5.6668$ reduced to $\gamma^* = 5.0952$, respectively, by replacing the block variable matrices (3.73) with (3.76) ones. Moreover, the reduced formulation derived in (3.26)-(3.28) corresponding to Theorem 3.2.1 associated with Lemma 3.2.2 solved by algorithm CCL1 shows a slight enhancement from $\gamma^* = 5.2818$ to $\gamma^* = 5.1002$. Finally, through the above analysis, some conclusions can state:

- The algorithm CCL provides more flexible stabilizing conditions by letting variables $\varepsilon_i, i = 1,2,3,$ tighten the gaps of Young's inequality. Besides, it shows an adaptation to integrate with structure parameterization, from simple form ε_i to parameter-dependent form $\varepsilon_i(\alpha)$ and affine scaling form $\Lambda_i(\alpha)$. The slack-variable reduces conservatism and reach to better optimal performance level.
- Algorithm CCL2 searches for the better local minimum value and faster than the iterative global optimization - algorithm CCL1. However, CCL2 returns positive results based on the solutions of parameters inherited from CCL1.
- Reduction - Redn (simplified) conditions shows better results thanks to a more compact and simpler conditional structure. However, if the slack-variable of the Young's inequalities reach their optimal values, both approaches (the original and the reduced form) approximately converge to the same optimal solutions (for example, in the case of affine scaling).
- Finally, the less conservative results observed in the 2nd catalog versus the 3rd and 4th catalog in Table 3.1.

In this example, the selection of T-S fuzzy model (3.71) with a distinction between the local linear systems leads to a disparate outcome in the 2nd catalog versus the 3rd and 4th catalogs in Table 3.1. The quadratic Lyapunov function used for stabilization analysis for the LPV system led to conservatism. It makes randomly choosing a set of scalars ε_i as (Dahmani et al., 2014, 2015; El Hajjaji et al., 2006; Kheloufi et al., 2013b; Zemouche et al., 2017) could be unsolvable.

For example, 3rd catalog of Table 3.1, where the design conditions are solved with algorithm CCL1 reach a minimal value $\gamma^* = 5.6668$ with the optimal set of $\varepsilon_{i,j}$ as follows:

$$\varepsilon_{11} = 270.7501, \varepsilon_{12} = 0.9656, \varepsilon_{21} = 25.0954, \varepsilon_{22} = 0.3815, \text{and } \varepsilon_3 = 0.3123.$$

It may not be an exaggeration to say that have no manipulation that can select this set of parameters to achieve optimal values (evenly gridding method, fine selection, etc.). Most of the work involves parametric uncertainty, in which these scalars often are randomly pre-selected. When dealing with numerical example (3.71), it is miserably hard to pick up a set of ε_{ij} for the feasible solution. Thereby, it authenticates the effectiveness of the proposed CCL algorithm.

3.4. Conclusions

In this chapter, we analyzed the conservation of the stabilization conditions delivered for the observer-based feedback system. The design structure of this controller is typically

based on the application of Young's inequality combined with a quadratic Lyapunov matrix. Both mentioned properties will end in strict stabilization conditions. Based on the CCL algorithm, an improvement using scaling-dependent sets has enhanced the performance of the closed-loop systems. The numerical simulation results and reducing disturbance optimization values have demonstrated the effectiveness of the proposed method. However, applying a quadratic Lyapunov function to analyze the stabilization of the parameter-dependent system is very conservative. So, in the next chapter, we present a synthesizing method of the parameter-dependent conditions derived from the stabilizing analysis for LPV/quasi-LPV system subject to actuator saturation.

Furthermore, the $\mathcal{L}_2$-norm bounded input does not accurately guarantee the saturation limit of the actuator. Therefore, in the next chapter, the saturated LPV controller stabilization is ensured by generalized sector condition.

Chapter 4.

Stabilization Synthesis for LPV/quasi-LPV Systems with Actuators Saturation

In this chapter, the sector bounding condition is predominantly used to enforce the bounds on the saturated control, and the parameter-dependent Lyapunov function is considered in stabilization analysis to enhance system performance. The following sections devote to the synthesis of controllers for saturated LPV systems including:

- The state feedback (section 4.1), the static output feedback (section 4.2), the observer-based feedback (section 4.3), and the dynamic output feedback (section 4.4) controllers are considered for LPV systems in the influence of disturbance and the uncertain parameter. Where the generalized sector condition (GSC) condition is employed to ensure the saturation limits. The saturated gain-scheduling controllers are obtained by the feasible solution of the parametric LMI stabilization conditions.
- The developments of observer-based control and dynamic output controller in sections 4.3 & 4.4 involve with the non-convex forms in the stabilization matrix inequality and the saturation condition. The bilinear terms will be handled by a less conservative congruence transformation.

It should note that of the feedback controller design architectures, the observer-based controller usually results in the most conservative stabilization condition. As a result, the scaling sets are considered for this control design strategy in chapter 3. However, the problem is still not fully covered, so a new design strategy is presented. Finally, the numerical simulation results in sections 4.1.2 and 4.5 will demonstrate the effectiveness of the proposed methods.

4.1. State Feedback Stabilization

4.1.1. *Sector Nonlinearity Models*

As discussed in section 2.3.2.1, by setting positive scalars $\sigma, \eta_0 > 0$, control bounds $\overline{u}_i > 0$, $i = 1, 2, \ldots m$, and using a PDLF associated with ellipsoidal domains (2.102) to analyze the stability of closed-loop system (2.111). Then, the stabilization condition combined with the $\mathscr{H}_\infty$-norm condition and the GSC condition (Corollary 2.3.1) are expressed as follows.

Theorem 4.1.1: *In the presence of disturbance, for the positive scalars* $\overline{u}_s, \eta_0, \eta, \gamma$, *if exists continuously differentiable matrices function* $X : \mathcal{U}_p \to \mathbb{S}^n_{++}$, $Y, Z : \mathcal{U}_p \to \mathbb{R}^{m \times n}$, *and diagonal matrix function* $T : \mathcal{U}_p \to \mathbb{S}^m_{++}$, *such that the following matrix inequalities hold:*

$$\left[\begin{array}{ccc|c} sym\{A(\rho)X(\rho)+B(\rho)Y(\rho)\}-\dot{X}(\rho) & * & * & * \\ Y(\rho)-Z(\rho)-T(\rho)B(\rho)^T & -2T(\rho) & * & * \\ \hline B_w(\rho)^T & 0 & -\gamma I_d & * \\ H(\rho)X(\rho)+J(\rho)Y(\rho) & -J(\rho)T(\rho) & J_w(\rho) & -\gamma I_r \end{array}\right] \prec 0, \qquad (4.1)$$

$$(a).\ \begin{bmatrix} \eta_0^{-1} & * \\ x(0) & X(\rho_0) \end{bmatrix} \succeq 0, \qquad (b).\ \begin{bmatrix} X(\rho) & * \\ Z(\rho)_{(s)} & \eta\overline{u}_s^2 \end{bmatrix} \succeq 0,\ s=1,2,..,m, \qquad (4.2)$$

$\forall x \in \mathcal{E}(X^{-1},\eta,\rho)$ *then state feedback controller with gains* $K(\rho)=Y(\rho)X(\rho)^{-1}$ *guarantees that*

(1) *for a bounded disturbance* $w(t)$, *from* $x(0)\in\mathcal{E}_0\subset\mathcal{E}$ *the trajectories of saturated closed-loop system* (2.111) *remain in the enclosed domain ellipsoid* $\mathcal{E}$ *corresponding to energy-to-energy index* γ.

(2) *for* $w(t)=0$, *the ellipsoid* $\mathcal{E}$ *is a region of asymptotical stability* (RAS) *for saturated LPV system* (2.111).

Proof.

On one side, as analyzed in section 2.3.2, the PLMIs (4.2) are equivalent to:

$$(4.2).a \ \rightarrow\ \eta_0 x(0)^T P(\rho_0)x(0)\le 1, \qquad \rightarrow\ V(0)\le\eta_0^{-1}, \qquad (4.3)$$

$$(4.2).b \ \rightarrow\ \left(\eta\overline{u}_s^2\right)^{-1} G(\rho)_{(s)}^T G(\rho)_{(s)} \le P(\rho). \qquad \rightarrow\ \left(\eta\overline{u}_s^2\right)^{-1}\left\|\vartheta_s(t)\right\|^2 \le V(t), \qquad (4.4)$$

with $G(\rho)=Z(\rho)P(\rho)$, $P(\rho)X(\rho)=I_n$, $Z(\rho)_{(s)}$ symbolizes s-th row of $Z(\rho)$.

Following Corollary 2.3.1, there exists a diagonal matrix function $T:\mathcal{U}_p\rightarrow\mathbb{S}_{++}^m$, such that sector nonlinearity $\Phi(u)$ defined in (2.91) with state feedback control $u(t)=K(\rho)x(t)$ and auxiliary control $\vartheta(t)=G(\rho)x(t)$ satisfy GSC condition (2.98), expressed as follows:

$$\Phi(u)^T T(\rho)^{-1}(K(\rho)x(t)-G(\rho)x(t)-\Phi(u)) \ \ge\ 0. \qquad (4.5)$$

On the other side, pre- and post-multiply $diag\{P(\rho),T(\rho)^{-1},I,I\}$ for the condition (4.1):

$$\left[\begin{array}{ccc|c} sym\{P(\rho)(A(\rho)+B(\rho)K(\rho))\}+\dot{P}(\rho) & * & * & * \\ (K(\rho)-G(\rho))-B(\rho)^T P(\rho) & -2T(\rho)^{-1} & * & * \\ \hline B_w(\rho)^T P(\rho) & 0 & -\gamma I_d & * \\ H(\rho)+J(\rho)K(\rho) & -J(\rho) & J_w(\rho) & -\gamma I_r \end{array}\right] \prec 0, \qquad (4.6)$$

where $\dot{P}(\rho)=-P(\rho)\dot{X}(\rho)P(\rho)$, and gain $K(\rho)=Y(\rho)P(\rho)$. By using Shur's complement to rearrange the above inequality, then consecutively *pre-* and *post*-multiplying with $[x(t)^T\ \ \Phi(u)^T\ \ w(t)^T]$ and its transposition that yields:

$$\begin{bmatrix} x(t) \\ \Phi(u) \\ w(t) \end{bmatrix}^T \begin{bmatrix} sym\{P(\rho)(A(\rho)+B(\rho)K(\rho))\}+\dot{P}(\rho) & * & * \\ (K(\rho)-G(\rho))-B(\rho)^T P(\rho) & -2T(\rho)^{-1} & * \\ B_w(\rho)^T P(\rho) & 0 & -\gamma I_d \end{bmatrix} \begin{bmatrix} x(t) \\ \Phi(u) \\ w(t) \end{bmatrix}$$

$$+\gamma^{-1}\begin{bmatrix} x(t) \\ \Phi(u) \\ w(t) \end{bmatrix}^T \begin{bmatrix} (H(\rho)+J(\rho)K(\rho))^T \\ -J(\rho)^T \\ J_w(\rho)^T \end{bmatrix} [H(\rho)+J(\rho)K(\rho) \quad -J(\rho) \quad J_w(\rho)] \begin{bmatrix} x(t) \\ \Phi(u) \\ w(t) \end{bmatrix} \prec 0, \qquad (4.7)$$

Expanding on the left-hand side we have:

$$\begin{aligned} 2x(t)^T P(\rho)(A(\rho)+B(\rho)K(\rho))x(t)+x(t)^T\dot{P}(\rho)x(t)+2x(t)^T P(\rho)B_w(\rho)w(t) \\ -2x(t)^T P(\rho)B(\rho)\Phi(u)+\gamma^{-1}z(t)^T z(t)-\gamma w(t)^T w(t) \\ +2\Phi(u)^T T(\rho)^{-1}(K(\rho)x(t)-G(\rho)x(t)-\Phi(u)) \;<\; 0. \end{aligned} \tag{4.8}$$

On the view of condition (4.5) that implies the derivative of Lyapunov function (2.102) along the trajectories of closed-loop system (2.111) $\dot{V}(t)+\gamma^{-1}\|z(t)\|^2-\gamma\|w(t)\|^2<0$, for all $x\in\mathcal{E}(P(\rho),\eta)\setminus\{0\}$.

Hence, from initial condition $x(0)\in\mathcal{E}_0(P(\rho_0),\eta_0)$ and for $x(t)\in\mathcal{E}$, we have:

- When $w(t)=0$, then $\dot{V}(t)<-\gamma^{-1}\|z(t)\|^2<0$ implies

$$\left(\eta\overline{u}_s^2\right)^{-1}\|\vartheta_s(t)\|^2 \overset{(4.2b)}{\leq} V(t) \overset{(4.1)}{<} V(0) \overset{(4.2a)}{\leq} \eta_0^{-1}\leq\eta^{-1}, \tag{4.9}$$

  that confirms ellipsoid set $\mathcal{E}(P(\rho),\eta)\subset\mathcal{S}(\vartheta,\overline{u})$ is the region of asymptotical stability of system (2.111) with $x_0\in\mathcal{E}_0\subseteq\mathcal{E}$.

- When $w(t)\neq 0, w(t)\in\mathcal{W}\setminus\{0\}$ (defined in section 2.3.1.4), then

$$\left(\eta\overline{u}_s^2\right)^{-1}\|\vartheta_s(t)\|^2 \overset{(4.2b)}{\leq} V(t) \overset{(4.1)}{<} \gamma\|w(t)\|_{\mathcal{L}_2}^2+V(0) \overset{(4.2a)}{\leq} \gamma\sigma^{-1}+\eta_0^{-1}\leq\eta^{-1}, \tag{4.10}$$

  condition (4.8) claims the trajectories of LPV system (2.111) do not leave the set $\mathcal{E}$ belong to the polyhedron $\mathcal{S}(\vartheta,\overline{u})$ from $x_0\in\mathcal{E}_0\subset\mathcal{E}$.

This ends the proof. □

From above analysis, the trade-offs between the performance requirement $-\gamma$, the estimation of RAS (ellipsoidal domain) - η, and the set of the admissible initial conditions - η_0 is a *mandatory* condition. The selection of appropriate constants combined with optimization of the remaining variables depends on the design purposes. For instance, preselecting η_0, then minimizing η such that conditions (4.1), (4.2) and $\gamma\sigma^{-1}+\eta_0^{-1}\leq\eta_{opt}^{-1}$ hold. However, this sub-optimization is conservative. Especially, the latter condition is expressed by a bilinear form relating to parameter-dependent conditions (4.1), (4.2). Furthermore, the minimization of γ results in the decline of the linear operating area (regions of unsaturated control signal), which predominantly affects the constraints like GSC (that is discussed in section 4.1.2.3).

4.1.2. *Example*

In the first part, the stabilization conditions design for the saturated system considering the effect disturbance and the time-varying parameters reveals the relaxation of GSC constraints (on the single input systems). Three relaxation methods of PLMI conditions will apply to Theorem 4.1.1 (i.e., gridding, SoS, and polytope). Then, the relaxation of multimodel (T-S fuzzy) is used to compare with the works in the literatures (A. T. Nguyen et al., 2015; Vafamand et al., 2016).

Concerning the stabilization of the saturated MIMO systems, some discussion is delivered about the high-gain problem of the bounding sector constraints. A typical example

used with the difference between the vertices of the local linear systems and the disproportion of the actuator's limits aggravates this numerical problem. As a result, a modification is proposed via LMI formulation to overcome the limitation.

4.1.2.1. *Ellipsoidal regions of stability*

Example 4.1.1: Consider a nonlinear open-loop unstable system introduced by (A. T. Nguyen et al., 2015) is presented by the following equations:

$$\begin{cases} \dot{x}_1 = -x_1 + (0.1 + 0.12x_2^2)x_2 + (1.48 + 0.16x_2^3)u + 0.1w \\ \dot{x}_2 = x_1 + 0.1w \\ z = x_2 + u + 0.1w \end{cases} \tag{4.11}$$

The saturation bound is $\overline{u} = 1$. For design purpose, let's set $\rho(x(t)) = x_2(t) \in [-1.5, 1.5]$, and $\dot{\rho}(x(t)) \in [-2, 2]$. Then, the LPV representation of the nonlinear system is given by

$$A(\rho) = \begin{bmatrix} -1 & 0.1 + 0.12\rho(x(t))^2 \\ -1 & 0 \end{bmatrix},\ B(\rho) = \begin{bmatrix} 1.48 + 0.16\rho(x(t))^3 \\ 0 \end{bmatrix},\ B_w(\rho) = \begin{bmatrix} 0.1 \\ 0.1 \end{bmatrix},$$
$$H(\rho) = [0 \quad 1],\ J(\rho) = 1,\ J_w(\rho) = 0.1. \tag{4.12}$$

Let's discuss the simultaneous optimization related to decision variables γ, η. It should realize that both relevant minimization criteria are the convex conditions. Considering the following optimization problem:

Problem 4.1.1.
Given compact set of the parameters $\rho(x(t)) \in \mathcal{U}_p$, *scalars* α_1, α_2, *find the variable decision matrices such that the following statement satisfies*:

$$\textbf{minimize}\ f(\gamma, \eta) = \alpha_1\gamma + \alpha_2\eta, \tag{4.13}$$

subject to inequalities (4.1)-(4.2) corresponding to the stabilization condition of Theorem 4.1.1.

The results in Table 4.1 (1st catalog) given by solving Theorem 4.1.1 corresponding to the PLMI conditions gridded over $N_p = 41$ points uniformly spaced $\rho(x(t)) \in [-1.5, 1.5]$. The LMI conditions are solved by the convex optimization Mosek (Erling D Andersen & Andersen, 2000) combined with the numerical calculation toolbox Yalmip (Lofberg, 2004). The second column is obtained from using the SoS toolbox (Papachristodoulou et al., 2013) to solve the parameter matrices polynomial according to the SoS decomposition approach with solver Sedumi (Sturm, 1999). And provided in catalog number 3, by deploying a conditional relaxation of Theorem 4.1.1 by convex combination of four vertices derived from the following T-S fuzzy system:

$$A_1 = A_2 = \begin{bmatrix} -1 & 0.1 \\ -1 & 0 \end{bmatrix},\ A_3 = A_4 = \begin{bmatrix} -1 & 0.37 \\ -1 & 0 \end{bmatrix},\ B_1 = B_3 = \begin{bmatrix} 0.94 \\ 0 \end{bmatrix},\ B_2 = B_4 = \begin{bmatrix} 2.02 \\ 0 \end{bmatrix},$$
$$B_{w,i} = [0.1 \quad 0.1]^T,\ H_i = [0 \quad 1],\ J_i = 1,\ J_{w,i} = 0.1,\ \text{with } i = 1,2,3,4. \tag{4.14}$$

The process of fuzzification of nonlinear system (4.11) and membership functions can be found in more detail at (A. T. Nguyen et al., 2015).

Table 4.1. *Multi-objective optimization* - *Problem* 4.1.1

	Parameter-dependent Stabilization & Actuator Saturation		
	Gridding (4.12)	SoS (4.11)	Polytope (4.14)
	Theorem 4.1.1	*Theorem* 4.1.1	*Theorem* 4.1.1
γ_{opt}	0.2924	0.6248	0.2341
η_{opt}	0.0557	0.1938	0.0039
t_{sol}	2.6829s	8.3878s	2.1272s
0	1	2	3

The optimization results are obtained by solving Theorem 4.1.1 with Problem 4.1.1 by these relaxed PLMI methods corresponding to the weighting scalar $\alpha_1 = \alpha_2 = 1$. It can be seen that the multi-convexities (T-S fuzzy) returns the best results with the optimal solve time. Meanwhile, the complexity in the conditional structure of the SoS decomposition method leads to a higher computation time. The finite-discreteness over the parameter domain provides a satisfactory result with reasonable time (this approach is the simplest relaxation of PLMI).

A *largest invariant ellipsoid contained in a polytope* (Boyd et al., 1994) is recalled to impose the constraints on the state. By defining a polyhedron $\mathcal{P}_x : \{x(t) \in \mathbb{R}^n \mid \ h_x^T x(t) \le 1\}$ encloses the ellipsoidal set $\mathcal{E} : \{x(t) \in \mathbb{R}^n \mid \ \eta x(t)^T X(\rho)^{-1} x(t) \le 1\}$ that yields:

$$\begin{bmatrix} X(\rho) & h_x^T \\ h_x & \eta \end{bmatrix} \succeq 0. \tag{4.15}$$

In this example, a vector $h_x = \begin{bmatrix} 0 & 1.5^{-1} \end{bmatrix}$ is chosen to enforce norm $\|x_2(t)\|^2 \le 1.5^2$. Combining conditions (4.13), (4.15) with the stabilization conditions solved with the relaxation methods at $\eta = 0.25$ and $\gamma = 2.75$, we obtain the regions of asymptotic stability of the LPV systems.

For the gridding and SoS methods, the discretization of ellipsoidal domain (at level set $\mathcal{E} = 1$) by uniformly grids 20 values of $\rho(t)$ over interval $[-1.5,\ 1.5]$ corresponding to 20 ellipses in the bounded region $|x_2(t)| \le 1.5$. On the other hand, 20 ellipsoids of FLF

$$\mathcal{E} : x(t) \in \mathbb{R}^n \mid \ \sum_{i=1}^{4} \lambda_i(t) x(t)^T X_i^{-1} x(t) \le 1. \tag{4.16}$$

is obtained by discretized the membership function $\lambda_1(t)$ uniformly over interval $[0,\ 1]$. It can be noticed that these ellipsoids are bounded by $\mathcal{E}(X_1^{-1})$ and $\mathcal{E}(X_4^{-1})$. Nonetheless, the condition (4.15) is very conservative constraint, and it is not always guaranteed that all of the trajectories of saturated closed-loop system is bounded in the definite domain. In this case, the hard-bounds imposed on the states are better fulfilled by the barrier function, see, e.g., (Ngo et al., 2005; Q. Nguyen & Sreenath, 2016; Tee et al., 2009).

4.1.2.2. *The comparison of conservativeness of conditions*

Example 4.1.2: Consider a T-S fuzzy system modified by (A. T. Nguyen et al., 2015) expressed by the following local linear matrices:

$$A_1 = \begin{bmatrix} 2 & -10 \\ 2 & 0 \end{bmatrix},\ A_2 = \begin{bmatrix} a & -5 \\ 1 & 2 \end{bmatrix},\ B_1 = \begin{bmatrix} 1 \\ 1 \end{bmatrix},\ B_2 = \begin{bmatrix} b \\ 2 \end{bmatrix},\ B_{w,i} = \begin{bmatrix} 0.1 \\ 0.1 \end{bmatrix},$$

$$C_i = H_i = [1 \quad 0],\ D_i = J_i = 0,\ D_{w,i} = J_{w,i} = 0,\ \text{with } i = 1,2. \tag{4.17}$$

In the second example, the objective is to compare the conservatives of the novel procedure for considering saturation constraint enforced by the GSC condition with those of the different approaches. The controller design conditions are applied for saturated T-S fuzzy systems without disturbance input. To facilitate comparison with work in the literature. A compact (no input disturbance) stabilization version of conditions (4.1)-(4.2) is presented as a relaxation of parameterized LMI as follows.

Corollary 4.1.1: *For the positive scalars* $\overline{u}_s, \eta$, *if there exist matrices* $X_k \in \mathbb{S}^n_{++}$, Y_{jk}, $Z_{jk} \in \mathbb{R}^{m\times n}$, *and diagonal matrix* $T \in \mathbb{S}^m_{++}$, *such that the following LMIs satisfy*:

$$\tfrac{1}{6}(\Upsilon_{ijk} + \Upsilon_{jik} + \Upsilon_{jki} + \Upsilon_{ikj} + \Upsilon_{kij} + \Upsilon_{kji}) \prec 0, \quad \textit{with } i \geq j,\ j \geq k \tag{4.18}$$

$$\frac{1}{2}\begin{bmatrix} X_k & * \\ Z_{jk} & \eta\overline{u}^2 \end{bmatrix} + \frac{1}{2}\begin{bmatrix} X_j & * \\ Z_{kj} & \eta\overline{u}^2 \end{bmatrix} \succeq 0, \quad \textit{with } j \geq k \tag{4.19}$$

where $\Upsilon_{ijk} = \begin{bmatrix} sym\{A_i X_k + B_i Y_{jk}\} - \nu(X_1 - X_2) & * \\ Y_{jk} - Z_{jk} - T_j B_i^T & -2T_j \end{bmatrix}$,

with $\forall x \in \mathcal{E}(X_k^{-1}, \eta)$, $i, j, k = 1,2$, *a bounded rate of membership function* $|\dot{\lambda}(t)| \leq \nu = 1$, *then state feedback controller gains are given by* $K_j = Y_{jk}(\sum_{k=1}^{2} \lambda_k(t) X_k)^{-1}$ *guarantees that the ellipsoid* $\mathcal{E}$ *is a region of asymptotical stability for saturated qLPV system* (4.17).

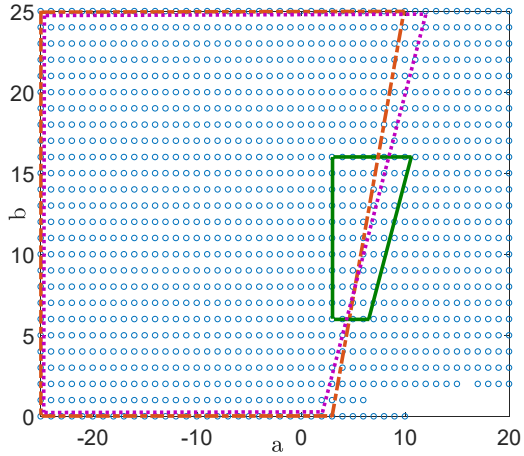

Colored dash-dotted trapezoid (A. T. Nguyen et al., 2015)

Violet dotted trapezoid (Guerra et al., 2012)

Green solid trapezoid (Vafamand et al., 2016)

Small blue circle (Corollary 4.1.1)

Figure 4-1. *The estimate of feasibility regions with* $a \in [-25,\ 20]$, $b \in [-0,\ 25]$.

By setting $\eta = 1$, the feasibility of T-S fuzzy system (4.17) is checked using the proposed relaxation (polytope) Corollary 4.1.1 for all 1,196 points of a 46×26 rectangle uniformly grid over the space $a \in [-25,\ 20]$, $b \in [-0,\ 25]$ with assumption $X_1 - X_2 \succeq 0$. The feasible region exhibits the proposed condition to be much less conservative than other approaches. In the work of (Vafamand et al., 2016), although the author intends to test on a smaller conditional region $a \in [2,\ 11]$, $b \in [6,\ 16]$, it can be objectively recognized that

there is a big difference compared with the feasibility region of the saturation constraint of Corollary 4.1.1. Besides, the optimization results of the stabilization conditions of Theorem 4.1, solved for the system (4.14), are also superior to the results of (A. T. Nguyen et al., 2015). However, the comparison will be more reasonable in analyzing with the same structure as the DOF control system provided in Section 4.4.

4.1.2.3. *Generalized Sector Condition*

As analyzed on the feasibility of the saturated LPV systems, the GSC shows a better performance. Now, let's study the numerical problem related to GSC for a two-rule T-S fuzzy system (example 3.4.2). The peculiarity of this example is that the saturation limits on the control inputs vary greatly. For simplified analysis, the parameter-dependent stabilization conditions (4.1)-(4.2) are employed by a quadratic Lyapunov function compare to a state-feedback controller constrained by norm bounded (Lemma 3.1.1).

$$\begin{aligned}
A_1 &= \begin{bmatrix} -10.3925 & -18.9120 \\ 0.7416 & -15.2311 \end{bmatrix}, & A_2 &= \begin{bmatrix} -0.0515 & -19.9951 \\ 0.0034 & -0.0752 \end{bmatrix}, \\
B_1 &= \begin{bmatrix} 117.3336 & 0 \\ 94.3627 & 0.0004 \end{bmatrix}, & B_2 &= \begin{bmatrix} 0.5840 & 0 \\ 0.4697 & 0.0004 \end{bmatrix}, \\
B_{w,1} &= \begin{bmatrix} 0.5459 & 0 & 117.3336 \\ 0 & 0.3720 & 94.3627 \end{bmatrix}, & B_{w,1} &= \begin{bmatrix} 0.5459 & 0 & 0.5840 \\ 0 & 0.3720 & 0.4697 \end{bmatrix}, \\
H &= I_2,\ J_i = 0,\ J_{w,i} = 0.
\end{aligned} \tag{4.20}$$

At first glance, we can realize a numerical problem using the quadratic Lyapunov form to stabilize the uncertain parameter system corresponding to the norm bounded and generalized sector constraints. However, **why** are only *high gain problems* observed in Table 4.2 with **GSC** conditions?

To understand this better, let's first remind some preliminary definitions of the generalized sector condition. Given a vector auxiliary control $\vartheta(t) = [\vartheta_1(t), \vartheta_2(t), ..., \vartheta_m(t)]^T \in \mathbb{R}^m$ belong to polyhedral set $\mathcal{S}(\vartheta(t), \overline{u}_i)$, a positive definite matrix $T = diag\{T_1, T_i, ..., T_m\}$, with $i = 1, 2, ..., m$, and dead-zone nonlinearities $\Phi(u_i) = u_i - sat(u_i)$. Then, the modified sector bounding separately imposed on each auxiliary control is presented by the following scalar multiplication:

$$\Phi^T(u_i) T_i^{-1} (u_i(t) - \vartheta_i(t) - \Phi(u_i)) \geq 0. \tag{4.21}$$

Meanwhile, condition (4.5) with $u(t) = K(\rho)x(t)$, and $\vartheta(t) = G(\rho)x(t)$ exhibits a vector and matrix multiplication

$$\Phi^T(u) T^{-1} (u(t) - \Phi(u) - \vartheta(t)) \geq 0. \tag{4.22}$$

So, if the design stabilization conditions (4.1)-(4.2) are satisfied, then condition (4.22) implicitly executes, that would be equivalent to

$$\sum_{i=1}^{m} \Phi^T(u_i) T_i^{-1} (u_i(t) - \Phi(u_i) - \vartheta_i(t)) \geq 0. \tag{4.23}$$

It's worthy to note that if conditions (4.21) hold, then condition (4.23) is kept, but the reverse is not correct. The problem does not reveal when the similarity limits enforced in

each control input are considered. In monographs (Tarbouriech et al., 2011) and references therein usually consider only single control input signal, or two control inputs with similarity bounds (e.g., $|u_1(t)| \le 5, |u_2(t)| \le 15$).

Table 4.2. *Robust Pole Placement in LMI Regions.*

$\mathcal{H}_\infty$	**Quadratic Stability**		
	Polytopic		*PDC-Fuzzy*
	NB	**GSC**	**GSC**
γ_{opt}	2.8887	$6.104 \cdot 10^{-3}$	$6.444 \cdot 10^{-3}$
		High gain	*High gain*
	& $\mathcal{D}$-Stable		
	$r = 20, \alpha = 5$	$r = 30, \alpha = 15$	$r = 30, \alpha = 15$
γ_{opt}	1.3054	0.0977	0.0978
0	1		2

NB – Norm bounded; GSC – generalized sector condition;

In this case, however, the bounds $\overline{u}_1 = 0.0524(rad)$, and $\overline{u}_2 = 2820(Nm)$ differ greatly. Hence, the problem becomes more severe in optimizing the reduction disturbance level with the stabilization conditions approached by the convex combination. For example, the fuzzy-feedback gains obtained corresponding to 1st catalog of Table 4.2 are given, respectively, with the Norm-Bounded (NB) constraint:

$$K_1 = \begin{bmatrix} 0.0021 & 0.1015 \\ 58.841 & -1549.8 \end{bmatrix}, \; K_2 = \begin{bmatrix} -0.0166 & 0.2075 \\ -932.78 & 10960. \end{bmatrix},$$

and the GSC condition:

$$K_1 = 10^9 \cdot \begin{bmatrix} 4.1942 & 3.240 \\ -15.072 & 16.881 \end{bmatrix}, \; K_2 = 10^9 \cdot \begin{bmatrix} 0.3195 & 0.2468 \\ -14.113 & 17.626 \end{bmatrix}.$$

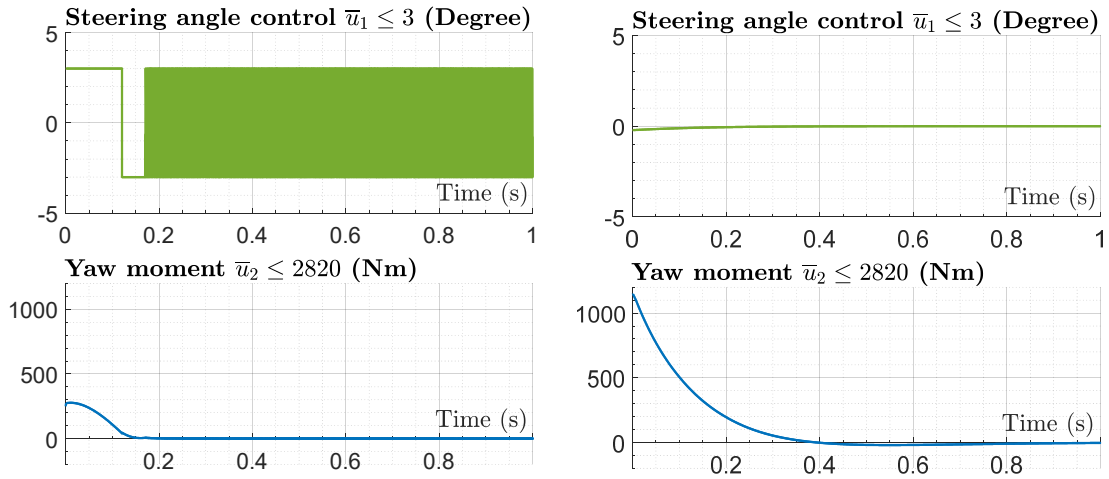

a. GSC constraint without $\mathcal{D}$-Stable *c. GSC constraint with $\mathcal{D}$-Stable*

Figure 4-2. *The improvement of the controller performance with LMI $\mathcal{D}$-Region, via Polytopic quadratic stability condition.*

It could realize that the magnitude of the first and second row of the gains solved by the

condition NB adequately obeys design limits $\overline{u}_1, \overline{u}_2$. But, if the GSC condition is applied, as explained from (4.21)-(4.23), this matching loses. Hence, the more minimized the disturbance attenuation level, the more amplified the controller gain. In addition, each local stabilizing gain K_i is characterized by the individual behaviors of each local linear system $A_i, B_i, B_{w,i}$, etc. These are the causes of chattering in the lower-limited control channel $\overline{u}_1 = 0.0524\ (rad)$ (as seen in Figure 4-2.*a*).

Let's recall the stabilization problems discussed on LTI systems with saturated actuators. The closed-loop poles are pushed away from the imaginary axis to the left at the optimized cancellation values. The features such as fast convergence and good response are ineffective when the control signal reaches its limit. The dead-zone nonlinear behavior can cause the system to become unstable and convergent about equilibria other than the origin (Gomes da Silva, 1997; Gomes da Silva et al., 2003; Tarbouriech et al., 2011). As a result, a deteriorated control performance (the chattering phenomenon) is observed. And presented in Figure 4-2.b, the poles get closer to the imaginary axis avoids chattering in the input signal control but the response characteristics are slower. This problem is alleviated by the method of displacing poles into the $\mathcal{D}$-stable region (Chilali et al., 1999; Chilali & Gahinet, 1996), a tradeoff between the system performance and the linear characteristic region. This approach could be implemented directly on design LMI conditions by relocating the eigenvalues of the matrix into region $\mathcal{D}$. The better control performance and the improved results are obtained.

Remark 4.1.1. This example was intentionally chosen to *discover* the limitation of the weakness of GSC condition in applied to the MIMO systems. It could remind that the structure of GSC conditional stabilization using quadratic Lyapunov was similar between Polytopic and PDC-fuzzy analyses.

Remark 4.1.2. The state-feedback controller construction yields a simplified control construction and a better characteristic of closed-loop system response. But it may be unimplemented in practice due to metrological and economic reasons. In this case, the more suitable approach would be the output feedback.

4.2. Static Output Feedback Stabilization

The static output design strategies often suffer from a bilinear structure due to the form of the measurement matrix. In this section, we present a decomposition structure of feedback controller gain that allows using simple congruence transformations. Besides, a more general problem could be included by considering a parameter-dependent formulation in the measurement matrix. By choosing the set of admissible initial conditions with $\eta_0 > 0$, and polyhedral set (2.92) related to level sets of ellipsoidal domains (2.102), the stability analysis of LPV system (2.113) to the following theorem.

Theorem 4.2.1: *For the positive scalars* $\varepsilon, \overline{u}_s, \eta_0, \eta, \gamma$, *if there exist continuously matrices function* $X : \mathcal{U}_p \to \mathbb{S}^n_{++}$, $Y : \mathcal{U}_p \to \mathbb{R}^{m\times p}$, $Z : \mathcal{U}_p \to \mathbb{R}^{m\times n}$, $W : \mathcal{U}_p \to \mathbb{R}^{p\times p}$, *and a diagonal matrix function* $T : \mathcal{U}_p \to \mathbb{S}^m_{++}$, *such that the following matrix inequalities satisfy:*

$$sym\left[\begin{array}{c|ccccc} -\varepsilon W(\rho) & C(\rho)X(\rho)-W(\rho)C(\rho) & 0 & 0 & 0 \\ \hline \varepsilon B(\rho)Y(\rho) & A(\rho)X(\rho)+B(\rho)Y(\rho)C(\rho)-\frac{1}{2}\dot{X}(\rho) & -B(\rho)T(\rho) & B_w(\rho) & 0 \\ \varepsilon Y(\rho) & Y(\rho)C(\rho)-Z(\rho) & -T(\rho) & 0 & 0 \\ 0 & 0 & 0 & -\frac{1}{2}\gamma I_d & 0 \\ \varepsilon J(\rho)Y(\rho) & H(\rho)X(\rho)+J(\rho)Y(\rho)C(\rho) & -J(\rho)T(\rho) & J_w(\rho) & -\frac{1}{2}\gamma I_r \end{array}\right] \prec 0, \tag{4.24}$$

$$(a).\ \begin{bmatrix} \eta_0^{-1} & * \\ x(0) & X(\rho_0) \end{bmatrix} \succeq 0, \qquad (b).\ \begin{bmatrix} X(\rho) & * \\ Z(\rho)_{(s)} & \eta\overline{u}_s^2 \end{bmatrix} \succeq 0, \tag{4.25}$$

$\forall x \in \mathcal{E}\left(X(\rho)^{-1},\eta\right)$ *then PDC feedback controller with gains* $K(\rho)=Y(\rho)W(\rho)^{-1}$ *guarantees that*

(1) *for* $w(t)=0$, *the ellipsoid* $\mathcal{E}$ *is a region of asymptotical stability for saturated LPV system* (2.113).

(2) *for bounded disturbance* $w(t)$, *from* $\forall x(0) \in \mathcal{E}_0 \subset \mathcal{E}$ *the trajectories of saturated closed-loop system* (2.113) *stay in the enclosed domain ellipsoid* $\mathcal{E}$ *corresponding to performance index* γ.

Proof.

Following the lines of Theorem 4.1.1, inequalities (4.25) directly imply the constraints of initial conditions and saturation condition on the *additional* control vector:

$$(4.25).a \ \rightarrow \ \eta_0 x(0)^T P(\rho_0) x(0) \le 1, \qquad \rightarrow V(0) \le \eta_0^{-1}, \tag{4.26}$$

$$(4.25).b \ \rightarrow \ \left(\eta\overline{u}_s^2\right)^{-1} G(\rho)_{(s)}^T G(\rho)_{(s)} \le P(\rho). \qquad \rightarrow \left(\eta\overline{u}_s^2\right)^{-1} \left\|\vartheta_s(t)\right\|^2 \le V(t), \tag{4.27}$$

with $G(\rho)=Z(\rho)P(\rho)$, and $P(\rho)=X(\rho)^{-1}$. And, the GSC condition can be presented by:

$$\Phi(u)^T T(\rho)^{-1}(K(\rho)C(\rho)x(t)-G(\rho)x(t)-\Phi(u)) \ \succeq \ 0. \tag{4.28}$$

Then, PDLMI (4.24) is reorganized by:

$$\Psi(\rho)+\mathcal{P}(\rho)^T\Theta(\rho)\mathcal{Q}(\rho)+\mathcal{Q}(\rho)^T\Theta(\rho)^T\mathcal{P}(\rho) \ \prec \ 0, \tag{4.29}$$

where $\Theta(\rho)=\varepsilon W(\rho)$,

$\mathcal{P}(\rho)=\left[-I \ \middle| \ K(\rho)^T B(\rho)^T \quad K(\rho)^T \quad 0 \quad K(\rho)^T J(\rho)^T\right]$, $\mathcal{Q}(\rho)=[I \ | \ 0 \quad 0 \quad 0 \quad 0]$,

$$\Psi(\rho)=sym\left[\begin{array}{c|ccccc} 0 & C(\rho)X(\rho)-W(\rho)C(\rho) & 0 & 0 & 0 \\ \hline 0 & A(\rho)X(\rho)+B(\rho)Y(\rho)C(\rho)-\frac{1}{2}\dot{X}(\rho) & -B(\rho)T(\rho) & B_w(\rho) & 0 \\ 0 & Y(\rho)C(\rho)-Z(\rho) & -T(\rho) & 0 & 0 \\ 0 & 0 & 0 & -\frac{1}{2}\gamma I_d & 0 \\ 0 & H(\rho)X(\rho)+J(\rho)Y(\rho)C(\rho) & -J(\rho)T(\rho) & J_w(\rho) & -\frac{1}{2}\gamma I_r \end{array}\right] \prec 0.$$

Now, given any matrices form $\mathcal{P}^{\perp}:=\mathrm{Ker}(\mathcal{P})$, $\mathcal{Q}^{\perp}:=\mathrm{Ker}(\mathcal{Q})$, base of the null spaces of $\mathcal{P}$ and $\mathcal{Q}$. For example, let's consider:

$$\ker(\mathcal{P})^T=\left[\begin{array}{c|cccc} B(\rho)K(\rho) & I & 0 & 0 & 0 \\ K(\rho) & 0 & I & 0 & 0 \\ 0 & 0 & 0 & I & 0 \\ J(\rho)K(\rho) & 0 & 0 & 0 & I \end{array}\right], \text{ and } \ker(\mathcal{Q})^T=\left[\begin{array}{c|cccc} 0 & I & 0 & 0 & 0 \\ 0 & 0 & I & 0 & 0 \\ 0 & 0 & 0 & I & 0 \\ 0 & 0 & 0 & 0 & I \end{array}\right].$$

Followed the projection lemma (see in Appendix A.5), the solvability of inequality (4.29) for $\Theta(\rho)$ is equivalent to the feasibility of the underlying LMIs:

$$\ker(\mathcal{P})^T \Psi(\rho) \ker(\mathcal{P}) \prec 0, \tag{4.30}$$

$$\ker(\mathcal{Q})^T \Psi(\rho) \ker(\mathcal{Q}) \prec 0, \tag{4.31}$$

with $Y(\rho) = K(\rho)W(\rho)$. Then, condition (4.30) is rearranged as follows:

$$sym\begin{bmatrix} A(\rho)X(\rho)+B(\rho)K(\rho)C(\rho)X(\rho)-\frac{1}{2}\dot{X}(\rho) & -B(\rho)T(\rho) & B_w(\rho) & 0 \\ K(\rho)C(\rho)X(\rho)-Z(\rho) & -T(\rho) & 0 & 0 \\ 0 & 0 & -\frac{1}{2}\gamma I & 0 \\ H(\rho)X(\rho)+J(\rho)K(\rho)C(\rho)X(\rho) & -J(\rho)T(\rho) & J_w(\rho) & -\frac{1}{2}\gamma I \end{bmatrix} \prec 0, \tag{4.32}$$

Applying a congruent transformation by $diag\{P(\rho), T(\rho)^{-1}, I, I\}$ for the latter matrix inequality that results in

$$\begin{bmatrix} \{P(\rho)(A(\rho)+B(\rho)K(\rho)C(\rho))\}^s + \dot{P}(\rho) & * & * & * \\ T(\rho)^{-1}(K(\rho)C(\rho)-G(\rho))-B(\rho)^T P(\rho) & -2T(\rho)^{-1} & * & * \\ B_w(\rho)^T P(\rho) & 0 & -\gamma I & * \\ H(\rho)+J(\rho)K(\rho)C(\rho) & -J(\rho) & J_w(\rho) & -\gamma I \end{bmatrix} \prec 0, \tag{4.33}$$

Firstly, by applied Schur's complement for above inequality, then *pre*- and *post*-multiplying with $[x(t)^T \ \Phi(u)^T \ w(t)^T]$ and its transposition that entails to the condition:

$$\begin{aligned} 2x(t)^T P(\rho)(A(\rho)+B(\rho)K(\rho)C(\rho))x(t) + x(t)^T \dot{P}(\rho)x(t) + 2x(t)^T P(\rho)B_w(\rho)w(t) \\ -2x(t)^T P(\rho)B(\rho)\Phi(u) + \gamma^{-1}z(t)^T z(t) - \gamma w(t)^T w(t) \\ +2\Phi(u)^T T(\rho)^{-1}(K(\rho)C(\rho)x(t) - G(\rho)x(t) - \Phi(u)) \ < \ 0. \end{aligned} \tag{4.34}$$

Combining with condition (4.28), we have the derivative of PDLF (2.102) along the trajectories of system (2.113) satisfies $\dot{V}(t) + \gamma^{-1}\|z(t)\|^2 - \gamma\|w(t)\|^2 < 0$. That ensues in the statements:

- When $w(t) = 0$, then $\dot{V}(t) < -\gamma^{-1}\|z(t)\|^2 < 0$ ensures that $\mathcal{E}(P(\rho), \eta)$ are the region of asymptotical stability of system (2.113) from $\forall x_0 \in \mathcal{E}_0 \subseteq \mathcal{E}$.
- When $w(t) \in \mathcal{W} \setminus \{0\}$, then (4.34) claims from $\forall x_0 \in \mathcal{E}_0 \subset \mathcal{E}$, the trajectories of LPV system (2.113) do not leave the set $\mathcal{E}(P, \eta, \rho)$, with $V(t) < \gamma\|w(t)\|_{\mathcal{L}_2}^2 + V(0) \leq \gamma\sigma^{-1} + \cdots$ $\eta_0^{-1} \leq \eta^{-1}$.

□

Remark 4.2.1. By using projection lemma (a generalization of Finsler's lemma), the nonlinearities in the stabilizing condition are converted to the *affine* parameter condition. The algebraic manipulation effectively permutes nonlinearities terms $K(\rho)C(\rho)X(\rho)$ related to the SOF controller analysis with substitution $K(\rho)C(\rho)X(\rho) = Y(\rho)C(\rho) + K(\rho)\cdot$ $(C(\rho)X(\rho) - W(\rho)C(\rho))$ and slack-variable $W(\rho)$. In addition, if W^{-1} does not involve in the controller structure, the stabilization conditions return to the general case of SOF controller synthesis for LPV systems. So, this approach provides a more general condition. Based on this development, a parameter-dependent SOF and a fuzzy PDC controller are addressed in the work of literature (Bui Tuan et al., 2021a).

4.3. Observer-based Feedback Stabilization

4.3.1. *Generalization of Young's Inequality*

As analyzed in section 2.3.2.3, the stabilization of the closed-loop system (2.115) using a parametric dependent ellipsoidal domain (2.116) corresponding to feedback controller (2.114) and auxiliary controller (2.118) is stated as follows.

Theorem 4.3.1: *In presence of disturbances, for the positive scalars* $\varepsilon, \overline{u}_s, \eta_0, \eta, \gamma$. *If there exist continuously differentiable matrices function* $X, P_2 : \mathcal{U}_p \to \mathbb{S}^n_{++}$, $Y_1, Z_1, Z_2 : \mathcal{U}_p \to \mathbb{R}^{m\times n}$, $Y_2 : \mathcal{U}_p \to \mathbb{R}^{n\times p}$, *and a diagonal matrix function* $T : \mathcal{U}_p \to \mathbb{S}^m_{++}$, *such that the following PLMI conditions:*

$$\begin{bmatrix} \Xi(\rho) & \Psi(\rho) \\ * & \Theta(\rho) \end{bmatrix} \prec 0, \tag{4.35}$$

$$(a).\begin{bmatrix} \eta_0^{-1} & * & * \\ x(0) & X(\rho_0) & * \\ P_2(\rho_0)e(0) & 0 & P_2(\rho_0) \end{bmatrix} \succeq 0, \quad (b).\begin{bmatrix} X(\rho) & 0 & Z_1(\rho)^T_{(s)} \\ * & P_2(\rho) & G_2(\rho)_{(s)} \\ * & * & \eta\overline{u}_s^2 \end{bmatrix} \succeq 0, \tag{4.36}$$

hold, $\forall x, e \in \mathcal{E}(X, P_2, \eta, \rho), s = 1,..,m$, *then feedback controller and observer with gains* $K(\rho) = Y_1(\rho)X(\rho)^{-1}$, $L(\rho) = P_2(\rho)^{-1}Y_2(\rho)$ *ensures that*

(1) *for* $w(t) = 0$, *the ellipsoid* $\mathcal{E}$ *is a region of asymptotical stability for saturated LPV system* (2.115) *and error estimate* $e(t)$ *converges asymptotically in the domain* $\mathcal{E}$.

(2) *for bounded disturbance* $w(t)$, *from* $\forall\, x(0),\ e(0) \in \mathcal{E}_0 \subset \mathcal{E}$ *the trajectories of saturated closed-loop system* (2.115) *stay in the domain ellipsoid* $\mathcal{E}$ *corresponding to performance index* γ.

where, $\Theta(\rho) = diag\{-\gamma I_d, -\gamma I_n, -\gamma I_n, -\varepsilon X(\rho), -\varepsilon^{-1}X(\rho)\}$,

$$\Xi(\rho) = \begin{bmatrix} \{A(\rho)X(\rho) + B(\rho)Y_1(\rho)\}^S - \dot{X}(\rho) & * & * \\ 0 & \{P_2(\rho)A(\rho) - Y_2(\rho)C(\rho)\}^S + \dot{P}_2(\rho) & * \\ Y_1(\rho) - Z_1(\rho) - T(\rho)B(\rho)^T & -G_2(\rho) & -2T(\rho) \end{bmatrix},$$

$$\Psi(\rho) = \begin{bmatrix} B_w(\rho) & (H(\rho)X(\rho) + J(\rho)Y_1(\rho))^T & 0 & 0 & B(\rho)Y_1(\rho) \\ P_2(\rho)B_w(\rho) & 0 & H_e(\rho)^T & I_n & 0 \\ 0 & (-J(\rho)T(\rho))^T & 0 & 0 & Y_1(\rho) \end{bmatrix}.$$

Proof.

In a repetitive manner, conditions (4.36).*a* brings to the initial condition:

$$x(0)^T P_1(\rho_0)x(0) + e(0)^T P_2(\rho_0)e(0) \le \eta_0^{-1} \qquad \to V(0) \le \eta_0^{-1}. \tag{4.37}$$

And the saturation constraints on the additional vector are derived from:

$$\left(\eta\overline{u}_s^2\right)^{-1} \left\| \begin{bmatrix} G_1(\rho)_{(s)} & G_2(\rho)_{(s)} \end{bmatrix} \begin{bmatrix} x(t) \\ e(t) \end{bmatrix} \right\|^2 \le \begin{bmatrix} x(t) \\ e(t) \end{bmatrix}^T \begin{bmatrix} P_1(\rho) & 0 \\ 0 & P_2(\rho) \end{bmatrix} \begin{bmatrix} x(t) \\ e(t) \end{bmatrix}. \tag{4.38}$$

with $G_i(\rho) = Z_i(\rho)P_1(\rho)$, $P_1(\rho) = X(\rho)^{-1}$, $i = 1,2$, and $s = 1,..,m$. Then, these PLMI conditions are organized as follows:

$$\begin{bmatrix} P_1(\rho) & 0 & G_1(\rho)_{(s)}^T \\ * & P_2(\rho) & G_2(\rho)_{(s)}^T \\ * & * & \eta\overline{u}_s^2 \end{bmatrix} \succeq 0. \tag{4.39}$$

By applying a simple transformation with $diag\{X(\rho), I, I\}$ and its transposition that entails in conditions (4.36).*b.*

On the other side, similar to the development of Theorem 3.1.1, we have the following stabilization conditions for the closed-loop system (2.115):

$$\left[\begin{array}{ccc:ccc} \Xi_{11}(\rho) & * & * & * & * & * \\ -K(\rho)^T B(\rho)^T & \Xi_{22}(\rho) & * & * & * & * \\ Y_1(\rho) - Z_1(\rho) - T(\rho)B(\rho)^T & -(K(\rho)+G_2(\rho)) & -2T(\rho) & * & * & * \\ \hdashline B_w(\rho)^T & 0 & 0 & -\gamma I_d & * & * \\ H(\rho)X(\rho)+J(\rho)Y_1(\rho) & 0 & -J(\rho)T(\rho) & 0 & -\gamma I_r & * \\ 0 & H_e(\rho) & 0 & 0 & 0 & -\gamma I_n \end{array}\right] \prec 0, \tag{4.40}$$

with, $\Xi_{11}(\rho) = \{A(\rho)X(\rho) + B(\rho)Y_1(\rho)\}^S - \dot{X}(\rho)$,
$\Xi_{22}(\rho) = \{P_2(\rho)A(\rho) - Y_2(\rho)C(\rho)\}^S + \dot{P}_2(\rho)$, and $Y_1(\rho) = K(\rho)X(\rho)$, $Y_2(\rho) = P_2(\rho)L(\rho)$.

In the literature (Tarbouriech et al., 2011), the presences of gain $K(\rho)$ in stabilizing condition (4.40) implies in the non-convex forms. In this work, by deploying Young's inequality for bilinear terms $K(\rho)^T B(\rho)^T$, $K(\rho)$ in conditions (4.40), we have:

$$\left\{\begin{bmatrix} B(\rho)K(\rho) \\ 0 \\ K(\rho) \\ 0 \\ 0 \\ 0 \end{bmatrix}\begin{bmatrix} 0 \\ I \\ 0 \\ 0 \\ 0 \\ 0 \end{bmatrix}^T\right\}^S \preceq \varepsilon^{-1}\begin{bmatrix} 0 \\ I \\ 0 \\ 0 \\ 0 \\ 0 \end{bmatrix} X(\rho)^{-1}\begin{bmatrix} 0 \\ I \\ 0 \\ 0 \\ 0 \\ 0 \end{bmatrix}^T + \varepsilon\begin{bmatrix} B(\rho)Y_1(\rho) \\ 0 \\ Y_1(\rho) \\ 0 \\ 0 \\ 0 \end{bmatrix} X(\rho)^{-1}\begin{bmatrix} B(\rho)Y_1(\rho) \\ 0 \\ Y_1(\rho) \\ 0 \\ 0 \\ 0 \end{bmatrix}^T, \tag{4.41}$$

Then, replacing the above decomposition to PLMIs (4.40), and reorganizing by Schur's complement that ensues in conditions (4.35). The remainder is settled similarly to the latter theorem.
That concludes the proof. □

Remark 4.3.1. A relaxing method for the stabilization condition using Young's inequality presents in Chapter 3. But the conservation of this inequality is also related to the organization of the right side. As observed in condition $\varepsilon > 0, X(\rho) \succ 0$, the right-hand side of this inequality is always positive, whereas the left side (the primary solution domain) can be positive or negative. That leads to the conservatism in the design conditions.

4.3.2. *Generalization of Finsler's Lemma*

The conservatism of OBF controllers using Young's inequality will reveal in the comparison section. To overcome the problem in Theorem 4.3.1, we introduce a new observer-based control structure using the generalization of Finsler's lemma. Then, the stabilization condition is stated as follows.

Theorem 4.3.2: *In presence of disturbances, for the positive scalars* $\varepsilon, \overline{u}_s, \eta_0, \eta, \gamma$. *If there exist continuously differentiable matrices function* $P_1, P_2 : \mathcal{U}_p \to \mathbb{S}^n_{++}$, $Y_1, G_1, G_2 : \mathcal{U}_p \to \mathbb{R}^{m\times n}$, $Y_2 : \mathcal{U}_p \to \mathbb{R}^{n\times p}$, *a matrix function* $X, Y_3 : \mathcal{U}_p \to \mathbb{R}^{m\times m}_{++}$, *and a diagonal matrix function* $T : \mathcal{U}_p \to \mathbb{S}^m_{++}$, *such that the following PLMI conditions:*

$$\left[\begin{array}{c|cccccc} -X(\rho)^S & * & * & * & * & * & * \\ \hline P_1(\rho)B(\rho)+Y_1(\rho)^T & \Psi_{22}(\rho) & * & * & * & * & * \\ -Y_1(\rho)^T & 0 & \Psi_{33}(\rho) & * & * & * & * \\ \frac{1}{2}I_m - Y_3(\rho)^T & -G_1(\rho) & -G_2(\rho) & -T(\rho) & * & * & * \\ 0 & B_w(\rho)^T P_1(\rho) & B_w(\rho)^T P_2(\rho) & 0 & \gamma I_d & * & * \\ J(\rho) & H(\rho) & 0 & 0 & J_w(\rho) & \gamma I_r & * \\ 0 & 0 & H_e(\rho) & 0 & 0 & 0 & \gamma I_n \end{array}\right] \prec 0, \tag{4.42}$$

$$(a).\ \begin{bmatrix} \eta_0^{-1} & * & * \\ P_1(\rho_0)x(0) & P_1(\rho_0) & * \\ P_2(\rho_0)e(0) & 0 & P_2(\rho_0) \end{bmatrix} \succeq 0, \qquad (b).\ \begin{bmatrix} P_1(\rho) & 0 & G_1(\rho)^T_{(s)} \\ * & P_2(\rho) & G_2(\rho)^T_{(s)} \\ * & * & \eta\overline{u}_s^2 \end{bmatrix} \succeq 0, \tag{4.43}$$

hold, $\forall x, e \in \mathcal{E}(P_1(\rho), P_2(\rho), \eta), s = 1,..,m$, *then feedback controller and observer with gains* $K(\rho) = X(\rho)^{-1}Y_1(\rho)$, $L(\rho) = P_2(\rho)^{-1}Y_2(\rho)$ *ensures that*

(1) *for* $w(t) = 0$, *the ellipsoid* $\mathcal{E}$ *is a region of asymptotical stability for saturated LPV system* (2.115)*, and error estimate* $e(t)$ *converges asymptotically in the domain* $\mathcal{E}$.

(2) *for bounded disturbance* $w(t)$, *from* $\forall\, x(0),\ e(0) \in \mathcal{E}_0 \subset \mathcal{E}$ *the trajectories of saturated closed-loop system* (2.115) *are contractive in the domain ellipsoid* $\mathcal{E}$ *corresponding to performance index* γ.

where, $\Psi_{22}(\rho) = \{P_1(\rho)A(\rho)\}^S + \dot{P}_1(\rho), \qquad \Psi_{33}(\rho) = \{P_2(\rho)A(\rho) - Y_2(\rho)C(\rho)\}^S + \dot{P}_2(\rho).$

Proof.

In a repetitive manner, conditions (4.43) proceed from the initial condition and saturation constraints on the additional controls such that:

$$x(0)^T P_1(\rho_0)x(0) + e(0)^T P_2(\rho_0)e(0) \le \eta_0^{-1}, \tag{4.44}$$

$$\left(\eta\overline{u}_s^2\right)^{-1} \left\| \begin{bmatrix} G_1(\rho)_{(s)} & G_2(\rho)_{(s)} \end{bmatrix} \begin{bmatrix} x(t) \\ e(t) \end{bmatrix} \right\|^2 \le \begin{bmatrix} x(t) \\ e(t) \end{bmatrix}^T \begin{bmatrix} P_1(\rho) & 0 \\ 0 & P_2(\rho) \end{bmatrix} \begin{bmatrix} x(t) \\ e(t) \end{bmatrix}. \tag{4.45}$$

Where the GSC condition can recall as follows:

$$\Phi(u)^T T(\rho)^{-1} \left(\begin{bmatrix} K(\rho) - G_1(\rho) & -K(\rho) - G_2(\rho) \end{bmatrix} \begin{bmatrix} x(t) \\ e(t) \end{bmatrix} - \Phi(u) \right) \ \ge\ 0. \tag{4.46}$$

On the other hand, PDLMI (4.42) is reorganized by:

$$\Psi(\rho) + \mathcal{P}(\rho)^T \Theta(\rho)\mathcal{Q}(\rho) + \mathcal{Q}(\rho)^T \Theta(\rho)^T \mathcal{P}(\rho) \ \prec\ 0, \tag{4.47}$$

where

$$\begin{array}{ll} \Theta(\rho) = X(\rho), & Y_2(\rho) = P_2(\rho)L(\rho), \\ Y_1(\rho) = X(\rho)K(\rho), & Y_3(\rho) = P_1(\rho)B(\rho)T(\rho), \end{array}$$

$$\Psi(\rho)=\left[\begin{array}{c|cccccc} 0 & * & * & * & * & * & * \\ \hline P_1(\rho)B(\rho) & \Psi_{22}(\rho) & * & * & * & * & * \\ 0 & 0 & \Psi_{33}(\rho) & * & * & * & * \\ \frac{1}{2}I_m & -G_1(\rho)-Y_3(\rho)^T & -G_2(\rho) & -T(\rho) & * & * & * \\ 0 & B_w(\rho)^T P_1(\rho) & B_w(\rho)^T P_1(\rho) & 0 & -\gamma I_d & * & * \\ J(\rho) & H(\rho) & 0 & 0 & J_w(\rho) & -\gamma I_r & * \\ 0 & 0 & H_e(\rho) & 0 & 0 & 0 & -\gamma I_n \end{array}\right]$$

$$\mathcal{P}(\rho)=[-I \mid K(\rho) \quad -K(\rho) \quad 0 \quad 0 \quad 0 \quad 0], \text{ and } \mathcal{Q}(\rho)=[I \mid 0 \quad 0 \quad 0 \quad 0 \quad 0 \quad 0].$$

Given any matrices base of the null spaces of $\mathcal{P}$, and $\mathcal{Q}$, e.g.,

$$\ker(\mathcal{P})^T=\left[\begin{array}{c|cccccc} K(\rho)^T & I & 0 & 0 & 0 & 0 & 0 \\ -K(\rho)^T & 0 & I & 0 & 0 & 0 & 0 \\ 0 & 0 & 0 & I & 0 & 0 & 0 \\ 0 & 0 & 0 & 0 & I & 0 & 0 \\ 0 & 0 & 0 & 0 & 0 & I & 0 \\ 0 & 0 & 0 & 0 & 0 & 0 & I \end{array}\right], \text{and } \ker(\mathcal{Q})^T=\left[\begin{array}{c|cccccc} 0 & I & 0 & 0 & 0 & 0 & 0 \\ 0 & 0 & I & 0 & 0 & 0 & 0 \\ 0 & 0 & 0 & I & 0 & 0 & 0 \\ 0 & 0 & 0 & 0 & I & 0 & 0 \\ 0 & 0 & 0 & 0 & 0 & I & 0 \\ 0 & 0 & 0 & 0 & 0 & 0 & I \end{array}\right].$$

Followed the projection lemma, the feasibility of inequality (4.47) entails in the feasibility of the underlying LMIs:

$$\ker(\mathcal{P})^T\Psi(\rho)\ker(\mathcal{P}) \prec 0, \tag{4.48}$$

$$\ker(\mathcal{Q})^T\Psi(\rho)\ker(\mathcal{Q}) \prec 0, \tag{4.49}$$

Applying a congruent transformation by $diag\{I,I,T(\rho)^{-1},I,I,I\}$ for condition (4.48), we have the following PDLMI:

$$\left[\begin{array}{cccccc} \Xi_{11}(\rho) & * & * & * & * & * \\ \Xi_{21}(\rho) & \Xi_{22}(\rho) & * & * & * & * \\ \Xi_{31}(\rho) & \Xi_{32}(\rho) & -2T(\rho)^{-1} & * & * & * \\ B_w(\rho)^T P_1(\rho) & B_w(\rho)^T P_1(\rho) & 0 & -\gamma I_d & * & * \\ H(\rho)+J(\rho)K(\rho) & -J(\rho)K(\rho) & -J(\rho)T(\rho) & J_w(\rho) & -\gamma I_r & * \\ 0 & H_e(\rho) & 0 & 0 & 0 & -\gamma I_n \end{array}\right] \prec 0, \tag{4.50}$$

with

$$\begin{aligned} \Xi_{11}(\rho) &= \Psi_{22}(\rho)+\{P_1(\rho)B(\rho)K(\rho)\}^S, \\ \Xi_{21}(\rho) &= -(P_1(\rho)B(\rho)K(\rho))^T, \\ \Xi_{31}(\rho) &= T(\rho)^{-1}(K(\rho)-G_1(\rho))+(P_1(\rho)B(\rho))^T \\ \Xi_{22}(\rho) &= \Psi_{33}(\rho)=\{P_2(\rho)A(\rho)-P_2(\rho)L(\rho)C(\rho)\}^S+\dot{P}_2(\rho), \\ \Xi_{32}(\rho) &= -T(\rho)^{-1}(K(\rho)+G_2(\rho)). \end{aligned}$$

Subsequently, applied Schur's complement for above inequality, then *pre*- and *post*-multiplying with $[x(t)^T \quad e(t)^T \quad \Phi(u)^T \quad w(t)^T]$ and its transposition that entails to:

$$\begin{aligned} &2\begin{bmatrix}x(t)\\e(t)\end{bmatrix}^T\begin{bmatrix}P_1(\rho) & 0\\ 0 & P_2(\rho)\end{bmatrix}\begin{bmatrix}A(\rho)+B(\rho)K(\rho) & -B(\rho)K(\rho)\\ 0 & A(\rho)-L(\rho)C(\rho)\end{bmatrix}\begin{bmatrix}x(t)\\e(t)\end{bmatrix}x(t) \\ &+\begin{bmatrix}x(t)\\e(t)\end{bmatrix}^T\begin{bmatrix}\dot{P}_1(\rho) & 0\\ 0 & \dot{P}_2(\rho)\end{bmatrix}\begin{bmatrix}x(t)\\e(t)\end{bmatrix}+2\begin{bmatrix}x(t)\\e(t)\end{bmatrix}^T\begin{bmatrix}P_1(\rho) & 0\\ 0 & P_2(\rho)\end{bmatrix}\begin{bmatrix}B_w(\rho)\\B_w(\rho)\end{bmatrix}w(t) \end{aligned}$$

$$-2\begin{bmatrix}x(t)\\e(t)\end{bmatrix}^T\begin{bmatrix}P_1(\rho) & 0\\ 0 & P_2(\rho)\end{bmatrix}\begin{bmatrix}-B(\rho)\\0\end{bmatrix}\Phi(u)+\gamma^{-1}z(t)^T z(t)-\gamma w(t)^T w(t)$$
$$+2\Phi(u)^T T(\rho)^{-1}\left(\begin{bmatrix}K(\rho)-G_1(\rho) & -K(\rho)-G_2(\rho)\end{bmatrix}\begin{bmatrix}x(t)\\e(t)\end{bmatrix}-\Phi(u)\right) < 0. \quad (4.51)$$

Following the line of the GSC condition for feedback control law (2.114), if the above condition holds, then the derivative of PDLF (2.102) along the trajectories of system (2.115) satisfies $\dot{V}(t)+\gamma^{-1}\|z(t)\|^2-\gamma\|w(t)\|^2<0,$ that implies in the statements:

- When $w(t)=0,$ then $\dot{V}(t)<-\gamma^{-1}\|z(t)\|^2<0$ ensures that $\mathcal{E}(P_1(\rho),P_2(\rho),\eta)$ are the region of asymptotical stability of the closed-loop system from $\forall x_0,e_0\in\mathcal{E}_0\subseteq\mathcal{E}.$
- When $w(t)\in\mathcal{W}\setminus\{0\}$ then (4.51) claims from $\forall x_0,e_0\in\mathcal{E}_0\subset\mathcal{E},$ the trajectories of LPV system (2.115) converge toward the set $\mathcal{E},$ with $V(t)<\gamma\|w(t)\|_{\mathcal{L}_2}^2+V(0)\leq\gamma\sigma^{-1}+\cdots$ $\eta_0^{-1}\leq\eta^{-1}.$

Which completes the proof. □

Remark 4.3.2. Instead of applying the generalization of Young's inequality in condition (4.41), the nonlinearities $P_1(\rho)B(\rho)K(\rho)$ is converted to the *convex* problem by using Finsler's lemma. The algebraic manipulation effectively decouples terms $B(\rho)K(\rho)$ involved the OBF development by replacing the slack-variable $X(\rho).$ The significant improvement of system performance is demonstrated in the results section 4.5.1, compared between the traditional method Theorem 4.3.1, the new design method Theorem 4.3.2, and the other developments.

4.4. Dynamic Output Feedback Stabilization

As described in section 2.3.2.4, we now address the necessary and sufficient conditions for the stabilization of closed-loop system (2.121) using dynamic control system (2.120) combined with auxiliary controller (2.126). A decomposition uses for the gain-scheduling DOF design strategy with the transformation matrix variables:

$$\Pi_1(\rho)=\begin{bmatrix}\boldsymbol{X}(\rho) & I\\ M(\rho)^T & 0\end{bmatrix},\ \Pi_2(\rho)=\begin{bmatrix}I & \boldsymbol{Y}(\rho)\\ 0 & N(\rho)^T\end{bmatrix}, \quad (4.52)$$

$$P(\rho)\Pi_1(\rho)=\Pi_2(\rho),\ \Pi_1(\rho)^T\Pi_2(\rho)=\begin{bmatrix}\boldsymbol{X}(\rho) & I\\ I & \boldsymbol{Y}(\rho)\end{bmatrix}. \quad (4.53)$$

The *crux* of the parameter-dependent stabilization synthesis is the derivatives of the parameter lied on the design conditions. The approach of (Gahinet, 1996; Scherer et al., 1997) meets the difficulties with the expansion of derivative $\dot{P}(\rho)$ involved in the derivative of $\star$. To avoid this problem, we can take advantage of the relationship (4.53) s.t.,

$$\Pi_1(\rho)^T\dot{P}(\rho)\Pi_1(\rho)=\Pi_1(\rho)^T\dot{\Pi}_2(\rho)-\Pi_1(\rho)^T P(\rho)\dot{\Pi}_1(\rho)$$
$$=\begin{bmatrix}-\dot{\boldsymbol{X}}(\rho) & \boldsymbol{X}(\rho)\dot{Y}(\rho)+M(\rho)\dot{N}(\rho)^T\\ \dot{\boldsymbol{Y}}(\rho)\boldsymbol{X}(\rho)+\dot{N}(\rho)M(\rho)^T & \dot{\boldsymbol{Y}}(\rho)\end{bmatrix}, \quad (4.54)$$

with $\dot{Y}(\rho)X(\rho)+\dot{N}(\rho)M(\rho)^T=-(Y(\rho)\dot{X}(\rho)+N(\rho)\dot{M}(\rho)^T).$ From the definition of state-space system (2.121), the production of variable matrices are deployed as follow:

$$\Pi_1(\rho)^T sym\{P(\rho)\mathbb{A}+\tfrac{1}{2}\dot{P}(\rho)\}\Pi_1(\rho)=$$
$$sym\begin{bmatrix}A(\rho)\boldsymbol{X}(\rho)+B(\rho)\hat{\boldsymbol{C}}(\rho)-\frac{1}{2}\dot{\boldsymbol{X}}(\rho) & A(\rho)+B(\rho)\hat{\boldsymbol{D}}(\rho)C(\rho)\\ \hat{\boldsymbol{A}}(\rho) & Y(\rho)A(\rho)+\hat{\boldsymbol{B}}(\rho)C(\rho)+\frac{1}{2}\dot{\boldsymbol{Y}}(\rho)\end{bmatrix}, \tag{4.55}$$

$$\Pi_2(\rho)^T\mathbb{B}_1=\begin{bmatrix}-B(\rho)\\ -\boldsymbol{Y}(\rho)B(\rho)\end{bmatrix},\ \text{and}\ \Pi_2(\rho)^T\mathbb{B}_2=\begin{bmatrix}B(\rho)\hat{\boldsymbol{D}}(\rho)D_w(\rho)+B_w(\rho)\\ \hat{B}(\rho)D_w(\rho)+\boldsymbol{Y}(\rho)B_w(\rho)\end{bmatrix}, \tag{4.56}$$

$$\mathbb{C}\Pi_1(\rho)=[H(\rho)\boldsymbol{X}(\rho)+J(\rho)\hat{\boldsymbol{C}}(\rho)\quad H(\rho)+J(\rho)\hat{\boldsymbol{D}}(\rho)C(\rho)], \tag{4.57}$$

$$\mathbb{G}\Pi_1(\rho)=[\hat{\boldsymbol{F}}(\rho)\quad \hat{\boldsymbol{G}}(\rho)C(\rho)],(\mathbb{K}-\mathbb{G})\Pi_1(\rho)=[\hat{\boldsymbol{C}}(\rho)-\hat{\boldsymbol{F}}(\rho)\quad (\hat{\boldsymbol{D}}(\rho)-\hat{\boldsymbol{G}}(\rho))C(\rho)], \tag{4.58}$$

where the change of controller variables:

$$\begin{aligned}\hat{\boldsymbol{A}}(\rho)&=\dot{\boldsymbol{Y}}(\rho)\boldsymbol{X}(\rho)+\dot{N}(\rho)M(\rho)^T+\boldsymbol{Y}(\rho)(A(\rho)+B(\rho)D(\rho)C(\rho))\boldsymbol{X}(\rho)+N(\rho)A_c(\rho)M(\rho)^T\\&\quad+\boldsymbol{Y}(\rho)B(\rho)C_c(\rho)M(\rho)^T+N(\rho)B_c(\rho)C(\rho)\boldsymbol{X}(\rho),\\ \hat{\boldsymbol{B}}(\rho)&=\boldsymbol{Y}(\rho)B(\rho)D_c(\rho)+N(\rho)B_c(\rho),\\ \hat{\boldsymbol{C}}(\rho)&=D_c(\rho)C(\rho)\boldsymbol{X}(\rho)+C_c(\rho)M(\rho)^T,\\ \hat{\boldsymbol{D}}(\rho)&=D_c(\rho),\\ \hat{\boldsymbol{F}}(\rho)&=G_c(\rho)C(\rho)\boldsymbol{X}(\rho)+F_c(\rho)M(\rho)^T,\\ \hat{\boldsymbol{G}}&=G_c(\rho).\end{aligned} \tag{4.59}$$

Based on the new transformation, we get the following stabilization conditions for the saturated system (2.121) with feedback control law (2.125).

Theorem 4.4.1: *In presence of disturbances, for the positive scalars* $\varepsilon,\overline{u}_s,\eta,\eta_0,\gamma$. *If there exist continuously differentiable matrices function* $\boldsymbol{X},\boldsymbol{Y}:\mathcal{U}_p\to\mathbb{S}^n_{++}$, $\hat{\boldsymbol{A}}:\mathcal{U}_p\to\mathbb{R}^{n\times n},\hat{\boldsymbol{B}}:\mathcal{U}_p\to\mathbb{R}^{n\times p},\hat{\boldsymbol{C}},\hat{\boldsymbol{F}}:\mathcal{U}_p\to\mathbb{R}^{m\times n},\hat{\boldsymbol{D}},\hat{\boldsymbol{G}}:\mathcal{U}_p\to\mathbb{R}^{m\times p}$, *and diagonal matrix* $T\in\mathbb{S}^m_{++}$, *such that the following conditions:*

$$(a).\ \begin{bmatrix}\Xi(\rho) & \Psi(\rho)\\ * & \Theta(\rho)\end{bmatrix}\prec 0, \qquad (b).\ \begin{bmatrix}\boldsymbol{X}(\rho) & \varepsilon I\\ \varepsilon I & \boldsymbol{Y}(\rho)\end{bmatrix}\succeq 0, \tag{4.60}$$

$$\begin{bmatrix}\eta_0^{-1} & * & *\\ x(0) & \boldsymbol{X}(\rho_0) & *\\ \boldsymbol{Y}(\rho_0)x(0)+N(\rho_0)x_c(0) & I & \boldsymbol{Y}(\rho_0)\end{bmatrix}\succeq 0, \tag{4.61}$$

$$\begin{bmatrix}\boldsymbol{X}(\rho) & I & \hat{\boldsymbol{F}}(\rho)_{(s)}^T\\ * & \boldsymbol{Y}(\rho) & C(\rho)^T\hat{\boldsymbol{G}}(\rho)_{(s)}^T\\ * & * & \eta\overline{u}_s^2\end{bmatrix}\succeq 0, \tag{4.62}$$

are satisfied, $\forall x(t),\ x_c(t)\in\mathcal{E}(P(\rho),\eta),\ s=1,..,m$, *then the controller gains are given by*

$$\begin{aligned}D_c(\rho)&=\hat{\boldsymbol{D}}(\rho),\\ C_c(\rho)&=(\hat{\boldsymbol{C}}(\rho)-\hat{\boldsymbol{D}}(\rho)C(\rho)\boldsymbol{X}(\rho))M(\rho)^{-T},\\ B_c(\rho)&=N(\rho)^{-1}(\hat{\boldsymbol{B}}(\rho)-\boldsymbol{Y}(\rho)B(\rho)\hat{\boldsymbol{D}}(\rho)),\\ A_c(\rho)&=N(\rho)^{-1}(\hat{\boldsymbol{A}}(\rho)-\dot{\boldsymbol{Y}}(\rho)\boldsymbol{X}(\rho)-\dot{N}(\rho)M(\rho)^T-\hat{\boldsymbol{B}}(\rho)C(\rho)\boldsymbol{X}(\rho)\cdots\\&\quad-Y(\rho)B(\rho)\hat{\boldsymbol{C}}(\rho)-\boldsymbol{Y}(\rho)(A(\rho)-B(\rho)\hat{\boldsymbol{D}}(\rho)C(\rho))\boldsymbol{X}(\rho))M(\rho)^{-T},\end{aligned} \tag{4.63}$$

ensures that,

(1) *for* $w(t)=0$, *the ellipsoid* $\mathcal{E}$ *is a region of asymptotical stability for saturated LPV system* (2.121).

(2) *for bounded disturbance* $w(t)$, *from* $\forall\, x(0),\ x_c(0) \in \mathcal{E}_0 \subset \mathcal{E}$ *the trajectories of saturated closed-loop system* (2.121) *converge in the enclosed domain ellipsoid* $\mathcal{E}$ *corresponding to performance index* γ.

where,

$$\Xi(\rho)=\begin{bmatrix} \{A(\rho)\boldsymbol{X}(\rho)+B(\rho)\hat{\boldsymbol{C}}(\rho)\}^S-\dot{\boldsymbol{X}}(\rho) & * & * \\ \hat{\boldsymbol{A}}(\rho)+(A(\rho)+B(\rho)\hat{\boldsymbol{D}}(\rho)C(\rho))^T & \{Y(\rho)A(\rho)+\hat{\boldsymbol{B}}(\rho)C(\rho)\}^S+\dot{\boldsymbol{Y}}(\rho) & * \\ \hat{\boldsymbol{C}}(\rho)-\hat{\boldsymbol{F}}(\rho)-T(\rho)B(\rho)^T & (\hat{\boldsymbol{D}}(\rho)-\hat{\boldsymbol{G}}(\rho))C(\rho)-T(\rho)B(\rho)^T\boldsymbol{Y}(\rho) & -2T(\rho) \end{bmatrix},$$

$$\Psi(\rho)=\begin{bmatrix} B(\rho)\hat{\boldsymbol{D}}(\rho)D_w(\rho)+B_w(\rho) & (H(\rho)\boldsymbol{X}(\rho)+J(\rho)\hat{\boldsymbol{C}}(\rho))^T \\ \hat{B}(\rho)D_w(\rho)+\boldsymbol{Y}(\rho)B_w(\rho) & (H(\rho)+J(\rho)\hat{\boldsymbol{D}}(\rho)C(\rho))^T \\ \hat{\boldsymbol{D}}(\rho)D_w(\rho) & -T(\rho)J(\rho)^T \end{bmatrix},$$

and $\Theta(\rho)=\begin{bmatrix} -\gamma I_d & (J(\rho)\hat{\boldsymbol{D}}(\rho)D_w(\rho)+J_w(\rho))^T \\ * & -\gamma I_r \end{bmatrix}$.

Proof.

Inherently, the above conditions are interpreted the same as previous theorems. Firstly, the saturation constraints involved in feedback controller (2.125) and auxiliary controller (2.126) will be analyzed. By using the congruence transformation (4.52), (4.53), and (4.58) we have LMIs (4.61)-(4.62) equivalent to the following conditions:

$$\begin{bmatrix} 1 & 0 \\ 0 & \Pi_2(\rho_0) \end{bmatrix}^T \begin{bmatrix} \eta_0^{-1} & \zeta(0)^T \\ \zeta(0) & P(\rho_0)^{-1} \end{bmatrix} \begin{bmatrix} 1 & 0 \\ 0 & \Pi_2(\rho_0) \end{bmatrix} \succeq 0, \tag{4.64}$$

$$\begin{bmatrix} \Pi_1(\rho) & 0 \\ 0 & 1 \end{bmatrix}^T \begin{bmatrix} P(\rho) & \mathbb{G}_{(s)}^T \\ \mathbb{G}_{(s)} & \eta\overline{u}_s^2 \end{bmatrix} \begin{bmatrix} \Pi_1(\rho) & 0 \\ 0 & 1 \end{bmatrix} \succeq 0,\ s=1,..,m. \tag{4.65}$$

It can realize that these are the initial condition and the saturation bounding on the controller. Now, applying Corollary 2.3.1 to the feedback control laws (2.125), we have:

$$\Phi^T(u)T(\rho)^{-1}(\mathbb{K}\zeta(t)-\Phi(u)-\mathbb{G}\zeta(t)-\hat{\boldsymbol{D}}(\rho)D_w(\rho)w(t)) \geq 0. \tag{4.66}$$

Repeating tedious mathematical transformations, combining the $\mathscr{H}_\infty$ performance, GSC condition (4.66) and derivative of Lyapunov function (2.123) along the trajectories of closed-loop system (2.121) for all $\zeta(t) \in \mathcal{E}(P(\rho),\eta)$, that yields to:

$$sym\begin{bmatrix} P(\rho)\mathbb{A}+\frac{1}{2}\dot{P}(\rho) & P(\rho)\mathbb{B}_1 & P(\rho)\mathbb{B}_2 & 0 \\ T(\rho)^{-1}(\mathbb{K}-\mathbb{G}) & -T(\rho)^{-1} & T(\rho)^{-1}\hat{\boldsymbol{D}}(\rho)D_w(\rho) & 0 \\ 0 & 0 & -\frac{1}{2}\gamma I & 0 \\ \mathbb{C} & \mathbb{D}_1 & \mathbb{D}_2 & -\frac{1}{2}\gamma I \end{bmatrix} \prec 0. \tag{4.67}$$

By pre- and post-multiply $diag\{\Pi_1(\rho)^T, T(\rho), I, I\}$ for above condition:

$$sym\begin{bmatrix} \Pi_1(\rho)^T(P(\rho)\mathbb{A}+\frac{1}{2}\dot{P}(\rho))\Pi_1(\rho) & \Pi_2(\rho)\mathbb{B}_1T(\rho) & \Pi_2(\rho)\mathbb{B}_2 & 0 \\ (\mathbb{K}-\mathbb{G})\Pi_1(\rho) & -T(\rho) & \hat{\boldsymbol{D}}(\rho)D_w(\rho) & 0 \\ 0 & 0 & -\frac{1}{2}\gamma I & 0 \\ \mathbb{C}\Pi_1(\rho) & \mathbb{D}_1T(\rho) & \mathbb{D}_2 & -\frac{1}{2}\gamma I \end{bmatrix} \prec 0. \tag{4.68}$$

Continuously, by using substitutions (4.54)-(4.58) that entails directly stabilization conditions (4.60).*a*. Whereas, condition (4.60).*b* is set to guarantee the definitively symmetrical positive of the matrix function $P(\rho)$, can indirectly determine by $\Pi_1(\rho)^T P(\rho)\Pi_1(\rho)$. Non-zero scalar ε ensures that matrix $\boldsymbol{X}(\rho)\boldsymbol{Y}(\rho)$ is nonsingular.

This end of the proof. □

Remark 4.4.1. Bilinearity $T(\rho)B(\rho)^T\boldsymbol{Y}(\rho)$ relates to the expression $T(\rho)\mathbb{B}_1^T\Pi_2(\rho)$ causes condition (4.60).*a* to no longer affine, because both $\boldsymbol{Y}(\rho)$ and $T(\rho)$ are already presented in this condition. In this case, the dead-zone nonlinearity is now included in dynamic controller (2.120) by following expression:

$$\begin{aligned}\dot{x}_c(t) &= A_c(\rho)x_c(t) + B_c(\rho)y(t) + E_c(\rho)\Phi(u),\\ u(t) &= C_c(\rho)x_c(t) + D_c(\rho)y(t).\end{aligned} \tag{4.69}$$

That entails a slight modification in extended system (2.121) such as:

$$\mathbb{B}_1 = \begin{bmatrix}-B(\rho)\\ E_c(\rho)\end{bmatrix}. \tag{4.70}$$

Then, the following the development, the bilinear problem is reformatted as:

$$\Pi_2(\rho)^T\mathbb{B}_1 T = \begin{bmatrix}-B(\rho)T\\ -\boldsymbol{Y}(\rho)B(\rho)T + N(\rho)E_c(\rho)T\end{bmatrix}. \tag{4.71}$$

Now, let's denote a new variable $\hat{\boldsymbol{E}}(\rho) = -\boldsymbol{Y}(\rho)B(\rho)T + N(\rho)E_c(\rho)T$, then the stabilization in Theorem 4.4.1 returns to convex form, where the dynamic gain is obtained by:

$$E_c(\rho) = N(\rho)^{-1}(\hat{\boldsymbol{E}}(\rho)T^{-1} + \boldsymbol{Y}(\rho)B(\rho)). \tag{4.72}$$

Remark 4.4.2. It should notice that the observer-based output feedback development in the previous section is a particular case of dynamic output feedback by setting:

$$x_c(t) \coloneqq \hat{x}(t);\ A_c \coloneqq A - LC + BK;\ B_c \coloneqq L;\ [D_cC \quad C_c] \coloneqq [K \quad -K]. \tag{4.73}$$

Besides, we only present the ordinary case where the order of the dynamical output-feedback controller equals to the plant system. The square matrices $N(\rho), M(\rho)$ provide the unique solutions for Eqs. (4.63) and (4.72).

4.5. Examples

In this section, the presented results relate to the following methodological arguments:

- The conservatism and implementation of the designed saturation controllers: the optimal level of reduced disturbance and the size criterion are addressed consistent to each proposed method (the state feedback and the output feedback strategy). In addition, the responses of the closed-loop systems governed by the design controllers expose an overall features and characteristics of the saturated control synthesis.
- The performance degradation and instability of the *nominal* (unconstrained) control system when the actuator saturates, compared with designed saturated systems.

- The analysis of the stabilization conditions using the parameter-dependent Lyapunov function shows the performance superiority over the quadratic Lyapunov condition.

In the first part, the stabilization analysis of a lateral axis dynamics for the L-1011 aircraft are deployed by the state feedback - SF (Theorem 4.1.1), the static output feedback - SOF (Theorem 4.2.1), the observer-based feedback – OBF (Theorem 4.3.1&Theorem 4.3.2), and the dynamic output feedback - DOF (Theorem 4.4.1). Based on these optimization results, we choose the appropriate feedback control structures to continue for the succeeding comparison. In which the gain-scheduling controllers stabilize the closed-loop LPV system demonstrate the effectiveness of the proposed method (ensures the stability of the corresponding designed saturation limits, and improves the system performance when the actuator reaches the saturation threshold).

Finally, the parameter-dependent stabilization conditions deployed for a quadratic Lyapunov stabilization condition and a non-quadratic Lyapunov function (NQLF). The latter discussion provides the less conservative stabilizing conditions of the parameter-dependent Lyapunov function toward the quadratic formulation.

4.5.1. *Saturated Feedback Controller Comparison*

Example 4.5.1: Consider the lateral axis dynamics of the L-1011 aircraft. The state-space representation for the L-1011 aircraft associated with the yaw rate, side slip angle, bank angle, and roll rate dynamics borrowed from (Andry et al., 1984; Galimidi & Barmish, 1986) and modified in (A. T. Nguyen et al., 2018) is given by:

$$A(\rho)=\begin{bmatrix}-2.980 & \rho(t) & 0 & -0.034\\ -\rho(t) & -0.210 & 0.035 & -0.001\\ 0 & 0 & 0 & 1.000\\ 0.390 & -1.350-3\rho(t) & 0 & -1.890\end{bmatrix},\ B(\rho)=\begin{bmatrix}-0.032\\ 0\\ 0\\ -\rho(t)\end{bmatrix},\ B_w(\rho)=\begin{bmatrix}0.10\\ 0.10\\ 0.18\\ 0.15\end{bmatrix},$$
$$C(\rho)=\begin{bmatrix}0 & 0 & 1 & 0\\ 0 & 0 & 0 & 1\end{bmatrix},\ H(\rho)=I_n,\ J(\rho)=J_w(\rho)=0. \tag{4.74}$$

For the simulation purpose, set $\overline{u}=5, \rho(t)\in[-0.57,\ 2.43]$ and $\dot{\rho}(t)\in[-1.5, 1.5]$. Now, let's discuss the simultaneous optimization related to decision variables γ, η. It should realize that both relevant minimization criteria are the convex conditions. Considering the optimization Problem 4.1.1. The obtained results in Table 4.3 are given by solving the theorems corresponding to the PLMI conditions gridded over $N_p=121$ points uniformly spaced $\rho(t)\in[-0.57,\ 2.43]$, with weighting scalars $\alpha_1=\alpha_2=1$. Through the prompt solutions, the comparison of the design stabilization conditions for the feedback controllers is delivered. It is interesting to point out that the stabilization conditions of the saturated gain-scheduling SOF (Theorem 4.2.1) and DOF (Theorem 4.4.1) roughly attain the same disturbance rejection optimization values with the SF (Theorem 4.1.1). However, as can be expected about conservativeness of the *old-fashioned* observer-based controller stabilization conditions. Briefly, it can explain that this approach has two critical drawbacks:

1. Young's inequality is typically deployed for the strategy design of observer-based controllers. But, using this bounding technique loses the equivalence of the solution domain of the conditions before and after applying the inequality (explained

in more detail in the Appendix A.4).

2. If it compares with the other structure of output feedback strategies, the use of a block-matrix diagonal Lyapunov candidature associated with the observer-based controller design is conservative.

Table 4.3. *Multi-objective optimization* – γ_{opt} and η_{opt}.

Parameter-dependent Stabilization & Actuator Saturation					
	State Feedback	***Output Feedback***			
	SF	SOF	OBF	# OBF	DOF
	Theorem 4.1.1	*Theorem* 4.2.1	*Theorem* 4.3.1	*Theorem* 4.3.2	*Theorem* 4.4.1
γ_{opt}	0.3656	0.3661	$1.0652\cdot10^{+6}$	0.7094	0.3753
η_{opt}	$2.2682\cdot10^{-3}$	$2.8827\cdot10^{-3}$	$4.4709\cdot10^{+4}$	$3.9896\cdot10^{-7}$	$2.4509\cdot10^{-3}$
0	1	2	3	4	5

SF: *State feedback*; *SOF*: *Static output feedback*; *OBF*: *Observer-based*; *DOF*: *Dynamic output feedback.*

Besides, a marked improvement on the results of the new OBF design method can be appreciated (compare 3rd and 4th catalogs). Solving problem (4.13) does not directly yield the optimums of the disturbance rejection levels or the size criterion (Volume Maximization, Minor Axis Maximization, or Trace Minimization, Etc.). But, based on the simultaneous minimization of γ_{opt} and η_{opt}, we acquire comparable optimal values of the state feedback, static output feedback, and dynamic output feedback approaches. On the contrary, the *traditional* approach for the observer-based control is not nearly as feasible. Therefore, this method (Theorem 4.3.1) is excluded in the following comparisons.

The simulations start from initial condition $x(0)=[-\pi/8 \;\; \pi/4 \;\; \pi/3 \;\; \pi/20]^T$ that belongs to the estimate of RAS. Using Yalmip LMI toolbox (Lofberg, 2004) integrated with interior-point optimizer Mosek® (E D Andersen et al., 2003; Erling D Andersen & Andersen, 2000) to solve optimization problem (4.13). Then, the parametric dependent forms of decision matrices are given corresponding to the design strategies:

Saturated State Feedback Controller

Solving the stabilization conditions of Theorem 4.1.1 with $\bar{u}=5$, we obtain the stabilizing gains $K(\rho)=Y(\rho)X^{-1}(\rho)$, where

$$\begin{aligned} X(\rho) &= X_0 + X_1\rho(t) + X_2\rho(t)^2, \\ Y(\rho) &= Y_0 + Y_1\rho(t) + Y_2\rho(t)^2, \end{aligned} \tag{4.75}$$

with

$$X_0 = \begin{bmatrix} 0.4182 & 0.0433 & 0.0541 & -0.1133 \\ 0.0433 & 0.0231 & 0.0234 & 0.0403 \\ 0.0541 & 0.0234 & 0.2408 & -0.3664 \\ -0.1133 & 0.0403 & -0.3664 & 0.9597 \end{bmatrix}, \quad Y_0^T = \begin{bmatrix} -0.3404 \\ -0.0370 \\ 0.2381 \\ -0.4977 \end{bmatrix},$$

$$X_1 = \begin{bmatrix} -0.0250 & 0.1503 & -0.0688 & 0.2838 \\ 0.1503 & 0.0589 & 0.0644 & 0.0215 \\ -0.0688 & 0.0644 & 0.0280 & 0.1620 \\ 0.2838 & 0.0215 & 0.1620 & -0.0085 \end{bmatrix}, \quad Y_1^T = \begin{bmatrix} 0.2201 \\ -0.1312 \\ -0.0076 \\ 0.3284 \end{bmatrix},$$

$$X_2 = \begin{bmatrix} 0.0255 & -0.0050 & 0.0226 & -0.0594 \\ -0.0050 & 0.0482 & -0.0283 & 0.0831 \\ 0.0226 & -0.0283 & 0.0028 & -0.0831 \\ -0.0594 & 0.0831 & -0.0831 & 0.2955 \end{bmatrix}, \qquad Y_2^T = \begin{bmatrix} -0.0460 \\ 0.0288 \\ -0.0367 \\ -0.0223 \end{bmatrix}.$$

Saturated Static Output Feedback Controller

Solving the stabilization conditions of Theorem 4.2.1 with $\overline{u} = 5$, we get the scheduling-gains $K(\rho) = Y(\rho)W(\rho)^{-1}$,

$$\begin{aligned} W(\rho) &= \begin{bmatrix} 0.2676 + 0.0550\rho(t) - 0.0111\rho(t)^2 & -0.4338 + 0.0424\rho(t) - 0.0213\rho(t)^2 \\ -0.2789 + 0.2545\rho(t) - 0.1378\rho(t)^2 & 0.7247 - 0.2771\rho(t) + 0.2814\rho(t)^2 \end{bmatrix}, \\ Y(\rho) &= \begin{bmatrix} 0.1053 - 0.0071\rho(t) - 0.0100\rho(t)^2 & -0.1854 + 0.1701\rho(t) + 0.0316\rho(t)^2 \end{bmatrix}. \end{aligned} \tag{4.76}$$

Saturated Observer-Based Feedback Controller

Solving the stabilization conditions of Theorem 4.3.2 with $\overline{u} = 5$, we get the scheduling-gains of controller $K(\rho) = X(\rho)^{-1}Y_1(\rho)$, and observer $L(\rho) = P_2(\rho)^{-1}Y_2(\rho)$, where

$$\begin{aligned} X(\rho) &= X_{10} + X_{11}\rho(t) + X_{12}\rho(t)^2 & P_2(\rho) &= P_{20} + P_{21}\rho(t) + P_{22}\rho(t)^2, \\ &= 110.1727 - 1.8489\rho(t) + 0.9927\rho(t)^2, & Y_2(\rho) &= Y_{20} + Y_{21}\rho(t) + Y_{22}\rho(t)^2, \end{aligned}$$

$$Y_1(\rho) = \begin{bmatrix} 3.0839 - 29.0680\rho(t) + 14.0751\rho(t)^2 \\ -12.2415 - 19.0330\rho(t) + 7.7953\rho(t)^2 \\ 1.8556 + 11.6742\rho(t) - 2.2475\rho(t)^2 \\ 11.1809 - 4.2657\rho(t) + 2.0248\rho(t)^2 \end{bmatrix}^T, \text{ with} \tag{4.77}$$

$$P_{20} = \begin{bmatrix} 72.5987 & 7.3403 & -29.8474 & -17.4622 \\ 7.3403 & 269.3097 & -130.7349 & -27.5461 \\ -29.8474 & -130.7349 & 160.1890 & -85.1585 \\ -17.4622 & -27.5461 & -85.1585 & 132.2066 \end{bmatrix}, \quad Y_{20} = \begin{bmatrix} 117.1381 & 135.8915 \\ 220.6554 & -213.0649 \\ 140.3023 & 116.8829 \\ 270.5934 & -203.1743 \end{bmatrix},$$

$$P_{21} = \begin{bmatrix} 72.5909 & 6.1269 & -29.7946 & -16.6734 \\ 6.1269 & 260.7905 & -127.7276 & -24.6514 \\ -29.7946 & -127.7276 & 159.7208 & -86.5901 \\ -16.6734 & -24.6514 & -86.5901 & 131.5089 \end{bmatrix}, \quad Y_{21} = \begin{bmatrix} 148.8636 & 2.0698 \\ 295.1686 & -394.3682 \\ 41.2966 & 56.4400 \\ 55.2109 & 33.4918 \end{bmatrix},$$

$$P_{22} = \begin{bmatrix} 72.6586 & 4.8619 & -29.7399 & -15.9047 \\ 4.8619 & 252.6758 & -124.8096 & -21.8857 \\ -29.7399 & -124.8096 & 159.2526 & -87.9657 \\ -15.9047 & -21.8857 & -87.9657 & 130.8414 \end{bmatrix}, \quad Y_{22} = \begin{bmatrix} -25.9682 & -2.1999 \\ -7.7522 & 8.5378 \\ -11.8909 & -17.1386 \\ -17.0664 & -10.3148 \end{bmatrix}.$$

Saturated Dynamic Output Feedback Controller

The optimal values achieve in Table 4.3 by solving the stabilization conditions of Theorem 4.4.1 with problem (4.13). Nonetheless, the high-gains cause the computation burden relating to the numerical simulation (it takes almost 10 minutes to complete a 10-second simulation). So, we slightly increase $\gamma = 0.3753 \rightarrow 0.4528$. Where, the dynamic gains and compensator gain are expressed, respectively, in Eqs. (4.63), (4.72) concerned with the following variable matrices:

$$\begin{aligned}
&\hat{A}(\rho)=\hat{A}_0+\hat{A}_1\rho(t)+\hat{A}_2\rho(t)^2, && \hat{C}(\rho)=\hat{C}_0+\hat{C}_1\rho(t)+\hat{C}_2\rho(t)^2,\\
&\hat{B}(\rho)=\hat{B}_0+\hat{B}_1\rho(t)+\hat{B}_2\rho(t)^2, && \hat{E}(\rho)=\hat{E}_0+\hat{E}_1\rho(t)+\hat{E}_2\rho(t)^2,\\
&\hat{D}(\rho)=[-1.1663-1.6885\rho(t)+1.1665\rho(t)^2 && -83.4450-6.7454\rho(t)+0.6718\rho(t)^2],\\
&X(\rho)=X_0+X_1\rho(t)+X_2\rho(t)^2, && Y(\rho)=Y_0+Y_1\rho(t)+Y_2\rho(t)^2,
\end{aligned} \tag{4.78}$$

with

$$\hat{A}_0=\begin{bmatrix} 1.0472 & -0.4428 & -0.1264 & -1.5672\\ -0.4428 & -0.7947 & -1.1774 & -0.7645\\ -0.1264 & -1.1774 & -2.9730 & -1.6918\\ -1.5672 & -0.7645 & -1.6918 & -1.9226\end{bmatrix},\quad \hat{B}_0=\begin{bmatrix} -25.9955 & -11.3784\\ -74.1838 & -52.88674\\ -48.8867 & -52.8867\\ -38.5519 & 10.6972\end{bmatrix},$$

$$\hat{A}_1=\begin{bmatrix} -0.8626 & 0.3398 & 1.0174 & -0.5004\\ 0.3398 & 0.9365 & 1.1496 & 0.9250\\ 1.0174 & 1.1496 & 1.6043 & 0.5748\\ -0.5004 & 0.9250 & 0.5748 & -82.4400\end{bmatrix},\quad \hat{B}_1=\begin{bmatrix} 33.7683 & -7.4510\\ 82.0784 & 82.7421\\ 60.4477 & 48.5540\\ 48.4422 & 16.1862\end{bmatrix},$$

$$\hat{A}_2=\begin{bmatrix} -0.1132 & -0.4806 & -0.4832 & -0.1904\\ -0.4806 & -0.1960 & -0.3073 & -0.5680\\ -0.4832 & -0.3073 & -0.6326 & -0.0573\\ -0.4832 & -0.5680 & -0.0573 & -6.5433\end{bmatrix},\quad \hat{B}_2=\begin{bmatrix} -13.8871 & 1.7507\\ -33.5962 & -12.4306\\ -25.2844 & -17.9354\\ -17.9352 & -5.1440\end{bmatrix},$$

$$X_0=\begin{bmatrix} 0.6947 & 0.0832 & 0.0193 & -0.0145\\ 0.0832 & 0.0643 & 0.0223 & 0.0755\\ 0.0193 & 0.0223 & 0.3153 & -0.4312\\ -0.0145 & 0.0755 & -0.4312 & 1.1586\end{bmatrix},\quad \hat{C}_0^T=\begin{bmatrix} -0.3240\\ -0.0733\\ 0.0903\\ -0.1929\end{bmatrix},$$

$$X_1=\begin{bmatrix} -0.0714 & 0.1864 & -0.0276 & 0.2290\\ 0.1864 & 0.0811 & 0.0399 & 0.0687\\ -0.0276 & 0.0399 & 0.0075 & 0.1796\\ 0.2290 & 0.0687 & 0.1796 & -0.0134\end{bmatrix},\quad \hat{C}_1^T=\begin{bmatrix} 0.1548\\ -0.2384\\ 0.2762\\ 7.3697\end{bmatrix},$$

$$X_2=\begin{bmatrix} 0.0342 & -0.0114 & 0.0104 & -0.0692\\ -0.0114 & 0.0489 & -0.0184 & 0.0698\\ 0.0104 & -0.0184 & 0.0234 & -0.0829\\ -0.0692 & 0.0698 & -0.0829 & 0.3236\end{bmatrix},\quad \hat{C}_2^T=\begin{bmatrix} -0.0982\\ -0.0130\\ -0.0951\\ -2.5728\end{bmatrix},$$

$$Y_0=\begin{bmatrix} 0.6947 & 0.0832 & 0.0193 & -0.0145\\ 0.0832 & 0.0643 & 0.0223 & 0.0755\\ 0.0193 & 0.0223 & 0.3153 & -0.4312\\ -0.0145 & 0.0755 & -0.4312 & 1.1586\end{bmatrix},\quad \hat{E}_0=\begin{bmatrix} -1.5122\\ 2.3779\\ 1.1625\\ 83.6383\end{bmatrix},$$

$$Y_1=\begin{bmatrix} -0.0714 & 0.1864 & -0.0276 & 0.2290\\ 0.1864 & 0.0811 & 0.0399 & 0.0687\\ -0.0276 & 0.0399 & 0.0075 & 0.1796\\ 0.2290 & 0.0687 & 0.1796 & -0.0134\end{bmatrix},\quad \hat{E}_1=\begin{bmatrix} 0.3470\\ 0.9507\\ 0.5614\\ 5.7743\end{bmatrix},$$

$$Y_2=\begin{bmatrix} 0.0342 & -0.0114 & 0.0104 & -0.0692\\ -0.0114 & 0.0489 & -0.0184 & 0.0698\\ 0.0104 & -0.0184 & 0.0234 & -0.0829\\ -0.0692 & 0.0698 & -0.0829 & 0.3236\end{bmatrix},\quad \hat{E}_2=\begin{bmatrix} -0.1521\\ 0.0137\\ -0.2395\\ -0.1082\end{bmatrix}.$$

An alternative for calculating the slack-variable matrices gives in the expression:

$$N(\rho)=(I-Y(\rho)X(\rho))M(\rho)^{-T}, \tag{4.79}$$

either by choosing $N(\rho)$ to calculate $M(\rho)$, or vice versa. But the choice of this parametric slack matrix leads to heterogeneity in matrix inversion (4.79). Therefore, in this example, we pick a full rank constant matrix

$$M = \begin{bmatrix} 0.4400 & 0.0923 & -1.7499 & 0.8985 \\ -0.6169 & 1.7298 & 0.9105 & 0.1837 \\ 0.2748 & -0.6086 & 0.8671 & 0.2908 \\ 0.6011 & -0.7371 & -0.0799 & 0.1129 \end{bmatrix}.$$

Applying the gains scheduling to the LPV system (4.74), we obtain the simulation results.

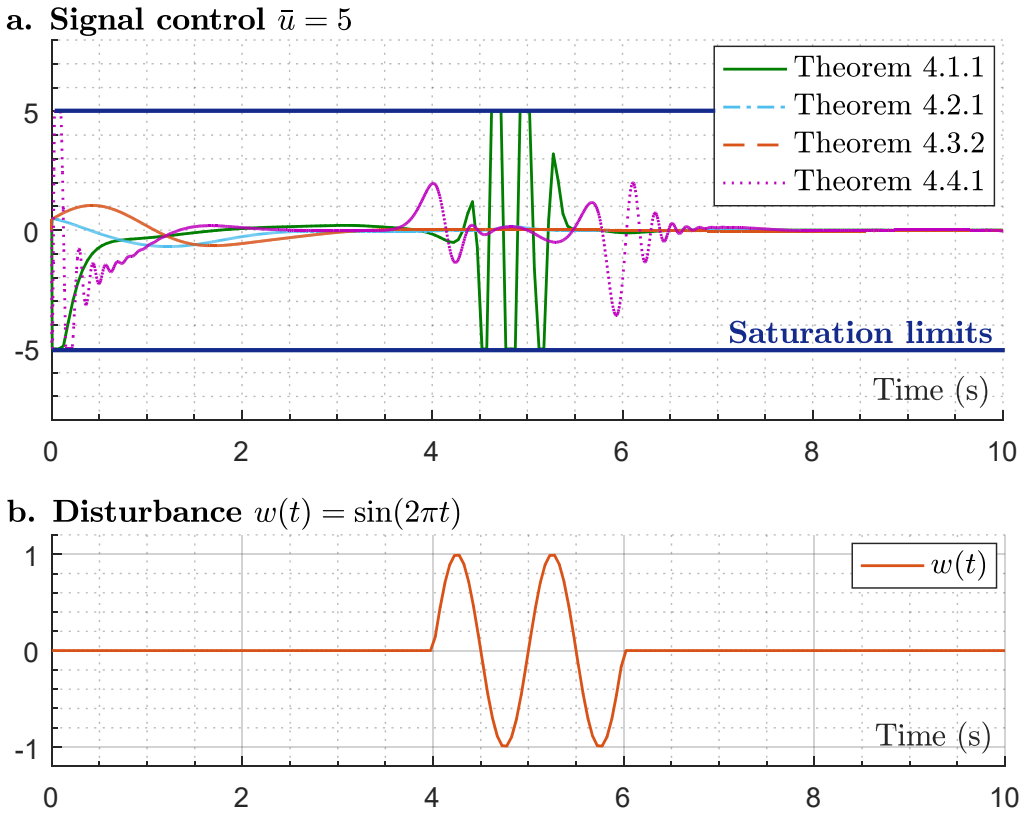

Figure 4-3. *a. The simulated constrained responses of the state-feedback SF controller* (*colored solid line*), *the static-output feedback SOF controller* (*colored dash-dotted line*), *the observer-based feedback OBF controller* (*colored dashed line*), *and the dynamic output feedback DOF controller* (*colored dotted line*). *b. The time-evolution of external disturbance.*

The signals of the dynamic output and state feedback control system exceed the saturation limits during the effect of exogenous signal (given in Figure 4-3) while the SOF controller and the new OBF exhibit a decent response corresponding to the design bound. The project lemma method demonstrates outstanding performance in designing static output controllers, which directly deliver a convex condition without applying mathematical constraints. When observing the time-evolution of the closed-loop states, the SOF system regulated a reasonable control signal conforming to the saturation limit. On the contrary, the convergence rate of the OBF control signal is too low (it can observe in the third and the fourth states). Furthermore, there exists a quasi-convex in condition (4.47) so this controller is also not deployed in the next comparison.

The robust performance and the stabilizability of the designed controllers evaluate under the influence of external disturbance from a non-zero initial condition. The time-evolution of the dynamical states shows in the 1st frame to the 4th frame and the time-varying

parameter given in the last frame in Figure 4-4.

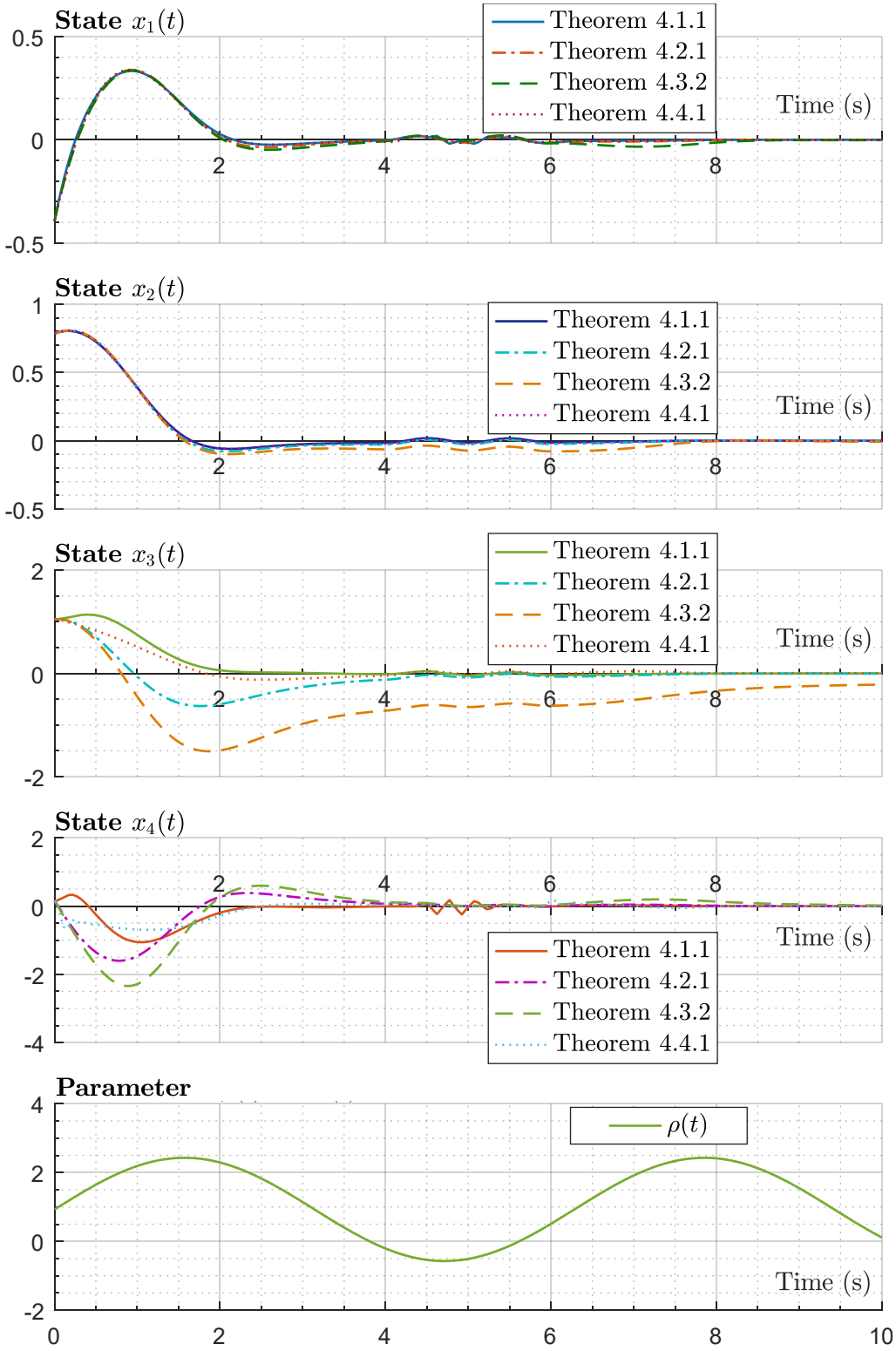

Figure 4-4. *The stabilized states of the closed-loop systems are regulated, respectively, by the gain-scheduled SF controller* (*colored solid line*), *SOF controller* (*colored dash-dotted line*), *OBF controller* (*colored dashed line*), *DOF controller* (*colored dotted line*) *conforming to the simulated parameter* (*green solid line in the last frame*).

There is no difference between states $x_1(t), x_2(t)$ governing by state feedback, static output feedback, and dynamic output feedback controllers. But it should note that the 3rd and 4th states are measurable, which leads to a *distinction* in the response of the respective systems. As seen in Figure 4-4, the disturbance (sine function with amplitude 1) affects the system during the 4th to 6th second minimized corresponding to the $\mathcal{L}_2$-norm values given in Table 4.3. The control systems show the effectiveness of ensuring saturation limits and reinforcing performance.

Now, let's discuss the size criteria associated with the ellipsoidal domain. The *volume maximization* delivers a linear and convex form relating to the decision variables. But it results in a disproportionate scale of the ellipsoidal region (that could entail an inaccurate estimate of the domain of attraction). The *trace minimization* and the *maximization along certain direction* method provide a multi-directional minimization of the ellipsoid characterized for the stability region. Nonetheless, the *minor axis maximization* exhibits the simplicity and the integrability with the stabilizing conditions. It should point out that the DOF stabilization conditions have a more complex structure. So, let's study the following minor axis maximization problem employed, respectively, for the saturated SF, SOF, and DOF control systems:

Problem 4.5.1.
Given compact set of the parameters $\rho(t) \in \mathcal{U}_p$, *scalars* α_1, α_2, *find a variable decision matrix* X *such that the following statement satisfies*:

minimize $f(\eta, \beta) = \alpha_1 \beta + \alpha_2 \eta,$ (4.80)

subject to inequalities (4.1)-(4.2), and (4.24)-(4.25) (the stabilization condition of Theorem 4.1.1, and Theorem 4.2.1, respectively), and

$$\begin{bmatrix} \beta I_n & I_n \\ I_n & X(\rho) \end{bmatrix} \succeq 0.$$

The latter LMI implies $P(\rho) \preceq \beta I_n$. So, the convex problem seeks for the optimization of the ellipsoid $\mathcal{E}(P(\rho), \eta)$ involved in the designed stabilization of state feedback controller and static output feedback controller. The variable substitutions of the DOF design condition prevents a direct application of the convex form as given in (4.80). By a slight adjustment, we have:

Problem 4.5.2.
Given compact set of the parameters $\rho(t) \in \mathcal{U}_p$, *scalars* α_1, α_2, *find variable decision matrices* X, Y *such that the following statement fulfills*:

minimize $f(\eta, \beta) = \alpha_1 \beta + \alpha_2 \eta,$ (4.81)

subject to inequalities (4.60)-(4.62) (the stabilization condition of Theorem 4.4.1), and

$$\begin{bmatrix} \beta I_n & \Pi_2 \\ \Pi_2^T & \Pi_1^T \Pi_2 \end{bmatrix} \succeq 0.$$

Using relation $\Pi_2^T P(\rho)^{-1} \Pi_2 = \Pi_1^T P(\rho) \Pi_1 = \Pi_1^T \Pi_2$, then perform a congruence transfor-

mation with $diag\{I_{2n}, \Pi_2\}$ that leads to the latter condition. Coupling matrix $\Pi_1^T \Pi_2$ contains the convex forms of variable matrices X, Y. But, the presence of matrix Π_2 ensues in a quasi-convex condition, where $N(\rho)$ is supposed to be an implicit slack-variable that reappears in the optimal conditions. One solution for this is to preset a full-rank matrix N, and then solve the design LMI conditions. Note that in this simulation, we consider the case where either M or N is a full-rank constant matrix, and the remaining matrix is parameter-dependent.

Table 4.4. *Minor Axis Maximization* $-\gamma = 10$.

	Parameter-dependent Stabilization & Actuator Saturation		
	State Feedback	***Output Feedback***	
	SF	SOF	DOF
	Theorem 4.1.1 *Problem* 4.5.1	*Theorem* 4.2.1 *Problem* 4.5.1	*Theorem* 4.4.1 *Problem* 4.5.2
$\eta = 0.01 \quad \rightarrow \beta_{opt}$	1.3106	1.3108	1.4373
$\eta = 0.1 \quad \rightarrow \beta_{opt}$	0.7324	0.7344	0.8361
0	1	2	3

SF: *State feedback*; *SOF*: *Static output feedback*; *DOF*: *Dynamic output feedback.*

Similar to the first case, we could optimize eta and beta values at the same time. But, for this time, we fixed $\gamma = 10$ and varied η from 0.01 to 0.1 to optimize β. Note that the smaller the value of η, the larger the linear behavior region.

It can observe in Table 4.3 and Table 4.4 that the static and dynamic output feedback controller solved by the conditions of Theorem 4.2.1 and Theorem 4.4.1 show good disturbance attenuation levels and reasonable estimations of RAS compared to state feedback controller. There is an insignificant difference of the optimal values. But it should be noted that the output feedback design method provides a practical implementation.

4.5.2. *Evaluation of the performance and stability of the saturated system*

In Example 4.5.1, only two states are measurable in four states of the system dynamic. But the vector spaces larger than two ensues in difficulty to exhibit the ellipsoidal domain. Using two out of four states in combination with the corresponding basis matrix (A. T. Nguyen et al., 2018) is incorrect to characterize the estimate of the convergence region. So, let's study the following example to discuss more the domain of attraction of the closed-loop systems governed by the proposed saturated feedback controllers and the performance deteriorate in the unsaturation design control systems.

Example 4.5.2: Consider the dynamic of the pitch-axis motion of an autopilot for a missile model. The aircraft associated with the angle of attack, the pitch rate discussed many times in the literature (Biannic & Apkarian, 1999; Daafouz et al., 2008; Pellanda et al., 2002; Wu et al., 1995) is represented by the state-space as follows:

$$A(\rho) = \begin{bmatrix} -0.89 - 0.89\rho(t) & 1 \\ -142.6 - 178.25\rho(t) & 0 \end{bmatrix}, B(\rho) = \begin{bmatrix} -0.119 \\ -130.8 \end{bmatrix}, B_w(\rho) = \begin{bmatrix} 0.01 \\ 0 \end{bmatrix}, C(\rho) = [-1.52 \quad 0],$$
$$D(\rho) = D_w(\rho) = 0, \; H(\rho) = [0 \quad 1], \; J(\rho) = 1, \; J_w(\rho) = 0. \tag{4.82}$$

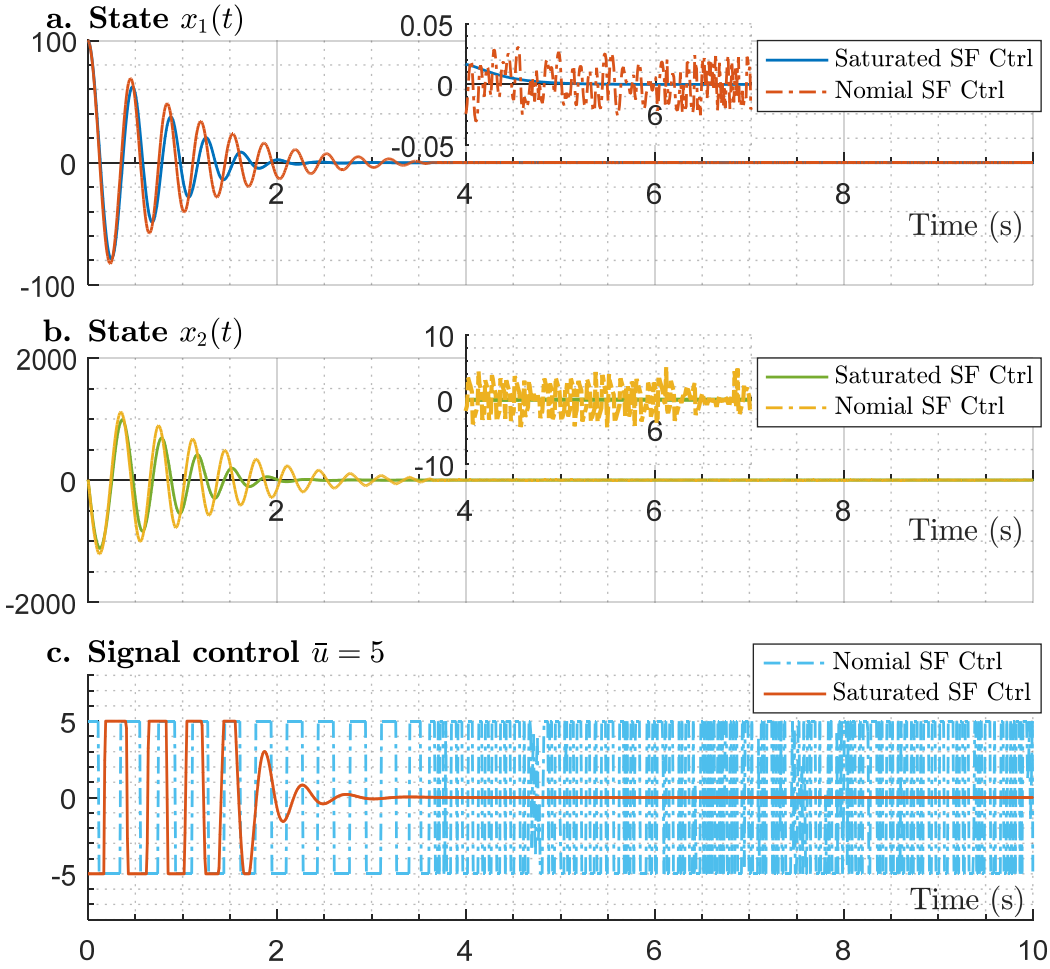

a-b. The time-evolution of state dynamics. c. The simulated constrained responses of the SF controller Theorem 4.1.1, and the nominal controller.

Figure 4-5. *The comparison of the closed-loop systems regulated, respectively, by the saturated gain-scheduled SF controller (colored solid line), and nominal state feedback controller (colored dotted line).*

The time-varying parameters $\rho(t) \in [-1, 1]$, $|\dot{\rho}(t)| \leq 1$, and the saturation limit sets on actuator $|u(t)| \leq \bar{u} = 5$. Similar to the discussed optimization methods, by solving Theorem 4.1.1, Theorem 4.2.1, and Theorem 4.4.1 gridded over $N_p = 121$ points uniformly spaced over parameter range, we attain the optimal results as given in Table 4.3. As noticed in the above table, the SOF controller is *exhausted* in this example, both in the two optimization categories. By varying coefficient ε_{SOF} from 10^{-3} to 10^{3}, the optimal values are obtained at $\varepsilon_{SOF} = 2 \cdot 10^{-2}$.

Now, we compare the design controller with GSC condition with the corresponding nominal controller. The control systems are set up for simulation of LPV system (4.82) with bounded actuators. Given in Figure 4-5 and Figure 4-6 are the comparisons of state-feedback and static output feedback controllers. The simulations start at the same initial condition $x(0) = [100 \;\; 0]^T$ regardless of the effect of disturbances.

In the first comparison of the state feedback systems, the performance degradation can be

discerned on the nominal system (does not include saturation constraints). An enlargement of the frame from 4th to 7th second (Figure 4-5.a&b) clarifies the instability of states corresponding to the chattering effect of the controller shown in Figure 4-5. In the opposite direction, the feedback controller designed by Theorem 4.1.1 exhibits a good performance and enforces stability when the actuator is saturated.

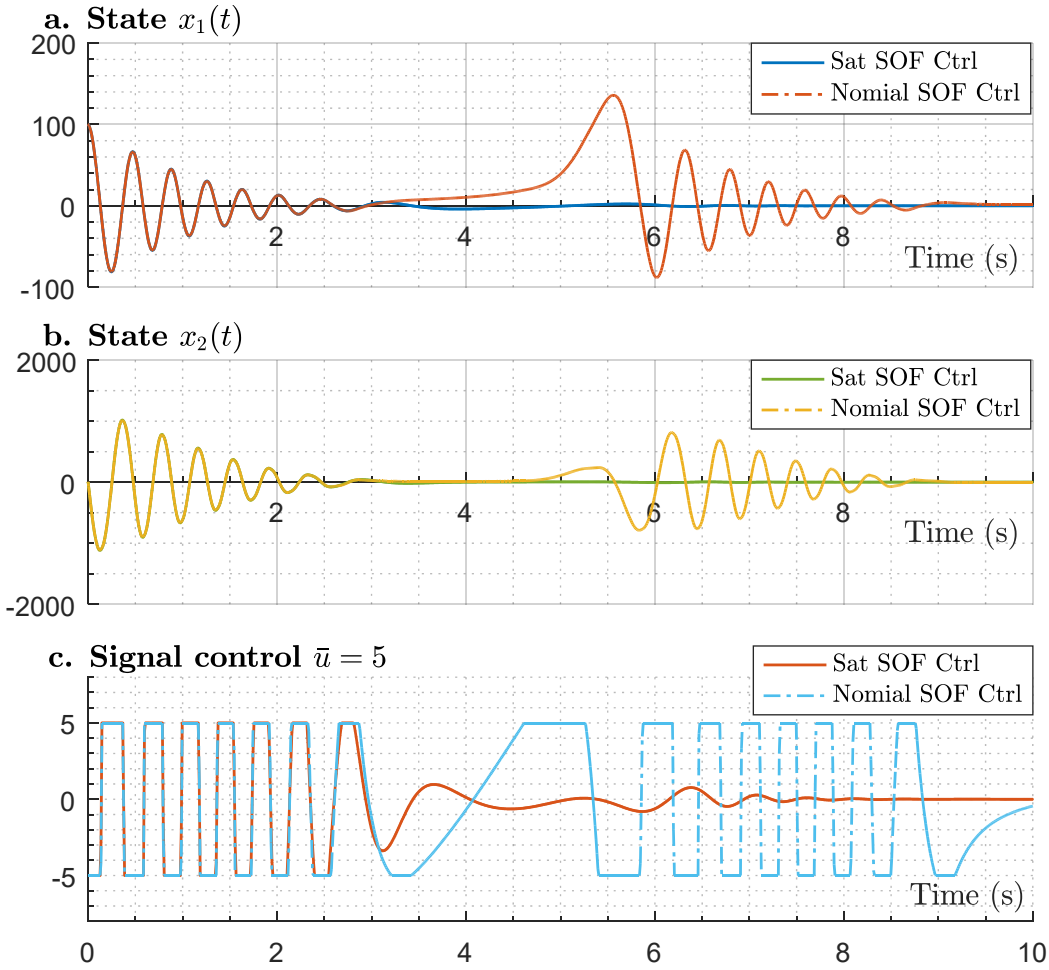

a-b. The time-evolution of state dynamics. c. The simulated constrained responses of the SOF controller Theorem 4.2.1, and the nominal controller.

Figure 4-6. *The comparison of the closed-loop systems regulated, respectively, by the saturated gain-scheduled SOF controller (colored solid line), and nominal static output feedback controller (colored dash-dotted line).*

In the second comparison, an instability behavior with increasing amplitude of oscillation is observed on the response of the nominal SOF control system, corresponding to this control signal being saturated all the simulated time. Once again, the SOF controller designed by Theorem 4.2.1 has demonstrated the enhanced performance compared to the nominal system without integrating saturation conditions. It should be noted that the phase plane diagrams of the nominal SOF closed-loop system are ellipses extending to infinity (the instability trajectories are given in Figure 4-7).

Through these simulation results, the control signals are regulated from stabilized control

systems obtained by design conditions with no saturation conditions (e.g., sector bounding GSC). It could be noticed the performance degradation and system instability when the actuator is saturated. On the opposite, from similar initial conditions, the designed controllers ensure stability and enhance system performance corresponding to the optimal values obtained in Table 4.3.

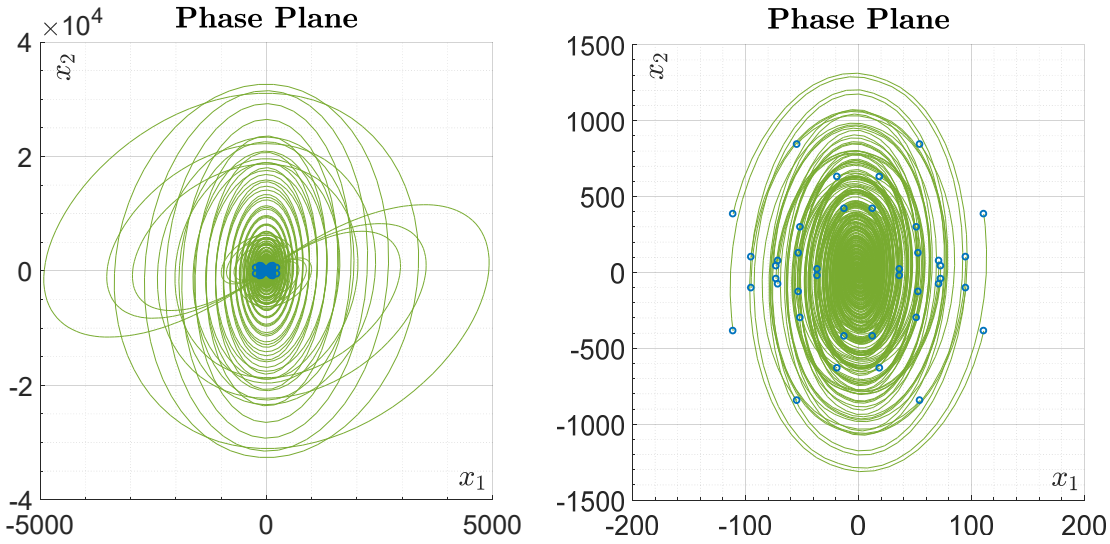

a. Destabilize trajectories governed by a nominal SOF controller.

b. Stabilize trajectories regulated by design saturated SOF controller.

Figure 4-7. *Region of stability. Trajectories of the closed-loop systems respond from the same initial conditions during 10 seconds of simulation.*

Table 4.5. *Actuator Saturation – Optimization Problems.*

Multi-objective optimization			
	State Feedback	***Output Feedback***	
	SF	SOF	DOF
	Theorem 4.1.1 *Problem* 4.1.1	*Theorem* 4.2.1 *Problem* 4.1.1	*Theorem* 4.4.1 *Problem* 4.1.1
γ_{opt}	$1.0448\cdot10^{-2}$	$5.3821\cdot10^{-2*}$	$1.0451\cdot10^{-2}$
η_{opt}	$2.6226\cdot10^{-4}$	$4.2281\cdot10^{-4*}$	$2.6020\cdot10^{-4}$
Minor Axis Maximization $-\gamma=10.$			
	Problem 4.5.1	*Problem* 4.5.1	Problem 4.5.2
$\eta=0.01\rightarrow\beta_{opt}$	1.9632	4.3569*	1.9664
$\eta=0.1\rightarrow\beta_{opt}$	0.8316	1.6935*	0.8337
0	1	2	3

SF: *State feedback*; *SOF*: *Static output feedback* (*: ε=0.02); *DOF*: *Dynamic output feedback.*

4.5.3. *Quadratic and Non-Quadratic Stabilization*

As mentioned in Chapter 3, there is a performance deteriorate of the stabilization conditions using quadratic Lyapunov function (QLF) candidature against the parameter-dependent form. In this section, Example 4.5.1 is adopted to deliver the optimization results

of the stabilization conditions for LPV saturation systems analyzed with a quadratic Lyapunov function compared to a parameter-dependent Lyapunov functional.

Table 4.6. *Multi-objective optimization - Example* 4.5.1.

Quadratic Stabilization & Actuator Saturation					
	State Feedback	***Output Feedback***		Compare with	**Table 4.3**
	SF	SOF	DOF		
	Theorem 4.1.1 *Problem* 4.1.1	*Theorem* 4.2.1 *Problem* 4.1.1	*Theorem* 4.4.1 *Problem* 4.1.1		
γ_{opt}	1.7416	3.8731	1.7416		
η_{opt}	$1.8071\cdot10^{-2}$	$7.6225\cdot10^{-2}$	$1.8069\cdot10^{-2}$		
Minor Axis Maximization $-\gamma=10.$					
	Problem 4.5.1	*Problem* 4.5.1	*Problem* 4.5.2		**Table 4.4**
$\eta=0.01 \rightarrow \beta_{opt}$	10.4753	16.3353	15.4075		
$\eta=0.1 \rightarrow \beta_{opt}$	6.1052	14.9865	8.7692		
0	1	2	3		

SF: *State feedback*; *SOF*: *Static output feedback*; *DOF*: *Dynamic output feedback.*

The quadratic stabilization expansion based on Theorem 4.1.1, Theorem 4.2.1, and Theorem 4.4.1 using the Lyapunov function (2.120) can interpret briefly as follows: considering the parameter-dependent condition (4.1)-(4.2) in Theorem 4.1.1, and the following adjustments: $X(\rho)\rightarrow X$, $\dot{X}(\rho)=0$, $T(\rho)\rightarrow T$. Then, analyze in a similar way for the other two theorems.

Implementing the minimization methods as in Table 4.3 and Table 4.4 for the quadratic optimization conditions, we obtain the results in Table 4.6. It can observe a performance degradation using a quadratic Lyapunov functional for the stabilization conditions as the optimization values γ_{opt} increase approximately five times and ten times for η_{opt} (the comparison between Table 4.6 QLF vs. Table 4.3 PDLF). Similarly, we also have conservatism for the minor axis optimization conditions (the comparison between Table 4.6 QLF vs. Table 4.4 PDLF) where the value β_{opt} also growths approximately ten times.

4.6. Conclusions

We have developed several feedback controls law to stabilize the saturated LPV/qLPV systems. The control system design strategy related to the desired performance ensures that the operation agrees to the actuator capacity. Accordingly, the necessary and sufficient stabilization conditions via the PLMI formulation are addressed for the feedback controllers conforming to the design requirements (i.e., the admissible set of the initial conditions, the estimated region of the asymptotic convergence domain, the robust stability against uncertain dynamics, and time-varying parameters, and the system performance with the influence of input disturbance, Etc.). Besides, the nonlinearities and concave problems involved the generalized sector condition converted to the tractable conditional forms. The extension of the gains-scheduling technique has been addressed for the saturated LPV systems. Then, specific criteria are compared based on optimization results.

Performance degradation and instability trajectories on a control system without a saturation design occurred when the actuator reached saturation bounds. The presented results persuade the essential of saturation design for control system strategy. In addition, the relaxation of the design conditions is claimed by the comparison between the quadratic Lyapunov and PDLF stabilization conditions.

It is worth noting that the design stabilization is presented in the generalized form as an expression of the parameterized linear matrix inequality (PLMI). So, it can adapt and develop for each specific strategy or a suitable relaxation method of the PLMI. Furthermore, it remains an open problem in the LPV control framework.

Chapter 5.

Stability Analysis of the LPV/Quasi-LPV Time-Delay Systems

Time-delay phenomena observe in various engineering systems such as chemical processes, mechanical transmissions, hydraulic transmissions, metallurgical processes, and networked control systems. They are often a source of instability and poor control performance. The stability and stabilization of the time-delay systems (TDS) have received considerable attention in the practice and control theory. The time delay can *sort* into different approaches depending on the characteristic or the response behavior of the delay to the system. The framework of time-delay systems represents by functional differential equations classified into four types: discrete delay, distributed delay, neutral delay, and scale delay (Briat, 2015b). The literature on stability and stabilization of time-delay systems is exhaustive and could find in the monographs for LTI systems (Dey et al., 2018; Gu et al., 2003) for LPV systems (Briat, 2008, 2015b), time domain-based Lyapunov stability analysis (Fridman, 2014; Sipahi et al., 2011), and the eigenvalue based approach (Michiels et al., 2002; Michiels & Niculescu, 2007).

Frequency-domain approaches dedicated to linear time-invariant (LTI) systems addressed a few cases of model transformations or varying delays. The stability of a system is verified from the distribution of the roots of its characteristic equation or the solutions of a complex Lyapunov matrix function equation. Interested readers can consult in more depth on this issue in the literature (Gu et al., 2003; Michiels, 2002; Michiels et al., 2005; Michiels & Niculescu, 2007; Michiels & Vyhlídal, 2005; Schoen, 1995). But the approach meets with difficulties in analyzing the robust performance of dynamic system with the uncertainty, disturbances, and nonlinearities. In this case, the time-domain analysis technique is more suitable for dealing with the control challenge of this class of LPV time-delay system.

During the last decade, significant effort has addressed the problem of stability analysis and controller design for time-delay systems. Based on the time-domain approach, the Lyapunov stability is deployed primarily by two famous stability theorems: namely (1) Lyapunov-Krasovskii (LK) theorem and (2) Lyapunov-Razumikhin (LR) theorem. A generalized analysis for both approaches outlines in the works of (Briat, 2015b; Fridman, 2014; Gu et al., 2003) and references therein. Generally, there are the major approaches to carrying out the stability analysis of TDS, depending upon the size and bound of the delay as follows:

- Delay-Independent Stability condition
- Delay-Dependent Stability condition
- Time-Varying-Delay and Delay-Range Stability condition

Recently, the primary research trend performed by the Lyapunov-Krasovskii functional analysis usually focuses on seeking less conservative (LC) stability conditions. There are two fundamental conservatism reduction approaches: (1) the reformulation of Lyapunov–Krasovskii functional and (2) the bounding techniques of its derivatives.

On the one hand, the tighter bounding integral inequalities can mention as the Wirtinger-based I (WBI) (Seuret & Gouaisbaut, 2012), the Wirtinger-based II (WBII) (M. Park et al., 2015; Seuret & Gouaisbaut, 2013), the Free-matrix-based II (FMBII) (Zeng et al., 2015, 2021), the Auxiliary-function-based II (AFBII) (P. G. Park et al., 2015), the reciprocal convex combination (Datta et al., 2021; P. Park et al., 2011; C. K. Zhang et al., 2017; X. M. Zhang et al., 2017), and the generalized vectors-based multiple integral inequalities (Y. Tian & Wang, 2020, 2021; Van Hien & Trinh, 2015; Zhao et al., 2017) significantly improve the asymptotic stability of TDS systems. The fundamental methodology of bounding techniques is to estimate better the lower bounds of the quadratic integral terms in the derivative of the Lyapunov-Krasovskii functional.

On the other hand, a suitable structure of LKF can refer to the additional integral terms, the increasing state vectors, and delay-partitioning/fragmented approaches showed superbly efficient on reducing the conservativeness of the stability conditions. It should note that the more slack-variable matrices used, the more complication is in analyzing the delay-dependent stability conditions. Accordingly, these approaches are the *trade-off of the relaxation of the stability condition with the computational complexity*.

In section 5.1, we discuss the Lyapunov-Krasovskii stability analysis for the time-delay LPV/qLPV system. An essential key point to relax the parameter-dependent stability condition founds on appropriate LKFs combined with reasonable bounding inequalities. In section 5.1.2, the convex function features, such as the auxiliary-function-based method (P. G. Park et al., 2015; Van Hien & Trinh, 2015; Zhao et al., 2017), fragmented/discretized Lyapunov functional (Y. Chen et al., 2017; Fridman, 2006; Gu et al., 2003; Han, 2008) are employed to tackle with the conservatism of Jensen's inequality.

Besides, a well-known problem in control design is capturing or measuring the exact-delay value. The input-output approach proposed in (Gu et al., 2003) provides a methodology where the delay treats as uncertain dynamics of the LTI system. Then, an improvement for the LPV time-delay system is presented in (Briat, 2008; Briat et al., 2009, 2010). This approach purposely *converts delay into* the uncertain parameter, so it can also deploy by the different LMI-based stability designs (e.g., LFT framework). Based on the delay approximation, also known as a δ-memory-resilient, a stability condition derives from a Lyapunov-Krasovskii functional presented in section 5.2. Moreover, the auxiliary-function-based method provides a less conservative stability condition than the traditional Jensen-based inequality (Briat, 2015a; Briat et al., 2010).

5.1. Introduction to LPV Time-Delay Systems

The first part of the chapter will reserve the definitions used in the rest of the thesis, such as delay space, convex function, etc. As discussed in the previous chapters, we are interested in the class of the parameter-dependent systems represented by LPV or quasi-LPV models (declaring properties such as time-continuous and having definite derivatives in

the specific domain). Second, the time-varying delay only considers the case of small and slow-varying values.

5.1.1. *Representation of LPV System with Single Delay*

Let's introduce a generic LPV time-delay system of the form:

$$\begin{aligned}\dot{x}(t) &= A(\rho)x(t) + A_h(\rho)x(t-h(t)) + B_w(\rho)w(t),\\ z(t) &= H(\rho)x(t) + H_h(\rho)x(t-h(t)) + J_w(\rho)w(t),\\ x(\theta) &= \varphi(\theta), \qquad\qquad \theta \in [-\bar{h}, 0].\end{aligned} \tag{5.1}$$

where parameter $\rho(t)$ and its unknown rate of variation are continuous and belong to parameter spaces (2.8)-(2.9), time-varying delay $h(t)$ belongs to the delay spaces

$$h(t) \in \mathcal{H}_0 = \{h \in \mathcal{C}^1(\mathbb{R}_+, [0, \bar{h}]) : |\dot{h}| < \mu\} \subset \mathbb{R}_+. \tag{5.2}$$

and $\varphi(\theta) \in \mathcal{C}(\mathbb{R}_+, [-\underline{h}, 0])$ is the functional initial condition. A Lyapunov-Krasovskii functional candidate associated to LPV time-delay system (5.1) generally has the form:

$$V(x(t), \rho(t)) = \underbrace{\varsigma(t)^T P(\rho)\varsigma(t)}_{V_1(t)} + \underbrace{\int_{t-h(t)}^{t} x(\theta)^T Q x(\theta) d\theta}_{V_2(t)} + \underbrace{\bar{h}\int_{t-\bar{h}}^{t}\int_{\theta}^{t} \dot{x}(s)^T R\dot{x}(s) ds d\theta}_{V_3(t)}, \tag{5.3}$$

where extended vector $\varsigma(t) = \begin{bmatrix} x(t)^T & \int_{t-h}^{t} x(\theta)^T d\theta & \cdots \end{bmatrix}^T$, a continuously differentiable matrix function $P : \mathcal{U}_p \to \mathbb{S}_{++}$ with appropriated dimension and the positive matrices $Q, R \in \mathbb{S}_{++}^n$ are to be sought. It could mention that function $V_2(t)$ has been deployed in some delay-independent stability conditions. Since it doesn't contain information on the implemented delay, the approach is excessively conservative, especially when the delay is small, see, e.g., (Fridman, 2014; Gu et al., 2003). Subsequently, the delay-dependent condition involved in the stability analysis contains the addition of a quadratic double-integral term $V_3(t)$, which capture the upper bound of delay. The derivative of $V_3(t)$ is expressed by

$$\dot{V}_3(t) = \bar{h}^2 \dot{x}(t)^T R\dot{x}(t) - \bar{h}\int_{t-\bar{h}}^{t} \dot{x}(\theta)^T R\dot{x}(\theta) d\theta. \tag{5.4}$$

entails an obstacle with the integral term on the right side. At first glance, it seems like a complicated integration and should find ways to cancel out rather than tackling it directly. During the first decade of the 21st century, considerable efforts and attention devoted to the study of delay-dependent stability can mention such as: the model transformations method (Descriptor, Parameterization, Cross-Term Bounding, and Free-Weighting Matrices, etc.), the input-output method (Delay Operators, Small gain Theorem, etc.), and the discretized Lyapunov-Krasovskii functional method. The outline of the methods and their *pros* and *cons* are discussed in more detail in Appendix C. Besides, one of the limitations of the delay space $\mathcal{H}_0$ and LKF (5.3) is that it does not include the lower bound of the delay. Which in practice this condition sometimes does not exactly characterize non-zero hysteresis systems. The delay-range stability research has attracted a lot of attention in recent decades for LTI systems such as (He et al., 2007; Liu et al., 2017; P. Park et al., 2011; Y. Tian & Wang, 2020, 2021; X. M. Zhang et al., 2017), for T-S fuzzy systems such as (Datta et al., 2021; Dey et al., 2014; Li et al., 2020; Lian et al., 2020, 2021; Peng

& Han, 2011; Y. Tian & Wang, 2022; Wang & Lam, 2018a, 2018b, 2019), etc. However, in this dissertation, we do not cover this issue but focus more on relaxing the stability conditions and handling the stabilization for the saturated control system.

Recently, the convex function inequalities have significantly contributed to the more accurate estimation of the upper bound of the derivative of the Lyapunov function. Accompanying these developments is the suitable modification of the LKF candidate from an old-style form (5.3) to an extended vector with double and triple integrals. Generally, these studies are based on the application of analytic functions (see e.g., Appendix C.1). The approaches should meet the requirements: reduce the conservativeness and optimize the numbers of decision-variable matrices. The following section is devoted to the analyses of the recent studies concerned with the less conservatism of Jensen's inequality.

5.1.2. *Delay-Dependent LKF Stability – Convex function*

We would deliver the alternative improvement for the tighter bounding inequalities involved with the LKF stability analysis via LMIs. All developments and postulates are based on characteristic analysis of convex functions such as Jensen, Wirtinger, Bessel–Legendre inequalities, etc., presented in Appendix C.1.

5.1.2.1. *Jensen's Inequality and Extended Approach*

There are considerable famous inequalities derived from *original* Jensen's inequality are characterized by convex function or variations of convexity. The definition and some properties of convex functions of higher order, the definitions of convex domain properties refer to Appendix A.1 or (Boyd & Vandenberghe, 2004; Mitrinović et al., 1993a). Among studies, the integral version of Jensen's inequality is frequently employed in control delay theory in the last decades. Jensen's inequality improvement also can be found in the mathematical literature (Fink & Jodeit, 1990; Mitrinović et al., 1993b).

The generalizations of Jensen-based inequality such as Wirtinger-based inequality (Appendix C.1.1 Corollary C1.2) and auxiliary functions (Appendix C.1.1 Corollary C1.3-4) show significantly the relaxation of the stability conditions. By substituting the function $\dot{x}(s)$ for $w(s)$ in these corollaries, that yields the following results.

Lemma 5.1.1. *For a positive matrix* $R \in \mathbb{R}^n_{++}$ *and any continuous differentiable function* $x(t):[a,\ b]\rightarrow\mathbb{R}^n, [a,\ b]\in\mathbb{R}_{++}$, *the following equalities*

$$\int_a^b \dot{x}(s)^T R\dot{x}(s)ds \geq \frac{1}{b-a}\Omega_1^T R\Omega_1, \tag{5.5}$$

$$\int_a^b \dot{x}(s)^T R\dot{x}(s)ds \geq \frac{1}{b-a}\left(\Omega_1^T R\Omega_1 + 3\Omega_2^T R\Omega_2\right), \tag{5.6}$$

$$\int_a^b \dot{x}(s)^T R\dot{x}(s)ds \geq \frac{1}{b-a}\left(\Omega_1^T R\Omega_1 + 3\Omega_2^T R\Omega_2 + 5\Omega_3^T R\Omega_3\right), \tag{5.7}$$

$$\int_a^b \dot{x}(s)^T R\dot{x}(s)ds \geq \frac{1}{b-a}\left(\Omega_1^T R\Omega_1 + 3\Omega_2^T R\Omega_2 + 5\Omega_3^T R\Omega_3 + 7\Omega_4^T R\Omega_4\right), \tag{5.8}$$

$$\int_a^b \int_s^b \dot{x}(\theta)^T R\dot{x}(\theta)^T d\theta ds \geq 2\Omega_5^T R\Omega_5 + 4\Omega_6^T R\Omega_6, \tag{5.9}$$

$$\int_a^b \int_s^b \dot{x}(\theta)^T R \dot{x}(\theta)^T d\theta ds \geq 2\Omega_5^T R \Omega_5 + 4\Omega_6^T R \Omega_6 + 6\Omega_7^T R \Omega_7, \tag{5.10}$$

holds where

$$\begin{aligned}
\Omega_1 &= x(b) - x(a), \\
\Omega_2 &= x(b) + x(a) - \frac{2}{b-a}\int_a^b x(s)ds, \\
\Omega_3 &= x(b) - x(a) + \frac{6}{b-a}\int_a^b x(s)ds - \frac{12}{(b-a)^2}\int_a^b \int_s^b x(\theta)d\theta\, ds, \\
\Omega_4 &= x(b) + x(a) - \frac{12}{b-a}\int_a^b x(s)ds + \frac{60}{(b-a)^2}\int_a^b \int_s^b x(\theta)d\theta\, ds - \frac{120}{(b-a)^3}\int_a^b \int_s^b \int_\theta^b x(\beta)d\beta\, d\theta\, ds, \\
\Omega_5 &= x(b) - \frac{1}{b-a}\int_a^b x(s)ds, \\
\Omega_6 &= x(b) + \frac{2}{b-a}\int_a^b x(s)ds - \frac{6}{(b-a)^2}\int_a^b \int_s^b x(\theta)d\theta\, ds, \\
\Omega_7 &= x(b) - \frac{3}{b-a}\int_a^b x(s)ds + \frac{24}{(b-a)^2}\int_a^b \int_s^b x(\theta)d\theta\, ds - \frac{60}{(b-a)^3}\int_a^b \int_s^b \int_\theta^b x(\beta)d\beta\, d\theta\, ds.
\end{aligned}$$

The proof of conditions (5.6), (5.7), and (5.9) is inferred directly from Appendix C.1.1 Corollary C1.1-4, and extended conditions (5.8), (5.10) can consult at (Y. Tian & Wang, 2020; Zhao et al., 2017). It should note that these methods provide better estimates of the lower bound of the expression $\int_{t-h}^t \dot{x}(s)^T R \dot{x}(s) ds$ and $\int_{t-h}^t \int_\theta^t \dot{x}(s)^T R \dot{x}(s) ds d\theta$. Accordingly, the most effective of these bounding conditions is accompanied by a reasonable choice of expansion vectors with single integral, double integral and triple integral, respectively. Let's consider the following LKF candidates associated to LPV time-delay system (5.1) as follows:

- The single integral case for application of Wirtinger-based inequality (WBII):

$$V(t) = V_1(t) + V_2(t) + V_3(t), \tag{5.11}$$

with the extended vector $\varsigma(t) = \begin{bmatrix} x(t)^T & \int_{t-h}^t x(s)^T ds \end{bmatrix}^T$, and functions

$$\begin{aligned}
V_1(t) &= \varsigma(t)^T P(\rho) \varsigma(t), \\
V_2(t) &= \int_{t-h(t)}^t x(\theta)^T Q x(\theta) d\theta, \\
V_3(t) &= \bar{h} \int_{t-\bar{h}}^t \int_\theta^t \dot{x}(s)^T R \dot{x}(s) ds d\theta,
\end{aligned} \tag{5.12}$$

where the decision variable matrices $P : \mathcal{U}_p \to \mathbb{S}_{++}^{2n}, Q, R \in \mathbb{S}_{++}^n$.

- The double/triple integral case for extensions:

$$V(t) = V_1(t) + V_2(t) + V_3(t) + V_4(t), \tag{5.13}$$

where augmented vector

$\varsigma(t) = \begin{bmatrix} x(t)^T & \int_{t-h}^t x(s)^T ds & \int_{t-h}^t \int_s^t x(\theta)^T d\theta\, ds & \int_{t-h}^t \int_s^t \int_\theta^t x(\beta)^T d\beta\, d\theta\, ds \end{bmatrix}^T$, and function

$V_4(t) = \int_{t-\bar{h}}^t \int_s^t \int_\theta^t \dot{x}(\beta)^T S \dot{x}(\beta) d\beta\, d\theta\, ds,$

Inequalities (5.6)-(5.8) is applied to derive a better estimate of the lower bound of expression $\int_{t-h}^{t} \dot{x}(s)^T R \dot{x}(s) ds$ relating to the derivative of the function $V_3(t)$. Correspondingly, inequalities (5.9), (5.10) are used to estimate the lower bound of the derivative $V_4(t)$. The effectiveness of the convex function is demonstrated in the works of (Datta et al., 2021; P. G. Park et al., 2015; Y. Tian & Wang, 2020, 2021; Zhao et al., 2017) with the significant improvement in the stability conditions. In section 5.2, the maximum allowable hysteresis are compared with recent work on stability analysis of LTI and LPV time-varying delay systems.

5.1.2.2. *Discretized Convex Function*

Along with the auxiliary function method, the *n*-convex discretization method also shows the effectiveness in relaxing the conservatism. The analyses of *n*-convex can find in the monographs (Boyd & Vandenberghe, 2004; Fink & Jodeit, 1990; Mitrinović et al., 1993a). It is interesting to emphasize that the gap of Jensen's inequality significantly decreases corresponding to the number of segments. The reduction of the inequality gap is obtained by discretizing, respectively, 1, 2, and 3 segments (in Appendix C.1.2) It shows that the *higher fragmentation*, the *less conservative* Jensen-based inequality.

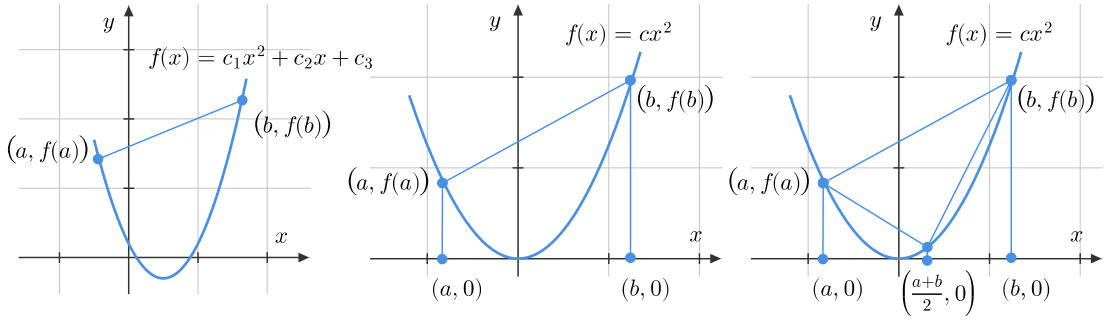

a. The chord of the parabola expresses convex inequality. *b. The integral region of the parabola is in the interval.* *c. The integral domain fragmentation.*

Figure 5-1. *Graph of a convex function.*

Using the simple Lyapunov-Krasovskii functional (5.3) cannot attain to the analytical delay limit (including using free-matrix conjoint with the decision matrices). So, let's consider a discretized Lyapunov-Krasovskii functional candidate associated to LPV time-delay system (5.1) under the form:

$$V(t) = V_1(t) + V_2(t) + V_3(t), \tag{5.14}$$

where functions

$$\begin{aligned} V_2(t) &= \int_{t-h(t)}^{t} x(\theta)^T Q(\theta) x(\theta) d\theta = \sum_{i=1}^{N} \int_{t-ih_\Delta(t)}^{t-(i-1)h_\Delta(t)} x(\theta)^T Q_i x(\theta) d\theta, \\ V_3(t) &= \int_{t-\bar{h}}^{t} \int_{\theta}^{t} \dot{x}(s)^T R(\theta) \dot{x}(s) ds d\theta = \sum_{i=1}^{N} \bar{h}_\Delta \int_{t-i\bar{h}_\Delta}^{t-(i-1)\bar{h}_\Delta} \int_{\theta}^{t} \dot{x}(s)^T R_i \dot{x}(s) ds d\theta. \end{aligned} \tag{5.15}$$

where $h_\Delta(t) = \frac{h(t)}{N}$, $\bar{h}_\Delta = \frac{\bar{h}}{N}$, and N is the number of divisions in the interval, i.e., $[-\bar{h}, 0]$.

This method significantly enhances the stability analysis of time-delay systems with the continuous and piecewise Lyapunov matrices. Then, the integral term $\int_{t-h}^{t} \dot{x}(s)^T R \dot{x}(s) ds$ involving in the derivative of function $V_3(t)$ bounded by the Jensen-based inequalities

(Jensen and Wirtinger). The minimizing gap in inequalities, making the condition least conservative. Some result has shown almost closer with analytical prediction (Briat et al., 2008; Gu et al., 2003; Han, 2008). The interesting point about the discretizing delay intervals is that it suits to all advanced bounding techniques (section 5.1.2).

5.1.3. *Delay-Dependent Stability – Input-Output Approach*

As discussed, the delay *decomposition* approach provides less conservative results for stability analysis and controller design. But the method is effective for systems that *access* the exact knowledge of the delay, which is ideal for numerical computation in practical design. Actually, the identifications or estimations of the continuous-time delay phenomenon in practice are tough challenges, see, e.g., (Anguelova & Wennberg, 2008; Belkoura et al., 2009; F. Chen et al., 2015; Ren et al., 2005; Zheng et al., 2011). It should to mention that almost all the works from the literature analyzes the stabilization problem with memoryless (conservative) or exact-memory (non-implementable) controllers. In this case, the uncertainty (approximation) delay method discussed in Section 8.6 (Gu et al., 2003) shows to be more suitable for implementing the strategy of control system design. Specifically, the time-varying delay that is not accurately known at the time of analysis and design is considered as the dynamical uncertainties of *nominal system*. The input-output approach is very convenient in analyzing the stability based on the reformulation of the original system to feedback interconnection with additional inputs and outputs of auxiliary systems. Based on this approach, the stability is formulated in the input-output framework where the characterized LMI conditions obtain by the Scaled Small-Gain theorem (Briat et al., 2009; Hmamed et al., 2015) or supply function (Briat et al., 2010).

The objective of this section is to deliver a delay-dependent stability condition with an uncertain knowledge of the implemented delay. This problem can be equivalently reformulated into a stability problem of a TDS with two time-varying delays expressed by an algebraic relation. Let's introduce a uncertain memory delay $\delta(t) \in [\underline{\delta}, \overline{\delta}]$ is defined by $\delta(t) = d(t) - h(t)$, with maximal non-fragility radius $|\delta(t)| \le \delta_m = \max\{\overline{\delta}, |\underline{\delta}|\}$.

Proposition 5.1.1. *Let's consider the operator* $\Delta_0 : \mathcal{L}_2[0,\infty) \to \mathcal{L}_2[0,\infty)$ *is expressed by the following equation:*

$$w_0(t) = \Delta_0(z_0(t)) = \frac{2}{\sqrt{7}\delta_m} \int_{t-d(t)}^{t-h(t)} z(\theta) d\theta. \tag{5.16}$$

This operator enjoys the property: Δ_0 *is* $\mathcal{L}_2$ *input-output stable and satisfies the bounded small gain constraint* $\|\Delta_0(z_0(t))\|_{\mathcal{L}_2} \le \|z_0(t)\|_{\mathcal{L}_2}$.

Temporarily ignore the effect of control input, TDS system (5.1) is transformed to the following differential equation using the internal topology with input-output structure:

$$\begin{aligned}
\dot{x}(t) &= A(\rho)x(t) + A_h(\rho)x(t-d(t)) + \tfrac{\sqrt{7}}{2}\delta_m A_h(\rho)w_0(t) + B_w(\rho)w(t) \\
z(t) &= H(\rho)x(t) + H_h(\rho)x(t-d(t)) + \tfrac{\sqrt{7}}{2}\delta_m H_h(\rho)w_0(t) + J_w(\rho)w(t) \\
z_0(t) &= \dot{x}(t) \\
w_0(t) &= \Delta_0(z_0(t))
\end{aligned} \tag{5.17}$$

In order to verify $\mathcal{L}_2$ input-output stable $w_0(t) \to z_0(t)$ and guarantee $\mathcal{L}_2$-gain on the transfer from $w(t) \to z(t)$, let's define a supply-function combining a parameter-dependent $\mathcal{D}$-scaling set and an energy-to-energy index $\gamma > 0$:

$$\mathcal{S}(\zeta(t), \rho(t)) = \begin{bmatrix} w(t) \\ z(t) \\ w_0(t) \\ z_0(t) \end{bmatrix}^T \begin{bmatrix} -\gamma I_d & 0 & 0 & 0 \\ 0 & \gamma I_r & 0 & 0 \\ 0 & 0 & -L(\rho) & 0 \\ 0 & 0 & 0 & L(\rho) \end{bmatrix} \underbrace{\begin{bmatrix} w(t) \\ z(t) \\ w_0(t) \\ z_0(t) \end{bmatrix}}_{\zeta(t)} \leq 0. \tag{5.18}$$

If the above condition holds, that suggests the satisfaction of the scaled small gain condition for uncertain norm-bounded operator $\Delta : z_0(t) \to w_0(t)$, and the $\mathscr{H}_\infty$ performance criterion of system i.e., $\|z(t)\|_{\mathcal{L}_2} \leq \gamma \|w(t)\|_{\mathcal{L}_2}$.

The equivalent between the Scaled Small-Gain and Lyapunov-based technique is discussed in (Boyd et al., 1994; Boyd & Yang, 1989; Doyle et al., 1991; J. Zhang et al., 2001; Zhou & Doyle, 1998) for LTI/LTV systems. Both constant and time-varying approximate delay approaches will be more detailed in Appendix C.3. The quadratic supply rate (5.18) will be integrated in the delay-dependent stability analysis so-called δ_m memory resilient (in Section 5.2.4), and developed for the saturated control design of the LPV time-delay system (in Chapter 6).

5.2. Stability Analysis of Lyapunov-Krasovskii functional

In this section, the stability of the time-varying delay LPV/quasi-LPV system is verified by using the parameter-dependent Lyapunov-Krasovskii function (PDLKF) candidate given in (5.3), (5.11), and (5.13). Besides, the advanced bounding techniques provide a better relaxation for the stability condition but return in the conditional complexity. That requires a delicate manipulation to decouple the bilinear components encountered in the control design strategy.

5.2.1. *Single Delay-Dependent LKF Stability and associated relaxation*

5.2.1.1. *Jensen's Inequality*

From the above discussion, PDLKF in Eqs. (5.3) is used to deliver a stability condition of system (5.1) combining with $\mathscr{H}_\infty$ performance that leads to the following results.

Lemma 5.2.1. *Given positive scalars $\overline{h}, \gamma$, delay and parameter belong to the sets*

$$h(t) \in \mathcal{H}_0 = \{h \in \mathcal{C}^1(\mathbb{R}_+, [0,\ \overline{h}]) : |\dot{h}| \leq \mu < 1\} \subset \mathbb{R}_+,$$
$$\rho(t) \in \mathcal{U}_p = \left\{ \rho_i \in \mathcal{C}^1([t_0,\ \infty), [\underline{\rho}_i,\ \overline{\rho}_i]) \;\middle|\; |\dot{\rho}_i| < \nu_i \in [\underline{\nu}_i,\ \overline{\nu}_i],\ i = 1, \ldots, N_p \right\} \subset \mathbb{R}^{N_p}.$$

Then, the LPV time-delay system (5.1) *is asymptotically stable corresponding to designed $\mathscr{H}_\infty$ performance attenuation, if there exist a continuously differentiable matrix function $P : \mathcal{U}_p \to \mathbb{S}^n_{++}$, matrices $Q, R \in \mathbb{S}^n_{++}$, such that the parameter-dependent matrix inequality satisfies*

$$\Upsilon(\rho)=\begin{bmatrix} \Upsilon_{11} & * & * & * & * \\ A_h(\rho)^T P(\rho)+R & -(1-\mu)Q-R & * & * & * \\ B_w(\rho)^T P(\rho) & 0 & -\gamma I_d & * & * \\ H(\rho) & H_h(\rho) & J_w(\rho) & -\gamma I_r & * \\ \bar{h}RA(\rho) & \bar{h}RA_h(\rho) & \bar{h}RB_w(\rho) & 0 & -R \end{bmatrix} \prec 0, \quad (5.19)$$

with: $\Upsilon_{11} = sym\{P(\rho)A(\rho)\} \pm \sum_i^{N_p} \nu_i \dfrac{\partial P(\rho)}{\partial \rho_i} + Q - R.$

Proof. The proof is detailed in Appendix D.1.

Remark 5.2.1. It should note that this stability analysis approach simplifies the stability PLMI condition, which concerns only the three decision matrices variables $P(\rho), Q$ and R from Lyapunov-Krasovskii functional (no slack matrices are included). Then, to avoid the use of the old-style techniques (e.g., cross-term inequality, model transformation), Jensen-based inequality (5.5) is employed to bound the integral $\int_{t-h}^{t} \dot{x}(s)^T R\dot{x}(s)ds$.

5.2.1.2. *Wirtinger-Based Inequality*

As we know, Wirtinger-Based inequality (5.6) has a better estimate of the lower bound of the expression $\int_{t-h}^{t} \dot{x}(s)^T R\dot{x}(s)ds$ than the traditional Jensen's inequality (5.5). The manipulation of this inequality accompanies a slight change in the LKF formulation from (5.3) to (5.11) combined with an augmented vector that yields the following lemma.

Lemma 5.2.2. *For positive scalars* $\bar{h}, \gamma$, *delay space* $h(t) \in \mathcal{H}_0$, *and* $\rho(t) \in \mathcal{U}_p$, *then LPV system* (5.1) *is asymptotically stable corresponding to* $\mathscr{H}_\infty$ *performance index, if there exist a continuously differentiable matrix function* $P_1 : \mathcal{U}_p \to \mathbb{S}_{++}^n$, *positive symmetric matrices* $P_3, Q, R \in \mathbb{S}_{++}^n$ and a *matrix* $P_2 \in \mathbb{R}^{n\times n}$, *such that the following PLMIs fulfill*

$$\begin{bmatrix} \Upsilon_{11}(\rho,\dot{\rho}) & * & * & * & * & * \\ \Upsilon_{21}(\rho) & -(1-\mu)Q-4R & * & * & * & * \\ \Upsilon_{31}(\rho) & \Upsilon_{32}(\rho) & -\frac{12}{\bar{h}^2}R & * & * & * \\ B_w(\rho)^T P_1(\rho) & 0 & B_w(\rho)^T P_2 & -\gamma I_d & * & * \\ H(\rho) & H_h(\rho) & 0 & J_w(\rho) & -\gamma I_r & * \\ \bar{h}RA(\rho) & \bar{h}RA_h(\rho) & 0 & \bar{h}RB_w(\rho) & 0 & -R \end{bmatrix} \prec 0, \quad (5.20)$$

$$P(\rho)=\begin{bmatrix} P_1(\rho) & P_2 \\ P_2^T & P_3 \end{bmatrix} \succ 0, \quad (5.21)$$

with $\Upsilon_{11}(\rho,\dot{\rho}) = sym\{P_1(\rho)A(\rho)+P_2\} \pm \sum_i^{N_p} \nu_i\, \partial P_1(\rho)/\partial\rho_i + Q - 4R,$
$\Upsilon_{21}(\rho) = A_h(\rho)^T P_1(\rho) - (1-\mu)P_2^T - 2R,$
$\Upsilon_{31}(\rho) = P_2^T A(\rho) + P_3 + \frac{6}{\bar{h}}R,$
$\Upsilon_{32}(\rho) = P_2^T A_h(\rho) - (1-\mu)P_3 + \frac{6}{\bar{h}}R.$

Proof.

Consider LKF (5.11) for LPV time-delay system (5.1). Then, this dynamic system is delay-dependent stable if the conditions:

$$\dot{V}(t) = 2\varsigma(t)^T P(\rho(t))\dot{\varsigma}(t) + x(t)^T Q x(t) - (1-\dot{h}(t))x(t-h(t))^T Q x(t-h(t))$$
$$\varsigma(t)^T \dot{P}(\rho(t))\varsigma(t) + \bar{h}^2 \dot{x}(t)^T R \dot{x}(t) - \bar{h}\int_{t-\bar{h}}^{t} \dot{x}(\theta)^T R \dot{x}(\theta) d\theta < 0, \tag{5.22}$$

hold along the trajectories of system, with

$$\varsigma(t) = \begin{bmatrix} x(t)^T & \int_{t-h}^{t} x(s)^T ds \end{bmatrix}^T,\ P(\rho(t)) = \begin{bmatrix} P_1(\rho(t)) & P_2 \\ P_2^T & P_3 \end{bmatrix}.$$

For the sake of simplicity, denote $x_t \coloneqq x(t)$, $x_h \coloneqq x(t-h(t))$. The integral of the positive real function is rearranged by Wirtinger-Based inequality WBII (5.6):

$$\begin{aligned} -\bar{h}\int_{t-\bar{h}}^{t} \dot{x}(\theta)^T R \dot{x}(\theta) d\theta &\le -\bar{h}\int_{t-h(t)}^{t} \dot{x}(\theta)^T R \dot{x}(\theta) d\theta \\ &\overset{WBII}{\le} -\frac{\bar{h}}{h(t)}(\Omega_1{}^T R \Omega_1 + 3\Omega_2{}^T R \Omega_2), \\ &\le -\begin{bmatrix} x_t \\ x_h \\ \int_{t-h}^{t} x(s) ds \end{bmatrix}^T \begin{bmatrix} 4R & 2R & -6R/\bar{h} \\ * & 4R & -6R/\bar{h} \\ * & * & 12R/\bar{h}^2 \end{bmatrix} \begin{bmatrix} x_t \\ x_h \\ \int_{t-h}^{t} x(s) ds \end{bmatrix}. \end{aligned} \tag{5.23}$$

where, $\Omega_1 = x_t - x_h$, $\Omega_2 = x_t + x_h - \dfrac{2}{h(t)}\displaystyle\int_{t-h(t)}^{t} x(s) ds$.

The well-posed problem of the inequality (5.23) at extreme point $h(t_i) \to 0$ at time $t = t_i$ is validated as analyzed in D.1. Then, considering the influence of external disturbance, performance constraint included in stability condition (5.22) and combines with condition (5.23) that entails in the following PLMI condition:

$$\dot{V}(t) + \gamma^{-1} z(t)^T z(t) - \gamma w(t)^T w(t) \le \xi(t)^T \Upsilon \xi(t) + \xi(t)^T \Gamma^T \begin{bmatrix} \gamma^{-1} I_r & 0 \\ 0 & R^{-1} \end{bmatrix} \Gamma \xi(t) < 0, \tag{5.24}$$

where

$$\xi^T = \begin{bmatrix} x_t^T & x_h^T & \int_{t-h}^{t} x(s)^T ds & w(t)^T \end{bmatrix},$$
$$\Gamma = \begin{bmatrix} H(\rho) & H_h(\rho) & 0 & J_w(\rho) \\ \bar{h}RA(\rho) & \bar{h}RA_h(\rho) & 0 & \bar{h}RB_w(\rho) \end{bmatrix},$$
$$\Upsilon = \begin{bmatrix} \{P_1(\rho)A(\rho) + P_2\}^S \pm \sum_i |\dot{\rho}_i| \frac{\partial P_1}{\partial \rho_i} + Q - 4R & * & * & * \\ A_h(\rho)^T P_1(\rho) - P_{2\mu}^T - 2R & -Q_\mu - 4R & * & * \\ P_2^T A(\rho) + P_3 + \frac{6}{\bar{h}} R & P_2^T A_h(\rho) - P_{3\mu} + \frac{6}{\bar{h}} R & -\frac{12}{\bar{h}^2} R & * \\ B_w(\rho)^T P_1(\rho) & 0 & B_w(\rho)^T P_2 & -\gamma I_d \end{bmatrix},$$

with notation $P_{2\mu} = (1-\mu)P_2$, $P_{3\mu} = (1-\mu)P_3$, $Q_\mu = (1-\mu)Q$, and $\{\cdot\}^S \coloneqq sym\{\cdot\}$. Then, using Schur's complement yields to (5.20).

□

Remark 5.2.2. The coupling decision matrices and system matrices in inequality (5.20) are more complicated than one in inequality (5.19). Consider condition (5.22), the expansion of $\bar{h}^2 \dot{x}(t)^T R \dot{x}(t)$ results in multiple product terms $RA(\rho)$ and $RA_h(\rho)$ etc., which could avoid if the conditional vector is expanded with $\dot{x}(t)$. But, the existence of the mul-

tiple productions terms $P_1(\rho)A(\rho)$, $P_2^T A(\rho)$ prevents performing a congruence transformation with the inverse of matrices $P_1(\rho)$, P_2^T. If the double and triple integrals include in LKF, then the design stabilization conditions are really in trouble.

From this point, a linearizing transformation with the slack-variables concerning a generalization of Finsler's lemma decouples the decision matrix variables and maintains the parametric characterization structure (provides flexibility for the LMI condition without the additional assumptions). Now, by using the projection lemma that results in the associated relaxation of PLMI condition.

Theorem 5.2.1: *For positive scalars* $\overline{h}, \gamma, \varepsilon$, *delay* $h(t) \in \mathcal{H}_0$, *and parameter* $\rho(t) \in \mathcal{U}_p$, *then LPV time-delay* (5.1) *is asymptotically stable conforming to the energy-to-energy index, if there exist a PD matrix* $X(\rho) \in \mathbb{R}^{n\times n}$, *positive matrices* $P_3, Q, R \in \mathbb{S}^n_{++}$, *a continuously differentiable matrix function* $P_1 : \mathcal{U}_p \to \mathbb{S}^n_{++}$, *and matrices* $P_2 \in \mathbb{R}^{n\times n}$, *such that the following PLMIs hold*

$$\begin{bmatrix} -X(\rho)^S & * & * & * & * & * & * & * \\ \Upsilon_{21}(\rho) & \Upsilon_{22}(\rho,\dot\rho) & * & * & * & * & * & * \\ A_h(\rho)^T X(\rho) & \Upsilon_{32}(\rho) & \Upsilon_{33}(\rho) & * & * & * & * & * \\ P_2^T & \Upsilon_{42}(\rho) & \Upsilon_{43}(\rho) & -\frac{12}{\overline{h}^2}R & * & * & * & * \\ B_w(\rho)^T X(\rho) & 0 & 0 & 0 & -\gamma I_d & * & * & * \\ 0 & H(\rho) & H_h(\rho) & 0 & J_w(\rho) & -\gamma I_r & * & * \\ \overline{h}R & 0 & 0 & 0 & 0 & 0 & -R & * \\ \varepsilon X(\rho) & 0 & 0 & -\varepsilon P_2 & 0 & 0 & -\varepsilon\overline{h}R & -P_1(\rho) \end{bmatrix} \prec 0, \quad (5.25)$$

$$P(\rho) = \begin{bmatrix} P_1(\rho) & P_2 \\ P_2^T & P_3 \end{bmatrix} \succ 0, \quad (5.26)$$

with:
$$\Upsilon_{21}(\rho) = A(\rho)^T X(\rho) + P_1(\rho) \qquad \Upsilon_{42}(\rho) = P_3 + \tfrac{6}{\overline{h}} R,$$
$$\Upsilon_{22}(\rho,\dot\rho) = P_2^S \pm \textstyle\sum_i^{N_p} \nu_i\, \partial P_1(\rho)/\partial\rho_i + Q - 4R - \varepsilon^2 P_1(\rho), \qquad \Upsilon_{33}(\rho) = -Q_\mu - 4R$$
$$\Upsilon_{32}(\rho) = -P_{2\mu}^T - 2R, \qquad \Upsilon_{43}(\rho) = -P_{3\mu} + \tfrac{6}{\overline{h}} R.$$

Proof.

The PDLMI (5.25) is reorganized as follows:

$$\Psi(\rho) + \mathcal{P}(\rho)^T \Theta(\rho) \mathcal{Q} + \mathcal{Q}^T \Theta(\rho)^T \mathcal{P}(\rho) \prec 0, \quad (5.27)$$

with $\Psi(\rho) =$
$$\left[\begin{array}{c|ccccccc} 0 & * & * & * & * & * & * & * \\ \hline P_1(\rho) & \Upsilon_{22}(\rho,\dot\rho) & * & * & * & * & * & * \\ 0 & \Upsilon_{32}(\rho) & \Upsilon_{33}(\rho) & * & * & * & * & * \\ P_2^T & \Upsilon_{42}(\rho) & \Upsilon_{43}(\rho) & -\frac{12}{\overline{h}^2}R & * & * & * & * \\ 0 & 0 & 0 & 0 & -\gamma I_d & * & * & * \\ 0 & H(\rho) & H_h(\rho) & 0 & J_w(\rho) & -\gamma I_r & * & * \\ \overline{h}R & 0 & 0 & 0 & 0 & 0 & -R & * \\ 0 & 0 & 0 & -\varepsilon P_2 & 0 & 0 & -\varepsilon\overline{h}R & -P_1(\rho) \end{array}\right],$$

and $\Theta(\rho) = X(\rho)$, $\mathcal{Q} = \left[I \mid 0 \quad 0 \quad 0 \quad 0 \quad 0 \quad 0 \quad 0\right]$,
$\mathcal{P}(\rho) = \left[-I \mid A(\rho) \quad A_h(\rho) \quad 0 \quad B_w(\rho) \quad 0 \quad 0 \quad \varepsilon I\right]$.

Let's consider matrices form base of the null spaces of $\mathcal{P}(\rho)$ and $\mathcal{Q}$:

$$\ker(\mathcal{P}) = \left[\begin{array}{c|cccccc} A(\rho) & A_h(\rho) & 0 & B_w(\rho) & 0 & 0 & \varepsilon I \\ \hline I & 0 & 0 & 0 & 0 & 0 & 0 \\ 0 & I & 0 & 0 & 0 & 0 & 0 \\ 0 & 0 & I & 0 & 0 & 0 & 0 \\ 0 & 0 & 0 & I & 0 & 0 & 0 \\ 0 & 0 & 0 & 0 & I & 0 & 0 \\ 0 & 0 & 0 & 0 & 0 & I & 0 \\ 0 & 0 & 0 & 0 & 0 & 0 & I \end{array}\right], \text{ and } \ker(\mathcal{Q}) = \left[\begin{array}{ccccccc} 0 & 0 & 0 & 0 & 0 & 0 & 0 \\ \hline I & 0 & 0 & 0 & 0 & 0 & 0 \\ 0 & I & 0 & 0 & 0 & 0 & 0 \\ 0 & 0 & I & 0 & 0 & 0 & 0 \\ 0 & 0 & 0 & I & 0 & 0 & 0 \\ 0 & 0 & 0 & 0 & I & 0 & 0 \\ 0 & 0 & 0 & 0 & 0 & I & 0 \\ 0 & 0 & 0 & 0 & 0 & 0 & I \end{array}\right].$$

Then, (5.27) is solvable for $\Theta(\rho)$ if and only if the two underlying LMIs are held.

$$\ker(\mathcal{P}(\rho))^T \Psi(\rho) \ker(\mathcal{P}(\rho)) \prec 0, \tag{5.28}$$

$$\ker(\mathcal{Q})^T \Psi(\rho) \ker(\mathcal{Q}) \prec 0, \tag{5.29}$$

Following the statement of Finsler's lemma, if condition (5.25) is fulfilled then the two sub-conditions (5.28), (5.29) will be satisfied. An expansion for sub-condition (5.28) can be simply performed as follows:

$$\left[\begin{array}{ccccccc} \Xi_{11}(\rho,\dot{\rho}) & * & * & * & * & * & * \\ \Xi_{21}(\rho) & -(1-\mu)Q-4R & * & * & * & * & * \\ \Xi_{31}(\rho) & \Xi_{32}(\rho) & -\frac{12}{\bar{h}^2}R & * & * & * & * \\ B_w(\rho)^T P_1(\rho) & 0 & B_w(\rho)^T P_2 & -\gamma I_d & * & * & * \\ H(\rho) & H_h(\rho) & 0 & J_w(\rho) & -\gamma I_r & * & * \\ \bar{h}RA(\rho) & \bar{h}RA_h(\rho) & 0 & \bar{h}RB_w(\rho) & 0 & -R & * \\ \hline \varepsilon P_1(\rho) & 0 & 0 & 0 & 0 & 0 & -P_1(\rho) \end{array}\right] \prec 0, \tag{5.30}$$

with

$$\begin{aligned} \Xi_{11}(\rho,\dot{\rho}) &= sym\{P_1(\rho)A(\rho)+P_2\} \pm \textstyle\sum_i^{N_p} \nu_i \, \partial P_1(\rho)/\partial\rho_i + Q - 4R - \varepsilon^2 P_1(\rho), \\ \Xi_{21}(\rho) &= A_h(\rho)^T P_1(\rho) - (1-\mu)P_2^T - 2R, \\ \Xi_{31}(\rho) &= P_2^T A(\rho) + P_3 + \tfrac{6}{\bar{h}}R, \\ \Xi_{32}(\rho) &= P_2^T A_h(\rho) - (1-\mu)P_3 + \tfrac{6}{\bar{h}}R. \end{aligned}$$

Finally, using Schur's complement for the latter condition that consistently ensues in stability condition (5.20).

□

Remark 5.2.3. The addition of the term $-\varepsilon^2 P_1(\rho) + \varepsilon P_1(\rho) P_1(\rho)^{-1} \varepsilon P_1(\rho)$ and the scalar ε produce extra-degrees of freedom for the designed condition (less conservative). But, the inclusion of condition (5.29) entails the unnecessary constraints for decision matrices. In the view of the LMI-Based relaxation methods, e.g., the *slack*-variable method (Ebihara et al., 2014; Zope et al., 2012) the slack-variable matrices couple $\Theta = diag\{X_1, X_2, X_3\}$ with system's matrices $A(\rho), A_h(\rho)$ and $B_w(\rho)$. Three *slack*-variables yields a more relaxed condition, and the second LMI condition $\ker(\mathcal{Q})^T \Psi(\rho) \ker(\mathcal{Q}) \prec 0$ is always feasibility. Nonetheless, too much coupling hinders the *scalability* of the controller design strategy. A linearization could derive from choosing $X_2 = \alpha X_1, X_3 = \beta X_1,$ but it reduces the interestingness of the SV method. By the way, one slack matrix is concerned in PDLMI (5.25).

5.2.1.3. *Auxiliary Function-Based Integral Inequality*

In this section, the stability condition delivers for the LPV time-delay system using an AFBII. As shown in the result section 5.2.5, this approach is the superior improvement of system performance compared to WBII and Jensen Inequality. Using the LKF equation (5.13) for stability analysis for the dynamical system (5.1), we have the following result.

Lemma 5.2.3. *For positive scalars* $\bar{h}, \gamma$, *delay space* $h(t) \in \mathcal{H}_0$, *and parameter* $\rho(t) \in \mathcal{U}_p$, *then LPV system* (5.1) *is asymptotically delay-dependent stable corresponding to* $\mathscr{H}_\infty$ *performance criterion, if there exist a continuously differentiable matrix function* $P_1 : \mathcal{U}_p \to \mathbb{S}^n_{++}$, *matrices* $P_2 \in \mathbb{R}^{n\times 3n}, P_3 \in \mathbb{S}^{3n}_{++}$, *and* $Q, R, S \in \mathbb{S}^n_{++}$ *such that the PDLMIs*

$$\left[\begin{array}{c|ccc} \Upsilon_{11}(\rho,\dot{\rho}) & * & * & * \\ \hline e_{11}(\rho) & -\gamma I_r & * & * \\ \bar{h}Re_0(\rho) & 0 & -R & * \\ \frac{\bar{h}}{2}Se_0(\rho) & 0 & 0 & -\frac{1}{2}S \end{array}\right] \prec 0, \tag{5.31}$$

$$P(\rho) = \begin{bmatrix} P_1(\rho) & P_2 \\ P_2^T & P_3 \end{bmatrix} \succ 0, \tag{5.32}$$

hold, where:

$$\begin{aligned}\Upsilon_{11}(\rho,\dot{\rho}) = {} & \{\Pi_1^T P(\rho)\Pi_2(\rho) + \tfrac{1}{2}\bar{P}(\rho,\dot{\rho})\}^S + e_1^T Q e_1 - e_2^T Q_\mu e_2 - e_3^T R e_3 - 3e_4^T R e_4 - 5e_5^T R e_5 \\ & - 7e_6^T R e_6 - 2e_7^T S e_7 - 4e_8^T S e_8 - 6e_9^T S e_9 - e_{10}^T \gamma e_{10},\end{aligned}$$

with

$$\begin{aligned}
e_0 &= [A(\rho) \quad A_h(\rho) \quad 0_n \quad 0_n \quad 0_n \quad B_w(\rho)], \\
e_1 &= [I_n \quad 0_n \quad 0_n \quad 0_n \quad 0_n \quad 0_{n\times d}], \\
e_2 &= [0_n \quad I_n \quad 0_n \quad 0_n \quad 0_n \quad 0_{n\times d}], \\
e_3 &= [I_n \quad -I_n \quad 0_n \quad 0_n \quad 0_n \quad 0_{n\times d}], \\
e_4 &= \left[I_n \quad I_n \quad -\frac{2}{\bar{h}}I_n \quad 0_n \quad 0_n \quad 0_{n\times d}\right], \\
e_5 &= \left[I_n \quad -I_n \quad \frac{6}{\bar{h}}I_n \quad -\frac{12}{\bar{h}^2}I_n \quad 0_n \quad 0_{n\times d}\right], \\
e_7 &= \left[I_n \quad 0_n \quad -\frac{1}{\bar{h}}I_n \quad 0_n \quad 0_n \quad 0_{n\times d}\right], \\
e_8 &= \left[I_n \quad 0_n \quad \frac{2}{\bar{h}}I_n \quad -\frac{6}{\bar{h}^2}I_n \quad 0_n \quad 0_{n\times d}\right], \\
\bar{P}(\rho,\dot{\rho}) &= \left[\begin{array}{c|c} \sum_i^{N_p} \pm\nu_i \frac{\partial P_1(\rho)}{\partial \rho_i} & 0_{n\times(4n+d)} \\ \hline 0_{(4n+d)\times n} & 0_{(4n+d)} \end{array}\right],
\end{aligned}$$

$$\begin{aligned}
e_6 &= \left[I_n \quad I_n \quad -\frac{12}{\bar{h}}I_n \quad \frac{60}{\bar{h}^2}I_n \quad -\frac{120}{\bar{h}^3}I_n \quad 0_{n\times d}\right], \\
e_9 &= \left[I_n \quad 0_n \quad -\frac{3}{\bar{h}}I_n \quad \frac{24}{\bar{h}^2}I_n \quad -\frac{60}{\bar{h}^3}I_n \quad 0_{n\times d}\right], \\
e_{10} &= [0_{d\times n} \quad 0_{d\times n} \quad 0_{d\times n} \quad 0_{d\times n} \quad 0_{d\times n} \quad I_d], \\
e_{11} &= [H(\rho) \quad H_h(\rho) \quad 0_{r\times n} \quad 0_{r\times n} \quad 0_{r\times n} \quad J_w(\rho)], \\
\Pi_1 &= \begin{bmatrix} I_n & 0_n & 0_n & 0_n & 0_n & 0_{n\times d} \\ 0_n & 0_n & I_n & 0_n & 0_n & 0_{n\times d} \\ 0_n & 0_n & 0_n & I_n & 0_n & 0_{n\times d} \\ 0_n & 0_n & 0_n & 0_n & I_n & 0_{n\times d} \end{bmatrix}^T, \\
\Pi_2(\rho) &= \begin{bmatrix} A(\rho) & A_h(\rho) & 0_n & 0_n & 0_n & B_w(\rho) \\ I_n & -I_\mu & 0_n & 0_n & 0_n & 0_{n\times d} \\ \bar{h}I_n & 0_n & -I_\mu & 0_n & 0_n & 0_{n\times d} \\ \frac{\bar{h}^2}{2}I_n & 0_n & 0_n & -I_\mu & 0_n & 0_{n\times d} \end{bmatrix}^T,
\end{aligned}$$

and $I_\mu = (1-\mu)I_n,\ Q_\mu = (1-\mu)Q.$

Proof.

The LPV time-delay system (5.1) is asymptotical stable if the derivative of LKF (5.13) along the trajectories of system satisfies:

$$\dot{V}(t)=\dot{V}_1(t)+\dot{V}_2(t)+\dot{V}_3(t)+\dot{V}_4(t)<0 \tag{5.33}$$

where,

$$\dot{V}_1(t)=2\varsigma_1(t)^T P(\rho)\dot{\varsigma}_1(t)+\varsigma_1(t)^T\dot{P}(\rho)\varsigma_1(t)\leq 2\varsigma_2(t)^T(\Pi_1^T P(\rho)\Pi_2(\rho)+\tfrac{1}{2}\overline{P}(\rho))\varsigma_2(t), \tag{5.34}$$

$$\dot{V}_2(t)=x(t)^T Qx(t)-x(t-h(t))^T Qx(t-h(t))\leq\varsigma_2(t)^T(e_1^T Qe_1-e_2^T Q_\mu e_2)\varsigma_2(t), \tag{5.35}$$

Applying bounding AFBII (5.8), (5.10) in Lemma 5.1.1, respectively, for $\dot{V}_3(t)$ and $\dot{V}_4(t)$, we obtain inequalities:

$$\begin{aligned}\dot{V}_3(t)=\overline{h}^2\dot{x}(t)^T R\dot{x}(t)-\overline{h}\int_{t-h}^{t}\dot{x}(s)^T R\dot{x}(s)ds\leq\varsigma_2(t)^T(\overline{h}^2 e_0^T Re_0-e_3^T Re_3\\ -3e_4^T Re_4-5e_5^T Re_5-7e_6^T Re_6)\varsigma_2(t),\end{aligned} \tag{5.36}$$

$$\begin{aligned}\dot{V}_4(t)=\frac{\overline{h}^2}{2}\dot{x}(t)^T S\dot{x}(t)-\int_{t-h}^{t}\int_{s}^{t}\dot{x}(\theta)^T R\dot{x}(\theta)d\theta\,ds\leq\varsigma_2(t)^T(\tfrac{\overline{h}^2}{2}e_0^T Se_0-2e_7^T Se_7\\ -4e_8^T Se_8-6e_9^T Se_9)\varsigma_2(t),\end{aligned} \tag{5.37}$$

with the augmented vectors

$$\varsigma_1(t)=\left[x(t)^T\quad\int_{t-h}^{t}x(s)^T ds\quad\int_{t-h}^{t}\int_{s}^{t}x(\theta)^T d\theta\,ds\quad\int_{t-h}^{t}\int_{s}^{t}\int_{\theta}^{t}x(\beta)^T d\beta\,d\theta\,ds\right]^T,$$

$$\varsigma_2(t)=\left[x(t)^T\quad x(t-h(t))^T\quad\int_{t-h}^{t}x(s)^T ds\quad\int_{t-h}^{t}\int_{s}^{t}x(\theta)^T d\theta\,ds\quad\int_{t-h}^{t}\int_{s}^{t}\int_{\theta}^{t}x(\beta)^T d\beta\,d\theta\,ds\quad w(t)^T\right]^T,$$

and the transformations: $\varsigma_1(t)=\Pi_1\varsigma_2(t),\ \dot{\varsigma}_1(t)=\Pi_2(\rho)\varsigma_2(t)$.

Including the $\mathscr{H}_\infty$ performance constraint to the stability condition and combines with upper bounds (5.34)-(5.37) that entails the following condition:

$$\begin{aligned}\dot{V}(t)+\gamma^{-1}z(t)^T z(t)-\gamma w(t)^T w(t)\leq\varsigma_2(t)^T(\Upsilon_{11}(\rho,\dot{\rho})+\overline{h}^2 e_0^T Re_0\\ +\tfrac{\overline{h}^2}{2}e_0^T Se_0+e_{11}^T\gamma^{-1}e_{11})\varsigma_2(t)<0,\end{aligned} \tag{5.38}$$

Finally, using Schur complement results in (5.31).

□

The upper bounds of $\dot{V}_3(t)$ in condition (5.36) considers two more negative term $-5e_5^T Re_5-7e_6^T Re_6$ on the right side for a better relaxation than the WBII condition (5.23). However, the addition of two double and triple integrals vectors in $\varsigma_1(t)$ increases the computational load, where $P(\rho)\in\mathbb{S}_{++}^{4n}$ compared to $P(\rho)\in\mathbb{S}_{++}^{2n}$ in Lemma 5.2.2.

5.2.2. *Decomposition Lyapunov-Krasovskii Functional Stability*

In the last sections, the tighter bounding techniques has delivered a less conservative condition with the augmented LKF. So, how could one improve the system performance by using *simple* Lyapunov-Krasovskii functional? The necessary and sufficient conditions are derived from the discretized delay method in the works (Gu, 2001; Gu et al., 2003) for the LTV systems, then refined to the LKF decomposition (Han, 2008).

First, let recall a discretized Lyapunov-Krasovskii function associated to LPV time-delay system (5.1) as follows:

$$V(t)=x(t)^T P(\rho(t))x(t)+V_2(t)+V_3(t), \tag{5.39}$$

where functions

$$\begin{aligned} V_2(t) &= \int_{t-h(t)}^{t} x(\theta)^T Q(\theta) x(\theta) d\theta = \sum\nolimits_{i=1}^{N} \int_{t-ih_\Delta(t)}^{t-(i-1)h_\Delta(t)} x(\theta)^T Q_i x(\theta) d\theta, \\ V_3(t) &= \int_{-\bar{h}}^{0} \int_{t+\theta}^{t} \dot{x}(s)^T R(\theta) \dot{x}(s) ds d\theta = \sum\nolimits_{i=1}^{N} \bar{h}_\Delta \int_{t-i\bar{h}_\Delta}^{t-(i-1)\bar{h}_\Delta} \int_{\theta}^{t} \dot{x}(s)^T R_i \dot{x}(s) ds d\theta. \end{aligned} \tag{5.40}$$

with $i = 1,2,...,N$, $h_\Delta(t) = \frac{h(t)}{N}$, and $\bar{h}_\Delta = \frac{\bar{h}}{N}$. For an uniform distribution N segments range from $t - h(t) \to t$, then it is possible to choose the same variation rates of all slow-varying delays bounds for each segment $\left|\dot{h}_\Delta(t)\right| \le \mu < 1$.

Lemma 5.2.4. *For time-varying delay $h(t) \in \mathcal{H}_0$, parameter $\rho(t) \in \mathcal{U}_p$, a positive scalar γ, and an integer number N, then LPV system* (5.1) *is asymptotically delay-dependent stable with corresponding to design $\mathcal{L}_2$ norm performance, if there exist matrices Q_i, R_i, $\in \mathbb{S}_{++}^n$, $i = 1,2,...,N$, and a continuously differentiable matrix function $P : \mathcal{U}_p \to \mathbb{S}_{++}^n$, such that the PDLMI*

$$\left[\begin{array}{c|ccc|cc|ccc} \Upsilon_{11}(\rho,\dot{\rho}) & * & \cdots & * & * & * & * & * & * \\ \hline R_1 & & & & & & & & \\ \vdots & \multicolumn{3}{c|}{\Upsilon_{[22]}} & * & * & * & * & * \\ 0 & & & & & & & & \\ \hline A_h(\rho)^T P(\rho) & 0 & \cdots & R_N & -(1-\mu_N)Q_N - R_N & * & * & * & * \\ \hline B_w(\rho)^T P(\rho) & \multicolumn{3}{c|}{\cdots} & 0 & -\gamma I_d & * & * & * \\ H(\rho) & & & & H_h(\rho) & J_w(\rho) & -\gamma I_r & * & * \\ \hline \bar{h}_\Delta R_1 A(\rho) & \multicolumn{3}{c|}{\cdots} & \bar{h}_\Delta R_1 A_h(\rho) & \bar{h}_\Delta R_1 B_w(\rho) & 0 & -R_1 & * \\ \vdots & & & & \vdots & & & \ddots & * \\ \bar{h}_\Delta R_N A(\rho) & \multicolumn{3}{c|}{\cdots} & \bar{h}_\Delta R_N A_h(\rho) & \bar{h}_\Delta R_1 B_w(\rho) & 0 & 0 \cdots & -R_N \end{array}\right] \prec 0, \tag{5.41}$$

holds, where: $\Upsilon_{11}(\rho,\dot{\rho}) = sym\{P(\rho)A(\rho)\} \pm \sum_{j=1}^{N_p} \nu_j (\partial P(\rho)/\partial \rho_j) + Q_1 - R_1$,

$$\Upsilon_{22} = \begin{bmatrix} \Theta_1 & * & * & * & * \\ R_2 & \ddots & * & * & * \\ 0 & \ddots & \Theta_{i-1} & * & * \\ \vdots & & \ddots & \ddots & * \\ 0 & \cdots & 0 & R_{N-1} & \Theta_{N-1} \end{bmatrix},$$

$$\Theta_i = -(1-\mu_i)(Q_i - Q_{i+1}) - R_i - R_{i+1},\ i = 1,\ldots,N-1,$$

and the decomposition of delay spaces into N-subsets

$$h_\Delta(t) \in \mathcal{H}_0(\Delta) := \{h_\Delta(t) \in \mathcal{C}^1(\mathbb{R}_+, [0, \bar{h}_\Delta]) : |\dot{h}_\Delta(t)| \le \mu < 1\} \subset \mathbb{R}_+.$$

Proof. The demonstration is delivered in D.2.

□

It is worth mentioning that when $N = 1$, the latter condition reverts to stability condition

(5.19) in Lemma 5.2.1. So, if we discretize the auxiliary convex function in the conditions of Lemma 5.2.2 and Lemma 5.2.3, that would yield the least conservative results. Now, let consider a discretization of extended Lyapunov-Krasovskii functional (5.11):

$$V(t)=\varsigma(t)^T P(\rho(t))\varsigma(t)+V_2(t)+V_3(t), \tag{5.42}$$

where $\varsigma(t)=\begin{bmatrix} x(t)^T & \int_{t-h}^{t} x(s)^T ds \end{bmatrix}^T$, $P(\rho)=\begin{bmatrix} P_1(\rho) & P_2 \\ P_2^T & P_3 \end{bmatrix}\in\mathbb{S}^{2n}_{++}$.

By using this Lyapunov-Krasovskii functional, we now study the asymptotic stability for LPV time-delay system (5.1) based on Lemma 5.2.2 as follows.

Lemma 5.2.5. *For time-delay $h(t)\in\mathcal{H}_0$, parameter $\rho(t)\in\mathcal{U}_p$, a positive scalar γ, and an integer number N, then LPV system* (5.1) *is asymptotically delay-dependent stable with corresponding to design $\mathcal{L}_2$ norm performance, if there exist matrices $P_3, Q_i, R_i, \in\mathbb{S}^n_{++}$, $i=1,2,...,N$, a continuously differentiable matrix function $P_1:\mathcal{U}_p\to\mathbb{S}^n_{++}$, and a matrix $P_2\in\mathbb{R}^{n\times n}$, such that the PLMI holds*

$$\left[\begin{array}{ccccc|ccc|ccc} \multicolumn{5}{c|}{\Upsilon_{[ii]}} & * & * & * & * & * & * & * & * \\ \hline \multicolumn{5}{c|}{} & \frac{-12R_1}{\bar{h}_\Delta^2} & & * & * & * & * & * & * \\ \multicolumn{5}{c|}{\Theta_{[ii]}} & \vdots & \ddots & & * & * & * & * & * \\ \multicolumn{5}{c|}{} & 0 & \cdots & \frac{-12R_N}{\bar{h}_\Delta^2} & * & * & * & * & * \\ \hline B_w^T P_1 & 0 & \cdots & 0 & 0 & B_w^T P_2 & \cdots & B_w^T P_2 & -\gamma I_d & * & * & * & * \\ H & 0 & \cdots & 0 & H_h & 0 & \cdots & 0 & J_w & -\gamma I_r & * & * & * \\ \hline \bar{h}_\Delta R_1 A & 0 & \cdots & 0 & \bar{h}_\Delta R_1 A_h & 0 & \cdots & 0 & \bar{h}_\Delta R_1 B_w & 0 & -R_1 & * & * \\ \vdots & & & & \vdots & \vdots & & \vdots & \vdots & \vdots & \vdots & \ddots & * \\ \bar{h}_\Delta R_N A & 0 & \cdots & 0 & \bar{h}_\Delta R_N A_h & 0 & \cdots & 0 & \bar{h}_\Delta R_1 B_w & 0 & 0 & \cdots & -R_N \end{array}\right] \prec 0, \tag{5.43}$$

$$P(\rho)=\begin{bmatrix} P_1(\rho) & P_2 \\ P_2^T & P_3 \end{bmatrix} \succ 0, \tag{5.44}$$

where:

$$\Upsilon_{[ii]}=\left[\begin{array}{c|ccc|c} \Upsilon_{00} & -2R_1 & \cdots & 0 & P_1(\rho)A_h(\rho)-I_\mu P_2 \\ \hline * & \ddots & \ddots & 0 & 0 \\ * & * & \Upsilon_{ii} & -2R_i & \vdots \\ * & * & * & \ddots & -2R_N \\ \hline * & * & * & * & -(1-\mu_N)Q_N-4R_N \end{array}\right],$$

with

$$\Upsilon_{00}(\rho,\dot{\rho})=sym\{P_1(\rho)A(\rho)+P_2\}\pm\sum\nolimits_i \nu_i\,\partial P_1(\rho)/\partial\rho_i+Q_1-4R_1,$$
$$\Upsilon_{ii}(\rho)=-(1-\mu_i)(Q_i-Q_{i+1})-4R_i-4R_{i+1},\ i=1,2,...,N-1,$$

the decomposition of delay spaces into N-subsets

$$h_\Delta(t)\in\mathcal{H}_0(\Delta):=\{h_\Delta(t)\in\mathcal{C}^1(\mathbb{R}_+,[0,\bar{h}_\Delta]):\ |\dot{h}_\Delta(t)|\le\mu<1\}\subset\mathbb{R}_+,$$

and

$$\Theta_{[ii]}=\left[\begin{array}{c|cccc|c} P_2^TA(\rho)+P_3+\frac{6R_1}{\bar{h}_\Delta} & \frac{6R_1}{\bar{h}_\Delta} & 0 & \cdots & 0 & P_2^TA_h(\rho)-I_\mu P_3 \\ \hline P_2^TA(\rho)+P_3 & \ddots & & \cdots & 0 & P_2^TA_h(\rho)-I_\mu P_3 \\ \vdots & \vdots & \frac{6R_i}{\bar{h}_\Delta} & \frac{6R_i}{\bar{h}_\Delta} & \vdots & \vdots \\ P_2^TA(\rho)+P_3 & 0 & \cdots & & \ddots & P_2^TA_h(\rho)-I_\mu P_3 \\ \hline P_2^TA(\rho)+P_3 & 0 & \cdots & 0 & \frac{6R_N}{\bar{h}_\Delta} & P_2^TA_h(\rho)-I_\mu P_3+\frac{6R_N}{\bar{h}_\Delta}, \end{array}\right].$$

Proof.

The sketch of demonstration is based on the lines of Lemma 5.2.4 combined with the use of Wirtinger-based inequality (5.23) in Lemma 5.2.2. The stability delay-dependent is verified if the conditions:

$$\begin{aligned}\dot{V}(t)&=2\varsigma(t)^TP(\rho)\dot{\varsigma}(t)+\frac{d}{dt}\left(\sum\nolimits_{i=1}^{N}\int_{t-ih_\Delta(t)}^{t-(i-1)h_\Delta(t)}x(\theta)^TQ_ix(\theta)d\theta\right)+\cdots\\ &\varsigma(t)^T\dot{P}(\rho)\varsigma(t)+\frac{d}{dt}\left(\sum\nolimits_{i=1}^{N}\bar{h}_\Delta\int_{t-i\bar{h}_\Delta}^{t-(i-1)\bar{h}_\Delta}\int_{\theta}^{t}\dot{x}(s)^TR_i\dot{x}(s)dsd\theta\right)<0. \end{aligned}\tag{5.45}$$

holds along the trajectories of LPV system (5.1). The key role of development lies in the application of the WBII inequality to the second term of the following expansion

$$\frac{d}{dt}\left(\sum_{i=1}^{N}\bar{h}_\Delta\int_{t-i\bar{h}_\Delta}^{t-(i-1)\bar{h}_\Delta}\int_{\theta}^{t}\dot{x}(s)^TR_i\dot{x}(s)dsd\theta\right)=\sum_{i=1}^{N}\left(\bar{h}_\Delta^2\dot{x}(t)^TR_i\dot{x}(t)-\bar{h}_\Delta\int_{t-i\bar{h}_\Delta}^{t-(i-1)\bar{h}_\Delta}\dot{x}(\theta)^TR_i\dot{x}(\theta)d\theta\right).$$

By denoting $x_0\coloneqq x_t\coloneqq x(t)$, $x_i\coloneqq x(t-ih_\Delta(t))$, $x_N\coloneqq x(t-h(t))$. The latter integrals of the positive real functions are reorganized by WBII:

$$\begin{aligned}-\bar{h}_\Delta\int_{t-i\bar{h}_\Delta}^{t-(i-1)\bar{h}_\Delta}\dot{x}(\theta)^TR_i\dot{x}(\theta)d\theta&\le-\bar{h}_\Delta\int_{t-ih_\Delta(t)}^{t-(i-1)h_\Delta(t)}\dot{x}(\theta)^TR_i\dot{x}(\theta)d\theta\\ &\le-\begin{bmatrix}x_{i-1}\\ x_i\\ \int_{t-ih_\Delta(t)}^{t-(i-1)h_\Delta(t)}x(\theta)d\theta\end{bmatrix}^T\begin{bmatrix}4R_i & 2R_i & -6R_i/\bar{h}_\Delta\\ * & 4R_i & -6R_i/\bar{h}_\Delta\\ * & * & 12R_i/\bar{h}_\Delta^2\end{bmatrix}\begin{bmatrix}x_{i-1}\\ x_i\\ \int_{t-ih_\Delta(t)}^{t-(i-1)h_\Delta(t)}x(\theta)d\theta\end{bmatrix}.\end{aligned}\tag{5.46}$$

It should be noted that

$$\begin{aligned}\frac{d}{dt}\left(\int_{t-h}^{t}x(\theta)d\theta\right)&=\frac{d}{dt}\left(\sum\nolimits_{i=1}^{N}\int_{t-ih_\Delta(t)}^{t-(i-1)h_\Delta(t)}x(\theta)d\theta\right)\\ &=\sum\nolimits_{i=1}^{N}\left((1-(i-1)\dot{h}_\Delta(t))x(t-(i-1)h_\Delta(t))-(1-i\dot{h}_\Delta(t))x(t-ih_\Delta(t))\right)\end{aligned}\tag{5.47}$$

Denoting $I_\mu\coloneqq(1-\mu)I$, and giving an extended vector:

$$\xi^T=\left[x_t^T\quad x_1^T\quad\cdots\quad x_{N-1}^T\quad x_N^T\quad\int_{t-h_\Delta(t)}^{t}x(\theta)d\theta\quad\cdots\quad\int_{t-h(t)}^{t-(N-1)h_\Delta(t)}x(\theta)d\theta\quad w^T\right].$$

In the view of uniform distribution, we have:

$$\varsigma(t)^T P(\rho)\dot{\varsigma}(t) = \xi(t)^T \begin{bmatrix} P_1(\rho) & P_2 \\ 0 & 0 \\ \vdots & \vdots \\ 0 & 0 \\ P_2^T & P_3 \\ P_2^T & P_3 \\ \vdots & \vdots \\ P_2^T & P_3 \\ P_2^T & P_3 \\ 0 & 0 \end{bmatrix} \begin{bmatrix} A(\rho) & 0 \cdots 0 & A_h(\rho) & 0 \cdots 0 & B_w(\rho) \\ I & 0 \cdots 0 & -I_\mu & 0 \cdots 0 & 0 \end{bmatrix} \xi(t), \quad (5.48)$$

Similar to the development in Appendix D.1, by combined the $\mathscr{H}_\infty$ performance criteria with the PDLKF stability condition (5.45), we have the following condition:

$$\dot{V}(t) + \gamma^{-1}\|z(t)\|^2 - \gamma\|w(t)\|^2 \le \xi(t)^T \left(\Upsilon(\rho,\dot{\rho}) + \Gamma(\rho)^T \left[\begin{array}{c|ccc} \gamma^{-1} I_r & * & * & * \\ \hline 0 & R_1^{-1} & * & * \\ \vdots & \vdots & \ddots & * \\ 0 & 0 & \cdots & R_N^{-1} \end{array}\right] \Gamma(\rho) \right) \xi(t) < 0, \quad (5.49)$$

where

$$\Upsilon(\rho,\dot{\rho}) = \left[\begin{array}{cccc|ccc|c} \Upsilon_{00}(\rho,\dot{\rho}) & * & * & * & * & * & * & * \\ -2R_1 & \Upsilon_{ii} & * & * & * & * & * & * \\ 0 & \ddots & \ddots & * & * & * & * & * \\ \Upsilon_{0N}(\rho) & 0 & -2R_N & \Upsilon_{NN} & * & * & * & * \\ \hline \Theta_{10}(\rho) & \frac{6R_1}{\bar{h}_\Delta} & \cdots & \Theta_{1N}(\rho) & \frac{-12}{\bar{h}_\Delta^2} R_1 & * & * & * \\ \Theta_{i0}(\rho) & \ddots & \ddots & \Theta_{iN}(\rho) & \vdots & \ddots & * & * \\ \Theta_{N0}(\rho) & \cdots & \frac{6R_N}{\bar{h}_\Delta} & \Theta_{NN}(\rho) & 0 & \cdots & \frac{-12}{\bar{h}_\Delta^2} R_N & * \\ \hline B_w(\rho)^T P_1(\rho) & \cdots & \cdots & 0 & B_w(\rho)^T P_2 & \cdots & B_w(\rho)^T P_2 & -\gamma I_d \end{array}\right],$$

with

$$\begin{aligned}
\Upsilon_{00}(\rho,\dot{\rho}) &= \{P_1(\rho)A(\rho) + P_2\}^S \pm \textstyle\sum_i \nu_i \, \partial P_1(\rho)/\partial\rho_i + Q_1 - 4R_1, \\
\Upsilon_{0N}(\rho) &= (P_1(\rho)A_h(\rho) - I_\mu P_2)^T, & \Upsilon_{NN}(\rho) &= -(1-\mu_N)Q_N - 4R_N, \\
\Upsilon_{ii}(\rho) &= -(1-\mu_i)(Q_i - Q_{i+1}) - 4R_i - 4R_{i+1}, & i &= 1,\ldots, N-1, \\
\Theta_{i0}(\rho) &= P_2^T A(\rho) + P_3, & i &= 2,\ldots, N, \\
\Theta_{iN}(\rho) &= P_2^T A_h(\rho) - I_\mu P_3, & i &= 1,\ldots, N-1, \\
\Theta_{10}(\rho) &= P_2^T A(\rho) + P_3 + \tfrac{6}{\bar{h}_\Delta} R_1, & \Theta_{NN}(\rho) &= P_2^T A_h(\rho) - I_\mu P_3 + \tfrac{6}{\bar{h}_\Delta} R_N,
\end{aligned}$$

and

$$\Gamma(\rho)=\left[\begin{array}{c|ccc|c|ccc|c} H(\rho) & 0 & \cdots & 0 & H_h(\rho) & 0 & \cdots & 0 & J_w(\rho) \\ \hline \bar{h}_\Delta R_1 A(\rho) & 0 & \cdots & 0 & \bar{h}_\Delta R_1 A_h(\rho) & 0 & \cdots & 0 & \bar{h}_\Delta R_1 B_w(\rho) \\ \vdots & & & & \vdots & & & & \vdots \\ \bar{h}_\Delta R_N A(\rho) & 0 & \cdots & 0 & \bar{h}_\Delta R_N A_h(\rho) & 0 & \cdots & 0 & \bar{h}_\Delta R_N B_w(\rho) \end{array}\right].$$

By using Schur complement yields to (5.43). □

5.2.3. *Uncertain Delay-Dependent Lyapunov-Krasovskii Functional Stability*

As discussed about the *obstacle* of knowing the exact-delay value in implementation of control system design, let's consider an uncertain time-delay system as follows:

$$\begin{aligned} \dot{x}(t) &= A(\rho)x(t)+A_h(\rho)x(t-h(t))+A_d(\rho)x(t-d(t))+B_w(\rho)w(t), \\ z(t) &= H(\rho)x(t)+H_h(\rho)x(t-h(t))+H_d(\rho)x(t-d(t))+J_w(\rho)w(t), \end{aligned} \tag{5.50}$$

with delay features as specified in the previous section. In the absence of exact knowledge of the delay $h(t)$, a *robust* stability addresses for the control and observation design strategy involved with two-delays (Briat, 2008). Concerning some design requirements such that the admissible maximum of the delay value, the permissible estimate (margin robust uncertain delay $|\delta(t)=d(t)-h(t)|\le\delta_m$), and the optimization of $\mathscr{H}_\infty$ performance criterion level might consider for the optimization problems.

A parameter-dependent Lyapunov-Krasovskii function is associated with system (5.50) as follows:

$$V(t)=V_0(t)+V_\Delta(t), \tag{5.51}$$

where the *nominal* and *uncertain* functions

$$V_0(t)=x(t)^TP(\rho)x(t)+\int_{t-h(t)}^{t}x(\theta)^TQx(\theta)d\theta+\bar{h}\int_{t-\bar{h}}^{t}\int_{\theta}^{t}\dot{x}(s)^TR\dot{x}(s)dsd\theta, \tag{5.52}$$

$$V_\Delta(t)=\int_{t-d(t)}^{t}x(\theta)^TQ_ux(\theta)d\theta+\delta_m\int_{\underline{\delta}}^{\bar{\delta}}\int_{t-h(t)+\theta}^{t}\dot{x}(\theta)^TR_u\dot{x}(\theta)d\theta d\tau. \tag{5.53}$$

and $\delta_m=\max\{\bar{\delta},|\underline{\delta}|\}$. By reformatting the integral limits, it is possible to capture the uncertainty variation of the approximate delay instead of just tracking the maximal relation. More specifics could find in section 5.7 (Gu et al., 2003) and section 4.7 (Briat, 2008). It should realize that the uncertain delay involves in the two following cases. At the times of t_i,t_j, belongs to the specified domain such that $d(t_i)=h(t_i),\delta(t_i)=0$, then the stability condition reforms to similar condition of a single delay dependent. And in the second case when $d(t_j)\neq h(t_j)$, that ensues on the following result.

Lemma 5.2.6. (Briat, 2008) *For positive scalars* $\bar{h},\gamma$, *parameter* $\rho(t)\in\mathcal{U}_p$, *then LPV time-varying delay* (5.50) *is asymptotically stable with* $h(t)\in\mathcal{H}_0$, $d(t)\in\mathcal{H}_d$, *corresponding to* H_∞ *performance criterion, if there exist matrices* Q, R, Q_u, $R_u\in\mathbb{S}^n_{++}$ *and a continuously differentiable matrix function* $P:\mathcal{U}_p\to\mathbb{S}^n_{++}$, *such that the following conditions are satisfied*

$$\begin{bmatrix} \Upsilon_{11}(\rho,\dot{\rho}) & * & * & * & * & * & * \\ A_h(\rho)^T P(\rho)+R & \Upsilon_{22}(\rho) & * & * & * & * & * \\ A_h(\rho)^T P(\rho) & (1-\mu_d)R_u & \Upsilon_{33}(\rho) & * & * & * & * \\ B_w(\rho)^T P(\rho) & 0 & 0 & -\gamma I_d & * & * & * \\ H(\rho) & H_h(\rho) & H_d(\rho) & J_w(\rho) & -\gamma I_r & * & * \\ \bar{h}RA(\rho) & \bar{h}RA_h(\rho) & \bar{h}RA_d(\rho) & \bar{h}RB_w(\rho) & 0 & -R & * \\ \delta_m R_u A(\rho) & \delta_m R_u A_h(\rho) & \delta_m R_u A_d(\rho) & \delta_m R_u B_w(\rho) & 0 & 0 & -R_u \end{bmatrix} \prec 0, \quad (5.54)$$

$$\begin{bmatrix} \Upsilon_{11}(\rho,\dot{\rho}) & * & * & * & * & * \\ (A_h(\rho)+A_d(\rho))^T P(\rho)+R & -(1-\mu)(Q+Q_u)-R & * & * & * & * \\ B_w(\rho)^T P(\rho) & 0 & -\gamma I_d & * & * & * \\ H(\rho) & H_h(\rho) & J_w(\rho) & -\gamma I_r & * & * \\ \bar{h}RA(\rho) & \bar{h}R(A_h(\rho)+A_d(\rho)) & \bar{h}RB_w(\rho) & 0 & -R & * \\ \delta_m R_u A(\rho) & \delta_m R_u (A_h(\rho)+A_d(\rho)) & \delta_m R_u B_w(\rho) & 0 & 0 & -R_u \end{bmatrix} \prec 0, \quad (5.55)$$

where $\Upsilon_{11}(\rho,\dot{\rho}) = sym\{P(\rho)A(\rho)\} \pm \sum_{i=1}^{N_p} \nu_i \, \partial P/\partial \rho_i + Q + Q_u - R,$

$\Upsilon_{22} = -(1-\mu)(Q+R_u)-R, \qquad \Upsilon_{33} = -(1-\mu_d)Q_u - (1-\mu)R_u,$

and the delay space $\mathcal{H}_d = \{d \in \mathcal{C}^1(\mathbb{R}_+,[0,\bar{d}]) : |\dot{d}| \le \mu_d < 1\} \subset \mathbb{R}_+.$

Proof. This section is represented in D.3.

5.2.4. *Memory-Resilient Delay-Dependent Lyapunov-Krasovskii Functional Stability*

Now, let's address uncertain delay-dependent as the input disturbance by using the relation of bounded delay operator (5.16). Then, the $\mathcal{L}_2$ scaled bounded real lemma is applied to ensure robust stability for the uncertain structure (satisfies a well-connected property (5.18)). The interesting point is the approximation of the exact-delay value varying within an uncertain ball, defined by an algebraic inequality $|\delta(t) = d(t) - h(t)| \le \delta_m$.

5.2.4.1. *Jensen's Inequality*

This methodology so-called δ-*memory resilient* where the stability PDLMI conditions are derived from the development of Lyapunov-Krasovskii function (5.14).

Lemma 5.2.7. (Briat, 2015a) *For positive scalar* $\gamma, \bar{h}, \delta_m$, *parameter* $\rho(t) \in \mathcal{U}_p$, *and delay* $h(t) \in \mathcal{H}_0$, *the LPV time-delay* (5.50) *is asymptotically stable consistent the* $\mathscr{H}_\infty$ *performance, if there exist continuously differentiable matrix function* $P, L : \mathcal{U}_p \to \mathbb{S}^n_{++}$, *and positive matrices* $Q, R \in \mathbb{S}^n_{++}$, *such that the following matrix inequality satisfies*

$$\begin{bmatrix} \Upsilon_{11}(\rho,\dot{\rho}) & * & * & * & * & * & * \\ \Upsilon_{21}(\rho) & \Upsilon_{22}(\rho) & * & * & * & * & * \\ \Upsilon_{31}(\rho) & \Upsilon_{32}(\rho) & \Upsilon_{33}(\rho) & * & * & * & * \\ \Upsilon_{41}(\rho) & 0 & 0 & -\gamma I_d & * & * & * \\ H(\rho) & \Upsilon_{52}(\rho) & \Upsilon_{53}(\rho) & J_w(\rho) & -\gamma I_r & * & * \\ L(\rho)A(\rho) & \Upsilon_{62}(\rho) & \Upsilon_{63}(\rho) & L(\rho)B_w(\rho) & 0 & -L(\rho) & * \\ \bar{h}RA(\rho) & \Upsilon_{72}(\rho) & \Upsilon_{73}(\rho) & \bar{h}RB_w(\rho) & 0 & 0 & -R \end{bmatrix} \prec 0, \quad (5.56)$$

with $\Upsilon_{11}(\rho,\dot\rho)=\{P(\rho)A(\rho)\}^S \pm \sum_i^{N_p}\nu_i\frac{\partial P(\rho)}{\partial \rho_i}+Q-R,$

$\Upsilon_{31}(\rho)=\frac{\sqrt{7}}{2}\delta_m A_h(\rho)^T P(\rho)+\frac{\sqrt{7}}{2}\delta_m R,$ $\quad \Upsilon_{22}(\rho)=-(1-\mu)Q-R,$

$\Upsilon_{21}(\rho)=(A_h(\rho)+A_d(\rho))^T P(\rho)+R,$ $\quad \Upsilon_{32}(\rho)=-\frac{\sqrt{7}}{2}\delta_m((1-\mu)Q+R),$

$\Upsilon_{41}(\rho)=B_w(\rho)^T P_1(\rho),$ $\quad \Upsilon_{52}(\rho)=H_h(\rho)+H_d(\rho),$

$\Upsilon_{72}(\rho)=\overline{h}R(A_h(\rho)+A_d(\rho)),$ $\quad \Upsilon_{62}(\rho)=L(\rho)(A_h(\rho)+A_d(\rho)),$

$\Upsilon_{33}(\rho)=-\frac{7}{4}\delta_m^2(1-\mu)Q-\frac{7}{4}\delta_m^2 R-L(\rho),$ $\quad \Upsilon_{63}(\rho)=\frac{\sqrt{7}}{2}\delta_m L(\rho)A_h(\rho),$

$\Upsilon_{53}(\rho)=\frac{\sqrt{7}}{2}\delta_m H_h(\rho),$ $\quad \Upsilon_{73}(\rho)=\frac{\sqrt{7}}{2}\delta_m \overline{h}RA_h(\rho),$

and notation $\{\cdot\}^S := sym\{\cdot\}$.

Proof. A sketch proof is given in the D.4, a the full version can find in the literature (Briat, 2015a).

5.2.4.2. *Wirtinger-Based Inequality*

Let's employ a bounding technique WBII (5.6) for the resilient delay-dependent stability analysis for LPV system (5.50) involved the $\mathcal{L}_2$-norm bounded delay operator (5.16) that results in the following theorem.

Theorem 5.2.2: *For positive scalars* $\gamma,\overline{h},\delta_m$, *delay* $h(t)\in_{\_0}$, *and parameter* $\rho(t)\in\mathcal{U}_p$, *then LPV time-delay* (5.1) *is asymptotically stable conforming to the energy-to-energy index, if there exist positive matrices* $P_3,Q,R\in\mathbb{S}^n_{++}$, *a continuously differentiable matrix function* $P_1:\ \mathcal{U}_p\to\mathbb{S}^n_{++}$, *a matrix function* $L:\mathcal{U}_p\to\mathbb{S}^n_{++}$, *and matrices* $P_2\in\mathbb{R}^{n\times n}$, *s.t. the following PLMI is fulfilled*

$$\begin{bmatrix}
\Upsilon_{11}(\rho,\dot\rho) & * & * & * & * & * & * & * \\
\Upsilon_{21}(\rho) & \Upsilon_{22}(\rho) & * & * & * & * & * & * \\
\Upsilon_{31}(\rho) & \Upsilon_{32}(\rho) & \Upsilon_{33}(\rho) & * & * & * & * & * \\
\Upsilon_{41}(\rho) & \Upsilon_{42}(\rho) & \Upsilon_{43}(\rho) & -\frac{12}{\overline{h}^2}R & * & * & * & * \\
\Upsilon_{51}(\rho) & 0 & 0 & B_w(\rho)^T P_2 & -\gamma I_d & * & * & * \\
H(\rho) & \Upsilon_{62}(\rho) & \Upsilon_{63}(\rho) & 0 & J_w(\rho) & -\gamma I_r & * & * \\
L(\rho)A(\rho) & \Upsilon_{72}(\rho) & \Upsilon_{73}(\rho) & 0 & L(\rho)B_w(\rho) & 0 & -L(\rho) & * \\
\overline{h}RA(\rho) & \Upsilon_{82}(\rho) & \Upsilon_{83}(\rho) & 0 & \overline{h}RB_w(\rho) & 0 & 0 & -R
\end{bmatrix} \prec 0, \quad (5.57)$$

with:

$\Upsilon_{11}(\rho,\dot\rho)=\{P_1(\rho)A(\rho)+P_2\}^S\pm\sum_i\nu_i\frac{\partial P_1}{\partial\rho_i}+Q-4R,$ $\quad \Upsilon_{22}(\rho)=-(1-\mu)Q-4R,$

$\Upsilon_{21}(\rho)=(A_h(\rho)+A_d(\rho))^T P_1(\rho)-(1-\mu)P_2^T-2R,$ $\quad \Upsilon_{32}(\rho)=-\frac{\sqrt{7}}{2}\delta_m((1-\mu)Q+4R),$

$\Upsilon_{31}(\rho)=\frac{\sqrt{7}}{2}\delta_m(A_h(\rho)^T P_1(\rho)-(1-\mu)P_2^T-2R),$ $\quad \Upsilon_{62}(\rho)=H_h(\rho)+H_d(\rho),$

$\Upsilon_{41}(\rho)=P_2^T A(\rho)+P_3+\frac{6}{\overline{h}}R,$ $\quad \Upsilon_{72}(\rho)=L(\rho)(A_h(\rho)+A_d(\rho)),$

$\Upsilon_{51}(\rho)=B_w(\rho)^T P_1(\rho),$ $\quad \Upsilon_{82}(\rho)=\overline{h}R(A_h(\rho)+A_d(\rho)),$

$\Upsilon_{42}(\rho)=P_2^T(A_h(\rho)+A_d(\rho))-(1-\mu)P_3+\frac{6}{\overline{h}}R,$ $\quad \Upsilon_{63}(\rho)=\frac{\sqrt{7}}{2}\delta_m H_h(\rho),$

$\Upsilon_{33}(\rho)=-\frac{7}{4}\delta_m^2((1-\mu)Q+4R)-L(\rho),$ $\quad \Upsilon_{73}(\rho)=\frac{\sqrt{7}}{2}\delta_m L(\rho)A_h(\rho),$

$\Upsilon_{43}(\rho)=\frac{\sqrt{7}}{2}\delta_m(P_2^T A_h(\rho)-(1-\mu)P_3+\frac{6}{\overline{h}}R),$ $\quad \Upsilon_{83}(\rho)=\frac{\sqrt{7}}{2}\delta_m\overline{h}RA_h(\rho).$

Proof.

Take the derivative the Lyapunov-Krasovskii functional (5.11) along trajectories of LPV time-delay system (5.50) and combined with $\mathcal{L}_2$-norm performance on the controlled output, that implies an accustomed delay-dependent stability condition:

$$\dot{V}(t)+\gamma^{-1}z(t)^Tz(t)-\gamma w(t)^Tw(t)\leq \xi(t)^T\left(\Upsilon+\Gamma^T\begin{bmatrix}\gamma^{-1}I_r & 0\\ 0 & R^{-1}\end{bmatrix}\Gamma\right)\xi(t)<0, \tag{5.58}$$

where

$$\begin{aligned}
\xi^T &= \begin{bmatrix}x_t^T & x_h^T & x_d^T & \int_{t-h}^t x(\theta)^T ds & w(\theta)^T\end{bmatrix},\\
\Upsilon &= \begin{bmatrix}
\Upsilon_{11}(\rho,\dot{\rho}) & * & * & * & *\\
A_h(\rho)^TP_1(\rho)-P_{2\mu}^T-2R & -Q_\mu-4R & * & * & *\\
A_d(\rho)^TP_1(\rho) & 0 & 0 & * & *\\
P_2^TA(\rho)+P_3+\frac{6}{\bar{h}}R & P_2^TA_h(\rho)-P_{3\mu}+\frac{6}{\bar{h}}R & P_2^TA_d(\rho) & -\frac{12}{\bar{h}^2}R & *\\
B_w(\rho)^TP_1 & 0 & 0 & B_w(\rho)^TP_2 & -\gamma I_d
\end{bmatrix},\\
\Gamma &= \begin{bmatrix}H(\rho) & H_h(\rho) & H_d(\rho) & 0 & J_w(\rho)\\ \bar{h}RA(\rho) & \bar{h}RA_h(\rho) & H_d(\rho) & 0 & \bar{h}RB_w(\rho)\end{bmatrix}.
\end{aligned}$$

Let's use operator (5.16) and interconnection (5.17) to express the relation between x_h and x_d through input perturbed delay w_0. So, we have a transformation of coordinate:

$$\xi(t)=\underbrace{\begin{bmatrix}I & 0 & 0 & 0 & 0\\ 0 & I & \frac{\sqrt{7}}{2}\delta_m & 0 & 0\\ 0 & I & 0 & 0 & 0\\ 0 & 0 & 0 & I & 0\\ 0 & 0 & 0 & 0 & I\end{bmatrix}}_{T}\underbrace{\begin{bmatrix}x_t\\ x_d\\ w_0(t)\\ \int_{t-h}^t x(s)^Tds\\ w(t)\end{bmatrix}}_{\zeta(t)}. \tag{5.59}$$

Considering a parameter-dependent $\mathcal{D}$-scaling $L(\rho)\in\mathbb{S}_{++}^n$ associated with the scaling sets and uncertain norm-bounded operator Δ_0. Applying the SSG lemma, with substituting (5.59) into condition (5.58) that yields the following parameter dependent LMI condition:

$$\zeta(t)^TT^T\left(\Upsilon+\Gamma^T\begin{bmatrix}\gamma^{-1}I_r & 0\\ 0 & R^{-1}\end{bmatrix}\Gamma\right)T\zeta(t)+z_0(t)^TL(\rho)L(\rho)^{-1}L(\rho)z_0(t)-w_0(t)^TL(\rho)w_0(t)<0, \tag{5.60}$$

with

$$\begin{aligned}
L(\rho)z_0(t) &= \begin{bmatrix}L(\rho)A(\rho) & L(\rho)(A_h(\rho)+A_d(\rho)) & \frac{\sqrt{7}}{2}\delta_mL(\rho)A_h(\rho) & 0 & L(\rho)B_w(\rho)\end{bmatrix}\zeta(t),\\
T^T\Upsilon T &= \begin{bmatrix}
\Upsilon_{11}(\rho,\dot{\rho}) & * & * & * & *\\
\Upsilon_{21}(\rho) & -Q_\mu-4R & * & * & *\\
\Upsilon_{31}(\rho) & \Upsilon_{32}(\rho) & -\frac{7}{4}\delta_m^2(Q_\mu+4R) & * & *\\
P_2^TA(\rho)+P_3+\frac{6}{\bar{h}}R & \Upsilon_{42}(\rho) & \Upsilon_{43}(\rho) & -\frac{12}{\bar{h}^2}R & *\\
B_w(\rho)^TP_1 & 0 & 0 & B_w(\rho)^TP_2 & -\gamma I_d
\end{bmatrix},\\
\Gamma T &= \begin{bmatrix}H(\rho) & H_h(\rho)+H_d(\rho) & \frac{\sqrt{7}}{2}\delta_mH_h(\rho) & 0 & J_w(\rho)\\ \bar{h}RA(\rho) & \bar{h}R(A_h(\rho)+A_d(\rho)) & \frac{\sqrt{7}}{2}\delta_m\bar{h}RA_h(\rho) & 0 & \bar{h}RB_w(\rho)\end{bmatrix}.
\end{aligned}$$

Finally, using Schur-complement to rearrange condition (5.60) that results PDLMI (5.57).

□

Remark 5.2.4. The satisfaction of small-gain stability for operator (5.16) is associated with finding a resilient-stable trajectory for an approximated delay $d(t)$ constrained within a ball of diameter δ_m centered along the trajectory of $h(t)$. It can be shown that if $\delta_m = 0$ ($d(t_i)$ is approached close to $h(t_i)$) and $L(\rho)$ sufficiently small, then inequality (5.57) brings about stability condition (5.20). This condition is therefore more general than the memory-delay dependent stability condition in Lemma 5.2.2.

Now, similar to Theorem 5.2.1, an associated relaxation condition of Theorem 5.2.2 is provided in next result.

Theorem 5.2.3: *For positive scalar* $\gamma, \bar{h}, \varepsilon, \delta_m$, *delay* $h(t) \in \mathtt{H}_0$, *and parameter* $\rho(t) \in \mathcal{U}_p$, *then the LPV time-delay* (5.1) *is asymptotically stable conforming to the energy-to-energy index, if there exist continuously matrices function* $X : \mathcal{U}_p \to \mathbb{R}^{n\times n}$, $L : \mathcal{U}_p \to \mathbb{S}^n_{++}$, *a continuously differential matrices function* $P_1 : \mathcal{U}_p \to \mathbb{S}^n_{++}$, *positive matrices* $P_3, Q, R \in \mathbb{S}^n_{++}$, *and a matrix* $P_2 \in \mathbb{R}^{n\times n}$, *such that the following PLMIs satisfy*

$$\begin{bmatrix}
-X(\rho)^S & * & * & * & * & * & * & * & * & * \\
\Upsilon_{21}(\rho) & \Upsilon_{22}(\rho,\dot{\rho}) & * & * & * & * & * & * & * & * \\
\Upsilon_{31}(\rho) & \Upsilon_{32}(\rho) & \Upsilon_{33}(\rho) & * & * & * & * & * & * & * \\
\Upsilon_{41}(\rho) & \Upsilon_{42}(\rho) & \Upsilon_{43}(\rho) & \Upsilon_{44}(\rho) & * & * & * & * & * & * \\
P_2^T & \Upsilon_{52}(\rho) & \Upsilon_{53}(\rho) & \Upsilon_{54}(\rho) & -\frac{12}{\bar{h}^2}R & * & * & * & * & * \\
\Upsilon_{61}(\rho) & 0 & 0 & 0 & 0 & -\gamma I_d & * & * & * & * \\
0 & H(\rho) & \Upsilon_{73}(\rho) & \Upsilon_{74}(\rho) & 0 & J_w(\rho) & -\gamma I_r & * & * & * \\
L(\rho) & 0 & 0 & 0 & 0 & 0 & 0 & -L(\rho) & * & * \\
\bar{h}R & 0 & 0 & 0 & 0 & 0 & 0 & 0 & -R & * \\
\varepsilon X(\rho) & 0 & 0 & 0 & -\varepsilon P_2 & 0 & 0 & -\varepsilon L(\rho) & -\varepsilon\bar{h}R & -P_1(\rho)
\end{bmatrix} \prec 0, \tag{5.61}$$

$$P(\rho) = \begin{bmatrix} P_1(\rho) & P_2 \\ P_2^T & P_3 \end{bmatrix} \succ 0. \tag{5.62}$$

with:

$$\begin{aligned}
\Upsilon_{21}(\rho) &= P_1(\rho) + A(\rho)^T X(\rho), \\
\Upsilon_{31}(\rho) &= (A_h(\rho) + A_d(\rho))^T X(\rho), \\
\Upsilon_{41}(\rho) &= \tfrac{\sqrt{7}}{2}\delta_m A_h(\rho)^T X(\rho), \\
\Upsilon_{61}(\rho) &= B_w(\rho)^T X(\rho), \\
\Upsilon_{22}(\rho,\dot{\rho}) &= P_2^S \pm \textstyle\sum_i \nu_i \frac{\partial P_1}{\partial \rho_i} + Q - 4R - P_1(\rho), \\
\Upsilon_{32}(\rho) &= -(1-\mu)P_2^T - 2R, \\
\Upsilon_{42}(\rho) &= -\tfrac{\sqrt{7}}{2}\delta_m((1-\mu)P_2^T + 2R), \\
\Upsilon_{52}(\rho) &= P_3 + \tfrac{6}{\bar{h}}R, \\
\Upsilon_{33}(\rho) &= -(1-\mu)Q - 4R, \\
\Upsilon_{43}(\rho) &= -\tfrac{\sqrt{7}}{2}\delta_m((1-\mu)Q + 4R), \\
\Upsilon_{53}(\rho) &= -(1-\mu)P_3 + \tfrac{6}{\bar{h}}R, \\
\Upsilon_{73}(\rho) &= H_h(\rho) + H_d(\rho), \\
\Upsilon_{44}(\rho) &= -\tfrac{7}{4}\delta_m^2((1-\mu)Q + 4R) - L(\rho), \\
\Upsilon_{54}(\rho) &= -\tfrac{\sqrt{7}}{2}\delta_m((1-\mu)P_3 - \tfrac{6}{\bar{h}}R), \\
\Upsilon_{74}(\rho) &= \tfrac{\sqrt{7}}{2}\delta_m H_h(\rho).
\end{aligned}$$

Proof.

First, stability condition (5.61) is rearranged as follows:

$$\Psi(\rho) + \mathcal{P}(\rho)^T X(\rho)\mathcal{Q} + \mathcal{Q}^T X(\rho)^T \mathcal{P}(\rho) \prec 0, \tag{5.63}$$

with

$$\Psi(\rho)=\left[\begin{array}{c|cccccccccc} 0 & * & * & * & * & * & * & * & * & * \\ \hline P_1(\rho) & \Upsilon_{22}(\rho,\dot\rho) & * & * & * & * & * & * & * & * \\ 0 & \Upsilon_{32}(\rho) & \Upsilon_{33}(\rho) & * & * & * & * & * & * & * \\ 0 & \Upsilon_{42}(\rho) & \Upsilon_{43}(\rho) & \Upsilon_{44}(\rho) & * & * & * & * & * & * \\ P_2^T & \Upsilon_{52}(\rho) & \Upsilon_{53}(\rho) & \Upsilon_{54}(\rho) & -\frac{12}{\bar h^2}R & * & * & * & * & * \\ 0 & 0 & 0 & 0 & 0 & -\gamma I_d & * & * & * & * \\ 0 & H(\rho) & \Upsilon_{73}(\rho) & \Upsilon_{74}(\rho) & 0 & J_w(\rho) & -\gamma I_r & * & * & * \\ L(\rho) & 0 & 0 & 0 & 0 & 0 & 0 & -L(\rho) & * & * \\ \bar hR & 0 & 0 & 0 & 0 & 0 & 0 & 0 & -R & * \\ 0 & 0 & 0 & 0 & -\varepsilon P_2 & 0 & 0 & -\varepsilon L(\rho) & -\varepsilon\bar hR & -P_1(\rho) \end{array}\right],$$

$$\mathcal{P}(\rho)=\left[-I \;\middle|\; A(\rho)\;\; A_h(\rho)\;\; 0\;\; 0\;\; B_w(\rho)\;\; 0\;\; 0\;\; 0\;\; \varepsilon I\right],$$

$$\mathcal{Q}=\left[I \;\middle|\; 0\;\; 0\;\; 0\;\; 0\;\; 0\;\; 0\;\; 0\;\; 0\;\; 0\right].$$

Let's introduce the matrices form base of the null spaces of $\mathcal{P}$, and $\mathcal{Q}$ respectively,

$$\mathcal{P}^\perp=\left[\begin{array}{ccccccccc} A(\rho) & A_h(\rho) & 0 & 0 & B_w(\rho) & 0 & 0 & 0 & \varepsilon I \\ \hline I & 0 & 0 & 0 & 0 & 0 & 0 & 0 & 0 \\ 0 & I & 0 & 0 & 0 & 0 & 0 & 0 & 0 \\ 0 & 0 & I & 0 & 0 & 0 & 0 & 0 & 0 \\ 0 & 0 & 0 & I & 0 & 0 & 0 & 0 & 0 \\ 0 & 0 & 0 & 0 & I & 0 & 0 & 0 & 0 \\ 0 & 0 & 0 & 0 & 0 & I & 0 & 0 & 0 \\ 0 & 0 & 0 & 0 & 0 & 0 & I & 0 & 0 \\ 0 & 0 & 0 & 0 & 0 & 0 & 0 & I & 0 \\ 0 & 0 & 0 & 0 & 0 & 0 & 0 & 0 & I \end{array}\right],\quad \mathcal{Q}^\perp=\left[\begin{array}{ccccccccc} 0 & 0 & 0 & 0 & 0 & 0 & 0 & 0 & 0 \\ \hline I & 0 & 0 & 0 & 0 & 0 & 0 & 0 & 0 \\ 0 & I & 0 & 0 & 0 & 0 & 0 & 0 & 0 \\ 0 & 0 & I & 0 & 0 & 0 & 0 & 0 & 0 \\ 0 & 0 & 0 & I & 0 & 0 & 0 & 0 & 0 \\ 0 & 0 & 0 & 0 & I & 0 & 0 & 0 & 0 \\ 0 & 0 & 0 & 0 & 0 & I & 0 & 0 & 0 \\ 0 & 0 & 0 & 0 & 0 & 0 & I & 0 & 0 \\ 0 & 0 & 0 & 0 & 0 & 0 & 0 & I & 0 \\ 0 & 0 & 0 & 0 & 0 & 0 & 0 & 0 & I \end{array}\right].$$

Followed the projection lemma, the feasibility of (5.61) entails the feasibility of the underlying conditions:

$$\ker(\mathcal{P}(\rho))^T\Psi(\rho)\ker(\mathcal{P}(\rho)) \prec 0, \tag{5.64}$$

$$\ker(\mathcal{Q})^T\Psi(\rho)\ker(\mathcal{Q}) \prec 0, \tag{5.65}$$

Similarly, rearranging condition (5.64), we obtain stability condition (5.57).

□

Remark 5.2.5. It should be noted that the satisfaction of parametric condition (5.61) implies the fulfillment of statements (5.64) and (5.65), but the reverse is not correct. By choosing $L(\rho)$ sufficiently small when $\delta_m = 0$, the approximate delay stability conditions (5.61) suggest to PDLMI (5.25). So this development provides a more general conditional form for delay-dependent stability analysis. Besides, the augmented Lyapunov-Krasovskii functional (as discussed in Sections 5.2.1 and 5.2.2) could consider delivering a further improvement of the inequality gap.

Remark 5.2.6. The feasible solutions of inequalities (5.57) depend on the parameters and its variation rates $(\rho(t), \dot\rho(t))$, nonetheless the *slack*-variable $X(\rho)$ in condition (5.61) only

depends on $\rho(t)$. That causes a degradation in the equivalent characterization of the congruence transformation. However, the obtained condition is convenient for the stabilization synthesis. It should be emphasized that the associated relaxation of delay-dependent stability conditions (5.25) and (5.61) will be thoroughly utilized in the controller design strategy for the saturated LPV time-delay system.

5.2.5. *Example*

In the first section, the two well-known examples in the domain of delay-dependent stability analysis for LTI time-delay system is used to deliverer a concise comparison of the proposed conditions with other works. Then, the proposed PLMI stability conditions is relaxed to the multiconvexities forms (linear combination, T-S fuzzy, as discussed in previous chapters) to compare with the literature of delay-dependent stability analysis for fuzzy systems. First, let's consider the simplifications of the time-delay system (5.1) with:

Example 5.2.1: (Gu et al., 2003)

$$A=\begin{bmatrix}-2 & 0\\ 0 & -0.9\end{bmatrix},\ A_h=\begin{bmatrix}-1 & 0\\ -1 & -1\end{bmatrix}. \tag{5.66}$$

The analytical maximal delay value for which system (5.66) is asymptotically stable $h_{analytics}=6.17$.

Example 5.2.2: (Kharitonov & Niculescu, 2003)

$$A=\begin{bmatrix}0 & 1\\ -1 & -2\end{bmatrix},\ A_h=\begin{bmatrix}0 & 0\\ -1 & 1\end{bmatrix}. \tag{5.67}$$

where the time-varying delay $h(t)\in\mathcal{H}_0$.

Table 5.1. *The maximum admissible upper bound MAUB for delay* $h(t)\in\mathcal{H}_0$.

Delay-dependent Stability LTI System					
	Example 5.2.1		**Example 5.2.2**		
	$\mu=0.5$	$\mu=0.9$	$\mu=0.3$	$\mu=0.5$	NoV
Lemma 5.2.1	1.5874	1.1798	2.1756		$1.5n^2+1.5n$
Lemma 5.2.4 ($N=2$)	2.3200	1.2012	2.3025		$2.5n^2+2.5n$
Lemma 5.2.4 ($N=3$)	5.0553	**4.2626**	5.9301		$3.5n^2+3.5n$
Lemma 5.2.2	2.1111	1.7576	2.1798		$3n^2+2n$
Lemma 5.2.3	**5.2312**	3.9416	**7.5882**	**6.1862**	$9.5n^2+3.5n$
Theorem 1 (Dey et al., 2014)	2.2594	1.8502	2.3370		$5n^2+2n$
Theorem 1 (Seuret & Gouaisbaut, 2019)		2.2130			$18.5n^2+5.5n$
Theorem 1 (Zhao et al., 2017)		3.1544	7.0463		$9.5n^2+3.5n$
Theorem 1 (Kwon et al., 2014)	2.4203			1.6962	$9n^2+3n$
Theorem 1 (T. H. Lee & Park, 2017)	3.1555			2.4963	$114n^2+18n$
Proposition 1 (X. M. Zhang et al., 2017)	3.2330			2.5090	$54.5n^2+6.5n$
Theorem 2 (Zeng et al., 2021) ($N=5$)	3.4810			2.8060	$103.5n^2+15.5n$
0	1	2	3	4	5

NoV: *Number of Variable.*

As can be observed from the above table, the delay-dependent reciprocally convex combination method (Seuret & Gouaisbaut, 2019; Zeng et al., 2021; C. K. Zhang et al., 2017; X. M. Zhang et al., 2017) considers amazed decision variables. However, the effectiveness is not as impressive as using the auxiliary convex function (Lemma 5.2.3). Actually, most of the maximal values of the upper bound delay (the bold values) solved by this lemma show superiority in all categories. So, the extending application of the bounding technique in conditions (5.5)-(5.10) Lemma 5.2.3 has expressively enhanced the MAUB.

Now, by using the multi-convexities conditional relaxation form of PLMI for Lemma 5.2.1-Lemma 5.2.3 for analyzing the delay-dependent stability of the following delayed quasi-LPV system:

Example 5.2.3: (Wu & Li, 2007) Let's consider a T-S fuzzy time-delay system with the local linear matrices are given by:

$$\begin{aligned} A_1 &= \begin{bmatrix} -3.2 & 0 \\ 0.0 & -2.1 \end{bmatrix}, \quad A_{h1} = \begin{bmatrix} 1.0 & 0.9 \\ 0.0 & 2.0 \end{bmatrix}, \\ A_2 &= \begin{bmatrix} -1.0 & 0.0 \\ 1.0 & -3.0 \end{bmatrix}, \quad A_{h2} = \begin{bmatrix} 0.9 & 0.0 \\ 1.0 & 1.6 \end{bmatrix}. \end{aligned} \tag{5.68}$$

Where the time-varying delay $h(t) \in \mathcal{H}_0, \rho(x(t)) \in \mathcal{U}_p,$ and the membership function:

$$\lambda_1(\rho(x(t))) = (1+e^{-2\rho(x(t))})^{-1}, \quad \lambda_2(\rho(x(t))) = 1-\lambda_1(\rho(x(t))).$$

Applying LMI relaxation methods similar to those in previous chapters to verify the stability for system (5.68) that yields the MAUB values in the catalogs 1 and 2.

Table 5.2. *The maximum admissible upper bound for delay* $h(t) \in \mathcal{H}_0$.

Delay-dependent Stability quasi-LPV System					
	Example 5.2.3		**Example 5.2.4**		
	$\mu = 0.5$	$\mu = 0.9$	$\mu = 0.5$	$\mu = 0.9$	NoV
Lemma 5.2.1 (*Multi-convexities*)	0.4917	0.4743	1.5782	0.9116	$2n^2+2n$
Lemma 5.2.2 (*Multi-convexities*)	0.9603	0.5113	1.6960	1.2316	$3.5n^2+2.5n$
Lemma 5.2.3 (*Multi-convexities*)	**2.4293**	**2.0616**	**3.7638**	**3.0913**	$10n^2+4n$
Theorem 1 (Yang & Yang, 2010)	0.4995	0.4988			$58n^2+4n$
Theorem 1 (Zeng et al., 2014)	0.7584	0.7524			$16.5n^2+6.5n$
Theorem 1 (Lian et al., 2017)	1.3123	1.2063			$51.5n^2+9.5n$
Theorem 1 (Li et al., 2020)	1.4819	1.3686			$38.5n^2+9.5n$
Theorem 1 (Y. Tian & Wang, 2022)	1.9914	1.8705			$86.5n^2+11.5n$
0	1	2	3	4	5

NoV: *Number of Variable.*

Recently, the stability and stabilization analysis for the delayed LPV/Quasi-LPV system has adopted the novel LKF constructions for the LTI time-delay system and the advanced bounding techniques s.t. Wirtinger-based II (Zeng et al., 2014; Z. Zhang et al., 2015), free-matrix-based II (Lian et al., 2016), auxiliary-function-based II (Datta et al., 2021; Li et al., 2020; Y. Tian & Wang, 2022), reciprocal convex combination (Lian et al., 2016, 2020), then combines with the relaxation methods of the PLMI condition (Wang & Lam,

2018a, 2018b, 2019) to deliver a less conservative condition.

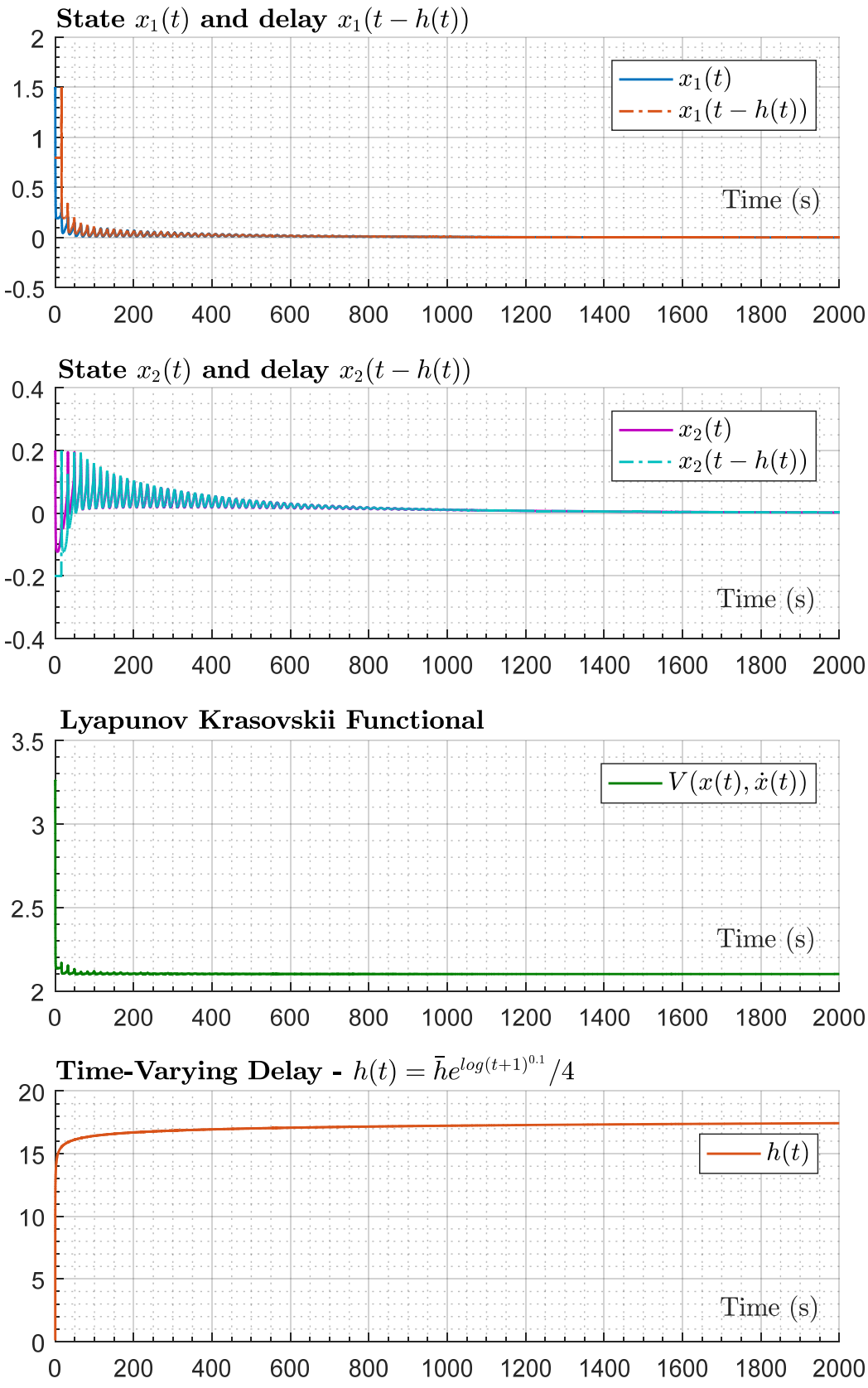

Figure 5-2. *The evolutions of quasi-LPV time-delay system* (5.68) with the slow-varying delay $h(t) \leq 20.4917$, $\dot{h}(t) \leq 0.1$.

In recent years much effort has been devoted to the delay-partitioning LKFs and augmented LKFs, and fruitful results have been achieved, see for example (Li et al., 2020; Lian et al., 2020; Y. Tian & Wang, 2022) and the reference therein. In order to further reduce the conservatism of the stability results, the new auxiliary polynomial-based functions (APFs) (S. Y. Lee et al., 2017; T. H. Lee & Park, 2017), the Intermediary-Polynomial-Based Functions (IPFs) (Li et al., 2020) and Flexible Polynomial-Based Functions (FPFs) (Y. Tian & Wang, 2022) are studied by introducing a set of orthogonal polynomials. These advanced techniques (i.e., generalized parameter-dependent reciprocally convex inequality) are proposed to better estimate the triple integral inequalities. However, it is possible to realize a significant improvement in system performance when comparing Lemma 5.2.3 with the mentioned works (as seen in the catalogs 1 and 2 of Table 5.2).

It can objectively acknowledge that the construction of polynomial-based functions aims to address the delay-range stability conditions. While the designed stability conditions in Lemma 5.2.2 and Lemma 5.2.3 are quite simple and have fewer computational complexities. With this advantage, these conditions would effortlessly adapt to the extension of the stabilized design strategy with the saturation constraints, approximation delay, etc. It's worth noting that both Lemma 5.2.1-Lemma 5.2.3 have validated delay-dependent stability for system (5.68) with a MAUB greater than 100s, corresponds to slowly varying delay cases $0 \le h(t) \le \overline{h},\ \dot{h}(t) \le 0.1$. Shown in Figure 5-2 is the evolution of the system dynamic with a slow-varying time function $h(t) = 0.25\overline{h}e^{\log(t+1)^{0.1}}$. The decision matrices $P(\rho) = \sum_{i=1}^{2} \lambda_i(\rho) P_i$, Q, R obtained from solving the stability condition of Lemma 5.2.1 are given as:

$$P_1 = \begin{bmatrix} 0.4626 & -0.2006 \\ -0.2006 & 0.3911 \end{bmatrix}, \quad P_2 = \begin{bmatrix} 1.1048 & -0.1188 \\ -0.1188 & 0.5204 \end{bmatrix}, \text{ and}$$

$$Q = \begin{bmatrix} 1.4094 & -0.2798 \\ -0.2798 & 0.9900 \end{bmatrix}, \quad R = 10^{-3}\begin{bmatrix} 0.3640 & -0.0941 \\ -0.0941 & 0.1969 \end{bmatrix}.$$

Currently, the numerical simulation tool Simulink® does not allow integrals in the variable interval, so we reformat the LKF as follows:

$$\begin{aligned} V(t) &= x(t)^T \sum_{i=1}^{2} \lambda_i(\rho) P_i x(t) + \int_{t-h(t)}^{t} x(\theta)^T Q x(\theta) d\theta + \overline{h} \int_{t-\overline{h}}^{t} (\overline{h} - t + \theta) \dot{x}(\theta)^T R \dot{x}(\theta) d\theta, \\ &\approx x(t)^T \sum_{i=1}^{2} \lambda_i(\rho) P_i x(t) \ + \ \left| \int_0^t f(x(\theta)) d\theta - \int_{h(t)}^{t} f(x(\theta - h(\theta))) d\theta \right| \ + \cdots \\ &\qquad \overline{h} \left| \int_0^t h(\theta) g(\dot{x}(\theta)) d\theta - \int_{\overline{h}}^{t} h(\theta) g\left(\dot{x}\left(\theta - \overline{h}\right)\right) d\theta \right|, \end{aligned} \tag{5.69}$$

with $f(x(\theta)) = x(\theta)^T Q x(\theta)$, and $g(\dot{x}(\theta)) = \dot{x}(\theta)^T R \dot{x}(\theta)$. Then, the approximation of LKF is given in the third frame of Figure 5-2.

Besides, another popular example has been used in the last decade in demonstrating the effectiveness of the proposed stability conditions for the T-S fuzzy system is given below. The results of the MAUB delay values are provided in the catalogs 3 and 4 of Table 5.2 respectively with Lemma 5.2.1-Lemma 5.2.3. However, the majority of studies use this example deal with the problem of delay-range stability. So, we could not deliver a further comparison result.

Example 5.2.4: (E. Tian & Peng, 2006)

$$\begin{aligned} A_1 &= \begin{bmatrix} 2.0 & 0 \\ 0.0 & -0.9 \end{bmatrix}, \quad A_{h1} = \begin{bmatrix} -1.0 & 0.0 \\ -1.0 & -1.0 \end{bmatrix}, \\ A_2 &= \begin{bmatrix} -1.0 & 0.5 \\ 0.0 & -1.0 \end{bmatrix}, \quad A_{h2} = \begin{bmatrix} -1.0 & 0.0 \\ 0.1 & -1.0 \end{bmatrix}. \end{aligned} \tag{5.70}$$

where the time-varying delay $h(t) \in \mathcal{H}_0, \rho(t) \in \mathcal{U}_p,$ and the membership function:

$$\lambda_1(\rho(t)) = (1 + e^{-2\rho(t)})^{-1}, \quad \lambda_2(\rho(t)) = 1 - \lambda_1(\rho(t)).$$

It's worthy to note that Wirtinger-based inequality (Lemma 5.2.2) could be considered as an exceptional case of the auxiliary-function-based method (Lemma 5.2.3). The vector expansion of this lemma employs only one single integral, showing an adequate trade-off between the number of variables to be solved (computational complexity) and the maximum value of the upper bound delay (conservatism). It provides a less conservative stability condition than traditional Jensen conditions, with an integrable conditional structure (without too much decoupling of the decision matrices to the dynamic system).

Furthermore, as mentioned about the multiple production complexity of the stability conditions using LKF formulation (5.13), in order to be compatible with control strategy designs for LPV time-delay systems subject to the saturated actuator, this appropriate LKF takes precedence over conservatism. Specifically, the analysis to the approximate delay and the memoryless gain-scheduled feedback controller with the saturation constraints are based on condition (5.25) in Theorem 5.2.1. It exhibits a well-proportioned stabilization condition between conservatism and numerical burden. These issues will be continued to discuss in detail in the next chapter.

5.3. Conclusions

In this chapter, the preliminary premises of the LPV delay system have been delivered. The delay-dependent stability is addressed on time-domain based on the Lyapunov Krasovskii functional technique. Where the convex properties of the analytical function are generalized the application to improve the stability conditions. Corresponding to each bounding technique (Jensen-based integral inequality, Wirtinger-based integral inequality, auxiliary-function-based integral inequality, etc.) is an appropriate selection of the augmented LKF to achieve the highest efficiency.

These delay-dependent stability conditions are analyzed for the parametric dependent system adopting the new structures LKF with double integral and triple integral. The parametric LMI stability conditions can be relaxed into LMI conditions and effectively solved by common convex optimization algorithms (barrier function, interior-point method, etc.). Along with the *original* stabilizing LFK conditions via PLMI, are associated-relaxation presented to decouple the multiple-production of the decision matrices and the dynamical matrices of state system. Furthermore, the transformation could adapt to all generalization of the proposed auxiliary-function condition structures were analyzed for the delay-dependent stability. A simple linearization method directly delivers a tractable condition that is suitable with the stabilization synthesis. The comparison results illustrate the effectiveness of the designed stability condition.

Chapter 6.

Stabilization Synthesis for the LPV/quasi-LPV Time-delay Systems with Actuators Saturation

This chapter inherits the implementations of the LPV saturation system in the previous chapter to develop the controller for the LPV delay system with constrained actuators. The analysis of the LPV delay control system typically entangles in multiple productions (for example, the stability conditions in sections 5.2.1, 5.2.4 are related to the matrix product expressions PA and RA with P, R being the decision variable matrices). The approaches such as descriptor or free weighting matrix will be more problematic when considering saturation constraints in the stabilization condition. Thus, this methodology settles these problems agreeing with the following design strategy:

1 - Develop the stability conditions for open-loop system (unsaturated)

2 - Employ the saturation conditions imposing on controller (generalized sector bounding), then multiple-productions will be decoupled using Finsler's lemma.

3 - Substitute the variable into the closed-loop expression (using the congruence transformations and setting the variable to obtain the parameter-dependent LMI condition).

4 - Relax the associated PLMI conditions, corresponding to the design requirements, then the PLMI conditions are converted to finite dimension LMIs by gridding, convex combination, $\mathcal{S}$-Variable methods, etc.

The “keywords” of modern control technology related to the control theory of LPV systems, the time-delay LPV systems, and the saturated system analysis, respectively, have been fully annotated in chapters 2, 4 and 5 with respective references. It should be noted that the characteristic of exact-memory controllers is non-implementable in practice due to the difficulty in estimating delays. Therefore, the uncertain delay gain-scheduled controller is more suitable for the delay-dependent stabilization condition. The features of the control system are:

- The delay considers to vary in a range or approximate, and thereby more applicable in practice.
- In the framework of modified sector condition, a suitable auxiliary controller strategy not only gives a more accurate estimation of the lower bound of LKF but also relaxes the saturation constraints.
- The use of Wirtinger inequality reduces the gap in Jensen's inequality, it has shown a reducing conservatism of the stability and stabilization delay-dependent conditions analysis. The improvements compare with the existing results by using fewer number of decision matrix variables.

In the first section, the rudimentary definitions such as the admissible set of the initial condition, saturation constraints, and structure of delay-dependent controllers will be present. The corresponding stabilization conditions then deliver for each design strategy.

6.1. Problem Formulation and Preliminaries

6.1.1. *Sector Nonlinearity Model Approach*

A time-delay LPV system with actuator saturation presents under the forms:

$$\begin{aligned}
\dot{x}(t) &= A(\rho)x(t) + A_h(\rho)x\big(t-h(t)\big) + B(\rho)\,\mathrm{sat}(u) + B_w(\rho)w(t),\\
y(t) &= C(\rho)x(t) + C_h(\rho)x\big(t-h(t)\big) + D(\rho)\,\mathrm{sat}(u) + D_w(\rho)w(t),\\
z(t) &= H(\rho)x(t) + H_h(\rho)x\big(t-h(t)\big) + J(\rho)\,\mathrm{sat}(u) + J_w(\rho)w(t),\\
x(\theta) &= \psi(\theta), \quad \theta \in [-\bar{h}, 0]
\end{aligned} \tag{6.1}$$

where $x(t) \in \mathbb{R}^n$ is state vector with initial condition $\psi(\cdot)$ and unknown time varying delay $h(t)$ assumes belong to spaces $\mathcal{H}_0$. $y(t) \in \mathbb{R}^p$ and $z(t) \in \mathbb{R}^r$ are outputs; $w(t) \in \mathbb{R}^d$ is disturbance inputs; and nonlinear saturation function $\mathrm{sat}(u)$. The parameters $\rho(t)$ and its unknown rate of variation belong to parameter spaces (2.8)-(2.9).

Saturation nonlinearity.

Control input vector $u(t) = [u_1(t), u_2(t), \ldots, u_m(t)]^T \in \mathbb{R}^m$ constrains by the limits of saturation $u_i(t) \in [-\overline{u}_i, \overline{u}_i], i = 1, 2, \ldots, m$. Let's recall a dead-zone nonlinearity associated with a symmetric saturation function $\mathrm{sat}(u) = u(t) - \Phi(u)$:

$$\Phi(u_i) = \begin{cases} u_i - \mathrm{sign}(u_i)\overline{u}_i & \text{if } |u_i| \geq \overline{u}_i \\ 0 & \text{if } |u_i| < \overline{u}_i \end{cases} \quad i = 1, 2 \ldots m. \tag{6.2}$$

Define an auxiliary control law $\vartheta(t)$ belong to the polyhedral set

$$\mathcal{S}(\vartheta, \overline{u}) = \left\{ \vartheta, u \in \mathbb{R}^m : |\vartheta_i| \leq \overline{u}_i,\ i = 1, 2 \ldots m \right\}. \tag{6.3}$$

Region of Attraction.

The saturation limits of actuators make the control design of the time delay LPV system more challenging. The system (6.1) attains global stability if the trajectories asymptotically converge to the origin from all initial conditions $\psi(\theta), \theta \in [-\bar{h}, 0]$, without effect of disturbance $w(t) = 0$. Nonetheless, this condition is hard to satisfy in practice. Instead of having to assurance all the initial conditions, an estimation of the region of attraction determines the initial conditions to which the system will converge asymptotically. The *key issue* relating to the estimate of the Region of Attraction (or *Domain of Attraction* - DoA) belongs to Banach space of continuous vector function of initial:

$$\mathcal{X}_0 = \left\{ \psi(\theta) \in \mathcal{C}^1\big([-\bar{h}, 0], \mathbb{R}^n\big) \,|\, \kappa_1 = \sup_{\theta \in [-\bar{h}, 0]} \|\psi(\theta)\|_2^2, \kappa_2 = \sup_{\theta \in [-\bar{h}, 0]} \|\dot{\psi}(\theta)\|_2^2 \right\}. \tag{6.4}$$

Ellipsoidal Set of Stability.

Lyapunov–Krasovskii functional candidate is used as a primary stability analysis tool for the dynamic systems. The estimations of DoA are associated to the following LKF:

Parameter-Dependent Lyapunov–Krasovskii functional (PDLKF) candidates:

$$V(x(t),\dot{x}(t)) = \varsigma(t)^T P(\rho)\varsigma(t) + \int_{t-h(t)}^{t} x(\theta)^T Q x(\theta) d\theta + \bar{h}\int_{t-\bar{h}}^{t}\int_{\theta}^{t} \dot{x}(s)^T R\dot{x}(s) ds d\theta. \quad (6.5)$$

with $P(\rho) = \begin{bmatrix} P_1(\rho) & P_2 \\ * & P_3 \end{bmatrix}$, $\varsigma(t) = \left[x(t)^T \int_{t-h(t)}^{t} x(\theta)^T d\theta \right]^T$.

In the next sections, the delay-dependent stabilization conditions derive for the state feedback, and the dynamic output feedback controller related to the determination of the delay in the system.

6.1.2. *Parameterized State Feedback Controller*

Considering a controller law is based on the compact sets of parameters $\rho(t)$:

$$u(t) = K(\rho)x(t) + K_d(\rho)x(t-d(t)), \quad (6.6)$$

with scheduling gain $K(\rho), K_d(\rho)$ are sought to stabilize the time delay system (6.1), and $d(t)$ is the delay approximation of the system delay $h(t)$ as presented in section 5.2.4.2. Let's recall the permissible delay estimate:

$$\mathcal{H}_d = \{d(t) \in \mathcal{C}(\mathbb{R}_+, \mathbb{R}_+) : \delta(t) = d(t) - h(t), \ \max|\delta(t)| \le \delta_m\} \subset \mathbb{R}_+. \quad (6.7)$$

Based on the understanding of $d(t)$ versus nominal delay value $h(t)$, we have the following controller design strategies:

- If $K_d(\rho) = 0$, the controller designates as a **memoryless controller**.
- If $d(t) \equiv h(t)$, the controller refers to as an **exact-memory controller**.
- If $|d(t) - h(t)| \le \delta_m$, the controller labels to as a **δ-memory-resilient controller**.

Most delay-dependent control strategies are typically concerned with the first case to simplify the design and be suitable for implementation (where delay values are unavailable for measurement). Since the gain $K_d(\rho)$ does not include in the feedback controller structure, this approach is conservative. The second case allows relaxation of the stabilization conditions but is inapplicable in practice. In the last case, the delay approximation (within the *robust margin*) indicates a practical implementation and is less conservative than a memoryless controller.

In the framework of saturation control using the generalized sector condition, the restriction on the feedback control law can be wiped off with the auxiliary controller. Specifically, let's consider the following controllers $\vartheta(t) \in \mathcal{S}$ associated with $u(t)$ (which must satisfy the GSC condition):

$$\vartheta(t) = G(\rho)x(t) + G_h(\rho)x(t-h(t)), \quad (6.8)$$

$$\vartheta(t) = G(\rho)x(t) + G_I(\rho)\int_{t-h(t)}^{t} x(\theta)d\theta, \text{ or} \quad (6.9)$$

$$\vartheta(t) = G(\rho)x(t) + G_h(\rho)x(t-h(t)) + G_I(\rho)\int_{t-h(t)}^{t} x(\theta)d\theta, \quad (6.10)$$

Substituting the control law (6.6) into system (6.1) we have a saturated closed-loop system as follows:

$$\begin{aligned}\dot{x}(t) &= A_{cl}(\rho)x(t) + A_h x(t-h(t)) + BK_d x(t-d(t)) - B(\rho)\Phi(u) + B_w(\rho)w(t),\\ z(t) &= H_{cl}(\rho)x(t) + H_h x(t-h(t)) + JK_d x(t-d(t)) - J(\rho)\Phi(u) + J_w(\rho)w(t),\\ x(\theta) &= \psi(\theta), \quad \theta \in [-\overline{h}, 0]\end{aligned} \tag{6.11}$$

with $A_{cl}(\rho) = A(\rho) + B(\rho)K(\rho), H_{cl}(\rho) = H(\rho) + J(\rho)K(\rho)$. The design requirements related to the $\mathscr{H}_\infty$-performance criterion is to search for bounded feedback controllers and auxiliary controllers, which guarantees the region stability of system (6.11). From initial condition (6.4), then condition (6.3) states briefly as follows: for the design saturation limits $\overline{u}_i$ look for the auxiliary control law $\vartheta(t)$ that satisfy $|\vartheta_i| \le \overline{u}_i, i = 1,2,...,m$. Generally, to ensure the stability of the closed-loop system under the influence of disturbance, the following necessary and sufficient conditions need to be fulfilled:

$$\frac{1}{\eta \overline{u}_i^2}\left\|\vartheta(t)_{(i)}\right\|^2 \le V(x(t), \dot{x}(t)), \tag{6.12}$$

$$\textit{if } w(t) = 0: \; V(x(t), \dot{x}(t)) \le V(0) \le \eta^{-1}, \tag{6.13}$$

$$\textit{if } w(t) \ne 0: \; V(x(t), \dot{x}(t)) \le V(0) + \gamma \left\|w(t)\right\|_{\mathcal{L}_2}^2 \le \eta^{-1}. \tag{6.14}$$

From the view of condition (6.12), the appropriate selection of an auxiliary controller ensues a better estimate of the lower bound of the Lyapunov function. That makes the stabilization conditions of the saturated control system less conservative. But conditions (6.13)-(6.14) are complicated to enforce directly for the time-delay LPV system unlike the method proposed in Chapter 4. Without loss of generality, we can assume that the energy bound of the disturbance is known $\|w(t)\|_{\mathcal{L}_2}^2 < \sigma^{-1}$, and the set of admissible initial condition is defined by the upper bounds in (6.4).

Optimization problems.

Combined with the estimation of DoA (6.4), the performance criterion, memory resilient and the upper-lower bounds of delay value, we formulate the following optimization problems:

- Given $\sigma, \overline{h}, \gamma, \delta_m$ then maximize the size of DoA.
- Given $\sigma, \overline{h}, \delta_m$ and a set of admissible initial condition then minimize γ (optimization disturbance rejection level).
- Given γ, σ a set of admissible initial condition then optimize $\overline{h}$ (the maximal upper bound on the delay value) or maximize δ_m (the allowable delay approximation).

It should be noted that the above cases consider a supposition on energy bounded exogenous signals (a $\mathcal{L}_2$-bound on the admissible disturbances defined by σ). In addition, the optimization problems such as minimizing energy-to-energy index γ, maximizing the upper bound of the delay value $\overline{h}$, and maximizing the delay approximation value δ_m are all convex problems. These values can be derived from a sub-optimization method or an iterative algorithm. However, the admissible set of the initial conditions usually relates to the concave problem. Therefore, we focus more on seek for the largest estimate of DoA

that satisfies the designed delay-dependent stabilization condition.

6.1.3. *Parameterized Dynamic Output Feedback Controller*

Let's consider a dynamic controller feedback system with approximate memory:

$$\begin{aligned}\dot{x}_c(t) &= A_c(\rho)x_c(t) + A_{dc}(\rho)x_c(t-d(t)) + B_c(\rho)y(t) + E_c(\rho)\Phi(u),\\ u(t) &= C_c(\rho)x_c(t) + C_{dc}(\rho)x_c(t-d(t)) + D_c(\rho)y(t).\\ y(t) &= C(\rho)x(t) + C_h x\big(t-h(t)\big) + D_w(\rho)w(t).\end{aligned} \tag{6.15}$$

Similar to the analysis for the feedback controller with uncertain delay value cases, when $d(t) \equiv h(t)$ refers to an exact-memory DOF controller. If $A_{dc}(\rho) = C_{dc}(\rho) = 0$, that represents a memoryless DOF controller, and if $d(t) \in \mathcal{H}_d$ we have a resilient memory DOF controller. Replacing the controller in the system (6.1), the extended closed-loop system is given by:

$$\begin{aligned}\dot{\zeta}(t) &= \mathbb{A}\zeta(t) + \mathbb{A}_h\zeta(t-h) + \mathbb{A}_d\zeta(t-d) + \mathbb{B}_1\Phi(u) + \mathbb{B}_2 w(t),\\ z(t) &= \mathbb{C}\zeta(t) + \mathbb{C}_h\zeta(t-h) + \mathbb{C}_d\zeta(t-d) + \mathbb{D}_1\Phi(u) + \mathbb{D}_2 w(t).\end{aligned} \tag{6.16}$$

with $\zeta(t) = [x(t)^T \quad x_c(t)^T]^T$, and

$$\mathbb{A} = \begin{bmatrix} A(\rho) + B(\rho)D_c(\rho)C(\rho) & B(\rho)C_c(\rho) \\ B_c(\rho)C(\rho) & A_c(\rho) \end{bmatrix}, \quad \mathbb{A}_h = \begin{bmatrix} A_h(\rho) + B(\rho)D_c(\rho)C_h(\rho) & 0 \\ B_c(\rho)C_h(\rho) & 0 \end{bmatrix},$$

$$\mathbb{C} = \begin{bmatrix} H(\rho) + J(\rho)D_c(\rho)C(\rho) & J(\rho)C_c(\rho) \end{bmatrix}, \quad \mathbb{C}_h = \begin{bmatrix} H_h(\rho) + J(\rho)D_c(\rho)C_h(\rho) & 0 \end{bmatrix},$$

$$\mathbb{A}_d = \begin{bmatrix} 0 & B(\rho)C_{dc}(\rho) \\ 0 & A_{dc}(\rho) \end{bmatrix}, \quad \mathbb{B}_1 = \begin{bmatrix} -B(\rho) \\ E_c(\rho) \end{bmatrix}, \quad \mathbb{B}_2 = \begin{bmatrix} B(\rho)D_c(\rho)D_w(\rho) + B_w(\rho) \\ B_c(\rho)D_w(\rho) \end{bmatrix},$$

$$\mathbb{C}_d = \begin{bmatrix} 0 & J(\rho)C_{dc}(\rho) \end{bmatrix}, \quad \mathbb{D}_1 = -J(\rho), \quad \mathbb{D}_2 = J(\rho)D_c(\rho)D_w(\rho) + J_w(\rho).$$

It is confusing to deploy the delay-dependent stability condition directly for the saturated LPV system considering a dynamic output feedback controller. Unlike the state feedback controller analysis, the stabilization analysis for closed-loop system (6.16) involves nonlinear structures. The use of congruence transformation only exacerbates the problem because of the coupling of the decision matrix LKF. Moreover, it can be seen that the quasi-convex related to the saturation conditions did not completely resolve in previous work (even the controller analysis for LTI systems). Inspired by the research of (Apkarian & Adams, 1998; Briat, 2008), we propose a new approach to solving the problem sequentially in the following steps:

- First, deliver a delay-dependent stability condition for unsaturated system (6.16) with inputs $\Phi(u)$ and $w(t)$ (employ Theorem 5.2.2 to address the stability condition with approximated delay value).
- Then, include the saturation conditions and integrate the GSC condition (developed similarly to Section 4.4).
- Lastly, use a congruence transformation to return the tractable condition.

It can see that stability analysis for resilient memory DOF controllers is more challenging than for exact-memory DOF controllers. The variable substitution is more problematic

when there is no match in the matrices $\mathbb{A}_h$ and $\mathbb{A}_d$ concerning $\mathbb{A}$ (which shows the impossibility of setting the variable as the method in section 4.4). The problem synthesis will be discussed and presented in Section 6.3.

6.2. State Feedback Controllers

This section concerns the synthesis of saturated state-feedback control laws with a memoryless and approximate delay value. The stabilization of closed-loop is addressed based on the delay-dependent stability conditions given in sections 5.2.1.2 and 5.2.4.2, respectively, for the single delay and approximate-delay case. These conditions are approached based on the application of the Wirtinger inequality, which are less conservative than the Jensen inequality (the comparison has shown in section 5.2.5).

6.2.1. *Memoryless Delay-Dependent Stabilization*

In the first case, we do not include the exact memory gain in the feedback controller structure, but the auxiliary controller $\vartheta(t)$ could employ with formulation (6.9) to relax the saturation condition. Now, the closed-loop system is obtained from the general form (6.11) with $K_d(\rho)=0$ as follows:

$$\begin{aligned} \dot{x}(t) &= A_{cl}(\rho)x(t)+A_h x(t-h(t))-B(\rho)\Phi(u)+B_w(\rho)w(t),\\ z(t) &= H_{cl}(\rho)x(t) \qquad\qquad -J(\rho)\Phi(u)+J_w(\rho)w(t),\\ x(\theta) &= \psi(\theta), \qquad\quad \theta\in[-\bar{h},0] \end{aligned} \tag{6.17}$$

Substituting this closed-loop system into the relaxed LMI condition (5.25) in section 5.2.1.2, with the dead-zone nonlinearity related in the GSC condition treated as in Chapter 4. Then, the memoryless state feedback controller attains by solving the following delay-dependent stability conditions.

Theorem 6.2.1: *For time-varying delay $h(t)\in\mathcal{H}_0$, parameter $(\rho(t),\dot{\rho}(t))\in\mathcal{U}_p\times\mathcal{U}_v$, positive scalars $\overline{u}_i,\nu_j,\eta,\gamma$ and presence of the $\mathcal{L}_2$-bound disturbance, if there exist continuously differentiable matrices function $\tilde{P}_1:\mathcal{U}_p\to\mathbb{S}^n_{++}$, Y, Z, $Z_I:\mathcal{U}_p\to\mathbb{R}^{m\times n}$, a diagonal matrix function $T:\mathcal{U}_p\to\mathbb{S}^m_{++}$, and matrices X, $\tilde{P}_2$, $\tilde{P}_3$, $\tilde{Q}$, $\tilde{R}\in\mathbb{R}^{n\times n}$, such that the following matrix inequalities hold:*

$$\begin{bmatrix} -X^S & * & * & * & * & * & * & * & * \\ \Upsilon_{21} & \Upsilon_{22} & * & * & * & * & * & * & * \\ (A_h(\rho)X)^T & \Upsilon_{32} & \Upsilon_{33} & * & * & * & * & * & * \\ P_2^T & \Upsilon_{42} & \Upsilon_{43} & -\frac{12}{\bar{h}^2}\tilde{R} & * & * & * & * & * \\ -(B(\rho)T(\rho))^T & \Upsilon_{52} & 0 & -Z_I(\rho) & -2T(\rho) & * & * & * & * \\ B_w(\rho)^T & 0 & 0 & 0 & 0 & -\gamma I_d & * & * & * \\ 0 & \Upsilon_{72} & 0 & 0 & -J(\rho)T(\rho) & J_w(\rho) & -\gamma I_r & * & * \\ \bar{h}\tilde{R} & 0 & 0 & 0 & 0 & 0 & 0 & -\tilde{R} & * \\ \varepsilon X^T & 0 & 0 & -\varepsilon\tilde{P}_2 & 0 & 0 & 0 & -\varepsilon\bar{h}\tilde{R} & -\tilde{P}_1(\rho) \end{bmatrix} \prec 0, \tag{6.18}$$

$$\begin{bmatrix} \tilde{P}_1(\rho)+2\bar{h}\tilde{R} & * & * \\ \tilde{P}_2^T-2\bar{h}\tilde{R} & \tilde{P}_3+\frac{1}{\bar{h}}(\tilde{Q}+2\tilde{R}) & * \\ Z(\rho)_{(i)} & Z_I(\rho)_{(i)} & \eta\bar{u}_i^2 \end{bmatrix} \succ 0, \quad i=1,2\ldots m, \tag{6.19}$$

where

$$\Upsilon_{21}=(A(\rho)X+B(\rho)Y(\rho))^T+\tilde{P}_1(\rho),$$
$$\Upsilon_{22}=\tilde{P}_2^S\pm\sum\nolimits_j \nu_j\left(\partial\tilde{P}_{1,j}(\rho)/\partial\rho_j\right)+\tilde{Q}-4\tilde{R}-\varepsilon^2\tilde{P}_1(\rho),$$
$$\Upsilon_{32}=-(1-\mu)\tilde{P}_2^T-2\tilde{R},$$
$$\Upsilon_{42}=\tilde{P}_3+\tfrac{6}{\bar{h}}\tilde{R},$$
$$\Upsilon_{52}=Y(\rho)-Z(\rho),$$
$$\Upsilon_{72}=H(\rho)X-J(\rho)Y(\rho),$$
$$\Upsilon_{33}=-(1-\mu)\tilde{Q}-4\tilde{R},$$
$$\Upsilon_{43}=-(1-\mu)\tilde{P}_3+\tfrac{6}{\bar{h}}\tilde{R},$$

$\bigcirc^S:=\bigcirc+\bigcirc^T$, *and* $Z_{(i)}$ *designates the i-th row of the matrix* Z, $j=1,2\ldots N_p$.

Then stabilizing gain $K(\rho)=Y(\rho)X^{-1}$ *guarantees the delay-dependent stability for the saturated LPV system* (6.17) *from initial condition belongs to DoA given by*

$$\mathcal{X}_0=\left\{\psi(\theta)\in\mathcal{C}^1\left([-\bar{h},0],\mathbb{R}^n\right)\middle|\ \eta_0^{-1}=\kappa_1^2\cdot((1+\bar{h}^2)\bar{\lambda}(\tilde{X}^{-T}\tilde{P}\tilde{X}^{-1})+\bar{h}\cdot\bar{\lambda}(X^{-T}\tilde{Q}X^{-1}))+\kappa_2^2\,\tfrac{\bar{h}^3}{2}\cdot\bar{\lambda}(X^{-T}\tilde{R}X^{-1})\le\eta^{-1}\right\},$$

such that

(1) *for bounded disturbance* $w(t)$, *the trajectories of closed-loop system are remained in the enclosed domain involving in design performance level* γ *and the upper bound* η^{-1}.

(2) *for* $w(t)=0$, *the contractive domain* (6.5) *is a region of asymptotical stability.*

with $\tilde{X}:=diag\{X,X\}$, $\tilde{P}=\begin{bmatrix}\tilde{P}_1(\rho) & \tilde{P}_2\\ * & \tilde{P}_3\end{bmatrix}\succ 0$, *and* κ_1,κ_2 *are defined in* (6.4).

Proof.

A sketch of the proof is presented sequentially as follows. First, by using Lyapunov–Krasovskii functional candidate (6.5), the parametric LMI condition (6.19) suggests the lower bound of the saturation constraints on auxiliary controller (6.9) are developed similar to Theorem 4.1.1:

$$\begin{aligned}(6.19)\ &\Leftrightarrow\ \frac{1}{\eta\mu_i^2}\begin{bmatrix}G(\rho) & G_I(\rho)\end{bmatrix}_{(i)}^T\begin{bmatrix}G(\rho) & G_I(\rho)\end{bmatrix}_{(i)}\preceq\begin{bmatrix}P_1(\rho)+2\bar{h}R & *\\ P_2^T-2\bar{h}R & P_3+\frac{1}{\bar{h}}(Q+2R)\end{bmatrix},\\ &\Leftrightarrow\ \frac{1}{\eta\mu_i^2}\vartheta_i^T\vartheta_i\le\varsigma(t)^T\begin{bmatrix}P_1(\rho)+2\bar{h}R & *\\ P_2^T-2\bar{h}R & P_3+\frac{1}{\bar{h}}(Q+2R)\end{bmatrix}\varsigma(t)\overset{\text{Lemma 5.1.1}}{\le}V(t).\end{aligned} \tag{6.20}$$

with $i=1,2\ldots m$. Then, in the view of the initial bounding set conditions (6.4), we have:

$$\begin{aligned}V(0)&\le\varsigma(0)^TP\varsigma(0)+\int_{-\bar{h}}^0x(\theta)^TQx(\theta)d\theta+\bar{h}\int_{-\bar{h}}^0\int_\theta^0\dot{x}(s)^TR\dot{x}(s)dsd\theta\\ &\le(1+\bar{h}^2)\cdot\|\psi(\theta)\|_2^2\cdot\bar{\lambda}(P)+\bar{h}\cdot\|\psi(\theta)\|^2\cdot\bar{\lambda}(Q)+\tfrac{\bar{h}^3}{2}\|\dot{\psi}(\theta)\|_2^2\cdot\bar{\lambda}(R)\\ &\le\kappa_1^2((1+\bar{h}^2)\bar{\lambda}(\tilde{X}^{-T}\tilde{P}\tilde{X}^{-1})+\bar{h}\cdot\bar{\lambda}(X^{-T}\tilde{Q}X^{-1}))+\kappa_2^2\,\tfrac{\bar{h}^3}{2}\cdot\bar{\lambda}(X^{-T}\tilde{R}X^{-1})\\ &\le\eta_0^{-1}.\end{aligned} \tag{6.21}$$

where $\bar{\lambda}(\cdot)$ is the largest eigenvalue of the matrix $(\cdot)$. Following Corollary 2.3.1 (chapter 2), there exists a diagonal matrix function $T:\mathcal{U}_p\to\mathbb{S}_{++}^m$, such that sector nonlinearity

$\Phi(u)$ defined in (2.91) with memoryless feedback control (6.6) and auxiliary control (6.9) satisfy GSC condition (2.98), expressed as follows:

$$\Phi(u)^T T^{-1}(\rho)\Big(K(\rho)x(t)-G(\rho)x(t)-G_I(\rho)\int_{t-h(t)}^{t}x(\theta)d\theta-\Phi(u)\Big)\geq 0, \tag{6.22}$$

The development of the delay-dependent stability is based on Lemma 5.2.2 by using Lyapunov–Krasovskii functional candidate (6.5) combined with $\mathscr{H}_\infty$ performance criterion, and GSC condition (6.22) that results in:

$$\begin{aligned}\dot{V}(t)+\tfrac{1}{\gamma}\|z(t)\|^2-\gamma\|w(t)\|^2+\Phi(u)^T T^{-1}(\rho)\Big(\big(K(\rho)-G(\rho)\big)x(t)-G_I(\rho)\int_{t-h(t)}^{t}x(\theta)d\theta-\Phi(u)\Big)\\ \leq \xi(t)^T\Xi(\rho)\xi(t)+\xi(t)^T\Gamma(\rho)^T\begin{bmatrix}\gamma^{-1}I_r & 0\\ 0 & R^{-1}\end{bmatrix}\Gamma(\rho)\xi(t)<0,\end{aligned} \tag{6.23}$$

where

$$\xi^T=\begin{bmatrix}x_t^T & x_h^T & \int_{t-h}^{t}x(s)^T ds & \Phi(u)^T & w(t)^T\end{bmatrix},$$

$$\Gamma(\rho)=\begin{bmatrix}H_{cl}(\rho) & 0 & 0 & -J(\rho) & J_w(\rho)\\ \bar{h}RA_{cl}(\rho) & \bar{h}RA_h(\rho) & 0 & -\bar{h}RB(\rho) & \bar{h}RB_w(\rho)\end{bmatrix},$$

$$\Xi(\rho)=\begin{bmatrix}\Xi_{11} & * & * & * & *\\ \Xi_{21} & \Xi_{22} & * & * & *\\ \Xi_{31} & \Xi_{32} & -\frac{12}{\bar{h}^2}R & * & *\\ \Xi_{41} & 0 & \Xi_{43} & -2T(\rho)^{-1} & *\\ B_w(\rho)^T P_1 & 0 & B_w(\rho)^T P_2 & 0 & -\gamma I_d\end{bmatrix},$$

with

$$\begin{aligned}\Xi_{11}&=(P_1(\rho)A_{cl}(\rho)+P_2)^S+\dot{P}_1(\rho)+Q-4R, & \Xi_{22}&=-(1-\mu)Q-4R,\\ \Xi_{21}&=(P_1(\rho)A_h(\rho))^T-(1-\mu)P_2^T-2R, & \Xi_{32}&=P_2^T A_h(\rho)-(1-\mu)P_3+\tfrac{6}{\bar{h}}R,\\ \Xi_{31}&=P_2^T A_{cl}(\rho)+P_3+\tfrac{6}{\bar{h}}R, & \Xi_{43}&=-T(\rho)^{-1}G_I(\rho)-B(\rho)^T P_2.\\ \Xi_{41}&=-(P_1(\rho)B(\rho))^T+T(\rho)^{-1}(K(\rho)-G(\rho)),\end{aligned}$$

Applying Schur's complement to the latter inequality, then similar to the associated relaxation of Theorem 5.2.1, this PLMI holds if the following condition

$$\Psi(\rho)+\mathcal{P}(\rho)^T X^{-1}\mathcal{Q}+\mathcal{Q}^T X^{-T}\mathcal{P}(\rho)\ \prec\ 0, \tag{6.24}$$

is satisfied, with $X\in\mathbb{R}^{n\times n}$ is a slack-variable matrix,

$$\Psi(\rho)=\left[\begin{array}{c|cccccccc}0 & * & * & * & * & * & * & * & *\\ \hline P_1(\rho) & \Psi_{22} & * & * & * & * & * & * & *\\ 0 & \Psi_{32} & \Psi_{33} & * & * & * & * & * & *\\ P_2^T & \Psi_{42} & \Psi_{43} & -12R & * & * & * & * & *\\ 0 & \Psi_{52} & 0 & -T(\rho)^{-1}G_I(\rho) & -2T(\rho)^{-1} & * & * & * & *\\ 0 & 0 & 0 & 0 & 0 & -\gamma I_d & * & * & *\\ 0 & H_{cl}(\rho) & 0 & 0 & -J(\rho) & J_w(\rho) & -\gamma I_r & * & *\\ \bar{h}R & 0 & 0 & 0 & 0 & 0 & 0 & -R & *\\ 0 & 0 & 0 & -\varepsilon P_2 & 0 & 0 & 0 & -\varepsilon\bar{h}R & -P_1(\rho)\end{array}\right],$$

and

$\mathcal{P}(\rho)=\left[-I \mid A_{cl}(\rho)\ \ A_h(\rho)\ \ 0\ \ -B(\rho)\ \ 0\ \ 0\ \ B_w(\rho)\ \ \varepsilon I\right],\ \mathcal{Q}=\left[I \mid 0\ \ 0\ \ 0\ \ 0\ \ 0\ \ 0\ \ 0\ \ 0\right],$
where

$$\Psi_{22}=P_2^S+\dot{P}_1(\rho)+Q-4R-P_1(\rho), \qquad \Psi_{52}=T(\rho)^{-1}(K(\rho)-G(\rho)),$$
$$\Psi_{32}=-(1-\mu)P_2^T-2R, \qquad \Psi_{33}=-(1-\mu)Q-4R,$$
$$\Psi_{42}=P_3+\tfrac{6}{\bar{h}}R, \qquad \Psi_{43}=-(1-\mu)P_3+\tfrac{6}{\bar{h}}R.$$

Pre- and post-multiplying condition (6.24), respectively, by following matrix and its transpose $diag\left\{X^T,X^T,X^T,X^T,T^{-1},X^T,X^T,I,I\right\}$, and using the variable substitutions:

$$A_{cl}(\rho)\leftarrow A(\rho)+B(\rho)K(\rho), \quad Y(\rho)\leftarrow K(\rho)X, \quad \tilde{Q}\leftarrow X^TQX, \quad \tilde{P}_2\leftarrow X^TP_2X,$$
$$\tilde{P}_1(\rho)\leftarrow X^TP_1(\rho)X, \quad Z(\rho)\leftarrow G(\rho)X, \quad \tilde{R}\leftarrow X^TRX, \quad \tilde{P}_3\leftarrow X^TP_3X.$$
$$\dot{\tilde{P}}_1(\rho)\leftarrow X^T\dot{P}_1(\rho)X, \quad Z_I(\rho)\leftarrow G_I(\rho)X,$$

that yields to PDLMI (6.18). It should remind that $\left|\dot{\tilde{P}}_1(\rho)\right|\le\sum_{i=1}^{N_p}\nu_i\left(\partial\tilde{P}_1(\rho)/\partial\rho_i\right)$ with parameters $(\rho(t),\dot{\rho}(t))\in\mathcal{U}_p\times\mathcal{U}_\nu$. Finally, if the stabilization condition (6.18) fulfills then the derivative of Lyapunov function (6.5) holds along the trajectories of closed-loop system (6.17), that ensues

- When $w(t)=0,$ then $\dot{V}(t)<-\gamma^{-1}\left\|z(t)\right\|^2<0,$ approves that
$$\frac{1}{\eta\mu_i^2}\vartheta_i^T\vartheta_i\overset{(6.19)}{\le}V(t)\overset{(6.18)}{\le}V(0)\le\eta_0^{-1}\le\frac{1}{\eta}. \tag{6.25}$$

- When $w(t)\neq 0, w(t)\in\mathcal{W}\backslash\{0\}$ then (6.18) claims
$$\frac{1}{\eta\mu_i^2}\vartheta_i^T\vartheta_i\overset{(6.19)}{\le}V(t)\overset{(6.18)}{\le}\gamma\left\|w(t)\right\|_{\mathcal{L}_2}^2+V(0)\le\gamma\sigma^{-1}+\eta_0^{-1}\le\frac{1}{\eta}. \tag{6.26}$$

This ends the proof. □

If the disturbance is not taken into account, we can choose $\eta=1$. Then, the DoA size optimization problem is formulated to seek the minimum value of the upper bound on condition (6.21). In contrast, the upper limit is indisposed to set by $\eta=1$ because it also relates to the energy bounded disturbance and the attenuation level $\gamma\sigma^{-1}$.

Since conditions (6.18)-(6.19) are linear matrix inequalities, seeking the upper bound of time-varying delay is not much of a challenge. However, condition (6.21) yields the non-convex formulations relating to decision matrix matrices $\tilde{Q}=XQX$, $\tilde{R}=XRX$,... make it not always possible to attain a good estimate of the initial condition domains. In Section 6.2.3, a linearization is proposed to handle the concave problem.

6.2.2. *Approximated Delay-Dependent Stabilization*

As discussed in section 5.2.4.2, the uncertain delay $d(t)$ provides a more general form of stability condition, in which a delay-dependent stability condition with memoryless or exact memory can derive from an approximate delay condition. By substituting the closed-loop system (6.11) into the relaxed LMI condition (5.61) and repeat the same analysis as in Theorem 6.2.1 that leads to following result.

Theorem 6.2.2: *For time-varying delay $h(t)\in\mathcal{H}_0, d(t)\in\mathcal{H}_d$, positive scalars $\overline{u}_i,\eta,\gamma,\varepsilon$, and $\mathcal{L}_2$-bound disturbances. If there exist matrices X, $\tilde{P}_2$, $\tilde{P}_3$, $\tilde{Q}$, $\tilde{R}\in\mathbb{R}^{n\times n}$, continuously differentiable matrices function $\tilde{P}_1:\mathcal{U}_p\to\mathbb{S}^n_{++}, Y$, Y_d, Z, $Z_h:\mathcal{U}_p\to\mathbb{R}^{m\times n}$, and a diagonal matrix function $T:\mathcal{U}_p\to\mathbb{S}^m_{++}$, s.t. the following PDLMIs satisfy:*

$$\begin{bmatrix}
-X^S & * & * & * & * & * & * & * & * & * & * \\
\Upsilon_{21} & \Upsilon_{22} & * & * & * & * & * & * & * & * & * \\
\Upsilon_{31} & \Upsilon_{32} & \Upsilon_{33} & * & * & * & * & * & * & * & * \\
\Upsilon_{41} & \Upsilon_{42} & \Upsilon_{43} & \Upsilon_{44} & * & * & * & * & * & * & * \\
\tilde{P}_2^T & \Upsilon_{52} & \Upsilon_{53} & \Upsilon_{54} & -\frac{12}{\bar{h}^2}\tilde{R} & * & * & * & * & * & * \\
\Upsilon_{61} & \Upsilon_{62} & Y_d(\rho) & 0 & -Z_I(\rho) & -2T(\rho) & * & * & * & * & * \\
B_w(\rho)^T & 0 & 0 & 0 & 0 & 0 & -\gamma I_d & * & * & * & * \\
0 & \Upsilon_{82} & \Upsilon_{83} & \Upsilon_{84} & 0 & -J(\rho)T(\rho) & J_w(\rho) & -\gamma I_r & * & * & * \\
\tilde{L} & 0 & 0 & 0 & 0 & 0 & 0 & 0 & -\tilde{L} & * & * \\
\bar{h}\tilde{R} & 0 & 0 & 0 & 0 & 0 & 0 & 0 & 0 & -\tilde{R} & * \\
\varepsilon X^T & 0 & 0 & 0 & -\varepsilon\tilde{P}_2 & 0 & 0 & 0 & -\varepsilon\tilde{L} & -\varepsilon\bar{h}\tilde{R} & -\tilde{P}_1(\rho)
\end{bmatrix} \prec 0, \tag{6.27}$$

$$\begin{bmatrix}
\tilde{P}_1(\rho)+2\bar{h}\tilde{R} & * & * \\
\tilde{P}_2^T-2\bar{h}\tilde{R} & \tilde{P}_3+\frac{1}{\bar{h}}(\tilde{Q}+2\tilde{R}) & * \\
Z(\rho)_{(i)} & Z_I(\rho)_{(i)} & \eta\overline{u}_i^2
\end{bmatrix} \succ 0, \quad i=1,2\ldots m, \tag{6.28}$$

where

$$\begin{aligned}
&\Upsilon_{21}=(A(\rho)X+B(\rho)Y(\rho))^T+\tilde{P}_1(\rho),\\
&\Upsilon_{31}=(A_h(\rho)X+B(\rho)Y_d(\rho))^T,\\
&\Upsilon_{41}=\tfrac{\sqrt{7}}{2}\delta_m(A_h(\rho)X)^T,\\
&\Upsilon_{61}=-(B(\rho)T(\rho))^T\\
&\Upsilon_{22}=\tilde{P}_2^S\pm\textstyle\sum_{j=1}^{N_p}\nu_j\left(\partial\tilde{P}_1(\rho)/\partial\rho_j\right)+\tilde{Q}-4\tilde{R}-\tilde{P}_1(\rho),\\
&\Upsilon_{32}=-(1-\mu)\tilde{P}_2^T-2\tilde{R},\\
&\Upsilon_{42}=-\tfrac{\sqrt{7}}{2}\delta_m((1-\mu)\tilde{P}_2^T+2\tilde{R})^T,\\
&\Upsilon_{52}=\tilde{P}_3+\tfrac{6}{\bar{h}}\tilde{R},\\
&\Upsilon_{62}=Y(\rho)-Z(\rho),\\
&\Upsilon_{82}=H(\rho)X+J(\rho)Y(\rho),\\
&\Upsilon_{33}=-(1-\mu)\tilde{Q}-4\tilde{R},\\
&\Upsilon_{43}=-\tfrac{\sqrt{7}}{2}\delta_m((1-\mu)\tilde{Q}+4\tilde{R}),\\
&\Upsilon_{53}=-(1-\mu)\tilde{P}_3+\tfrac{6}{\bar{h}}\tilde{R},\\
&\Upsilon_{83}=(H_h(\rho)X+J(\rho)Y_d(\rho)),\\
&\Upsilon_{44}=-\tfrac{7}{4}\delta_m^2((1-\mu)\tilde{Q}+4\tilde{R})-\tilde{L}(\rho),\\
&\Upsilon_{54}=-\tfrac{\sqrt{7}}{2}\delta_m((1-\mu)\tilde{P}_3-\tfrac{6}{\bar{h}}\tilde{R}),\\
&\Upsilon_{84}=\tfrac{\sqrt{7}}{2}\delta_m H_h(\rho)X.
\end{aligned}$$

Then, stabilizing gains $K(\rho)=Y(\rho)X^{-1}$, $K_d(\rho)=Y_d(\rho)X^{-1}$ guarantee the delay-dependent stability for the saturated LPV system (6.11) *from initial condition belongs to DoA*

$$\mathcal{X}_0=\left\{\psi(\theta)\in\mathcal{C}^1\left([-\bar{h},0],\mathbb{R}^n\right)\,\middle|\,\begin{array}{r}\eta_0^{-1}=\kappa_1^2\cdot((1+\bar{h}^2)\overline{\lambda}(\tilde{X}^{-T}\tilde{P}\tilde{X}^{-1})+\bar{h}\cdot\overline{\lambda}(X^{-T}\tilde{Q}X^{-1}))\\ +\kappa_2^2\,\tfrac{\bar{h}^3}{2}\cdot\overline{\lambda}(X^{-T}\tilde{R}X^{-1})\le\eta^{-1}\end{array}\right\},$$

such that

(1) *for bounded disturbance $w(t)$, the trajectories of closed-loop system are detained in the enclosed domain involving in design performance level γ and the upper bound η^{-1}.*

(2) *for $w(t)=0$, the contractive domain* (6.5) *is a region of asymptotical stability.*

with $\tilde{X} := diag\{X, X\}, \tilde{P} = \begin{bmatrix} \tilde{P}_1(\rho) & \tilde{P}_2 \\ * & \tilde{P}_3 \end{bmatrix} \succ 0$, *and* κ_1, κ_2 *are defined in* (6.4).

Proof.

This part will be omitted because it is similar to the development of memoryless control laws in the last theorem. By substituting closed-loop system (6.17) into delay-dependent stability condition (2.194) in Theorem 5.2.3 combined with GSC condition

$$\Phi(u)^T T^{-1}(\rho)(u(t) - \vartheta(t) - \Phi(u)) \geq 0, \tag{6.29}$$

where approximated feedback control $u(t) = K(\rho)x(t) + K_d(\rho)x(t - d(t))$ defines in (6.6) and auxiliary control $\vartheta(t) = G(\rho)x(t) + G_I(\rho)\int_{t-h(t)}^{t} x(\theta)d\theta$ gives in (6.9).

□

Remark 6.2.1. The delay approximation transformation is derived from the delay-dependent stability condition in Theorem 5.2.2. The difference between conditions (6.27) and (6.18) lies in the fourth and eleventh row and column. As a result, the approximated memory state-feedback controller provides the implementation feasibility compared to the exact-memory controller and gives less conservative stabilizing conditions than the memoryless controller.

6.2.3. *Optimization problem – Maximization Domain of Attraction*

The optimization problems usually involve to the size criteria of the admissible initial condition and the maximum allowable level of the disturbances. Specifically, let's consider the following criteria relate to inequalities (6.13), (6.14), that includes:

- Preselect γ, σ then minimizing η

  When $w(t) = 0$: $\eta_0^{-1} \leq \eta_{opt}^{-1}$, that implies maximizing the estimation of DoA.
  When $w(t) \neq 0$: $\eta_0^{-1} \leq \eta_{opt}^{-1} - \gamma\sigma^{-1}$, that results in the certain *allowable level* of the initial conditions (it should note that in the cases $\eta_{opt}^{-1} \leq \gamma\sigma^{-1}$, then we adjust the bounds on the external disturbances).

- Preselect σ, η then minimizing γ

  When $w(t) = 0$: the admissible initial conditions satisfy $\eta_0^{-1} \leq \eta^{-1}$.
  When $w(t) \neq 0$: the admissible initial conditions validate $\eta_0^{-1} \leq \eta^{-1} - \gamma_{opt}\sigma^{-1}$.

As discussed, the optimization problems such as minimizing energy-to-energy index γ, maximizing the upper bound of the delay value $\overline{h}$, and maximizing the delay approximation value δ_m are all affine conditions. These values can be found by optimization methods or by iterative algorithms. However, the expressions of the admissible set of the initial conditions are involved in the bilinear forms (e.g., condition (6.21)). In this section, we seek for the largest estimate of DoA that satisfies the delay-dependent stabilization conditions in Theorem 6.2.1 & Theorem 6.2.2 conforming to the design delay space $\mathcal{H}_0$.

Followed the definition of the domain of attraction $\mathcal{X}_0$, maximizing the size of DoA means minimizing of the greatest eigenvalue of nonlinear matrices $\tilde{X}^{-T}\tilde{P}\tilde{X}^{-1}, X^{-T}\tilde{Q}X^{-1}$,

$X^{-T}\tilde{R}X^{-1}$. By utilized the *minor axis maximization*, the non-convex problems are converted to the following linear criteria.

Problem 6.2.1. *Given delay space* $h(t)\in\mathcal{H}_0$, *compact sets of parameters* $\rho(t)\in\mathcal{U}_p$, *and the definition of the initial set* $\mathcal{X}_0$. *Find the variable decision matrices* X, $\tilde{P}$, $\tilde{Q}$, $\tilde{R}$ *such that the initial conditions meet condition* (6.21)*, and the following statement fulfills*:

$$\textbf{Minimize}\ f(\beta)=(1+\bar{h}^2)\beta_1+\bar{h}\beta_2+0.5\bar{h}^3\beta_3+\chi\beta_4 \tag{6.30}$$

subject to (6.18), (6.19), $\tilde{P}\prec\beta_1 I$, $\tilde{Q}\prec\beta_2 I$, $\tilde{R}\prec\beta_3 I$, and

$$\begin{bmatrix}\beta_4 I & I\\ * & \alpha(X^T+X)-\alpha^2 I\end{bmatrix}\succeq 0. \tag{6.31}$$

for pre-selected scalar α, *weighting scalar* χ.

It's worth noting that inequality $(X-\alpha I)(X-\alpha I)^T\succeq 0$ always hold for all scalar $\alpha\in\mathbb{R}$, matrix $X\in\mathbb{R}^{n\times n}$. So, the constraint (6.31) implies $(XX^T)^{-1}\preceq(\alpha(X^T+X)-\alpha^2 I)^{-1}\preceq\beta_4 I$, shows less conservatism than a directly imposed condition $X^{-1}\preceq\beta_4 I$. This method depends on the selection of $\alpha\in\mathbb{R}$, and condition $XX^T\succeq\alpha(X^T+X)-\alpha^2 I$ for all X,α, but the opposite holds only when $\alpha(X^T+X)-\alpha^2 I\succeq 0$. Thus, it is possible to miss the solution belong to the negative side: $\alpha(X^T+X)-\alpha^2 I\prec 0$.

Besides, we have $Q\triangleq X^{-T}\tilde{Q}X^{-1}\preceq\ \beta_2(XX^T)^{-1}\preceq\beta_2\beta_4 I$, and similarly for $R\preceq\beta_3\beta_4 I$, $P\preceq\beta_1\beta_4 I$. So, optimization problem (6.30) also means looking for the minimization of the greatest eigenvalue of variable matrices P, Q, R of Lyapunov–Krasovskii functional (6.5). By such expansions, the concave problem is transformed into a linear optimization problem with the objective of finding variables $\beta_i\in\mathbb{R}_{++}, i=1,2,3,4,$ such that the cost function (6.30) reaches the smallest value corresponding to the design stabilization conditions and the linearity conditions (6.31).

6.2.4. *Example*

This section is devoted to the analysis of the results and discussion of the proposed method. First, an example of the LPV delay system discussed in (Briat et al., 2010; Zhang & Grigoriadis, 2005) is applied to demonstrate the performance of a designed controller with the approximate delay value (in the case of with and without external disturbance). Second, the efficiency of the saturation constraints is validated on an unstable open-loop LPV system with the bounded signal control (due to physical limitation or safety mechanism, etc.). Then, the performance degradation and instability will observe in the systems without the saturated control design.

In the next part - section 6.2.4.2, we borrow a well-known example (Fridman et al., 2003; Gomes da Silva et al., 2011) to show the adaptation of the proposed method. In which the local stabilization enforces the saturated LTI time-delay system. After that, a comparison of the maximizing estimation of the domain of attraction is provided.

6.2.4.1. *Memory-resilient saturated controller synthesis*

The optimal disturbance reduction levels solving by the stabilization condition of Theorem 6.2.1 and Theorem 6.2.2 deliver for unsaturated system (6.32) that will compare with other unsaturated control systems. So, the constrained saturation on controller temporarily is ignored. Specifically, condition (6.19), the *fifth* columns and row of condition (6.18) of Theorem 6.2.1, condition (6.28), the *sixth* columns and row of condition (6.27) in Theorem 6.2.2 will be not included in the first controller comparison.

Example 6.2.1: Let's consider an LPV time-delay system:

$$\begin{aligned}\dot{x}(t)&=\begin{bmatrix}0 & 1+\phi\sin(t)\\ -2 & -3+\delta\sin(t)\end{bmatrix}x(t)+\begin{bmatrix}\phi\sin(t) & 0.1\\ -0.2+\delta\sin(t) & -0.3\end{bmatrix}x(t-h(t))\\ &\quad+\begin{bmatrix}\phi\sin(t)\\ 0.1+\delta\sin(t)\end{bmatrix}u(t)+\begin{bmatrix}0.2\\ 0.2\end{bmatrix}w(t),\\ z(t)&=\begin{bmatrix}0 & 10\\ 0 & 0\end{bmatrix}x(t)+\begin{bmatrix}0\\ 0.1\end{bmatrix}u(t).\end{aligned}\tag{6.32}$$

where $\phi=0.2, \delta=0.1$. By setting parameter $\rho(t)=\sin(t)$ that implies $\rho(t), \dot{\rho}(t)\in[-1, 1]$ and assuming time-varying delay belong to $h(t)\in\mathcal{H}_0$.

Table 6.1. *The optimization of $\mathscr{H}_\infty$ performance criterion – γ_{opt}.*

			Delay-Dependent Stabilization					
Example 6.2.1			$\bar{h}=0.5$, $\mu=0.5$	$\bar{h}=10$ $\mu=0.9$			$\bar{h}=3$ $\mu=0.99$	$\bar{h}=3.3$ $\mu=0.99$
(Briat, 2010)	Theorem 4.1		1.9089	12.8799	(Briat, 2015)	Corollary 8.1.3	10.2210	–
	Theorem 4.2	$\delta_m=\bar{h}$	–	13.0604		Theorem 8.1.5 $\delta_m=\bar{h}$	10.2210	–
		$\delta_m=0$	–	4.1658		$\delta_m=0$	3.4691	–
	Theorem 6.2.1		1.0821	3.1444			3.4924	4.5415
	Theorem 6.2.2	$\delta_m=\bar{h}$	1.0821	3.1444		$\delta_m=\bar{h}$	3.4924	4.5415
		$\delta_m=0$	1.0761	2.6648		$\delta_m=0$	2.1131	2.2758
0			1	2	3		4	5

–: *does not include.*

Parameter $\rho(t)$ is gridded over $N_p=41$ points uniformly spaced $[-1, 1]$. The optimal results are solved by the *modified* conditions of Theorem 6.2.1 and Theorem 6.2.2 consistent with given delay values in Table 6.1 and the assumption of zero initial conditions. The proposed stabilizations show the flexibility when it can comfortably apply to the unsaturated controller system analysis. Moreover, performance improvement has been attained with the memoryless and memory-resilient controllers compared to (Briat, 2015; Briat et al., 2010), demonstrated the relaxation of the proposed method. It is interesting to point out that the stabilization conditions with an approximated delay value could deliver the same disturbance rejection optimization levels with the exact-memory and memoryless, respectively, when $\delta_m=0$ and $\delta_m=\bar{h}$. However, the effects of saturation are less attractive analyzing the stabilizable system (LPV time delay system (6.32) has $A(\rho)+A_h(\rho)$ Hurwitz). So, let's consider a modification of the previous example.

Example 6.2.2: Let's introduce a quasi-LPV time-delay system:

$$\begin{aligned}\dot{x}(t) &= \begin{bmatrix} 2 & 1+0.2\sin(x_1(t)) \\ -2 & -3+0.1\sin(x_1(t)) \end{bmatrix} x(t) + \begin{bmatrix} 0.2\sin(x_1(t)) & 0.1 \\ -0.2+0.1\sin(x_1(t)) & 2.2 \end{bmatrix} x(t-h(t)) \\ &\quad + \begin{bmatrix} 1+0.2\sin(x_1(t)) \\ 2+0.1\sin(x_1(t)) \end{bmatrix} u(t) + \begin{bmatrix} 0.2 \\ 1.8 \end{bmatrix} w(t), \\ z(t) &= \begin{bmatrix} 0 & 10 \\ 0 & 0 \end{bmatrix} x(t) + \begin{bmatrix} 0 \\ 0.1 \end{bmatrix} u(t). \end{aligned} \tag{6.33}$$

where $\bar{u} = 5$, and $A(\rho), A_h(\rho), A(\rho) + A_h(\rho)$ are not Hurwitz matrices for all time-varying parameter $\rho(x(t)) = \sin(x_1(t)) \in [-1, 1]$ assumed $\dot{\rho}(t) = \dot{x}_1(t)\cos(x_1(t)) \in [-3, 3]$.

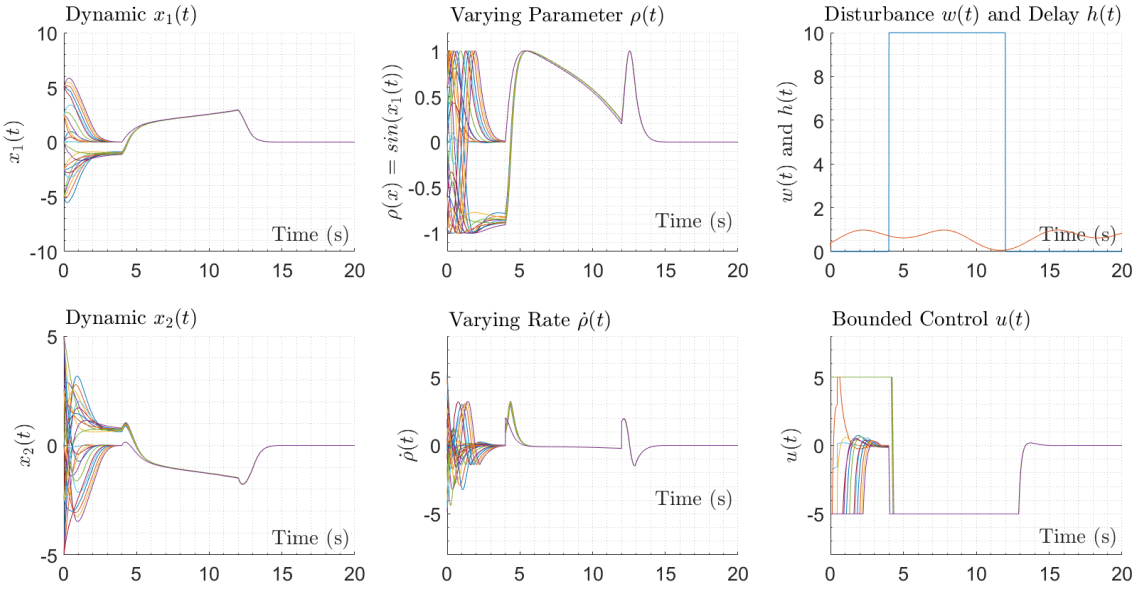

Figure 6-1. *The responses of the bounded controllers correspond to saturation limit* $\bar{u} = 5$, *with* $\bar{h} = 1, \mu = 0.9$.

In this example, the simulation starts from *safe* initial conditions that belongs to the estimate of DoA. Then, the disturbance amplitude gradually increases but does not exceed the maximum allowable bounded energy $\|w(t)\|_{\mathcal{L}_2}^2 < \sigma^{-1}$. The purpose of this process is to estimate the evolutions of the state-dependent parameter as well as the saturation response of the unbounded feedback controllers. It clears to realize that $\dot{\rho}(t)$ is bounded between $[-5, 5]$. But most of the response characteristics are in the range of $[-3, 3]$ (even when system is influenced by a large magnitude external disturbance). So we proceed to solve the proposed theorems with parameter values selected in the assumed range.

The actuator saturation usually takes place in many practical applications where its existence may lead to the degradation performance or even cause the instability of the closed-loop system. In the monographs (Hu & Lin, 2001; Tarbouriech et al., 2011), the authors thoroughly explained all the behavior of the closed-loop states *frozen* when the actuator is saturated. In which the state dynamics can destabilize or converge to a *parasitic equilibrium* instead of toward to the origin. The gain-scheduling controllers solved by the proposed methods could be compared with the system without the saturation conditions. The constrained conditions (6.19), and (6.28) ensure the local stabilization contrasting to the system without a saturated design.

However, these results may be less objective than in Table 6.1, when we reconstruct stabilization conditions of Theorem 8.1.5 and Theorem 4.2 of the literature (Briat, 2015; Briat et al., 2010) to implement controls applicable for the saturated LPV time-delay system (6.33). Nevertheless, the scheduling gains of the proposed theorems have shown the stability regulation efficiency for the LPV time-delay system conforming to actuator limits. The parametric dependent gains are given by:

Memoryless Saturated Controller

Solving the stabilization condition of Theorem 6.2.1 with $\overline{h}=1, \mu=0.9$, we obtain stabilizing gains $K(\rho)=Y(\rho)X^{-1}$,

$$K(\rho)=\begin{bmatrix}-240.2029+62.2704\rho(t)-45.2684\rho(t)^2\\ -22.4705+8.0147\rho(t)-4.0625\rho(t)^2\end{bmatrix}. \tag{6.34}$$

Saturated Controller with Approximate Memory

Solving the stabilization condition of Theorem 6.2.2 with $\overline{h}=1, \mu=0.9, \delta_m=0.19$, we get stabilizing gains $K(\rho)=Y(\rho)X^{-1}, K_d(\rho)=Y_d(\rho)X^{-1}$,

$$\begin{aligned}K(\rho)|_{\delta_m=0.19}&=\begin{bmatrix}-227.0362+65.2742\rho(t)-42.6110\rho(t)^2\\ -22.3907+8.4960\rho(t)-4.0884\rho(t)^2\end{bmatrix},\\ K_d(\rho)|_{\delta_m=0.19}&=\begin{bmatrix}0.0809-0.0645\rho(t)+0.0528\rho(t)^2\\ -0.0308-0.0020\rho(t)+0.0067\rho(t)^2\end{bmatrix}.\end{aligned} \tag{6.35}$$

In the stability analysis of LPV delay systems, the gain $K_h(\rho)$ plays a key role in relaxing the conservativeness of the condition. When δ_m closes to $\overline{h}$, gain $K_d(\rho)$ will decline, and when δ_m approaches to 0, gain $K_d(\rho)$ will converge to memory gain $K_h(\rho)$. As we have seen in Table 6.1, the best attenuation criteria are achieved with the memory controllers (or memory-resilient controller with $\delta_m=0$). It's interesting to admit that controllers with approximate memory demonstrate a generality and unified formulation for memoryless controllers and controllers with memory.

For simulation purposes, let:

$$h(t)=0.5\overline{h}+0.5\overline{h}\sin\left(\frac{2\mu t}{\overline{h}}+\pi/2\right), \tag{6.36}$$

and $d(t)$ is approximate delay value agreeing with the design memory-resilient δ_m.

In the bounded controller framework, the signal is sensitive to saturation limit if the designed gain is too high. Explicitly, the higher rejection disturbance level ensues in smaller linear behavior region. As a way of repeating, it is a trade-off between system performance, estimation of domain asymptotical stability, and the admissible set of the initial conditions.

6.2.4.2. *Maximization of the set of admissible initial conditions*

Now, we present the results of the optimization method discussed in Section 6.2.3 for estimating the allowable initial conditions. There are inconsiderable studies on this aspect for the LPV time-varying delay system with the saturated actuator, so we employ the

proposed implementation methods for an LTI system.

Example 6.2.3: Consider the following linear time-delay system (LTDS):

$$A=\begin{bmatrix} 1 & 1.5 \\ 0.3 & -2 \end{bmatrix},\ A_h=\begin{bmatrix} 0 & -1 \\ 0 & 0 \end{bmatrix},\ B=\begin{bmatrix} 10 \\ 1 \end{bmatrix},\ \text{and } \bar{u}=15. \tag{6.37}$$

The stabilizations of LTDS (6.37) address by Theorem 6.2.1 and Theorem 6.2.2, respectively, for a delay bound of $\bar{h}=1, \mu=0,$ and $\mu=0.1$. The estimates of DoA are carried out by the optimization Problem 6.2.1.

The estimate domain of attraction solving by Theorem 6.2.1 (a stabilization of memoryless controller) bounds by $11.3125\kappa_1^2+2.0022\kappa_2^2\leq 10^5$ (for the case of $\kappa_1\neq\kappa_2$) and $\kappa=$ 86.6633 (for the case of $\kappa_1=\kappa_2$). The maximum radius of the stability ball stabilizing state-feedback controller obtains for all delays that are less than or equal to $\bar{h}=1$ corresponding to $\mu=0,$ and 0.1.

The more *slack*-matrix variables usually lead to high computation complexity. The proposed method provides good results with less conservative stabilization conditions for a reasonable number of variables to be determined. To solve the stabilization conditions for system (6.37), we only use 27 variables compared to 36, 37 variables of the reciprocally convex combination (RCC) and free matrix based (FMB) method (Dey et al., 2014), and 82, 35 variable of the free-weighting matrix (FWM) method (Chen et al., 2015, 2017), respectively.

Table 6.2. *Domain of attraction, with* $\bar{h}=1$.

			Delay-Dependent Stabilization		
Example 6.2.3	$\mu=0.1$	$\mu=0.0$	*Number of Variables*		Parameters
	$\kappa_1=\kappa_2$	$\kappa_1=\kappa_2$	$n=2,\ m=1$		α,χ
Theorem 3 (Dey, 2014)	–	106.2856	$n(7n+2m+2)+m$	37	$\chi=10^{11}$
Theorem 1 (Chen, 2017)	–	92.5966	$\frac{(2N+1)(n^2+n)}{2}+(Nm+3m+2)n$	35	$\alpha=0.4, \chi=10^9, N=3$
Theorem 6.2.1	84.8793	86.6634	$2n(n+3)+m(3n+1)$	27	$\alpha=1, \chi=10^{10}, \varepsilon=1.15$
Theorem 1 (Chen, 2015)	–	84.6074	$n(5n+27)+4mn$	82	$\alpha=0.4, \chi=10^9$
(Gomes da Silva, 2011)	83.55	–	$\frac{3}{2}n^2+\frac{11}{2}n+2mn+m$	22	–
Theorem 2 (Dey, 2014)	–	80.3239	$n(7n+2m+2)$	36	$\chi=10^9$
Th1 (Fridman, 2003)	–	79.43	$\frac{3}{2}n^2+\frac{23}{2}n+2mn$	33	–
0	1	2	3		4

–: *does not include*; Th1: *Theorem* 1.

The methods outlined in Table 6.2 focus on the LTI system. The trade-off of conditional relaxation with the computational complexity of the condition makes these approaches hard to implement on a parameter-dependent stabilization. The proposed condition balances the number of variable matrices, the conservatism, and the scalability of the control synthesis. To the best of our knowledge, the stabilization problem for LPV/quasi-LPV time-delay system subject to actuator saturation has not been well addressed, although

the problematics have significant practical applications. In the next section, the proposed structure conditions are used to deliver the stabilization of the dynamic output controller. Then, the optimization problems for LPV time-varying delay systems relate to the size criteria of the admissible initial condition and the maximum disturbances attenuation are provided in section 6.3.4.

6.3. Dynamic Output Feedback Controllers

6.3.1. *Exact Memory Delay-Dependent Stabilization*

In practice, the value of the delay is difficult to measure with precision. So, implementations for systems with time-varying delays are occasionally accompanied by the assumption that this value is known accurately. In the first part, a stability condition is delivered for the following time-delay system with exact-memory value (the case of $d(t) \equiv h(t)$):

$$\begin{aligned} \dot{\zeta}(t) &= \mathbb{A}\zeta(t) + \mathbb{A}_h\zeta(t-h) + \mathbb{B}_1\Phi(u) + \mathbb{B}_2 w(t), \\ z(t) &= \mathbb{C}\zeta(t) + \mathbb{C}_h\zeta(t-h) + \mathbb{D}_1\Phi(u) + \mathbb{D}_2 w(t). \end{aligned} \tag{6.38}$$

with

$$\mathbb{A} = \begin{bmatrix} A(\rho) + B(\rho)D_c(\rho)C(\rho) & B(\rho)C_c(\rho) \\ B_c(\rho)C(\rho) & A_c(\rho) \end{bmatrix}, \quad \mathbb{A}_h = \begin{bmatrix} A_h(\rho) + B(\rho)D_c(\rho)C_h(\rho) & B(\rho)C_{dc}(\rho) \\ B_c(\rho)C_h(\rho) & A_{dc}(\rho) \end{bmatrix},$$

$$\mathbb{C} = \begin{bmatrix} H(\rho) + J(\rho)D_c(\rho)C(\rho) & J(\rho)C_c(\rho) \end{bmatrix}, \quad \mathbb{C}_h = \begin{bmatrix} H_h(\rho) + J(\rho)D_c(\rho)C_h(\rho) & J(\rho)C_{dc}(\rho) \end{bmatrix},$$

$$\mathbb{B}_1 = \begin{bmatrix} -B(\rho) \\ E_c(\rho) \end{bmatrix}, \mathbb{B}_2 = \begin{bmatrix} B(\rho)D_c(\rho)D_w(\rho) + B_w(\rho) \\ B_c(\rho)D_w(\rho) \end{bmatrix}, \mathbb{D}_1 = -J(\rho), \mathbb{D}_2 = J(\rho)D_c(\rho)D_w(\rho) + J_w(\rho).$$

Let's re-present the input control of the actuator saturation

$$u(t) = \mathbb{K}\zeta(t) + \mathbb{K}_h\zeta(t-h) + D_c(\rho)D_w(\rho)w(t), \tag{6.39}$$

and define an auxiliary controller

$$\vartheta(t) = \mathbb{G}\zeta(t) + \mathbb{G}_I \int_{t-h(t)}^{t} \zeta(\theta)d\theta, \tag{6.40}$$

with $\mathbb{K} = [D_c(\rho)C(\rho) \quad C_c(\rho)]$, $\mathbb{K}_h = [D_c(\rho)C_h(\rho) \quad C_{dc}(\rho)]$, and $\mathbb{G}, \mathbb{G}_I$ will be defined after to suit the design structure. From now on, the stabilization analysis interprets the same as previous theorems, with the implementation variable substitutions similar to section 4.4.

Now, let's introduce the block variable matrices:

$$W = \begin{bmatrix} \boldsymbol{Y} & N \\ N^T & \star \end{bmatrix}, \; W^{-1} = \begin{bmatrix} \boldsymbol{X} & M \\ M^T & \star \end{bmatrix}, \; \Pi_1 = \begin{bmatrix} \boldsymbol{X} & I \\ M^T & 0 \end{bmatrix}, \text{ and } \Pi_2 = \begin{bmatrix} I & \boldsymbol{Y} \\ 0 & N^T \end{bmatrix}. \tag{6.41}$$

We have $W\Pi_1 = \Pi_2$, and matrices $W \in \mathbb{S}_{++}^{2n}, \boldsymbol{X}, \boldsymbol{Y} \in \mathbb{S}_{++}^{n}, M, N \in \mathbb{R}^{n\times n}$. Using the definition of state-space system (6.38), the block matrix multiplications are expanded by:

$$\Pi_2^T \mathbb{A}\Pi_1 = \begin{bmatrix} A(\rho)\boldsymbol{X} + B(\rho)\hat{\boldsymbol{C}}(\rho) & A(\rho) + B(\rho)\hat{\boldsymbol{D}}(\rho)C(\rho) \\ \hat{\boldsymbol{A}}(\rho) & \boldsymbol{Y}A(\rho) + \hat{\boldsymbol{B}}(\rho)C(\rho) \end{bmatrix}, \tag{6.42}$$

$$\Pi_2^T \mathbb{A}_h\Pi_1 = \begin{bmatrix} A_h(\rho)\boldsymbol{X} + B(\rho)\hat{\boldsymbol{C}}_h(\rho) & A_h(\rho) + B(\rho)\hat{\boldsymbol{D}}(\rho)C_h(\rho) \\ \hat{\boldsymbol{A}}_h(\rho) & \boldsymbol{Y}A_h(\rho) + \hat{\boldsymbol{B}}(\rho)C_h(\rho) \end{bmatrix}, \tag{6.43}$$

$$\Pi_2^T\mathbb{B}_1=\begin{bmatrix}-B(\rho)\\ -\boldsymbol{Y}B(\rho)+N(\rho)E_c(\rho)\end{bmatrix},\ \Pi_2^T\mathbb{B}_2=\begin{bmatrix}B(\rho)\hat{\boldsymbol{D}}(\rho)D_w(\rho)+B_w(\rho)\\ \hat{\boldsymbol{B}}(\rho)D_w(\rho)+\boldsymbol{Y}B_w(\rho)\end{bmatrix}, \tag{6.44}$$

$$\mathbb{C}\Pi_1=[H(\rho)\boldsymbol{X}+J(\rho)\hat{\boldsymbol{C}}(\rho)\quad H(\rho)+J(\rho)\hat{\boldsymbol{D}}(\rho)C(\rho)], \tag{6.45}$$

$$\mathbb{C}_h\Pi_1=[H_h(\rho)\boldsymbol{X}+J(\rho)\hat{\boldsymbol{C}}_h(\rho)\quad H_h(\rho)+J(\rho)\hat{\boldsymbol{D}}(\rho)C_h(\rho)], \tag{6.46}$$

and choose $\mathbb{G}\Pi_1=[\hat{\boldsymbol{F}}(\rho)\quad \hat{\boldsymbol{G}}(\rho)C(\rho)]$ to match with $\mathbb{K}\Pi_1$, respectively, we have

$$(\mathbb{K}-\mathbb{G})\Pi_1=[\hat{\boldsymbol{C}}(\rho)-\hat{\boldsymbol{F}}(\rho)\quad (\hat{\boldsymbol{D}}(\rho)-\hat{\boldsymbol{G}}(\rho))C(\rho)], \tag{6.47}$$

$$\mathbb{K}_h\Pi_1=[\hat{\boldsymbol{C}}_h(\rho)\quad \hat{\boldsymbol{D}}(\rho)C_h(\rho)],\ \mathbb{G}_I\Pi_1=[\hat{\boldsymbol{F}}_I(\rho)\quad \hat{\boldsymbol{G}}_I(\rho)C_h(\rho)], \tag{6.48}$$

with the change of controller variables:

$$\begin{aligned}
\hat{\boldsymbol{A}}(\rho)&=\boldsymbol{Y}(A(\rho)+B(\rho)D_c(\rho)C(\rho))\boldsymbol{X}+NA_c(\rho)M^T+\boldsymbol{Y}B(\rho)C_c(\rho)M^T+NB_c(\rho)C(\rho)\boldsymbol{X},\\
\hat{\boldsymbol{A}}_h(\rho)&=\boldsymbol{Y}(A_h(\rho)+B(\rho)D_c(\rho)C_h(\rho))\boldsymbol{X}+NA_{dc}(\rho)M^T+\boldsymbol{Y}B(\rho)C_{dc}(\rho)M^T+NB_c(\rho)C_h(\rho)\boldsymbol{X},\\
\hat{\boldsymbol{B}}(\rho)&=\boldsymbol{Y}B(\rho)D_c(\rho)+NB_c(\rho),\\
\hat{\boldsymbol{C}}(\rho)&=D_c(\rho)C(\rho)\boldsymbol{X}+C_c(\rho)M^T,\\
\hat{\boldsymbol{C}}_h(\rho)&=D_c(\rho)C_h(\rho)\boldsymbol{X}+C_{dc}(\rho)M^T,\\
\hat{\boldsymbol{D}}(\rho)&=D_c(\rho),\\
\hat{\boldsymbol{E}}(\rho)&=-\boldsymbol{Y}B(\rho)T(\rho)+NE_c(\rho)T(\rho),
\end{aligned} \tag{6.49}$$

where $\hat{\boldsymbol{E}}(\rho)$ will appear from the stabilization analysis, and $\hat{\boldsymbol{F}}(\rho),\hat{\boldsymbol{F}}_h(\rho),\hat{\boldsymbol{G}}(\rho),\hat{\boldsymbol{G}}_h(\rho)$ are variable matrices with appropriate dimensions. Based on these transformations, we deploy associated relaxation of the stabilization condition (provided in section 5.2.1.2) for extended system (6.38) as follows.

Theorem 6.3.1: *For time-varying delay $h(t)\in\mathcal{H}_0$, positive scalars $\varepsilon_1,\varepsilon_2,\overline{u}_i,\eta,\gamma$, and $\mathcal{L}_2$-bounded disturbance, if there exist continuously differentiable matrices function $\tilde{P}_1:\mathcal{U}_p\to\mathbb{S}^{2n}_{++}$, $\hat{\boldsymbol{A}}:\mathcal{U}_p\to\mathbb{R}^{n\times n}$, $\hat{\boldsymbol{B}}:\mathcal{U}_p\to\mathbb{R}^{n\times p}$, $\hat{\boldsymbol{C}},\hat{\boldsymbol{F}},\hat{\boldsymbol{F}}_I:\mathcal{U}_p\to\mathbb{R}^{m\times n}$, $\hat{\boldsymbol{D}},\hat{\boldsymbol{G}},\hat{\boldsymbol{G}}_I:\mathcal{U}_p\to\mathbb{R}^{m\times p}$, $\hat{\boldsymbol{E}}:\mathcal{U}_p\to\mathbb{R}^{m\times n}$, a diagonal matrix function $T:\mathcal{U}_p\to\mathbb{R}^m_{++}$, and matrices $\tilde{P}_2$, $\tilde{P}_3$, $\tilde{Q}$, $\tilde{R}\in\mathbb{R}^{2n\times 2n}$, $\boldsymbol{X},\boldsymbol{Y}\in\mathbb{S}^n_{++}$, such that the following conditions hold:*

$$\begin{bmatrix}
-\{\Pi_2^T\Pi_1\}^S & * & * & * & * & * & * & * & *\\
\tilde{\Upsilon}_{21} & \tilde{\Upsilon}_{22} & * & * & * & * & * & * & *\\
(\Pi_2^T\mathbb{A}_h\Pi_1)^T & \tilde{\Upsilon}_{32} & \tilde{\Upsilon}_{33} & * & * & * & * & * & *\\
\tilde{P}_2^T & \tilde{\Upsilon}_{42} & \tilde{\Upsilon}_{43} & -\frac{12}{\overline{h}^2}\tilde{R} & * & * & * & * & *\\
(\Pi_2^T\mathbb{B}_1T(\rho))^T & \tilde{\Upsilon}_{52} & \mathbb{K}_h\Pi_1 & -\mathbb{G}_I\Pi_1 & -2T(\rho) & * & * & * & *\\
(\Pi_2^T\mathbb{B}_2)^T & 0 & 0 & 0 & 0 & -\gamma I_d & * & * & *\\
0 & \mathbb{C}\Pi_1 & \mathbb{C}_h\Pi_1 & 0 & \mathbb{D}_1T(\rho) & \mathbb{D}_2 & -\gamma I_r & * & *\\
\overline{h}\tilde{R} & 0 & 0 & 0 & 0 & 0 & 0 & -\tilde{R} & *\\
\varepsilon_1\Pi_2^T\Pi_1 & 0 & 0 & -\varepsilon_1\tilde{P}_2 & 0 & 0 & 0 & -\varepsilon_1\overline{h}\tilde{R} & -\tilde{P}_1(\rho)
\end{bmatrix}\prec 0, \tag{6.50}$$

$$(a).\ \begin{bmatrix}\tilde{P}_1(\rho)+2\overline{h}\tilde{R} & * & *\\ \tilde{P}_2^T-2\overline{h}\tilde{R} & \tilde{P}_3+\frac{1}{\overline{h}}(\tilde{Q}+2\tilde{R}) & *\\ (\mathbb{G}\Pi_1)_{(i)} & (\mathbb{G}_I\Pi_1)_{(i)} & \eta\overline{u}_i^2\end{bmatrix}\succ 0,\qquad (b).\ \begin{bmatrix}\boldsymbol{X} & \varepsilon_2 I\\ \varepsilon_2 I & \boldsymbol{Y}\end{bmatrix}\succeq 0, \tag{6.51}$$

where $i=1,2\ldots m$,

$$\begin{aligned}
&\tilde{\Upsilon}_{21}=(\Pi_2^T\mathbb{A}\Pi_1)^T+\tilde{P}_1(\rho), && \tilde{\Upsilon}_{52}=(\mathbb{K}-\mathbb{G})\Pi_1,\\
&\tilde{\Upsilon}_{22}=\tilde{P}_2^S\pm\textstyle\sum_{j=1}^{N_p}\nu_j\big(\partial\tilde{P}_1(\rho)/\partial\rho_j\big)+\tilde{Q}-4\tilde{R}-\varepsilon_1^2\tilde{P}_1(\rho), && \tilde{\Upsilon}_{33}=-(1-\mu)\tilde{Q}-4\tilde{R},\\
&\tilde{\Upsilon}_{32}=-(1-\mu)\tilde{P}_2^T-2\tilde{R}, && \tilde{\Upsilon}_{43}=-(1-\mu)\tilde{P}_3+\tfrac{6}{\bar{h}}\tilde{R},\\
&\tilde{\Upsilon}_{42}=\tilde{P}_3+\tfrac{6}{\bar{h}}\tilde{R}, &&
\end{aligned}$$

and the matrix transformations are detailed from (6.41) to (6.49). Then, the controller gains are given by

$$\begin{aligned}
E_c(\rho)&=N^{-1}(\hat{\boldsymbol{E}}(\rho)T(\rho)^{-1}+\boldsymbol{Y}B(\rho)),\\
D_c(\rho)&=\hat{\boldsymbol{D}}(\rho),\\
C_c(\rho)&=(\hat{\boldsymbol{C}}(\rho)-\hat{\boldsymbol{D}}(\rho)C(\rho)\boldsymbol{X})M^{-T},\\
C_{dc}(\rho)&=(\hat{\boldsymbol{C}}_h(\rho)-\hat{\boldsymbol{D}}(\rho)C_h(\rho)\boldsymbol{X})M^{-T},\\
A_c(\rho)&=N^{-1}(\hat{\boldsymbol{A}}(\rho)-\hat{\boldsymbol{B}}(\rho)C(\rho)X-\boldsymbol{Y}B(\rho)\hat{\boldsymbol{C}}(\rho)-\boldsymbol{Y}(A(\rho)-B(\rho)\hat{\boldsymbol{D}}(\rho)C(\rho))\boldsymbol{X})M^{-T},\\
A_{dc}(\rho)&=N^{-1}(\hat{\boldsymbol{A}}_h(\rho)-\hat{\boldsymbol{B}}(\rho)C(\rho)X-\boldsymbol{Y}B(\rho)\hat{\boldsymbol{C}}_h(\rho)-\boldsymbol{Y}(A_h(\rho)-B(\rho)\hat{\boldsymbol{D}}(\rho)C_h(\rho))\boldsymbol{X})M^{-T},\\
B_c(\rho)&=N^{-1}(\hat{\boldsymbol{B}}(\rho)-\boldsymbol{Y}B(\rho)\hat{\boldsymbol{D}}(\rho)),
\end{aligned}\tag{6.52}$$

guarantee the delay-dependent stability for the saturated LPV system (6.38) *from initial condition belongs to DoA given by*

$$\mathcal{X}_0=\left\{\psi(\theta)\in\mathcal{C}^1\big([-\bar{h},0],\mathbb{R}^n\big)\;\middle|\;\begin{array}{c}\eta_0^{-1}=\kappa_1^2\cdot\Big((1+\bar{h}^2)\bar{\lambda}(\tilde{\Pi}^{-T}\tilde{P}\tilde{\Pi}^{-1})+\bar{h}\cdot\bar{\lambda}\big(\Pi_1^{-T}\tilde{Q}\Pi_1^{-1}\big)\Big)\\ +\kappa_2^2\,\frac{\bar{h}^3}{2}\cdot\bar{\lambda}(\Pi_1^{-T}\tilde{R}\Pi_1^{-1})\le\eta^{-1}\end{array}\right\},$$

such that

(1) *for bounded disturbance* $w(t)$*, the trajectories of closed-loop system stay in the enclosed domain involving in design performance level* γ *and the upper bound* η^{-1}.

(2) *for* $w(t)=0$*, the contractive domain* (6.5) *is a region of asymptotical stability.*

with $\tilde{\Pi}:=diag\{\Pi_1,\Pi_1\},\tilde{P}=\begin{bmatrix}\tilde{P}_1(\rho) & \tilde{P}_2\\ * & \tilde{P}_3\end{bmatrix}\succ 0$*, and* κ_1,κ_2 *are bounds of initial conditions.*

Proof.

A sketch of the proof is provided as follows. Firstly, using the transformation (6.41), we have LMI (6.51).*a* equivalent to the following condition:

$$\begin{bmatrix}\Pi_1 & 0 & 0\\ 0 & \Pi_1 & 0\\ 0 & 0 & 1\end{bmatrix}^T\begin{bmatrix}\tilde{P}_1(\rho)+2\bar{h}\tilde{R} & * & *\\ \tilde{P}_2^T-2\bar{h}\tilde{R} & \tilde{P}_3+\frac{1}{\bar{h}}(\tilde{Q}+2\tilde{R}) & *\\ (\mathbb{G}\Pi_1)_{(i)} & (\mathbb{G}_I\Pi_1)_{(i)} & \eta\overline{u}_i^2\end{bmatrix}\begin{bmatrix}\Pi_1 & 0 & 0\\ 0 & \Pi_1 & 0\\ 0 & 0 & 1\end{bmatrix}\succeq 0,\ i=1\tag{6.53}$$

with the change of variable: $\tilde{P}_1(\rho)\leftarrow\Pi_1^TP_1(\rho)\Pi_1,\quad\tilde{P}_2\leftarrow\Pi_1^TP_2\Pi_1,\quad\tilde{P}_3\leftarrow\Pi_1^TP_3\Pi_1,$

We consider the Lyapunov-Krasovskii functional (6.5) for extended system (6.38) consistent with the dynamic state $\zeta(t)$. It can realize that (6.53) are the saturation constraints involved in feedback controller (6.39) and auxiliary controller (6.40).

$$\frac{1}{\eta\mu_i^2}\vartheta_i^T\vartheta_i\le\varsigma(t)^T\begin{bmatrix}P_1(\rho)+2\bar{h}R & *\\ P_2^T-2\bar{h}R & P_3+\frac{1}{\bar{h}}(Q+2R)\end{bmatrix}\varsigma(t)\le V(t).\tag{6.54}$$

where $i=1,2\ldots m.$ Condition (6.51).*b* sets to guarantee the definitively symmetrical positive matrix W (which can be indirectly determined by $\Pi_1^TW\Pi_1$) and scalar ε_2 to ensure that $\boldsymbol{XY}$ is nonsingular. Then, substituting system (6.38) into stability condition (5.25) of

Theorem 5.2.1, with matrix W given in (6.41) replaces the slack-variable X, that lead to the following PLMI

$$\begin{bmatrix} -W^S & * & * & * & * & * & * & * & * \\ \Upsilon_{21} & \Upsilon_{22} & * & * & * & * & * & * & * \\ (W\mathbb{A}_h)^T & \Upsilon_{32} & \Upsilon_{33} & * & * & * & * & * & * \\ \bar{h}P_2^T & \Upsilon_{42} & \Upsilon_{43} & -\frac{12}{\bar{h}^2}R & * & * & * & * & * \\ (W\mathbb{B}_1)^T & \Upsilon_{52} & T(\rho)^{-1}\mathbb{K}_h & -T(\rho)^{-1}\mathbb{G}_I & -2T(\rho)^{-1} & * & * & * & * \\ (W\mathbb{B}_2)^T & 0 & 0 & 0 & 0 & -\gamma I_d & * & * & * \\ 0 & \mathbb{C} & \mathbb{C}_h & 0 & \mathbb{D}_1 & \mathbb{D}_2 & -\gamma I_r & * & * \\ \bar{h}R & 0 & 0 & 0 & 0 & 0 & 0 & -R & * \\ \varepsilon_1 W & 0 & 0 & -\varepsilon_1 P_2 & 0 & 0 & 0 & -\varepsilon_1\bar{h}R & -P_1(\rho) \end{bmatrix} \prec 0, \quad (6.55)$$

where
$\Upsilon_{21} = (W\mathbb{A})^T + P_1(\rho)$,
$\Upsilon_{22} = P_2^S \pm \sum_{j=1}^{N_p}\nu_j\left(\partial P_1(\rho)/\partial\rho_j\right) + Q - 4R - \varepsilon^2 P_1(\rho)$,
$\Upsilon_{32} = -(1-\mu)P_2^T - 2R$,
$\Upsilon_{42} = P_3 + \frac{6}{\bar{h}}R$,
$\Upsilon_{52} = T(\rho)^{-1}(\mathbb{K} - \mathbb{G})$,
$\Upsilon_{33} = -(1-\mu)Q - 4R$,
$\Upsilon_{43} = -(1-\mu)P_3 + \frac{6}{\bar{h}}R$,

Afterward, pre and post-multiplying (6.55) by matrix

$$diag\{\Pi_1^T, \Pi_1^T, \Pi_1^T, \Pi_1^T, T^{-1}, \Pi_1^T, \Pi_1^T, I, I\},$$

and its transpose, respectively, that entails directly stabilization conditions (6.50), with the linearizing change of variable: $W\Pi_1 \leftarrow \Pi_2$, $\tilde{Q} \leftarrow \Pi_1^T Q \Pi_1$, $\tilde{R} \leftarrow \Pi_1^T R \Pi_1$,

$$\left|\dot{\tilde{P}}_1(\rho) \leftarrow \Pi_1^T \dot{P}_1(\rho)\Pi_1\right| \le \sum_{j=1}^{N_p}\nu_j\left(\partial\tilde{P}_1(\rho)/\partial\rho_j\right).$$

By inversing variable assignments (6.49), we get the dynamic output controller (6.52). The rest of the demonstration will follow the lines as in Theorem 6.2.1.

□

For using the congruence transformation, the slack-matrix W is chosen as a symmetric matrix. Besides, as discussed in the previous sections $W, \Pi_1, \Pi_2,$ must be parameter-independent variable matrices to avoid nonlinear components appearing in the condition. Analysis of stability conditions for system (6.38) takes full advantage of the commensurate structure between matrices $\mathbb{A}$ and $\mathbb{A}_h$, so the variable substitutions are not much of a problem. However, the uncertain delay value typically leads to incompatibility between the matrices $\Pi_2^T\mathbb{A}_h\Pi_1$ and $\Pi_2^T\mathbb{A}_d\Pi_1$, which produce non-convex forms. By modifying the structure of the output and controller

$$\begin{aligned} \dot{x}_c(t) &= A_c(\rho)x_c(t) + A_{dc}(\rho)x_c(t-d(t)) + B_c(\rho)y(t) + B_{dc}(\rho)y(t-d(t)) + E_c(\rho)\Phi(u), \\ u(t) &= C_c(\rho)x_c(t) + C_{dc}(\rho)x_c(t-d(t)) + D_c(\rho)y(t) + D_{dc}(\rho)y(t-d(t)), \\ y(t) &= C(\rho)x(t), \end{aligned} \quad (6.56)$$

will suppress the bilinear terms and deliver a convex condition. Nonetheless, it loses the generality and interestingness of the approximated delay method. In the next section, Young's inequality is recalled to deal with these nonlinear problems.

6.3.2. *Approximate Delay-Dependent Stabilization*

Let's introduce an input control

$$u(t) = \mathbb{K}\zeta(t) + \mathbb{K}_h\zeta(t-h) + \mathbb{K}_d\zeta(t-h) + D_c(\rho)D_w(\rho)w(t), \tag{6.57}$$

where $\mathbb{K} = [D_c(\rho)C(\rho) \quad C_c(\rho)]$, $\mathbb{K}_h = [D_c(\rho)C_h(\rho) \quad 0]$, $\mathbb{K}_d = [0 \quad C_{dc}(\rho)]$, conforming to auxiliary controller (6.40), with $\mathbb{G}, \mathbb{G}_I$ given in equation (6.47).

Similarly, the development analyzes the same as previous approach, with the variable substitutions based on the variable matrices (6.41). Applying the definition of state-space system (6.16), the block matrix multiplications $\Pi_2^T\mathbb{A}\Pi_1$, $\Pi_2^T\mathbb{B}_1$, $\Pi_2^T\mathbb{B}_2$, $\mathbb{C}\Pi_1$, $(\mathbb{K}-\mathbb{G})\Pi_1$, $\mathbb{G}_I\Pi_1$ refer to (6.42)-(6.47), and

$$\Pi_2^T(\mathbb{A}_h + \mathbb{A}_d)\Pi_1 = \begin{bmatrix} A_h(\rho)\boldsymbol{X} + B(\rho)\hat{\boldsymbol{C}}_h(\rho) & A_h(\rho) + B(\rho)\hat{\boldsymbol{D}}(\rho)C_h(\rho) \\ \hat{\boldsymbol{A}}_h(\rho) & \boldsymbol{Y}A_h(\rho) + \hat{\boldsymbol{B}}(\rho)C_h(\rho) \end{bmatrix}, \tag{6.58}$$

$$\Pi_2^T\mathbb{A}_h\Pi_1 = \begin{bmatrix} (A_h(\rho) + B(\rho)\hat{\boldsymbol{D}}(\rho)C_h(\rho))\boldsymbol{X} & A_h(\rho) + B(\rho)\hat{\boldsymbol{D}}(\rho)C_h(\rho) \\ (\boldsymbol{Y}A_h(\rho) + \hat{\boldsymbol{B}}(\rho)C_h(\rho))\boldsymbol{X} & \boldsymbol{Y}A_h(\rho) + \hat{\boldsymbol{B}}(\rho)C_h(\rho) \end{bmatrix}, \tag{6.59}$$

$$(\mathbb{C}_h + \mathbb{C}_d)\Pi_1 = [J(\rho)\hat{\boldsymbol{C}}_h(\rho) \quad J(\rho)\hat{\boldsymbol{D}}(\rho)C(\rho)], \tag{6.60}$$

$$\mathbb{C}_h\Pi_1 = [J(\rho)\hat{\boldsymbol{D}}(\rho)C_h(\rho)\boldsymbol{X} \quad J(\rho)\hat{\boldsymbol{D}}(\rho)C_h(\rho)], \tag{6.61}$$

$$(\mathbb{K}_h + \mathbb{K}_d)\Pi_1 = [\hat{\boldsymbol{C}}_h(\rho) \quad \hat{\boldsymbol{D}}(\rho)C_h(\rho)],\ \mathbb{K}_h\Pi_1 = [\hat{\boldsymbol{D}}(\rho)C_h(\rho)\boldsymbol{X} \quad \hat{\boldsymbol{D}}(\rho)C_h(\rho)]. \tag{6.62}$$

with the variables substitutions are given in (6.49). Now, we separate the linear and nonlinear terms from equations (6.59), (6.61), and (6.62) as follows:

$$\Pi_2^T\mathbb{A}_h\Pi_1 = \mathbb{A}_l + \mathbb{A}_n[\boldsymbol{X} \ \ 0],\ \mathbb{C}_h\Pi_1 = \mathbb{C}_l + \mathbb{C}_n[\boldsymbol{X} \ \ 0], \text{ and } \mathbb{K}_h\Pi_1 = \mathbb{K}_l + \mathbb{K}_n[\boldsymbol{X} \ \ 0], \tag{6.63}$$

where

$$\begin{aligned} \mathbb{A}_l &= \begin{bmatrix} A_h(\rho)\boldsymbol{X} & A_h(\rho) + B(\rho)\hat{\boldsymbol{D}}(\rho)C_h(\rho) \\ 0 & \boldsymbol{Y}A_h(\rho) + \hat{\boldsymbol{B}}(\rho)C_h(\rho) \end{bmatrix}, \quad \mathbb{A}_n = \begin{bmatrix} B(\rho)\hat{\boldsymbol{D}}(\rho)C_h(\rho) \\ (\boldsymbol{Y}A_h(\rho) + \hat{\boldsymbol{B}}(\rho)C_h(\rho)) \end{bmatrix}, \\ \mathbb{C}_l &= [0 \quad J(\rho)\hat{\boldsymbol{D}}(\rho)C_h(\rho)], \qquad \mathbb{C}_n = J(\rho)\hat{\boldsymbol{D}}(\rho)C_h(\rho), \\ \mathbb{K}_l &= [0 \quad \hat{\boldsymbol{D}}(\rho)C_h(\rho)], \qquad \mathbb{K}_n = \hat{\boldsymbol{D}}(\rho)C_h(\rho). \end{aligned} \tag{6.64}$$

Based on these transformations, we substitute the closed-loop system (6.16) into the relaxed LMI condition (5.61) in section 5.2.4.2 and repeat the same analysis as the previous theorems that leads to following results.

Theorem 6.3.2: *For time-varying delay $h(t) \in \mathcal{H}_0$, positive scalars $\varepsilon_1, \varepsilon_2, \varepsilon_3, \mu_i, \eta, \gamma$ and presence of the $\mathcal{L}_2$-bounded disturbance. If there exist continuously differentiable matrices function $\tilde{P}_1 : \mathcal{U}_p \to \mathbb{S}^{2n}_{++}$, $\hat{\boldsymbol{A}} : \mathcal{U}_p \to \mathbb{R}^{n\times n}$, $\hat{\boldsymbol{B}} : \mathcal{U}_p \to \mathbb{R}^{n\times p}$, $\hat{\boldsymbol{C}}, \hat{\boldsymbol{F}}, \hat{\boldsymbol{F}}_I : \mathcal{U}_p \to \mathbb{R}^{m\times n}$, $\hat{\boldsymbol{D}}, \hat{\boldsymbol{G}}$, $\hat{\boldsymbol{G}}_I : \mathcal{U}_p \to \mathbb{R}^{m\times p}$, $\hat{\boldsymbol{E}} : \mathcal{U}_p \to \mathbb{R}^{m\times n}$, a diagonal matrix function $T : \mathcal{U}_p \to \mathbb{R}^m_{++}$, and matrices $\tilde{P}_2, \tilde{P}_3, \tilde{Q}, \tilde{R} \in \mathbb{R}^{2n\times 2n}$, $\boldsymbol{X}, \boldsymbol{Y} \in \mathbb{S}^n_{++}$, such that the following LMIs are satisfied:*

$$(a).\ \begin{bmatrix} \tilde{P}_1(\rho) + 2\bar{h}\tilde{R} & * & * \\ \tilde{P}_2^T - 2\bar{h}\tilde{R} & \tilde{P}_3 + \frac{1}{\bar{h}}(\tilde{Q} + 2\tilde{R}) & * \\ (\mathbb{G}\Pi_1)_{(i)} & (\mathbb{G}_I\Pi_1)_{(i)} & \eta\overline{u}_i^2 \end{bmatrix} \succ 0, \qquad (b).\ \begin{bmatrix} \boldsymbol{X}(\rho) & \varepsilon_2 I \\ \varepsilon_2 I & \boldsymbol{Y}(\rho) \end{bmatrix} \succeq 0, \tag{6.65}$$

$$\begin{bmatrix}
\Upsilon_{11} & * & * & * & * & * & * & * & * & * & * & * & * \\
\Upsilon_{21} & \Upsilon_{22} & * & * & * & * & * & * & * & * & * & * & * \\
\Upsilon_{31} & \Upsilon_{32} & \Upsilon_{33} & * & * & * & * & * & * & * & * & * & * \\
\Upsilon_{41} & \Upsilon_{42} & \Upsilon_{43} & \Upsilon_{44} & * & * & * & * & * & * & * & * & * \\
\overline{h}\tilde{P}_2^T & \Upsilon_{52} & \Upsilon_{53} & \Upsilon_{54} & -12\tilde{R} & * & * & * & * & * & * & * & * \\
\Upsilon_{61} & \Upsilon_{62} & \Upsilon_{63} & \Upsilon_{64} & \Upsilon_{65} & -2T(\rho) & * & * & * & * & * & * & * \\
\Upsilon_{71} & 0 & 0 & 0 & 0 & 0 & -\gamma I_d & * & * & * & * & * & * \\
0 & \Upsilon_{82} & \Upsilon_{83} & \Upsilon_{84} & 0 & \Upsilon_{86} & \mathbb{D}_2 & -\gamma I_r & * & * & * & * & * \\
\tilde{L} & 0 & 0 & 0 & 0 & 0 & 0 & 0 & -\tilde{L} & * & * & * & * \\
\overline{h}\tilde{R} & 0 & 0 & 0 & 0 & 0 & 0 & 0 & 0 & -\tilde{R} & * & * & * \\
\varepsilon_1\Pi_1^T\Pi_2 & 0 & 0 & 0 & -\varepsilon_1\tilde{P}_2 & 0 & 0 & 0 & -\varepsilon_1\tilde{L} & -\varepsilon_1\overline{h}\tilde{R} & -\tilde{P}_1(\rho) & * & * \\
\Upsilon_{121} & 0 & 0 & 0 & 0 & \Upsilon_{126} & 0 & \Upsilon_{128} & 0 & 0 & 0 & -\varepsilon_3^{-1}I_n & * \\
0 & 0 & 0 & \Upsilon_{134} & 0 & 0 & 0 & 0 & 0 & 0 & 0 & 0 & -\varepsilon_3 I_n
\end{bmatrix} \prec 0, \tag{6.66}$$

where $i = 1, 2 \ldots m$,

$$\begin{aligned}
\Upsilon_{11} &= -\{\Pi_2^T\Pi_1\}^S \\
\Upsilon_{21} &= (\Pi_2^T\mathbb{A}\Pi_1)^T + \tilde{P}_1(\rho), \\
\Upsilon_{31} &= (\Pi_2^T(\mathbb{A}_h + \mathbb{A}_d)\Pi_1)^T, \\
\Upsilon_{41} &= \tfrac{\sqrt{7}}{2}\delta_m\mathbb{A}_l^T, \\
\Upsilon_{61} &= (\Pi_2^T\mathbb{B}_1 T(\rho))^T, \\
\Upsilon_{71} &= (\Pi_2^T\mathbb{B}_2)^T, \\
\Upsilon_{121} &= \tfrac{\sqrt{7}}{2}\delta_m\mathbb{A}_n^T, \\
\Upsilon_{22} &= \tilde{P}_2^S \pm \textstyle\sum_{j=1}^{N_p}\nu_j(\partial\tilde{P}_1(\rho)/\partial\rho_j) + \tilde{Q} - 4\tilde{R} - \varepsilon_1^2\tilde{P}_1(\rho), \\
\Upsilon_{32} &= -(1-\mu)\tilde{P}_2^T - 2\tilde{R}, \\
\Upsilon_{42} &= -\tfrac{\sqrt{7}}{2}\delta_m((1-\mu)\tilde{P}_2^T + 2\tilde{R})^T, \\
\Upsilon_{52} &= \tilde{P}_3 + \tfrac{6}{h}\tilde{R}, \\
\Upsilon_{62} &= (\mathbb{K} - \mathbb{G})\Pi_1, \\
\Upsilon_{82} &= \mathbb{C}\Pi_1, \\
\Upsilon_{33} &= -(1-\mu)\tilde{Q} - 4\tilde{R}, \\
\Upsilon_{43} &= -\tfrac{\sqrt{7}}{2}\delta_m((1-\mu)\tilde{Q} + 4\tilde{R}), \\
\Upsilon_{53} &= -(1-\mu)\tilde{P}_3 + \tfrac{6}{h}\tilde{R}, \\
\Upsilon_{63} &= (\mathbb{K}_h + \mathbb{K}_d)\Pi_1, \\
\Upsilon_{83} &= (\mathbb{C}_h + \mathbb{C}_d)\Pi_1, \\
\Upsilon_{44} &= -\tfrac{7}{4}\delta_m^2((1-\mu)\tilde{Q} + 4\tilde{R}) - \tilde{L}, \\
\Upsilon_{54} &= -\tfrac{\sqrt{7}}{2}\delta_m((1-\mu)\tilde{P}_3 - \tfrac{6}{h}\tilde{R}), \\
\Upsilon_{64} &= \tfrac{\sqrt{7}}{2}\delta_m\mathbb{K}_l, \\
\Upsilon_{84} &= \tfrac{\sqrt{7}}{2}\delta_m\mathbb{C}_l, \\
\Upsilon_{134} &= [\boldsymbol{X} \;\; 0_n], \\
\Upsilon_{65} &= -\mathbb{G}_I\Pi_1, \\
\Upsilon_{86} &= \mathbb{D}_1 T(\rho), \\
\Upsilon_{126} &= \tfrac{\sqrt{7}}{2}\delta_m\mathbb{K}_n^T, \\
\Upsilon_{128} &= \tfrac{\sqrt{7}}{2}\delta_m\mathbb{C}_n^T,
\end{aligned}$$

with the substitutions are defined in (6.42)-(6.47) *and* (6.58)-(6.64)*. Then, the controller gains are given by*

$$\begin{aligned}
E_c(\rho) &= N^{-1}(\hat{\boldsymbol{E}}(\rho)T(\rho)^{-1} + \boldsymbol{Y}B(\rho)), \\
D_c(\rho) &= \hat{\boldsymbol{D}}(\rho), \\
C_c(\rho) &= (\hat{\boldsymbol{C}}(\rho) - \hat{\boldsymbol{D}}(\rho)C(\rho)\boldsymbol{X})M^{-T}, \\
C_{dc}(\rho) &= (\hat{\boldsymbol{C}}_h(\rho) - \hat{\boldsymbol{D}}(\rho)C_h(\rho)\boldsymbol{X})M^{-T}, \\
A_c(\rho) &= N^{-1}(\hat{\boldsymbol{A}}(\rho) - \hat{\boldsymbol{B}}(\rho)C(\rho)X - \boldsymbol{Y}B(\rho)\hat{\boldsymbol{C}}(\rho) - \boldsymbol{Y}(A(\rho) - B(\rho)D(\rho)C(\rho))\boldsymbol{X})M^{-T}, \\
A_{dc}(\rho) &= N^{-1}(\hat{\boldsymbol{A}}_h(\rho) - \hat{\boldsymbol{B}}(\rho)C(\rho)X - \boldsymbol{Y}B(\rho)\hat{\boldsymbol{C}}_h(\rho) - \boldsymbol{Y}(A_h(\rho) - B(\rho)D(\rho)C_h(\rho))\boldsymbol{X})M^{-T}, \\
B_c(\rho) &= N^{-1}(\hat{\boldsymbol{B}}(\rho) - \boldsymbol{Y}B(\rho)\hat{\boldsymbol{D}}(\rho)),
\end{aligned} \tag{6.67}$$

ensure the delay-dependent stability for the saturated LPV system (6.16) *from initial condition belongs to DoA given by*

$$\mathcal{X}_0 = \left\{ \psi(\theta) \in \mathcal{C}^1\left([-\overline{h},0],\mathbb{R}^n\right) \;\middle|\; \begin{array}{r} \eta_0^{-1} = \kappa_1^2 \cdot \left((1+\overline{h}^2)\overline{\lambda}(\tilde{\Pi}^{-T}\tilde{P}\tilde{\Pi}^{-1}) + \overline{h}\cdot\overline{\lambda}\left(\Pi_1^{-T}\tilde{Q}\Pi_1^{-1}\right)\right) \\ +\kappa_2^2\,\frac{\overline{h}^3}{2}\cdot\overline{\lambda}(\Pi_1^{-T}\tilde{R}\Pi_1^{-1}) \le \eta^{-1} \end{array} \right\},$$

such that

(1) *for bounded disturbance* $w(t)$, *the trajectories of closed-loop system remain in the enclosed domain relating to design performance index* γ *and upper bound* η^{-1}.
(2) *for* $w(t)=0$, *the contractive domain* (6.5) *is a region of asymptotical stability.*

with $\tilde{\Pi} := diag\{\Pi_1,\Pi_1\}, \tilde{P} = \begin{bmatrix} \tilde{P}_1(\rho) & \tilde{P}_2 \\ * & \tilde{P}_3 \end{bmatrix} \succ 0$, *and* κ_1,κ_2 *are bounds of initial conditions.*

Proof.

Substituting closed-loop system (6.16) into stability condition (5.61) of Theorem 5.2.3, with the slack-variable matrix W in (6.41) replaces the slack-variable X. Then, performing a congruence transformation with respect to matrix

$$diag\{\Pi_1^T,\Pi_1^T,\Pi_1^T,\Pi_1^T,\Pi_1^T,T^{-1},\Pi_1^T,\Pi_1^T,I,I,\Pi_1^T\},$$

with the variable substitutions:

$$\begin{array}{llll} W\Pi_1 \leftarrow \Pi_2, & \tilde{Q} \leftarrow \Pi_1^T Q \Pi_1, & \tilde{P}_2 \leftarrow \Pi_1^T P_2 \Pi_1, & \dot{\tilde{P}}_1(\rho) \leftarrow \Pi_1^T \dot{P}_1(\rho)\Pi_1, \\ \tilde{P}_1(\rho) \leftarrow \Pi_1^T P_1(\rho)\Pi_1, & \tilde{R} \leftarrow \Pi_1^T R \Pi_1, & \tilde{P}_3 \leftarrow \Pi_1^T P_3 \Pi_1, & \left|\dot{\tilde{P}}_1(\rho)\right| \le \sum\nolimits_j \nu_j \left(\partial \tilde{P}_{1,j}(\rho)/\partial\rho_j\right), \end{array}$$

that results in the following condition

$$\Upsilon(\rho) + \mathcal{P}^T\mathcal{Q} + \mathcal{Q}^T\mathcal{P} \prec 0, \tag{6.68}$$

where

$$\Upsilon(\rho) = \begin{bmatrix} \Upsilon_{11} & * & * & * & * & * & * & * & * & * & * \\ \Upsilon_{21} & \Upsilon_{22} & * & * & * & * & * & * & * & * & * \\ \Upsilon_{31} & \Upsilon_{32} & \Upsilon_{33} & * & * & * & * & * & * & * & * \\ \Upsilon_{41} & \Upsilon_{42} & \Upsilon_{43} & \Upsilon_{44} & * & * & * & * & * & * & * \\ \overline{h}\tilde{P}_2^T & \Upsilon_{52} & \Upsilon_{53} & \Upsilon_{54} & -12\tilde{R} & * & * & * & * & * & * \\ \Upsilon_{61} & \Upsilon_{62} & \Upsilon_{63} & \Upsilon_{64} & \Upsilon_{65} & -2T(\rho) & * & * & * & * & * \\ \Upsilon_{71} & 0 & 0 & 0 & 0 & 0 & -\gamma I_d & * & * & * & * \\ 0 & \Upsilon_{82} & \Upsilon_{83} & \Upsilon_{84} & 0 & \Upsilon_{86} & \mathbb{D}_2 & -\gamma I_r & * & * & * \\ \tilde{L} & 0 & 0 & 0 & 0 & 0 & 0 & 0 & -\tilde{L} & * & * \\ \overline{h}\tilde{R} & 0 & 0 & 0 & 0 & 0 & 0 & 0 & 0 & -\tilde{R} & * \\ \varepsilon_1\Pi_1^T\Pi_2 & 0 & 0 & 0 & -\varepsilon_1\tilde{P}_2 & 0 & 0 & 0 & -\varepsilon_1\tilde{L} & -\varepsilon_1\overline{h}\tilde{R} & -\tilde{P}_1(\rho) \end{bmatrix},$$

$$\mathcal{P} = \begin{bmatrix} \frac{\sqrt{7}}{2}\delta_m\mathbb{A}_n^T & 0_{n\times 2n} & 0_{n\times 2n} & 0_{n\times 2n} & 0_{n\times 2n} & \frac{\sqrt{7}}{2}\delta_m\mathbb{K}_n^T & 0_{n\times 2n} & 0_{n\times 2n} & 0_{n\times d} & \frac{\sqrt{7}}{2}\delta_m\mathbb{C}_n^T & 0_{n\times 2n} \end{bmatrix},$$

$$\mathcal{Q} = \begin{bmatrix} 0_{n\times 2n} & 0_{n\times 2n} & 0_{n\times 2n} & \Upsilon_{134} & 0_{n\times 2n} & 0_{n\times m} & 0_{n\times 2n} & 0_{n\times 2n} & 0_{n\times d} & 0_{n\times r} & 0_{n\times 2n} \end{bmatrix}.$$

Applying Young's inequality for above PLMI condition, then using Schur to rearrange the matrix inequality that entails in the stability condition (6.66). The rest follows the same lines as the one of Theorem 6.3.1. □

It can be noticed the difference between the analysis of a dynamic output controller with an approximated delay and a state feedback controller. Where the exact-delay value is

still *stuck* in the controller structure (6.57). We could assume a simplification of output measurement, but the hysteresis also affects the measured signals in practice. Thus, system (6.15) presents a more general form. But, to deal with the concave problem, we have to use Young's inequality for condition (6.68), which has limitation.

6.3.3. *Optimization problem – Maximization Domain of Attraction*

As shown in the results section 6.2.4, the minimum values of attenuation criterion can be obtained by directly optimizing γ in PLMI stabilization conditions. The maximum allowable value of the delay margin $\overline{h}$ can be found by the iterative sweeping technique. It should note that both approaches carry out with preselected values of $\eta, \eta_0, \gamma,$ or $\overline{h}$, etc. As we discussed in section 6.2.3, the estimates of the domain of attraction are concerned with the coupling of the variable matrices in the conditions. In which minimizing $\tilde{P}, \tilde{Q}, \tilde{R}$, concomitant with maximizing $\tilde{X}$ makes the global optimization sometimes not converge to the correct solution. Nonetheless, so far, the recent methods have solved the optimization problem of the stabilization condition according to this approach. By substituting Π_1 in place of X and slightly modifies Problem 6.2.1, we have the following result.

Problem 6.3.1. *Given delay space* $h(t) \in \mathcal{H}_0$, *compact sets of parameters* $\rho(t) \in \mathcal{U}_p$, *and the initial condition definitions* $\mathcal{X}_0$. *Find the variable decision matrices* $\Pi_1, \tilde{P}, \tilde{Q}, \tilde{R}$ *such that the following statement satisfies*:

$$\textbf{Minimize } f(\beta) = (1+\overline{h}^2)\beta_1 + \overline{h}\beta_2 + 0.5\overline{h}^3\beta_3 + \chi\beta_4 \tag{6.69}$$

subject to (6.50), (6.51), $\tilde{P} \prec \beta_1 I$, $\tilde{Q} \prec \beta_2 I$, $\tilde{R} \prec \beta_3 I$, and

$$\begin{bmatrix} \beta_4 I_{2n} & I_{2n} & 0_{2n} \\ * & 2\alpha\Pi_2^T\Pi_1 & \alpha\Pi_2^T \\ * & * & I_{2n} \end{bmatrix} \succeq 0. \tag{6.70}$$

for pre-selected scalar $\alpha \in \mathbb{R}_{++}$, *weighting scalar* $\chi \in \mathbb{R}_{++}$.
With $\tilde{Q}, \tilde{R} \in \mathbb{S}_{++}^{2n}$, $\tilde{P}(\rho) \in \mathbb{S}_{++}^{4n}$, and $\Pi_1 \in \mathbb{R}^{2n}$.

Condition (6.70) is interpreted similar to condition (6.31), with expansions:

$$(\Pi_1 - \alpha\Pi_2)^T(\Pi_1 - \alpha\Pi_2) \succeq 0, \text{ infers} \tag{6.71}$$

$$(\Pi_1^T\Pi_1)^{-1} \preceq (2\alpha\Pi_2^T\Pi_1 - \alpha^2\Pi_2^T\Pi_2)^{-1} \preceq \beta_4 I, \tag{6.72}$$

The methodology avoids concave-problem and singular matrix forms. But, it has a drawback in approaching the dynamic output controller stabilization. That will be revealed in section 6.3.4.2.

6.3.4. *Example*

The stabilization implementations analyzed in this chapter use the generalized sector bounding condition to enforce the control saturation. Nevertheless, the saturation constraints set for the state feedback controller in Theorem 6.2.2, distinguishes from the dynamic output controller in Theorem 6.3.1. What lies in the feedback signal of the deadzone function $\Phi(u)$ considered the input of the controller system (6.15). And dynamic gain $E_c(\rho)$ plays the role of the saturated compensation and enhances the performance of

the closed-loop system.

In addition, most of the work on developing stabilization conditions with delay and actuator saturation is generally applied to LTI systems and employs a quadratic Lyapunov function. In section 6.3.4.1, the parameter-dependent stabilization conditions are addressed for an LPV time-delay system. Then, the comparison of gain-scheduled controllers, and the maximizing the estimation of DoA concern to the parameter-dependent Lyapunov function will be provided in section 6.3.4.2.

6.3.4.1. *Memory saturated controller synthesis*

Example 6.3.1: Let's introduce the following system modified from (Zhang & Grigoriadis, 2005):

$$\begin{aligned}\dot{x}(t) &= \begin{bmatrix} 2 & 1+0.2\sin(t) \\ -2 & -3+0.1\sin(t)) \end{bmatrix} x(t) + \begin{bmatrix} 0.2\sin(t) & 0.1 \\ -0.2+0.1\sin(t) & 2.2 \end{bmatrix} x(t-h(t)) \\ &\quad + \begin{bmatrix} 1+0.2\sin(t) \\ 2+0.1\sin(t) \end{bmatrix} u(t) + \begin{bmatrix} 0.2 \\ 0.2 \end{bmatrix} w(t), \\ y(t) &= \begin{bmatrix} 1-0.2\sin(t) & 0 \end{bmatrix} x(t) + \begin{bmatrix} 0.2 & -0.2+0.1\sin(t) \end{bmatrix} x(t-hh(t)), \\ z(t) &= \begin{bmatrix} 0 & 2 \\ 2 & -1 \end{bmatrix} x(t) + \begin{bmatrix} 0.2 \\ 0.1\sin(t) \end{bmatrix} u(t). \end{aligned} \tag{6.73}$$

where $\overline{u} = 5$, and parameter $\rho(t) = \sin(t) \in [-1, 1]$, $|\dot{\rho}(t)| \in [0, 1]$. The simulation starts from an initial condition $x(0) = [4.2 \quad -3.8]^T$, with a $\mathcal{L}_2$-Bounded disturbance:

$$\mathcal{W}(w(t), \sigma) := \{w(t) = a\sin(t) \mid \|w(t)\|_{\mathcal{L}_2}^2 < \sigma^{-1}\}, \tag{6.74}$$

The parameter-dependent stabilization conditions of Theorem 6.2.2 and Theorem 6.3.1 grid over $N_p = 41$ points uniformly spaced $[-1, 1]$. Then, the linear programming problems are handled by semidefinite program, cone program Yalmip (Lofberg, 2004) with solver Mosek (Andersen et al., 2003).

Following the definition of domain of attraction $\mathcal{X}_0$, provides the maximal values of η_0^{-1} varying in the range $[17.4748, \ 20.8667]$ corresponding to $\rho(t)$ discretizes uniformly 41 points of uniformly spaced from $[-1, 1]$. Since $\eta_0^{-1} \ll \eta_{opt}^{-1} - \gamma\sigma^{-1}$, the stability system ensures even surge the amplitude of the disturbance within the allowable level (e.g., tunes up $a = 1 \rightarrow 30$). On the contrary, if the initial conditions do not belong to $\mathcal{X}_0$, then the trajectories of the closed-loop system won't leave the RAS corresponding to the optimal value η_{opt}^{-1}. It is noteworthy that compared with the results in section 6.2.4.1 (optimizing γ), the scheduling gains (6.75) are smaller. The system trades between performance and stability in the size criterion optimization (e.g., minimizing eta). As explained in Chapter 4, since the linear response region expands, the feedback control signal rarely exceeds the saturation threshold. These properties will illustrate in the next figures.

Saturated State Feedback Controller with Approximate Memory

Solving the stabilization condition of Theorem 6.2.2 with $\overline{h} = 1, \mu = 0.5, \delta_m = 0, \gamma = 2.5$, we attain an optimization value $\eta_{opt}^{-1} = 332.6817$, with the stabilizing gains:

$$
\begin{aligned}
K(\rho)|_{\delta_m=0.0} &= \begin{bmatrix} -3.3989 + 0.7881\rho(t) - 0.5155\rho(t)^2 \\ -0.8972 - 0.0118\rho(t) - 0.0913\rho(t)^2 \end{bmatrix}, \\
K_d(\rho)|_{\delta_m=0.0} &= \begin{bmatrix} 0.1521 - 0.2451\rho(t) + 0.0380\rho(t)^2 \\ -0.1771 + 0.0438\rho(t) - 0.0261\rho(t)^2 \end{bmatrix}.
\end{aligned} \tag{6.75}
$$

Where the decision variable matrices of the Lyapunov–Krasovskii functional:

$$
\begin{aligned}
P_1(\rho) &= \begin{bmatrix} 0.0347 - 0.0010\rho(t) + 0.0072\rho(t)^2 & 0.0076 - 0.0030\rho(t) + 0.0410\rho(t)^2 \\ 0.0076 - 0.0030\rho(t) + 0.0410\rho(t)^2 & 0.8352 - 0.0040\rho(t) + 0.2373\rho(t)^2 \end{bmatrix}, \\
P_2 &= \begin{bmatrix} -0.0118 & 0.0081 \\ 0.0081 & -0.2387 \end{bmatrix}, \qquad P_3 = \begin{bmatrix} 0.0076 & -0.0098 \\ -0.0098 & 0.1452 \end{bmatrix}, \\
Q &= \begin{bmatrix} 0.0169 & -0.0726 \\ -0.0726 & 0.5489 \end{bmatrix}, \qquad R = \begin{bmatrix} 0.0054 & -0.0203 \\ -0.0203 & 0.1007 \end{bmatrix}.
\end{aligned} \tag{6.76}
$$

Memory Saturated Dynamic Output Controller

Solving the stabilization condition of Theorem 6.3.1 with $\bar{h} = 1$, $\mu = 0.5$, and $\gamma = 2.5$, we reach an optimal value $\eta_{opt}^{-1} = 41.0729$, and obtain the slack-matrices:

$$
\begin{aligned}
X &= \begin{bmatrix} 0.0677 & 0.0042 \\ 0.0042 & 1.4025 \end{bmatrix}, \qquad Y = \begin{bmatrix} 23.0542 & -8.5374 \\ -8.5374 & 18.4990 \end{bmatrix}, \text{ and} \\
M^T &= \begin{bmatrix} -0.5708 & 0.9914 \\ 0.4942 & 1.0771 \end{bmatrix}, \qquad N = \begin{bmatrix} 5.8257 & 5.6638 \\ -11.6309 & -12.4189 \end{bmatrix}.
\end{aligned}
$$

With the PD matrix variables:

$$
\begin{aligned}
\hat{A}(\rho) &= \begin{bmatrix} -0.2591 + 0.1705\rho(t) - 0.3174\rho(t)^2 & -1.5847 + 0.0573\rho(t) + 0.1494\rho(t)^2 \\ -1.5847 + 0.0573\rho(t) + 0.1494\rho(t)^2 & -3.4808 + 0.8396\rho(t) + 0.5230\rho(t)^2 \end{bmatrix}, \\
\hat{A}_h(\rho) &= \begin{bmatrix} -0.7610 - 0.0419\rho(t) + 0.2293\rho(t)^2 & 1.0004 + 0.1539\rho(t) - 0.0758\rho(t)^2 \\ 1.0004 + 0.1539\rho(t) - 0.0758\rho(t)^2 & 1.6823 + 0.3610\rho(t) - 0.2280\rho(t)^2 \end{bmatrix}, \\
\hat{B}(\rho) &= \begin{bmatrix} -146.5727 - 24.7124\rho(t) - 5.9875\rho(t)^2 \\ 81.1942 + 8.7893\rho(t) + 1.2349\rho(t)^2 \end{bmatrix}, \\
\hat{C}(\rho) &= \begin{bmatrix} -0.345 - 0.0137\rho(t) - 0.0577\rho(t)^2 & -1.6326 - 0.0504\rho(t) - 0.0951\rho(t)^2 \end{bmatrix}, \\
\hat{C}_h(\rho) &= \begin{bmatrix} -0.0002 + 0.0009\rho(t) + 0.0029\rho(t)^2 & -0.1322 + 0.0203\rho(t) + 0.0014\rho(t)^2 \end{bmatrix}, \\
\hat{D}(\rho) &= -3.8703 + 0.1108\rho(t) - 0.3005\rho(t)^2, \\
\hat{E}(\rho) &= \begin{bmatrix} -0.3074 - 0.0914\rho(t) + 0.0178\rho(t)^2 \\ -0.0042 + 0.2330\rho(t) - 0.0678\rho(t)^2 \end{bmatrix},
\end{aligned} \tag{6.77}
$$

The dynamic controller gains schedule online consistent with the expressions given in (6.49). From the allowable set of the initial conditions, we can observe from Figure 6-3 that the control feedback signals exceed the saturation threshold from the 0th to the 1st second. The state feedback controller continues to surpass the control limit from the 3.5rd to the 5.5th second. That can be referred to as the states of the feedback control system in Figure 6-2. If there is no saturation bound, then the system will converge asymptotically

at this moment.

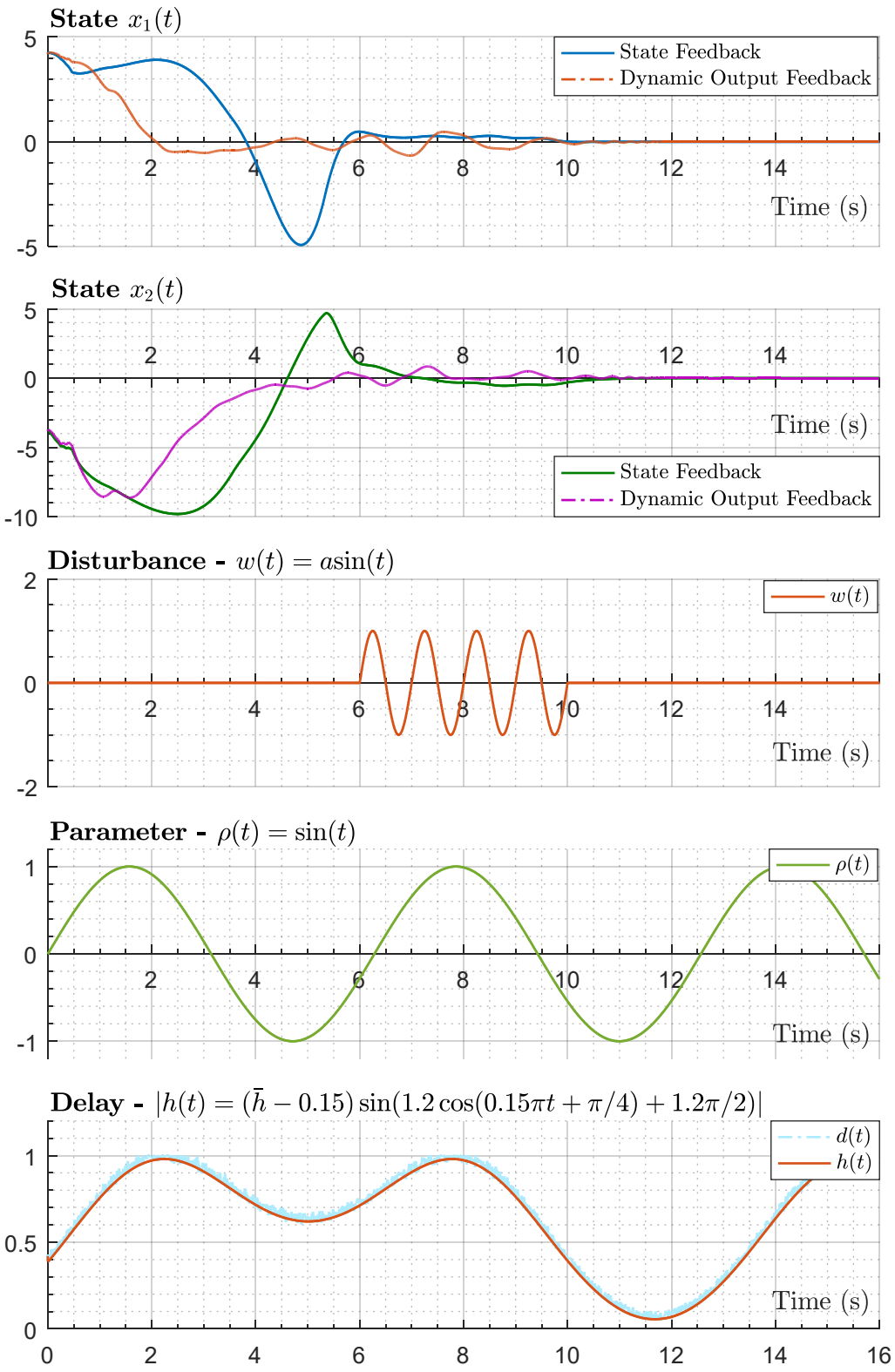

Figure 6-2. *The evolutions of the LPV time-delay system regulate by saturated state feedback and dynamic output feedback controllers.*

The evolutions of the system state regulated by the state feedback controller and the dy-

namic output controller perform in Figure 6-2. The behaviors of the dynamic system governed by state feedback controller are *underdamped* (in comparison to the dynamic output feedback controller). In this example, an exchange between system performance and the set of the admissible initial conditions could deduce from expression: $\eta_0^{-1} + \gamma\sigma^{-1} \leq \eta_{opt}^{-1}$. is pre-set for both theorems, and a disturbance input $w(t) = \sin(t)$ effects from the 6^{th} to the 10^{th} second. Explicitly, both LPV time-delay systems ensure stable asymptotes consistent with the design values.

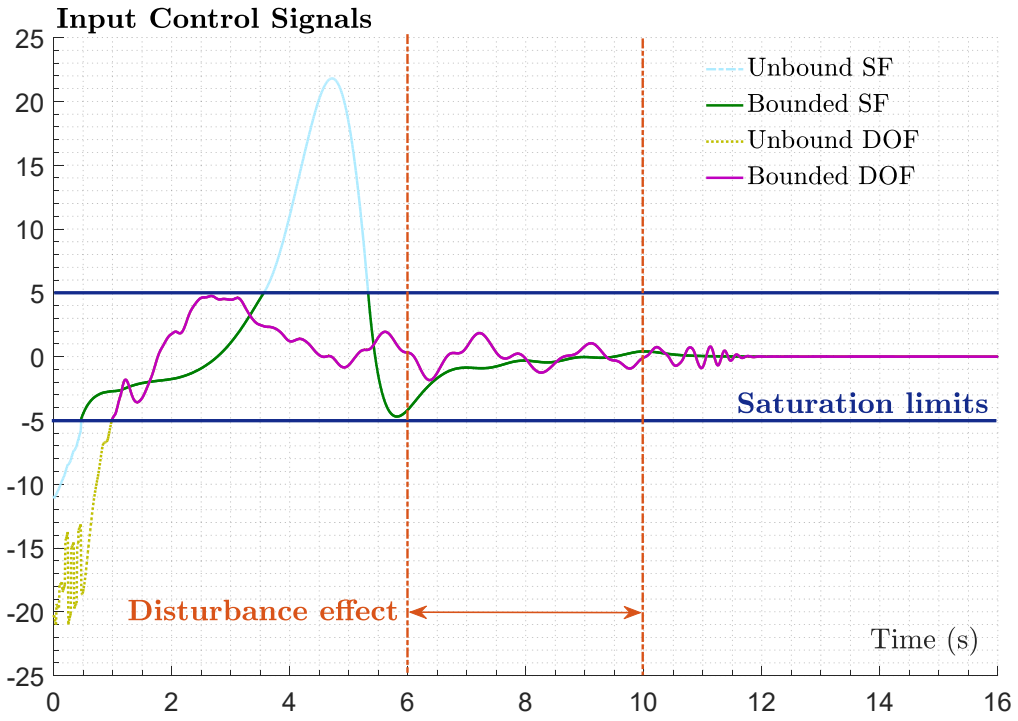

Figure 6-3. *The responses of the stabilizing gain-scheduling controllers solved by Theorem* 6.2.2, *and Theorem* 6.3.1 *corresponding to saturation limit* $\bar{u} = 5$, *with* $\bar{h} = 1, \mu = 0.5,$ and $\gamma = 2.5$.

The time-varying delay expressed like the one in Eqs. (6.36) and the approximate delay are presented in the bottom frame of Figure 6-2. The feedback controller gains (6.75) with an uncertain delay value obtained from the solution of Theorem 6.2.2. Besides, the scheduling gains of the dynamic control system (6.52) are indirectly found from the variable matrices (6.77), which attain from the feasible solution of Theorem 6.3.1. The results demonstrate the effectiveness of the proposed method with the guarantee of local stability for the delayed LPV system respect to the saturated constraints. It should note that in practice, it is difficult to reach all states (cause the limitations of measurement, the effect of delay on measurement output, etc.). Therefore, the approach of Theorem 6.3.1 shows more practical significance.

6.3.4.2. *Optimization Problems*

We deliver a comparison of the minor axis maximization of the ellipsoid η, the minimization of disturbance attenuation index γ, the maximization of the upper bounds of the

delay, and the maximization of the set of admissible initial conditions $\mathcal{X}_0(\eta_0^{-1})$. The comparison between the two theorems are detailed in Table 6.3.

As can be easily visualized, Theorem 6.2.2 dominates Theorem 6.3.1 in all optimization categories. From the estimation of RAS, the rejection disturbance criterion or the maximum allowable value of the delay are all better. It is reasonable because the stabilizability synthesis of the state feedback controller always attains the best relaxation compared to the output feedback controller. It should note that the difficulty of optimization problems increases from categories 1 to 4. In which the optimizations of η and γ could achieve directly from the stabilization conditions. And the maximum delay is solved by an incremental loop algorithm. But, maximizing the set of the admissible initial conditions must meet the satisfaction of Problem 6.2.1 and Problem 6.3.1, respectively, combines with the stabilization condition of Theorem 6.2.2 and Theorem 6.3.1.

Table 6.3. *Multi-criteria optimization*.

Delay-Dependent Stabilization				
Example 6.3.1	$\bar{h}=1.0 \quad \gamma=2.5$ $\mu=0.5$	$\bar{h}=1.0 \quad \eta^{-1}=10$ $\mu=0.5$	$\mu=0.5 \quad \eta^{-1}=10$ $\gamma=2.5$	$\bar{h}=1.0 \quad \eta^{-1}=40$ $\mu=0.5 \quad \gamma=2.5$
	η_{opt}^{-1}	γ_{opt}	$\bar{h}$	$\kappa_1=\kappa_2$
Theorem 6.2.2	332.6817	0.4852	2.8908	0.7740
Theorem 6.3.1	41.0729	2.0741	1.0612	0.2985
0	1	2	3	4

Theorem 6.2.2: *State Feedback Controller*; Theorem 6.3.1: *Dynamic Output Feedback Controller*.

Let's recall the upper bound expression of the initial condition (6.21) combined with the analysis of the stabilization with and without the influence of external disturbance (6.13)-(6.14), we have:

$$V(0)+\gamma\|w(t)\|_{\mathcal{L}_2}^2 \le \kappa_1^2((1+\bar{h}^2)\bar{\lambda}(\tilde{X}^{-T}\tilde{P}\tilde{X}^{-1})+\bar{h}\cdot\bar{\lambda}(X^{-T}\tilde{Q}X^{-1}))+\kappa_2^2\tfrac{\bar{h}^3}{2}\cdot\bar{\lambda}(X^{-T}\tilde{R}X^{-1})+\gamma\sigma^{-1} \le \eta^{-1}.$$

The optimal values provided in catalog 4 of Table 6.3 is derived from the expression:

$$\kappa_1=\kappa_2 \le \sqrt{\frac{\eta^{-1}-\gamma\sigma^{-1}}{((1+\bar{h}^2)\bar{\lambda}(\tilde{X}^{-T}\tilde{P}(\rho)\tilde{X}^{-1})+\bar{h}\cdot\bar{\lambda}(X^{-T}\tilde{Q}X^{-1}))+\frac{\bar{h}^3}{2}\cdot\bar{\lambda}(X^{-T}\tilde{R}X^{-1})}}. \quad (6.78)$$

More precisely, solving the optimization Problem 6.2.1, we obtain the estimation of the domain of attraction is the circle with a diameter of 0.7709. As shown in Figure 6-4.*a*, all the trajectories of the closed-loop system from the initial conditions within the disc will asymptotically convergence to origin. Figure 6-4.*b* displays the convergence region from the initial conditions inside the elliptical domain, where the parameter-dependent ellipsoid $\mathcal{E}(P(\rho),\eta)$ is defined by:

$$\eta\varsigma(t)^T P(\rho)\varsigma(t) \le \eta V(t) \le 1. \quad (6.79)$$

with $V(t)$ given in (6.5) and $P(\rho)=\begin{bmatrix} P_1(\rho) & P_2 \\ * & P_3 \end{bmatrix}$, $\varsigma(t)=\left[x(t)^T \quad \int_{t-h(t)}^{t} x(\theta)^T d\theta\right]^T$.

In the simulation with the feedback controller (relating to Theorem 6.2.2, illustrating in

Figure 6-4.*a&b*), we chose $x(0) \in [-10,10]\times[-30,30]$, and $\psi(\theta) = 0, \theta \in [-h(0),0]$. In contrast to Chapter 4, the characterization of the asymptotic stable domain of an LPV time-delay system meets difficulties with the extended vector and the initial condition. It can notice that the level set of ellipsoids (6.79) could not completely cover the behavior of $V(t)$ (cause that does not characterize the integrals). So, it could not accurately describe the domain of attraction. Specifically, some initial conditions outside the ellipsoidal set, such as $x(0) = (6,-22),\ (7,-20),\ (8,-18)\ldots$will *converge* to origin.

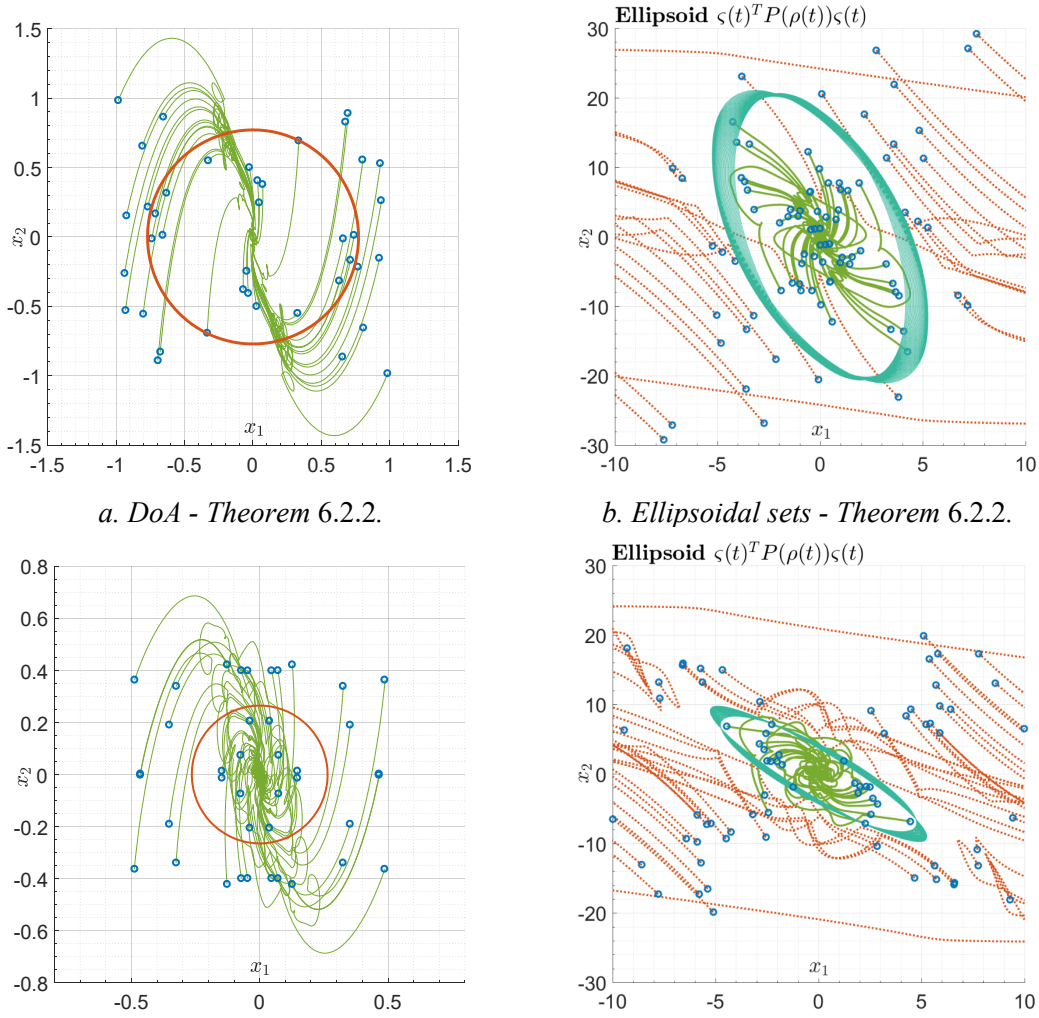

a. DoA - Theorem 6.2.2. *b. Ellipsoidal sets - Theorem* 6.2.2.

c. DoA - Theorem 6.3.1. *d. Ellipsoidal sets - Theorem* 6.3.1.

Figure 6-4. *Example 6.3.1 — designed controllers. The estimates of region of stability using sector nonlinearities approaches with different criteria. Asymptotically stabilized* (*green solid-lines*) *and destabilized trajectories* (*brown dotted-lines*) *of the closed-loop systems from the initial conditions* (o).

The estimates of the domain of attraction presented in Figure 6-4.*c&d* are the solution of solving Theorem 6.3.1&Problem 6.3.1. It is apparent to recognize that the region of attraction of the closed-loop system regulated by the state feedback controller is larger than that of the dynamic output feedback controller.

The optimal results of Theorem 6.3.1 given in Table 6.3 are approached similarly to Theorem 6.2.2. However, inequality (6.70) contains a quasi-convex form, if Π_2 is present in

this condition. As a result, minimizing the estimation of the set of the admissible initial conditions leads N to be a singular matrix. To avoid this, based on the relationship $YX + NM^T = I_n$, we propose two solutions:

- Choose a small value of η such that the stability conditions of Theorem 6.3.1 to have a solution, then use this matrix N to solve the optimal Problem 6.3.1.
- Use the optimal value of η_{opt} to calculate the upper bound of η_0^{-1}, then indirectly obtains the boundary of the DoA estimation domain by

$$\kappa_1 = \kappa_2 \le \sqrt{\frac{\eta_{opt}^{-1} - \gamma\sigma^{-1}}{((1+\bar{h}^2)\bar{\lambda}(\tilde{\Pi}_1^{-T}\tilde{P}(\rho)\tilde{\Pi}_1^{-1}) + \bar{h}\cdot\bar{\lambda}(\Pi_1^{-T}\tilde{Q}\Pi_1^{-1})) + \frac{\bar{h}^3}{2}\cdot\bar{\lambda}(\Pi_1^{-T}\tilde{R}\Pi_1^{-1})}}. \quad (6.80)$$

Using the second approach, we obtain a disc of DOA with a diameter of 0.2985 and an ellipsoidal domain shown in Figure 6-4.*c*&*d*.

6.4. Conclusions

We have addressed the feedback control laws to stabilize the LPV time-delay systems with the saturated actuators. The control analysis and synthesis with the state feedback and the dynamic output feedback structure is provided. Where the nonlinearities and concave problems in the stabilization conditions handle effectively by using a simple transformation. The multi-criteria optimizations implement both memoryless, approximation delay controllers subject to the control saturation. The results show an enhancement of system performance and robust stability against the effect of the external disturbance and time-varying parameters.

Chapter 7.

Conclusions and Perspectives

Summary

Through the contents discussed in this thesis, there are main contributions which are briefly summarized by the following conclusions:

- PLMI conditions have been considered to solve the analysis and design problems for LPV and quasiLPV systems. The derived conditions have a general formulation which is convenient for various design purpose. Some numerical results in Chapter 2 have given to illustrate the advantage this methodology.

- By considering the scaling structure, the non-convex optimization related to the robust controller design is linearized into the multiple-convex optimization problem through an iterative algorithm CCL. The relaxation results given in Chapter 3 have shown the effectiveness of the proposed method.

- In Chapter 4, the control synthesis conforming to saturation constraints is investigated to address the stabilization of the feedback controller design for saturated LPV systems. The derived PLMI formulations allow relaxation for an individual implementation. The simulation results emphasize the reducing conservativeness of the presented condition compared to the existing works and provide an LPV analysis tool for gain-scheduling feedback controller subject to saturation constraints.

- The following chapter has focused on the stability of time-delay systems based on Lyapunov-Krasovskii functional. This chapter is a slightly different construction in which an appropriate stability analysis method is addressed for the LPV delay systems before proceeding with the stabilization analysis. The comparisons presented in chapter 5 demonstrate the less conservative results of refined LKF conditional forms using expanded vectors. The best results are obtained by the investigated method compared with the recent works in the literature.

- Based on this design strategy, the saturation conditions combined with the delay-dependent stabilization scheme allow the balance between the conservatism and computational efforts. The estimation of attraction domains shown in the last chapter has demonstrated this point of view. Furthermore, the simulation results also reveal the system's enhancement when actuators are saturated. In addition, the resilient-memory controller has shown good performance with respect to saturation limits and the robustness with uncertain knowledge of time-varying delay values. Finally, a linearization method fruitfully is converted the nonlinear matrix inequality constraints

involving the optimization of the DOA of dynamic output feedback controllers to the tractable LMI conditions. The estimation of DOA also exposes some characterized ellipsoidal domains associated with LKF.

Remaining problems and future work

The work of this dissertation is covered by five chapters related to stability analysis and stabilization for LPV systems and time-varying delay subject to actuator saturation. The main objectives of the thesis have been achieved through theoretical results. In which the proposed methods have quite productively treated the problems corresponding to specific contexts. However, it is possible to point out some open problems involving in the particular case as follows:

- The CCL algorithm in Chapter 3 is convenient for linearizing design problems using QLF. However, if the more general forms i.e., PDLF are considered, it must be quite confusing to deploy this algorithm. On the other hand, the application of CCL algorithm mainly involves refining the slack scalars in Young's inequality. Unfortunately, the use of this inequality to decompose uncertain structures or bilinear matrices is a very conservative manner. Similar to the concave optimization problem discussed in Chapter 6, mathematical tools are needed to properly treat these nonlinear matrix structures.

- Regarding the developed saturation conditions, limits only consider the symmetry case. In fact, there are many asymmetric bounded saturation systems for which the design constraints (GSC) needs to be developed to be more suitable for the general case. Moreover, the guarantee of regional stability conditions corresponding to the state constraints has not really been completely solved. One of the promising approaches that can be integrated with the saturation condition via LMI technique is the shaping Lyapunov function (control barrier function) method.

- Almost all the examples consider time-delay systems are stabilizable/detectable for $h(t) \in \mathcal{H}_0,\ \underline{h} = 0$, which makes the designed conditions not accurately describe (conservative) the stability characteristic of the system with $\underline{h} \neq 0$. In these cases, to take into account the information of the lower bound of delay, a delay-range-dependent condition makes more sense.

- The generalization of proposed methods have been developed for: systems with uncertain parameters $\hat{\rho}(t)$, systems with asymmetrical limits on derivative $\underline{\nu} \leq \dot{\rho}(t) \leq \overline{\nu},$ systems with delayed parameters $\rho(t-h(t))$. Or consider an extension of the parameter-dependent decision matrices such that $Q(\rho(t)),\ R(\rho(t))$ are other perspectives that will be developed.

- Application for dynamic systems such as vehicle body stability system (ESC, ESP, ADS, etc.), remote robot control for slave – master system (e.g., for medical service), or other engineering systems.

Appendix A

Linear algebra

This section is not intended to provide complete definitions of matrix algebra, ring fields, matrix determinants, eigenvalues, and etc. Instead, it is mainly concerned with the essential algebraic mathematical techniques relating to system and control theory. Specifically, the postulates and properties of convex functions, integrable functions, and convex optimization involved in the analysis of system and control expressed by linear/bilinear matrix inequality conditions.

A.1 Affine space

The rudimental concepts (i.e. convex sets, convex functions, and linear combinations, etc.) involved in this work could be illustrated by *n*-dimensional vector space in the following figure.

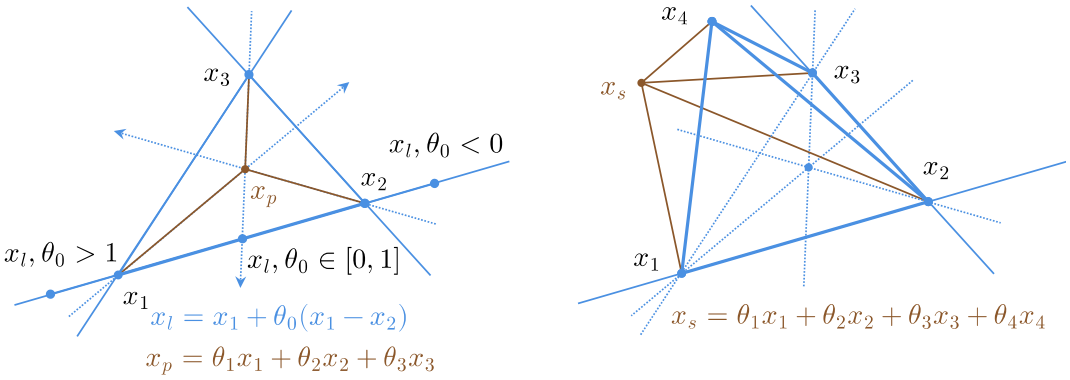

a. Affine hull in $\wp \subseteq \mathbb{R}^2$ *b. Affine hull in* $\wp \subseteq \mathbb{R}^3$

Figure A-1. *The linear transformation of given vectors* $x = \{x_1, x_2, \ldots, x_n\}$ *in n-dimensional coordinate space is expressed linearly independent based on the basis set and the corresponding coordinate parameters* $\theta_i \in \mathbb{R}$.

It is conceivable that the coordinates of a point belonging to subspace $\wp \subseteq \mathbb{R}^n$ can be expressed by linear expressions (convex or quasi-convex). Now, let's review some basis of the linear formulations.

A.1.1 *Affine sets*

Given affine set $\wp \subseteq \mathbb{R}^n$, and $\theta_i \in \mathbb{R}$, $\forall x_1, x_2 \in \wp$, then the coordinates of the point x_l on the line $d(x)$ passing through two points x_1, x_2 are geometrically presented in Figure A-1.*a*, expressed in the form:

$$d(x): x_l = \theta_0 x_1 + (1 - \theta_0) x_2 \in \wp \tag{A.1}$$

For all $x_3 \in C, x_3 \notin d(x)$, and the set of parameters $\theta = \{\theta_i \in R \mid \theta_1 + \theta_2 + \theta_3 = 1\}$, then the

affine combination of x_p slide on the plane $p(x)$ (shows in Figure A-1.*a*) is given:

$$p(x): x_p = \theta_1 x_1 + \theta_2 x_2 + \theta_3 x_3 \in \wp \tag{A.2}$$

With $x_4 \in C, x_4 \notin p(x)$, and the set of parameters $\theta = \{\theta_i \in \mathbb{R} \mid \sum_{i=1}^{4} \theta_i = 1\}$, then the affine combination of x_s in space $\mathbb{R}^3$ (shows in Figure A-1.*b*) is obtained:

$$s(x): x_s = \sum_{j=1}^{4} \theta_j x_j \in \wp \tag{A.3}$$

A.1.2 *Convex sets*

The convex set contains all points such that the segment connecting any two points of the set is stay inside the convex set. And the convex hull is the smallest outer boundary that contains of this set.

a. Convex *b. Non-convex* (*Concave*)

Figure A-2. *Illustrates some simple convex and nonconvex sets* $\mathbb{R}^2$.

Example A.1.1. In the plane $p(x)$ (Figure A-2.a) the smallest convex hull containing three points $x_1, x_2, x_3 \in p(x)$, is the triangle domain $x_1 x_2 x_3 \subset p(x)$, then as defined in (Boyd & Vandenberghe, 2004) the convex set is the set of all convex combinations of points in $\wp$:

$$\mathbf{conv}\ \wp = \left\{ x_p = \theta_1 x_1 + \theta_2 x_2 + \theta_3 x_3 \;\middle|\; x_p \in \wp,\ \theta_i \in \mathbb{R}_+,\ \theta_1 + \theta_2 + \theta_3 = 1 \right\} \tag{A.4}$$

A.1.3 *Convex functions*

Now, let's recall some definitions provided in the literature (Boyd & Vandenberghe, 2004; Mitrinović et al., 1993a) as follows:

Definition A.1.1 *Given a continuous function* $f: \mathbb{R}^n \mapsto \mathbb{R}$ *is convex if its domain of definition denoted as* $dom(f)$ *is convex set, and if for* $\forall a, b \in dom(f)$ *and set* $\theta \in [0, 1]$, *we have the following inequality*

$$f(\theta a + (1-\theta)b) \leq \theta f(a) + (1-\theta) f(b). \tag{A.5}$$

The geometric significance of this condition can be illustrated in Figure C-1. *a.* Then the consequences of this condition can be expressed as follows: function f is strictly convex if the strict inequality (A.5) holds with $\forall a \neq b$ and $\theta \in (0, 1)$.

Definition A.1.2 *For* $a, b \in dom(f)$, *and* $\lambda_1 + \lambda_2 > 0$ *then (A.5) is equivalent to*

$$f\left(\frac{\lambda_1 a+\lambda_2 b}{\lambda_1+\lambda_2}\right) \leq \frac{\lambda_1 f(a)+\lambda_2 f(b)}{\lambda_1+\lambda_2}. \tag{A.6}$$

The Fenchel-Young inequality is widely applied in control fields (stability control and time-varying delay) is based on the conjugate function as follows.

Definition A.1.3 *Let* $f: \mathbb{R}^n \mapsto \mathbb{R}$, *for* $a,b \in dom(f)$, *and a convex function is defined as the conjugate of* f *given by*

$$f^*(b) = \sup_{x \in dom(f)} (b^T a - f(a)), \tag{A.7}$$

then the following condition hold $\forall a,b$,

$$\langle a,b \rangle := a^T b \leq f(a) + f^*(b) \tag{A.8}$$

A corollary is directly obtained from the above conditions, gives a matrix $R \in \mathbb{S}^n_{++}$ by choosing differentiable function $f = a^T R a$ that results in the well-known inequality

$$a^T b \leq a^T R a + b^T R^{-1} b. \tag{A.9}$$

Further discussion with the application of this inequality will be presented in the following sections.

A.1.4 *Polytope Partition*

"Polytopic" extensively used in robust analysis and control strategy for the LPV system in recent decades. The application of the quadratic Lyapunov function is straight-forward for stabilization conditions but results in conservatism. Since then, many methods proposed to improve the performance of LPV systems. The representation of the system as a polytopic model using all the vertices of the convex hull covering the parameter domain directly yields a multi-LTIs formulation. However, in some case, it might cause a conservativeness and numerical burden. The partitioning illustrated in Figure A-3 significantly decreases the vertices of the polytope and results in the less conservative condition.

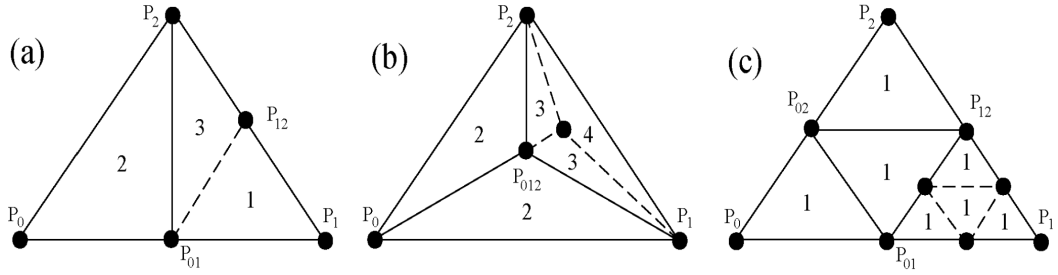

Figure A-3. *Two steps of three possible subdivisions of a triangle* (Gonçalves et al., 2006). (a) *Division by two, or bisection*. (b) *Division by three*. (c) *Division by four, or edgewise subdivision*.

The representation of the LPV system as the uncertain polytope is proposed by (Gonçalves et al., 2006) known as *Polytope-Bounded Uncertainty* method. It promises to

reduce computational load but increase complexity with parametric uncertainties. An application can be mentioned, see for example, a relaxing result of $\mathscr{H}_2/\mathscr{H}_\infty$ performance condition presented in the articles (H. Zhang et al., 2014, 2015).

A.1.4.1 *Switching Multiple-Affine*

Now, let's discuss a generalization of converting the coordinate parameter dependence to the fundamental coordinate system of the convex domain. Given compact parameter set $\rho(t) \in \mathcal{U}_p$. There exists a linear mapping to transform the basis linear/bilinear conservation from the parametric dependent function

$$\mathcal{F}_{\mathcal{P}} \coloneqq \{\rho \in \mathcal{C}^1([t_0,\ \infty), \mathbb{R}^{N_p}) |\ \rho_i(t) \in \mathcal{U}_p,\ i = 1,...,N_p\}, \quad \text{to}$$
$$\mathcal{F}_{\mathcal{Q}} \coloneqq \left\{\theta \in \mathcal{C}^1([t_0,\ \infty), \mathbb{R}_+^{N_p}) |\ \theta_i(t) \in \mathcal{U}_q,\ i = 1,...,N_p\right\}.$$

where $\mathcal{U}_q = \{\theta_i \in [0,\ 1], i = 1,...,N_p\} \subset \mathbb{R}^{N_p}$. Then, the set of all partitions containing N_p and $(N_p - 1)$ of the elements of set $\mathcal{N} \coloneqq \left\{1,\ 2,...,\ N_p\right\}$, is defined by:

$$\Omega(\mathcal{N}) \coloneqq \left\{(\mathcal{A}_i,\ \mathcal{B}_i) |\ \mathcal{A}_i \cap \mathcal{B}_i = \varnothing,\ \mathcal{A}_i \cup \mathcal{B}_i = \mathcal{N},\ i = 1,...,2^{N_p}\right\}.$$
$$\Omega(\mathcal{N}^1) \coloneqq \left\{(\mathcal{A}_i^1,\ \mathcal{B}_i^1) |\ \mathcal{A}_i^1 \cap \mathcal{B}_i^1 = \varnothing,\ \mathcal{A}_i^1 \cup \mathcal{B}_i^1 = \mathcal{N}^1,\ i = 1,...,2^{N_p-1}\right\}.$$

where $\mathcal{N}^1$ is a set of $(N_p - 1)$ elements, of which any elements are removed from $\mathcal{N}$. And then the membership function will be represented by:

$$\lambda_i(t) = \prod_{j \in \mathcal{A}_i} (1 - \theta_j(t)) \prod_{k \in \mathcal{B}_i} \theta_k(t), \text{ with } (\mathcal{A}_i, \mathcal{B}_i) \in \Omega(\mathcal{N}),\ i = 1,...,N_l, \text{ and } N_l = 2^{N_p}. \quad \text{(A.10)}$$

Lemma A.1.1. *Given nonnegative homogeneous set $\mathcal{U}_q$ is convex cone, then the generalized transformation of linear combination of $\theta(t) \in \mathcal{U}_q$ retain in convex hull and preserve convex properties as follows:*

$$\sum_{i=1}^{N_l} \lambda_i(t) = 1,\ \forall \lambda_i(t) \in [0,\ 1],\ i = 1,...,N_l, \quad \text{(A.11)}$$

and there exists a piecewise function $\sigma_{i,j} = 0$ if $j \in \mathcal{A}_i$ and $\sigma_{i,j} = 1$ if $j \in \mathcal{B}_i$ so that

$$\sum_{i=1}^{N_l} \lambda_i(t) \sigma_{i,j} = \theta_j(t) \prod_{k \in \mathcal{A}_i^1} (1 - \theta_k(t)) \prod_{l \in \mathcal{B}_i^1} \theta_l(t) = \theta_j(t),\ \forall j = 1,...,N_p,\ N_l = 2^{N_p}. \quad \text{(A.12)}$$

Coordinate Eqs. (A.12) presents a generalization of the combinatorial convex from the defined parameter hyper-rectangle set. Furthermore, the combinatorial formulation introduced in Eq. (A.10) is convenient for the expansion of derivatives that makes the relaxation method (Guerra & Bernal, 2009; Sala & Ariño, 2009) to deploy more efficiently.

Example A.1.2. Let consider an affine system

$$\dot{x}(t) = \sum_{i=1}^{N_p} \theta_i(t)(A_i x(t) + B_{w,i} w(t)),\ \theta_i(t) \in \mathcal{U}_q. \quad \text{(A.13)}$$

Applying the transient binary switching (A.12) to converts the LPV system to the following switched LTI systems:

$$\dot{x}(t) = \sum_{j=1}^{2^{N_p}} \lambda_j(t) \sum_{i=1}^{N_p} \sigma_{i,j} \left(A_i x(t) + B_{w,i} w(t) \right), \tag{A.14}$$

with $N_l = 2^{N_p}, \sum_{i=1}^{N_l} \lambda_i(\rho(t)) = 1,\ \lambda_j(t) \in [0,\ 1],\ j = 1, \ldots, N_l.$

A.1.4.2 *Piecewise Affine Space*

On the other hand, the piecewise affine parameter-dependent (PAPD) approaches introduced as multi-switch partitioned parameter space, see, e.g., (Apkarian & Tuan, 1998; Lim, 1998), could provide less conservative stability conditions. The parametric switch subsystem is illustrated in the following figure.

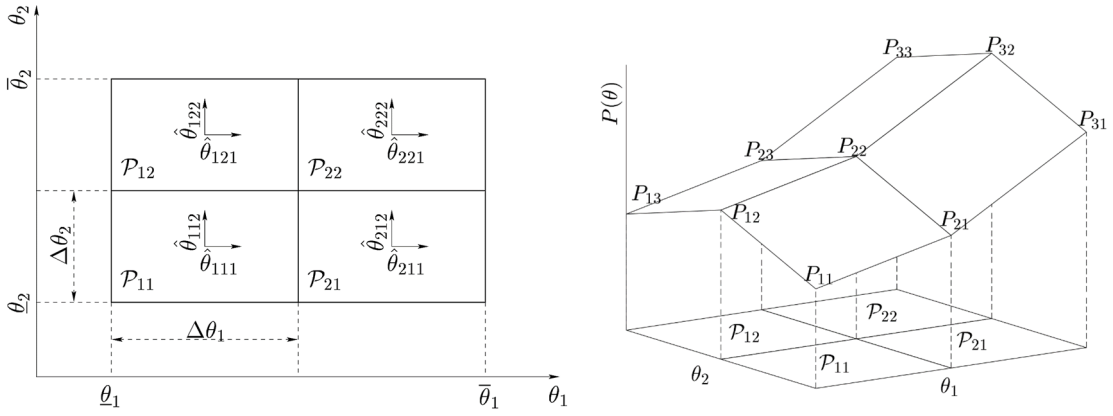

a. Distributed parameter subspaces *b. Continuous piecewise-affine*

Figure A-4. *Visualization PALPV model discretization* (Lim, 1998).

For simplicity, we assume the affine system depends on the parameter vector $\theta(t) = [\theta_1(t)\ \ \theta_2(t)]^T \in \mathcal{U}_\theta$ Then the *piecewise discretization* of the parameters is given by:

$$\begin{aligned} \hat{\theta}_{ij1}(t) &= \theta_1(t) - \underline{\theta}_1 - (i - 0.5)\Delta\theta_1, \\ \hat{\theta}_{ij2}(t) &= \theta_2(t) - \underline{\theta}_2 - (j - 0.5)\Delta\theta_2, \end{aligned} \tag{A.15}$$

where $\hat{\theta}_{ijk}(t) \in [-\Delta\theta_k,\ \Delta\theta_k] \subset \mathcal{P}_{ij} \subset \mathcal{U}_\theta$ and $\dot{\hat{\theta}}_{ijk}(t) \in [-\nu_k,\ \nu_k]$, with $k = 1, 2.$ Then, the Piecewise Affine Linear Parameter Varying is expressed by:

$$\theta(t) = \sum_{i=1}^{N_1} \sum_{j=1}^{N_2} \alpha_{ij}(\theta) \left(\theta_{ij0} + \sum_{k=1}^{2} \hat{\theta}_{ijk}(t) \right), \qquad i = 1, 2, \ldots, N_1, \text{ and } j = 1, 2, \ldots, N_2, \tag{A.16}$$

With Π_{ij} -partitioned parameter subspace *ij-th*, the switching rule is defined as:

$$\sigma_{ij}(t) = \begin{cases} 1 & \text{if } \theta(t) \in \mathcal{P}_{ij} - \left(\mathcal{P}_{i(j+1)} \cup \mathcal{P}_{(i+1)j} \right) \\ 0 & \text{else} \end{cases} \tag{A.17}$$

Lipschitz parameter-dependent Lyapunov function is chosen as:

$$P(\theta) = \sum_{i=1}^{N_1} \sum_{j=1}^{N_2} \sigma_{ij}(\theta) \left(P_{ij0} + \sum_{k=1}^{2} \hat{\theta}_{ijk}(t) P_{ijk} \right), \text{ and} \tag{A.18}$$

$$P_{ij} + P_{(i+1)(j+1)} = P_{(i+1)j} + P_{i(j+1)}. \tag{A.19}$$

where P_{ij0} is the center point (as seen in Figure A-4.*b*), and the parallelogram rules (A.19) is set to ensure finite matrices P_{ij}, so $P(\theta)$ is Lipchitz function in $\theta(t)$. As this reason, the approach leads to less conservative stability conditions. But the number of LMI condition that must check is overwhelming. For example, given a LPV system depend on *p* parameters, each parameter is partitioned into N_i subspace, so the number of conditions that need to be checked is about $2^p \prod_{i=1}^{p} N_i$.

A.2 Linear Matrix Inequality

In recent decades there has been a wide variety of problems in system control theory related to convex optimization expressed in the linear matrix inequalities LMIs. For a more detailed history of the linear matrix inequality, readers can refer to (Boyd et al., 1994). Since these resulting optimization problems can be solved numerically very efficiently using interior-point methods (also referred to as barrier methods), and are very convenient compared to seeking an analytic or frequency-domain solution. So, many constraints including convex quadratic inequalities, matrix norm inequalities, and Lyapunov function, can be expressed as convex optimization problems

$$\begin{aligned} &\textbf{Minimize } c^T x \\ &\text{subject to } F(x) = F_0 + \sum_{i=1}^{m} x_i F_i \succeq 0, \text{ or } F(x) = F_0 + \sum_{i=1}^{m} x_i F_i \succ 0. \end{aligned} \tag{A.20}$$

where vector $x \in \mathbb{R}^m$ and real symmetric matrices F_i. The reader intends to study in-depth about interior points, refers to the following monograph (Nesterov & Nemirovskii, 1994).

A.2.1 *Linear Programming*

The problem statement and optimality condition of the linear programming relates to minimization of linear function subject to linear constraints can represented in the inequality form

$$\textbf{Minimize } c^T x \quad \text{subject to } \mathrm{A}x \succeq b, \tag{A.21}$$

or *standard form*

$$\textbf{Minimize } c^T x \quad \text{subject to } \mathrm{A}x = b, \; x \succeq 0. \tag{A.22}$$

The logarithmic *barrier function* associated with problem (A.21) is

$$B(x,\mu) = c^T x - \mu \sum_{j=1}^{m} \ln x_j, \tag{A.23}$$

where positive scalar μ is called the *barrier parameter*. For a sequence of monotonically decreasing and sufficiently small values of μ, there exists an associated sequence $\{x_\mu\}$ called barrier trajectory (or central path) that converges to the feasible solution x^* from the strict interior of the feasible region (Wright, 1992).

The gradient of barrier function and barrier Hessian have simple forms:

$$g_B(x,\mu) = c - \mu X^{-1}\mathbf{1}, \quad H_B(x,\mu) = \mu X^{-2}. \tag{A.24}$$

where $\mathbf{1} = (1,\ldots,1)^T$, and X means the diagonal matrix whose diagonal elements are those

of vector x.

A.2.1.1 *The Primal Barrier Method for Linear Programming*

Consider a standard-form linear program, then a barrier sub-problem associated with linear problem (A.22) is

$$\textbf{Minimize } c^T x - \mu \sum_{j=1}^{m} \ln x_j \quad \text{subject to } \mathrm{A}x = b, \tag{A.25}$$

with the assumptions

(1) the set of x satisfies $\mathrm{A}x = b$, and $x \succ 0$ is nonempty,

(2) given the set $(y,\ z)$ satisfies $A^T y + z = c,$ and $z \succ 0$ is nonempty, and

(3) $\text{rank}(A) = m.$

At the optimal solution, there is an estimate of the Lagrange multipliers for the equality constraints y_μ such that:

$$g_B(x,\mu) = c - \mu X^{-1}\mathbf{1} = A^T y \ \Rightarrow \ c = \mu X^{-1}\mathbf{1} + A^T y. \tag{A.26}$$

The barrier trajectory for standard-from LP (A.22) is defined by vectors $(x_k,\ y_k)$

$$\begin{aligned} Ax_k &= b, \ \text{ for } x_k \succ 0, \\ \mu X_k^{-1}\mathbf{1} + A^T y_k &= c. \end{aligned} \tag{A.27}$$

Starting from $x \succ 0,$ using gradient and barrier Hessian give in (A.24), the Newton equation of sub-problem (A.25) corresponding to Newton step p_k is

$$\begin{bmatrix} \mu_k X_k^{-2} & A^T \\ A & 0 \end{bmatrix} \begin{bmatrix} p_k \\ -y_{k+1} \end{bmatrix} = \begin{bmatrix} \mu_k X_k^{-1}\mathbf{1} - c \\ Ax_k - b \end{bmatrix}. \tag{A.28}$$

In which the Newton step p_k satisfies

$$\mu_k X_k^{-2} p_k - \mu_k X_k^{-1}\mathbf{1} = A^T y_{k+1}, \tag{A.29}$$

for some Lagrange multiplier vector y_{k+1}. Using the relation $Ax_k = b, Ap_k = 0,$ by multiplying the latter equation with AX_k^2, we have

$$AX_k^2 A^T y_{k+1} = AX_k(Xc - \mu_k \mathbf{1}), \tag{A.30}$$

has a unique solution y_{k+1} since $\text{rank}(A) = m,$ and $AX_k^2 A^T$ is positive definite. So, the new step is defined in term of y_{k+1} as follows

$$p_{k+1} = x_k + \mu_k^{-1} X_k^2 (A^T y_{k+1} - c). \tag{A.31}$$

In the late 1980s, the analysis of polynomial-time complexity for an interior method should recognize the work of (Nesterov & Nemirovskii, 1994) with the contribution of the defining of a *self-concordant barrier function*. A convex function $F(x) : \wp \in \mathbb{R}^n \mapsto \mathbb{R}^n$ is μ *self-concordant* in $\wp$ if

(1) $F(x)$ is three time continuously differentiable in $\wp$, and

(2) for all $x \in \wp, h \in \mathbb{R}^n :\ \left|\nabla^3 F(x)[h,h,h]\right| \le 2\mu (h^T \nabla^2 F(x) h)^{3/2}.$

where $\nabla^3 F(x)[h,h,h]$ is the third differential of $F(x)$ taken at x along the collection of direction $[h_1,h_2,h_3]$. Using the concept of self-concordance, new barrier functions have been devised for certain convex programming problems, e.g., semidefinite programming.

A.2.1.2 *The Primal-Dual Barrier Method for Linear Programming*

In the last decades of the last century, innumerable papers have been written about the interior revolution relates to the primal-dual family. Both methods are based on applying Newton's method, but the Primal barrier algorithm is formulated in terms of only seeking primal variables x. Let's consider the optimal solution of the sub-problem (A.25) that satisfies (A.27) for some vector y. By defining a vector z such that

$$\begin{aligned} c &= A^T y + z, \\ Xz &= \mu \mathbf{1}. \end{aligned} \tag{A.32}$$

Make the use of Lagrange multiplier estimate to seek dual variables y and z satisfying the following barrier trajectory

$$\begin{aligned} Ax_k &= b, \quad \text{for } x_k \succ 0, \\ A^T y_k + z_k &= c, \quad \text{for } z_k \succ 0, \\ X_k z_k &= \mu \mathbf{1}. \end{aligned} \tag{A.33}$$

With the presence of nonlinear problem in the third equation. Following Newton's method, we obtain a linear system for Newton step p_k in x, y, and z:

$$\begin{bmatrix} A & 0 & 0 \\ 0 & A^T & I \\ Z_k & 0 & X_k \end{bmatrix} \begin{bmatrix} p_{x,k} \\ p_{y,k} \\ p_{z,k} \end{bmatrix} = \begin{bmatrix} b - Ax_k \\ c - A^T y_k - z_k \\ \mu_k \mathbf{1} - X_k Z_k \mathbf{1} \end{bmatrix}. \tag{A.34}$$

using the similar transformation as (A.29)-(A.30) to eliminate $p_{x,k}$ and $p_{z,k}$, we have

$$AZ_k^{-1} X_k A^T p_{y,k} = AZ_k^{-1} X_k (c - A^T y_k - \mu_k X_k^{-1} \mathbf{1}) + b - Ax_k. \tag{A.35}$$

For specified value $p_{y,k}$ will find the corresponding value $p_{x,k}$ and $p_{z,k}$.

A.2.2 *The Semidefinite Programming Problem*

Semidefinite programming may be viewed as a generalization of linear programming, but they are not much harder to solve. Semidefinite programming unifies some standard problems and could be found in many applications of control system theory and combinatorial optimization, for details, see the survey (Vandenberghe & Boyd, 1996) and reference therein. The semidefinite programming problem could be expressed as follows:

$$\begin{aligned} &\textbf{Minimize } \operatorname{trace}(CX) \\ &\text{subject to } \operatorname{trace}(A_i X) = b_i, \quad i = 1,\ldots,m, \quad X \succeq 0, \end{aligned} \tag{A.36}$$

with an appropriated real matrix C, a symmetric matrix $A_i \in \mathbb{S}^n$, and a vector $b_i \in \mathbb{R}^m$. Presenting the SDP in this form is quite similar to the standard-form LP problem. In the work (Nesterov & Nemirovskii, 1994), the author has shown that the function $\log\det(X)$ is a self-concordant barrier function for the semidefinite programming problem, which can be solved in polynomial time via a sequence of barrier parameter μ:

$$\begin{aligned} &\textbf{Minimize } \operatorname{trace}(CX) - \mu \log\det(X) \\ &\text{subject to } \operatorname{trace}(A_i X) = b_i,\ \ i = 1,\ldots,m,\ \ X \succeq 0. \end{aligned} \tag{A.37}$$

This sub-problem associated with semidefinite programming problem is analyzed similarly to the previous section. Under suitable assumption, given symmetric matrix X_μ obeys the equality constraints and a vector $y_\mu \in \mathbb{R}^m$ such that the sequence $\{X_\mu, y_\mu\}$ is unique and satisfies the following condition:

$$X(C - \textstyle\sum_{i=1}^{m} y_i A_i) \ = \ \mu I, \ \ C - \sum_{i=1}^{m} y_i A_i \ \succeq \ 0. \tag{A.38}$$

However, the left-hand side of equation is not symmetric, so a primal approach is proposed by the alternative condition

$$X(C - \textstyle\sum_{i=1}^{m} y_i A_i) + (C - \sum_{i=1}^{m} y_i A_i)X \ = \ 2\mu I. \tag{A.39}$$

Similarly, a primal-dual interior-point method for semidefinite programming problem is involved by seeking $\{X_\mu, y_\mu, Z_\mu\}$, with matrices $X_\mu, Z_\mu \succ 0$ satisfies:

$$\begin{aligned} &\operatorname{trace}(A_i X) = b_i, \\ &C - \textstyle\sum_{i=1}^{m} y_i A_i = Z, \\ &XZ + ZX = 2\mu I. \end{aligned} \tag{A.40}$$

From this point, it can be seen that the similarity is quite clear between last equations and the one in linear programming problem (A.33).

A.3 Schur Complement

The Schur complement is a fundamental and core mathematical tool used in matrix analysis in the field of theoretical control systems. In the context of LMIs formulation, the conditions for positive definiteness and semi-definiteness that can be expressed by:

Lemma A.3.1. *The following statements are equivalent*:

(1) *Let a real symmetric* $X = \begin{bmatrix} A & B \\ B^T & C \end{bmatrix} \succ 0.$

(2) *A is invertible,* $A \succ 0$, *and complement* $X/A = C - B^T A^{-1} B \succ 0.$

(3) *C is invertible,* $C \succ 0$, *and complement* $X/C = A - BC^{-1}B^T \succ 0.$

From this view, it could be realized that the nonlinear matrix inequalities in statements 2 and 3 also deliver convex problems in the form of affine LMI (statement 1).

A.4 Young's inequality

Let's recall Young's inequality (Mitrinović et al., 1993b) and its matricial generalization (Ando, 1995) for further discussion about its application for the LMI analysis.

Lemma A.4.1. (Mitrinović et al., 1993b) *Let a continuous function* $f:(0,\infty)\mapsto\mathbb{R}$ *is increasing function defined for nonnegative real numbers* x, *with initial condition* $f(0)=0$. *Give* a,b *are positive real numbers such that* a *is in the domain of* f *and* b *is in the image of* f . *Then*

$$ab\leq\int_0^a f(x)dx+\int_0^b f^{-1}(x)dx, \tag{A.41}$$

with equality if and only if $b=f(a)$.

From left to right of Figure A-5, respectively, shows the left and right side of the inequality, and the gap of this inequality.

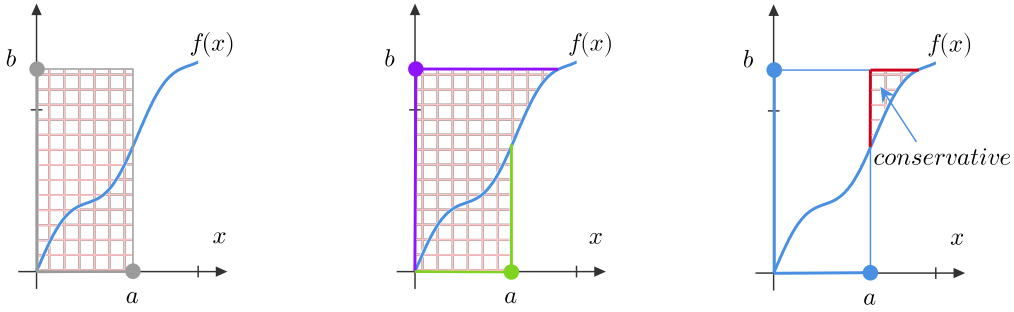

Figure A-5. *The visualization of Young's inequality.*

Generalization of Young's inequality

Lemma A.4.2. *Given real matrices with appropriate dimensions* X,Z, *a time-varying matrix* $\|Y(t)\|^2\leq I$, *and a symmetric matrix* $W\succ 0$. *Then for any scalar* $\varepsilon>0$, *we have the following inequalities*:

$$\pm XY(t)Z\pm Z^TY(t)^TX^T\leq\varepsilon^{-1}XX^T+\varepsilon Z^TZ. \tag{A.42}$$

$$\pm XZ\pm Z^TX^T\leq\varepsilon^{-1}XW^{-1}X^T+\varepsilon Z^TWZ. \tag{A.43}$$

Proof.

For any matrix $X,Y(t),Z$ that satisfies the assumption, the condition (A.42) is ensued on:

$$\begin{aligned}&\left(\varepsilon^{-0.5}X^T\mp\varepsilon^{0.5}Y(t)Z\right)^T\left(\varepsilon^{-0.5}X^T\mp\varepsilon^{0.5}Y(t)Z\right)\geq 0,\\ \Leftrightarrow\quad &\varepsilon^{-1}XX^T+\varepsilon Z^TZ\geq\varepsilon^{-1}XX^T+\varepsilon Z^TY(t)^TY(t)Z\\ &\geq\pm XY(t)Z\pm Z^TY(t)^TX^T.\end{aligned}$$

Performing the deployment in a similar manner with

$$(\varepsilon^{-0.5}W^{-0.5}X^T\mp\varepsilon^{0.5}W^{-0.5}Z)^T(\varepsilon^{-0.5}W^{-0.5}X^T\mp\varepsilon^{0.5}W^{-0.5}Z)\geq 0,$$

that implies the inequality (A.43). □

Actually, these conditions are the matricial generalization of Young's inequality (Ando, 1995). These inequalities are well-known in the control system theory, while condition (A.42) is regularly used to eliminate uncertainty matrices, condition (A.43) is typically encountered in general in output feedback control design (SOF and OBF, see for example (Benzaouia & Hajjaji, 2014; He et al., 2008; Leibfritz, 2001; Peng & Han, 2011; Sadabadi

& Peaucelle, 2016), etc.). Moreover, this bounded technique is also encountered in deployments of stability of time-delay system. In this aspect, this generalization known as cross term bounding technique (He et al., 2004b; Moon et al., 2001; PooGyeon Park, 1999; M. Wu et al., 2004) did not include the scaling scalar but rather free weighting matrices (FWM). As has been analyzed by (Briat, 2015a; Han, 2005b, 2005a), these methods do not seem to yield satisfactory results.

A.5 Finsler's Lemma

Yakubovich's $\mathcal{S}$-lemma is a consequence quadratic result known as non-strict Finsler's lemma. In its original form it is widely used in optimization and control theory. A comprehensive state-of-the-art review of the $\mathcal{S}$-Lemma and its applications was given by Polik and Terlaky in (Pólik & Terlaky, 2007). Following the well-known concepts in optimization, relaxation methods, and functional analysis in the work of the literature (Briat, 2008; Cimprič, 2015; Pólik & Terlaky, 2007; Skelton et al., 1998; Tuy & Tuan, 2013), the lemma was briefly represented in a general form as follows.

Lemma A.5.1. *The following statements are equivalent*

(1) *For* $\forall x \in \mathbb{R}^n \setminus \{0\},\ Bx = 0,$ *given a matrix* $M \in \mathbb{R}^{n\times n}$ *such that* $x^T Mx < 0.$

(2) *There exists a scalar* $\tau \in \mathbb{R}$ *satisfies* $M - \tau B^T B < 0,$ *and*

$$\tau > \lambda_{\max}(D^T(M - MB_\perp(B_\perp^T MB_\perp)^{-1}B_\perp M)D),$$

where $D = (B_r B_l^T)^{-1/2} B_l^+,$ *with any factor of* $B := B_l B_r.$

(3) *There exists a symmetric matrix X such that* $M - B^T XB \prec 0$ *holds.*

(4) *There exists an unconstrained matrix N such that* $M + N^T B + B^T N \prec 0.$

(5) *Given any basis of the null space of* $B : B_\perp$ *such that* $B_\perp^T MB_\perp \prec 0$ *holds.*

(6) *There exists a matrix* $W \in \mathbb{S}_+^{m+n},\ \operatorname{rank}(W) = m,$ *and a scalar* $\sigma \in \mathbb{R}_{++}$ *such that*

$$\begin{bmatrix} M & B^T \\ B & -\sigma I_m \end{bmatrix} \prec W.$$

For further discussions and demonstrations can be found in the mentioned documents.

Generalization of Finsler's Lemma

The following statement, known as Projection Lemma (or also as Elimination Lemma), is particularly related to robust control and linear matrix inequalities

Lemma A.5.2. Projection Lemma (Gahinet & Apkarian, 1994) *Let matrices of appropriate dimensions* $\Psi \in \mathbb{S}^n$, *and* $\mathcal{P}, \mathcal{Q},$ *then the following statements are equivalent*

(1) *There exists an unconstrained matrix* Θ *such that* $\Psi + \mathcal{P}^T \Theta \mathcal{Q} + \mathcal{Q}^T \Theta \mathcal{P} \prec 0.$

(2) *The two following underlying LMIs fulfill*

$$\ker(\mathcal{P})^T \Psi \ker(\mathcal{P}) \prec 0,$$
$$\ker(\mathcal{Q})^T \Psi \ker(\mathcal{Q}) \prec 0.$$

(3) *There exists two scalars* $\tau_p, \tau_q \in \mathbb{R}$ *such that*

$$\Psi - \tau_p \mathcal{P}^T \mathcal{P} \prec 0,$$
$$\Psi - \tau_q \mathcal{Q}^T \mathcal{Q} \prec 0.$$

This lemma is usually used in signal and system control analysis (common for both time and frequency domains) based on the LMI technique. In this thesis, we could only utilize a small application for dealing with the nonlinear structures in controller synthesis for LPV saturated systems.

Appendix B

Robust Stability and Performances Analysis via LMIs

In this section, the design specifications and requirements analyze on the state-space using the Lyapunov stability via linear matrix inequality formulation. The performance and robustness analysis for the LTI system systematically introduced by (Boyd et al., 1994; Scherer et al., 1997) deploys on the concept of the input-output properties. The terms such as $\mathcal{L}_2$-norm, $\mathcal{L}_2$-gain and $\mathscr{H}_\infty$-norm have been widespread in the stability and performance evaluation consistent with the (Scaled) Small-Gain Theorem (Boyd et al., 1994; Doyle, 1985; Zhou et al., 1996), the (Scaled) Bounded Real Lemma (Apkarian & Gahinet, 1995; Gahinet & Apkarian, 1994; Scherer, 1990), the full-block $\mathcal{S}$-procedure (Scherer, 2001, 1997; Scherer & Weiland, 2005), or the Integral Quadratic Constraints (IQC) (Jönsson, 1997; Megretski & Rantzer, 1997). This issue is also considered for the LPV delay systems in (Briat, 2008, 2015a), and the TS-fuzzy systems in (Tanaka & Wang, 2001). We briefly recall the general definitions for control system design criteria discussed in the work of (Scherer et al., 1997) and references therein.

The approximate deviations, and the uncertain knowledge about the parameters in the modeling are often referred to as the parametric uncertainty. Whereas the nonlinearities components are considered as dynamical uncertainty. The distinction demarcates between robust control theory and the LPV gain-scheduling technique (typically related to measurable parameters). Since the scheduling controller design are introduced by (Shamma, 1988; Shamma & Athans, 1990) that shown an efficient way to analyze and synthesize for this class of system. In recent decades, applications of LPV gain-scheduling controllers pervades in a wide range of system engineering from aeronautical engineering (aircraft, missiles, helicopters, AUVs...) to road traffic engineering (cars, trucks, trains), robotics, energy engineering (renewable energy systems), etc. It's also easy to find the applications in the same areas are addressed by the robust stability theory.

Definition A.5.1. *On the n-dimensional complex space* $\mathbb{C}^n$, *given a vector* $z : \mathbb{R}_+ \to \mathbb{C}^n$. *The* $\mathcal{L}_2$*-norm of* z *can be expressed as*

$$\|z\|_{\mathcal{L}_2} = \sqrt{\int_0^\infty z(s)^* z(s) ds}. \tag{B.1}$$

The space of signal mapping from $\mathbb{R}_+$ *to* $\mathbb{C}^n$ *with finite* $\mathcal{L}_2$*-norm could be denoted as* (Briat, 2015a) *by* $\mathcal{L}_2(\mathbb{R}_+, \mathbb{C}^n)$.

Now, let's consider an open-loop LPV system:

$$\begin{aligned} \dot{x}(t) &= A(\rho)x(t) + B_w(\rho)w(t) \\ z(t) &= H(\rho)x(t) + J_w(\rho)w(t) \end{aligned} \tag{B.2}$$

where $x(t) \in \mathbb{R}^n$ is state vector; $z(t) \in \mathbb{R}^r$ is regulated output; $w(t) \in \mathbb{R}^d$ is input disturbance. The parameters $\rho(t) = [\rho_1(t), \rho_2(t), ..., \rho_{Np}(t)]$ belong to parameter spaces (2.8)-(2.9).

B.1 Bounded Real Lemma - $\mathscr{H}_\infty$ performance

In the presence of external disturbance, giving a so-called energy-to-energy performance criterion γ involved in the stability analysis for LPV time-delay system (B.2) which meets the following requirements:

- for $w(t) = 0$, the LPV system (B.2) is asymptotically stable.
- for $w(t) \neq 0$, guarantees $\mathcal{L}_2$-norm on output of (B.2) bounded with $\gamma > 0$:

$$\gamma^{-1} \|z(t)\|_{\mathcal{L}_2}^2 \leq \gamma \|w(t)\|_{\mathcal{L}_2}^2 \tag{B.3}$$

This margin robustness and performance are typically required for the design specification of the systems affected by external disturbance and parametric uncertainty. The bounded real lemma (Scherer, 1990) is a well–known criterion allowing for the computation of the $\mathscr{H}_\infty$–norm, coincides with the $\mathcal{L}_2$-norm, that is, the highest input–output gain for finite energy. Generally speaking, the sensitiveness of the disturbance input $w(t)$ on the regulated output $z(t)$ is evaluated by the performance norm

$$\gamma_\infty := \sup_{w \in \mathcal{L}_2, \|w\| \neq 0} \frac{\|z\|_{\mathcal{L}_2}}{\|w\|_{\mathcal{L}_2}}. \tag{B.4}$$

Specifically, it promises that the LPV system (B.2) is asymptotically stable for disturbance inputs, where system gain from $\|w(t)\|_{\mathcal{L}_2}$ to $\|z(t)\|_{\mathcal{L}_2}$ not larger than $\gamma_\infty > 0$ if and only if there exist a symmetric positive matrix $P \in \mathbb{S}_{++}^n$ such that

$$\begin{bmatrix} A(\rho)^T P + PA(\rho) & PB_w(\rho) & H(\rho)^T \\ * & -\gamma_\infty I_d & J_w(\rho)^T \\ * & * & -\gamma_\infty I_r \end{bmatrix} \prec 0. \tag{B.5}$$

Energy-to-energy index $-\gamma_\infty$ also refers to a level of rejection disturbance. This criterion is usually encountered in the design objective, e.g., the robust stability and performance.

B.2 Block-Structured Uncertainty – Scaled Bounded Real Lemma

The representation of LPV system in a linear fractional transformation (LFT) form, the original system is separate in two interconnected subsystems Figure B-1. Where the sta-

bility analysis of *nominal* system affected by the dynamical uncertainties, and the parametric dynamic is reformulated in the input-output framework. The characterized LMI stability conditions are derived from Scaled Small-Gain theorem (Doyle, 1985; Doyle et al., 1991; Dullerud & Paganini, 2000; Feron et al., 1996; Packard & Doyle, 1993).

Let's introduce a LPV plant with dynamical uncertain governed by state-space equations of the generalized form:

$$\begin{aligned} \dot{x}(t) &= A(\cdot)x(t) + B_w(\cdot)w(t) \\ z(t) &= H(\cdot)x(t) + J_w(\cdot)w(t) \\ w_i(t) &= \Delta_i z_i(t) \end{aligned} \tag{B.6}$$

a. Uncertain system model. *b. Block-Structured LPV.*

Figure B-1. *The interconnection structure.*

Where the block-diagonal uncertainty set Δ_i is subset of the unit ball in $\mathcal{L}_2$ space.

$$\Delta_u := \left\{ diag(\Delta_1, \Delta_2, ..., \Delta_d) : \Delta_i \in \mathcal{L}_2, \text{ and } \left\|\Delta_i\right\| < 1,\ i = 1, 2, ..., d \right\}. \tag{B.7}$$

The operator Δ_i are normally referred to as the uncertainty structure. The condition of robust well-connectedness over the set Δ_u can be guaranteed by considering the set of positive definite similarity scaling associated with the structure Δ_i as follows.

$$\mathcal{D}_\Delta := \left\{ diag(L_1, L_2, ..., L_d) : L_i \in \mathbb{R}_{++}^{m_i \times m_i}, \text{ and } L_i \Delta_i = \Delta_i L_i,\ i = 1, 2, ..., d \right\}. \tag{B.8}$$

The commuting of the uncertainty is devoted to reduce the conservatism of the small gain condition (Doyle, 1985; Dullerud & Paganini, 2000; Zhou et al., 1996) that leads to the following results.

Proposition B.2.1. Supposing M is bounded LTI operator mapping $w \to z$ and A is Hurwitz matrix. Then the uncertainty structure (M, Δ_u) is robustly well-connected, and the system (B.6) is asymptotically stable if one of the following conditions hold:

- there exists $L \in \mathcal{D}_\Delta$ such that $\left\| LML^{-1} \right\|_{\mathcal{L}_2} < 1$.
- there exists matrix $P \in \mathbb{S}_{++}^n$, such that

$$\begin{bmatrix} H^T \\ J_w^T \end{bmatrix} L \begin{bmatrix} H & J_w \end{bmatrix} + \begin{bmatrix} PA + A^T P & PB_w \\ * & -L \end{bmatrix} \prec 0. \tag{B.9}$$

Following the arguments of (Apkarian & Gahinet, 1995; Packard & Doyle, 1993), an improvement of condition (B.5) is derived from the block diagonal operator:

$$\Theta(\rho) = diag\{\lambda_1 I_{\nu_1}, \lambda_2 I_{\nu_2}, ..., \lambda_{N_p} I_{\nu_{N_p}}\},\ \lambda_i \in [-1,\ 1],\ i = 1, ..., N_p. \tag{B.10}$$

Consider the set of positive $\mathcal{D}$-scaling associated with $\Theta(\rho)$ is denoted by

$$\mathcal{D}_\Theta := \{L \in \mathbb{S}^{\nu}_{++} : \Theta L^{\frac{1}{2}} = L^{\frac{1}{2}}\Theta\}, \text{ with } \nu = \sum_{i=1}^{N_p} \nu_i. \tag{B.11}$$

According the definition, the set of positive definite symmetric enjoys the commutation property, then the Scaled Bounded-Real Lemma introduces as follows:

$$\begin{bmatrix} A(\rho)^T P + PA(\rho) & PB_w(\rho) & H(\rho)^T L(\rho) \\ * & -\gamma L(\rho) & J_w(\rho)^T L(\rho) \\ * & * & -\gamma L(\rho) \end{bmatrix} \prec 0. \tag{B.12}$$

Condition (B.12) could interpret from bounded real lemma applied for reformulated structure system, then respectively, do a congruence transformation by $diag\{I, L^{\frac{1}{2}}, L^{\frac{1}{2}}\}$. This formulation offers an extra degree of freedom provides more relaxation than the small-gain theorem. The necessary and sufficient condition are delivered for LTI systems could find in (Packard & Doyle, 1993) and (Apkarian & Gahinet, 1995; Briat, 2015a) for LPV systems. Following the linear fractional transformation, the uncertain structures appear to detach from the plant. The stability problem of an LPV system based on this approach does not require much essential information from uncertain parameters, except for its range of variations. It should note that the LMI (B.12) is a quadratic stability, in which *P* is independent-parameter decision matrix. So, this condition in some circumstances is a strict condition.

B.3 Full-Block $\mathcal{S}$-Procedure

Finsler's lemma has been widely recognized in control system theory by the well-known - projection lemma introduced in the early 1990s (Gahinet, 1996; Gahinet & Apkarian, 1994; Iwasaki & Skelton, 1994; Skelton et al., 1998). Another generalization can be mentioned as the $\mathcal{S}$-procedure (or $\mathcal{S}$-lemma) provides an efficient polynomial-time powerful approach for system analysis and synthesis via convex optimization problems. The analytic solutions can be losslessly reformulated as the feasibility of SDPs and deliver an alternative approach to the stability control synthesis based-LMI condition. A comprehensive state-of-the-art review is given in the monographs (Boyd & Vandenberghe, 2004; Pólik & Terlaky, 2007).

Now, we would like to discuss the $\mathcal{S}$-Variable LMI-based method (Ebihara et al., 2015) using a generalization of Finsler's lemma to carry the unconventional conditions of the $\mathscr{H}_\infty$-performance. From the expression of system (B.2), take full advantage of null cancelation equation:

$$\underbrace{\begin{bmatrix} A(\rho) & B_w(\rho) & -I \end{bmatrix}}_{\Phi} \underbrace{\begin{bmatrix} x(t)^T & w(t)^T & \dot{x}(t)^T \end{bmatrix}^T}_{\ker(\Phi)} = 0. \tag{B.13}$$

Consider a quadratic Lyapunov function candidate $V(x(t)) = x(t)^T P x(t)$ for LPV system (B.2). Then, the derivation of this function along the trajectories of system dynamics combining with $\mathscr{H}_\infty$-norm can be represented by:

$$\dot{V}(x(t)) = \ker(\Phi)^T \Psi \ \ker(\Phi) \ \prec \ 0, \tag{B.14}$$

$$\text{where } \Psi = \begin{bmatrix} 0 & 0 & P \\ 0 & -\gamma I & 0 \\ P & 0 & 0 \end{bmatrix} + \begin{bmatrix} H(\rho)^T \\ J_w(\rho)^T \\ 0 \end{bmatrix}^T \gamma^{-1} \begin{bmatrix} H(\rho) & J_w(\rho) & 0 \end{bmatrix},$$

Then, following the argument of $\mathcal{S}$-variable LMI based on Finsler's lemma that yields:

$$\Psi + \Omega\Phi + \Phi^T\Omega^T \prec 0, \tag{B.15}$$

with an injected matrix $\Omega = \begin{bmatrix} U_1^T & U_2^T & U_3^T \end{bmatrix}^T$ are slack variable (SV) matrices of adequate dimension. The formulation (B.15) is dependent on the decision variable P and slack variables. It should remark that the equivalence of the two conditions (B.14) and (B.15) is still held in the case of taking into account the PDLF $P(\rho)$. By applying Schur's complement for the latter inequality that entails in the LMI condition:

$$\begin{bmatrix} U_1A(\rho) + A(\rho)^T U_1 & U_1B_w(\rho) + A(\rho)^T U_2 & -U_1 + A(\rho)^T U_3 + P & H(\rho)^T \\ * & -\gamma I + U_2B_w(\rho) + B_w(\rho)^T U_2 & -U_2 + B_w(\rho)^T U_3 & J_w(\rho)^T \\ * & * & -U_3 - U_3^T & 0 \\ * & * & * & -\gamma I \end{bmatrix} \prec 0. \tag{B.16}$$

The stability condition (B.14) is satisfied if condition (B.16) is fulfilled. Furthermore, the matrices $U_i, i = 1, 2, 3$ are slack variables in the above inequality, do not require definite positive symmetry like *P*. And, if $U_1 = P, U_2 = 0, U_3 = 0$, then condition (B.16) reverts to $\mathscr{H}_\infty$-performance (B.5), so this condition provides the more general stability formulation. The main advantage is the decoupling between the decision variable and the dynamic system (*P* and $A(\rho), B_w(\rho)$, respectively). This transformation is the key for conservatism reduction of the new robust stability analysis. In the work of literature (Ebihara et al., 2015) shows a relaxation of the robust stabilization condition compared with the traditional LMI based Lyapunov method.

It is worth recognizing that it is also used for the stability analysis of time-delay systems known as the free-weighting matrix. In section 5.2, this decoupling technique is applied essentially to handle with the couples between the Lyapunov-Krasovskii matrices with the dynamics system in the stability analysis of the LPV time-delay system.

The full-block $\mathcal{S}$-procedure provides a general result and comprehends the (scaled) small-gain, $\mathscr{H}_\infty$-norm results of the previous sections. The term *full-block* comes from the fact that the scaling involved are general matrices, as opposed to the block-diagonal scaling in (B.9), (B.12). Besides, a variety of methods has been developed within the area of robust control (includes all the previous results), which can be reformulated to fall within the framework of integral quadratic constraints IQCs (Megretski & Rantzer, 1997; Pfifer & Seiler, 2015). This important mathematical object that can implicitly characterize the operators in an input/output framework, e.g., small-gains theorem, bounded real lemma, the full-block $\mathcal{S}$-procedure, etc.

Definition B.3.1. (Scherer, 2001) *Gives two signals $w, z \in \mathcal{L}_2$ satisfies the IQC performance specification from the channel $w \to z$, if the following condition holds*

$$\mathcal{J} = \int_0^\infty \begin{bmatrix} w(s) \\ z(s) \end{bmatrix}^T \begin{bmatrix} Q & S \\ S^T & R \end{bmatrix} \begin{bmatrix} w(s) \\ z(s) \end{bmatrix} ds \;\leq\; 0. \tag{B.17}$$

Let us now rewrite the full-block problem formulation with the $\mathcal{S}$-variable approach by taking the derivative of the Lyapunov function candidate $V(x(t)) = x(t)^T P x(t)$ along the trajectories of system dynamics combining with IQC (B.17) as follows

$$\begin{aligned} \dot{V}(x(t)) + \dot{\mathcal{J}} &= \ker(\Phi)^T (\Psi) \ker(\Phi) \\ &\triangleq \ker(\Phi)^T \left(\Psi + \Omega\Phi + \Phi^T\Omega^T\right) \ker(\Phi) \;\prec\; 0, \end{aligned} \tag{B.18}$$

where $\ker\Phi = \begin{bmatrix} x(t)^T & \dot{x}(t)^T & w(t)^T \end{bmatrix}^T$,

$$\begin{aligned} \Psi &= \begin{bmatrix} I & 0 & 0 \\ 0 & I & 0 \end{bmatrix}^T \begin{bmatrix} 0 & P \\ P & 0 \end{bmatrix} \begin{bmatrix} I & 0 & 0 \\ 0 & I & 0 \end{bmatrix} + \begin{bmatrix} 0 & 0 & I \\ H(\rho) & 0 & J_w(\rho) \end{bmatrix}^T \begin{bmatrix} Q & S \\ S^T & R \end{bmatrix} \begin{bmatrix} 0 & 0 & I \\ H(\rho) & 0 & J_w(\rho) \end{bmatrix} \\ &= \left[\begin{array}{ccc} I & 0 & 0 \\ 0 & I & 0 \\ \hline 0 & 0 & I \\ H(\rho) & 0 & J_w(\rho) \end{array}\right]^T \left[\begin{array}{cc|cc} 0 & P & 0 & 0 \\ P & 0 & 0 & 0 \\ \hline 0 & 0 & Q & S \\ 0 & 0 & S^T & R \end{array}\right] \left[\begin{array}{ccc} I & 0 & 0 \\ 0 & I & 0 \\ \hline 0 & 0 & I \\ H(\rho) & 0 & J_w(\rho) \end{array}\right]. \end{aligned}$$

Similar to the previous argument, there exists an SV matrix Ω such that

$$\Psi + \Omega\Phi + \Phi^T\Omega^T \prec 0, \tag{B.19}$$

with $\Phi = \begin{bmatrix} A(\rho) & -I & B_w(\rho) \end{bmatrix}$, $\Omega = \begin{bmatrix} U_1^T & U_2^T & U_3^T \end{bmatrix}^T$.

The latter condition can be recognized as a more general form when both conditions (B.12) and (B.16) are included. Therefore, it is expected to cover a wider class of systems with a reduced conservatism.

B.4 Pole-Placement LMI regions

Following the performance constraints of $\mathcal{H}_\infty$ synthesis (Chilali et al., 1999; Chilali & Gahinet, 1996) has proposed an effective pole placement method based on the LMI formulation of Lyapunov stability condition. The objective is looking for the pole clustering in suitable stability sub-regions consistent to good behavior such as rational controller dynamics, well damping, fast decay, etc. This LMI-based representation of $\mathcal{D}$-stability regions is characterized by relocating its poles in sub-region $\mathcal{D}$ of the complex plane (half-planes, disks, sectors, vertical/horizontal stripes, and any intersection (as illustrated in Figure B-2)). Besides, Chilali delivers a sufficient LMI-based condition for quadratic $\mathcal{D}$-stability and robust $\mathcal{D}$-stability along with the *design criteria* of the controller system.

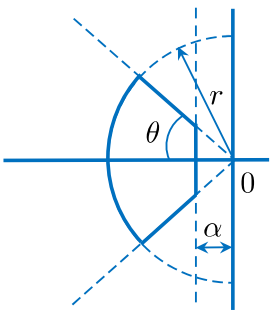

Region $\mathcal{S}(\alpha, r, \theta)$.

Figure B-2. Pole-placement of LMI regions (Chilali & Gahinet, 1996).

Definition B.4.1. (LMI regions - Chilali & Gahinet, 1996) *A subset $\mathcal{D}$ of complex plane is called an LMI region if there exist a real symmetric matrix $\mathcal{L}$, real matrix M such that*

$$\mathcal{D} = \{z \in \mathbb{C}:\ f_{\mathcal{D}}(z) = \mathcal{L} + zM + \overline{z}M < 0\}, \tag{B.20}$$

where $f_{\mathcal{D}}(z)$ is characteristic function of $\mathcal{D}$. Given below the examples of LMI regions

1 - *Half-plane* $\mathrm{Re}(z) < -\alpha : f_{\mathcal{D}}(z) = 2\alpha + z + \overline{z} < 0.$

2 - *Disk centered at* $(-q, 0)$ *with radius* $r : f_{\mathcal{D}}(z) = \begin{bmatrix} -r & q+z \\ q+\overline{z} & -r \end{bmatrix} \prec 0,$

and some dynamic e.g., oscillations $\mathrm{Re}(z) < -\alpha,\ |z| < r$; *bandwidth* $\alpha_1 < \mathrm{Re}(z) < \alpha_2$; *horizontal strip* $\mathrm{Im}(z) < \alpha$; *and damping cone* $\mathrm{Re}(z)\tan\theta < -|\mathrm{Im}(z)|$.

Example B.4.1. Giving a dynamic system:

$$\dot{x}(t) = Ax(t). \tag{B.21}$$

Then, matrix A is said $\mathcal{D}$-stable when its spectrum $\sigma_A := \{\lambda_i(A)\}$ belongs to region $\mathcal{D}$. Let's consider a Lyapunov characterization of LMI stability of system (B.21):

$$PA + A^T P \prec 0, \tag{B.22}$$

Then, a disk of radius r and center $(-q, 0)$ is an LMI region with characteristic function $f_{\mathcal{D}}$ if there exists a symmetric matrix P such that:

$$f_{\mathcal{D}}(PA) = \begin{bmatrix} -rP & q + PA \\ q + A^T P & -r \end{bmatrix} \prec 0, \text{ with } P \succ 0. \tag{B.23}$$

Pole clustering in LMI regions can formulate as a more general region, e.g., $\mathcal{S}(\alpha, r, \theta)$.

Let's analysis the $\mathscr{H}_\infty$–performance LMI constraint (B.5) belong to this disk region. Specifically, system (B.2) is quadratically $\mathcal{D}$-stable in LMI region disk of center $(-q, 0)$ and radius r, if there exists a symmetric matrix P such that condition (B.24) holds,

$$\begin{bmatrix} -rP & qP + PA(\rho) & PB_w(\rho) & 0 \\ * & -rP & 0 & H(\rho)^T \\ * & * & -\gamma I_d & J_w(\rho)^T \\ * & * & * & -\gamma I_r \end{bmatrix} \prec 0. \tag{B.24}$$

where: $\mathcal{L} = \begin{bmatrix} -r & q \\ q & -r \end{bmatrix}$, and $M = \begin{bmatrix} 0 & 1 \\ 0 & 0 \end{bmatrix} = \underbrace{\begin{bmatrix} 1 \\ 0 \end{bmatrix}}_{M_1^T} \underbrace{\begin{bmatrix} 0 & 1 \end{bmatrix}}_{M_2}$.

Since condition (B.24) is parameter-dependent, according to the analysis in reference (Chilali et al., 1999) it is recommended to check overall characteristic function for each region $\mathcal{D}_i$ in order to be more efficient and less conservative to test the robust $\mathcal{D}$-stability.

B.5 $\mathscr{H}_2$ Performance

The $\mathscr{H}_2$-norm is more effective in dealing with stochastic characteristics such as measurement noise and random disturbance (tremors, wind loads, wind gusts, surface profiles, turbulent, etc.). Rather than bounding the output energy, it may be desirable to keep the

peak amplitude of the output below a certain level. The $\mathscr{H}_2$–norm of a system measures the output energy in the impulse responses of the system. Suppose LPV system (B.2) with $D(\rho)=0$ is asymptotically stable, if and only if exists a performance index $\gamma>0,$ and a symmetric positive matrix $P\in\mathbb{S}^n_{++}, Q\in\mathbb{S}^r_{++}$ such that the following LMIs:

$$\begin{bmatrix} A(\rho)^T P + PA(\rho) & PB(\rho) \\ * & -I \end{bmatrix} \prec 0, \qquad \begin{bmatrix} P & C(\rho)^T \\ * & Q \end{bmatrix} \succ 0, \qquad \text{trace}\,(Q) < \gamma^2. \tag{B.25}$$

are satisfied. These conditions restrict the limits of the impulse response of the system to be smaller than some admissible values conforming to the design specification. Indeed, that implies in a less conservative condition.

B.6 Generalized $\mathscr{H}_2$ Performance

The multi-objective typically relates to the conflicting requirements e.g., satisfying time-domain hard constraints, capturing the peak amplitude of the output signal over all unit-energy inputs, etc. So, the energy-to-peak strategy shows a reasonable choice to relax the conservation of the stability condition involved in the robust control design. Similarly, supposing $D(\rho)=0,$ then the so-called generalized $\mathscr{H}_2$-norm is defined for LPV system (B.2) as $\mathcal{L}_2$–$\mathcal{L}_\infty$ induced norm:

$$\|z(t)\|^2_{\mathcal{L}_\infty} < \gamma^2 \|w(t)\|^2_{\mathcal{L}_2}, \tag{B.26}$$

is guaranteed if and only if there exists an energy-to-peak performance index $\gamma>0$ and a symmetric positive matrix $P\in\mathbb{S}^n_{++},$ such that the following conditions hold:

$$\begin{bmatrix} A(\rho)^T P + PA(\rho) & PB(\rho) \\ * & -I \end{bmatrix} \prec 0, \qquad \begin{bmatrix} P & C(\rho)^T \\ * & \gamma^2 I \end{bmatrix} \succ 0. \tag{B.27}$$

This *modified* condition keeps the peak amplitude of the output $z(t)$ bounded by an allowable value corresponding to the design specifications, e.g., to guarantee the safety constraints, to avoid the actuator saturations (saving energy), etc. The generalized $\mathscr{H}_2$–norm uses to ensure robust stability that appears less conservative than the $\mathscr{H}_\infty$-norm (since it bounds the peak amplitude of the output over the input disturbances - white noise or impulse). However, the specification of time-domain hard constraints is sometimes in the sense of probability.

Appendix C

Technical Results in Time-Delay Systems

Delay-Dependent Lyapunov-Krasovskii functional Stability

C.1 Convex function.

We would discuss here the alternative improvement for the tighter bounding inequalities relate to the LKF stability conditions. Some definitions of convex domain properties refer to Appendix A.1.3.

In order to better estimate the lower bound on the quadratic integral term derived from the stability conditions, the application of the following inequalities plays a core role in the developments:

Lemma C.1.1. (PooGyeon Park, 1999) *Given vector functions* $a,b:\Omega\mapsto\mathbb{R}^n$. *Then for any matrices* $M\in\mathbb{R}^n$, *and* $X\in\mathbb{S}_+^n$, *the following inequality hold:*

$$-2\int_{\Omega} b(\theta)^T a(\theta)d\theta \leq \int_{\Omega}\begin{bmatrix}a(\theta)\\ b(\theta)\end{bmatrix}^T\begin{bmatrix}X & XM\\ * & (M^TX+I)X^{-1}(XM+I)\end{bmatrix}\begin{bmatrix}a(\theta)\\ b(\theta)\end{bmatrix}d\theta, \tag{C.1}$$

by choosing matrix $M=0$, *the above condition returns to its basic form.*

Lemma C.1.2. (Moon et al., 2001) *Assume that* $a:\Omega\mapsto\mathbb{R}^n$ *and* $b:\Omega\mapsto\mathbb{R}^m$ *are given vector function, and* $N\in\mathbb{R}^{n\times m}$ *is given matrix. Then for any matrices* $X\in\mathbb{S}^n$ $Y\in\mathbb{R}^{n\times m}$, $Z\in\mathbb{S}^m$ *if the following condition is satisfied:*

$$\begin{bmatrix}X & Y\\ * & Z\end{bmatrix}\succeq 0\,, \tag{C.2}$$

then the inequality hold

$$-2\int_{\Omega} b(\theta)^T N^T a(\theta)d\theta \leq \int_{\Omega}\begin{bmatrix}a(\theta)\\ b(\theta)\end{bmatrix}^T\begin{bmatrix}X & Y-N\\ * & Z\end{bmatrix}\begin{bmatrix}a(\theta)\\ b(\theta)\end{bmatrix}d\theta. \tag{C.3}$$

by choosing matrix $M=0$, *the above condition returns to its basic form.*

C.1.1 *Jensen's Inequality and Extensions Approach*

There are considerable famous inequalities are derived from original Jensen's inequality to some applied convex function or variations of characterize convexity. Among studies, the integral version of Jensen's inequality is frequently employed in control delay theory in the last decades.

Lemma C.1.3. (Mitrinović et al., 1993a) *Let* $\mathbb{I}$ *be an interval in* $\mathbb{R}$. *For* $a,b\in\mathbb{I}$, *then an integrable function* $\varphi:\mathbb{I}\mapsto\mathbb{R}$, *is said to be J-convex on* $[a,b]$ *if the following inequality*

$$\varphi\left(\int_a^b f(\cdot)d\sigma\Big/\int_a^b d\sigma\right)\leq\int_a^b\varphi(f(\cdot))d\sigma\Big/\int_a^b d\sigma\,, \tag{C.4}$$

is valid for all integrable function $f\in dom(\varphi)$.

By choosing $\varphi(f(x))=f(x)^TQf(x), f(x)=\dot{x}$, with $x\in\mathbb{I}^n$, and $Q\in\mathbb{S}_{++}^n$, that entails in the *original form* of Jensen inequality that might be found in the time delay literature (Briat, 2015b; Fridman, 2014; Gu et al., 2003) and references mentioned therein. Jensen's inequality improvement also can be found in the mathematical literature (Fink & Jodeit, 1990; Mitrinović et al., 1993c). Thereby, it provides a judicious generalization of this inequality including the finite *n*-segments on the specified interval $[a,b]$. The convexity application is proposed to reduce the conservation of Jensen integral inequality (C.4).

In addition, the higher monotonicity derive from the use of Chebyshev's inequality. These consist essentially of functions for which several derivatives are also convex. In the literature (Fink & Jodeit, 1990), they have invested the "*best possible*" of Jensen's inequality

for all φ convex and σ is *end-positive*. The article also covers the case of function φ is *n*-convex, which is widely applied in two development directions. Those are the discrete interval integrals (Gu et al., 2003; Han, 2008) and high-order convex functions (Park et al., 2015; Tian & Wang, 2020; Zhao et al., 2017).

Lemma C.1.4. (Fink & Jodeit, 1990) *For* $a,b\in\mathbb{I}$, *and an integrable function* $f(x):[a,\ b]\to\mathbb{R}^n$ *such that the following equality*

$$\int_x^b dx_1\int_{x_1}^b dx_2\cdots\int_{x_n}^b f(x_{n+1})dx_{n+1}=\frac{1}{n!}\int_a^b (y-x)^n f(y)dy. \tag{C.5}$$

holds for any $x\in[a,b]$

Proof. The demonstration is referred to (Fink & Jodeit, 1990; Tian & Wang, 2020).

Lemma C.1.5. (Park et al., 2015) *Gives an integrable function* $w(x):[a,\ b]\to\mathbb{R}^n$, *and an auxiliary scalar function* $\overline{p}(x):[a,\ b]\to\mathbb{R}^n$ *satisfies* $\int_a^b\overline{p}(s)ds=0$, *exits a positive matrix* $R\in\mathbb{R}_{++}^n$ *such that the following equality holds*

$$\begin{aligned}\int_a^b w(s)^T Rw(s)ds\geq&\frac{1}{b-a}\left(\int_a^b w(s)ds\right)^T R\left(\int_a^b w(s)ds\right)\\&+\left(\int_a^b\overline{p}(s)^2ds\right)^{-1}\left(\int_a^b\overline{p}(s)w(s)ds\right)^T R\left(\int_a^b\overline{p}(s)w(s)ds\right).\end{aligned} \tag{C.6}$$

Proof. The proof is given in appendix 2.2 or referred to (Park et al., 2015).

Inequality (C.6) is essentially a generalization of Jensen's inequality from which the following consequences can be deduced.

Corollary C.1.1. Jensen's Inequality (Gu et al., 2003) *For all continuous integrable function* $w(x):[a,\ b]\to\mathbb{R}^n$, *exits a positive matrix* $R\in\mathbb{R}_{++}^n$ *such that the following equality holds*

$$\int_a^b w(s)^T Rw(s)ds\geq\frac{1}{b-a}\Omega_1^T R\Omega_1. \tag{C.7}$$

where $\Omega_1=\int_a^b w(s)ds$.

Corollary C.1.2. Wirtinger-Based Inequality (Seuret & Gouaisbaut, 2013) *For all continuous integrable function* $w(x):[a,\ b]\to\mathbb{R}^n$, *exits a positive matrix* $R\in\mathbb{R}_{++}^n$ *such that the following equality holds*

$$\int_a^b w(s)^T Rw(s)ds\geq\frac{1}{b-a}\Omega_1^T R\Omega_1+\frac{3}{b-a}\Omega_{20}^T R\Omega_{20}. \tag{C.8}$$

where $\Omega_{20}=\Omega_1-\frac{2}{b-a}\int_a^b\int_a^s w(\theta)d\theta\,ds$.

Corollary C.1.3. Auxiliary-Function-Based Inequality (Park et al., 2015) *For a positive matrix* $R\in\mathbb{R}_{++}^n$ *and any continuous integrable function* $w(x):[a,\ b]\to\mathbb{R}^n$, *the following equality holds*

$$\int_a^b w(s)^T R w(s) ds \geq \frac{1}{b-a}\Omega_1^T R \Omega_1 + \frac{3}{b-a}\Omega_2^T R \Omega_2 + \frac{5}{b-a}\Omega_3^T R \Omega_3. \tag{C.9}$$

where

$$\Omega_2 = \Omega_1 - \frac{2}{b-a}\int_a^b \int_s^b w(\theta) d\theta\, ds,$$
$$\Omega_3 = -2\Omega_1 + 3\Omega_2 + \frac{12}{(b-a)^2}\int_a^b \int_s^b \int_\theta^b w(\beta) d\beta\, d\theta\, ds.$$

Corollary C.1.4. Auxiliary-Function-Based Inequality (Park et al., 2015) *For a positive matrix* $R \in \mathbb{R}^n_{++}$ *and any continuous integrable function* $w(x):[a,\ b] \to \mathbb{R}^n$, *the following equality holds*

$$\int_a^b \int_s^b w(\theta)^T R w(\theta) d\theta\, ds \geq 2\Omega_4^T R \Omega_4 + 4\Omega_5^T R \Omega_5. \tag{C.10}$$

where $\Omega_4 = \frac{1}{2}(\Omega_1 + \Omega_2),\ \Omega_5 = \frac{1}{2}(\Omega_2 + \Omega_3)$.

Another proof of Corollary C.1.4 can be found at (Van Hien & Trinh, 2015). Recently, a general case of the double integral inequalities deployed for the 2nd order formulation (similar to Corollary C.1.4) and the 3rd order formulation provided in the literature (Zhao et al., 2017) are attracting works.

Lemma C.1.6. (Zhao et al., 2017) *For an auxiliary scalar function* $\varphi(x):[a,\ b] \to \mathbb{R}^n$, *satisfies* $\int_a^b \int_a^b \varphi_i(\theta)\varphi_j(\theta) d\theta\, ds = 0$, *a positive matrix* $R \in \mathbb{R}^n_{++}$ *and any continuous integrable function* $w(x):[a,\ b] \to \mathbb{R}^n$, *the following equality*

$$\int_a^b \int_s^b w(\theta)^T R w(\theta) d\theta\, ds \geq \sum_{i=1}^{\infty} \frac{1}{p_i}\Omega_i(w)^T R \Omega_i(w), \tag{C.11}$$

holds with $\Omega_i(w) = \int_a^b \int_s^b \varphi_i(\theta) w(\theta) d\theta\, ds,\ p_i = \int_a^b \int_s^b \varphi_i^2(\theta) d\theta\, ds$.

C.1.2 *Discretized Convex Function*

We use an example to show the effective reduction of the conservation of inequality by the discretizing method of the *n*-convex function.

Example C.1.1: By considering the following integrals:

$$I_0 = \int_a^b cx^2 dx, I_1 = \frac{1}{b-a}\left(\int_a^b c^{\frac{1}{2}} x dx\right)^2, \text{and } I_2 = \frac{2}{b-a}\left(\int_a^{\frac{1}{2}(a+b)} c^{\frac{1}{2}} x dx\right)^2 + \frac{2}{b-a}\left(\int_{\frac{1}{2}(a+b)}^b c^{\frac{1}{2}} x dx\right)^2.$$

where $f(x) = cx^2$, $c \in \mathbb{R}_{++}$ is *J*-convex functions satisfying the definitions given in Appendix A.1.3 (convex geometry gives in Figure C-1.*b*&*c*). The gap in Jensen's inequality is characterized by a positive difference between integrals $\Delta_i = I_i - I_0, i = 1, \ldots, N$. Let's analyze the first three orders $i = 1, 2, 3,$ as follows:

$$\begin{aligned}
\Delta_1 &= I_0 - I_1 \\
&= \frac{c}{3}x^3\Big|_a^b - \frac{c}{b-a}\left(\frac{x^2}{2}\Big|_a^b\right)^2 \\
&= \frac{c}{3}(b^3 - a^3) - \frac{c}{4}((b^3 - a^3) - ab(b-a)) = \frac{c(b-a)^3}{12} = \frac{c(b-a)^3}{12 \cdot \mathbf{1}^2}.
\end{aligned}$$

And,

$$\begin{aligned}\Delta_2 &= I_0 - I_2.\\ &= \frac{c}{3}x^3\Big|_a^b - \frac{2c}{b-a}\left(\frac{x^2}{2}\Big|_a^{\frac{a+b}{2}}\right)^2 - \frac{2c}{b-a}\left(\frac{x^2}{2}\Big|_{\frac{a+b}{2}}^{b}\right)^2.\\ &= \frac{c}{3}(b^3-a^3) - \frac{c}{16}(b-a)(5a^2+6ab+5b^2) = \frac{c(b-a)^3}{48} = \frac{c(b-a)^3}{12\cdot\mathbf{2}^2}.\end{aligned}$$

Similarly, by dividing interval $[a,b]$ into 3 equal segments, we have integral

$$I_3 = \frac{3}{b-a}\left(\int_a^{\frac{1}{3}(a+b)} c^{\frac{1}{2}}xdx\right)^2 + \frac{3}{b-a}\left(\int_{\frac{1}{3}(a+b)}^{\frac{2}{3}(a+b)} c^{\frac{1}{2}}xdx\right)^2 + \frac{3}{b-a}\left(\int_{\frac{2}{3}(a+b)}^{b} c^{\frac{1}{2}}xdx\right)^2,$$

and 3th-*order* integral inequality gap

$$\begin{aligned}\Delta_3 &= I_0 - I_3.\\ &= \frac{c}{3}x^3\Big|_a^b - \frac{3c}{b-a}\left(\frac{x^2}{2}\Big|_a^{\frac{1}{3}(a+b)}\right)^2 - \frac{3c}{b-a}\left(\frac{x^2}{2}\Big|_{\frac{1}{3}(a+b)}^{\frac{2}{3}(a+b)}\right)^2 - \frac{3c}{b-a}\left(\frac{x^2}{2}\Big|_{\frac{2}{3}(a+b)}^{b}\right)^2.\\ &= \frac{c}{3}(b^3-a^3) - \frac{c}{4\cdot 3^3(b-a)}((a+b)^2(74a^2-140ab+74b^2)+2\cdot 3^4a^2b^2)\\ &= \frac{c(b-a)^3}{108} = \frac{c(b-a)^3}{12\cdot\mathbf{3}^2}.\end{aligned}$$

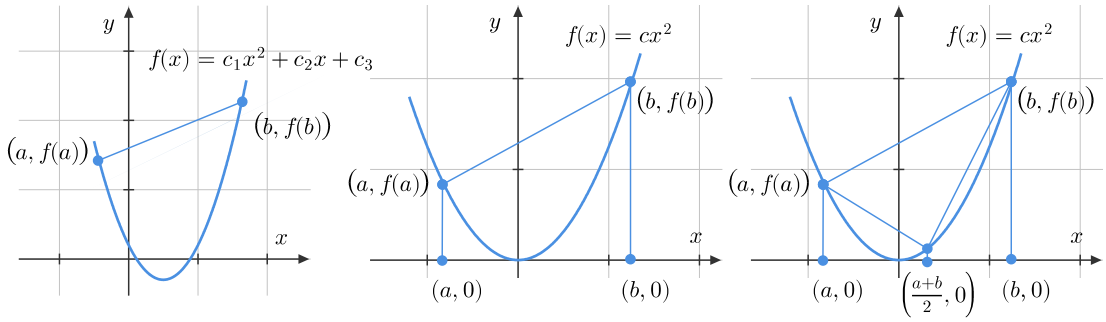

a. The chord of the parabola expresses convex inequality. *b. The integral region of the parabola is in the interval.* *c. The integral domain fragmentation.*

Figure C-1. *Graph of a convex function.*

This method significantly enhances the stability analysis of time-delay systems with the least conservative results by minimizing gap in matrix inequalities constraint.

C.2 Model Transformation

There are considerable researches using model Transformation methods for analyzing delay-dependent stability conditions using the Lyapunov-Krasovskii function as outlined in (Briat, 2015b; Fridman, 2014; Fridman & Shaked, 2003). Actually, it can be recapitulated in two approaches: explicit model transformations and implicit model transformations (Gu et al., 2003). The model transformation methods and the improvement inequalities were proposed to reduce the conservatism of delay-dependent conditions of the LTI delay system. According to the analysis in (Briat, 2015b; Fridman, 2014; Fridman &

Shaked, 2003; Gu et al., 2003), nonetheless these methods have yet to be thoroughly improved. Let's consider the features of model transformations.

C.2.1 *Model transformation I - Newton-Leibniz Model Transformation*

The delayed terms $x(t-h)$ in the LTI delay systems are substituted to yield the fixed model transformations:

$$\dot{x}(t) = (A + A_h)x(t) - A_h \int_{t-h}^{t} (Ax(\theta) + A_h x(t-h))d\theta. \tag{C.12}$$

$$\dot{x}(t) = (A + A_h)x(t) - A_h \int_{t-h}^{t} \dot{x}(\theta)d\theta. \tag{C.13}$$

and parametrized model transformation (PMT):

$$\dot{x}(t) = (A + C)x(t) + (A_h - C)x(t-h) - C\int_{t-h}^{t} (Ax(\theta) + A_h x(t-h))d\theta. \tag{C.14}$$

The following Lyapunov-Krasovskii functional is used to determine a delay-dependent stability condition for system (C.12) and (C.14):

$$V(x,t) = V_1(t) + V_2(t) + V_3(t), \tag{C.15}$$

where $V_1(t) = x(t)^T Px(t) + \int\limits_{t-h(t)}^{t} x(\theta)^T Qx(\theta)d\theta$, $V_2(t) = \int\limits_{-h}^{0}\int\limits_{t+\theta}^{t} x(s)^T Rx(s)dsd\theta$,

and $V_3(t) = \int\limits_{-2h}^{-h}\int\limits_{t+\theta}^{t} x(s)^T R_1 x(s)dsd\theta$. A LKF candidate is considered for system (C.13):

$$V(x,t) = V_1(t) + V_4(t), \text{ where } V_4(t) = \int\limits_{-h}^{0}\int\limits_{t+\theta}^{t} \dot{x}(s)^T R\dot{x}(s)dsd\theta. \tag{C.16}$$

Consequently, the derivative of the LKFs result in the following expression,

$$-2x(t)^T PA_h \int_{t-h}^{t} (Ax(\theta) + A_h x(\theta - h))d\theta, \text{ and } -2x(t)^T PA_h \int_{t-h}^{t} \dot{x}(\theta)d\theta, \tag{C.17}$$

that cannot seem to be directly suppressed by model transformation. By imposed the bounding cross-term inequality we have:

$$-2x(t)^T PA_h \int_{t-h}^{t} \dot{x}(\theta)d\theta \le hx(t)^T PA_h R^{-1} A_h^T Px(t) + \int_{t-h}^{t} \dot{x}(\theta)^T R\dot{x}(\theta)d\theta, \tag{C.18}$$

and, $-2x(t)^T PA_h \int_{t-h}^{t} (Ax(\theta) + A_h x(\theta - h))d\theta \le hx(t)^T PA_h \begin{bmatrix} A \\ A_h \end{bmatrix}^T \begin{bmatrix} R^{-1} & 0 \\ 0 & R_1^{-1} \end{bmatrix} \begin{bmatrix} A \\ A_h \end{bmatrix} A_h^T Px(t)$

$$+ \int_{t-h}^{t} x(\theta)^T Rx(\theta)d\theta + \int_{t-2h}^{t-h} x(\theta)^T R_1 x(\theta)d\theta. \tag{C.19}$$

Remark C.2.1. Model transformation given in (C.13) has the same purpose as the fixed model transformation (C.12). Where the term $h\dot{x}(\theta)^T R\dot{x}(\theta)$ produced in derivative stability problem analysis is replaced by original system, but that entails in the persisted delay terms $x(t-h)$. The inconsistent elimination of the integral terms and delay terms in this explicit model transformation leads to conservativeness. On the other hand, the use of

parametrized model transformation method produces a new matrix parameter in cross-term, where the compensation of the additional dynamics is reformatted into variable matrix optimization problem. However, the basic bounding inequality applied for cross-terms resulting in conservatism, whereas the application of Park's inequality to PMT stability condition as analysis (Fridman & Shaked, 2003) shows no more improvement in conditional relaxation.

C.2.2 *Model transformation II – Neutral type Transformation*

As an alternative introduction to system (C.12), we have the following LTI delay system:

$$\frac{d}{dt}\left[x(t)+A_h\int_{t-h}^{t}x(\theta)d\theta\right]=(A+A_h)x(t). \tag{C.20}$$

The aim of above model transformations is to convert the integral term into the functional differential equation so as to produce both cross terms and quadratic integral terms in the derivative of a Lyapunov-Krasovskii functional along the trajectories of the systems. But because of the following disadvantages that leads to their supersession by other methods.

1 - The original system is recovered in (C.17) then the effect of the transformed model would be lost.

2 - Both transformation methods introduce additional dynamics into the system, then the transformed system is not equivalent to the original one.

3 - By applied the bounding inequality for cross-term (C.17) entails in conservatism since the right-hand side of (C.18), (C.19) are always positive.

4 - Eliminating the integral expression in the derivative of LKF has also lost important information in negative definite stability conditions.

As point out by (Briat, 2015b; Fridman & Shaked, 2003; Gu & Niculescu, 2001) the use of the Newton-Leibniz model transformation might lead to more conservative stability conditions and lose its generality for the reasons outlined above. In order to improve these results certainly count on either by using less restrictive model-transformations (or even no model-transformation at all) or by employing more accurate bounding techniques (as given in Lemma C.1.1 and Lemma C.1.2). The application these inequalities reduces the conservative LMI stability conditions, and can be incorporated with others model transformations. However, when the computational complexity of the conditions increase (parameter dependent Lyapunov function PDLF, optimization of the attraction domain - saturation control, robust stability...) then the generality of the inequality lost.

C.2.3 *Model transformation III – Descriptor (Fridman) Transformation*

The following descriptor model transformation is proposed by (Fridman, 2001) has attracted significant attentions in last decade:

$$\dot{x}(t)=y(t),\qquad y(t)=(A+A_h)x(t)-A_h\int_{t-h}^{t}y(\theta)d\theta. \tag{C.21}$$

The Lyapunov-Krasovskii functional is employed for this class of system:

$$V(x,t)=\begin{bmatrix}x(t)\\ y(t)\end{bmatrix}^T\underbrace{\begin{bmatrix}I & 0\\ 0 & 0\end{bmatrix}}_{E}\underbrace{\begin{bmatrix}P_1 & 0\\ P_2 & P_3\end{bmatrix}}_{P}\begin{bmatrix}x(t)\\ y(t)\end{bmatrix}+\int_{t-h(t)}^{t}x(\theta)^TQx(\theta)d\theta+V_2(t). \tag{C.22}$$

After derivative of LKF equation (C.22) similar to the previous methods, we obtained the following cross terms:

$$-2\int_{t-h}^{t}\begin{bmatrix}x(t)\\ y(t)\end{bmatrix}^TP^T\begin{bmatrix}0\\ A_h\end{bmatrix}y(\theta)d\theta. \tag{C.23}$$

The bounding of this cross terms eliminates the quadratic integral terms in the derivative of the Lyapunov-Krasovskii functional (the one related to the derivative of the double integral $\dot{V}_2(t)$). Even though the descriptor method relies on a non-conservative model transformation and make an interesting result, however, it still has some limitations.

1 - It is still based on cross-terms bounding inequality ensuing to conservatism.

2 - Inconsistent substitution of delay term in system and in stability condition and the adding zero-equivalent term with weighting matrices lead to the requirement of determining optimization of the fixed weighting matrices.

The use of Moon's inequality (Lemma C.1.2) in combination with this transformation method yield to less conservativeness delay-dependent conditions that seems useful in stability, stabilization analysis and control synthesis. Besides, the computational complexity of the above result can be improved by relaxation method (Briat, 2015b) that provide a better construction of the variable matrices.

C.2.4 *Model transformation IV – Free Weighting Matrix Approach*

In the above sections, we have analyzed the transformation methods and the inequalities that enhance the LK dependent stability conditions. As has been mentioned, the distribution of heterogeneous matrix weight functions corresponding to variables $x(t)$, $x(t-h)$, and $\int_{t-h}^{t}\dot{x}(\theta)d\theta$ (there are a relationship between them), that can interfere with solution of stability conditions. Consequently, the Free Weighting Matrix (FWM) method is introduced in (He et al., 2004a, 2007) generally called by *lifting-variables* that gives more degree of freedom in design condition stability. In which the fixed weighting matrices are replaced by appropriate dimensional *slack* matrices by the following *null* algebraic matrix equations:

$$2\left(x(t)^TN_1+x(t-h)N_2\right)\left(x(t)-x(t-h)-\int_{t-h}^{t}\dot{x}(\theta)d\theta\right)=0. \tag{C.24}$$

These additional free matrices not only produce *linkage information* weighting matrices between the dynamic variables $x(t)$, $x(t-h)$,$\int_{t-h}^{t}\dot{x}(\theta)d\theta$, but also neutralize constraint of Newton-Leibniz formula and associate with information on maximizing the upper bound on delay value.

A methodological improvement is found in the works (Briat, 2015b; M. Wu et al., 2010), however there are the matrix variables to be determined along with decision matrices of

stability conditions including *P–system dynamic*, Q and R–*delay dependent*. And as pointed out (Briat, 2015b), after using the reduction in computational complexity method for FWM inequality that leads to in similar results to the inequality introduced hereafter.

C.3 Input-Output Approach

As discussed, the delay *decomposition* approach is less conservative results for stability analysis and controller design. But the method is effective for systems that *access* the exact knowledge of the delay, which is ideal for numerical computation in practical design. The identifications or estimations of the continuous-time delay phenomenon in practice are tough challenges, see, e.g., (Anguelova & Wennberg, 2008; Belkoura et al., 2009; Chen et al., 2015; Ren et al., 2005; Zheng et al., 2011). In this case, the uncertainty (approximation) delay method discussed in Section 8.6 (Gu et al., 2003) shows to be more suitable for implementing the strategy of control system design. Specifically, the time-varying delay that is not accurately known at the time of analysis and design is considered as the dynamical uncertainties of a nominal system. Based on this approach, the stability is formulated in the input-output framework where the characterized LMI conditions obtain by the Scaled Small-Gain theorem (Briat et al., 2009; Hmamed et al., 2015) or supply function (Briat et al., 2010). The equivalent between the Scaled Small-Gain and Lyapunov-based technique is discussed in (Boyd et al., 1994; Boyd & Yang, 1989; Doyle et al., 1991; J. Zhang et al., 2001; Zhou & Doyle, 1998) for LTI/LPV systems.

C.3.1 *Approximate Delay-Range Approach*

The input-output approach is very convenient in analyzing the stability based on the representation of the original system to feedback interconnection with additional inputs and outputs of auxiliary systems. The analysis of uncertain LPV systems deployed by the small-gain theorem has attracted much interest in the literature in the last century. Besides, the robust stability and performance problems could reformulate in LMIs formulation can efficiently solve by convex programming.

The approximate delay value around the nominal values derived from the uncertain delay-range-dependent approach (Gu et al., 2003), or the time-varying approximation delay (Briat, 2008). Temporarily ignore the effect of disturbance, the TDS system is transformed to the following differential equation:

$$\begin{aligned}\dot{x}(t) &= Ax(t) + A_h x(t-h_a) \\ &\quad - A_h \int_{t-h_a-\delta(t)}^{t-h_a} (Ax(\tau) + A_h x(\tau - h_a - \delta(t)))d\tau,\end{aligned} \tag{C.25}$$

with the assumption of knowing the variation of the delay $0 < \underline{h} \le h(t) \le \overline{h}$, by choosing a constant approximate value $h_a \in [\underline{h}, \overline{h}]$, and defining a limit of uncertain interval delay $\delta(t) = h(t) - h_a, |\delta(t)| \le h_u = \max\{h_a - \underline{h}, \overline{h} - h_a\}$. The distributed delay is now considered as an input disturbance. The stability analysis for system (C.25) would infer to system

$$\dot{x}(t) = Ax(t) + A_h x(t-h), \tag{C.26}$$

but without the initial condition there does not guarantee an equivalence.

By using the internal topology with input-output structure:

$$z(t) = Gw(t), \text{ and } w(t) = \Delta z(t). \tag{C.27}$$

The system (C.25) is represented by a generalization (Gu et al., 2003),

$$\begin{aligned} \dot{x}(t) &= Ax(t) + A_h x(t-h_a) + h_u A_h w_2(t), \\ z_1(t) &= (1-\mu)^{-\frac{1}{2}} x(t), \\ z_2(t) &= Ax(t) + A_h w_1(t), \end{aligned} \tag{C.28}$$

where the operators are defined as

$$w_1(t) = (1-\mu)^{\frac{1}{2}} z_1(t-h_a-\delta(t)). \tag{C.29}$$

$$w_2(t) = -h_u^{-1} \int_{t-h_a-\delta(t)}^{t-h_a} z_2(\tau) d\tau. \tag{C.30}$$

Proposition C.3.1. *These operators enjoy the following immediate property*

- Δ *is* $\mathcal{L}_2$ *input-output stable and satisfies the scaled small gain condition*.

Proof.

Let's consider a set of block-diagonal appropriate dimension matrices

$$\mathcal{D}_\Delta := \left\{ diag(L_1, L_2) \;\middle|\; L_1, L_2 \in \mathbb{S}_{++}^n \right\}. \tag{C.31}$$

The interconnected system feedback $\mathcal{F}_u(G, \Delta)$ is well–defined and input–output stable if the following integral quadratic constraints satisfy

$$\mathcal{I}_k = \int_0^t w_k^T(\tau) L_k w_k(\tau) d\tau \leq \int_0^t z_k^T(\tau) L_k z_k(\tau) d\tau \tag{C.32}$$

For $k = 1$, replace (C.29) to the left side of (C.32) that results in:

$$\mathcal{I}_1 = (1-\mu) \int_0^t z_1^T(\tau - h_a - \delta(\tau)) L_1 z_1(\tau - h_a - \delta(\tau)) d\tau \tag{C.33}$$

By using substitution $\theta = \tau - h_a - \delta(\tau)$, that implies $d\theta = (1-\dot{\delta}(t))d\tau$, and assuming the zero-initial condition. It should be reminded the derivate uncertain delay $\dot{\delta}(t) = \dot{h}(t) \leq \mu$. We thus get:

$$\mathcal{I}_1 = (1-\mu) \int_0^{t-h_a-\delta(t)} \frac{z_1(\theta)^T L_1 z_1(\theta)}{(1-\dot{\delta}(t))} d\theta \leq \int_0^t z_1^T(\theta) L_1 z_1(\theta) d\theta. \tag{C.34}$$

And similarly, for $k = 2$.

$$\mathcal{I}_2 = h_u^{-2} \int_0^t \left[\int_{\tau-h_a-\delta(\tau)}^{\tau-h_a} z_2(\theta) d\theta \right]^T L_2 \left[\int_{\tau-h_a-\delta(\tau)}^{\tau-h_a} z_2(\theta) d\theta \right] d\tau \,. \tag{C.35}$$

By using Jensen's Inequality, we have:

$$\mathcal{I}_2 \leq h_u^{-2} \int_0^t |\delta(\tau)| \int_{\tau-h_a-\max\{0,\delta(\tau)\}}^{\tau-h_a-\min\{0,\delta(\tau)\}} z_2^T(\theta) L_2 z_2(\theta) d\theta d\tau. \tag{C.36}$$

With $\max\{\tau - h_a, \tau - h_a - \delta(\tau)\} = \tau - h_a - \min\{0, \delta(\tau)\}$, then by changing order of integration in double integrals as illustrated in Figure C-2.*a*, with assumption of the zero initial condition we obtain:

$$\begin{aligned}\mathcal{I}_2 &\le h_u^{-2}\int_{-h_a-\max\{0,\delta(0)\}}^{t-h_a-\min\{0,\delta(t)\}} z_2^T(\theta)L_2z_2(\theta)\left(\int_{\max\{0,\min\{\theta+h_a,\,\theta+h_a+\delta(\tau)\}\}}^{\min\{t,\,\max\{\theta+h_a,\,\theta+h_a+\delta(\tau)\}\}}|\delta(\tau)|d\tau\right)d\theta,\\ &\le h_u^{-2}\int_{-h_a-\max\{0,\delta(0)\}}^{t-h_a-\min\{0,\delta(t)\}} h_u^2 z_2^T(\theta)L_2z_2(\theta)d\theta,\\ &\le \int_0^t z_2^T(\theta)L_2z_2(\theta)d\theta. \end{aligned} \tag{C.37}$$

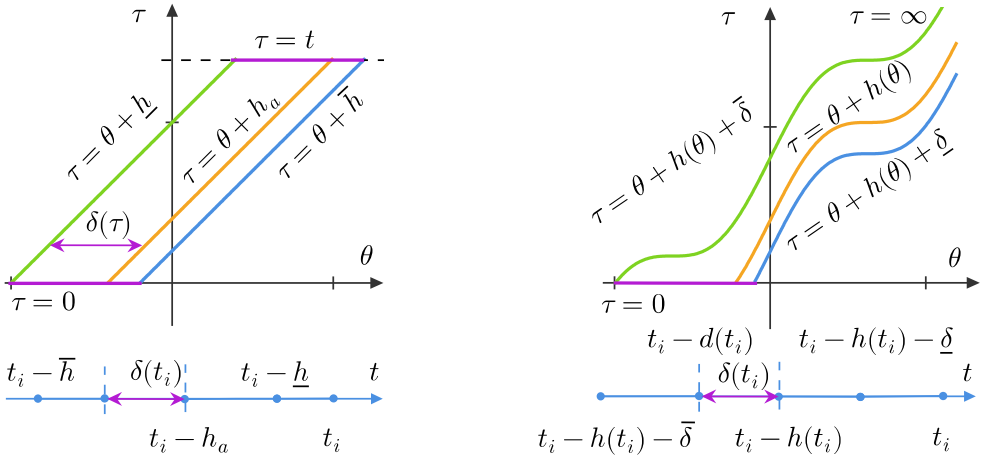

a. Constant approximation. *b. Uncertain approximation.*

Figure C-2. *Changing order of integration of double integrals.*

From condition (C.36) an *alternative proof* may be assigned.

$$\begin{aligned}\mathcal{I}_2 &\le h_u^{-2}\int_0^t|\delta(\tau)|\int_{\tau-h_a-\bar{h}}^{\tau-h_a-\underline{h}} z_2^T(\theta)L_2z_2(\theta)d\theta d\tau.\\ &\le h_u^{-2}\int_{-h_a-\bar{h}}^{t-h_a-\underline{h}} z_2^T(\theta)L_2z_2(\theta)\left(\int_{\max\{0,\theta+h_a+\underline{h}\}}^{\min\{t,\theta+h_a+\bar{h}\}}|\delta(\tau)|d\tau\right)d\theta,\\ &\le h_u^{-2}\int_{-h_a-\bar{h}}^{t-h_a-\underline{h}} h_u^2 z_2^T(\theta)L_2z_2(\theta)d\theta,\\ &\le \int_0^t z_2^T(\theta)L_2z_2(\theta)d\theta. \end{aligned} \tag{C.38}$$

C.3.2 *Uncertain Delay-Dependent Approach*

The previous stability of the comparison system is analyzed at a *constant* approximated delay in the varying dependency range, that purposely approached by the small gain theorem. Followed this approach, a time-varying approximation delay $d(t)$ was discussed in (Briat, 2008; Briat et al., 2010) along with a specified LK function to be able to capture both the maximal *nominal delay value* $\bar{h}=\max h(t)$, and the maximal resilient delay $\bar{\delta}=\max(h(t)-d(t))$. This delay-dependent approach is based on Lyapunov-Krasovskii technique with a resilient uncertain $\delta(t)\in[\underline{\delta},\bar{\delta}]$ is introduced by relation $d(t)=h(t)+\delta(t)$. By consider an additional Lyapunov-Krasovskii functions as follow:

$$V_{un}(t)=\int_{t-d(t)}^{t} x(\theta)^T Q_u x(\theta)d\theta+\delta_m\int_{\underline{\delta}}^{\bar{\delta}}\int_{t-h(t)+\theta}^{t}\dot{x}(\theta)^T R_u\dot{x}(\theta)d\theta d\tau. \tag{C.39}$$

with $\delta_m=\max\{\bar{\delta},|\underline{\delta}|\}$. The derivative of this LK function results to the following integral inequalities with approximately limited integral range:

$$
\begin{aligned}
-\delta_m \int_{t-h(t)+\underline{\delta}}^{t-h(t)+\overline{\delta}} \dot{x}(s)^T R_u \dot{x}(s) ds &\leq -\delta_m \int_{\min\{t-h(t),t-d(t)\}}^{\max\{t-h(t),t-d(t)\}} \dot{x}(s)^T R_u \dot{x}(s) ds, \\
&\overset{Jensen}{\leq} -\tfrac{\delta_m}{|h(t)-d(t)|} \left(\int_{t-h(t)}^{t-d(t)} \dot{x}(s) ds \right)^T R_u \int_{t-h(t)}^{t-d(t)} \dot{x}(s) ds, \\
&\overset{(*)}{=} -\tfrac{\delta_m}{|h(t)-d(t)|} (x_d - x_h)^T R (x_d - x_h).
\end{aligned} \tag{C.40}
$$

with denoted variables $x_d \coloneqq x(t-d(t)), x_h \coloneqq x(t-h(t))$. And an asymmetric bound of integration limits which are generalized in the approximate delay-dependent stability and stabilization analysis. Note that $x(t)$ has derivatives across the defined domain, the condition $(*)$ needs to be validated at the critical extreme time $d(t) \to h(t)$, that is explained detail in Appendix D.1. Besides, the delay approximation analyzed in (Briat et al., 2009, 2010) is more general than that introduced of (Gu et al., 2003) and enhances stability condition. But there is a restriction when $d(t)$ is involved in the system with two dependent delays, that need more design memory for the observer and controller structure.

In the framework of *non-small* delay, the upper bound on gains $w(t) = \Delta z(t)$ given by (Shustin & Fridman, 2007) with assumption of zero-initial condition as follows

$$
\gamma_0(\Delta) = \mu \sqrt{f(d)}, \qquad f(d) = \begin{cases} 1 & \text{if } -\infty \leq d \leq 1, \\ (2d-1)/d & \text{if } 1 < d < 2, \\ (7d-8)/(4d-4) & \text{if } d \geq 2, \\ 7/4 & \text{if } d \text{ is unknown.} \end{cases} \tag{C.41}
$$

From this point, (Briat et al., 2010) deliverers an operator to represent the interconnection input-output and have implemented both on LK and LFT stabilization approaches for delay-dependent LPV systems.

Proposition C.3.2. *Let's consider the operator $\Delta_0 : \mathcal{L}_2[0,\infty) \to \mathcal{L}_2[0,\infty)$ is expressed by the following equation:*

$$
w_0(t) = \Delta_0(z_0(t)) = \frac{2}{\sqrt{7}\delta_m} \int_{t-d(t)}^{t-h(t)} z(\tau) d\tau. \tag{C.42}
$$

This operator enjoys the property: Δ_0 is $\mathcal{L}_2$ input-output stable and satisfies the bounded small gain constraint $\|\Delta_0(z_0(t))\|_{\mathcal{L}_2} \leq \|z_0(t)\|_{\mathcal{L}_2}$.
Let's introduce an interconnection as follow:

$$
\begin{aligned}
z_0(t) &= \dot{x}(t), \\
w_0(t) &= \Delta_0(z_0(t)) = 2/(\sqrt{7}\delta_m)(x_h - x_d).
\end{aligned} \tag{C.43}
$$

The demonstration of operator Δ_0 satisfies SSG condition is addressed the same as proposition. The interconnected system is well-defined and input–output mapping stable if the following Integral Quadratic Constraints (IQC) satisfy:

$$
\mathcal{I} = \int_0^\infty w(\tau)^T L w(\tau) d\tau \leq \int_0^\infty z(\tau)^T L z(\tau) d\tau. \tag{C.44}
$$

For all positive definite matrix $Q \in \mathbb{S}_{++}^n$, we have:

$$\begin{aligned}\mathcal{I} &= \frac{4}{7\delta_m^2}\int_0^\infty \left[\int_{\tau-d(\tau)}^{\tau-h(\tau)} z(\theta)d\theta\right]^T L\int_{\tau-d(\tau)}^{\tau-h(\tau)} z(\theta)d\theta d\tau \\ &\overset{Jensen}{\leq} \frac{4}{7\delta_m^2}\int_0^\infty |\delta(\tau)|\int_{\tau-h(\tau)-\max\{0,\delta(\tau)\}}^{\tau-h(\tau)-\min\{0,\delta(\tau)\}} z(\theta)^T Lz(\theta)d\theta\, d\tau, \\ &\leq \frac{4}{7\delta_m^2}\int_0^\infty |\delta(\tau)|\int_{\tau-h(\tau)-\bar{\delta}}^{\tau-h(\tau)-\underline{\delta}} z(\theta)^T Qz(\theta)d\theta\, d\tau. \end{aligned} \tag{C.45}$$

The transforming the limits of integration into the domain of double integrals are described in Figure C-2.*b*. With assumption of the zero initial condition, we get:

$$\begin{aligned}\mathcal{I} &\leq \frac{4}{7\delta_m^2}\int_{-h(0)-\bar{\delta}}^{\infty} z(\theta)^T Lz(\theta)\left(\int_{\min\{0,\theta+h(\theta)+\underline{\delta}\}}^{\theta+h(\theta)+\bar{\delta}} |\delta(\tau)|d\tau\right)d\theta, \\ &\leq \frac{4}{7\delta_m^2}\int_0^\infty \delta_m^2 z(\theta)^T Lz(\theta)d\theta, \\ &\leq \int_0^\infty z(\theta)^T Lz(\theta)d\theta. \end{aligned} \tag{C.46}$$

C.3.3 *Delay-Scheduled LFT Approach*

In the framework of input-output stabilizing, the delay operators could let the time-varying delay play a role as the parametric uncertain, where the characterized stability synthesis of the approximate dependent delay can be addressed by the Lyapunov technique or by the small-gain theorem. In addition, similar to the uncertain structure framework, time-varying delay values can be cast as a gain-scheduled parameter. The gain scheduling in the analytical robust stability control framework for LTI/LPV systems are well-developed. Unlikely, the delay scheduling analysis for delay-dependent LPV systems has not been adequately studied and analyzed, see, for example (Briat, 2008, 2015b; Briat et al., 2008, 2007). An LPV plant with linear fractional depends on parameter and delay can represent as an upper LFT interconnection structure with delay operators Δ and parameter sets Θ (illustrated in Figure B-1). Let's consider the following operators.

Proposition C.3.3. *Let's consider the operators* $\Delta_i : \mathcal{L}_2[0,\infty) \to \mathcal{L}_2[0,\infty)$ *are expressed by the following equation:*

$$w_1(t) = \Delta_1(z_0(t)) = \frac{h_{\min}}{h_{\max}}\int_{t-h(t)}^{t} \frac{z_0(\tau)}{h(\tau)}d\tau. \tag{C.47}$$

$$w_2(t) = \Delta_2(z_0(t)) = \frac{1}{\sqrt{h_{\max}}}\int_{t-h(t)}^{t} \frac{z_0(\tau)}{\sqrt{h(\tau)}}d\tau. \tag{C.48}$$

These operators enjoy the property: Δ_i *are* $\mathcal{L}_2$ *input-output stable and satisfies the bounded small gain constraint* $\|\Delta_i(z_0(t))\|_{\mathcal{L}_2} \leq \|z_0(t)\|_{\mathcal{L}_2}$, with $i = 1, 2..$

The operator mentioned in Equation (C.47) has a singularity at zero, so the delay dependent is limited in the interval $[h_{\min}, h_{\max}]$ does not contain zero. Besides, operator (C.48) is quite similar to operator (C.42) with a defined interval conforming to the delay space $\mathcal{H}_0$ and transformed $\mathcal{L}_2$-norm encouraging for tightening conditions. By using structural LFT, the stabilizing condition is resolved via small gain theorem in (Briat, 2008).

Appendix D

Demonstration

D.1 The proof of Lemma 5.2.1.

The LPV system (5.1) is delay-dependent stable if the conditions:

$$\dot{V}\big(x(t),\dot{x}(t),\rho(t)\big)=\dot{x}(t)^{T}P(\rho(t))x(t)+x(t)^{T}P(\rho(t))\dot{x}(t)+x(t)^{T}\dot{P}(\rho(t))x(t)+x(t)^{T}Qx(t)$$

$$-(1-\dot{h}(t))x(t-h(t))^{T}Qx(t-h(t))+\overline{h}^{2}\dot{x}(t)^{T}R\dot{x}(t)-\overline{h}\int_{t-\overline{h}}^{t}\dot{x}(\theta)^{T}R\dot{x}(\theta)d\theta<0 \qquad \text{(D.1)}$$

hold along the trajectories of system. From the above condition, $\dot{x}(t)$ are substituted by the original dynamic system, the derivative of the time-varying delay is bounded, the derivative of the matrix dependent $P(\rho(t))$ analyzed as in Chapter 2, while the integral of the positive real function is organized by Jensen's inequality as follows.

$$\begin{aligned}-\overline{h}\int_{t-\overline{h}}^{t}\dot{x}(\theta)^{T}R\dot{x}(\theta)d\theta &\le -\overline{h}\int_{t-h(t)}^{t}\dot{x}(\theta)^{T}R\dot{x}(\theta)d\theta\\ &\overset{Jensen}{\le} -\frac{\overline{h}}{h(t)}\left(\int_{t-h(t)}^{t}\dot{x}(\theta)d\theta\right)^{T}R\int_{t-h(t)}^{t}\dot{x}(\theta)d\theta.\\ &=-\frac{\overline{h}}{h(t)}\big(x(t)-x(t-h(t))\big)^{T}R\big(x(t)-x(t-h(t))\big).\end{aligned} \qquad \text{(D.2)}$$

In order to verify the well-posed of the inequality (D.2) at extreme point $h(t)\to 0$, it is necessary to prove the defined domain included point $h(t_i)=0$ at time $t=t_i$. We have,

$$\begin{aligned}&\lim_{h(t_i)\to 0}\frac{\overline{h}}{h(t_i)}\big(x(t_i)-x(t_i-h(t_i))\big)^{T}R\big(x(t_i)-x(t_i-h(t_i))\big)\\ &=\lim_{h(t_i)\to 0}\overline{h}h(t_i)\frac{\big(x(t_i)-x(t_i-h(t_i))\big)^{T}}{h(t_i)}R\,\frac{\big(x(t_i)-x(t_i-h(t_i))\big)}{h(t_i)}\\ &=\lim_{h(t_i)\to 0}\overline{h}h(t_i)\dot{x}(t_i)^{T}R\dot{x}(t_i)=0.\end{aligned} \qquad \text{(D.3)}$$

For all $t\to t_i$, $h(t_i)\to 0$, $x(t)$ has a derivative at t_i, so condition (D.2) is defined for all $x(t)$ and $h(t)$ satisfying the initial assumption.

Henceforward, for the sake of simplicity, the time-dependent expressions "(t)", and scheduling parameter "(ρ)" are omitted in equations, denote $x_t \coloneqq x(t)$, $x_h \coloneqq x(t-h(t))$. In presence of external perturbations, combined the performance constraint (B.3) with the PDLKF stability condition (D.1) that results in the following stability condition:

$$\dot{V}+\gamma^{-1}z^{T}z-\gamma w^{T}w\le\xi^{T}\Upsilon\big(\rho,\dot{\rho}\big)\xi+\xi^{T}\Gamma^{T}\begin{bmatrix}\gamma^{-1}I_{r} & 0\\ 0 & R\end{bmatrix}\Gamma\xi<0, \qquad \text{(D.4)}$$

where $\xi^T = \begin{bmatrix} x_t^T & x_h^T & w^T \end{bmatrix}$, $\Gamma = \begin{bmatrix} H & H_h & J_w \\ \bar{h}A & \bar{h}A_h & \bar{h}B_w \end{bmatrix}$, and

$$\Upsilon(\rho,\dot{\rho}) = \begin{bmatrix} PA + A^T P + \sum_i \frac{\partial P}{\partial \rho_i} |\dot{\rho}_i| + Q - R & * & * \\ A_h^T P + R & -(1-\mu)Q - R & * \\ B_w^T P & 0 & -\gamma I_d \end{bmatrix}.$$

By using Schur complement (Boyd et al., 1994) yields to

$$\begin{bmatrix} PA + A^T P + \sum_i \pm\nu_i \frac{\partial P}{\partial \rho_i} + Q - R & * & * & * & * \\ A_h{}^T P + R & -(1-\mu)Q - R & * & * & * \\ E^T P & 0 & -\gamma I_d & * & * \\ H & H_h & J_w & -\gamma I_r & * \\ \bar{h}RA & \bar{h}RA_h & \bar{h}RB_w & 0 & -R \end{bmatrix} \prec 0, \tag{D.5}$$

Q.E.D.

D.2 The proof of Lemma 5.2.4.

The stability delay-dependent of LPV system (5.1) is ensured if the condition holds along the trajectories of system.

$$\begin{aligned} \dot{V}(t) = \dot{x}(t)^T P(\rho)x(t) + x(t)^T P(\rho)\dot{x}(t) + \frac{d}{dt}\left(\sum_{i=1}^N \int_{t-ih_\Delta(t)}^{t-(i-1)h_\Delta(t)} x(\theta)^T Q_i x(\theta) d\theta\right) \\ + x(t)^T \dot{P}(\rho)x(t) + \frac{d}{dt}\left(\sum_{i=1}^N \bar{h}_\Delta \int_{t-i\bar{h}_\Delta}^{t-(i-1)\bar{h}_\Delta} \int_\theta^t \dot{x}(s)^T R_i \dot{x}(s) ds d\theta\right) < 0. \end{aligned} \tag{D.6}$$

where the derivatives are developed as follows

$$\begin{aligned} \frac{d}{dt}\left(\sum_{i=1}^N \int_{t-ih_\Delta(t)}^{t-(i-1)h_\Delta(t)} x(\theta)^T Q_i x(\theta) d\theta\right) = \sum_{i=1}^N \Big(-(1-i\dot{h}_\Delta(t))x(t-ih_\Delta(t))^T Q_i x(t-ih_\Delta(t)) \cdots \\ + (t-(i-1)\dot{h}_\Delta(t))x(t-(i-1)h_\Delta(t))^T Q_i x(t-(i-1)h_\Delta(t))\Big). \end{aligned} \tag{D.7}$$

$$\begin{aligned} \frac{d}{dt}\left(\sum_{i=1}^N \bar{h}_\Delta \int_{t-i\bar{h}_\Delta}^{t-(i-1)\bar{h}_\Delta} \int_\theta^t \dot{x}(s)^T R_i \dot{x}(s) ds d\theta\right) = \sum_{i=1}^N \Big(\bar{h}_\Delta^2 \dot{x}(t)^T R_i \dot{x}(t) \cdots \\ - \bar{h}_\Delta \int_{t-i\bar{h}_\Delta}^{t-(i-1)\bar{h}_\Delta} \dot{x}(\theta)^T R_i \dot{x}(\theta) d\theta\Big). \end{aligned} \tag{D.8}$$

Then, following the line of the proof in D.1, we have:

$$\dot{V} + \gamma^{-1} z^T z - \gamma w^T w \le \xi^T \left(\Upsilon(\rho,\dot{\rho}) + \Gamma(\rho)^T \begin{bmatrix} \gamma^{-1} I_r & * & * & * \\ 0 & R_1 & * & * \\ \vdots & & \ddots & * \\ 0 & \cdots & 0 & R_N \end{bmatrix} \Gamma(\rho) \right) \xi < 0, \tag{D.9}$$

where $\xi^T = \begin{bmatrix} x_t^T & x_1^T & \cdots & x_{N-1}^T & x_N^T & w^T \end{bmatrix}$, $x_i := x(t-ih_\Delta(t))$, $x_N := x(t-h(t))$,

$$\Upsilon(\rho,\dot{\rho})=\begin{bmatrix} \Upsilon_{11} & * & * & * & * \\ R_1 & \ddots & & & * \\ \vdots & \ddots & \Theta_i & * & * \\ 0 & & R_{i+1} & \ddots & * \\ A_h(\rho)^T P & \cdots & 0 & R_N & -(1-\mu_N)Q_N - R_N & * \\ B_w(\rho)^T P & \cdots & 0 & 0 & 0 & -\gamma I_d \end{bmatrix},$$

with $\Upsilon_{11}(\rho,\dot{\rho}) = P(\rho)A(\rho) + A(\rho)^T P(\rho) + \sum_{j=1}^{N_p} \pm\nu_j(\partial P/\partial\rho_j) + Q_1 - R_1$,

$\Theta_i = -(1-\mu_i)(Q_i - Q_{i+1}) - R_i - R_{i+1},\ i = 1,\ldots,N-1,$

and $\Gamma = \begin{bmatrix} H(\rho) & 0 & \cdots & 0 & H_h(\rho) & J_w(\rho) \\ \overline{h}_\Delta A(\rho) & 0 & \cdots & 0 & \overline{h}_\Delta A_h(\rho) & \overline{h}_\Delta B_w(\rho) \\ \vdots & \vdots & & & \vdots & \vdots \\ \overline{h}_\Delta A(\rho) & 0 & \cdots & 0 & \overline{h}_\Delta A_h(\rho) & \overline{h}_\Delta B_w(\rho) \end{bmatrix}.$

Finally, by using Schur complement and rearrange rows and columns that results (5.41). Q.E.D.

D.3 The proof of Lemma 5.2.6.

The stability LMIs are derived from the derivative expansion of Lyapunov-Krasovskii functional (5.51) along trajectories of LPV time-delay system (5.50). Firstly, by expanding the $\dot{V}_0(t)$ and combining with $\mathcal{L}_2$-norm performance on the controlled output (5.50), that entails a similar condition with Lemma 5.2.1 as follows:

$$\dot{V}_0(t) + \gamma^{-1} z(t)^T z(t) - \gamma w(t)^T w(t) \le \xi(t)^T \Upsilon_0 \xi(t) + \xi(t)^T \Gamma_0^T \begin{bmatrix} \gamma^{-1} I_r & 0 \\ 0 & R \end{bmatrix} \Gamma_0 \xi(t), \qquad \text{(D.10)}$$

where $\xi(t)^T = \begin{bmatrix} x_t^T & x_h^T & x_d^T & w(t)^T \end{bmatrix}$, $\Gamma_0 = \begin{bmatrix} H & H_h & H_d & J_w \\ \overline{h}A & \overline{h}A_h & \overline{h}A_d & \overline{h}B_w \end{bmatrix}$, and

$$\Upsilon_0(\rho,\dot{\rho}) = \begin{bmatrix} PA + A^T P + \sum_i \dfrac{\partial P}{\partial \rho_i} |\dot{\rho}_i| + Q - R & * & * & * \\ A_h^T P + R & -(1-\mu)Q - R & * & * \\ A_d^T P & 0 & 0 & * \\ B_w^T P & 0 & 0 & -\gamma I_d \end{bmatrix}.$$

On the other hand, applying the analysis in (C.40) we have

$$\begin{aligned} \dot{V}_\Delta(t) &= x_t^T Q_u x_t - \big(1-\dot{d}(t)\big) x_d^T Q_u x_d + \delta_m^2 \dot{x}_t^T R \dot{x}_t - \delta_m \big(1-\dot{h}(t)\big) \int_{t-h(t)+\underline{\delta}}^{t-h(t)+\overline{\delta}} \dot{x}(s)^T R_u \dot{x}(s) ds \\ &\le x_t^T Q_u x_t - (1-\mu_d) x_t^T Q_u x_d + \delta_m^2 \dot{x}_t^T R_u \dot{x}_t - (1-\mu)(x_d - x_h)^T R_u (x_d - x_h). \qquad \text{(D.11)} \end{aligned}$$

As latter discussion, from the above inequality we have the two possibilities: at time t_i, the delay approximates $d(t)$ is close to $h(t)$. According to analysis in (D.3) when $\delta(t) \to 0$ so $(x_d - x_h)^T R (x_d - x_h)$ approaching 0. And, the second case is $d(t_j) \neq h(t_j)$.

Case 1: (*Time uniformity*) $d(t_i) = h(t_i)$, then the derivative LKF conditions associate

(D.10) with (D.11) will gather into the following form.

$$\dot{V}_0+\dot{V}_\Delta+\gamma^{-1}z^Tz-\gamma w^Tw\le\xi_1^T\Upsilon_1\xi_1+\xi_1^T\Gamma_1^T\begin{bmatrix}\gamma^{-1}I_r & * & *\\ 0 & R & *\\ 0 & 0 & R_u\end{bmatrix}\Gamma_1\xi_1<0 \tag{D.12}$$

where time expression (t) is dropped $\xi_1^T=\begin{bmatrix}x_t^T & x_h^T & w^T\end{bmatrix}$,

$$\Gamma=\begin{bmatrix}H & H_h+H_d & J_w\\ \bar{h}A & \bar{h}(A_h+A_d) & \bar{h}B_w\\ \delta_mA & \delta_m(A_h+A_d) & \delta_mB_w\end{bmatrix},$$

$$\Upsilon_1(\rho,\dot{\rho})=\begin{bmatrix}PA+A^TP+\sum_{i=1}^{N_p}\pm\nu_i\dfrac{\partial P}{\partial\rho_i}+Q+Q_u-R, & * & *\\ \left(A_d+A_h\right)^TP+R & -(1-\mu)(Q+Q_u)-R & *\\ E^TP & 0 & -\gamma I_d\end{bmatrix}.$$

By using the Schur complement that leads to the condition (5.54).

Case 2: (*Uncertain delay*) the study involved when the two delays were different $d(t_j)\neq h(t_j)$. Consequently, by expanded of conditions (D.10) and (D.11), we obtain:

$$\dot{V}_0(t)+\dot{V}_\Delta(t)+\gamma^{-1}z^Tz-\gamma w^Tw\le\xi^T\Upsilon_2\xi+\xi^T\Gamma_2^T\begin{bmatrix}\gamma^{-1}I_r & * & *\\ 0 & R & *\\ 0 & 0 & R_u\end{bmatrix}\Gamma_2\xi_2<0 \tag{D.13}$$

where $\Gamma_2=\begin{bmatrix}H & H_h & H_d & J_w\\ \bar{h}A & \bar{h}A_h & \bar{h}A_d & \bar{h}B_w\\ \delta_mA & \delta_mA_h & \delta_mA_d & \delta_mB_w\end{bmatrix}$, and

$$\Upsilon_2(\rho,\dot{\rho})=\begin{bmatrix}\Upsilon_{11}(\rho,\dot{\rho}) & * & * & *\\ A_h^TP+R & -(1-\mu)\left(Q+R_u\right)-R & * & *\\ A_d^TP & (1-\mu)R_u & -(1-\mu_d)Q-(1-\mu)R_u & *\\ E^TP & 0 & 0 & -\gamma I_d\end{bmatrix}.$$

Lastly, by continuing to apply Schur complement method we get condition (5.55).

Q.E.D.

D.4 The proof of Lemma 5.2.7.

Derivative the *simple* Lyapunov-Krasovskii functional along trajectories of LPV time-delay system (5.50) and integrating with $\mathcal{L}_2$-norm performance on the controlled output (5.50), that implies accustomed stability delay-dependent condition:

$$\dot{V}_0(t)+\gamma^{-1}z^Tz-\gamma w^Tw\le\xi^T\Upsilon_0\xi+\xi^T\Gamma_0^T\begin{bmatrix}\gamma^{-1}I_r & 0\\ 0 & R\end{bmatrix}\Gamma_0\xi, \tag{D.14}$$

Let's use operator (C.42) and interconnection (C.43) to express the relation between x_h

and x_d as input perturbed delay w_0 is bounded by the IQC (C.44). Accordingly, we have a transformation of coordinate:

$$\xi = \underbrace{\begin{bmatrix} I & 0 & 0 & 0 \\ 0 & I & \frac{\sqrt{7}}{2}\delta_m & 0 \\ 0 & I & 0 & 0 \\ 0 & 0 & 0 & I \end{bmatrix}}_{T} \underbrace{\begin{bmatrix} x_t \\ x_d \\ w_0 \\ w \end{bmatrix}}_{\zeta}. \tag{D.15}$$

By considering a parameter dependent $\mathcal{D}$-scaling $L(\rho) \in \mathbb{S}^n_{++}$ implicated in the scaling commuting sets $\mathcal{D}_\Delta$ and uncertain bounded operator Δ_0. Then applied the scaled bounded real lemma for uncertainty, with substituting (D.15) into condition (D.14) that lead to the following parameter dependent LMI condition:

$$\zeta^T \Upsilon \zeta + \zeta^T \Gamma^T \begin{bmatrix} \gamma^{-1} I_r & 0 & 0 \\ 0 & L(\rho) & 0 \\ 0 & 0 & R \end{bmatrix} \Gamma \zeta, \tag{D.16}$$

where $\zeta^T = \xi^T T^T = \begin{bmatrix} x_t^T & x_d^T & w_0^T & w^T \end{bmatrix}$,

$$\Gamma = \begin{bmatrix} H & H_h + H_d & \frac{\sqrt{7}}{2}\delta_m H_h & J_w \\ A & A_h + A_d & \frac{\sqrt{7}}{2}\delta_m A_h & B_w \\ \bar{h}A & \bar{h}\left(A_h + A_d\right) & \frac{\sqrt{7}}{2}\bar{h}\delta_m A_h & \bar{h}B_w \end{bmatrix}, \text{ and}$$

$$\Upsilon = \begin{bmatrix} \Upsilon_{11} & * & * & * \\ \left(A_d^T + A_h^T\right)P + R & -(1-\mu)Q - R & * & * \\ \frac{\sqrt{7}}{2}\delta_m A_h^T P + \frac{\sqrt{7}}{2}\delta_m R & \frac{-\sqrt{7}}{2}\delta_m (1-\mu)Q - \frac{\sqrt{7}}{2}\delta_m R & \frac{-7}{4}\delta_m^2 (1-\mu)Q - \frac{7}{4}\delta_m^2 R - L(\rho) & * \\ E^T P & 0 & 0 & -\gamma I_d \end{bmatrix}.$$

Finally, using Schur-complement that results in the PDLMI condition:

$$\begin{bmatrix} \Upsilon_{11} & * & * & * & * & * & * \\ \left(A_d^T + A_h^T\right)P + R & \Upsilon_{22} & * & * & * & * & * \\ \frac{\sqrt{7}}{2}\delta_m A_h^T P + \frac{\sqrt{7}}{2}\delta_m R & \frac{\sqrt{7}}{2}\delta_m \Upsilon_{22} & \frac{7}{4}\delta_m^2 \Upsilon_{22} - L & * & * & * & * \\ E^T P & 0 & 0 & -\gamma I_d & * & * & * \\ H & H_h + H_d & \frac{\sqrt{7}}{2}\delta_m H_h & F & -\gamma I_r & * & * \\ LA & L\left(A_h + A_d\right) & \frac{\sqrt{7}}{2}\delta_m L A_h & LE & 0 & -L & * \\ \bar{h}RA & \bar{h}R\left(A_h + A_d\right) & \frac{\sqrt{7}}{2}\bar{h}\delta_m R A_h & \bar{h}RE & 0 & 0 & -R \end{bmatrix} \prec 0. \tag{D.17}$$

Q.E.D.

For the associated relaxation by continuingly deploys similarly to Theorem 5.2.1:

$$\begin{bmatrix} -X-X^T & * & * & * & * & * & * & * & * \\ A^TX+P & \tilde{\Upsilon}_{11} & * & * & * & * & * & * & * \\ (A_d^T+A_h^T)X & R & \Upsilon_{22} & * & * & * & * & * & * \\ \frac{\sqrt{7}}{2}\delta_m A_h^T X & \frac{\sqrt{7}}{2}\delta_m R & \frac{\sqrt{7}}{2}\delta_m \Upsilon_{22} & \frac{7}{4}\delta_m^2\Upsilon_{22}-L & * & * & * & * & * \\ E^TX & 0 & 0 & 0 & -\gamma I_d & * & * & * & * \\ 0 & H & H_h+H_d & \frac{\sqrt{7}}{2}\delta_m H_h & F & -\gamma I_r & * & * & * \\ X & 0 & 0 & 0 & 0 & 0 & -P & * & * \\ L & 0 & 0 & 0 & 0 & 0 & -L & -L & * \\ \bar{h}R & 0 & 0 & 0 & 0 & 0 & \bar{h}R & 0 & -R \end{bmatrix} \prec 0, \quad \text{(D.18)}$$

with: $\tilde{\Upsilon}_{11} = \sum_{i=1}^{N_p} \pm\nu_i \frac{\partial P}{\partial \rho_i} + Q - R - P.$

Appendix E

Provisions for The Numerical Simulation

E.1 Chapter 3 – Quadruple-Tank System

The nonlinearity $f_k(t) = \sqrt{h_k(t)}$ of the liquid level in tank–*k*, *k* = 1...4 is described in two regions as following rule–based system:

1 - If $h_k(t)$ is M_1 then $f_k(t) = C_{fz1} h_k(t)$

2 - If $h_k(t)$ is M_2 then $f_k(t) = C_{fz2} h_k(t)$

Then T–S fuzzy model is presented as:

$$f_k(t) = \left(\lambda_1(h_k) C_{fz1} + \lambda_2(h_k) C_{fz2}\right) h_k(t) \quad \text{(E.1)}$$

where the membership functions are given by the expression:

$$\lambda_j(h_i) = \omega_j(h_k) \Big/ \sum_{j=1}^{2} \omega_j(h_k),\ j = 1,2,\ k = 1,2,3,4 \quad \text{(E.2)}$$

and satisfied the properties:

$$\sum_{j=1}^{2} \lambda_j(h_k) = 1,\ \lambda_j(h_i) \in [0,\ 1],\ j = 1,2,\ k = 1,2,3,4. \quad \text{(E.3)}$$

Obtained by the generalization of the Cauchy distribution (also known as the Bell MF), which is specified by three parameters $\{a_j,\ b_j,\ c_j\}$:

$$\omega_j(h_k) = \frac{1}{\left(1 + \left|(h_k - c_j)/a_j\right|\right)^{2b_j}},\ j = 1,2,\ k = 1,2,3,4. \quad \text{(E.4)}$$

The generalized method is based on the Levenberg–Marquardt algorithm combined with the least square method. The details of the fuzzy parameters are given Table E.1.

Table E.1. *The Parameter of Membership Functions.*

Parameters	Description	Values
$a_1,\ a_2$	The width of MFs (Standard deviation)	0.0021, 0.3078
$b_1,\ b_2$		0.7219, 5.3137
$c_1,\ c_2$	The center of MFs (mean)	–0.1656, 0.3155
C_{fz1}	The coefficient of fuzzy set in region M_1	2.389×10^3
C_{fz2}	The coefficient of fuzzy set in region M_2	0.8149

Assumption 1: By sharing the same fuzzy structure and same nonlinear function characteristics, so the proposed rules could determine by only $\lambda_j(h_1), j = 1, 2$.

This assumption reduced the number of the membership functions from 8 to 2.

Table E.2. *The Nominal Parameter Value of Tank Process.*

Parameters	Description	Values
$A_{s1},\ A_{s3}$	Areas of tanks 1,3 (m^2)	2.8×10^{-3}
$A_{s2},\ A_{s4}$	Areas of tanks 2,4 (m^2)	3.2×10^{-3}
$a_{s1},\ a_{s3}$	Areas of outlet in tanks 1,3 (m^2)	7.1×10^{-6}
$a_{s2},\ a_{s4}$	Areas of the outlet in tanks 2,4 (m^2)	5.7×10^{-6}
k_{vi}	Coefficient of pump–*i*, *i* =1,2 (ml $V^{-1}s^{-1}$)	3.33, 3.35
h_i	The liquid level in tank–*i* (m)	
γ_i	The value scaling of flow at valve–*i*	
v_i	The voltage control signal at pump–*i* (V)	

Remark 1. Time–varying parameters $\gamma_i(t), i = 1, 2$ is the flow rate value of valve–*i* correspond tanks, by assumed to be measurable and transformed to the convex combination parameters as follows:

$$\theta_1(t) = \gamma_1(t)/2,\ \theta_2(t) = (1-\gamma_1(t))/2,\ \theta_3(t) = \gamma_2(t)/2,\ \theta_4(t) = (1-\gamma_2(t))/2, \tag{E.5}$$

then $\sum_{k=1}^{4} \theta_k(t) = 1$.

The gains of observer-based controller derived from the design conditions in Theorem 3.2.1 solving by toolbox Matlab Yalmip (Lofberg, 2004) with solver Mosek (Andersen et al., 2003) are given by:

The fuzzy controller gains:

$$K_1 = Q_{1,1}W^{-1} = 10^4 \times \begin{bmatrix} 2.1222 & 0.9691 & 1.9389 & 2.0599 \\ 1.9466 & 1.4708 & 3.1558 & 2.6800 \end{bmatrix},$$

$$K_2 = Q_{1,2}W^{-1} = 10^4 \times \begin{bmatrix} 1.7406 & 1.4158 & 1.9525 & 2.9458 \\ 1.6465 & 1.6527 & 2.6095 & 3.1714 \end{bmatrix},$$

…

$$K_7 = Q_{1,7}W^{-1} = 10^{-4} \times \begin{bmatrix} 14.6370 & 3.4505 & 46.1479 & 8.9414 \\ 0.8152 & 3.4842 & 8.3322 & 2.4140 \end{bmatrix},$$

$$K_8 = Q_{1,8}W^{-1} = 10^{-4} \times \begin{bmatrix} 4.8534 & 1.6037 & 0.8016 & 5.7585 \\ 0.8625 & -7.7916 & 5.0404 & -44.0952 \end{bmatrix},$$

and observer gains:

$$L_1 = P_2^{-1}Q_{2,1} = 10^4 \times \begin{bmatrix} 0.6220 & 0.3379 & 0.6439 & 0.4826 \\ 0.3572 & 1.2129 & 0.4416 & 1.7370 \end{bmatrix}^T,$$
$$L_2 = P_2^{-1}Q_{2,2} = 10^4 \times \begin{bmatrix} 0.6227 & 0.3385 & 0.6446 & 0.4836 \\ 0.3563 & 1.2114 & 0.4406 & 1.7348 \end{bmatrix}^T,$$
$$\dots$$
$$L_8 = P_2^{-1}Q_{28} = 10^3 \times \begin{bmatrix} 2.1734 & 1.1239 & 2.2192 & 1.6058 \\ 1.2273 & 4.4262 & 1.5359 & 6.3062 \end{bmatrix}^T.$$

E.2 Chapter 3 – Lateral Vehicle Dynamic

The accurate estimation of the tire friction's side force plays an important role in the design vehicle stability system. Among the static tire models, it can be mentioned the HSRI model (Dugoff et al., 1970), the semi-empirical Pacejka model (Pacejka, 2012), and the Kiencke model (Kiencke & Nielsen, 2005), etc. Since, the Pacejka model describes the lateral forces that could have an effective/linear cornering stiffness and nonlinear characteristics. In this literature, the nonlinear forces are modeled by TS-fuzzy method as in (Bui Tuan & El Hajjaji, 2018; Dahmani et al., 2014; Dahmani, Chadli, et al., 2015; Dahmani, Pages, et al., 2015; El Hajjaji et al., 2006), with the front and rear lateral forces are represented by

$$\begin{cases} F_{yf}(\hat{\alpha}_f) = \varpi_1\left(\left|\hat{\alpha}_f\right|\right)C_{f,1}\alpha_f + \varpi_2\left(\left|\hat{\alpha}_f\right|\right)C_{f,2}\alpha_f \\ F_{yr}(\hat{\alpha}_r) = \varpi_1\left(\left|\hat{\alpha}_r\right|\right)C_{r,1}\alpha_r + \varpi_2\left(\left|\hat{\alpha}_r\right|\right)C_{r,2}\alpha_r \end{cases} \tag{E.6}$$

where $C_{f,i}$ and $C_{r,i}, i = 1,2$, the effective cornering stiffness in front and rear of SUV E-Class car model are fuzzificated as the *local linear* gain between tire sideslip angle and tire force. For the simplicity, expression $(\hat{\alpha}_f, \hat{\alpha}_r)$ may be shorten to only (α).

The membership functions satisfy the following properties

$$\varpi_i(\hat{\alpha}_f), \varpi_i(\hat{\alpha}_r) \in \mathcal{U}_l = \{\varpi_i(\cdot) \in [0,1], i = 1,2, \sum_{i=1}^{2} \varpi_i(\cdot) = 1\} \subset \mathbb{R}^2. \tag{E.7}$$

and are expressed by:

$$\varpi_i(\cdot) = \frac{\kappa_i(\cdot)}{\sum_{i=1}^{2}\kappa_i(\cdot)}, \text{ with } \kappa_i(\cdot) = \left(1 + \left|\frac{|\cdot| - c_i}{a_i}\right|\right)^{-2b_i}, \; i = 1, 2. \tag{E.8}$$

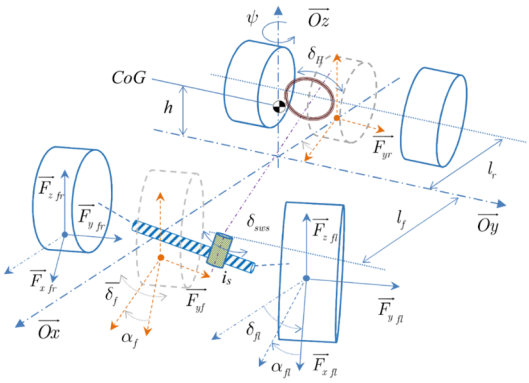

Figure E-1. *The forces acting on two-tracks 3D vehicle model.*

Table E.3. *Coefficient of Pacejka tire model: 265/75 R16.*

Tire characteristics				**Parameter of the Membership Function**			
Front tires		Rear tires		Front tires		Rear tires	
B_1	= 9.2916	B_2	= 9.3449	C_{f1}	= 1.0748e5	C_{r1}	= 8.2913e4
C_1	= 1.6307	C_2	= 1.6307	C_{f2}	= 534.98	C_{r2}	= 407.68
D_1	= 4339.4	D_2	= 3393.2	a_1	= 0.0801	a_2	= 112.64
E_1	= 0.2290	E_2	= 0.2292	b_1	= 0.7309	b_2	= 676.78
				c_1	= 0.0202	c_2	= 112.61

Table E.4. *Simulation vehicle parameters - SUV E-Class car model.*

Parameters	**Descriptions**	**Values**
m	Total vehicle mass (kg)	1832
$\overline{F_{zfl}}$	Nominal vertical forces at front left wheel (N)	5193.0
$\overline{F_{zfr}}$	Nominal vertical forces at front right wheel (N)	5153.5
$\overline{F_{zrl}}$	Nominal vertical forces at rear left wheel (N)	3915.4
$\overline{F_{zrr}}$	Nominal vertical forces at rear right wheel (N)	3847.6
υ	Vehicle speed (m s^{-1})	
υ_x	Longitudinal velocity (m s^{-1})	
υ_y	Lateral velocity (m s^{-1})	
$\underline{v}_x$	The lower bound of the longitudinal velocity (m s^{-1})	10
$\overline{v}_x$	The upper bound of the longitudinal velocity (m s^{-1})	40
I_z	Yaw moment of inertia at center of gravity (CG) (kg m^2)	2988
l_r	Distance from CoG to rear axle (m)	1.77
l_f	Distance from CoG to front axle (m)	1.18
M_z	Driving/Braking force control (Nm)	
δ_f	Front steering angle (rad)	
δ_{sw}	Steering wheel angle (deg)	
i_S	Steering ration	20.0312

The local time-varying matrices $A_i \in \mathbb{R}^{2\times2}$, $B_i \in \mathbb{R}^{2\times2}$, and $C \in \mathbb{R}^{1\times2}$ are given as:

$$A_i = \begin{bmatrix} \frac{-2}{mv_x}C_{0i} & \frac{-2}{mv_x}C_{1i} - v_x(t) \\ \frac{-2}{I_z v_x}C_{1i} & \frac{-2}{I_z v_x}C_{2i} \end{bmatrix}, B_i = \begin{bmatrix} \frac{2}{m}C_{f,j} & 0 \\ \frac{2}{I_z}C_{f,j}l_f & \frac{1}{I_z} \end{bmatrix}, B_{\delta,i} = \begin{bmatrix} \frac{2}{m}C_{f,j} \\ \frac{2}{I_z}C_{f,j}l_f \end{bmatrix} \text{ and } B_d = \begin{bmatrix} \frac{1}{m} & 0 \\ 0 & \frac{1}{I_z} \end{bmatrix}.$$

where $C_{0i} = C_{fj} + C_{rk}$, $C_{1i} = C_{fj}l_f - C_{rk}l_r$, and $C_{2i} = C_{fj}l_f^2 + C_{rk}l_r^2$, and i follows the rule: if $j = k$, then $i = 1,4$ and if $j \neq k$ then $i = 2,3$, with $j,k = 1,2,$ and $i = 1,2,3,4$.

It should be noted that the combination of membership function (E.7) is:

$$\lambda_i(\alpha) = \varpi_j(\hat{\alpha}_f)\varpi_k(\hat{\alpha}_r), \text{ with } j,k = 1,2, \text{ and } i = 1,2,3,4. \tag{E.9}$$

When simplifying the model of system based on two vertices of the front wheel slip angle that consider only $\lambda_i(\alpha) \coloneqq \varpi_i(\hat{\alpha}_f) \cong \varpi_i(\hat{\alpha}_r)$, then $i = 1,2$.

Bibliography

Ahmad, S., Rehan, M., & Hong, K. S. (2016). Observer-based robust control of one-sided Lipschitz nonlinear systems. *ISA Transactions*, *65*, 230–240.

Alwan, M. S., & Liu, X. (2018). *Theory of Hybrid Systems: Deterministic and Stochastic*. Springer Singapore.

Andersen, E D, Roos, C., & Terlaky, T. (2003). On implementing a primal-dual interior-point method for conic quadratic optimization. *Mathematical Programming*, *95*(2), 249–277.

Andersen, Erling D, & Andersen, K. D. (2000). The Mosek Interior Point Optimizer for Linear Programming: An Implementation of the Homogeneous Algorithm. In H. Frenk, K. Roos, T. Terlaky, & S. Zhang (Eds.), *High Performance Optimization* (pp. 197–232). Springer US.

Ando, T. (1995). Matrix Young Inequalities. In C. B. Huijsmans, M. A. Kaashoek, W. A. J. Luxemburg, & B. de Pagter (Eds.), *Operator Theory in Function Spaces and Banach Lattices: Essays dedicated to A.C. Zaanen on the occasion of his 80th birthday* (pp. 33–38). Birkhäuser Basel.

Andry, A. N., Chung, J. C., & Shapiro, E. Y. (1984). Modalized Observers. *IEEE Transactions on Automatic Control*, *29*(7), 669–672.

Anguelova, M., & Wennberg, B. (2008). State elimination and identifiability of the delay parameter for nonlinear time-delay systems. *Automatica*, *44*(5), 1373–1378.

Apkarian, P., & Adams, R. J. (1998). Advanced gain-scheduling techniques for uncertain systems. *IEEE Transactions on Control Systems Technology*, *6*(1), 21–32.

Apkarian, P., Feron, E., & Gahinet, P. (1995). Parameter-Dependent Lyapunov Functions for Robust Control of Systems with Real Parametric Uncertainty. *IEEE Transactions on Automatic Control*, *41*, 436--442.

Apkarian, P., & Gahinet, P. (1995). A convex characterization of gain-scheduled H/sub ∞/ controllers. *IEEE Transactions on Automatic Control*, *40*(5), 853–864.

Apkarian, P., Gahinet, P., & Becker, G. (1995). Self-scheduled H∞ control of linear parameter-varying systems: a design example. In *Automatica* (Vol. 31, Issue 9, pp. 1251–1261).

Apkarian, P., & Tuan, H. D. (2000a). Robust control via concave minimization local and global algorithms. *IEEE Transactions on Automatic Control*, *45*(2), 299–305.

Apkarian, P., & Tuan, H. D. (2000b). Parameterized LMIs in Control Theory. *SIAM Journal on Control and Optimization*, *38*(4), 1241–1264.

Apkarian, P., & Tuan, H. D. (1998). Parametrized LMIs in control theory. *Proceedings of the 37th IEEE Conference on Decision and Control (Cat. No.98CH36171)*, *1*, 152–157.

Ariola, M., & Pironti, A. (2016). *Magnetic Control of Tokamak Plasmas*. Springer International Publishing.

Azuma, T., Watanabe, R., Kenko, U., & Fujita, M. (2000). A new LMI approach to

analysis of linear systems depending on scheduling parameter in polynomial forms. *At-Automatisierungstechnik*, *48*(4), 199–204.

Bakker, E., Pacejka, H. B., & Lidner, L. (1989). A New Tire Model with an Application in Vehicle Dynamics Studies. *SAE International*, 890087.

Balas, G. J., Fialho, I. J., Packard, A., Renfrow, J., & Mullaney, C. (1997). On the design of LPV controllers for the F-14 aircraft lateral-directional axis during powered approach. *Proceedings of the 1997 American Control Conference (Cat. No.97CH36041)*, *June*, 123–127 vol.1.

Balas, G. J., Mueller, J., & Barker, J. (n.d.). Application of gain-scheduled, multivariable control techniques to the F/A-18 system research aircraft. In *Guidance, Navigation, and Control Conference and Exhibit*.

Becker, G., & Packard, A. (1994). Robust performance of linear parametrically varying systems using parametrically-dependent linear feedback. *Systems and Control Letters*, *23*(3), 205–215.

Belkoura, L., Richard, J. P., & Fliess, M. (2009). Parameters estimation of systems with delayed and structured entries. *Automatica*, *45*(5), 1117–1125.

Benzaouia, A., & Hajjaji, A. El. (2014). Advanced Takagi–Sugeno Fuzzy Systems: Delay and Saturation. In *Studies in Systems, Decision and Control* (Vol. 8).

Bertsimas, D. (1999). Nonlinear programming. In *Mathematical Programming* (p. 802).

Bertsimas, D., & Tsitsiklis, J. (1997). *Introduction to Linear Optimization (Athena Scientific Series in Optimization and Neural Computation, 6)* (p. 608).

Biannic, J.-M., & Apkarian, P. (1999). Missile autopilot design via a modified LPV synthesis technique. *Aerospace Science and Technology*, *3*(3), 153–160.

Bosche, J., & El Hajjaji, A. (2008). An output feedback controller design for lateral vehicle dynamic. *IFAC Proceedings Volumes (IFAC-PapersOnline)*, *17*(1 PART 1), 5670–5675.

Boukas, E. K. (2006). Stochastic Switching Systems. In *Angewandte Chemie International Edition, 6(11), 951–952.* Birkhäuser Boston.

Boyd, S., El Ghaoui, L., Feron, E., & Balakrishnan, V. (1994). Linear Matrix Inequalities in System and Control Theory. In *Linear Matrix Inequalities in System and Control Theory*. Society for Industrial and Applied Mathematics (SIAM, 3600 Market Street, Floor 6, Philadelphia, PA 19104).

Boyd, S., & Vandenberghe, L. (2004). *Convex Optimization* (Issue pt. 1). Cambridge University Press.

Boyd, S., & Yang, Q. (1989). Structured and simultaneous lyapunov functions for system stability problems. *International Journal of Control*, *49*(6), 2215–2240.

Briat, C. (2008). *Commande et Observation Robuste des Systemes LPV Retardés*. Grenoble INP.

Briat, C. (2015a). *Linear Parameter-Varying and Time-Delay Systems* (Vol. 3). Springer Berlin Heidelberg.

Briat, C. (2015b). Stability analysis and control of a class of LPV systems with piecewise constant parameters. *Systems and Control Letters*, *82*, 10–17.

Briat, C. (2018). Stability analysis and state-feedback control of LPV systems with piecewise constant parameters subject to spontaneous poissonian jumps. *IEEE*

Control Systems Letters, *2*(2), 230–235.

Briat, C. (2021). Stability analysis and stabilization of LPV systems with jumps and (piecewise) differentiable parameters using continuous and sampled-data controllers. *Nonlinear Analysis: Hybrid Systems*, *41*, 101040.

Briat, C., Sename, O., & Lafay, J.-F. (2008). Delay-Scheduled State-Feedback Design for Time-Delay Systems with Time-Varying Delays. In *IFAC Proceedings Volumes* (Vol. 41, Issue 2). IFAC.

Briat, C., Sename, O., & Lafay, J.-F. (2009). Delay-scheduled state-feedback design for time-delay systems with time-varying delays—A LPV approach. *Systems & Control Letters*, *58*(9), 664–671.

Briat, C., Sename, O., & Lafay, J.-F. (2010). Memory-resilient gain-scheduled state-feedback control of uncertain LTI/LPV systems with time-varying delays. *Systems and Control Letters*, *59*(8), 451–459.

Briat, C., Sename, O., & Lafay, J.-F. (2007). A LFT/$\mathscr{H}$<inf>∞</inf> state feedback design for linear parameter varying time delay systems. *2007 European Control Conference (ECC)*, 4882–4888.

Bribiesca Argomedo, F., Prieur, C., Witrant, E., & Brémond, S. (2011). Polytopic control of the magnetic flux profile in a tokamak plasma. *IFAC Proceedings Volumes (IFAC-PapersOnline)*, *44*(1 PART 1), 6686–6691.

Bribiesca Argomedo, F., Witrant, E., & Prieur, C. (2014). Safety Factor Profile Control in a Tokamak. In *SpringerBriefs in Control, Automation and Robotics* (Issue 9783319019574). Springer International Publishing.

Bribiesca Argomedo, F., Witrant, E., Prieur, C., Georges, D., & Brémond, S. (2010). Model-based control of the magnetic flux profile in a Tokamak plasma. *49th IEEE Conference on Decision and Control (CDC)*, 6926–6931.

Bui Tuan, V. L., & El Hajjaji, A. (2018). Robust Observer-Based Control for TS Fuzzy Models Application to Vehicle Lateral Dynamics. *2018 26th Mediterranean Conference on Control and Automation (MED)*, 1–6.

Bui Tuan, V. L., El Hajjaji, A., & Naami, G. (2019). Robust TS-Fuzzy observer-based control for Quadruple-Tank system. *2019 12th Asian Control Conference, ASCC 2019*.

Bui Tuan, V. L., El Hajjaji, A., & Pages, O. (2021). $\mathscr{L}$2 -Stabilization of anti-windup compensators subject to actuator saturation and disturbances. *2021 Australian & New Zealand Control Conference (ANZCC)*, 80–85.

Bui Tuan, V. L., Pages, O., & Hajjaji, A. El. (2021). Robust TS-Fuzzy output feedback controller synthesis for saturated vehicle System. *Proceedings of the American Control Conference*, *2021-May*, 142–147.

Cao, Y. Y., James, L., & Sun, Y. X. (1998). Static output feedback stabilization: An ILMI approach. *Automatica*, *34*(12), 1641–1645.

Cao, Y. Y., Lin, Z., & Shamash, Y. (2002). Set invariance analysis and gain-scheduling control for LPV systems subject to actuator saturation. *Systems and Control Letters*, *46*(2), 137–151.

Cao, Y. Y., Lin, Z., & Ward, D. G. (2002). An antiwindup approach to enlarging domain of attraction for linear systems subject to actuator saturation. *IEEE Transactions on Automatic Control*, *47*(1), 140–145.

Chang, X.-H., & Yang, G.-H. (2014). New Results on Output Feedback <formula formulatype="inline"> <tex Notation="TeX">$H_{\infty} $</tex></formula> Control for Linear Discrete-Time Systems. *IEEE Transactions on Automatic Control*, *59*(5), 1355–1359.

Chatterjee, D., & Liberzon, D. (2006). Stability analysis of deterministic and stochastic switched systems via a comparison principle and multiple Lyapunov functions. *SIAM Journal on Control and Optimization*, *45*(1), 174–206.

Chen, F., Garnier, H., & Gilson, M. (2015). Robust identification of continuous-time models with arbitrary time-delay from irregularly sampled data. *Journal of Process Control*, *25*, 19–27.

Chen, J., Gu, D., Postlethwaite, I., & Natesan, K. (2008). Robust LPV Control of UAV with Parameter Dependent Performance. In *IFAC Proceedings Volumes* (Vol. 41, Issue 2). IFAC.

Chen, Y., Fei, S., & Li, Y. (2015). Stabilization of neutral time-delay systems with actuator saturation via auxiliary time-delay feedback. *Automatica*, *52*, 242–247.

Chen, Y., Fei, S., & Li, Y. (2017). Robust Stabilization for Uncertain Saturated Time-Delay Systems: A Distributed-Delay-Dependent Polytopic Approach. *IEEE Transactions on Automatic Control*, *62*(7), 3455–3460.

Chilali, M., & Gahinet, P. (1996). H∞ design with pole placement constraints: an LMI approach. *IEEE Transactions on Automatic Control*, *41*(3), 358–367.

Chilali, M., Gahinet, P., & Apkarian, P. (1999). Robust pole placement in LMI regions. *IEEE Transactions on Automatic Control*, *44*(12), 2257–2270.

Chilali, M., Gahinet, P., & Scherer, C. W. (1996). Multi-Objective Output-Feedback Control via LMI Optimization. *IFAC Proceedings Volumes*, *29*(1), 1691–1696.

Cimprič, J. (2015). Finsler's Lemma for matrix polynomials. *Linear Algebra and Its Applications*, *465*, 239–261.

Colaneri, P. (2009). Dwell time analysis of deterministic and stochastic switched systems. *European Journal of Control*, *15*(3–4), 228–248.

Cristi, R., Healey, A. J., & Papouias, F. (1990). Dynamic Output Feedback by Robust Observer and Variable Structure Control. *1990 American Control Conference*, 2649–2653.

Daafouz, J., Bernussou, J., & Geromel, J. C. (2008). On inexact LPV control design of continuous-time polytopic systems. *IEEE Transactions on Automatic Control*, *53*(7), 1674–1678.

Dahmani, H., Chadli, M., Rabhi, A., & El Hajjaji, A. (2015). Detection of impending vehicle rollover with road bank angle consideration using a robust fuzzy observer. *International Journal of Automation and Computing*, *12*(1), 93–101.

Dahmani, H., Pages, O., & El Hajjaji, A. (2015). Robust control with parameter uncertainties for vehicle chassis stability in critical situations. *Proceedings of the IEEE Conference on Decision and Control*, *54rd IEEE*(Cdc), 209–214.

Dahmani, H., Pages, O., El Hajjaji, A., & Daraoui, N. (2014). Observer-Based Robust Control of Vehicle Dynamics for Rollover Mitigation in Critical Situations. *IEEE Transactions on Intelligent Transportation Systems*, *15*(1), 274–284.

Dahmani, H., Pages, O., El Hajjaji, A., & Pages, O. (2015). Observer-Based State

Feedback Control for Vehicle Chassis Stability in Critical Situations. *IEEE Transactions on Control Systems Technology*, *32*(2), 1–1.

Datta, R., Saravanakumar, R., Dey, R., Bhattacharya, B., & Ahn, C. K. (2021). Improved stabilization criteria for Takagi–Sugeno fuzzy systems with variable delays. *Information Sciences*, *579*, 591–606.

Dey, R., Ghosh, S., Ray, G., & Rakshit, A. (2014). Improved delay-dependent stabilization of time-delay systems with actuator saturation. *International Journal of Robust and Nonlinear Control*, *24*(5), 902–917.

Dey, R., Ray, G., & Emilia Balas, V. (2018). Stability and Stabilization of Linear and Fuzzy Time-Delay Systems. In *International Journal of Robust and Nonlinear Control* (Vol. 141, Issue 9). Springer International Publishing.

Do, A. L. (2011). *Approche LPV pour la commande robuste de la dynamique des véhicules : amélioration conjointe du confort et de la sécurité* (Issue 2011GRENT114) [Université de Grenoble].

Do, A. L., Sename, O., & Dugard, L. (2010). An LPV control approach for semi-active suspension control with actuator constraints. *Proceedings of the 2010 American Control Conference, ACC 2010*, 4653–4658.

Dong, J., & Yang, G. H. (2013). Robust static output feedback control synthesis for linear continuous systems with polytopic uncertainties. *Automatica*, *49*(6), 1821–1829.

Doumiati, M., Sename, O., Dugard, L., Martinez-Molina, J. J., Gaspar, P., & Szabo, Z. (2013). Integrated vehicle dynamics control via coordination of active front steering and rear braking. *European Journal of Control*, *19*(2), 121–143.

Doumiati, M., Sename, O., Martinez-Molina, J. J., Dugard, L., & Poussot-vassal, C. (2012). Gain-scheduled LPV/H∞ controller based on direct yaw moment and active steering for vehicle handling improvements. *49th IEEE Conference on Decision and Control (CDC)*, 6427–6432.

Doyle, J. C. (1985). Structured uncertainty in control system design. *1985 24th IEEE Conference on Decision and Control*, 260–265.

Doyle, J. C., Packard, A., & Zhou, K. (1991). Review of LFTs, LMIs, and μ. *Proceedings of the IEEE Conference on Decision and Control*, *2*, 1227–1232.

Dugoff, H., Fancher, P. S., & Segel, L. (1970). An analysis of tire traction properties and their influence on vehicle dynamic performance. *SAE Technical Papers*.

Dullerud, G. E., & Paganini, F. (2000). A Course in Robust Control Theory. In *Springer* (Vol. 36, Issue 9). Springer New York.

Ebihara, Y., Peaucelle, D., & Arzelier, D. (2014). LMI approach to linear positive system analysis and synthesis. *Systems and Control Letters*, *63*(1), 50–56.

Ebihara, Y., Peaucelle, D., & Arzelier, D. (2015). *S-Variable Approach to LMI-Based Robust Control*. Springer London.

Ebihara, Y., Peaucelle, D., Arzelier, D., & Hagiwara, T. (2006). Robust H2 Performance Analysis Of Uncertain Lti Systems Via Polynomially Parameter-Dependent Lyapunov Functions. *IFAC Proceedings Volumes*, *39*(9), 435–440.

El Ghaoui, L., & Niculescu, S. (Eds.). (2000). *Advances in Linear Matrix Inequality Methods in Control*. Society for Industrial and Applied Mathematics.

El Ghaoui, L., Oustry, F., & AitRami, M. (1997). A cone complementarity linearization

algorithm for static output-feedback and related problems. *IEEE Transactions on Automatic Control*, *42*(8), 1171–1176.

El Hajjaji, A., Chadli, M., Oudghiri, M., & Pages, O. (2006). Observer-based robust fuzzy control for vehicle lateral dynamics. *Proceedings of the American Control Conference*, *2006*, 4664–4669.

Fakhri, P. (2005). *Application of Polytopic Separation Techniques to Nonlinear Observer Design* [University of Toronto].

Farrelly, J., & Wellstead, P. (1996). Estimation of vehicle lateral velocity. *IEEE Conference on Control Applications - Proceedings*, 552–557.

Feron, E., Apkarian, P., & Gahinet, P. (1996). Analysis and synthesis of robust control systems via parameter-dependent Lyapunov functions. *IEEE Transactions on Automatic Control*, *41*(7), 1041–1046.

Fink, A. M., & Jodeit, M. (1990). Jensen inequalities for functions with higher monotonicities. *Aequationes Mathematicae*, *40*(1), 26–43.

Forni, F., & Galeani, S. (2007). Model based, gain-scheduled anti-windup control for LPV systems. *Proceedings of the IEEE Conference on Decision and Control*, 1174–1179.

Forni, F., & Galeani, S. (2010). Gain-scheduled, model-based anti-windup for LPV systems. *Automatica*, *46*(1), 222–225.

Fridman, E. (2001). New Lyapunov-Krasovskii functionals for stability of linear retarded and neutral type systems. *Systems and Control Letters*, *43*(4), 309–319.

Fridman, E. (2006). Descriptor discretized Lyapunov Functional method. *IFAC Proceedings Volumes (IFAC-PapersOnline)*, *5*(PART 1), 638–643.

Fridman, E. (2014). Tutorial on Lyapunov-based methods for time-delay systems. *European Journal of Control*, *20*(6), 271–283.

Fridman, E., Pila, A., & Shaked, U. (2003). Regional stabilization and H∞ control of time-delay systems with saturating actuators. *International Journal of Robust and Nonlinear Control*, *13*(9), 885–907.

Fridman, E., & Shaked, U. (2003). Delay-dependent stability and H∞ control: Constant and time-varying delays. *International Journal of Control*, *76*(1), 48–60.

Fukada, Y. (1999). Slip-angle estimation for vehicle stability control. *Vehicle System Dynamics*, *32*(4), 375–388.

Furqon, R., Chen, Y. J., Tanaka, M., Tanaka, K., & Wang, H. O. (2017). An SOS-Based Control Lyapunov Function Design for Polynomial Fuzzy Control of Nonlinear Systems. *IEEE Transactions on Fuzzy Systems*, *25*(4), 775–787.

Gahinet, P. (1996). Explicit controller formulas for LMI-based H∞ synthesis. *Automatica*, *32*(7), 1007–1014.

Gahinet, P., & Apkarian, P. (1994). A linear matrix inequality approach to H∞ control. *International Journal of Robust and Nonlinear Control*, *4*(4), 421–448.

Gahinet, P., Apkarian, P., & Chilali, M. (1994). Affine parameter-dependent lyapunov functions for real parametric uncertainty. *Proceedings of the IEEE Conference on Decision and Control*, *3*, 2026–2031.

Gahinet, P., Apkarian, P., & Chilali, M. (1996). Affine parameter-dependent Lyapunov functions and real parametric uncertainty. *IEEE Transactions on Automatic Control*,

41(3), 436–442.

Gahinet, P., & Laub, A. J. (1994). LMI Control Toolbox For Use with MATLAB. In *Matrix* (Vol. 3). IEEE.

Gahlawat, A., Peet, M. M., & Witrant, E. (2011). Control and verification of the safety-factor profile in Tokamaks using sum-of-squares polynomials. *IFAC Proceedings Volumes (IFAC-PapersOnline)*, *44*(1 PART 1), 12556–12561.

Galeani, S., Massimetti, M., Teel, A. R., & Zaccarian, L. (2006). Reduced order linear anti-windup augmentation for stable linear systems. *International Journal of Systems Science*, *37*(2), 115–127.

Galeani, S., Tarbouriech, S., Turner, M., & Zaccarian, L. (2009). A Tutorial on Modern Anti-windup Design. *European Journal of Control*, *15*(3–4), 418–440.

Galimidi, A. R., & Barmish, B. R. (1986). The Constrained Lyapunov Problem and Its Application to Robust Output Feedback Stabilization. *IEEE Transactions on Automatic Control*, *31*(5), 410–419.

Ganguli, S., Marcos, A., & Balas, G. J. (2002). Reconfigurable LPV control design for Boeing 747-100/200 longitudinal axis. *Proceedings of the American Control Conference*, *5*, 3612–3617.

Gassara, H., El Hajjaji, A., & Chaabane, M. (2017). Design of polynomial fuzzy observer–controller for nonlinear systems with state delay: sum of squares approach. *International Journal of Systems Science*, *48*(9), 1954–1965.

Giri, F., & Bai, E. W. (2013). Robust Control and Linear Parameter Varying Approaches. In O. Sename, P. Gaspar, & J. Bokor (Eds.), *Lecture Notes in Control and Information Sciences* (Vol. 437). Springer Berlin Heidelberg.

Gomes da Silva, J.M., & Tarbouriech, S. (1998). Local stabilization of discrete-time linear systems with saturating controls: an LMI-based approach. *Proceedings of the 1998 American Control Conference. ACC (IEEE Cat. No.98CH36207)*, *46*(1), 92–96 vol.1.

Gomes da Silva, João Manoel. (1997). *Sur la Stabilité Locale de Systèmes Linéaires avec Saturation des Commandes*. Université Paul Sabatier.

Gomes da Silva, João Manoel, Seuret, A., Fridman, E., & Richard, J. P. (2011). Stabilisation of neutral systems with saturating control inputs. *International Journal of Systems Science*, *42*(7), 1093–1103.

Gomes da Silva, João Manoel, & Tarbouriech, S. (2001). Local stabilization of discrete-time linear systems with saturating controls: an LMI-based approach. *IEEE Transactions on Automatic Control*, *46*(1), 119–125.

Gomes da Silva, João Manoel, & Tarbouriech, S. (2005). Antiwindup design with guaranteed regions of stability: An LMI-based approach. *IEEE Transactions on Automatic Control*, *50*(1), 106–111.

Gomes da Silva, João Manoel, & Tarbouriech, S. (1999). Contractive polyhedra for linear continuous-time systems with saturating controls. *Proceedings of the 1999 American Control Conference (Cat. No. 99CH36251)*, *3*, 2007–2011 vol.3.

Gomes da Silva, João Manoel, Tarbouriech, S., & Garcia, G. (2003). Local stabilization of linear systems under amplitude and rate saturating actuators. *IEEE Transactions on Automatic Control*, *48*(5), 842–847.

Gonçalves, E. N., Palhares, R. M., Takahashi, R. H. C., & Mesquita, R. C. (2006). New Approach to Robust$ cal D$-Stability Analysis of Linear Time-Invariant Systems With Polytope-Bounded Uncertainty. *IEEE Transactions on Automatic Control*, *51*(10), 1709–1714.

Gossmann, F., & Svaricek, F. (2019). Parameter dependent static output feedback control-An LPV approach. *2019 18th European Control Conference, ECC 2019*, *3*, 3322–3327.

Grimm, G., Hatfield, J., Postlethwaite, I., Teel, A. R., Turner, M. C., & Zaccarian, L. (2003). Antiwindup for Stable Linear Systems with Input Saturation: An LMI-Based Synthesis. *IEEE Transactions on Automatic Control*, *48*(9), 1509–1525.

Gu, K. (2001). A further refinement of discretized Lyapunov functional method for the stability of time-delay systems. *International Journal of Control*, *74*(10), 967–976.

Gu, K., Kharitonov, V. L., & Chen, J. (2003). *Stability of Time-Delay Systems* (Vol. 53, Issue 9). Birkhäuser Boston.

Gu, K., & Niculescu, S.-I. (2001). Further remarks on additional dynamics in various model transformations of linear delay systems. *IEEE Transactions on Automatic Control*, *46*(3), 497–500.

Guerra, T. M., & Bernal, M. (2009). A way to escape from the quadratic framework. *IEEE International Conference on Fuzzy Systems*, *1*, 784–789.

Guerra, T. M., Bernal, M., Guelton, K., & Labiod, S. (2012). Non-quadratic local stabilization for continuous-time Takagi-Sugeno models. *Fuzzy Sets and Systems*, *201*, 40–54.

Guldner, J., Tan, H. S., & Patwardhan, S. (1996). Analysis of automatic steering control for highway vehicles with look-down lateral reference systems. *Vehicle System Dynamics*, *26*(4), 243–269.

Halalchi, H., Laroche, E., & Bara, G. I. (2014). Flexible-Link Robot Control Using a Linear Parameter Varying Systems Methodology. *International Journal of Advanced Robotic Systems*, *11*(3), 46.

Han, Q.-L. (2005a). A new delay-dependent stability criterion for linear neutral systems with norm-bounded uncertainties in all system matrices. *International Journal of Systems Science*, *36*(8), 469–475.

Han, Q.-L. (2005b). Absolute stability of time-delay systems with sector-bounded nonlinearity. *Automatica*, *41*(12), 2171–2176.

Han, Q.-L. (2008). A Delay Decomposition Approach to Stability of Linear Neutral Systems. *IFAC Proceedings Volumes*, *41*(2), 2607–2612.

He, Y., & Wang, Q. G. (2006). An Improved ILMI Method for Static Output Feedback Control With Application to Multivariable PID Control. *IEEE Transactions on Automatic Control*, *51*(10), 1678–1683.

He, Y., Wang, Q. G., Lin, C., & Wu, M. (2007). Delay-range-dependent stability for systems with time-varying delay. *Automatica*, *43*(2), 371–376.

He, Y., Wu, M., Liu, G.-P., & She, J.-H. (2008). Output Feedback Stabilization for a Discrete-Time System With a Time-Varying Delay. *IEEE Transactions on Automatic Control*, *53*(10), 2372–2377.

He, Y., Wu, M., She, J.-H., & Liu, G.-P. (2004a). Parameter-Dependent Lyapunov

Functional for Stability of Time-Delay Systems With Polytopic-Type Uncertainties. *IEEE Transactions on Automatic Control*, *49*(5), 828–832.

He, Y., Wu, M., She, J. H., & Liu, G. P. (2004b). Delay-dependent robust stability criteria for uncertain neutral systems with mixed delays. *Systems and Control Letters*, *51*(1), 57–65.

Heemels, W. P. M. H., Daafouz, J., & Millerioux, G. (2010). Observer-based control of discrete-time LPV systems with uncertain parameters. *IEEE Transactions on Automatic Control*, *55*(9), 2130–2135.

Henrion, D., & Tarbouriech, S. (1999). LMI relaxations for robust stability of linear systems with saturating controls. *Automatica*, *35*(9), 1599–1604.

Henrion, D., Tarbouriech, S., & Kučera, V. (2005). Control of linear systems subject to time-domain constraints with polynomial pole placement and LMIs. *IEEE Transactions on Automatic Control*, *50*(9), 1360–1364.

Hiriart-Urruty, J.-B., & Lemaréchal, C. (1993a). *Convex Analysis and Minimization Algorithms I* (Vol. 305). Springer Berlin Heidelberg.

Hiriart-Urruty, J.-B., & Lemaréchal, C. (1993b). *Convex Analysis and Minimization Algorithms II* (Vol. 306). Springer Berlin Heidelberg.

Hmamed, A., El Aiss, H., & El Hajjaji, A. (2015). Stability analysis of linear systems with time varying delay: An input output approach. *Proceedings of the IEEE Conference on Decision and Control*, *54rd IEEE*(Cdc), 1756–1761.

Hoffmann, C., Hashemi, S. M., Abbas, H. S., & Werner, H. (2014). Synthesis of LPV controllers with low implementation complexity based on a reduced parameter set. *IEEE Transactions on Control Systems Technology*, *22*(6), 2393–2398.

Hoffmann, C., & Werner, H. (2014). Linear parameter-varying control of complex mechanical systems. In *IFAC Proceedings Volumes (IFAC-PapersOnline)* (Vol. 19, Issue 3). IFAC.

Hoffmann, C., & Werner, H. (2015). A survey of linear parameter-varying control applications validated by experiments or high-fidelity simulations. *IEEE Transactions on Control Systems Technology*, *23*(2), 416–433.

Hosoe, Y., & Peaucelle, D. (2017). S-variable approach to robust stabilization state feedback synthesis for systems characterized by random polytopes. *2016 European Control Conference, ECC 2016*, 2023–2028.

Hu, T., & Lin, Z. (2001). Control Systems with Actuator Saturation. In Intergovernmental Panel on Climate Change (Ed.), *Journal of Chemical Information and Modeling* (Vol. 53, Issue 9). Birkhäuser Boston.

Hu, T., & Lin, Z. (2003). Composite quadratic Lyapunov functions for constrained control systems. *IEEE Transactions on Automatic Control*, *48*(3), 440–450.

Hu, T., Lin, Z., & Chen, B. M. (2002). An analysis and design method for linear systems subject to actuator saturation and disturbance. *Automatica*, *38*(2), 351–359.

Hu, T., Teel, A. R., & Zaccarian, L. (2006). Stability and performance for saturated systems via quadratic and nonquadratic Lyapunov functions. *IEEE Transactions on Automatic Control*, *51*(11), 1770–1786.

Hu, T., Teel, A. R., & Zaccarian, L. (2008). Anti-windup synthesis for linear control systems with input saturation: Achieving regional, nonlinear performance.

Automatica, *44*(2), 512–519.

Ibrir, S., Wen, F. X., & Su, C. Y. (2005). Observer-based control of discrete-time Lipschitzian non-linear systems: Application to one-link flexible joint robot. *International Journal of Control*, *78*(6), 385–395.

Isidori, A. (1995). Nonlinear Control Systems. In *Journal of Chemical Information and Modeling* (Vol. 53, Issue 9). Springer London.

Iwasaki, T., & Skelton, R. E. (1994). All controllers for the general H∞ control problem: LMI existence conditions and state space formulas. *Automatica*, *30*(8), 1307–1317.

Jaadari, A. (2013). *Continuous quasi-LPV Systems: how to leave the quadratic Framework?*

Johansson, K. H. (1997). Relay Feedback and Multivariable Control [Department of Automatic Control, Lund Institute of Technology (LTH)]. In *Engineering Sciences*.

Johansson, M. (1999). *Piecewise Linear Control Systems*. Department of Automatic Control, Lund Institute of Technology (LTH).

Jönsson, U. (1997). Stability analysis with Popov multipliers and integral quadratic constraints. *Systems and Control Letters*, *31*(2), 85–92.

Kajiwara, H., Apkarian, P., & Gahinet, P. (1999). LPV techniques for control of an inverted pendulum. *IEEE Control Systems Magazine*, *19*(1), 44–54.

Kapila, V., & Grigoriadis, K. (Eds.). (2002). *Actuator Saturation Control*. CRC Press.

Kau, S. W., Lee, H. J., Yang, C. M., Lee, C. H., Hong, L., & Fang, C. H. (2007). Robust H∞ fuzzy static output feedback control of T-S fuzzy systems with parametric uncertainties. *Fuzzy Sets and Systems*, *158*(2), 135–146.

Kawamoto, S., Tada, K., Ishigame, A., & Taniguchi, T. (1992). An approach to stability analysis of second order fuzzy systems. *[1992 Proceedings] IEEE International Conference on Fuzzy Systems*, 1427–1434.

Khalil, H. K. (1996). Nonlinear Systems. In *Advances in the Astronautical Sciences* (Vol. 57). Prentice Hall.

Khargonekar, P. P., Petersen, I. R., & Zhou, K. (1990). Robust stabilization of uncertain linear systems: quadratic stabilizability and H/sup infinity / control theory. *IEEE Transactions on Automatic Control*, *35*(3), 356–361.

Kharitonov, V., & Niculescu, S.-I. (2003). On the stability of linear systems with uncertain delay. *IEEE Transactions on Automatic Control*, *48*(1), 127–132.

Kheloufi, H., Zemouche, A., Bedouhene, F., & Boutayeb, M. (2013a). A new observer-based stabilization method for linear systems with uncertain parameters. *2013 European Control Conference, ECC 2013*, 1120–1125.

Kheloufi, H., Zemouche, A., Bedouhene, F., & Boutayeb, M. (2013b). On LMI conditions to design observer-based controllers for linear systems with parameter uncertainties. *Automatica*, *49*(12), 3700–3704.

Kiencke, U., & Nielsen, L. (2005). *Automotive Control Systems*. Springer Berlin Heidelberg.

Konno, H., Thach, P. T., & Tuy, H. (1997). *Optimization on Low Rank Nonconvex Structures* (Vol. 15, Issue 9). Springer US.

Kwon, O., Park, M. J., Park, J. H., Lee, S. M., & Cha, E. J. (2014). Improved results on

stability of linear systems with time-varying delays via Wirtinger-based integral inequality. *Journal of the Franklin Institute*, *351*(12), 5386–5398.

Labit, Y., Peaucelle, D., & Henrion, D. (n.d.). SEDUMI INTERFACE 1.02: a tool for solving LMI problems with SEDUMI. *Proceedings. IEEE International Symposium on Computer Aided Control System Design*, 272–277.

Lam, H.-K. (2016). *Polynomial Fuzzy Control Systems Stability Analysis and Control Synthesis Using Membership Function-dependent*.

Latrech, C., El Hajjaji, A., Rabhi, A., & Kchaou, M. (2015). Vehicle dynamics decentralized networked control. *2015 IEEE International Conference on Fuzzy Systems (FUZZ-IEEE)*, *2015-Novem*, 1–7.

Lee, S. Y., Lee, W. Il, & Park, P. (2017). Polynomials-based integral inequality for stability analysis of linear systems with time-varying delays. *Journal of the Franklin Institute*, *354*(4), 2053–2067.

Lee, T. H., & Park, J. H. (2017). A novel Lyapunov functional for stability of time-varying delay systems via matrix-refined-function. *Automatica*, *80*, 239–242.

Leibfritz, F. (2001). An LMI-Based Algorithm for Designing Suboptimal Static $\cal H_2/\cal H_\infty$ Output Feedback Controllers. *SIAM Journal on Control and Optimization*, *39*(6), 1711–1735.

Li, X., & Yang, G. (2014). Fault Detection for T–S Fuzzy Systems With Unknown Membership Functions. *IEEE Transactions on Fuzzy Systems*, *22*(1), 139–152.

Li, Z., Yan, H., Zhang, H., Sun, J., & Lam, H. K. (2020). Stability and Stabilization with Additive Freedom for Delayed Takagi-Sugeno Fuzzy Systems by Intermediary-Polynomial-Based Functions. *IEEE Transactions on Fuzzy Systems*, *28*(4), 692–705.

Lian, Z., He, Y., & Wu, M. (2021). Stability and stabilization for delayed fuzzy systems via reciprocally convex matrix inequality. *Fuzzy Sets and Systems*, *402*, 124–141.

Lian, Z., He, Y., Zhang, C. K., & Wu, M. (2016). Stability analysis for T-S fuzzy systems with time-varying delay via free-matrix-based integral inequality. *International Journal of Control, Automation and Systems*, *14*(1), 21–28.

Lian, Z., He, Y., Zhang, C. K., & Wu, M. (2017). Further robust stability analysis for uncertain Takagi–Sugeno fuzzy systems with time-varying delay via relaxed integral inequality. *Information Sciences*, *409–410*, 139–150.

Lian, Z., He, Y., Zhang, C. K., & Wu, M. (2020). Stability and Stabilization of T-S Fuzzy Systems with Time-Varying Delays via Delay-Product-Type Functional Method. *IEEE Transactions on Cybernetics*, *50*(6), 2580–2589.

Lien, C. H. (2004). Robust observer-based control of systems with state perturbations via LMI approach. *IEEE Transactions on Automatic Control*, *49*(8), 1365–1370.

Lim, S. (1998). *Parameter-Varying Systems*.

Lim, S., & How, J. P. (1997). Analysis of LPV systems using a piecewise affine parameter-dependent Lyapunov function. *Proceedings of the IEEE Conference on Decision and Control*, *2*(December), 978–983.

Liu, K., Seuret, A., & Xia, Y. (2017). Stability analysis of systems with time-varying delays via the second-order Bessel–Legendre inequality. *Automatica*, *76*, 138–142.

Lofberg, J. (2004). YALMIP : a toolbox for modeling and optimization in MATLAB. *2004 IEEE International Conference on Robotics and Automation (IEEE Cat.*

No.04CH37508), 284–289.

Lovera, M., Bergamasco, M., & Casella, F. (2013). *LPV Modelling and Identification: An Overview* (pp. 3–24).

Marcos, A. (2001). *A Linear Parameter Varying Model of the Boeing 747- 100/200 Longitudinal Motion*. Minnesota.

Marcos, A., & Balas, G. J. (2001). Linear parameter varying modeling of the boeing 747-100/200 longitudinal motion. *AIAA Guidance, Navigation, and Control Conference and Exhibit*, *August*, 1–11.

Marcos, A., & Balas, G. J. (2004). Development of Linear-Parameter-Varying Models for Aircraft. *Journal of Guidance, Control, and Dynamics*, *27*(2), 218–228.

Marcos, A., & Bennani, S. (2009). LPV modeling, analysis and design in space systems: Rationale, objectives and limitations. *AIAA Guidance, Navigation, and Control Conference and Exhibit*, *August*, 1–23.

Megretski, A., & Rantzer, A. (1997). System analysis via integral quadratic constraints. *IEEE Transactions on Automatic Control*, *42*(6), 819–830.

Michiels, W. (2002). *Stability and stabilization of time-delay systems*.

Michiels, W., Engelborghs, K., Vansevenant, P., & Roose, D. (2002). Continuous pole placement for delay equations. *Automatica*, *38*(5), 747–761.

Michiels, W., & Niculescu, S.-I. (2007). *Stability and Stabilization of Time-Delay Systems*. Society for Industrial and Applied Mathematics.

Michiels, W., Van Assche, V., & Niculescu, S.-I. (2005). Stabilization of time-delay systems with a controlled time-varying delay and applications. *IEEE Transactions on Automatic Control*, *50*(4), 493–504.

Michiels, W., & Vyhlídal, T. (2005). An eigenvalue based approach for the stabilization of linear time-delay systems of neutral type. *Automatica*, *41*(6), 991–998.

Mitrinović, D. S., Pečarić, J. E., & Fink, A. M. (1993a). Convex Functions and Jensen's Inequality. In *Classical and New Inequalities in Analysis* (pp. 1–19). Springer Netherlands.

Mitrinović, D. S., Pečarić, J. E., & Fink, A. M. (1993b). Young's Inequality. In *Classical and New Inequalities in Analysis* (pp. 379–389). Springer Netherlands.

Mitrinović, D. S., Pečarić, J. E., & Fink, A. M. (1993c). Classical and New Inequalities in Analysis. In *aequationes mathematicae* (Vol. 40, Issue 1). Springer Netherlands.

Mohammadpour, J., & Scherer, C. W. (Eds.). (2012). *Control of Linear Parameter Varying Systems with Applications*. Springer US.

Moon, Y. S., Park, P., Kwon, W. H., & Lee, Y. S. (2001). Delay-dependent robust stabilization of uncertain state-delayed systems. *International Journal of Control*, *74*(14), 1447–1455.

Mozelli, L. A., Palhares, R. M., Souza, F. O., & Mendes, E. M. A. M. (2009). Reducing conservativeness in recent stability conditions of TS fuzzy systems. *Automatica*, *45*(6), 1580–1583.

Natesan, K., Gu, D. W., & Postlethwaite, I. (2007). Design of static H∞ linear parameter varying controllers for unmanned aircraft. *Journal of Guidance, Control, and Dynamics*, *30*(6), 1822–1827.

Nesterov, Y., & Nemirovskii, A. (1994). Interior-Point Polynomial Algorithms in Convex Programming. In *Interior-Point Polynomial Algorithms in Convex Programming*. Society for Industrial and Applied Mathematics.

Ngo, K. B., Mahony, R., & Jiang, Z. P. (2005). Integrator backstepping using barrier functions for systems with multiple state constraints. *Proceedings of the 44th IEEE Conference on Decision and Control, and the European Control Conference, CDC-ECC '05*, *2005*, 8306–8312.

Nguyen, A. T., Chevrel, P., & Claveau, F. (2018). Gain-scheduled static output feedback control for saturated LPV systems with bounded parameter variations. *Automatica*, *89*, 420–424.

Nguyen, A. T., Dequidt, A., & Dambrine, M. (2015). Anti-windup based dynamic output feedback controller design with performance consideration for constrained Takagi-Sugeno systems. *Engineering Applications of Artificial Intelligence*, *40*, 76–83.

Nguyen, A. T., Guerra, T. M., & Sentouh, C. (2018). Simultaneous Estimation of Vehicle Lateral Dynamics and Driver Torque using LPV Unknown Input Observer. *IFAC-PapersOnLine*, *51*(26), 13–18.

Nguyen, A. T., Tanaka, K., Dequidt, A., & Dambrine, M. (2017). Static output feedback design for a class of constrained Takagi–Sugeno fuzzy systems. *Journal of the Franklin Institute*, *354*(7), 2856–2870.

Nguyen, M. Q. (2016). *LPV approaches for modelling and control of vehicle dynamics : application toa small car pilot plant with ER dampers* (Issue 2016GREAT091) [Université Grenoble Alpes].

Nguyen, Q., & Sreenath, K. (2016). Exponential Control Barrier Functions for enforcing high relative-degree safety-critical constraints. *Proceedings of the American Control Conference*, *2016-July*(3), 322–328.

Ono, E., Hosoe, S., Asano, K., Sugai, M., & Doi, S. (1999). Robust stabilization of the vehicle dynamics by gain-scheduled H/sub /spl infin// control. *Proceedings of the 1999 IEEE International Conference on Control Applications (Cat. No.99CH36328)*, *2*, 1679–1685 vol. 2.

Ono, E., Hosoe, S., Doi, S., Asano, K., & Hayashi, Y. (1998). Theoretical approach for improving the vehicle robust stability and maneuverability by active front wheel steering control. *Vehicle System Dynamics*, *29*(SUPPL.), 748–753.

Pacejka, H. B. (2012). Tire Characteristics and Vehicle Handling and Stability. In *Tire and Vehicle Dynamics*.

Packard, A. (1994). Gain scheduling via linear fractional transformations. *Systems & Control Letters*, *22*(2), 79–92.

Packard, A., & Doyle, J. C. (1993). The complex structured singular value. *Automatica*, *29*(1), 71–109.

Papachristodoulou, A., Anderson, J., Valmorbida, G., Prajna, S., Seiler, P., & Parrilo, P. A. (2013). *SOSTOOLS: Sum of squares optimization toolbox for MATLAB*.

Papachristodoulou, A., & Prajna, S. (2002). On the construction of Lyapunov functions using the sum of squares decomposition. *Proceedings of the IEEE Conference on Decision and Control*, *3*(December), 3482–3487.

Papageorgiou, G., Glover, K., D'Mello, G., & Patel, Y. (2000). Taking robust LPV control into flight on the VAAC Harrier. *Proceedings of the IEEE Conference on*

Decision and Control, *5*, 4558–4564.

Park, M., Kwon, O., Park, J. H., Lee, S., & Cha, E. (2015). Stability of time-delay systems via Wirtinger-based double integral inequality. *Automatica*, *55*, 204–208.

Park, P., Ko, J. W., & Jeong, C. (2011). Reciprocally convex approach to stability of systems with time-varying delays. *Automatica*, *47*(1), 235–238.

Park, P., Lee, W. Il, & Lee, S. Y. (2015). Auxiliary function-based integral inequalities for quadratic functions and their applications to time-delay systems. *Journal of the Franklin Institute*, *352*(4), 1378–1396.

Parrilo, P. A. (2000). Structured semidefinite programs and semialgebraic geometry methods in robustness and optimization. *PhD Thesis, California Institute of Technology, Pasadena, CA*, *2000*, 117.

Parrilo, P. A. (2003). Semidefinite programming relaxations for semialgebraic problems. *Mathematical Programming*, *96*(2), 293–320.

Peaucelle, D., & Arzelier, D. (2001). An efficient numerical solution for H2 static output feedback synthesis. *2001 European Control Conference, ECC 2001*, 3800–3805.

Peaucelle, D., & Ebihara, Y. (2014). LMI results for robust control design of observer-based controllers, the discrete-time case with polytopic uncertainties. *IFAC Proceedings Volumes (IFAC-PapersOnline)*, *19*, 6527–6532.

Peaucelle, D., Henrion, D., Labit, Y., & Taitz, K. (2002). User's guide for SeDuMi interface 1.04. *LAAS-CNRS, Toulouse*.

Pellanda, P. C., Apkarian, P., & Tuan, H. D. (2002). Missile autopilot design via a multi-channel LFT/LPV control method. *International Journal of Robust and Nonlinear Control*, *12*(1), 1–20.

Peng, C., & Han, Q.-L. (2011). Delay-range-dependent robust stabilization for uncertain T–S fuzzy control systems with interval time-varying delays. *Information Sciences*, *181*(19), 4287–4299.

Pfifer, H., & Seiler, P. (2015). Integral quadratic constraints for delayed nonlinear and parameter-varying systems. *Automatica*, *56*, 36–43.

Pipeleers, G., Demeulenaere, B., Swevers, J., & Vandenberghe, L. (2009). Extended LMI characterizations for stability and performance of linear systems. *Systems and Control Letters*, *58*(7), 510–518.

Pólik, I., & Terlaky, T. (2007). A Survey of the S-Lemma. *SIAM Review*, *49*(3), 371–418.

PooGyeon Park. (1999). A delay-dependent stability criterion for systems with uncertain time-invariant delays. *IEEE Transactions on Automatic Control*, *44*(4), 876–877.

Poussot-vassal, C. (2008). *Commande Robuste LPV Multivariable de Châssis Automobile*.

Prajna, S., Papachristodoulou, A., & Wu, F. (2004). Nonlinear control synthesis by sum of squares optimization: A Lyapunov-based approach. *2004 5th Asian Control Conference*, *1*, 157–165.

Prempain, E., & Postlethwaite, I. (2001). Static output feedback stabilisation with H∞ performance for a class of plants. *Systems & Control Letters*, *43*(3), 159–166.

Qiu, J., Feng, G., & Gao, H. (2013). Static-output-feedback H∞ control of continuous-time T-S fuzzy affine systems via piecewise lyapunov functions. *IEEE Transactions on Fuzzy Systems*, *21*(2), 245–261.

Ren, X. M., Rad, A. B., Chan, P. T., & Lo, W. L. (2005). Online identification of continuous-time systems with unknown time delay. *IEEE Transactions on Automatic Control*, *50*(9), 1418–1422.

Rheex, B. J., & Won, S. (2006). A new fuzzy Lyapunov function approach for a Takagi-Sugeno fuzzy control system design. *Fuzzy Sets and Systems*, *157*(9), 1211–1228.

Robert, D., Sename, O., & Simon, D. (2010). An H∞ LPV design for sampling varying controllers: Experimentation with a T-inverted pendulum. *IEEE Transactions on Control Systems Technology*, *18*(3), 741–749.

Roos, C., Biannic, J.-M., Tarbouriech, S., & Prieur, C. (2007). On-Ground Aircraft Control Design Using an LPV Anti-windup Approach. In D. Bates & M. Hagström (Eds.), *Nonlinear Analysis and Synthesis Techniques for Aircraft Control* (pp. 117–145). Springer Berlin Heidelberg.

Roose, A. I., Yahya, S., & Al-Rizzo, H. (2017). Fuzzy-logic control of an inverted pendulum on a cart. *Computers and Electrical Engineering*, *61*, 31–47.

Rotondo, D., Cristofaro, A., Gryte, K., & Johansen, T. A. (2017). LPV model reference control for fixed-wing UAVs. *IFAC-PapersOnLine*, *50*(1), 11559–11564.

Rotondo, D., Nejjari, F., & Puig, V. (2013). Quasi-LPV modeling, identification and control of a twin rotor MIMO system. *Control Engineering Practice*, *21*(6), 829–846.

Rotondo, D., Nejjari, F., & Puig, V. (2014). Robust state-feedback control of uncertain LPV systems: An LMI-based approach. *Journal of the Franklin Institute*, *351*(5), 2781–2803.

Sadabadi, M. S., & Peaucelle, D. (2016). From static output feedback to structured robust static output feedback: A survey. *Annual Reviews in Control*, *42*(12), 11–26.

Sala, A. (2009). On the conservativeness of fuzzy and fuzzy-polynomial control of nonlinear systems. *Annual Reviews in Control*, *33*(1), 48–58.

Sala, A. (2010). The polytopic/fuzzy polynomial approach for non-linear control: advantages and drawbacks. *18Th Mediterranean Conference on Control and Automation*, *1*, 1670–1678.

Sala, A. (2019). Stability analysis of LPV systems: Scenario approach. *Automatica*, *104*, 233–237.

Sala, A., & Arino, C. (2008). Relaxed Stability and Performance LMI Conditions for Takagi--Sugeno Fuzzy Systems With Polynomial Constraints on Membership Function Shapes. *IEEE Transactions on Fuzzy Systems*, *16*(5), 1328–1336.

Sala, A., & Ariño, C. (2009). Polynomial fuzzy models for nonlinear control: A taylor series approach. *IEEE Transactions on Fuzzy Systems*, *17*(6), 1284–1295.

Sato, M., & Peaucelle, D. (2006). Robust stability/performance analysis for linear time-invariant polynomially parameter-dependent systems using polynomially parameter-dependent Lyapunov functions. *Proceedings of the IEEE Conference on Decision and Control*, 5807–5813.

Sato, M., & Peaucelle, D. (2007a). Comparison between SOS approach and Slack Variable approach for non-negativity check of polynomial functions: Multiple variable case. *2007 European Control Conference, ECC 2007*, 3016–3025.

Sato, M., & Peaucelle, D. (2007b). Robust stability/performance analysis for uncertain

linear systems via multiple slack variable approach: Polynomial LTIPD systems. *Proceedings of the IEEE Conference on Decision and Control*, 5031–5037.

Sato, M., & Peaucelle, D. (2013). Gain-scheduled output-feedback controllers using inexact scheduling parameters for continuous-time LPV systems. *Automatica*, *49*(4), 1019–1025.

Savaresi, S. M., Poussot-vassal, C., Spelta, C., Sename, O., & Dugard, L. (2010). Semi-Active Suspension Control Design for Vehicles. In *Semi-Active Suspension Control Design for Vehicles*. Elsevier.

Scherer, C. W. (1990). *The Riccati inequality and state-space H∞-optimal control.*

Scherer, C. W. (2001). LPV control and full block multipliers. *Automatica*, *37*(3), 361–375.

Scherer, C. W. (2006). LMI relaxations in robust control. *European Journal of Control*, *12*(1), 3–29.

Scherer, C. W. (1997). A full block S-procedure with applications. *Proceedings of the 36th IEEE Conference on Decision and Control*, *3*(December), 2602–2607.

Scherer, C. W., Gahinet, P., & Chilali, M. (1997). Multiobjective output-feedback control via LMI optimization. *IEEE Transactions on Automatic Control*, *42*(7), 896–911.

Scherer, C. W., & Weiland, S. (2005). Linear matrix inequalities in control. In W. S. Levine (Ed.), *The Control Systems Handbook, Second Edition: Control System Advanced Methods* (Vol. 56, Issue 11, pp. 24/1--24/30). CRC Press.

Schoen, G. M. (1995). Stability and stabilization of time-delay systems. In *PhD thesis*.

Schug, A., Seiler, P., & Pfifer, H. (2016). *Robustness Margins for Linear Parameter Varying Systems*. *13*, 1–9.

Sename, O., Simon, D., & Gaid, M. Ben. (2008). A LPV approach to control and real-time scheduling codesign: Application to a robot-arm control. *Proceedings of the IEEE Conference on Decision and Control*, 4891–4897.

Seuret, A., & Gouaisbaut, F. (2012). On the use of the Wirtinger inequalities for time-delay systems. In *IFAC Proceedings Volumes (IFAC-PapersOnline)* (Vol. 45, Issue 14 PART 1). IFAC.

Seuret, A., & Gouaisbaut, F. (2013). Wirtinger-based integral inequality: Application to time-delay systems. *Automatica*, *49*(9), 2860–2866.

Seuret, A., & Gouaisbaut, F. (2019). *Delay-Dependent Reciprocally Convex Combination Lemma for the Stability Analysis of Systems with a Fast-Varying Delay* (pp. 187–197).

Shamma, J. S. (1988). Analysis and design of gain scheduled control systems [Massachusetts Institute of Technology]. In *Massachusetts Institute of Technology*.

Shamma, J. S. (2012). An Overview of LPV Systems. In *Control of Linear Parameter Varying Systems with Applications* (pp. 3–26). Springer US.

Shamma, J. S., & Athans, M. (1990). Analysis of gain scheduled control for nonlinear plants. *IEEE Transactions on Automatic Control*, *35*(8), 898–907.

Shamma, J. S., & Cloutier, J. R. (1992). Linear parameter varying approach to gain scheduled missile autopilot design. *Proceedings of the American Control Conference*, *2*, 1317–1321.

Shin, J. Y., Balas, G. J., & Kaya, A. M. (2001). Blending approach of linear parameter varying control synthesis for F-16 aircraft. *AIAA Guidance, Navigation, and Control Conference and Exhibit*.

Shustin, E., & Fridman, E. (2007). On delay-derivative-dependent stability of systems with fast-varying delays. *Automatica*, *43*(9), 1649–1655.

Sipahi, R., Niculescu, S.-I., Abdallah, C. T., Michiels, W., & Gu, K. (2011). Stability and Stabilization of Systems with Time Delay. *IEEE Control Systems*, *31*(1), 38–65.

Skelton, R. E., Iwasaki, T., & Grigoriadis, K. M. (1998). A Unified Algebraic Approach To Control Design. In *A Unified Algebraic Approach to Control Design* (Issue January). Routledge.

Sturm, J. F. (1999). Using SeDuMi 1.02, A Matlab toolbox for optimization over symmetric cones. *Optimization Methods and Software*, *11*(1–4), 625–653.

Sun, J., Liu, G. P., & Chen, J. (2009). Delay-dependent stability and stabilization of neutral time-delay systems. *International Journal of Robust and Nonlinear Control*, *19*(12), 1364–1375.

Syrmos, V. L., Abdallah, C. T., Dorato, P., & Grigoriadis, K. M. (1997). Static output feedback - A survey. *Automatica*, *33*(2), 125–137.

Takagi, T., & Sugeno, M. (1985). Fuzzy identification of systems and its applications to modeling and control. *IEEE Transactions on Systems, Man, and Cybernetics*, *SMC-15*(1), 116–132.

Tanaka, K., Hori, T., & Wang, H. O. (2003). A multiple Lyapunov function approach to stabilization of fuzzy control systems. *IEEE Transactions on Fuzzy Systems*, *11*(4), 582–589.

Tanaka, K., Ikeda, T., & Wang, H. O. (1998). Fuzzy regulators and fuzzy observers: relaxed stability conditions and LMI-based designs. *IEEE Transactions on Fuzzy Systems*, *6*(2), 250–265.

Tanaka, K., & Wang, H. O. (2001). Fuzzy Control Systems Design and Analysis: A Linear Matrix Inequality Approach. In *Automatica* (Vol. 39, Issue 11). John Wiley & Sons, Inc.

Tanaka, K., Yoshida, H., Ohtake, H., & Wang, H. O. (2009). A sum-of-squares approach to modeling and control of nonlinear dynamical systems with polynomial fuzzy systems. *IEEE Transactions on Fuzzy Systems*, *17*(4), 911–922.

Tarbouriech, S., Garcia, G., Gomes da Silva, J. M., & Queinnec, I. (2011). *Stability and Stabilization of Linear Systems with Saturating Actuators*. Springer London.

Tarbouriech, S., Prieur, C., & Gomes da Silva, J. M. (2006). Stability analysis and stabilization of systems presenting nested saturations. *IEEE Transactions on Automatic Control*, *51*(8), 1364–1371.

Tee, K. P., Ge, S. S., & Tay, E. H. (2009). Barrier Lyapunov Functions for the control of output-constrained nonlinear systems. *Automatica*, *45*(4), 918–927.

Teel, A. R., Subbaraman, A., & Sferlazza, A. (2014). Stability analysis for stochastic hybrid systems: A survey. *Automatica*, *50*(10), 2435–2456.

Theis, J., Sedlmair, N., Thielecke, F., & Pfifer, H. (2020). Observer-based LPV control with anti-windup compensation: A flight control example. *IFAC-PapersOnLine*, *53*(2), 7325–7330.

Theory of Robot Control. (1996). In C. Canudas-de-Wit, B. Siciliano, & G. Bastin (Eds.), *Journal of Chemical Information and Modeling* (Vol. 53, Issue 9). Springer London.

Tian, E., & Peng, C. (2006). Delay-dependent stability analysis and synthesis of uncertain T-S fuzzy systems with time-varying delay. *Fuzzy Sets and Systems*, *157*(4), 544–559.

Tian, Y., & Wang, Z. (2020). A new multiple integral inequality and its application to stability analysis of time-delay systems. *Applied Mathematics Letters*, *105*, 106325.

Tian, Y., & Wang, Z. (2021). Composite slack-matrix-based integral inequality and its application to stability analysis of time-delay systems. *Applied Mathematics Letters*, *120*, 107252.

Tian, Y., & Wang, Z. (2022). Stability Analysis and Generalized Memory Controller Design for Delayed T-S Fuzzy Systems via Flexible Polynomial-Based Functions. *IEEE Transactions on Fuzzy Systems*, *30*(3), 728–740.

Tóth, R. (2010). Modeling and Identification of Linear Parameter-Varying Systems. In *Lecture Notes in Control and Information Sciences* (Vol. 403). Springer Berlin Heidelberg.

Tuan, H. D., & Apkarian, P. (1999). Relaxations of parameterized LMIs with control applications. *International Journal of Robust and Nonlinear Control*, *9*(2), 59–84.

Tuan, H. D., & Apkarian, P. (2002). Monotonic relaxations for robust control: new characterizations. *IEEE Transactions on Automatic Control*, *47*(2), 378–384.

Tuan, H. D., Apkarian, P., Narikiyo, T., & Kanota, M. (2004). New Fuzzy Control Model and Dynamic Output Feedback Parallel Distributed Compensation. *IEEE Transactions on Fuzzy Systems*, *12*(1), 13–21.

Tuan, H. D., Apkarian, P., Narikiyo, T., & Yamamoto, Y. (2001). Parameterized linear matrix inequality techniques in fuzzy control system design. *IEEE Transactions on Fuzzy Systems*, *9*(2), 324–332.

Tuan, H. D., Ono, E., Apkarian, P., & Hosoe, S. (2001). Nonlinear H/sub ∞/ control for an integrated suspension system via parameterized linear matrix inequality characterizations. *IEEE Transactions on Control Systems Technology*, *9*(1), 175–185.

Tuy, H. (2016). *Convex Analysis and Global Optimization* (Vol. 110, Issue 9). Springer International Publishing.

Tuy, H., & Tuan, H. D. (2013). Generalized S-Lemma and strong duality in nonconvex quadratic programming. *Journal of Global Optimization*, *56*(3), 1045–1072.

Vafamand, N., Asemani, M. H., & Khayatiyan, A. (2016). A robust L1 controller design for continuous-time TS systems with persistent bounded disturbance and actuator saturation. *Engineering Applications of Artificial Intelligence*, *56*(April), 212–221.

Van Hien, L., & Trinh, H. (2015). Refined Jensen-based inequality approach to stability analysis of time-delay systems. *IET Control Theory and Applications*, *9*(14), 2188–2194.

Vandenberghe, L., & Boyd, S. (1996). Semidefinite Programming. *SIAM Review*, *38*(1), 49–95.

Vidyasagar, M. (1992). Nonlinear Systems Analysis. In *Automatica* (Vol. 30, Issue 10). Society for Industrial and Applied Mathematics.

Vu, V. T., Sename, O., Dugard, L., & Gaspar, P. (2016). Active anti-roll bar control using electronic servo valve hydraulic damper on single unit heavy vehicle. *IFAC-PapersOnLine*, *49*(11), 418–425.

Wang, L.-X. (1996). *A Course in Fuzzy Systems and Control*. Prentice-Hall, Inc.

Wang, L., & Lam, H.-K. (2018a). Local Stabilization for Continuous-time Takagi–Sugeno Fuzzy Systems With Time Delay. *IEEE Transactions on Fuzzy Systems*, *26*(1), 379–385.

Wang, L., & Lam, H. K. (2018b). A new approach to stability and stabilization analysis for continuous-time takagi-sugeno fuzzy systems with time delay. *IEEE Transactions on Fuzzy Systems*, *26*(4), 2460–2465.

Wang, L., & Lam, H. K. (2019). New stability criterion for continuous-time Takagi-Sugeno fuzzy systems with time-varying delay. *IEEE Transactions on Cybernetics*, *49*(4), 1551–1556.

Watanabe, R. (1993). *Hinf Control of Gasturbine Engines for Helicopters Helicopters Control of Gasturbine Engines for Gasturbine Engines for Helicopters*. *Actuator 2*, 1123–1127.

Wesson, J., & Campbell, D. J. (2004). *Tokamaks*. Clarendon Press.

Witrant, E., Joffrin, E., Brémond, S., Giruzzi, G., Mazon, D., Barana, O., & Moreau, P. (2007). A control-oriented model of the current profile in tokamak plasma. *Plasma Physics and Controlled Fusion*, *49*(7), 1075–1105.

Wright, M. H. (1992). Interior methods for constrained optimization. *Acta Numerica*, *1*, 341–407.

Wu, F. (1995). *Control of linear parameter varying systems*. University of California.

Wu, F., Grigoriadis, K. M., & Packard, A. (2000). Anti-windup controller design using linear parameter-varying control methods. *International Journal of Control*, *73*(12), 1104–1114.

Wu, F., Packard, A., & Balas, G. J. (1995). LPV control design for pitch-axis missile autopilots. *Proceedings of the IEEE Conference on Decision and Control*, *1*(December), 188–193.

Wu, F., & Prajna, S. (2004). A new solution approach to polynomial LPV system analysis and synthesis. *Proceedings of the American Control Conference*, *2*, 1362–1367.

Wu, F., Yang, X. H., Packard, A., & Becker, G. (1996). Induced L2-norm control for LPV systems with bounded parameter variation rates. *International Journal of Robust and Nonlinear Control*, *6*(910), 983–998.

Wu, H.-N., & Li, H.-X. (2007). New Approach to Delay-Dependent Stability Analysis and Stabilization for Continuous-Time Fuzzy Systems With Time-Varying Delay. *IEEE Transactions on Fuzzy Systems*, *15*(3), 482–493.

Wu, M., He, Y., & She, J. H. (2010). Stability analysis and robust control of time-delay systems. In *Stability Analysis and Robust Control of Time-Delay Systems*.

Wu, M., He, Y., She, J. H., & Liu, G. P. (2004). Delay-dependent criteria for robust stability of time-varying delay systems. *Automatica*, *40*(8), 1435–1439.

Xie, L., Shishkin, S., & Fu, M. (1997). Piecewise Lyapunov functions for robust stability of linear time-varying systems. *Systems & Control Letters*, *31*(3), 165–171.

Yang, C., Jiang, Y., Na, J., Li, Z., Cheng, L., & Su, C. Y. (2019). Finite-Time

Convergence Adaptive Fuzzy Control for Dual-Arm Robot with Unknown Kinematics and Dynamics. *IEEE Transactions on Fuzzy Systems*, *27*(3), 574–588.

Yang, Z., & Yang, Y.-P. (2010). New delay-dependent stability analysis and synthesis of T-S fuzzy systems with time-varying delay. *International Journal of Robust and Nonlinear Control*, *20*(3), 313–322.

Yi, J., & Yubazaki, N. (2000). Stabilization fuzzy control of inverted pendulum systems. *Artificial Intelligence in Engineering*, *14*(2), 153–163.

Zaccarian, L., & Teel, A. R. (2002). A common framework for anti-windup, bumpless transfer and reliable designs. *Automatica*, *38*(10), 1735–1744.

Zaccarian, L., & Teel, A. R. (2005). The scriptLsign; (l2) bumpless transfer problem for linear plants: Its definition and solution. *Automatica*, *41*(7), 1273–1280.

Zaccarian, L., & Teel, A. R. (2011). *Modern Anti-windup Synthesis: Control Augmentation for A tuator Saturation* (Princeton). Princeton University Press.

Zemouche, A., & Boutayeb, M. (2013). On LMI conditions to design observers for Lipschitz nonlinear systems. *Automatica*, *49*(2), 585–591.

Zemouche, A., Rajamani, R., Kheloufi, H., & Bedouhene, F. (2017). Robust observer-based stabilization of Lipschitz nonlinear uncertain systems via LMIs - discussions and new design procedure. *International Journal of Robust and Nonlinear Control*, *27*(11), 1915–1939.

Zemouche, A., Rajamani, R., Trinh, H., & Zasadzinski, M. (2017). A new LMI based H∞ observer design method for Lipschitz nonlinear systems. *2016 European Control Conference, ECC 2016*, 2011–2016.

Zeng, H. B., He, Y., Wu, M., & She, J. (2015). Free-Matrix-Based Integral Inequality for Stability Analysis of Systems With Time-Varying Delay. *IEEE Transactions on Automatic Control*, *60*(10), 2768–2772.

Zeng, H. B., Park, J. H., Xia, J. W., & Xiao, S. P. (2014). Improved delay-dependent stability criteria for T-S fuzzy systems with time-varying delay. *Applied Mathematics and Computation*, *235*, 492–501.

Zeng, H. B., Zhai, Z. L., & Wang, W. (2021). Hierarchical stability conditions of systems with time-varying delay. *Applied Mathematics and Computation*, *404*, 126222.

Zhang, C. K., He, Y., Jiang, L., Wu, M., & Wang, Q. G. (2017). An extended reciprocally convex matrix inequality for stability analysis of systems with time-varying delay. *Automatica*, *85*, 481–485.

Zhang, F., & Grigoriadis, K. M. (2005). Delay-dependent stability analysis and H∞ control for state-delayed LPV system. *Proceedings of the 20th IEEE International Symposium on Intelligent Control, ISIC '05 and the 13th Mediterranean Conference on Control and Automation, MED '05*, *2005*, 1532–1537.

Zhang, H., Huang, X., Wang, J., & Karimi, H. R. (2015). Robust energy-to-peak sideslip angle estimation with applications to ground vehicles. *Mechatronics*, *30*, 338–347.

Zhang, H., & Wang, J. (2017). Active steering actuator fault detection for an automatically-steered electric ground vehicle. *IEEE Transactions on Vehicular Technology*, *66*(5), 3685–3702.

Zhang, H., Zhang, X., & Wang, J. (2014). Robust gain-scheduling energy-to-peak control of vehicle lateral dynamics stabilisation. *Vehicle System Dynamics*, *52*(3), 309–340.

Zhang, J., Knopse, C. R., & Tsiotras, P. (2001). Stability of time-delay systems: Equivalence between Lyapunov and scaled small-gain conditions. *IEEE Transactions on Automatic Control*, *46*(3), 482–486.

Zhang, X. M., Han, Q.-L., Seuret, A., & Gouaisbaut, F. (2017). An improved reciprocally convex inequality and an augmented Lyapunov–Krasovskii functional for stability of linear systems with time-varying delay. *Automatica*, *84*, 221–226.

Zhang, Z., Lin, C., & Chen, B. (2015). New stability and stabilization conditions for T-S fuzzy systems with time delay. *Fuzzy Sets and Systems*, *263*, 82–91.

Zhao, N., Lin, C., Chen, B., & Wang, Q. G. (2017). A new double integral inequality and application to stability test for time-delay systems. *Applied Mathematics Letters*, *65*, 26–31.

Zheng, G., Barbot, J. P., & Boutat, D. (2011). Delay identification for nonlinear time-delay systems with unknown inputs. *Proceedings of the IEEE Conference on Decision and Control*, 6302–6307.

Zhou, K., & Doyle, J. C. (1998). *Essentials of Robust Control* (Vol. 12, Issue 2). Prentice Hall.

Zhou, K., Doyle, J. C., & Glover, K. (1996). *Robust and Optimal Control* (Vol. 40). Prentice Hall.

Zhou, K., & Khargonekar, P. P. (1988). Robust stabilization of linear systems with norm-bounded time-varying uncertainty. *Systems and Control Letters*, *10*(1), 17–20.

Zope, R., Mohammadpour Velni, J. M., Grigoriadis, K. M., & Franchek, M. (2012). Delay-Dependent Output Feedback Control of Time-Delay LPV Systems. In J. Mohammadpour & C. W. Scherer (Eds.), *Control of Linear Parameter Varying Systems with Applications* (pp. 279–299). Springer US.

Abstract

The dissertation is devoted to developing a methodology of stability and stabilization for the linear parameter-dependent (PD) and time-delay systems (TDSs) subject to control saturation. In the industrial process, control signal magnitude is usually bounded by the safety constraints, the physical cycle limits, and so on. For this reason, a suitable synthesis and analysis tool is needed to accurately describe the characteristics of the saturated linear parameter-varying (LPV) systems.

In the part one, a parameter-dependent form of the generalized sector condition (GSC) is considered to solve the saturated stabilization problem. Several feedback control strategies are investigated to stabilize the saturated LPV/qLPV systems. Necessary and sufficient stabilization conditions via the parameterized linear matrix inequality (PLMI) formulation proposed for the feedback controllers conforming to the design requirements (i.e., the admissible set of the initial conditions, the estimated region of the asymptotic convergence domain, the robust stability and performance with the influence of perturbations, Etc.). The relaxation of the designed PLMIs is shown through the comparison results using a parameter-dependent Lyapunov function (PDLF).

In the second part, the delay-dependent stability developments based on Lyapunov-Krasovskii functional (LKF) are presented. The modern advanced bounding techniques are utilized with a balance between conservatism and computational complexity. Then, saturation stabilization analyzes for the gain-scheduling controllers are proposed. Inspired by uncertain delay system methods, a novel stabilization condition is derived from the delay-dependent stabilizing analysis for the LPV time-delay system subject to saturation constraints. In this aspect, the stabilizing gain-scheduling feedback controllers improve the performance and stability of the saturated system and provide a large attraction domain. It can be emphasized that the derived formulation is general and can be used for the design control of many dynamic systems. Finally, to maximize the attraction region while guaranteeing the asymptotic stability of the closed-loop system, an optimization problem is included to the proposed control design strategy.

Key-Words: *LPV/quasi-LPV Systems*, *Actuators Saturation*, *Time-Delay Systems*, *Robust Control*, *Parametrized LMIs*.

Résumé

La thèse est consacrée au développement d'une méthodologie de stabilité et de stabilisation pour les systèmes linéaires à paramètres variables (LPV) et à retard soumis à la saturation de la commande. Dans les procédés industriel, l'amplitude du signal de commande est généralement limitée par les contraintes de sécurité, etc. Une synthèse de commande est donc nécessaire pour les systèmes saturés à paramètres linéaires variables.

Dans la première partie, une nouvelle expression de la condition de secteur généralisée (GSC) est considérée pour résoudre le problème de stabilisation saturée. Plusieurs stratégies de contrôle sont étudiées pour stabiliser les systèmes LPV/quasi-LPV saturés. Des conditions de stabilisation nécessaires et suffisantes via la résolution des inégalités matricielles linéaires paramétrées sont proposées pour les contrôleurs par retour d'état respectant les exigences de conception (c'est-à-dire l'ensemble admissible des conditions initiales, la région estimée du domaine de convergence asymptotique, la stabilité et les performances robustes sous l'influence des perturbations, etc.). La relaxation des conditions LMI paramétrées est illustrée par des résultats proposant une fonction de Lyapunov dépendant des paramètres.

Dans la deuxième partie, les conditions de stabilité dépendant du retard basé sur la fonction de Lyapunov-Krasovskii (LKF) sont présentées. Les techniques modernes et avancées de délimitation sont utilisées avec un compromis entre conservatisme et complexité de calcul. Ensuite, des conditions de stabilisation avec saturation sont proposés pour les contrôleurs à gain préprogrammé. Inspirée des méthodes de systèmes à retard incertains, une nouvelle condition de stabilisation est dérivée pour le systèmes à retard LPV soumis à des contraintes de saturation. Les contrôleurs de rétroaction à gain préprogrammé améliorent les performances et la stabilité du système saturé et fournissent un grand domaine d'attraction. Nous pouvons souligner que la formulation dérivée des conditions est générale et peut être utilisée pour le contrôle de nombreux systèmes dynamiques. Enfin, pour maximiser la région d'attraction tout en garantissant la stabilité asymptotique du système en boucle fermée, un problème d'optimisation est inclus dans la stratégie de conception de commande proposée.

Mots-clés : *Systèmes LPV/quasi-LPV*, *Saturation des Actionneurs*, *Systèmes à Retard*, *Commande Robuste*, *LMI Paramétrés*.